BEILSTEIN JOURNAL OF ORGANIC CHEMISTRY

Progress in metathesis chemistry II

Edited by Karol Grela

Imprint

Beilstein Journal of Organic Chemistry
www.bjoc.org
ISSN 1860-5397
Email: journals-support@beilstein-institut.de

The *Beilstein Journal of Organic Chemistry* is published by the Beilstein-Institut zur Förderung der Chemischen Wissenschaften.

Beilstein-Institut zur Förderung der Chemischen Wissenschaften
Trakehner Straße 7–9
60487 Frankfurt am Main
Germany
www.beilstein-institut.de

BEILSTEIN JOURNAL OF ORGANIC CHEMISTRY

Progress in metathesis chemistry II

Karol Grela[1,2]

Editorial

Open Access

Address:
[1]Biological and Chemical Research Centre, Faculty of Chemistry, University of Warsaw, Żwirki i Wigury 101, 02-089 Warsaw, Poland and [2]Institute of Organic Chemistry, Polish Academy of Sciences, Kasprzaka 44/52, 01-224 Warsaw, Poland

Email:
Karol Grela - karol.grela@gmail.com

Keywords:
olefin metathesis

Beilstein J. Org. Chem. **2015,** *11,* 1639–1640.
doi:10.3762/bjoc.11.179

Received: 06 August 2015
Accepted: 17 August 2015
Published: 15 September 2015

This article is part of the Thematic Series "Progress in metathesis chemistry II".

Guest Editor: K. Grela

"*And the time, too, goes on – till one perceives ahead a shadow-line warning one that the region of early youth, too, must be left behind*"

Joseph Conrad – The Shadow-Line

Five years have passed since the first publication of the Thematic Series on Olefin Metathesis in the *Beilstein Journal of Organic Chemistry* [1]. During these years the research continued to progress at full speed. Astute readers of this Thematic Series, as well as readers of the recent books devoted to olefin metathesis [2,3], can easily see that a great number of studies in this field have advanced from the basic research phase to the commercial application stage. While new, active and more selective catalysts that solve some longstanding limitations are still being developed, a growing number of projects deal only with applications using olefin metathesis as one of many stock transformations.

However, this does not imply that the research phase is over, that all problems have been solved, that the technology is widely recognized and used, and that catalyst manufacturers have become millionaires. It only means that olefin metathesis is now a full-grown technology, which has already crossed the shadow line – the term coined by the Polish–British novelist Józef Teodor Konrad Korzeniowski (Joseph Conrad) to indicate the point where maturity is gained. This maturity will bring new promise, new expectations, and new challenges. During the application of this technology, new problems on various levels will surely emerge. I am therefore fully convinced that in the forthcoming years scientists dealing with olefin metathesis will have many opportunities for exciting research and for hard work, too.

On a personal level, it was for me a great pleasure to serve as the editor of this Thematic Series. I am very thankful to all authors for their first-class contributions. At the same time, I would like to thank the colleagues at the Beilstein-Institut for their professional support and patience.

Karol Grela

Warsaw, August 2015

References

1. Grela, K. *Beilstein J. Org. Chem.* **2010,** *6,* 1089–1090. doi:10.3762/bjoc.6.124
2. Grubbs, R. H.; Wenzel, A. G.; O'Leary, D. J.; Khosravi, E., Eds. *Handbook of Metathesis,* 2nd ed.; Wiley-VCH: Weinheim, 2015; Vol. 3.
3. Grela, K. *Olefin Metathesis: Theory and Practice;* John Wiley & Sons: Hoboken, 2014.

License and Terms

BEILSTEIN JOURNAL OF ORGANIC CHEMISTRY

Hybrid macrocycle formation and spiro annulation on *cis-syn-cis*-tricyclo[6.3.0.0^{2,6}]undeca-3,11-dione and its congeners via ring-closing metathesis

Sambasivarao Kotha*, Ajay Kumar Chinnam and Rashid Ali

Full Research Paper

Open Access

Address:
Department of Chemistry, Indian Institute of Technology-Bombay, Powai, Mumbai-400 076, India, Fax: 022-2572 7152

Email:
Sambasivarao Kotha* - srk@chem.iitb.ac.in

* Corresponding author

Keywords:
aza-polyquiananes; Fischer indolization; macrocycles; ring-closing metathesis; spiropolyquinanes

Beilstein J. Org. Chem. **2015,** *11,* 1123–1128.
doi:10.3762/bjoc.11.126

Received: 23 February 2015
Accepted: 23 June 2015
Published: 06 July 2015

This article is part of the Thematic Series "Progress in metathesis chemistry II".

Guest Editor: K. Grela

Abstract

We have developed a simple methodology to transform *cis-syn-cis*-triquinane derivative **2** into the diindole based macrocycle **6** involving Fischer indolization and ring-closing metathesis (RCM). Various spiro-polyquinane derivatives have been assembled via RCM as a key step.

Introduction

Design and synthesis of polyquinanes is an active area of research during the last three decades [1-10]. Various theoretically interesting as well as biologically active molecules such as dodecahedrane, [5.5.5.5]fenestrane and retigeranic acid A contain the quinane framework in their structures (Figure 1). A variety of quinane-based natural products isolated from terrestrial, microbial and marine sources have stimulated the growth of polyquinane chemistry. In this context, there is a continuous demand for the development of new methodologies to assemble cyclopentanoids (or quinanes) [11-21]. Several approaches are available for the synthesis of carbocyclic quinanes, however, only a limited number of methods is available for oxa- [22-25] and aza-polyquinanes [26-28]. The indole unit is present in a variety of plant alkaloids (e.g., reserpine, strychnine, physostigmine) and several important drugs contain indole as a key component [29-32]. Therefore, we are interested in designing new strategies to hybrid molecules containing both quinane and indole ring systems. On several occasions, the spirocyclic moiety seems to be a recurring motif in bioactive molecules. Consequently, assembling architecturally complex spirocycles is of great relevance to the diversity-oriented synthesis of biologically active spirocycles. In this context, new synthetic methods to generate multiple spirocenters in a simple manner remain a challenging task. Although, a variety of strategies have been investigated, a limited number of general methods are available [33-46] for the generation of multiple spirocenters in a

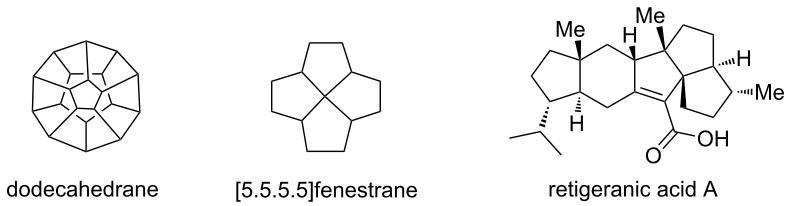

Figure 1: Natural and non-natural products containing quinane systems.

single step [43]. To expand the chemical space of aza-polyquinanes we conceived a new strategy based on Fischer indolization and ring-closing metathesis as the key steps.

To develop a simple synthetic methodology to aza-polycycles and spiropolycycles from readily available starting materials [47-52], bicyclic, tricyclic and pentacyclic diones (**1**–**3**) were identified as useful building blocks (Figure 2). The selection of these diones is based on their easy accessibility and also the symmetry involved with them. For example, with diones **1** and **2** one can apply a two-directional synthesis [53] to increase the brevity [54] of the overall synthesis. Earlier, we have shown that Weiss–Cook dione **1** [49-51] is a useful substrate for double Fischer indolization with a low melting mixture of L-(+)-tartaric acid and *N*,*N*′-dimethylurea (L-(+)-TA:DMU) [55] at 70 °C to generate an unusual C_s-symmetric diindole derivative along with the known C_2-symmetric diindole [56]. Also, based on Fischer indolization and ring-closing metathesis (RCM), we have developed a new strategy to indole-based propellane derivatives [57].

Here, the tricyclic dione **2** required was prepared starting with the Cookson's dione **4** in two steps involving flash vacuum pyrolysis (FVP) and hydrogenation steps (Scheme 1). A variety of synthetic transformations involving tricyclic diones **5** and **2** were reported in the literature [47].

To expand the utility of building block **2** in organic synthesis, we conceived a simple retrosynthetic approach to macrocylic aza-polyquinane **6** and spiro-polyquinane derivative **7** (Figure 3). The key steps involved here are: double Fischer indolization and RCM. To install the alkane chain connecting the two nitrogen atoms, we plan to use alkylation with allyl-bromide followed by RCM and hydrogenation protocols. It is known that a mono-indole derivative was obtained via Fischer indolization starting with dione **2** and two equivalents of phenylhydrazine hydrochloride, but the diindole derivative **8** [58] was not obtained under these conditions. Our experience with Fischer indolization of **1** using the low melting mixture protocol gave unusual results as compared with conventional Fischer indolization conditions. Therefore, the reactivity of **2**

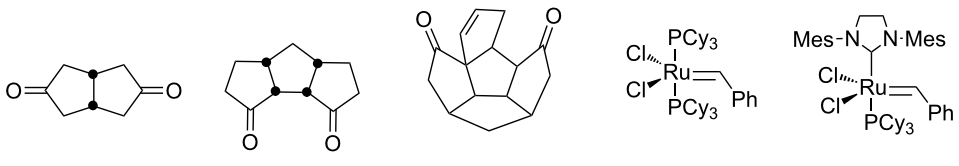

Figure 2: Quinane building blocks (**1**–**3**) and metathetic catalyst used in our strategy.

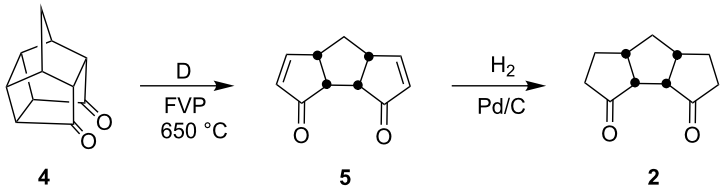

Scheme 1: Synthesis of tricyclic diones **5** and **2**.

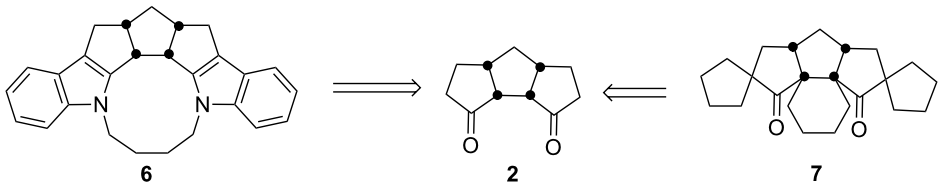

Figure 3: Retrosynthetic approach to aza-polyquinane **6** and spiro-polyquinane **7**.

under conditions of the low melting mixture is worthy of systematic investigation. Here, we are pleased to report our successful results in generating the diindole derivative **8** by utilizing a low melting mixture of L-(+)-TA:DMU and its subsequent utility in assembling the macrocyclic system **6** via RCM. During this venture, we also found that the tricyclic dione **2** is a useful substrate for the synthesis of spiro-polyquinane derivative **7** via a six fold allylation followed by a three-fold RCM and a hydrogenation sequence.

Results and Discussion

To realize the strategy shown in Figure 3, the tricyclic dione **2** was subjected to a two-fold Fischer indolization in the presence of two equivalents of phenylhydrazine hydrochloride with the aid of a low melting mixture of L-(+)-TA:DMU to generate the diindole derivative **8** (62%, Scheme 2). The structure of the diindole **8** has been established on the basis of ^{1}H NMR and ^{13}C NMR spectral data. The presence of 12 signals in the ^{13}C NMR spectrum clearly indicated that the C_s-symmetry is present in molecule **8**. Later, the diindole derivative was treated with methyl iodide in the presence of NaH/DMF at room temperature to deliver the dimethyl derivative **9**. Again, the C_s-symmetry present in **9** is evidenced by the appearance of 13 signals in the ^{13}C NMR spectrum. Alternatively, the diindole derivative **9** has been generated in a single step by reacting the dione **2** with *N*-methyl-*N*-phenyl-hydrazine under conditions using the described low melting mixture.

Next, the *N*-allylation of the diindole derivative **8** with allyl bromide in the presence of NaH/DMF gave diallyl derivative **10**, which was subjected to the RCM sequence in the presence of Grubbs' 2nd generation catalyst to produce the cyclized compound **11** (84%). Subsequently, the macrocyclic diindole derivative **11** was hydrogenated in the presence of H_2/Pd/C to afford the saturated compound **6** (Scheme 3).

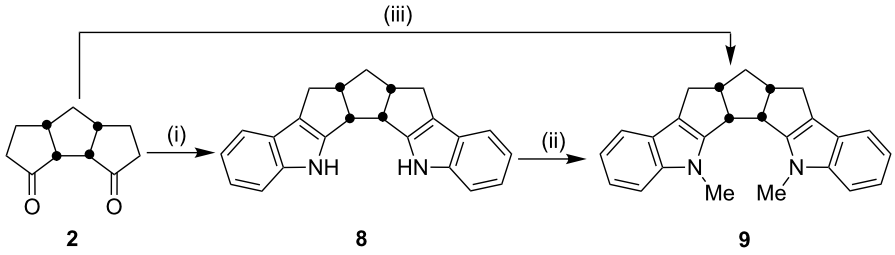

Scheme 2: Synthesis of the diindole derivative **9** Reagents and conditions: (i) TA:DMU, $PhNHNH_3Cl$, 70 °C, 6 h, 62%; (ii) NaH, MeI, DMF, rt, 24 h, 87%; (iii) TA:DMU, 70 °C, $PhNMeNH_2$, 6 h, 76%.

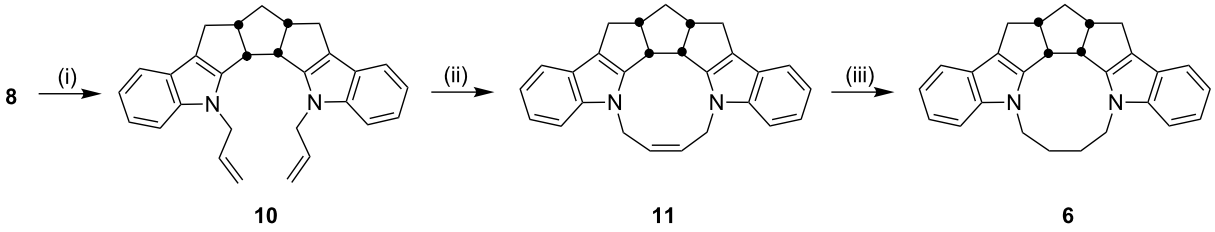

Scheme 3: Synthesis of the macrocyclic aza-polyquinane derivative **6**. Reagents and conditions: (i) NaH, allyl bromide, DMF, rt, 24 h, 65%; (ii) G-II, CH_2Cl_2, rt, 12 h, 84%; (iii) Pd/C, H_2, EtOAc, rt, 18 h, 95%.

To assemble the intricate spiro-polyquinane **7** via RCM as a key step [59-62], we started with the triquinane derivative **2**. To this end, the *cis-syn-cis*-triquinane dione **2** was treated with an excess amount of allyl bromide in the presence of NaH to generate the hexaallyl derivative **12** in 59% yield. Later, it was subjected to RCM with Grubbs' 1st generation catalyst to deliver the three-fold RCM product **13** in 80% yield. Furthermore, treatment of the hexacyclic dione **13** with Pd/C in EtOAc under hydrogen atmosphere (1 atm) gave the saturated spiro-polyquinane **7** in 90% yield (Scheme 4). Very few examples are known in the literature where multiple RCM was performed in a single operation to generate the molecules of medium molecular weight [63]. The present example involving the generation of triple spirocyclic compound **7** is unique and demonstrates the power and scope of the RCM approach. It is worth mentioning that previous attempts to functionalize **2** were unsuccessful [47].

To generalize the spiroannulation sequence, allylation of pentacyclic diones **3a–c** [48] gave the tetraallyl diones **14a–c** in respectable yields. Next, treatment of these allylated derivatives **14a–c** with G-I catalyst gave the double RCM products **15a**, **15b** and **15c** in 92%, 92% and 91% yields, respectively (Scheme 5 and Table 1). Later, these double RCM products were subjected to the hydrogenation protocol in the presence of H_2/Pd/C to deliver the saturated bis-spiro-polyquinane derivatives **16a**, **16b** and **16a** in an excellent yield (Table 1). Similarly, the dione **3a** in the presence of an excess amount of NaH and allyl bromide gave the pentaallyl dione **14d** in 67% yield (Table 1). Next, the pentaallyl derivative **14d** was treated with G-I catalyst to produce the bis-spiro-polyquinane **15d**. ^{1}H NMR and ^{13}C NMR spectral data clearly indicated the presence of intact allyl residue along with the unsaturated double bonds. The bis-spiro-polyquinane **15d** was then subjected to hydrogenation sequence to deliver the saturated bis-spiro-polyquinane **16d** in good yield (Table 1).

Conclusion

In summary, we have developed a protocol for the synthesis of a diindole-based hybrid macrocycle through Fischer indoliza-

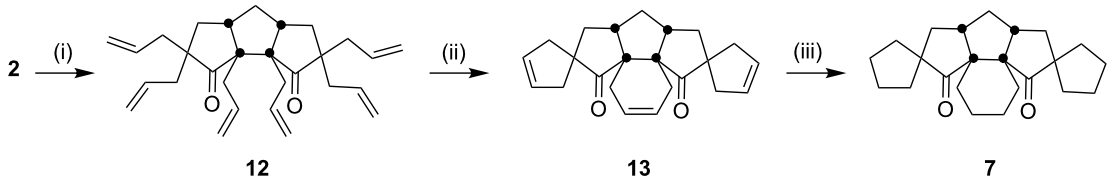

Scheme 4: Synthesis of the spiro-polyquinane **7**. Reagents and conditions: (i) NaH, allyl bromide, THF, rt, 24 h, 59%; (ii) G-I, CH_2Cl_2, rt, 15 h, 80%; (iii) Pd/C, H_2, EtOAc, rt, 24 h, 90%.

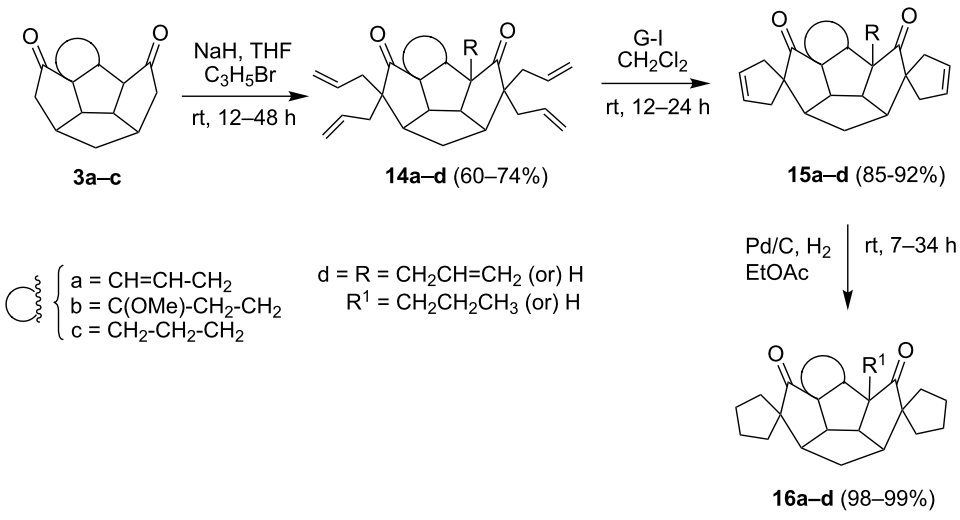

Scheme 5: General strategy to bis-spirocycles via RCM.

Table 1: List of bis-spirocycles assembled by RCM.

Allylation product (%)	Time	RCM product (%)	Time	Hydrogenation product (%)	Time
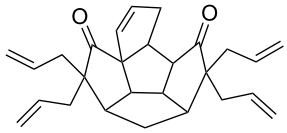 **14a** (74%)	12 h	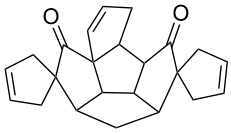 **15a** (92%)	12 h	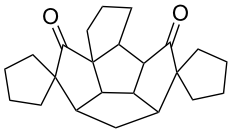 **16a** (98%)	7 h
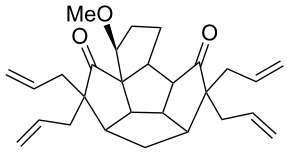 **14b** (60%)	14 h	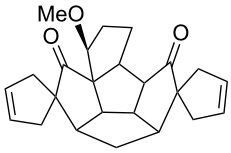 **15b** (92%)	10 h	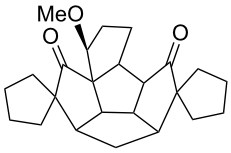 **16b** (99%)	7 h
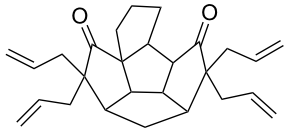 **14c** (70%)	12 h	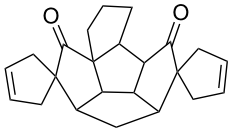 **15c** (91%)	12 h	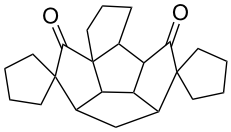 **16a** (99%)	7 h
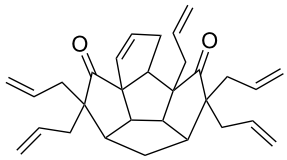 **14d** (67%)	48 h	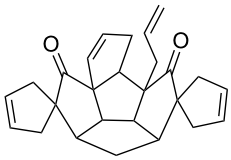 **15d** (85%)	24 h	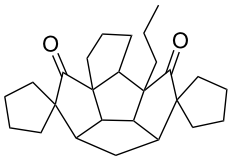 **16d** (97%)	12 h

tion of the triquinane **2** followed by bis-*N*-allylation and RCM. The allylation-RCM sequence has also been extended to construct structurally intricate spiro-polyquinanes.

Supporting Information

Supporting Information File 1

Experimental and analytical data.
[http://www.beilstein-journals.org/bjoc/content/supplementary/1860-5397-11-126-S1.pdf]

Supporting Information File 2

NMR spectra.
[http://www.beilstein-journals.org/bjoc/content/supplementary/1860-5397-11-126-S2.pdf]

Acknowledgements

AKC and RA acknowledge the University Grant Commission, New Delhi for the award of research fellowships. SK thanks the DST for the award of a J. C. Bose fellowship. We also thank the CSIR (New Delhi) and the Department of Science and Technology (DST), New Delhi for the financial support. We thank Prof. G. Mehta for valuable suggestions.

References

1. Greenberg, A.; Liebman, J. F. *Strained Organic Molecules;* Academic Press: New York, 1978.
2. Olah, G. A. *Cage Hydrocarbons;* John-Wiley: New York, 1990.
3. Vögtle, F. *Fascinating Molecules in Organic Chemistry;* Wiley : Chichester, 1992.
4. Ōsawa, E.; Yonemitsu, O. *Carbocyclic Cage Compounds: Chemistry and Applications;* VCH: New York, 1992.
5. Hopf, H. *Classics in Hydrocarbon Chemistry;* Wiley-VCH: Weinheim, 2000.
6. Mehta, G.; Srikrishna, A. *Chem. Rev.* **1997,** *97,* 671. doi:10.1021/cr9403650
7. Wender, P. A.; Dore, T. M.; deLong, M. A. *Tetrahedron Lett.* **1996,** *37,* 7687. doi:10.1016/0040-4039(96)01740-6
8. Tzvetkov, N. T.; Neumann, B.; Stammler, H.-G.; Mattay, J. *Eur. J. Org. Chem.* **2006,** 351. doi:10.1002/ejoc.200500546
9. Camps, P.; Fernández, J. A.; Vázquez, S. *ARKIVOC* **2010,** No. iv, 74. doi:10.3998/ark.5550190.0011.407
10. Paquette, L. A.; Doherty, A. M. *Polyquinane Chemistry, Synthesis and Reactions;* Springer-Verlag: New York, 1987.
11. Ramaiah, M. *Synthesis* **1984,** 529. doi:10.1055/s-1984-30893
12. Singh, V.; Thomas, B. *Tetrahedron* **1998,** *54,* 3647. doi:10.1016/S0040-4020(97)10426-4
13. Toyota, M.; Nishikawa, Y.; Motoki, K.; Yoshida, N.; Fukumoto, K. *Tetrahedron* **1993,** *49,* 11189. doi:10.1016/S0040-4020(01)81806-8
14. Liao, C.-C. *Pure Appl. Chem.* **2005,** *77,* 1221. doi:10.1351/pac200577071221
15. Srikrishna, A.; Dethe, D. H. *Indian J. Chem.* **2011,** *50B,* 1092.

16. Tolstikov, G. A.; Ismailov, S. A.; Gimalova, F. A.; Ivanova, N. A.; Miftakhov, M. S. *Russ. Chem. Bull.* **2013,** *62,* 226. doi:10.1007/s11172-013-0035-z
17. Heasley, B. *Curr. Org. Chem.* **2014,** *18,* 641. doi:10.2174/1385272813176660150
18. Chaplin, J. H.; Jackson, K.; White, J. M.; Flynn, B. L. *J. Org. Chem.* **2014,** *79,* 3659. doi:10.1021/Jo500040b
19. Álvarez-Fernández, A.; Suárez-Rodriguez, T.; Suárez-Sobrino, Á. L. *J. Org. Chem.* **2014,** *79,* 6419. doi:10.1021/Jo500378z
20. Tymann, D.; Klüppel, A.; Hiller, W.; Hiersemann, M. *Org. Lett.* **2014,** *16,* 4062. doi:10.1021/Ol501204m
21. Nagaraju, C.; Prasad, K. R. *Angew. Chem., Int. Ed.* **2014,** *53,* 10997. doi:10.1002/anie.201407680
22. Hext, N. M.; Hansen, J.; Blake, A. J.; Hibbs, D. E.; Hursthouse, M. B.; Shishkin, O. V.; Mascal, M. *J. Org. Chem.* **1998,** *63,* 6016. doi:10.1021/jo980788s
23. Jevric, M.; Zheng, T.; Meher, N. K.; Fettinger, J. C.; Mascal, M. *Angew. Chem., Int. Ed.* **2011,** *50,* 717. doi:10.1002/anie.201006470
24. Li, Y.; Meng, Y.; Meng, X.; Li, Z. *Tetrahedron* **2011,** *67,* 4002. doi:10.1016/j.tet.2011.04.031
25. Ramakrishna, K.; Kaliappan, K. P. *Synlett* **2011,** 2580. doi:10.1055/s-0030-1289518
26. McClure, C. K.; Kiessling, A. J.; Link, J. S. *Org. Lett.* **2003,** *5,* 3811. doi:10.1021/ol035202p
27. Singh, V.; Sahu, B. C.; Mobin, S. M. *Synlett* **2008,** 1222. doi:10.1055/s-2008-1072588
28. Bandaru, A.; Kaliappan, K. P. *Synlett* **2012,** 1473. doi:10.1055/s-0031-1290375
29. Wilson, L. J.; Yang, C.; Murray, W. V. *Tetrahedron Lett.* **2007,** *48,* 7399. doi:10.1016/j.tetlet.2007.08.006
30. Simonov, A. Y.; Bykov, E. E.; Lakatosh, S. A.; Luzikov, Y. N.; Korolev, A. M.; Reznikova, M. I.; Perobrazhenskaya, M. N. *Tetrahedron* **2014,** *70,* 625. doi:10.1016/j.tet.2013.12.004
31. Torney, P.; Shirsat, R.; Tilve, S. *Synlett* **2014,** *25,* 2121. doi:10.1055/s-0034-1378536
32. Davis, F.; Higson, S. *Macrocycles: Construction, Chemsitry and Nanotechnology Applications;* John Wiley & Sons: Chichester, 2011.
33. Kotha, S.; Manivannan, E.; Ganesh, T.; Sreenivasachary, N.; Deb, A. *Synlett* **1999,** 1618. doi:10.1055/s-1999-2896
34. Kotha, S.; Sreenivasachary, N. *Indian J. Chem.* **2001,** *40B,* 763.
35. Wybrow, R. A. J.; Edwards, A. S.; Stenvenson, N. G.; Adams, H.; Johnstone, C.; Harrity, J. P. A. *Tetrahedron* **2004,** *60,* 8869. doi:10.1016/j.tet.2004.07.025
36. Justus, J.; Beck, T.; Noltemeyer, M.; Fitjer, L. *Tetrahedron* **2009,** *65,* 5192. doi:10.1016/j.tet.2009.05.005
37. Meyer-Wilmes, I.; Gerke, R.; Fitjer, L. *Tetrahedron* **2009,** *65,* 1689. doi:10.1016/j.tet.2008.12.025
38. Widjaja, T.; Fitjer, L.; Meindl, K.; Herbst-Irmer, R. *Tetrahedron* **2008,** *64,* 4304. doi:10.1016/j.tet.2008.02.073
39. Kotha, S.; Srinivas, V.; Krishna, N. G. *Heterocycles* **2012,** *86,* 1555. doi:10.3987/COM-12-S(N)89
40. Kotha, S.; Deb, A. C.; Kumar, R. V. *Bioorg. Med. Chem. Lett.* **2005,** *15,* 1039. doi:10.1016/j.bmcl.2004.12.034
41. Kotha, S.; Chavan, A. S.; Mobin, S. M. *J. Org. Chem.* **2012,** *77,* 482. doi:10.1021/jo2020714
42. Kotha, S.; Dipak, M. K. *Tetrahedron* **2012,** *68,* 397. doi:10.1016/j.tet.2011.10.018
43. D'yakonov, V. A.; Trapeznikova, O. A.; de Meijere, A.; Dzhemilev, U. M. *Chem. Rev.* **2014,** *114,* 5775. doi:10.1021/cr400291c
44. Kotha, S.; Mandal, K. *Tetrahedron Lett.* **2004,** *45,* 1391. doi:10.1016/j.tetlet.2003.12.075
45. Kotha, S.; Mandal, K.; Deb, A. C.; Banerjee, S. *Tetrahedron Lett.* **2004,** *45,* 9603. doi:10.1016/j.tetlet.2004.11.012
46. Kotha, S.; Mandal, K. *Chem. – Asian J.* **2009,** *4,* 354. doi:10.1002/asia.200800244
47. Mehta, G.; Srikrishna, A.; Reddy, A. V.; Nair, M. S. *Tetrahedron* **1981,** *37,* 4543. doi:10.1016/0040-4020(81)80021-X
48. Mehta, G.; Kotha, S. R. *J. Org. Chem.* **1985,** *50,* 5537. doi:10.1021/jo00350a021
49. Bertz, S. H.; Cook, J. M.; Gawish, A.; Weiss, U. *Org. Synth.* **1986,** *64,* 27. doi:10.15227/orgsyn.064.0027
50. Gupta, A. K.; Fu, X.; Snydert, J. P.; Cook, J. M. *Tetrahedron* **1991,** *47,* 3665. doi:10.1016/S0040-4020(01)80896-6
51. Fu, X.; Cook, J. M. *Aldrichimica Acta* **1992,** *25,* 43.
52. Kotha, S.; Sivakumar, R.; Damodharan, L.; Pattabhi, V. *Tetrahedron Lett.* **2002,** *43,* 4523. doi:10.1016/S0040-4039(02)00815-8
53. Magnuson, S. R. *Tetrahedron* **1995,** *51,* 2167. doi:10.1016/0040-4020(94)01070-G
54. Hudlicky, T.; Reed, J. W. *The Way of Synthesis;* Wiley-VCH: Weinheim, 2007; p 89.
55. Gore, S.; Baskaran, S.; König, B. *Org. Lett.* **2012,** *14,* 4568. doi:10.1021/ol302034r
56. Kotha, S.; Chinnam, A. K. *Synthesis* **2013,** *46,* 301. doi:10.1055/s-0033-1340341
57. Kotha, S.; Chinnam, A. K.; Tiwari, A. *Beilstein J. Org. Chem.* **2013,** *9,* 2709. doi:10.3762/bjoc.9.307
58. Mehta, G.; Prabhakar, C. *Indian J. Chem.* **1995,** *34B,* 267.
59. Kotha, S.; Ali, R.; Tiwari, A. *Synlett* **2013,** *24,* 1921. doi:10.1055/s-0033-1339489
60. Kotha, S.; Ali, R. *Heterocycles* **2014,** *88,* 789. doi:10.3987/COM-13-S(S)48
61. Kotha, S.; Ali, R.; Chinnam, A. K. *Tetrahedron Lett.* **2014,** *55,* 4492. doi:10.1016/j.tetlet.2014.06.049
62. Kotha, S.; Ali, R.; Tiwari, A. *Synthesis* **2014,** *46,* 2471. doi:10.1055/s-0034-1378280
63. Wallace, D. J. *Tetrahedron Lett.* **2003,** *44,* 2145. doi:10.1016/S0040-4039(03)00161-8

License and Terms

BEILSTEIN JOURNAL OF ORGANIC CHEMISTRY

Design and synthesis of fused polycycles via Diels–Alder reaction and ring-rearrangement metathesis as key steps

Sambasivarao Kotha* and Ongolu Ravikumar

Full Research Paper

Open Access

Address:
Department of Chemistry, Indian Institute of Technology-Bombay, Powai, Mumbai-400 076, India, Fax: 022-25767152

Email:
Sambasivarao Kotha* - srk@chem.iitb.ac.in

* Corresponding author

Keywords:
Diels–Alder reaction; Grignard addition; ring-rearrangement metathesis; polycycles

Beilstein J. Org. Chem. **2015,** *11,* 1259–1264.
doi:10.3762/bjoc.11.140

Received: 09 April 2015
Accepted: 08 July 2015
Published: 27 July 2015

This article is part of the Thematic Series "Progress in metathesis chemistry II".

Guest Editor: K. Grela

Abstract

Atom efficient processes such as the Diels–Alder reaction (DA) and the ring-rearrangement metathesis (RRM) have been used to design new polycycles. In this regard, ruthenium alkylidene catalysts are effective in realizing the RRM of bis-norbornene derivatives prepared by DA reaction and Grignard addition. Here, fused polycycles are assembled which are difficult to produce by conventional synthetic routes.

Introduction

Design and synthesis of complex polycycles in a minimum number of steps will enhance the overall synthetic economy of the preparation of a target molecule. The ring-rearrangement metathesis (RRM) is a conceptually novel, synthetically useful atom-economic method for the construction of complex molecules and by this process compounds containing several stereocenters are produced starting from simple starting materials. RRM involves a combination of two or more metathetic transformations, wherein multiple bond forming and bond breaking events take place in a one-pot operation [1-20]. Interestingly, the stereochemical information from the starting material is transferrred to the product. Moreover, RRM enables unprecedented and indirect routes to polycycles. For successful application of this strategy it is desirable that the starting materials have ring strain so that they can readily undergo a C=C double bond cleavage. Release of ring strain is the main driving force for RRM. In this regard, bicyclo[2.2.1] and bicyclo[2.2.2] systems are well suited. Here, we demonstrate that an endocyclic bis-norbornene system undergoes an RRM with a suitably placed olefin moiety to generate complex polycyclic compounds. RRM of norbornene derivatives are common, however, reports dealing with RRM of bis-norbornene derivatives are rare [21,22]. Herein, we report two unique examples where the synthesis of hexacyclic systems containing 10 stereocenters have been generated by the application of RRM of readily available bis-norbornene derivatives using Grubbs' catalysts (Figure 1).

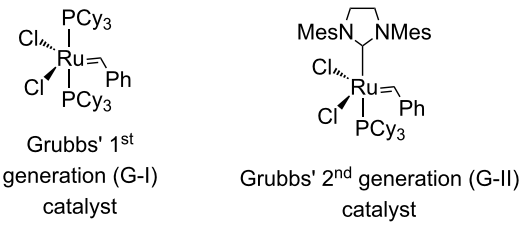

Figure 1: Commercially available ruthenium catalysts used in RRM metathesis.

The higher analogue related to the bicyclo[2.2.2] system is also studied.

Results and Discussion

Our strategy to polycycles involves a Diels–Alder reaction (DA) [23-25], a Grignard addition [26] and a RRM as key steps. To begin with, a double DA reaction of cyclopentadiene (**1**) with 1,4-benzoquinone (**2**) gave the known bis-adduct **3** [27,28]. Later, it was reacted with allylmagnesium bromide to produce 1,2-addition product **4**. A molecular model of compound **3** reveals that its exo-face is more accessible for Grignard addition than the endo-face. Also, the X-ray structure of compound **5** indicates the stereostructure of **4**. Further, the diol **4** was treated with four equivalents of allyl bromide in the presence of an excess amount of NaH to generate the mono-*O*-allyl compound **5** and surprisingly the di-*O*-allyl compound was not formed. The stereostructure of **5** has been established on the basis of single-crystal X-ray diffraction studies [29] and it shows the steric hindrance associated with one of the hydroxy groups (Figure 2).

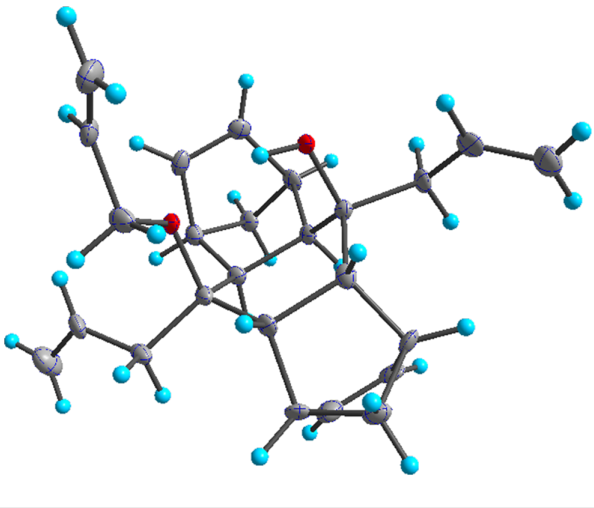

Figure 2: Crystal structure of **5** with thermal ellipsoids drawn at 50% probability level.

Later, the triallyl compound **5** was subjected to RRM in the presence of G-II catalyst (Figure 1) under ethylene atmosphere to deliver the hexacyclic rearranged product **6a** in 70% yield and ring-closing spiro product **6b** in 28% yield (Scheme 1).

To expand this strategy, next we focussed on the preparation of an analogous bicyclo[2.2.2] system and to this end, the DA reaction of 1,3-cyclohexadiene (**7**) with 1,4-benzoquinone (**2**) furnished the known bis-adduct **8** [27,28], which on treatment with allylmagnesium bromide delivered diol **9**. Later, *O*-allylation of diol **9** with four equivalents of allyl bromide in the presence of NaH in DMF gave the mono *O*-allyl compound **10**.

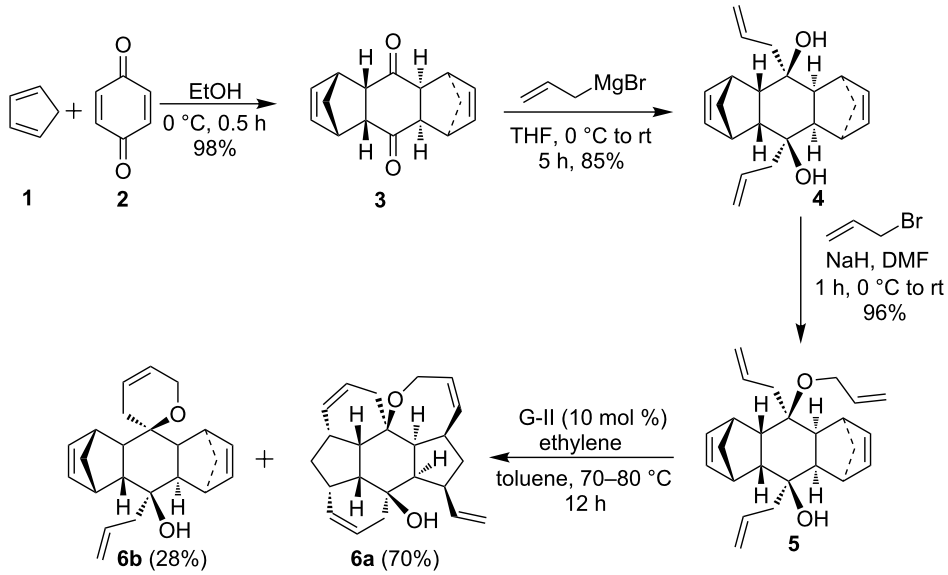

Scheme 1: Synthesis of hexacyclic compound **6a** by using an RRM approach.

Attempts to achieve complete allylation of **10** were not successful. Finally, the RRM of compound **10** in the presence of G-I catalyst (Figure 1) under ethylene atmosphere gave the hexacyclic derivative **11** in 92% yield (Scheme 2). The structures of various polycyclic derivatives have been established on the basis of ^{1}H and ^{13}C NMR spectral data and further supported by HRMS data.

Conclusion

We have demonstrated a simple, useful and atom-economic methodology for the synthesis of polycycles via DA reaction and RRM as key steps. Here, we generated polycyclic compounds with 10 stereocenters involving six fused rings in four steps starting with readily available starting materials such as 1,3-cyclopentadiene, 1,3-cyclohexadiene and 1,4-benzoquinone. Further studies to expand the scope of this strategy are underway. The strategy demonstrated here is likely to find useful applications in complex targets.

Experimental

General remarks

All reactions were monitored by employing thin layer chromatography (TLC) technique using an appropriate solvent system for development. Reactions involving oxygen-sensitive reagents or catalysts were performed in degassed solvents. Dry tetrahydrofuran (THF) and dry ether were obtained by distillation over sodium benzophenone ketyl freshly prior to use. Dichloromethane (DCM) and toluene were distilled over P_2O_5 and DMF over CaH_2. Sodium sulfate was dried in an oven at 130 °C for one day. All solvent extracts were washed successively with water and brine (saturated sodium chloride solution), dried over anhydrous sodium sulfate, and concentrated at reduced pressure on a rotary evaporator. Yields refer to the chromatographically isolated sample. All the commercial grade reagents were used without further purification. NMR samples were generally made in chloroform-*d* solvent, and chemical shifts were reported in δ scale using tetramethylsilane (TMS) as an internal standard. The standard abbreviations s, d, t, q and m, refer to singlet, doublet, triplet, quartet, and multiplet, respectively. Coupling constants (*J*) are reported in Hertz.

Experimental procedures

Synthesis of compound 4

Analogously as described in [2], to a stirred solution of diketone **3** (0.2 g, 0.83 mmol) in dry THF (10 mL) was added allylmagnesium bromide (4.2 mL, 1 M solution in ether) at 0 °C under nitrogen atmosphere, and the reaction mixture was stirred for 5 h at rt. After completion of the reaction (TLC monitoring), the reaction mixture was quenched with saturated ammonium chloride and extracted with ethyl acetate. The combined organic layer was washed with water, brine and dried over sodium sulfate. The organic layer was concentrated under reduced pressure and the crude product was purified by silica gel column chromatography by eluting with 5% ethyl acetate in petroleum ether to afford **4** as a white solid (0.23 g, 85%). mp 130–131 °C; ^{1}H NMR (500 MHz, DMSO) δ 6.12 (s, 2H), 6.05–5.98 (m, 2H), 5.92 (s, 2H), 5.14 (d, *J* = 17.1 Hz, 2H), 5.06 (d, *J* = 10.2 Hz, 2H), 4.68 (s, 2H), 2.78 (d, *J* = 16.8 Hz, 4H), 2.48–2.42 (m, 2H), 2.26 (s, 2H), 2.15 (dd, *J* = 14.3, 8.3 Hz, 2H), 1.61 (s, 2H), 1.19 (d, *J* = 8.0 Hz, 1H), 1.11 (d, *J* = 7.6 Hz, 2H),

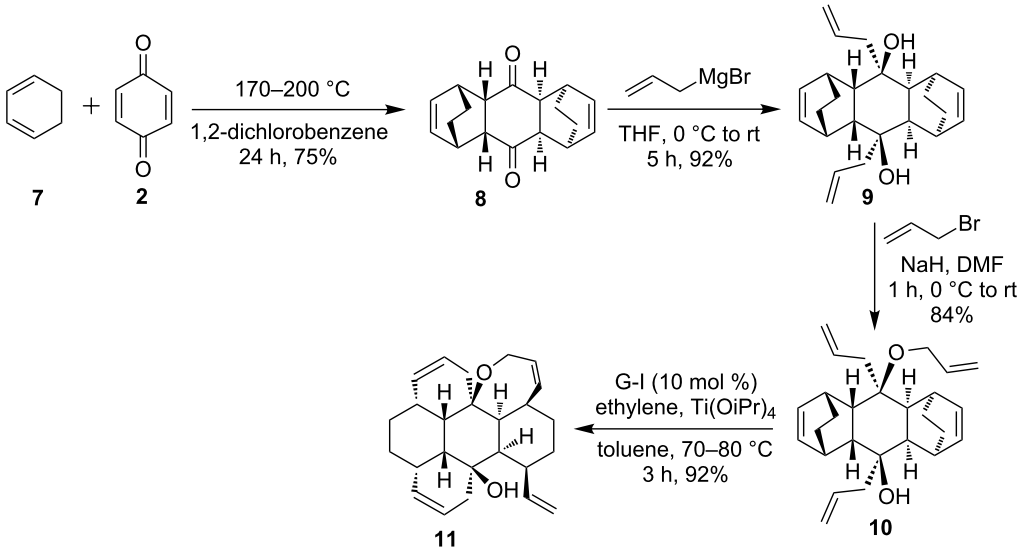

Scheme 2: Synthesis of hexacyclic compound **11** by using an RRM route.

0.99 (d, J = 7.3 Hz, 1H) ppm; ^{13}C NMR (125 MHz, $CDCl_3$) δ 135.5, 134.7, 134.4, 118.3, 73.4, 52.3, 52.3, 50.6, 49.2, 45.8, 45.7, 44.8 ppm; HRMS (Q–ToF) m/z: $[M + Na]^+$ calcd for $C_{17}H_{20}ONa$, 347.1982; found, 347.1980.

Synthesis of compound **9**

Analogously as described in [2], to a stirred solution of diketone **8** (0.5 g, 1.8 mmol) in dry THF (10 mL) was added allylmagnesium bromide (11 mL, 1 M solution in ether) at 0 °C under nitrogen atmosphere, and the reaction mixture was stirred for 5 h at rt. After completion of the reaction (TLC monitoring), the reaction mixture was quenched with saturated ammonium chloride and extracted with ethyl acetate. The combined organic layer was washed with water, brine and dried over sodium sulfate. The organic layer was concentrated under reduced pressure and the crude product was purified by silica gel column chromatography by eluting with 10% ethyl acetate in petroleum ether to afford **9** as a white solid (0.6 g, 92%). mp 122–125 °C; ^{1}H NMR (400 MHz, $CDCl_3$) δ 6.29 (dd, J = 4.7, 3.3 Hz, 2H), 6.18 (dd, J = 4.6, 3.3 Hz, 2H), 6.05–5.95 (m, 2H), 5.16 (dd, J = 5.7, 1.4 Hz, 4H), 3.78 (s, 2H), 2.71 (d, J = 14.2 Hz, 4H), 2.62 (dd, J = 14.6, 6.2, 2H), 2.26 (dd, J = 14.6, 7.5, 2H), 2.07 (s, 2H), 1.63 (s, 2H), 1.42 (t, J = 6.9 Hz, 4H), 1.24–1.21 (m, 2H), 1.15–1.12 (m, 2H) ppm; ^{13}C NMR (100 MHz, $CDCl_3$) δ 134.9, 134.2, 132.4, 117.9, 73.7, 49.2, 48.7, 44.7, 32.4, 31.1, 26.6, 26.4 ppm; HRMS (Q–ToF) m/z: $[M + Na]^+$ calcd for $C_{24}H_{32}O_2Na$, 375.2295; found, 375.2293.

Synthesis of compound **5**

Analogously as described in [2], to a suspension of NaH (26 mg, 1.08 mmol) in dry DMF (10 mL), was added solution of compound **4** (50 mg, 0.15 mmol) in DMF (5 mL) and allyl bromide (0.074 g, 0.62 mmol) at 0 °C under nitrogen atmosphere and stirred at rt for 1 h. After completion of the reaction (TLC monitoring), the reaction mixture was quenched with saturated ammonium chloride and extracted with ethyl acetate. The combined organic layer washed with water, brine dried over sodium sulfate. The organic layer was concentrated under reduced pressure and purified by silica gel column chromatography by eluting with 5% ethyl acetate in petroleum ether to afford **5** as a white solid (60 mg, 96%). mp 105–108 °C; ^{1}H NMR (500 MHz, $CDCl_3$) δ 6.09–6.17 (m, 2H), 6.05–5.97 (m, 3H), 5.93 (dd, J = 5.4, 3.0 Hz, 1H), 5.84–5.76 (m, 1H), 5.22 (dq, J = 17.2, 1.5 Hz, 1H), 5.19–5.17 (m, 1H), 5.17–5.07 (m, 4H), 4.43 (d, J = 1.9 Hz, 1H), 3.94 (dd, J = 11.6, 5.7 Hz, 1H), 3.85–3.82 (m, 1H), 3.00 (s, 1H), 2.94 (s, 1H), 2.84 (s, 1H), 2.79 (s, 1H), 2.76–2.70 (m, 1H), 2.65 (dd, J = 9.8, 3.5 Hz, 1H), 2.54 (dd, J = 14.2, 6.2 Hz, 1H), 2.41 (dd, J = 9.8, 3.5 Hz, 1H), 2.32 (dd, J = 15.6, 8.2 Hz, 1H), 2.18–2.13 (m, 1H), 1.75–1.73 (m, 2H), 1.42–1.39 (m, 1H), 1.28 (d, J = 4.0 Hz, 1H), 1.22–1.20 (m, 1H), 1.0 (d, J = 7.7 Hz, 1H) ppm; ^{13}C NMR (125 MHz, $CDCl_3$) δ 135.9, 135.3, 135.1, 134.9, 134.4, 134.1, 133.5, 117.0, 116.9, 116.6, 79.4, 72.1, 62.6, 52.4, 51.6, 51.4, 49.6, 49.5, 45.9, 45.7, 45.6, 45.5, 45.1, 44.4, 42.5 ppm; HRMS (Q–ToF) m/z: $[M + Na]^+$ calcd for $C_{25}H_{32}O_2Na$, 387.2295; found, 387.2295.

Synthesis of compound **10**

Analogously as described in [2], to a suspension of NaH (115 mg, 4.77 mmol) in dry DMF (10 mL), was added a solution of compound **9** (240 mg, 0.68 mmol) in DMF (10 mL) and allyl bromide (0.33 g, 2.72 mmol) at 0 °C under nitrogen atmosphere and stirred at rt for 1 h. After completion of the reaction (TLC monitoring), the reaction mixture was quenched with saturated ammonium chloride and extracted with ethyl acetate. The combined organic layer was washed with water, brine and dried over sodium sulfate. The organic layer was concentrated under reduced pressure and purified by silica gel column chromatography by eluting with 5% ethyl acetate in petroleum ether to afford **11** as a yellow semisolid (224 mg, 84%). ^{1}H NMR (400 MHz, $CDCl_3$) δ 6.22–6.18 (m, 1H), 6.17–6.07 (m, 3H), 6.07–6.00 (m, 1H), 5.99–5.92 (m, 1H), 5.84–5.73 (m, 1H), 5.31 (d, J = 2.5 Hz, 1H), 5.27 (dq J = 17.2, 1.7 Hz, 1H), 5.20–5.14 (m, 1H), 5.13–5.06 (m, 3H), 3.96–3.87 (m, 2H), 2.80–2.56 (m, 7H), 2.32 (d, J = 1.5 Hz, 1H), 2.21–2.14 (m, 1H), 2.40 (d, J = 1.6 Hz, 1H), 1.67 (d, J = 7.0 Hz, 2H), 1.58 (d, J = 7.5 Hz, 1H), 1.57–1.42 (m, 2H), 1.31–1.41 (m, 2H), 1.26–1.11 (m, 4H) ppm; ^{13}C NMR (100 MHz, $CDCl_3$) δ 136.0, 135.5, 134.3, 132.9, 132.6, 132.4, 131.9, 117.1, 116.6, 116.4, 79.9, 71.9, 62.4, 50.4, 49.7, 48.6, 44.9, 44.4, 42.9, 32.3, 31.9, 30.7, 30.6, 27.5, 26.7, 26.1 ppm; HRMS (Q–ToF) m/z: $[M + Na]^+$ calcd for $C_{27}H_{36}O_2Na$, 415.2608; found, 415.2605.

Synthesis of compounds **6a** and **6b**

Analogously as described in [2], to a stirred solution of compound **5** (40 mg, 0.11 mmol) in toluene (40 mL) degassed with nitrogen for 10 minutes, purged with ethylene gas for another 10 minutes and then G-II catalyst (8 mg, 10 mol %) was added and stirred at 70 °C for 12 h under ethylene atmosphere. After completion of the reaction (TLC monitoring), the solvent was removed on a rotavapor under reduced pressure and purified by silica gel column chromatography by eluting with 5–10% ethyl acetate in petroleum ether provided **6a** and **6b** as a colourless liquids (25 mg and 10 mg, 70% and 28%, respectively). **6a**; ^{1}H NMR (500 MHz, $CDCl_3$) δ 6.31–6.24 (m, 1H), 6.10 (dd, J = 5.6, 3.0 Hz, 1H), 6.05 (dd, J = 5.6, 2.7 Hz, 1H), 5.85 (dt, J = 9.8, 2.8 Hz, 1H), 5.80–5.76 (m, 1H), 5.68–5.65 (m, 2H), 4.99 (dd, J = 17.1, 2.4 Hz, 1H), 4.88 (dd, J = 9.9, 2.4 Hz, 1H), 4.33–4.29 (m, 1H), 4.22–4.18 (m, 1H), 2.95–2.88 (m, 2H), 2.82 (s, 1H), 2.68–2.61 (m, 2H), 2.56 (dd, J = 10.1, 3.5 Hz, 1H), 2.35–2.29 (m, 1H), 2.21–1.92 (m, 3H), 1.85–1.60 (m, 5H), 1.44 (dt, J = 7.9, 1.8 Hz, 1H), 1.35 (d, J = 8.0 Hz, 1H) ppm; ^{13}C NMR (125 MHz, $CDCl_3$) δ = 142.5, 135.3, 132.5, 129.2,

123.9, 123.8, 123.1, 114.3, 76.2, 68.4, 60.2, 52.3, 50.7, 49.6, 47.6, 46.7, 45.9, 42.7, 41.2, 41.1, 40.9, 37.0, 32.3 ppm; HRMS (Q–ToF) *m*/*z*: $[M + Na]^+$ calcd for $C_{25}H_{32}NaO_2$, 359.1982; found, 359.1988; IR (neat) ν_{max}: 3050, 2954, 1691, 1610, 1266 cm^{-1}.

6b; ^1H NMR (500 MHz, CD_3OD) δ 6.23 (dd, *J* = 5.6, 3.0 Hz, 1H), 6.17 (dd, *J* = 5.7, 2.8 Hz, 1H), 6.15–6.08 (m, 1H), 5.95 (t, *J* = 2.4 Hz, 2H), 5.99–5.89 (m, 1H), 5.72 (dd, *J* = 10.3, 2.4 Hz, 1H), 5.22 (dd, *J* = 17.1, 1.4 Hz, 1H), 5.14 (d, *J* = 10.2 Hz, 1H), 4.22–4.10 (m, 2H), 2.97 (s, 1H), 2.93 (dd, *J* = 10.0, 3.7 Hz, 1H), 2.87 (s, 1H), 2.68 (s, 1H), 2.59–2.53 (m, 2H), 2.48 (dd, *J* = 10.0, 3.4 Hz, 1H), 2.29 (dd, *J* = 14.4, 8.0 Hz, 1H), 2.09–2.03 (m, 1H), 1.90–1.84 (m, 2H), 1.43–1.41 (m, 1H), 1.35–1.30 (m, 4H), 1.15 (d, *J* = 7.6 Hz, 1H) ppm; ^{13}C NMR (125 MHz, $CDCl_3$) δ 134.8, 134.7, 133. 9, 133.5, 124.1, 122.6, 116.0, 73.8, 73.1, 59.9, 51.5, 51.1, 50.9, 49.5, 45.6, 44.6, 44.5, 44.1, 40.1, 32.1 ppm; HRMS (Q–ToF) *m*/*z*: $[M + Na]^+$ calcd for $C_{25}H_{32}NaO_2$, 359.1982; found, 359.1986.

Synthesis of compound **11**

Analogously as described in [2], to a stirred solution of compound **10** (20 mg, 0.05 mmol) in toluene (20 mL) degassed with nitrogen for 10 minutes, purged with ethylene gas for another 10 minutes and then added titanium isopropoxide and G-I catalyst (4 mg, 10 mol %) and stirred at 70–80 °C for 3 h under ethylene atmosphere. After completion of the reaction (TLC monitoring), solvent was removed on rotavapor under reduced pressure and purified by silica gel column chromatography by eluting with 5% ethyl acetate in petroleum ether provided **11** as a yellow semisolid (17 mg, 92%). ^1H NMR (500 MHz, $CDCl_3$) δ 6.24 (t, *J* = 7.1 Hz, 1H), 6.24–6.11 (m, 2H), 6.07–5.99 (m, 2H), 5.89–5.84 (m, 1H), 5.63 (dq , *J* = 10.2, 2.6 Hz, 1H), 5.15–5.08 (m, 3H), 4.19–4.07 (m, 2H), 2.71–2.57 (m, 5H), 2.42–2.34 (m, 2H), 2.24–2.18 (m, 1H), 2.05 (d, *J* = 10.1 Hz, 1H), 1.99–1.94 (m, 1H), 1.62–1.54 (m, 2H), 1.52–1.45 (m, 1H), 1.44–1.36 (m, 3H), 1.30–1.17 (m, 4H) ppm; ^{13}C NMR (125 MHz, $CDCl_3$) δ 135.8, 133.8, 133.1, 132.1, 131.2, 124.9, 123.4, 116.7, 74.7, 72.5, 61.1, 49.4, 49.2, 49.1, 44.5, 39.6, 34.2, 32.3, 31.5, 31.2, 30.6, 28.1, 27.4, 26.1, 25.3 ppm; HRMS (Q–ToF) *m*/*z*: $[M + Na]^+$ calcd for $C_{25}H_{32}NaO_2$, 387.2295; found, 387.2292.

Supporting Information

Supporting Information File 1

Copies of ^1H and ^{13}C NMR spectra of new compounds; X-ray crystallographic data for compound **5**.
[http://www.beilstein-journals.org/bjoc/content/supplementary/1860-5397-11-140-S1.pdf]

Acknowledgements

We thank the Department of Science and Technology (DST), New Delhi for the financial support and the Sophisticated Analytical Instrument Facility (SAIF), IIT-Bombay for recording spectral data and also thank Gaddamedi Sreevani and Darshan Mhatre for their help in collecting the X-ray data and structure refinement. S. K. thanks the Department of Science and Technology for the award of a J. C. Bose fellowship. O. R. thanks the University Grants Commission, New Delhi for the award of a research fellowship.

References

1. Kotha, S.; Dipak, M. K. *Tetrahedron* **2012,** *68,* 397. doi:10.1016/j.tet.2011.10.018
2. Kotha, S.; Ravikumar, O. *Eur. J. Org. Chem.* **2014,** 5582. doi:10.1002/ejoc.201402273
3. Kotha, S.; Ravikumar, O. *Tetrahedron Lett.* **2014,** *55,* 5781. doi:10.1016/j.tetlet.2014.08.108
4. Zuercher, W. J.; Hashimoto, M.; Grubbs, R. H. *J. Am. Chem. Soc.* **1996,** *118,* 6634. doi:10.1021/ja9606743
5. Blechert, S.; Holub, N. *Chem. – Asian J.* **2007,** *2,* 1064. doi:10.1002/asia.200700072
6. Arjona, O.; Csákÿ, A. G.; Plumet, J. *Eur. J. Org. Chem.* **2003,** 611. doi:10.1002/ejoc.200390100
7. Schmidt, Y.; Lam, J. K.; Pham, H. V.; Houk, K. N.; Vanderwal, C. D. *J. Am. Chem. Soc.* **2013,** *135,* 7339. doi:10.1021/ja4025963
8. Lam, J. K.; Pham, H. V.; Houk, K. N.; Vanderwal, C. D. *J. Am. Chem. Soc.* **2013,** *135,* 17585. doi:10.1021/ja409618p
9. Standen, P. E.; Kimber, M. C. *Tetrahedron Lett.* **2013,** *54,* 4098. doi:10.1016/j.tetlet.2013.05.112
10. Lee, D.; Li, J. *Eur. J. Org. Chem.* **2011,** 4269. doi:10.1002/ejoc.201100438
11. Carreras, J.; Avenoza, A.; Busto, J. H.; Peregrina, J. M. *J. Org. Chem.* **2011,** *76,* 3381. doi:10.1021/jo200321t
12. Bose, S.; Ghosh, M.; Ghosh, S. *J. Org. Chem.* **2012,** *77,* 6345. doi:10.1021/jo300945b
13. Minger, T. L.; Phillips, A. J. *Tetrahedron Lett.* **2002,** *43,* 5357. doi:10.1016/S0040-4039(02)00905-X
14. North, M.; Banti, D. *Adv. Synth. Catal.* **2002,** *344,* 694. doi:10.1002/1615-4169(200208)344:6/7<694::AID-ADSC694>3.0.CO;2-X
15. Nguyen, N. N. M.; Leclère, M.; Stogaitis, N.; Fallis, A. G. *Org. Lett.* **2010,** *12,* 1684. doi:10.1021/ol100150f
16. Schrock, R. R.; Hoveyda, A. H. *Angew. Chem., Int. Ed.* **2003,** *42,* 4592. doi:10.1002/anie.200300576
17. Malik, C. K.; Hossain, Md. F.; Ghosh, S. *Tetrahedron Lett.* **2009,** *50,* 3063. doi:10.1016/j.tetlet.2009.04.033
18. Vincent, G.; Kouklovsky, C. *Chem. – Eur. J.* **2011,** *17,* 2972. doi:10.1002/chem.201002558
19. Gao, F.; Stamp, C. T. M.; Thornton, P. D.; Cameron, T. S.; Doyle, L. E.; Miller, D. O.; Burnell, D. J. *Chem. Commun.* **2012,** *48,* 233. doi:10.1039/C1CC15452D
20. Miege, F.; Meyer, C.; Cossy, J. *Org. Lett.* **2010,** *12,* 248. doi:10.1021/ol9025606
21. Malik, C. K.; Ghosh, S. *Org. Lett.* **2007,** *9,* 2537. doi:10.1021/ol070906a

22. Higashibayashi, S.; Tsuruoka, R.; Soujanya, Y.; Purushotham, U.; Sastry, G. N.; Seki, S.; Ishikawa, T.; Toyoto, S.; Sakurai, H. *Bull. Chem. Soc. Jpn.* **2012,** *85,* 450. doi:10.1246/bcsj.20110286
23. Nicolaou, K. C.; Snyder, S. A.; Montagnon, T.; Vassilikogiannakis, G. *Angew. Chem., Int. Ed.* **2002,** *41,* 1668. doi:10.1002/1521-3773(20020517)41:10<1668::AID-ANIE1668>3.0.CO;2-Z
Angew. Chem. **2002,** *114,* 1742. doi:10.1002/1521-3757(20020517)114:10<1742::AID-ANGE1742>3.0.CO;2-Y.
24. Kotha, S.; Banerjee, S. *RSC Adv.* **2013,** *3,* 7642. doi:10.1039/C3RA22762F
25. Kotha, S.; Misra, S.; Srinivas, V. *Eur. J. Org. Chem.* **2012,** 4052. doi:10.1002/ejoc.201200484
26. Richey, H. G. *Grignard Reagents: New Developments;* Wiley: Heidelberg, Germany, 2000; pp 418 ff.
27. Valiulin, R. A.; Arisco, T. M.; Kutateladze, A. G. *Org. Lett.* **2010,** *12,* 3398. doi:10.1021/ol101297b
28. Rathore, R.; Kochi, J. K. *J. Org. Chem.* **1995,** *60,* 4399. doi:10.1021/jo00119a017
29. CCDC-1051925 contains the supplementary crystallographic data for this paper. These data can be obtained free of charge from The Cambridge Crystallographic Data Centre (CCDC).

License and Terms

BEILSTEIN JOURNAL OF ORGANIC CHEMISTRY

Spiro annulation of cage polycycles via Grignard reaction and ring-closing metathesis as key steps

Sambasivarao Kotha*, Mohammad Saifuddin, Rashid Ali and Gaddamedi Sreevani

Full Research Paper

Open Access

Address:
Department of Chemistry, Indian Institute of Technology-Bombay, Powai, Mumbai-400 076, India, Phone: +91-22-2576 7160, Fax: +91(22)-2572 7152

Email:
Sambasivarao Kotha* - srk@chem.iitb.ac.in

* Corresponding author

Keywords:
cage molecules; Diels–Alder reaction; Grignard reaction; ring-closing metathesis; spirocycles

Beilstein J. Org. Chem. **2015,** *11,* 1367–1372.
doi:10.3762/bjoc.11.147

Received: 14 April 2015
Accepted: 14 July 2015
Published: 05 August 2015

This article is part of the Thematic Series "Progress in metathesis chemistry II".

Guest Editor: K. Grela

Abstract

A simple synthetic strategy to C_2-symmetric bis-spiro-pyrano cage compound **7** involving ring-closing metathesis is reported. The hexacyclic dione **10** was prepared from simple and readily available starting materials such as 1,4-naphthoquinone and cyclopentadiene. The synthesis of an unprecedented octacyclic cage compound through intramolecular Diels–Alder (DA) reaction as a key step is described. The structures of three new cage compounds **7**, **12** and **18** were confirmed by single crystal X-ray diffraction studies.

Introduction

Design and synthesis of architecturally intricate cage molecules is a worthwhile challenge. The unique properties associated with the carbocyclic cage frameworks are the main reasons for pursuing their synthesis [1,2]. They are valuable synthons to assemble natural as well as non-natural products [3,4]. In addition, the cage molecules are interesting targets because of their unusual structural features such as the deformation of the ideal C–C bond angles, high degree of symmetry and the enhanced ring strain etc. [5-18].

The structures of a variety of intricate cage systems, for example, snoutane (**1**) [5], pentaprismane (**2**) [10], dodecahedrane (**3**) [11-19], cage crown ether **4** [20], amantadine (**5**) and pushpakenediol (**6**) [21] along with the target molecule **7** are shown in Figure 1. Interestingly the amino group containing cage molecule amantadine (**5**) exhibits antiviral properties [22].

Although, several methods are available for the construction of cage compounds [7,23-33], the synthesis of symmetrical spiro-cage molecule **7** seems to be a synthetic challenge due to the proximity of the two carbonyl groups in dione **10** which provides a hemiketal with various nucleophiles [34-39]. In view of various applications of cage molecules and the documented difficulties in their synthesis, we conceived a short synthetic

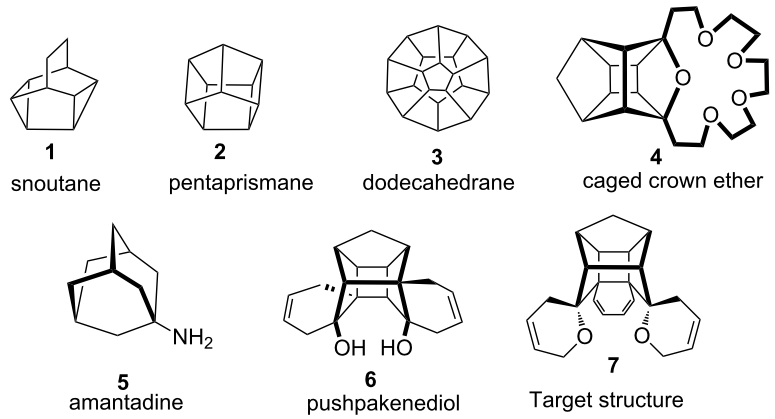

Figure 1: Structures of diverse biologically as well as theoretically interesting molecules.

route to C_2-symmetric bis-spiro-pyrano cage compound **7**. To this end, the Grignard addition and ring-closing metathesis (RCM) are considered as viable options. The retrosynthetic analysis to the target bis-spiro-cage compound **7** is shown in Figure 2. The target compound **7** could be obtained from *O*-allylation of the Grignard addition product **11** followed by the two-fold RCM sequence. The required cage dione **10** could be constructed in two steps from readily available starting materials such as 1,4-naphthoquinone (**9**) and cyclopentadiene (**8**) [40,41].

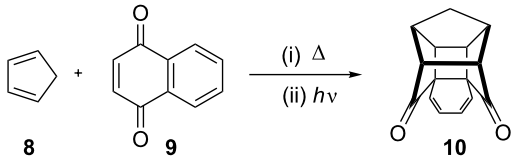

Scheme 1: Synthesis of hexacyclic cage dione **10**.

Results and Discussion

In connection with the synthesis of new cage molecules, we reported a new approach to the hexacyclic dione **10** and related systems via Claisen rearrangement and RCM as key steps [21,30]. Here, we have prepared the cage dione **10** by the known route involving two atom-economic protocols such as Diels–Alder reaction and [2 + 2] photocycloaddition [42-45] (Scheme 1).

Later, the hexacyclic cage dione **10** was subjected to a Grignard reaction with comercially available allylmagnesium bromide in diethyl ether. Under these conditions, we realized the formation of hemiketal **12** in 84.7% yield instead of the expected diallylated product **11** (Scheme 2). In similar fashion, the cage dione **10** was treated with comercially available vinylmagnesium bromide and the hemiketal **13** [46,47] was obtained in 89.2% yield instead of the desired divinylated compound **14** (Scheme 2). The proximity of the carbonyl groups may be responsible for the formation of hemiketals.

The structures of both these heptacyclic hemiketals **12** and **13** have been confirmed by ^{1}H and ^{13}C NMR spectral data and further supported by HRMS data. Finally their structures have been unambiguously established by single crystal X-ray diffraction studies [48] (Figure 3).

Since our goal was to synthesize the diallylated compound **11**, we screened various reaction conditions and finally, we found that the addition of the etheral solution of the hexacyclic dione

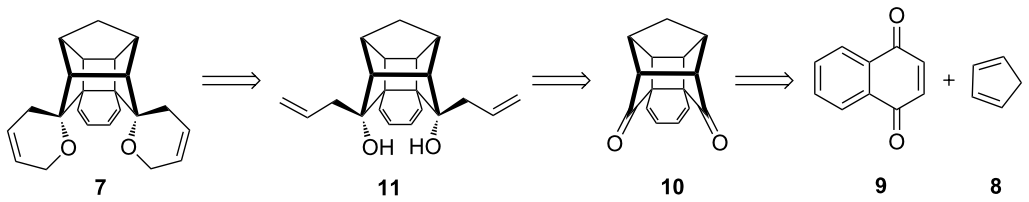

Figure 2: Retrosynthetic analysis of bis-spiro-pyrano cage compound **7**.

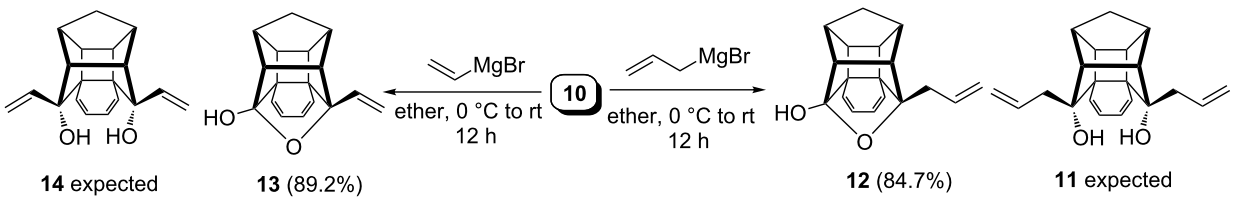

Scheme 2: Synthesis of tetrahydrofuran-based cage compounds **12** and **13**.

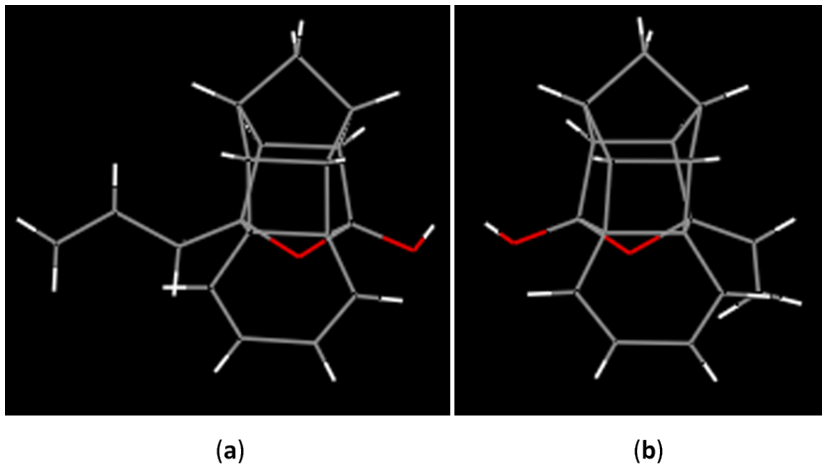

Figure 3: (a)Optimized structure of **12**, (b) optimized structure of **13**.

10 to a freshly prepared allyl Grignard reagent at 0 °C gave the expected diallylated compound **11** in 88% yield (Scheme 3). The Grignard reagent at higher concentration (1.0 M solution) exists as a mixture of dimer, trimer and polymeric components. However, the home-made Grignard reagent at low concentration (0.1 M solution) exists mostly in the monomeric form. So, we speculate that the difference in the concentration may be responsible for the formation of diol **11** [49-51]. Alternatively, when the diketone was reacted with an excess amount of Grignard reagent, the carbonyl groups are attacked simultaneously by the Grignard reagent and resulted in the formation of diol **11**. When an excess amount of substrate containing carbonyl group was reacted with a limited amount of Grignard reagent, the oxyanion formed by the Grignard reagent attacks the other carbonyl group in a transannular fashion to generate hemiketal derivatives **12** and **13**.

Later, the diallyldiol **11** was subjected to an *O*-allylation sequence under NaH/allyl bromide conditions in DMF to deliver the desired tetraallyl compound **15** (53%) along with the triallyl compound **16** (34.3%) (Scheme 4). Subsequently, the tetraallyl compound **15** was subjected to an RCM sequence with the aid of Grubbs' first generation catalyst (G-I) in dry CH_2Cl_2. Surprisingly under these conditions the reaction was found to be sluggish.

Therefore, various other reaction conditions were screened to optimize the yields. Finally, we found that the Grubbs' first

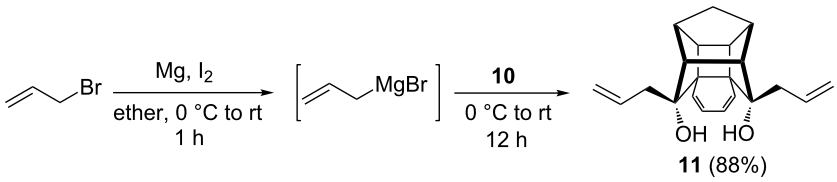

Scheme 3: Synthesis di-allyl cage compound **11**.

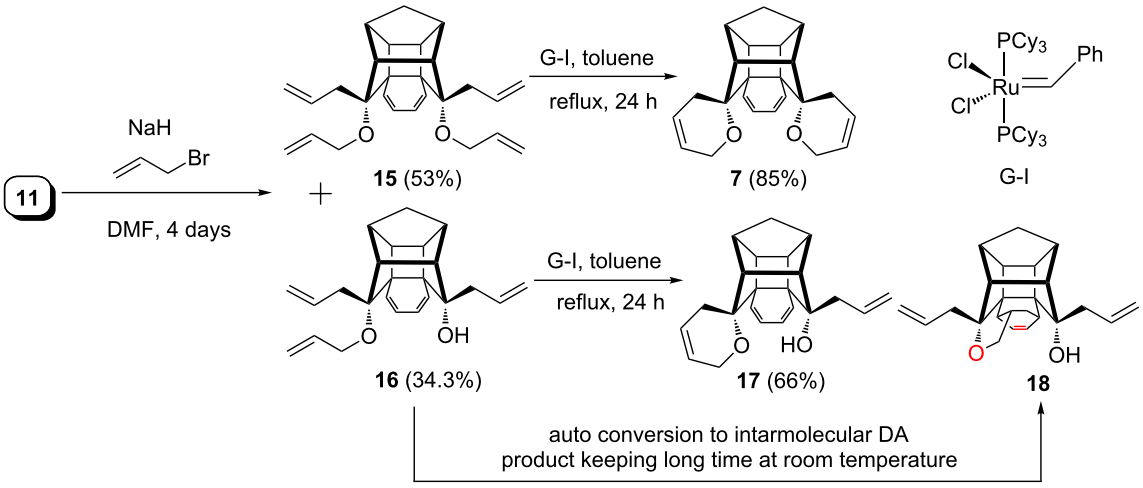

Scheme 4: Synthesis of spiro-pyrano cage molecules **7** and **17**.

generation catalyst (G-I) in refluxing toluene gave the desired RCM product **7** in 85% yield. Along similar lines, the triallyl compound **16** gave the RCM product **17** in 66% yield (Scheme 4).

The structures of the annulated cage compounds **7** and **17** have been confirmed by ^{1}H and ^{13}C NMR spectral data and also supported by HRMS data with a molecular weight of 355.16 for **7** and 343.16 for compound **17**, respectively. Furthermore, the structure of the bis-spiro pyrano cage compound **7** was confirmed by single crystal X-ray diffraction studies [52] (Figure 4). Fortunately, we observed that the liquid compound **16** kept at room temperature for a long time converted into a solid material. Therefore, we were keen to investigate the reason for this observation. In this context, the ^{1}H and ^{13}C NMR spectra of this compound were again recorded, indicating the occurence of an intramolecular DA reaction. Later, it was confirmed by single crystal X-ray diffraction studies [53] (Figure 4).

Next, the formation of compound **18** has been confirmed by an independent synthesis. To this end, triallyl compound **16** was subjected to intramolecular DA reaction in refluxing toluene to deliver the DA adduct **18** in 80% yield (Scheme 5).

Surprisingly the related system **19**, prepared from **12** did not undergo DA reaction to produce the intramolecular DA adduct **20**. Even under prolonged toluene reflux reaction conditions, we did not realize the formation of the required DA product **20** (Scheme 6).

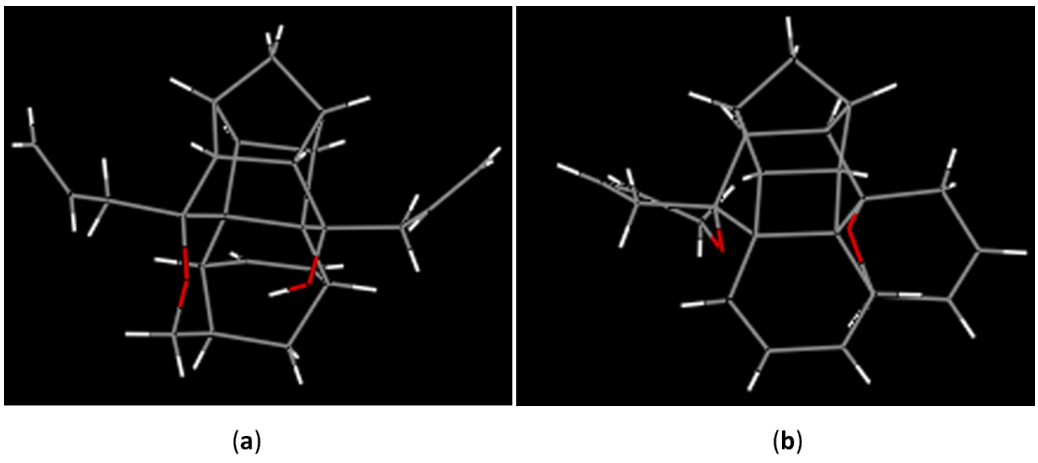

Figure 4: (a) Optimized structure of **18**, (b) optimized structure of **7**.

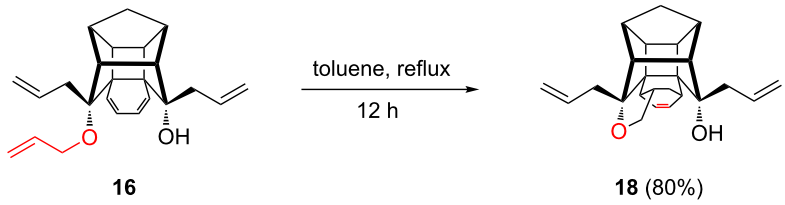

16 18 (80%)

Scheme 5: Synthesis of octacyclic cage compound **18** via intramolecular DA reaction.

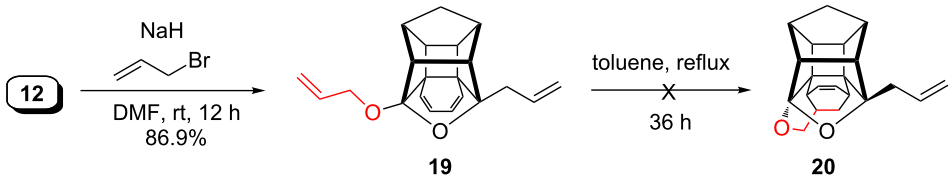

19 20

Scheme 6: Attempted synthesis to cage compound **20**.

Conclusion

In summary, we have demonstrated a new approach to intricate C_2-symmetric cage bis-spirocyclic pyran derivative **7** through an allyl Grignard reaction and an RCM sequence. The strategy demonstrated here involves an atom economic process. The synthetic sequence demonstrated here opens up a new route to complex cage targets. Additionally, intramolecular DA reaction opens up a new strategy for the synthesis of highly complex cage compounds that are inaccessible by other routes. Studies to extend the scope of the intramolecular as well as intermolecular DA reaction for the synthesis of interesting cage molecules are in progress.

Supporting Information

Supporting Information File 1

Detailed experimental procedures, characterization data and copies of ^{1}H and ^{13}C NMR spectra for all new compounds.
[http://www.beilstein-journals.org/bjoc/content/supplementary/1860-5397-11-147-S1.pdf]

Acknowledgements

We thank the Department of Science and Technology (DST), New Delhi for the financial support and the Sophisticated Analytical Instrument Facility (SAIF), IIT-Bombay for recording spectral data. S.K. thanks the Department of Science and Technology for the award of a J. C. Bose fellowship. M.S. thanks IIT-Bombay for the Istitute post-doc fellowship. R.A thanks the University Grants Commission (UGC), New Delhi and G.S thanks CSIR, New Delhi for the award of a research fellowship.

References

1. Marchand, A. P. *Aldrichimica Acta* **1995,** *28,* 95.
2. Marchand, A. P. In *Advances in Theoretically Interesting Molecules;* Thumel, R. P., Ed.; JAI: Greenwich, CT, 1989; Vol. 1, pp 357 ff.
3. Mehta, G.; Srikrishna, A. *Chem. Rev.* **1997,** *97,* 671. doi:10.1021/cr9403650
4. D'yakonov, V. A.; Trapeznikova, O. A.; de Meijere, A.; Dzhemilev, U. M. *Chem. Rev.* **2014,** *114,* 5775. doi:10.1021/cr400291c
5. Chamot, E.; Paquette, L. A. *J. Org. Chem.* **1978,** *43,* 4527. doi:10.1021/jo00417a031
6. Eaton, P. E.; Cassar, L.; Halpern, J. *J. Am. Chem. Soc.* **1970,** *92,* 6366. doi:10.1021/ja00724a061
7. Maier, G.; Pfriem, S.; Schäfer, U.; Matusch, R. *Angew. Chem., Int. Ed. Engl.* **1978,** *17,* 520. doi:10.1002/anie.197805201
8. Katz, T. J.; Acton, N. *J. Am. Chem. Soc.* **1973,** *95,* 2738. doi:10.1021/ja00789a084
9. Eaton, P. E.; Cole, T. W. *J. Am. Chem. Soc.* **1964,** *86,* 962. doi:10.1021/ja01059a072
10. McKennis, J. S.; Brener, L. J.; Ward, J. S.; Pettit, R. *J. Am. Chem. Soc.* **1971,** *93,* 4957. doi:10.1021/ja00748a076
11. Ternansky, R. J.; Balogh, D. W.; Paquette, L. A. *J. Am. Chem. Soc.* **1982,** *104,* 4503. doi:10.1021/ja00380a040
12. Carreño, M. C.; Garcia Ruano, J. L.; Urbano, A.; López-Solera, M. I. *J. Org. Chem.* **1997,** *62,* 976. doi:10.1021/jo9618942
13. Nair, M. S.; Sudhir, U.; Joly, S.; Rath, N. P. *Tetrahedron* **1999,** *55,* 7653. doi:10.1016/S0040-4020(99)00381-6
14. Pandey, B.; Saravanan, K.; Rao, A. T.; Nagamani, D.; Kumar, P. *Tetrahedron Lett.* **1995,** *36,* 1145. doi:10.1016/0040-4039(94)02442-E
15. Chou, T.-C.; Lin, G.-H.; Yeh, Y.-L.; Lin, K.-J. *J. Chin. Chem. Soc.* **1997,** *44,* 477. doi:10.1002/jccs.199700073
16. Griesbeck, A. G. *Tetrahedron Lett.* **1988,** *29,* 3477. doi:10.1016/0040-4039(88)85194-3
17. Griesbeck, A. G.; Deufel, T.; Hohlneicher, G.; Rebentisch, R.; Steinwascher, J. *Eur. J. Org. Chem.* **1998,** 1759. doi:10.1002/(SICI)1099-0690(199809)1998:9<1759::AID-EJOC1759>3.0.CO;2-I

18. Govender, T.; Hariprakasha, H. K.; Kruger, H. G.; Marchand, A. P. *Tetrahedron: Asymmetry* **2003,** *14,* 1553. doi:10.1016/S0957-4166(03)00272-6
19. Paquette, L. A.; Ternansky, R. J.; Balogh, D. W.; Kentgen, G. *J. Am. Chem. Soc.* **1983,** *105,* 5446. doi:10.1021/ja00354a043
20. Marchand, A. P.; Kumar, K. A.; McKim, A. S.; Mlinarié-Majerski, K.; Kragol, G. *Tetrahedron* **1997,** *53,* 3467. doi:10.1016/S0040-4020(97)00075-6
21. Kotha, S.; Dipak, M. K. *Beilstein J. Org. Chem.* **2014,** *10,* 2664. doi:10.3762/bjoc.10.280
22. Suwalsky, M.; jemiola-Rzeminska, M.; Altamirano, M.; Villena, F.; Dukes, N.; Strzalka, K. *Biophys. Chem.* **2015,** *202,* 13. doi:10.1016/j.bpc.2015.04.002
23. Kotha, S.; Seema, V.; Singh, K.; Deodhar, K. D. *Tetrahedron Lett.* **2010,** *51,* 2301. doi:10.1016/j.tetlet.2010.02.131
24. Paquette, L. A.; Beckley, R. S. *J. Am. Chem. Soc.* **1975,** *97,* 1084. doi:10.1021/ja00838a023
25. Abdelkafi, H.; Herson, P.; Nay, B. *Org. Lett.* **2012,** *14,* 1270. doi:10.1021/ol300133x
26. Ng, S. M.; Beaudry, C. M.; Trauner, D. *Org. Lett.* **2003,** *5,* 1701. doi:10.1021/ol0343414
27. Gupta, S.; Choudhury, R.; Krois, D.; Wagner, G.; Brinker, U. H.; Ramamurthy, V. *Org. Lett.* **2011,** *13,* 6074. doi:10.1021/ol202568s
28. Eey, S. T.-C.; Lear, M. J. *Org. Lett.* **2010,** *12,* 5510. doi:10.1021/ol102390t
29. Schneider, T. F.; Werz, D. B. *Org. Lett.* **2010,** *12,* 772. doi:10.1021/ol902904z
30. Kotha, S.; Dipak, M. K. *Chem. – Eur. J.* **2006,** *12,* 4446. doi:10.1002/chem.200501366
31. Vasquez, T. E., Jr.; Bergset, J. M.; Fierman, M. B.; Nelson, A.; Roth, J.; Khan, S. I.; O'Leary, D. J. *J. Am. Chem. Soc.* **2002,** *124,* 2931. doi:10.1021/ja016879f
32. Kruger, H. G.; Ramdhani, R. *Magn. Reson. Chem.* **2006,** *44,* 1058. doi:10.1002/mrc.1889
33. Anderson, C. E.; Pickrell, A. J.; Sperry, S. L.; Vasquez, T. E., Jr.; Custer, T. G.; Fierman, M. B.; Lazar, D. C.; Brown, Z. W.; Iskenderian, W. S.; Hickstein, D. D.; O'Leary, D. J. *Heterocycles* **2007,** *72,* 469. doi:10.3987/COM-06-S(K)40
34. Osawa, E.; Yonemitsu, O. *Carbocyclic Caged Compounds: Chemistry and Applications;* Wiley: New York, 1992.
35. Mehta, G.; Srikrishna, A.; Reeddy, A. V.; Nair, M. S. *Tetrahedron* **1981,** *37,* 4543. doi:10.1016/0040-4020(81)80021-X
36. Marchand, A. P. *Chem. Rev.* **1989,** *89,* 1011. doi:10.1021/cr00095a004
37. Kotha, S.; Chakraborty, K. *Indian J. Chem., Sect. B* **2000,** *39,* 382.
38. Sasaki, T.; Eguchi, S.; Kiriyama, T.; Hiroaki, O. *Tetrahedron* **1974,** *30,* 2707. doi:10.1016/S0040-4020(01)97433-2
39. Cookson, R. C.; Crundwell, E.; Hill, R. R.; Hudec, J. *J. Chem. Soc.* **1964,** 3062. doi:10.1039/JR9640003062
40. Kushner, A. S. *Tetrahedron Lett.* **1971,** *35,* 3275. doi:10.1016/S0040-4039(01)97154-0
41. Valiulin, R. A.; Arisco, T. M.; Kutateladze, A. G. *J. Org. Chem.* **2011,** *76,* 1319. doi:10.1021/jo102221q
42. Kotha, S.; Chavan, A. S.; Goyal, D. *ACS Comb. Sci.* **2015,** *17,* 253. doi:10.1021/co500146u
43. Suresh, R.; Muthusubramanian, S.; Senthilkumaran, R.; Manickam, G. *J. Org. Chem.* **2012,** *77,* 1468. doi:10.1021/jo202256z
44. Bhuyan, D.; Sarma, R.; Dommaraju, Y.; Prajapati, D. *Green Chem.* **2014,** *16,* 1158. doi:10.1039/c3gc42389a
45. Trost, B. M. *Angew. Chem., Int. Ed. Engl.* **1995,** *34,* 259. doi:10.1002/anie.199502591
46. Bott, S. G.; Marchand, A. P.; Kumar, K. A. *J. Chem. Crystallogr.* **1996,** *26,* 429. doi:10.1007/BF01665824
47. Bott, S. G.; Marchand, A. P.; Alihodzic, S.; Kumar, K. A. *J. Chem. Crystallogr.* **1998,** *28,* 251. doi:10.1023/A:1021893001351
48. CCDC 1053504 (**12**) and CCDC 1053505 (**13**) contain the supplementary crystallographic data for this paper. These data can be obtained free of charge from The Cambridge Crystallographic Data Centre via http://www.ccdc.cam.ac.uk/data_request/cif. (Hydrogen atoms are removed for better visualization).
49. Smith, M. B. *Advanced Organic Chemistry: Reaction, Mechanism, Structure;* Wiley: New York, 2013; p 231.
50. Ashby, E. C.; Smith, M. B. *J. Am. Chem. Soc.* **1964,** *86,* 4363. doi:10.1021/ja01074a026
51. Benn, R.; Lehmkuhl, H.; Mehler, K.; Rufińska, A. *Angew. Chem., Int. Ed. Engl.* **1984,** *23,* 534. doi:10.1002/anie.198405341
52. CCDC 1053506 (**7**) contain the supplementary crystallographic data for this paper. The data can be obtained free of charge from The Cambridge Crystallographic Data Centre via http://www.ccdc.cam.ac.uk/data_request/cif. (Hydrogen atoms are removed for better visualization).
53. CCDC 1053507 (**18**) contain the supplementary crystallographic data for this paper. The data can be obtained free of charge from The Cambridge Crystallographic Data Centre via http://www.ccdc.cam.ac.uk/data_request/cif. (Hydrogen atoms are removed for better visualization).

License and Terms

BEILSTEIN JOURNAL OF ORGANIC CHEMISTRY

Design and synthesis of polycyclic sulfones via Diels–Alder reaction and ring-rearrangement metathesis as key steps

Sambasivarao Kotha* and Rama Gunta

Full Research Paper

Open Access

Address:
Department of Chemistry, Indian Institute of Technology-Bombay, Powai, Mumbai-400 076, India, Fax: 022-25767152

Email:
Sambasivarao Kotha* - srk@chem.iitb.ac.in

* Corresponding author

Keywords:
alkenylation; Diels–Alder reaction; ring-rearrangement metathesis; sulfones

Beilstein J. Org. Chem. **2015,** *11,* 1373–1378.
doi:10.3762/bjoc.11.148

Received: 16 April 2015
Accepted: 20 July 2015
Published: 06 August 2015

This article is part of the Thematic Series "Progress in metathesis chemistry II".

Guest Editor: K. Grela

Abstract

Here, we describe a new and simple synthetic strategy to various polycyclic sulfones via Diels–Alder reaction and ring-rearrangement metathesis (RRM) as the key steps. This approach delivers tri- and tetracyclic sulfones with six (n = 1), seven (n = 2) or eight-membered (n = 3) fused-ring systems containing *trans*-ring junctions unlike the conventional all *cis*-ring junctions generally obtained during the RRM sequence. Interestingly the starting materials used are simple and commercially available.

Introduction

Sulfones [1-8] are popular building blocks [9] in organic synthesis. They are also useful substrates for the Ramberg–Bäcklund reaction [10] and they can be alkylated via carbanion chemistry. Moreover, they are suitable synthons in Diels–Alder (DA) reactions [11-14]. In view of various applications of sulfone derivatives, we envisioned a new synthetic strategy based on ring-rearrangement metathesis (RRM) as a key step. It is worth mentioning that the RRM strategy [15-23] with a variety of substrates affords intricate products that are inaccessible by conventional retrosynthetic routes. Several bicyclo[2.2.1]heptane systems [24-26] are known to undergo RRM. However, in almost all instances the products produced are *cis*-configured at the ring junctions. The main driving force for the RRM of these systems is the release of ring strain. The configuration is transferred from the starting material to the product. In connection with our interest to design new polycycles by RRM [27,28] as a key step, here we conceive unique examples where *cis* and *trans* ring junctions are produced in the RRM reactions.

Results and Discussion

Strategy

Our retrosynthetic strategy to diverse sulfone derivatives is shown in Figure 1. The target sulfone derivatives **1** could be

synthesized from the functionalized tricyclic sulfone **2** by RRM sequence. The sulfone **2** may be prepared from the dimesylate **3**, which in turn, can be assembled from the known anhydride **4** via reduction followed by mesylation of the resulting diol. Compound **4** could be prepared via DA reaction starting with freshly cracked cyclopentadiene and maleic anhydride (Figure 1).

To realize the strategy shown in Figure 1, we started with the preparation of the known compound **4** [29,30]. Later, the DA adduct **4** was reduced with $LiAlH_4$ to deliver the corresponding diol (95%) [31], which was subsequently treated with methanesulfonyl chloride in the presence of triethylamine as a base to obtain the dimesylate **3** (89%). Next, compound **3** was subjected to a cyclization reaction by treating with sodium sulfide nonahydrate ($Na_2S{\cdot}9H_2O$) using 20% Aliquat® 336 as a phase–transfer catalyst (PTC) to produce the known sulfide **5** (83%) [31].

Having the sulfide **5** in hand, our next task was to prepare sulfone **6**. In this regard, Trost and Curran [32] have reported the conversion of sulfides to sulfones in the presence of other common functional groups such as olefins by reacting with the oxidizing agent, potassium hydrogen persulfate ($KHSO_5$, commercially available as Oxone®) in aqueous methanol. Equipped with this information, oxidation of compound **5** was attempted under similar reaction conditions to get the desired sulfone **6** [33] (Scheme 1, Table 1).

Initially, when the reaction was carried out at 0 °C, the epoxy sulfone **7** was the major product (Table 1, entry 1). However, after a considerable amount of experimentation (Table 1), the desired sulfone **6** has been produced in 89% yield (Table 1, entry 2) but it was not possible to eliminate the formation of the epoxy sulfone **7**.

Next, our efforts were directed towards the synthesis of various alkenylated sulfone derivatives. In this regard, Bloch and co-workers reported a useful preparation of monoallylated sulfone **8a** [34]. To this end, we carried out the allylation of sulfone **6** with allyl bromide (1.2 equiv) and *n*-BuLi (2.7 equiv) at −75 °C to rt. The monoallylated sulfone **8a** was obtained in 22% yield and the diallylated sulfone **2a** in 5% yield. Also, 25% of the starting material was recovered. To optimize the yield of diallylated sulfone **2a** various conditions were studied (e.g., NaH and LDA). In this regard, increasing the

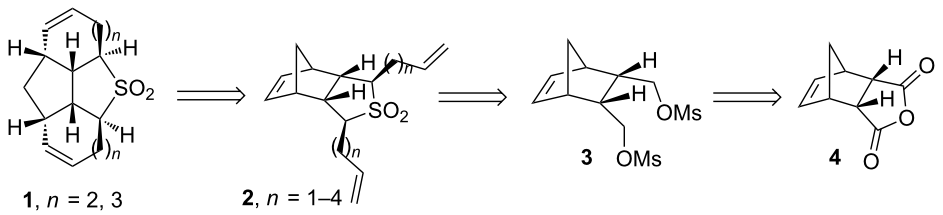

Figure 1: Retrosynthetic approach to polycyclic sulfones.

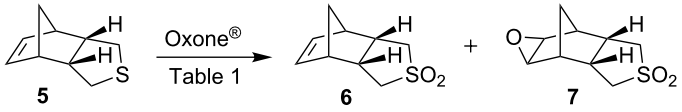

Scheme 1: Preparation of the sulfone **6** via oxidation.

Table 1: Different reaction conditions used to improve the yield of the sulfone **6**.

Entry	Reaction conditions	**6** yield [%]	**7** yield [%]
1	Oxone® (3 equiv), MeOH, H_2O, 0 °C, 22 h	29	40
2	**Oxone® (2.5 equiv), MeOH, H_2O, −5 °C, 6 h**	**89**	**8**
3	Oxone® (2.5 equiv), MeOH, H_2O, −5 °C, 5.5 h	83	15
4	Oxone® (2.2 equiv), MeOH, H_2O, −8 °C, 4.5 h	82	5
5	Oxone® (2 equiv), MeOH, H_2O, −20 °C, 5 h	71	5

equivalents of allyl bromide and *n*-BuLi produced the diallylated sulfone **2a** in 80% yield and the monoallylated compound **8a** in 10% yield (Table 2, entry 1a) [35] along with a minor amount (3%) of triallylated sulfone **9** (Scheme 2). However, with an excess amount of base (5 equiv) and allyl bromide the diallylated sulfone **2a** was isolated as a major product and the triallylated sulfone **9** in 6% yield (Table 2, entry 1b). Later, the monoallylated sulfone **8a** has been converted to the desired diallyl compound **2a** (88%) under similar reaction conditions. The structures of the diallyl (**2a**) and triallyl (**9**) sulfones have been confirmed by ^{1}H and ^{13}C NMR spectral data and further supported by HRMS data. In addition, the structure and stereochemistry of the allyl groups present in compound **2a** have been confirmed by single-crystal X-ray diffraction studies and this data clearly indicated that the allylation had occurred at α-position of the sulfone moiety and the two allyl groups are in *cis*-arrangement with each other [35-37].

Analogously, the alkenylation of sulfone **6** was optimized with other electrophiles and the results are summarized in Table 2 (entries 2–4). In this regard, sulfone **6** was butenylated with 4-bromo-1-butene and *n*-BuLi in the presence of HMPA at −74 °C to rt to deliver the monobutenylated sulfone **8b** in 75% yield. Surprisingly, here a minor amount of the desired dibutenylated sulfone **2b** (21%) was isolated (Table 2, entry 2). However, the monobutenylated sulfone **8b** can be converted to the dibutenylated sulfone **2b** under similar conditions. Next, the same synthetic sequence has been extended to the dipentenyl and the dihexenyl sulfone derivatives. Thus, treatment of sulfone **6** with 5-bromo-1-pentene and *n*-BuLi using HMPA at −78 °C to rt (Table 2, entry 3) gave the desired dipentenylated sulfone **2c** (57%) and a minor amount of monopentenylated sulfone **8c** (5%).

Similarly, we synthesized the hexenyl sulfone derivatives **8d** and **2d** by treating compound **6** with 6-bromo-1-hexene using HMPA and *n*-BuLi at −78 °C. The desired dihexenylated sulfone **2d** has been furnished in 75% yield along with monohexenyl sulfone derivative **8d** (9%, Table 2, entry 4). Based on these optimization studies, it was concluded that it is necessary to use the appropriate number of equivalents of the alkenyl bromide and the suitable base to generate the dialkenylated products (Table 2 and Scheme 2).

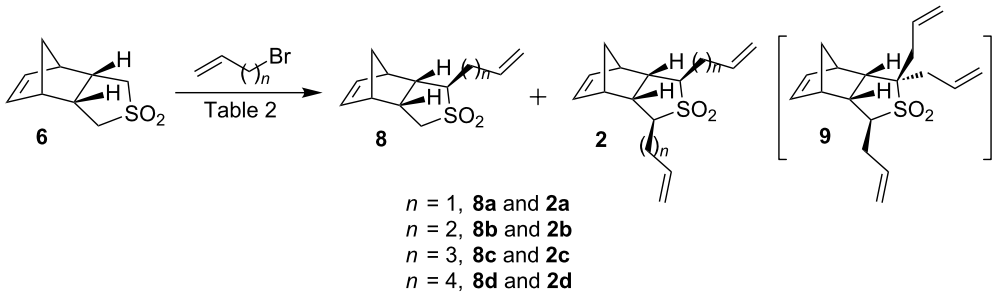

Scheme 2: Synthesis of alkenylated sulfone derivatives.

Table 2: Optimized reaction conditions to realize mono and dialkenylated sulfones.

Entry	*n*	Reaction conditions	Monoalkenylated product yield [%]	Dialkenylated product yield [%]
1a	1	allyl bromide (3 equiv), *n*-BuLi THF, −75 °C to rt, 25 h	**8a** (10)	**2a** (80) & **9**[a] (3)
1b		allyl bromide (10 equiv), *n*-BuLi THF, −58 °C to rt, 26 h	**8a** (0)	**2a** (80) & **9**[a] (6)
2	2	4-bromo-1-butene (3 equiv), *n*-BuLi HMPA, THF, −74 °C to rt, 20 h	**8b** (75[b])	**2b** (21[b])
3	3	5-bromo-1-pentene (2.5 equiv), *n*-BuLi HMPA, THF, −78 °C to rt, 17.5 h	**8c** (5)	**2c** (57)
4	4	6-bromo-1-hexene (2.8 equiv), *n*-BuLi HMPA, THF, −78 °C to rt, 17 h	**8d** (9)	**2d** (75)

[a]Triallylated product, [b]isolated yield based on starting material recovered.

After the successful synthesis of various dialkenyl sulfone derivatives **2a–d**, we focussed our attention towards the RRM step. Initially, the diallyl sulfone **2a** (~0.0141 M solution in dry CH_2Cl_2) was subjected to RRM using G-I catalyst in the presence of ethylene gas in refluxing CH_2Cl_2 to get the tetracyclic sulfone **1a**, however, we isolated the tricyclic sulfone **10** in 48% yield. When the G-I catalyst was replaced with G-II a complex mixture of products was observed as indicated by ^{1}H and ^{13}C NMR spectral data. Later, compound **10** was treated with conventional Grubbs catalysts under different reaction conditions (Table 3) to obtain the RRM product **1a** (Scheme 3). Unfortunately, the expected compound **1a** was not obtained. The strain present in the *trans*-fused compound **1a** may be responsible for its absence in the RRM sequence.

Interestingly, dibutenyl sulfone **2b** (~0.0034 M solution in toluene) smoothly underwent RRM with Grubbs 2nd generation (G-II) catalyst in the presence of ethylene in refluxing toluene to produce the anticipated tetracyclic sulfone **1b** (97%) (Scheme 4). The sulfone **1b** has been characterized by ^{1}H and ^{13}C NMR and DEPT-135 spectral data including HRMS data.

Next, the RRM of dipentenyl sulfone **2c** (~0.0031 M solution in toluene) was carried out under similar reaction conditions to furnish **1c**. Interestingly, the tricyclic sulfone **11** was isolated in 60% along with the expected tetracyclic sulfone **1c** (32%) and a minor amount of ring-opened product **12** (6%, Scheme 5). A complex mixture of products was obtained when compound **2c** was exposed to the metathesis catalyst for a longer period of time as indicated by ^{1}H and ^{13}C NMR spectral data.

Analogously, dihexenyl sulfone **2d** (~0.0024 M solution in toluene) was treated with G-II catalyst to deliver the RRM product in the presence of ethylene in refluxing toluene. In this regard, only ring-opened sulfone **13** was produced in 88% yield (Scheme 6) and no cyclized product was observed. Presumably, this observation may be explained on the basis that the nine-membered ring product was not formed due to the unfavourable steric interactions involved.

Conclusion

Several interesting polycyclic sulfone derivatives were designed and assembled involving RRM. The RRM outcome of various

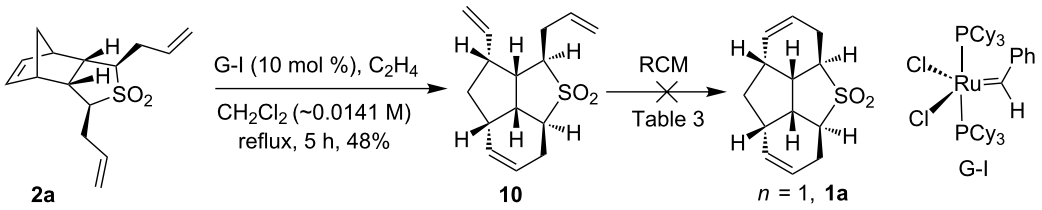

Scheme 3: Synthesis of **10** by RRM of **2a**.

Table 3: Toluene (~0.004 M) reflux conditions to convert **10** to **1a**.

Entry	Conditions	Result
1	G-I (10 mol %), C_2H_4, 19 h	SM[a] recovered
2	G-II (10 mol %), $Ti(OiPr)_4$, C_2H_4, 24 h	No product[b]
3	HG-II[c] (10 mol %), $Ti(OiPr)_4$, C_2H_4, 24 h	No product[b]

[a]Starting material. [b]SM not recovered, [c]Hoveyda–Blechert–Grubbs catalyst.

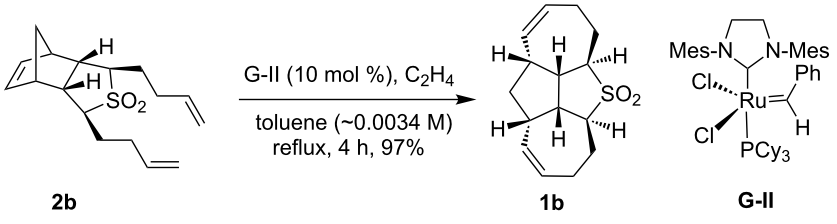

Scheme 4: Synthesis of **1b** using RRM.

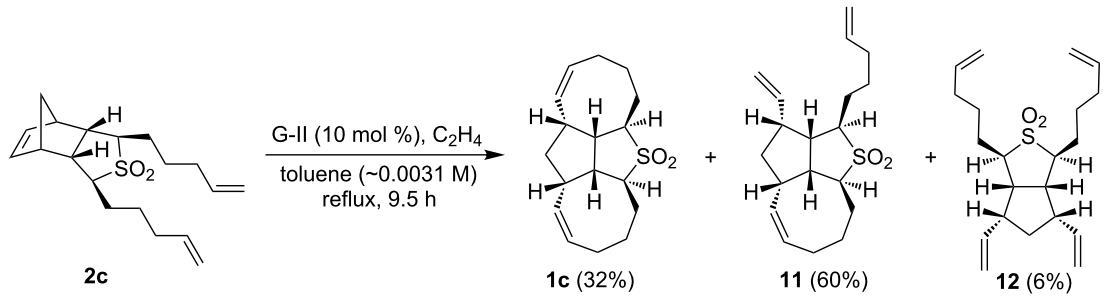

Scheme 5: RRM of the dipentenyl sulfone **2c**.

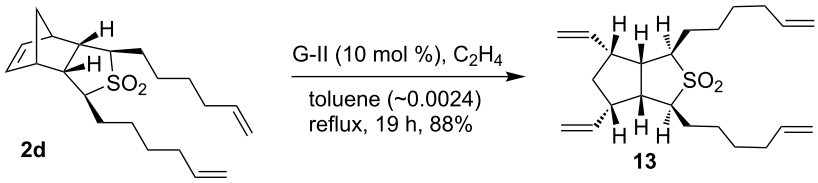

Scheme 6: RRM of the dihexenyl sulfone **2d**.

sulfones (**2a–d**) depends on the length of the alkenyl chain. In this context, the dibutenyl sulfone derivative **2b** is the most-promising candidate for the RRM protocol. In other instances, for example with propenyl analogue **2a** the partial ring-closing product **10** was obtained. With substrate **2c**, the eight-membered RRM compound **1c** was formed as a minor product and partial ring-closing compound **11** as a major product. With substrate **2d**, only ring-opened product **13** was produced. Interestingly, we demonstrated *trans*-ring junction products are possible in the RRM protocol. It is clear that RRM has a unique place in olefin metathesis [38-45] and further interesting examples are expected in future.

Supporting Information

Supporting Information File 1

Detailed experimental procedures, characterization data and copies of ^{1}H,^{13}C NMR and HRMS spectra for all new compounds.
[http://www.beilstein-journals.org/bjoc/content/supplementary/1860-5397-11-148-S1.pdf]

Acknowledgements

We thank the Department of Science and Technology (DST), New Delhi for the financial support and the Sophisticated Analytical Instrument Facility (SAIF), IIT-Bombay for recording spectral data. S.K. thanks the Department of Science and Technology for the award of a J. C. Bose fellowship. R.G. thanks the University Grants Commission (UGC), New Delhi for the award of a research fellowship.

References

1. Alba, A.-N. R.; Companyó, X.; Rios, R. *Chem. Soc. Rev.* **2010,** *39,* 2018–2033. doi:10.1039/B911852G
2. Meadows, D. C.; Gervay-Hague, J. *Med. Res. Rev.* **2006,** *26,* 793–814. doi:10.1002/med.20074
3. Bäckvall, J.-E.; Chinchilla, R.; Nájera, C.; Yus, M. *Chem. Rev.* **1998,** *98,* 2291–2312. doi:10.1021/cr970326z
4. García Ruano, J. L.; Alemán, J.; Parra, A.; Marzo, L. *Eur. J. Org. Chem.* **2014,** 1577–1588. doi:10.1002/ejoc.201301483
5. Alonso, D. A.; Fuensanta, M.; Nájera, C.; Varea, M. *Phosphorus, Sulfur Silicon Relat. Elem.* **2005,** *180,* 1119–1131. doi:10.1080/10426500590910657
6. Roy, K.-M. Sulfones and Sulfoxides. *Ullmann's Encyclopedia of Industrial Chemistry;* Wiley-VCH: Weinheim, 2000. doi:10.1002/14356007.a25_487
7. Kotha, S.; Ali, R. *Tetrahedron Lett.* **2015,** *56,* 2172–2175. doi:10.1016/j.tetlet.2015.03.021
8. Kotha, S.; Ali, R. *Tetrahedron* **2015,** *71,* 1597–1603. doi:10.1016/j.tet.2015.01.009
9. Kotha, S. *Acc. Chem. Res.* **2003,** *36,* 342–351. doi:10.1021/Ar020147q
10. Harvey, J. E.; Bartlett, M. J. *Chem. N. Z.* **2010,** *74,* 63–69. And references cited therein.
11. Metz, P.; Fleischer, M.; Fröhlich, R. *Tetrahedron* **1995,** *51,* 711–732. doi:10.1016/0040-4020(94)00969-2
12. Barbarella, G.; Cinquini, M.; Colonna, S. *J. Chem. Soc., Perkin Trans. 1* **1980,** 1646–1649. doi:10.1039/P19800001646
13. Kotha, S.; Bandi, V. *Heterocycles* **2015,** *90,* 226–237. doi:10.3987/Com-14-S(K)9

14. Kotha, S.; Khedkar, P. *J. Org. Chem.* **2009,** *74,* 5667–5670. doi:10.1021/jo900658z
15. Holub, N.; Blechert, S. *Chem. – Asian J.* **2007,** *2,* 1064–1082. doi:10.1002/asia.200700072
And references cited therein.
16. Vincent, G.; Kouklovsky, C. *Chem. – Eur. J.* **2011,** *17,* 2972–2980. doi:10.1002/chem.201002558
17. Nolan, S. P.; Clavier, H. *Chem. Soc. Rev.* **2010,** *39,* 3305–3316. doi:10.1039/B912410c
18. Clavier, H.; Broggi, J.; Nolan, S. P. *Eur. J. Org. Chem.* **2010,** 937–943. doi:10.1002/ejoc.200901316
19. Tsao, K.-W.; Devendar, B.; Liao, C.-C. *Tetrahedron Lett.* **2013,** *54,* 3055–3059. doi:10.1016/j.tetlet.2013.03.142
20. Standen, P. E.; Kimber, M. C. *Tetrahedron Lett.* **2013,** *54,* 4098–4101. doi:10.1016/j.tetlet.2013.05.112
21. Li, J.; Lee, D. *Chem. Sci.* **2012,** *3,* 3296–3301. doi:10.1039/C2sc20812a
22. Imhof, S.; Blechert, S. *Synlett* **2003,** 609–614. doi:10.1055/s-2003-38367
23. Arjona, O.; Csákÿ, A. G.; Plumet, J. *Eur. J. Org. Chem.* **2003,** 611–622. doi:10.1002/ejoc.200390100
24. Nguyen, N. N. M.; Leclère, M.; Stogaitis, N.; Fallis, A. G. *Org. Lett.* **2010,** *12,* 1684–1687. doi:10.1021/Ol100150f
25. Datta, R.; Bose, S.; Viththlbhai, P. B.; Ghosh, S. *Tetrahedron Lett.* **2014,** *55,* 3538–3540. doi:10.1016/j.tetlet.2014.04.091
26. Lam, J. K.; Pham, H. V.; Houk, K. N.; Vanderwal, C. D. *J. Am. Chem. Soc.* **2013,** *135,* 17585–17594. doi:10.1021/ja409618p
27. Kotha, S.; Ravikumar, O. *Tetrahedron Lett.* **2014,** *55,* 5781–5784. doi:10.1016/j.tetlet.2014.08.108
28. Kotha, S.; Ravikumar, O. *Eur. J. Org. Chem.* **2014,** 5582–5590. doi:10.1002/ejoc.201402273
29. Goll, J. M.; Fillion, E. *Organometallics* **2008,** *27,* 3622–3625. doi:10.1021/Om800390w
30. Wilcox, C. F., Jr.; Craig, R. R. *J. Am. Chem. Soc.* **1961,** *83,* 3866–3871. doi:10.1021/ja01479a030
31. Zhang, M.; Flynn, D. L.; Hanson, P. R. *J. Org. Chem.* **2007,** *72,* 3194–3198. doi:10.1021/Jo0620260
32. Trost, B. M.; Curran, D. P. *Tetrahedron Lett.* **1981,** *22,* 1287–1290. doi:10.1016/S0040-4039(01)90298-9
33. Bloch, R.; Abecassis, J. *Tetrahedron Lett.* **1982,** *23,* 3277–3280. doi:10.1016/S0040-4039(00)87591-7
34. Bloch, R.; Abecassis, J.; Hassan, D. *Can. J. Chem.* **1984,** *62,* 2019–2024. doi:10.1139/V84-345
35. Kotha, S.; Gunta, R. *Acta Crystallogr., Sect. E* **2014,** *70,* o1163–o1164. doi:10.1107/S1600536814022053
36. Bloch, R.; Abecassis, J. *Synth. Commun.* **1985,** *15,* 959–963. doi:10.1080/00397918508076826
37. Bloch, R.; Abecassis, J. *Tetrahedron Lett.* **1983,** *24,* 1247–1250. doi:10.1016/S0040-4039(00)81626-3
38. Grubbs, R. H. *Handbook of Metathesis,* 1st ed.; Wiley-VCH: Weinheim, 2003.
39. Kotha, S.; Sreenivasachary, N. *Indian J. Chem., Sect. B* **2001,** *40,* 763–780.
40. Kotha, S.; Lahiri, K. *Synlett* **2007,** 2767–2784. doi:10.1055/s-2007-990954
41. Kotha, S.; Mandal, K. *Chem. – Asian J.* **2009,** *4,* 354–362. doi:10.1002/asia.200800244
42. Kotha, S.; Misra, S.; Sreevani, G.; Babu, B. V. *Curr. Org. Chem.* **2013,** *17,* 2776–2795. doi:10.2174/13852728113179990118
43. Kotha, S.; Meshram, M.; Tiwari, A. *Chem. Soc. Rev.* **2009,** *38,* 2065–2092. doi:10.1039/B810094m
44. Kotha, S.; Dipak, M. K. *Tetrahedron* **2012,** *68,* 397–421. doi:10.1016/j.tet.2011.10.018
45. Kotha, S.; Krishna, N. G.; Halder, S.; Misra, S. *Org. Biomol. Chem.* **2011,** *9,* 5597–5624. doi:10.1039/c1ob05413a

License and Terms

BEILSTEIN JOURNAL OF ORGANIC CHEMISTRY

Cross-metathesis reaction of α- and β-vinyl *C*-glycosides with alkenes

Ivan Šnajdr[1], Kamil Parkan[2], Filip Hessler[1] and Martin Kotora[*1]

Full Research Paper

Open Access

Address:
[1]Department of Organic Chemistry, Charles University in Prague, Hlavova 8, 153 00 Praha 2, Czech Republic, Fax: (+) 420 221 951 326 and [2]Department of Chemistry of Natural Compounds, University of Chemistry and Technology, Prague, Technická 5, 160 00 Praha 6, Czech Republic

Email:
Martin Kotora[*] - martin.kotora@natur.cuni.cz

* Corresponding author

Keywords:
C-glycosides; catalysis; carbohydrates; cross-metathesis; ruthenium

Beilstein J. Org. Chem. **2015,** *11,* 1392–1397.
doi:10.3762/bjoc.11.150

Received: 17 April 2015
Accepted: 20 July 2015
Published: 10 August 2015

This article is part of the Thematic Series "Progress in metathesis chemistry II".

Guest Editor: K. Grela

Abstract

Cross-metathesis of α- and β-vinyl *C*-deoxyribosides and α-vinyl *C*-galactoside with various terminal alkenes under different conditions was studied. The cross-metathesis of the former proceeded with good yields of the corresponding products in $ClCH_2CH_2Cl$ the latter required the presence of CuI in CH_2Cl_2 to achieve good yields of the products. A simple method for the preparation of α- and β-vinyl *C*-deoxyribosides was also developed. In addition, feasibility of deprotection and further transformations were briefly explored.

Introduction

Natural and unnatural *C*-substituted glycosides are important compounds with a plethora of attractive biological properties and they often have been used as artificial DNA components [1]. Among various synthetic procedures providing *C*-deoxyribosides the one based on the use of a protected *C*-(2-deoxyribofuranosyl)ethyne, easily accessed by a coupling of a protected D-ribosyl halide and ethynylmagnesium chloride [2], offers a considerable synthetic flexibility since the triple bond could be transformed directly into various functional groups [3-13]. Thus the ethyne moiety was used in [2 + 2 + 2] cyclotrimerization to yield aryl *C*-deoxyribosides [3] and in a Sonogashira reaction for the synthesis of butenolidyl *C*-deoxyribosides [4]. Substituted alkynyl *C*-deoxyribosides [5,10,11] were used in other types of cycloaddition reactions providing indolyl *C*-deoxyribosides [6], cyclopentenonyl *C*-deoxyribosides [9], triazolyl *C*-deoxyribosides [12,13], carboranyl *C*-deoxyribosides [7], and finally also in Diels–Alder reaction with cyclobutadiene derivatives [8]. Despite of the above mentioned transformations, alkynyl *C*-deoxyribosides could also be used as a suitable starting material for hitherto rarely studied transformations.

One such a potential transformation is their hydrogenation to the corresponding vinyl *C*-deoxyribosides that could serve as

intermediates for further functionalization. Interestingly, just a couple of reports regarding synthesis of vinyl *C*-deoxyribosides have been published so far. Among them is the Lindlar catalyst mediated hydrogenation of ethynyl β-*C*-deoxyriboside (prepared by a rather lengthy synthetic procedure) that provided vinyl β-*C*-deoxyribofuranosides [9]. Another procedure leading to pure vinyl β-*C*-deoxyribofuranoside was based on transformation of 6-*O*-*tert*-butyldiphenylsilyl-3,5-dideoxy-5-iodo-L-lyxo-hexofuranose [14]. A reaction sequence relying on Horner–Wadsworth–Emmons/ring closure–halogenation/Ramberg–Bäcklund/Wittig reaction gave rise to the equimolar mixture of styryl α- and β-*C*-deoxyribosides [15].

Finally, there is also a method utilizing an excess of vinylmagnesium bromide in the reaction with 3,5-bis-*O*-TBDPS-protected 2-deoxy-D-ribofuranose giving rise to a mixture of diastereoisomeric diols. The diasteroisomers were separated and cyclized in the presence of MsCl to the corresponding vinyl α-*C*-deoxyriboside α-**2** and β-*C*-deoxyriboside β-**2** [16]. As far as further transformation of vinyl *C*-deoxyribosides relying on the metathesis reaction is concerned, only one paper dealing with successful cross-metathesis with 4-vinyl-5-methyl-2-oxazolone has been reported [16]. This finding is rather surprising, because the metathesis reaction has been frequently used as a tool for chain elongation of various saccharides [17].

In view of the aforementioned, it is obvious that a development of a new and simple route to anomerically pure α- and β-vinyl *C*-deoxyribosides is desirable as well as to study the scope of their participation in cross-metathesis reactions. This procedure could thus open a new pathway for preparation of a number of alkenyl and alkyl *C*-deoxyriboside derivatives.

Results and Discussion

Synthesis of vinyl α- and β-*C*-deoxyribosides **2**

Although the simplest pathway for the preparation of vinyl α-*C*-deoxyriboside α-**2** and β-*C*-deoxyriboside β-**2** seems the reaction of a halogenose with ethynylmagnesium chloride followed by hydrogenation, this approach has not been reported yet (to the best of our knowledge). Presumably, difficulties regarding separation of a mixture of ethynyl α-*C*-deoxyriboside α-**1** and β-*C*-deoxyriboside β-**1** precluded any attempts. Notwithstanding this, we decided to test this approach. We found that hydrogenation of the epimeric mixture of ethynyl α-*C*-deoxyriboside α-**1** and β-*C*-deoxyriboside β-**1** on Lindlar catalyst at 1 atm of H_2 provided, as expected, a mixture of the corresponding vinyl α-*C*-deoxyriboside α-**2** and vinyl β-*C*-deoxyriboside β-**2**. The mixture was easily separated into pure epimers (59% for α-**2** and 30% β-**2**) just by using a simple column chromatography (Scheme 1). Their identity was confirmed by comparison of the obtained spectral data with the published ones for related compounds [9,14,16]. This two-step reaction sequence is very simple and provides access to both epimers from a simply available starting material.

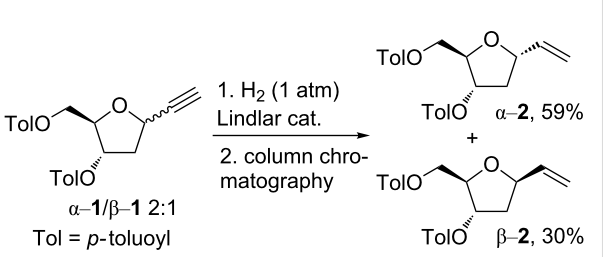

Scheme 1: Synthesis of vinyl *C*-deoxyribosides α-**2** and β-**2**.

Cross-metathesis reactions with vinyl α- and β-*C*-deoxyribosides **2**

There is a general interest in synthesis of borylated [18] or carboranylated [8,19] saccharides and derivatives thereof because of their interesting properties. Bearing this in mind, we decided to explore the possibility of attaching the carborane moiety by using a cross-metathesis reaction. Cross-metathesis of α-**2** with the allylated carborane **3a** (Figure 1) was used as a model reaction [20-22]. Since it has been shown that the solvent [23] may profoundly affect the course of the cross-metathesis reaction in terms of activity and selectivity, we screened various reaction conditions to secure the highest yield of the desired cross-product of the reaction between α-**2** and **3a** (Table 1). The reactions were carried out in the presence of Hoveyda–Grubbs 2nd generation catalyst (HG II), which has been shown to be the best catalyst for cross-metathesis reactions [24]. Running the reaction under the standard conditions in dichloromethane or toluene under reflux, the desired cross-metathesis product α-**4a** was isolated in low 10% and 3% yields (Table 1, entries 1 and 2). Although it has been observed that the use of octafluorotoluene [23,25-27] as the solvent had a positive effect on yields, its use provided α-**4a** in a low 12% yield (Table 1, entry 3), but its use under microwave irradiation [26,28-30] gave rise to α-**4a** in 33% isolated yield (Table 1, entry 4). A similar result (36% yield) was obtained with a 1:1 octafluorotoluene/$ClCH_2CH_2Cl$ mixture (Table 1, entry 5). Although microwave irradiation had a positive effect on the cross-metathesis reaction, see examples above, carrying out the reaction in a mixture of 1:1 octafluorotoluene/$ClCH_2CH_2Cl$ under irradiation provided α-**4a** in only 3% (Table 1, entry 6). Finally, carrying out the reaction in pure $ClCH_2CH_2Cl$ under reflux furnished the product in a nice 70% isolated yield (Table 1, entry 7), while microwave irradiation resulted in decreased yield of 58% (Table 1, entry 8). According to the obtained data in some cases microwave irradiation had a positive effect on the course of the

reaction (Table 1, entry 4), whereas as in some cases it had a detrimental effect (Table 1, entries 6 and 8). Currently we do not know how to account for these observations; however, decomposition of the catalyst under these conditions cannot be excluded. In all of the above mentioned cases the unreacted starting material was recovered from the reaction mixtures.

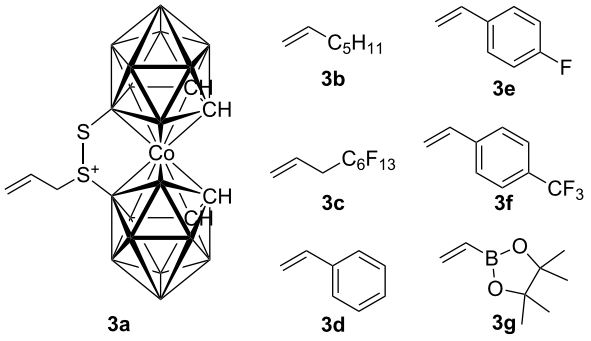

Figure 1: Alkenes **3** used in cross-metathesis reactions with **2**.

Table 1: Conditions tested for cross-metathesis of α-**2** with **3a**.

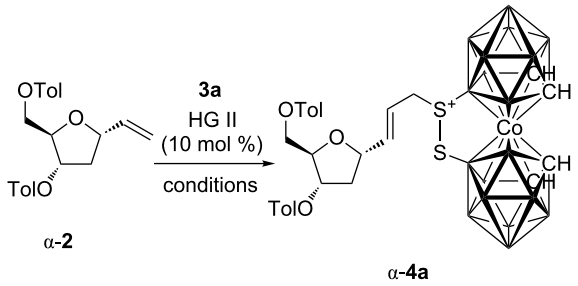

Entry	Reaction conditions[a]	Yield (%)[b]
1	CH_2Cl_2, reflux, 24 h	10
2	toluene, reflux, 24 h	3
3	$C_6F_5CF_3$, reflux, 16 h	12
4	$C_6F_5CF_3$, mw[c]	33
5	$C_6F_5CF_3$/$ClCH_2CH_2Cl$ 1:1, 16 h	36
6	$C_6F_5CF_3$/$ClCH_2CH_2Cl$ 1:1, mw[c]	3
7	$ClCH_2CH_2Cl$, reflux, 12 h	70
8	$ClCH_2CH_2Cl$, mw, 110 °C, 2 h[c]	58

[a]α-**2** (0.26 mmol), solvent (5 mL). [b]Isolated yields. [c]mw = microwave irradiation.

With these results in hand we decided to screen the scope of cross-metathesis reactions with other terminal alkenes **3b**–**3g** (Figure 1, Table 2). Our first choice was 1-heptene (**3b**), which reacted under the above mentioned conditions (i.e., with HG II in $ClCH_2CH_2Cl$ under reflux) to give the corresponding product α-**4b** in 59% isolated yield (Table 2, entry 2). We also carried out the reaction with perfluorohexylpropene (**3c**), because of our long term interest in the synthesis of perfluoroalkylated compounds [21,30-34] and their application [35]. The reaction furnished the desired compound α-**4c** in a good 50% isolated yield (Table 2, entry 3). Next we switched our attention to styrenes **3d**–**3f**. In all cases the corresponding products α-**4d**–α-**4f** were obtained in good 68, 60, and 59% isolated yields, respectively (Table 2, entries 4–6). Finally, cross-metathesis with vinylboronic acid pinacol ester (**3g**) was attempted. Once again the reaction proceeded well, furnishing boronate α-**4g** in 66% isolated yield (Table 2, entry 7). Then we turned to reactions of the above mentioned terminal alkenes with β-**2**. In all cases the corresponding products were obtained in good isolated yields in the range similar to α-**2**. The metathesis with the allylated carborane **3a** provided β-**4a** in 77% yield (Table 2, entry 8). The reaction with 1-heptene (**3b**) and perfluorohexylpropene (**3c**) gave the corresponding products β-**4b** and β-**4c** in 64 and 48% yields (Table 2, entries 9 and 10). In a similar manner also the styrenes **3d**–**3f** furnished the desired products β-**4d**–β-**4f** in 69, 58, and 61% yields, respectively (Table 2, entries 11–13). Similarly compound **3g** reacted well providing the boronate β-**4g** in a nice 64% yield (Table 2, entry 14). The latter boronate was subjected to coupling with iodobenzene under Suzuki conditions and the corresponding product β-**4d** was obtained in 51% isolated yield.

Table 2: Cross-coupling of **2α** and β-**2** with alkenes **3**.

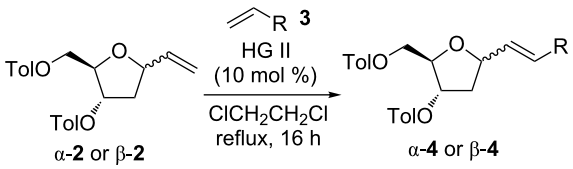

Entry	**2**	**3**	**4**	Yield (%)[a]
1	α-**2**	**3a**	α-**4a**	74
2		**3b**	α-**4b**	59
3		**3c**	α-**4c**	50
4		**3d**	α-**4d**	68
5		**3e**	α-**4e**	60
6		**3f**	α-**4f**	59
7		**3g**	α-**4g**	66
8	β-**2**	**3a**	β-**4a**	77
9		**3b**	β-**4b**	64
10		**3c**	β-**4c**	48
11		**3d**	β-**4d**	69
12		**3e**	β-**4e**	58
13		**3f**	β-**4f**	61
14		**3g**	β-**4g**	64

[a]Isolated yields.

With the *C*-deoxyribosides on hand, the feasibility of catalytic hydrogenation was also briefly explored. Compounds possessing the heptenyl side chain (β-**4b**), tridecafluorononenyl side chain (β-**4c**), and the styryl side chain (β-**4d**) were chosen as substrates. In all cases the hydrogenation by using Pd/C under low pressure of hydrogen (1 atm) proceeded uneventfully to give rise to products with the saturated side chain β-**5b**, β-**5c**, and β-**5d** in good isolated yields of 88, 57, and 87% (Scheme 2). In addition, deprotection of the toluoyl groups was tested on compounds bearing an unsaturated side chain such as β-**4e** and a saturated side chain such as β-**5b** by using K_2CO_3 in a mixture of MeOH/H_2O. In both cases the reaction proceeded almost quantitatively providing the corresponding *C*-deoxyribosides β-**6e** and β-**7b** in 89 and 93% isolated yields (Scheme 3).

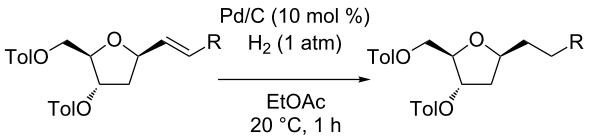

β-**4b**, R = *n*-pentyl
β-**4c**, R = $CF_3(CF_2)_5CH_2$
β-**4d**, R = Ph

β-**5b**, R = *n*-pentyl, 88%
β-**5c**, R = $CF_3(CF_2)_5CH_2$, 57%
β-**5d**, R = Ph, 87%

Scheme 2: Hydrogenation of β-**4b**–β-**4d** to β-**5b**–β-**5d**.

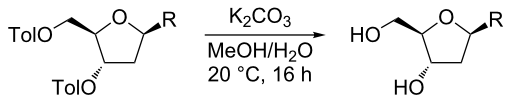

β-**4e**, R = 4-F-C_6H_4CH=CH
β-**5b**, R = *n*-heptyl

β-**6e**, R = 4-F-C_6H_4CH=CH, 89%
β-**7b**, R = *n*-heptyl, 93%

Scheme 3: Deprotection of β-**4e** and β-**5b** to β-**6e** and β-**7b**.

Cross-metathesis reactions with 1-(tetra-*O*-acetyl-α-D-galactopyranosyl)ethene (**8**)

There have been, to the best of our knowledge, just a handful of reports of cross-metathesis reactions of other vinyl *C*-glycosides. Among these reports metatheses of 1-(D-glucopyranosyl)prop-2-ene derivatives with various alkenes [36-40] and one report regarding a 1-(α-D-galactopyranosyl)ethene derivative with allyl amines [41]. Because of our interest in the synthesis of various D-galactose derivatives, we decided to explore the scope of their metathesis reaction with several different alkenes.

The starting material – 1-(tetra-*O*-acetyl-α-D-galactopyranosyl)ethene (**8**) – was prepared according to the previously reported procedure. A solution of penta-*O*-acetyl-D-galactose, allyltrimethylsilane and $BF_3{\cdot}Et_2O$ was refluxed in acetonitrile giving a 6:1 mixture of α- and β-epimers of 1-(tetra-*O*-acetyl-D-galactopyranosyl)prop-2-ene in 98% yield. Zemplén deacetylation afforded quantitatively the same mixture of epimeric 1-(D-galactopyranosyl)prop-2-enes that were dissolved in ethanol and treated with ether. This allowed the α-epimer to precipitate and it could afterwards be isolated as a pure crystalline product in 60% yield [42]. Its acetylation afforded 1-(tetra-*O*-acetyl-α-D-galactopyranosyl)prop-2-ene in high yield and purity. It was then isomerized [43] to 1-(tetra-*O*-acetyl-α-D-galactopyranosyl)prop-1-ene (80% yield) that was subjected to cross-metathesis with ethene to give the desired compound **8** in 82% yield [41].

The above mentioned metathesis conditions – HG II, reflux in 1,2-dichloroethane – were also tested in the reactions of **8** with alkenes **3d**–**3f** (Table 3). However, the yields of the corresponding products **9d**–**9f** were around 60% (Table 3, entries 1–3, column IV). Switching the solvent to dichloromethane did not have any substantial effect on the yields of the corresponding products (57–70%) (Table 3, entries 1–3, column V). Moreover, in all above mentioned cases the starting material remained partially unreacted and could not be easily separated from the desired products.

Table 3: Cross-metathesis of **8** with alkenes **3**.

Entry	**3**	**9**	Yield (%)[a] (in $ClCH_2CH_2Cl$)	Yield (%)[a] (in CH_2Cl_2)
1	**3d**	**9d**	58	70
2	**3e**	**9e**	61	57
3	**3f**	**9f**	56	58

[a]Isolated yield.

A considerable improvement was observed when the metatheses were run in dichloromethane and in the presence of CuI (Table 4) [44]. In all cases the reactions provided the corresponding products in very good isolated yields. The first metatheses were carried out with 1-heptene (**3b**) and perfluorohexylpropene (**3c**) furnishing **9b** and **9c** in nice 80 and 79% isolated yields, respectively (Table 4, entries 1 and 2). Then we switched our attention to styrenes **3d**–**3f**. In all cases the corresponding products **9d**–**9f** were obtained in good 82, 79, and 78% isolated yields, respectively (Table 4, entries 3–5). In addition, in all cases deprotection under basic conditions provided the corresponding *C*-alkenylated D-galactoses in very good isolated yields (86–93%).

Conclusion

In conclusion, the cross-metathesis reaction of anomerically pure vinyl *C*-deoxyriboses (easily accessible from a mixture of ethynyl α/β-*C*-deoxyribosides) with alkenes bearing various

Table 4: Cross-metathesis of **8** with alkenes **3** in the presence of CuI.

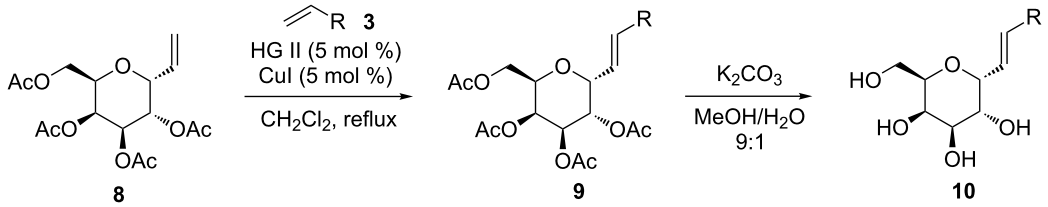

8 **9** **10**

Entry	3	9	Yield (%)[a]	10	Yield (%)[a]
1	**3b**	**9b**	80	**10b**	88
2	**3c**	**9c**	79	**10c**	80
3	**3d**	**9d**	82	**10d**	93
4	**3e**	**9e**	79	**10e**	90
5	**3f**	**9f**	78	**10f**	87

[a]Isolated yield.

functional groups proceeded in the presence of a catalytic amount of HG II catalysts in refluxing 1,2-dichloroethane giving rise to the corresponding alkenylated derivatives in good yields and without loss of stereochemical information. Deprotection as well as hydrogenation is also feasible providing the desired compounds as exemplified in selected examples. In addition, this methodology is also applicable to vinyl α-*C*-D-galactopyranoside, albeit the best results were obtained when the reaction was carried out in refluxing dichloromethane and in the presence of CuI. Deprotection of the prepared alkenylated derivatives proceeded without any problems.

Since homodimerization of the starting alkenes **2** and **8** has not been observed under the reaction conditions used (however, we cannot exclude that minor undetected amounts of homodimers of **2** or **8** were formed), they could be preliminarily considered as type II or III olefins according to the Grubbs classification of olefins [45].

Supporting Information

Supporting Information File 1

Detailed experimental procedures for all compounds, characterization of the synthesized compounds, and copies of $^{1}H/^{13}C$ NMR spectra for all compounds.
[http://www.beilstein-journals.org/bjoc/content/supplementary/1860-5397-11-150-S1.pdf]

Acknowledgements

This work was supported by Czech Science Foundation (grant No. 13-15915S and 15-17572S).

References

1. Teo, Y. N.; Wilson, J. N.; Kool, E. T. *J. Am. Chem. Soc.* **2009,** *131,* 3923–3933. doi:10.1021/ja805502k
2. Wamhoff, H.; Warnecke, H. *ARKIVOC* **2001,** *9,* 5–100.
3. Novák, P.; Číhalová, S.; Otmar, M.; Hocek, M.; Kotora, M. *Tetrahedron* **2008,** *64,* 5200–5207. doi:10.1016/j.tet.2008.03.046
4. Novák, P.; Pour, M.; Špulák, M.; Votruba, I.; Kotora, M. *Synthesis* **2008,** 3465–3472. doi:10.1055/s-0028-1083181
5. Bobula, T.; Hocek, M.; Kotora, M. *Tetrahedron* **2010,** *66,* 530–536. doi:10.1016/j.tet.2009.11.030
6. Nečas, D.; Hidasová, D.; Hocek, M.; Kotora, M. *Org. Biomol. Chem.* **2011,** *9,* 5934–5937. doi:10.1039/c1ob05844d
7. Šnajdr, I.; Janoušek, Z.; Takagaki, M.; Císařová, I.; Hosmane, N. S.; Kotora, M. *Eur. J. Med. Chem.* **2014,** *83,* 389–397. doi:10.1016/j.ejmech.2014.06.005
8. Hessler, F.; Kulhavá, L.; Císařová, I.; Otmar, M.; Kotora, M. *Synth. Commun.* **2014,** *44,* 1232–1239. doi:10.1080/00397911.2013.848896
9. Takase, M.; Morikawa, T.; Abe, H.; Inouye, M. *Org. Lett.* **2003,** *5,* 625–628. doi:10.1021/ol027210w
10. Adamo, M. F. A.; Pergoli, R. *Org. Lett.* **2007,** *9,* 4443–4446. doi:10.1021/ol701794u
11. Heinrich, D.; Wagner, T.; Diederichsen, U. *Org. Lett.* **2007,** *9,* 5311–5314. doi:10.1021/ol7025334
12. Nakahara, M.; Kuboyama, T.; Izawa, A.; Hari, Y.; Imanishi, T.; Obika, S. *Bioorg. Med. Chem. Lett.* **2009,** *19,* 3316–3319. doi:10.1016/j.bmcl.2009.04.063
13. Kaliappan, K. P.; Kalanidhi, P.; Mahapatra, S. *Synlett* **2009,** 2162–2166. doi:10.1055/s-0029-1217570
14. Egron, D.; Durand, T.; Roland, A.; Vidal, J.-P.; Rossi, J.-C. *Synlett* **1999,** *4,* 435–437. doi:10.1055/s-1999-3157
15. Jeanmart, S.; Taylor, R. J. K. *Tetrahedron Lett.* **2005,** *46,* 9043–9048. doi:10.1016/j.tetlet.2005.10.099
16. Rothman, J. H. *J. Org. Chem.* **2009,** *74,* 925–928. doi:10.1021/jo801910u
17. Aljarilla, A.; López, J. C.; Plumet, J. *Eur. J. Org. Chem.* **2010,** 6123–6143. doi:10.1002/ejoc.201000570

18. Martin, A. R.; Mohanan, K.; Luvino, D.; Floquet, N.; Baraguey, C.; Smietana, M.; Vasseur, J.-J. *Org. Biomol. Chem.* **2009,** *7,* 4369–4377. doi:10.1039/b912616c
19. Tietze, L. F.; Griesbach, U.; Schubert, I.; Bothe, U.; Marra, A.; Dondonni, A. *Chem. – Eur. J.* **2003,** *9,* 1296–1302. doi:10.1002/chem.200390148
20. Wei, X.; Carroll, P. J.; Sneddon, L. G. *Organometallics* **2006,** *25,* 609–621. doi:10.1021/om050851l
21. Eignerová, B.; Janoušek, Z.; Dračínský, M.; Kotora, M. *Synlett* **2010,** 885–888. doi:10.1055/s-0029-1219546
22. Sedlák, D.; Eignerová, B.; Dračínský, M.; Janoušek, Z.; Bartůněk, P.; Kotora, M. *J. Organomet. Chem.* **2013,** *747,* 178–183. doi:10.1016/j.jorganchem.2013.06.013
23. Rost, D.; Porta, M.; Gessler, S.; Blechert, S. *Tetrahedron Lett.* **2008,** *49,* 5968–5971. doi:10.1016/j.tetlet.2008.07.161
24. Vougioukalakis, G. C.; Grubbs, R. H. *Chem. Rev.* **2010,** *110,* 1746–1787. doi:10.1021/cr9002424
25. Samojłowicz, C.; Bienek, M.; Zarecki, A.; Kadyrov, R.; Grela, K. *Chem. Commun.* **2008,** *47,* 6282–6284. doi:10.1039/b816567j
26. Samojłowicz, C.; Borré, E.; Maudit, M.; Grela, K. *Adv. Synth. Catal.* **2011,** *353,* 1993–2002. doi:10.1002/adsc.201100053
27. Samojłowicz, C.; Bienik, M.; Pazio, A.; Makal, A.; Woźniak, K.; Poater, A.; Cavallo, L.; Wójcik, J.; Zdanowski, K.; Grela, K. *Chem. – Eur. J.* **2011,** *17,* 12981–12993. doi:10.1002/chem.201100160
28. Bargiggia, F. C.; Murray, W. V. *J. Org. Chem.* **2005,** *70,* 9636–9639. doi:10.1021/jo0514624
29. Michaut, A.; Boddaert, T.; Coquerel, Y.; Rodriguez, J. *Synthesis* **2007,** 2867–2871. doi:10.1055/s-2007-983825
30. Prchalová, E.; Votruba, I.; Kotora, M. *J. Fluorine Chem.* **2012,** *141,* 49–57. doi:10.1016/j.jfluchem.2012.06.005
31. Eignerová, B.; Dračínský, M.; Kotora, M. *Eur. J. Org. Chem.* **2008,** 4493–4499. doi:10.1002/ejoc.200800230
32. Eignerová, B.; Slavíková, B.; Buděšínský, M.; Dračínský, M.; Klepetářová, B.; Šťastná, E.; Kotora, M. *J. Med. Chem.* **2009,** *52,* 5753–5757. doi:10.1021/jm900495f
33. Eignerova, B.; Sedlák, D.; Dračínský, M.; Bartůněk, P.; Kotora, M. *J. Med. Chem.* **2010,** *53,* 6947–6953. doi:10.1021/jm100563h
34. Řezanka, M.; Eignerová, B.; Jindřich, J.; Kotora, M. *Eur. J. Org. Chem.* **2010,** 6256–6262. doi:10.1002/ejoc.201000807
35. Prchalová, E.; Štěpánek, O.; Smrček, S.; Kotora, M. *Future Med. Chem.* **2014,** *6,* 1201–1229. doi:10.4155/fmc.14.53
36. Dondoni, A.; Giovannini, P. P.; Marra, A. *J. Chem. Soc., Perkin Trans. 1* **2001,** 2380–2388. doi:10.1039/b106029p
37. Postema, M. H. D.; Piper, J. L. *Tetrahedron Lett.* **2002,** *43,* 7095–7099. doi:10.1016/S0040-4039(02)01617-9
38. Dominique, R.; Das, S. K.; Liu, B.; Nahra, J.; Schmor, B.; Gan, Z.; Roy, R. *Methods Enzymol.* **2003,** *362,* 17–28. doi:10.1016/S0076-6879(03)01002-4
39. Nolen, N. G.; Kurish, A. J.; Wong, K. A.; Orlando, M. D. *Tetrahedron Lett.* **2003,** *44,* 2449–2453. doi:10.1016/S0040-4039(03)00350-2
40. Lin, Y. A.; Chalker, J. M.; Davis, B. G. *J. Am. Chem. Soc.* **2010,** *132,* 16805–16811. doi:10.1021/ja104994d
41. Chen, G.; Schmieg, J.; Tsuji, M.; Franck, R. W. *Org. Lett.* **2004,** *6,* 4077–4080. doi:10.1021/ol0482137
42. Štěpánek, P.; Vích, O.; Werner, L.; Kniežo, L.; Dvořákova, H.; Vojtíšek, P. *Collect. Czech. Chem. Commun.* **2005,** *70,* 1411–1428. doi:10.1135/cccc20051411
43. Liu, S.; Ben, R. N. *Org. Lett.* **2005,** *7,* 2385–2388. doi:10.1021/ol050677x
44. Voigtritter, K.; Ghorai, S.; Lipshutz, B. H. *J. Org. Chem.* **2011,** *76,* 4697–4702. doi:10.1021/jo200360s
45. Chatterjee, A. K.; Choi, T.-L.; Sanders, D. P.; Grubbs, R. H. *J. Am. Chem. Soc.* **2003,** *125,* 11360–11370. doi:10.1021/ja0214882

License and Terms

BEILSTEIN JOURNAL OF ORGANIC CHEMISTRY

Consequences of the electronic tuning of latent ruthenium-based olefin metathesis catalysts on their reactivity

Karolina Żukowska*[1], Eva Pump[2], Aleksandra E. Pazio[3], Krzysztof Woźniak[3], Luigi Cavallo[4] and Christian Slugovc*[2]

Full Research Paper

Open Access

Address:
[1]Institute of Organic Chemistry, Polish Academy of Sciences, Kasprzaka 44/52, 01-224 Warszawa, Poland, [2]Institute of Chemistry and Technology of Materials, Graz University of Technology, NAWI Graz, Stremayrgasse 9, 8010 Graz, Austria, [3]Biological and Chemical Research Centre, Faculty of Chemistry, University of Warsaw, Żwirki i Wigury 101, 02-089; Warszawa, Poland and [4]Kaust Catalysis Center, Physical Sciences and Engineering Division, King Abdullah University of Science and Technology, Thuwal 23955-6900, Saudi Arabia

Email:
Karolina Żukowska* - karolina.zukowska@gmail.com;
Christian Slugovc* - slugovc@tugraz.at

* Corresponding author

Keywords:
DFT calculations; olefin metathesis; ring closing metathesis; ring-opening metathesis polymerisation; ruthenium

Beilstein J. Org. Chem. **2015,** *11,* 1458–1468.
doi:10.3762/bjoc.11.158

Received: 20 May 2015
Accepted: 07 August 2015
Published: 20 August 2015

This article is part of the Thematic Series "Progress in metathesis chemistry II".

Guest Editor: K. Grela

Abstract

Two ruthenium olefin metathesis initiators featuring electronically modified quinoline-based chelating carbene ligands are introduced. Their reactivity in RCM and ROMP reactions was tested and the results were compared to those obtained with the parent unsubstituted compound. The studied complexes are very stable at high temperatures up to 140 °C. The placement of an electron-withdrawing functionality translates into an enhanced activity in RCM. While electronically modified precatalysts, which exist predominantly in the *trans*-dichloro configuration, gave mostly the RCM and a minor amount of the cycloisomerization product, the unmodified congener, which preferentially exists as its *cis*-dichloro isomer, shows a switched reactivity. The position of the equilibrium between the *cis*- and the *trans*-dichloro species was found to be the crucial factor governing the reactivity of the complexes.

Introduction

Olefin metathesis is a catalytic process during which C–C double bonds are exchanged [1]. Since the first examples were published in the 1950s, many stunning accomplishments have been made in the field resulting in ever increasing interests in the method. Establishment of well-defined molybdenum- and ruthenium-based complexes lead to multitude of applications [2-4]. Especially, the latter class of compounds have gained attention due to their user-friendly character caused by a wide

functional group-tolerance and high oxygen and moisture stability. Although a great progress has been made, the unsuitability of ruthenium complexes for high temperature applications remains one of the greatest challenges in the field.

Modifications in the basic structure of ruthenium-based olefin metathesis catalysts led to a diversification of catalytic profiles (Figure 1) [5,6]. Perhaps the most important one was the introduction of bidentate benzylidene ligands instead of simple alkylidenes, thus giving rise to the class of Hoveyda-type complexes with the parent compound **2** [7]. Further modifications of such systems followed. One of the most common is tuning of the properties of the benzylidene ligand so that modified reactivity of the resulting complex is achieved [8]. Various examples of such approaches have been published over the years. Particularly interesting results were obtained by substituting the oxygen atom with sulfur or nitrogen leading to a group of structurally diverse ruthenium chelates [9-11].

N-Based chelating complexes offer the advantage of a great availability of precursors for amine ligands making the number of possible structures virtually unlimited. Complexes incorporating alkylidene ligands based on aromatic [12-15] or aliphatic amines [16,17] and Schiff base patterns [18-22] have been prepared so far, exhibiting diverse activities ranging from very fast to very slow initiation. Furthermore, in those compounds, a *trans–cis* isomerization of the chloride ligands was observed in many cases (Scheme 1) [16]. This phenomenon has been widely discussed in literature with multiple reports of superior activity of *trans*-configured complexes. The general hypothesis is that the *trans*-dichloro form of the complex promotes metathesis whereas the *cis*-dichloro form is postulated to be metathetically inactive [23,24]. Thus, the *trans–cis* isomerization can be exploited for slowly releasing the olefin metathesis active species [25,26].

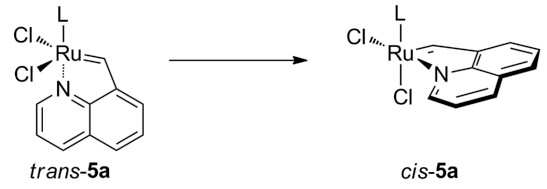

Scheme 1: *trans–cis* Isomerization.

Aside from the interesting conformational behavior, nitrogen-chelated complexes possess some practical properties, namely they tend to be thermally stable, enabling applications at elevated temperatures. Being aware of the various advantages of such systems, we set out to study substituted quinolone–ruthenium chelates in view of their *trans–cis* susceptibility and its consequences.

Results and Discussion

Synthesis and characterization

The shortest pathway to obtain the desired ligands was chosen to provide access to starting materials. It was envisioned as a two-step sequence of triflation of commercially available substituted 8-hydroxyquinolines **8** and **9** followed by a Suzuki coupling as shown in Scheme 2 [14].

The cyano-substituted compound **10** was obtained without difficulty, but esterification of compound **9** was problematic

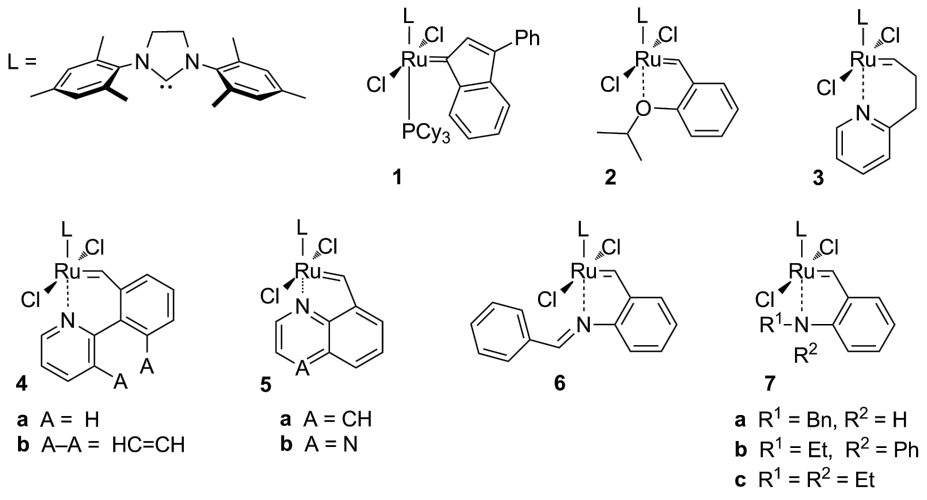

Figure 1: Selected ruthenium-based complexes.

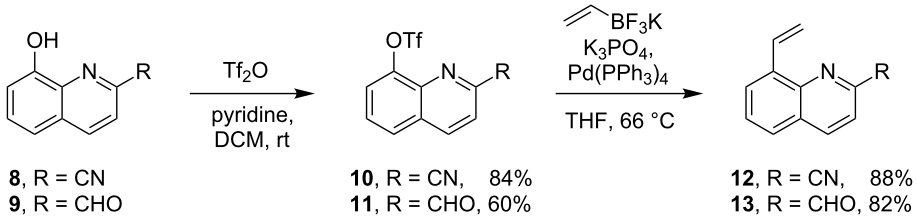

Scheme 2: Synthesis of the ligand precursors.

because of purification issues (cf. Supporting Information File 1) so an alternative pathway was established. Starting from 2-bromoaniline upon Doebner–Miller reaction and oxidation, we obtained the corresponding bromide derivative which was subsequently converted via Suzuki coupling into the carbene precursor **13**. Both compounds **12** and **13** were then used in a carbene exchange reaction with compound **1** conducted in toluene at 80 °C (see Scheme 3), releasing the desired complexes **14** and **15** as *trans*-dichloro isomers in good yields.

Based on the previously reported *trans–cis* isomerization of the parent quinoline-based complex **5a**, a potential isomerization of **14** and **15** was investigated. Reaction conditions for the isomerization of **5a** (complete isomerization after 6 days at 23 °C in CD_2Cl_2) [14] were proven to be ineffective for the isomerization of **14** and **15**, so that more forcing conditions were applied: Compounds **5a**, **14** or **15** were dissolved in $CDCl_3$ and heated to 140 °C for 1 h in a microwave reactor.

When the reactions were performed in air, only decomposition of the complexes was observed. Upon using oxygen-free conditions a complete rearrangement of *trans*-**5a** to *cis*-**5a** in 30 min was obtained. Attempts, to prepare the *cis*-isomers of electronically modified complexes **14** and **15** in a similar fashion, however, turned out to be difficult. Using methods, such as starting from a pyridine containing the ruthenium complex, which is known to increase the *cis*-content, or increasing the exposure time of the catalyst up to 8 h in microwave at 140 °C in $CDCl_3$ resulted in limited success.

The formyl-substituted complex **15** underwent isomerization, but only a mixture of 11% *cis*-**15** and 89% *trans*-**15** was obtained (cf. Supporting Information File 1). In the case of the CN-substituted compound **14**, on the other hand, no evidence for any isomerization could have been retrieved. These results suggest, that the introduction of the electron withdrawing substituent in 2-position changes the thermodynamic equilibrium favoring the *trans*- over the *cis*-isomers. In any case, a remarkable thermal stability of all studied compounds was found.

Intrigued by the observed phenomenon, we turned to structural studies. Structures of **14** and **15** have been determined using single-crystal X-ray diffraction. Each of them includes two molecules of the studied compound in the *trans*-conformation and one molecule of the solvent (dichloromethane) in the asymmetric part of the unit cell (Figure 2). Both crystals are isotypic, so the crystal packing is identical and lattice dimensions are very similar (Figure 3).

Bond lengths and angles of **5a**, **14** and **15** are very similar, so their different tendencies to form the corresponding *cis*-complexes could not be rationalized based on this dataset. The

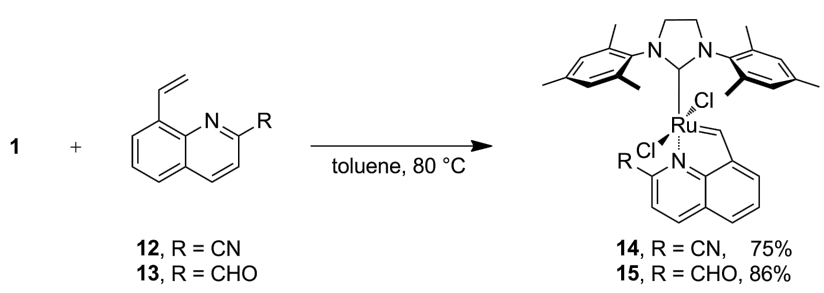

Scheme 3: Synthesis of the ruthenium complexes.

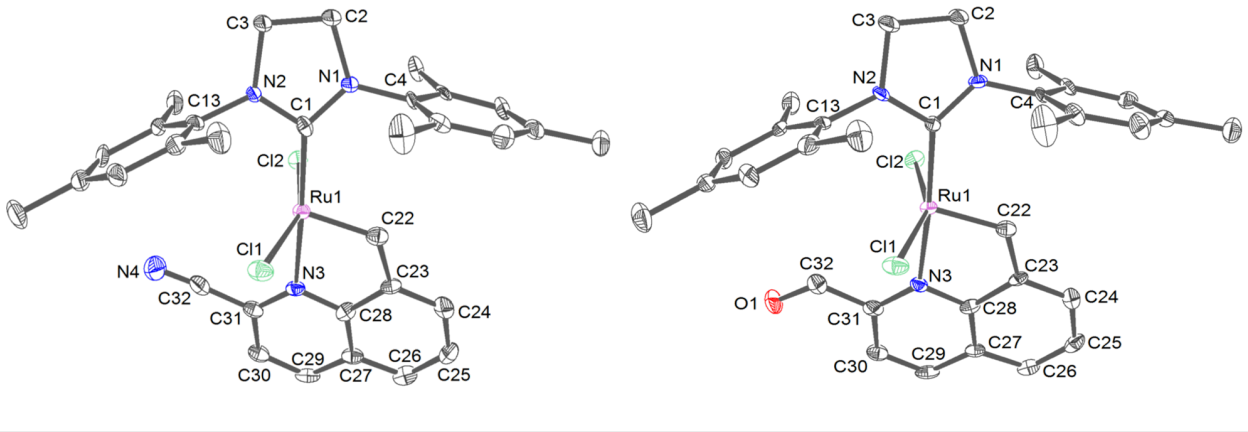

Figure 2: ADPs (atomic displacement parameters) and atoms labeling of the first molecule in the asymmetric part for **14** (left) and **15** (right). Thermal ellipsoids at 50% level of probability. Hydrogen atoms were omitted for clarity.

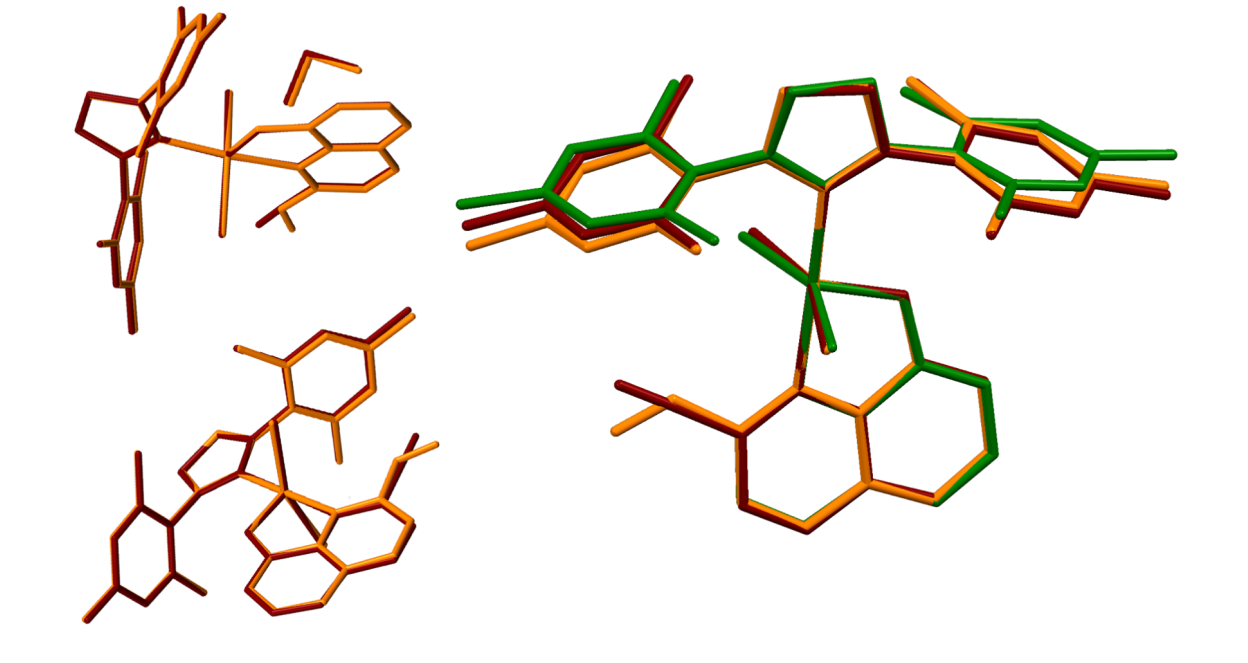

Figure 3: Superposition of the asymmetric parts of units' cells in both investigated structures: an example of isostructural packing (left). Superposition (right side) *trans* forms of all studied molecules **5a** (green), **14** (ruby) and **15** (orange).

only feature worth mentioning is a slightly decreased Ru(1)-C(22) bond length in compound **15** compared to **5a** or **14** (1.829, 1.845 and 1.842 Å, respectively).

DFT calculations

Density functional theory (DFT) calculations were performed with the aim to learn more about the compounds under investigation especially in view of their peculiar *trans–cis* isomerization behavior. Geometry optimizations were conducted by BP86//SVP, solvent effects were added by single point calculations using M06//TZVP functional (cf. Supporting Information File 1). The first question tackled concerned the anticipated coordination of the carbonyl group in compound **15** to form the corresponding 18-electron complex. Formation of the 18-electron compound is in principle feasible although it is endothermic by 2.6 kcal/mol. Thus, it can be concluded that preferably the corresponding 16-electron species is present in solution. Next, we investigated the relative stabilities of the *trans*-dichloro versus the *cis*-dichloro isomers. As already stated in literature, DFT calculations suggested a more preferential

arrangement of **5a** in the *cis*-dichloro configuration [23,24]. Here, the equilibrium was investigated assuming solvation in CH_2Cl_2 and results revealed a preference for the *cis*-dichloro isomer in the case of **5a** (*cis*-**5a** is 4.1 kcal/mol more stable than *trans*-**5a**) and **15** (*cis*-**15** is 2.4 kcal/mol more stable than *trans*-**15**). In contrast, the cyano-group substituted compound **14** exists preferably in the *trans* configuration of the chloride ligands (*trans*-**14** is 1.4 kcal/mol more stable than *cis*-**14**). Because the *cis* isomer is better stabilized in solvents with high dielectric constants (such as CH_2Cl_2) than in solvents with low dielectric constants [27], the *trans*–*cis* energies were calculated in toluene (as an example for a solvent with low dielectric constant). In this case, **5a** is still preferably in the *cis* configuration (*cis*-**5a** is 1.3 kcal/mol more stable than *trans*-**5a**), while in **14** and **15** the *trans* configuration is favored (by 0.7 kcal/mol in case of **15** and 4.2 kcal/mol in case of **14**). Further, the energy profile for the isomerization reaction was investigated taking a dissociative and a concerted pathway into consideration (cf. Figure 4).

As disclosed earlier [23,24], the concerted pathway is the most likely operative for the isomerization of **5a**. The transition state **TS2** (which is the transition state for the concerted pathway) is 5.3 kcal lower in energy than the transition state for closing the chelating ligand towards the *cis*-dichloro configured form (**TS1**$_{cis}$). The energetic preference of the concerted over the dissociative pathway is decreasing when substituents in 2 position of the quinoline ligand are present. For **14** and **15** the transition state for the generation of the catalytically active 14-electron species (**TS1**$_{trans}$) is considerably lower compared to **5a**. These results go in hand with studies on electronically modified Hoveyda-type catalysts [28,29] and electronically modified ester-chelating benzylidene complexes [30]. Moreover, as already discussed, **TS2** becomes energetically more demanding so that for **14** and **15** the pathways for the isomerization (leading to the olefin metathesis inactive *cis*-dichloro form) becomes less important. Consequently, complex **15** and in particular **14** should be metathetically more active than their unsubsituted version **5a**.

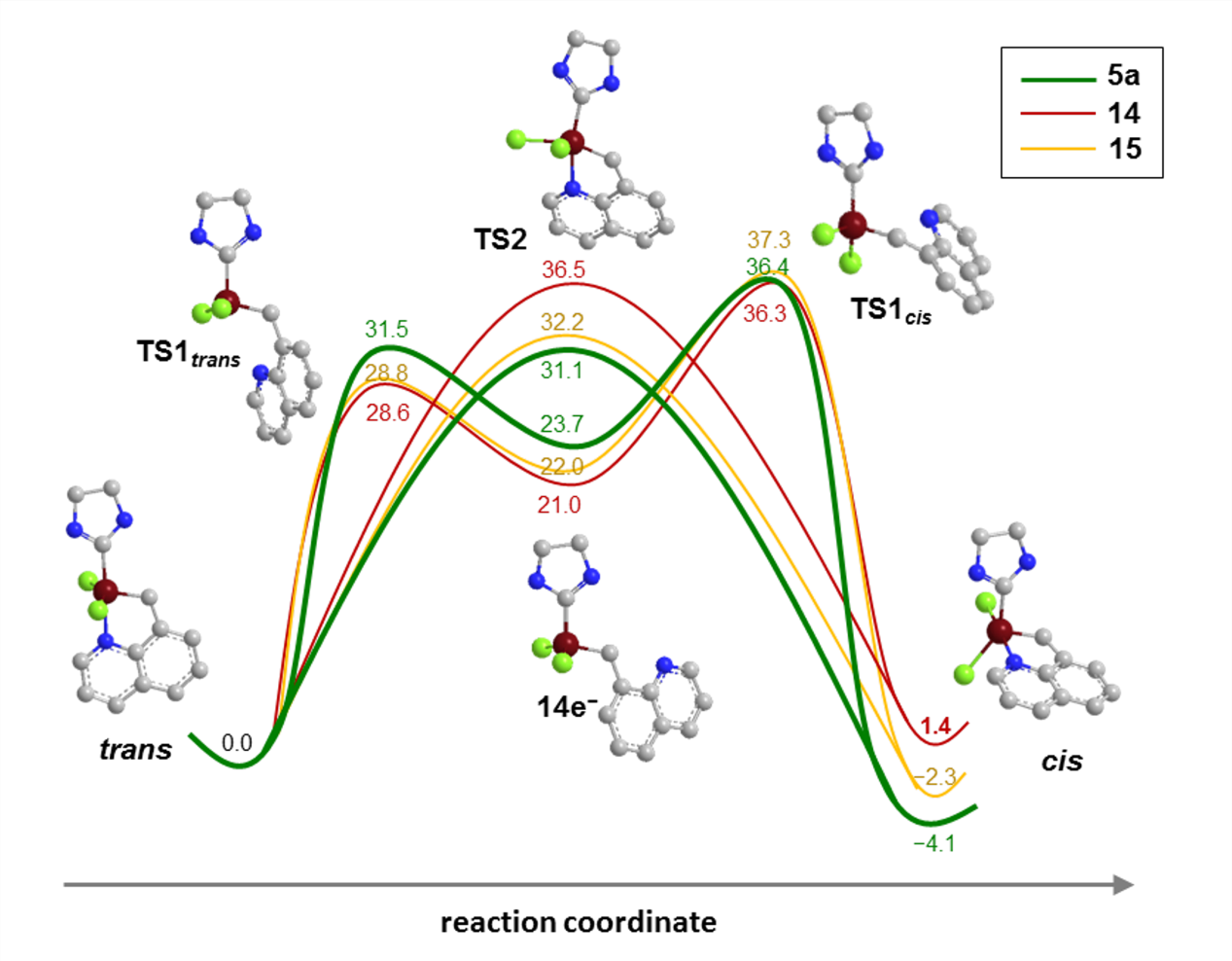

Figure 4: Energy profile of *trans*–*cis* isomerization, modelled in CH_2Cl_2, (ΔE in kcal/mol). Geometry optimizations BP86//SVP, solvent effects included by single point calculations, using M06//TZVP.

Activity in RCM

The consecutive step of the research was devoted to exploring the activity of the obtained complexes in metathesis reactions. The preliminary choice was to conduct ring-closing metathesis (RCM) of diethyl diallylmalonate (**16**, Scheme 4).

Initially examined conditions (DCM, rt) originate from the papers previously published by Grela's group on the subject [14,31]. Unfortunately, along with F. Hoffmann-La Roche AG researchers [32] we were unable to fully reproduce the aforementioned results. The complex was inert at ambient conditions and only tests at elevated temperatures (80 or 140 °C) revealed catalytic activity of **5a**. When substrate **16** was subjected to RCM in high temperature conditions, a complex mixture of products was obtained (Figure 5). Upon GC and GC–MS analysis, structures of compounds **17**–**19** were determined (cf. Supporting Information File 1).

The substituted complexes were inert in ambient conditions similarly to the parent complex. The experiments at elevated temperature (toluene, 80 °C) revealed that precatalysts **14** and **15** led to higher conversions than the unsubstituted version **5a**. What is more interesting, both complexes exhibit prolonged activity and similar overall activity under the studied conditions. An interesting observation is that reactions catalyzed with **14** and **15** gave predominantly the RCM product (compound **17**) accompanied by a minor amount of a cycloisomerization-derived compound **19**. It is worth noting, that even after heating at 80 °C for 100 h the catalysts were still active, as can be assessed from the time/conversion plots (cf. Figure 5a and b). In contrast, the precatalyst **5a** promoted predominantly cycloisomerization albeit conversion was poor (cf. Figure 5c). Because all transformations were very slow at 80 °C the next series of test reactions was conducted at 140 °C in xylenes as the solvent (cf. Figure 5d–f). Electronically modified derivatives **14** and **15** promoted a faster transformation of **16**. In the first 10 min. about 90% of **16** was converted into about 80% cycloisomerization product **19** and about 12–16% RCM-product **17**, thus the selectivity changed upon raising the temperature. In addition, a minor amount of the isomerized RCM-product **18** and isomerized diethyl diallylmalonate **20** were detected in the reaction mixture. After about 1 h reaction time, the composition of the reaction mixture remained virtually unchanged upon prolonged heating.

At this high temperature, the precatalyst *trans*-**5a** resulted in a complete conversion of **16** which gave more than 90% cycloisomerization product **19** in 8 h. A small amount of isomerized diethyl diallylmalonate **20** and RCM-product **17** were also observed (cf. Figure 5f). Using *cis*-**5a** as the precatalyst resulted in similar results as can be seen in Figure 6. This is not especially peculiar as isomerization is conducted in the very same temperature range within less than 30 minutes meaning that the corresponding equilibrium is reached quickly.

Basing on the described experiments, it can be stated that precatalysts are thermally stable in the absence of oxygen and diethyl diallylmalonate at temperatures as high as 140 °C. Electronically modified precatalysts **14** and **15** initiate significantly faster than the parent precatalyst **5a** and when employed in RCM of diethyl diallylmalonate at 80 °C, those complexes gave predominantly the RCM product **17** accompanied with minor amounts of the cycloisomerization product **19**, while **5a** released predominantly the cycloisomerization product **19**.

Switching to 140 °C reaction temperature, all precatalysts released the cycloisomerization product **19** as the main product. These observations make again clear that the thermal stability of the precatalyst becomes irrelevant once it is in the presence of the substrate [33], because it is the thermal stability of the actual active species in the reaction mixture that governs the reaction outcome. In the present case, the methylidene complex formed during metathesis with the terminal olefin diethyl diallylmalonate is probably the most fragile species [32,34-36]. A

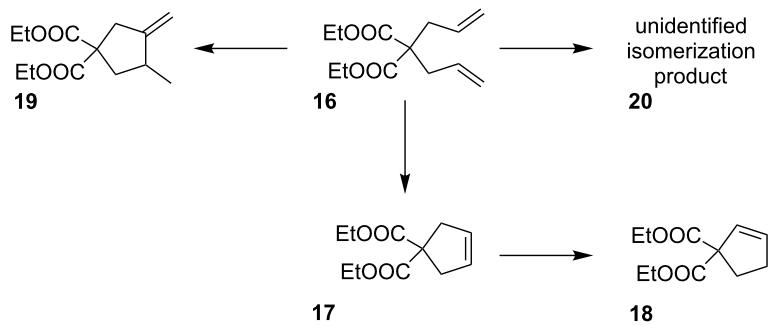

Scheme 4: Possible reaction pathways of **16**.

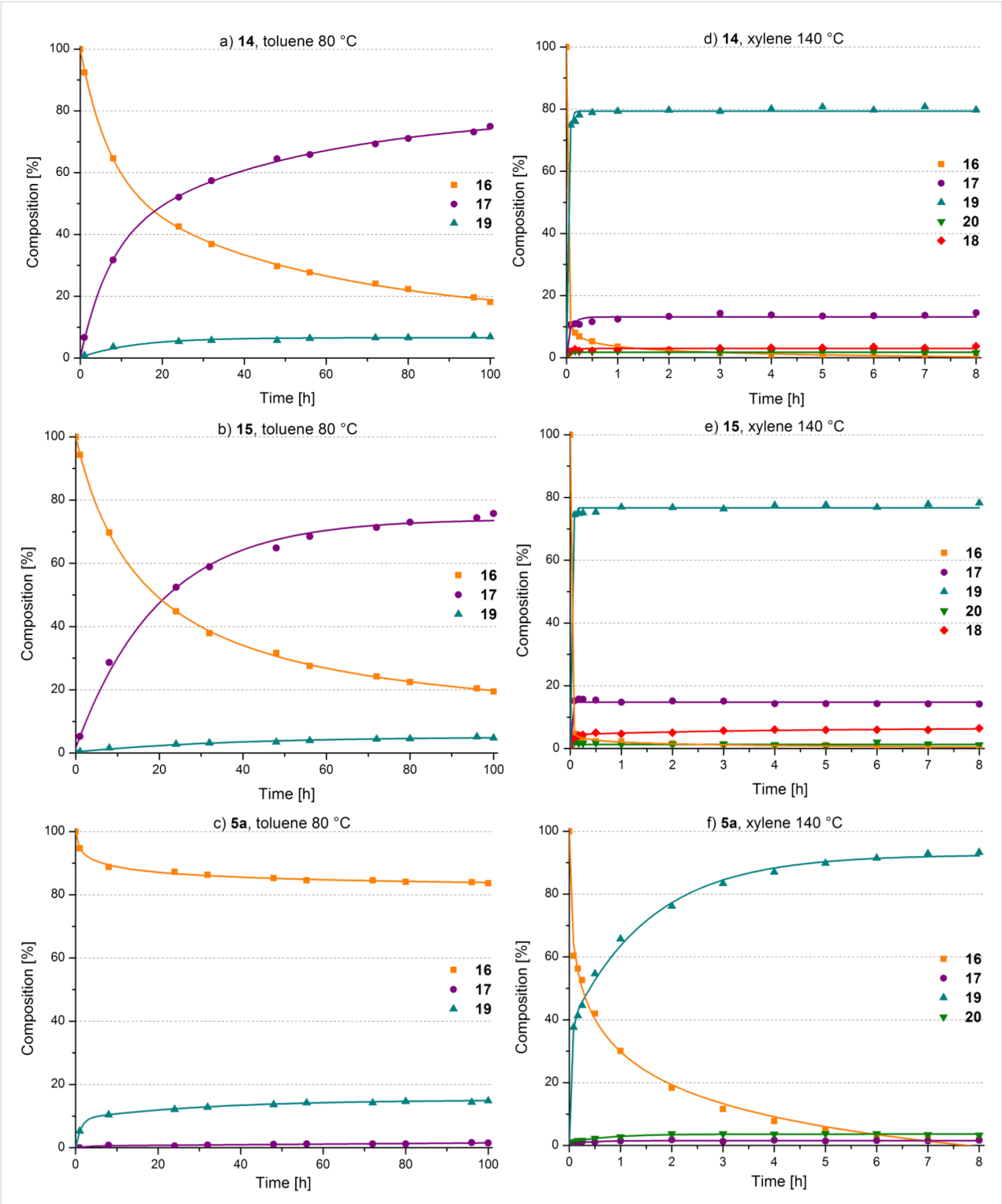

Figure 5: Time/conversion plots for the transformation of **16** catalyzed by 5 mol % of the *trans* isomers of *trans*-**5a**, **14** and **15**. Lines are intended as visual aids.

recent work provides evidence that the catalytic species responsible for (cyclo)isomerization originates from decomposition of the methylidene [37]. Generally, the ability of olefin metathesis precatalysts to promote cycloisomerization [38] is known and has been widely researched both theoretically [39,40] and experimentally [41-43]. Moreover, the methylidene species

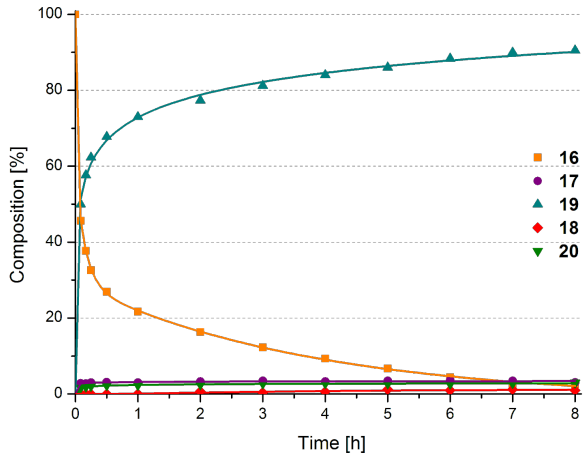

Figure 6: Composition of a reaction mixture after subjecting **16** to 5 mol % *cis*-**5a** in xylene, 140 °C. Lines are intended as visual aids.

alone are characterized by a certain degree of stability that is dramatically reduced in the presence of olefins, in particular, ethylene [38]. Accordingly, RCM reactions can be improved in terms of efficiency when ethylene is removed [44-46]. Based on these facts, the catalytic performance of the precatalysts **14** and **15** can be explained as follows: At 80 °C the actual active species is slowly released and performs mainly metathesis with diethyl diallylmalonate (**16**) leading, amongst other species, to the methylidene complex [47]. The latter is moderately stable under these conditions and participates in the catalytic RCM cycle. A concurring decomposition reaction of the methylidene or another Ru-species is responsible for the cycloisomerization side reaction. Further, the latter species is not able to isomerize the educt or the RCM product. Upon increasing the temperature to 140 °C, the said decomposition reaction is faster leading to the observed switch of reactivity in favor of the cycloisomerization pathway and isomerization of the educt as well as that of the product is observed. However, the results for **5a** as the precatalyst make clear that the thermal stability of the methylidene is not the only factor governing the outcome of the studied reactions. If the stability of the methylidene were the only crucial factor in all cases, the product distributions from reactions with **5a** would be similar to those from **14** and **15**. This is definitely not the case. Therefore, it can be assumed that in case of **5a** another, yet unknown decomposition reaction is responsible for the occurrence of the cycloisomerization reaction.

Use as initiators in ROMP

In the next step, compounds **5a**, **14** and **15** were tested as initiators in ring-opening metathesis polymerization (ROMP). The active species in ROMP (i.e., the propagating species) can be considered more stable than the methylidene intermediate in RCM, particularly when norbornenes such as *endo*,*exo*-bicyclo[2.2.1]hept-5-ene-2,3-dicarboxylic acid dimethyl ester (**21**) are polymerized (Figure 7) [48].

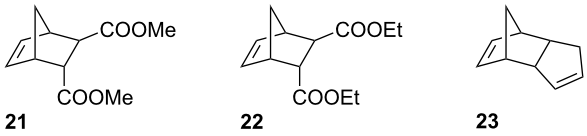

Figure 7: Monomers utilized in model ROMP reactions.

First, 300 equivalents of monomer **21** were polymerized with 1 equivalent initiator (**5a**, **14** or **15**) at 110 °C in toluene ([**21**] = 0.1 M) for 2 days. Initiator **5a** polymerized 90% of **21** and the corresponding polymer was characterized by a number average molecular weight (M_n) of 557.0 kg·mol^{-1} (polydispersity index, PDI = 1.9) as examined by size exclusion chromatography (SEC) in THF against poly(styrene) standards. Initiator **15** gave 93% monomer-conversion and the resulting polymer exhibited a M_n of 516.0 kg·mol^{-1} (PDI = 2.2) and **14** gave the highest conversion (98%) and the shortest polymer strands (M_n = 326.7 kg·mol^{-1}; PDI = 2.2).

The M_n values allow for an indirect relative assessment of the initiation efficacy [49-54], because they are proportional to the ratio of the propagation rate (k_p) and the initiation rate constant (k_i), provided that no secondary metathesis occurs. In this case, M_n is only dependent on k_i, because in all cases the same propagating species occurs and k_p is the same. Accordingly, initiator **14** exhibits the highest initiation efficacy and initiator **5a** the lowest. Analyzing these data as disclosed previously, a linear correlation between the M_n values and the difference between the calculated thermodynamic stabilities of the *trans*- and the *cis*-dichloro configured isomers ($\Delta E_{trans-cis}$) can be established (Figure 8). This correlation suggests that the initiation efficacy is above all determined by the position of the *trans*–*cis* equilibrium which can be quickly reached at 110 °C [29,55].

In the second step, the initiators were tested in neat monomer using simultaneous thermal analysis (STA) for monitoring the polymerizations. As the monomer, either *endo*,*exo*-bicyclo[2.2.1]hept-5-ene-2,3-dicarboxylic acid diethyl ester (**22**) or dicylcopentadiene (**23**) were used (cf. Figure 7). A distinctly changed initiation trend was observed under these reaction conditions. Initiator **5a** started the polymerization at the lowest temperature (onset of the polymerization exotherm at approx. 60 °C; cf. Figure 9, left) while the highest latency was found for initiator **14** (onset at approx. 75 °C). While initiators **14** and **15** exhibited rather sharp exotherms for the polymerization of monomer **22**, a much broader shape was found in the case of **5a**. This shape can be explained by assuming, that the

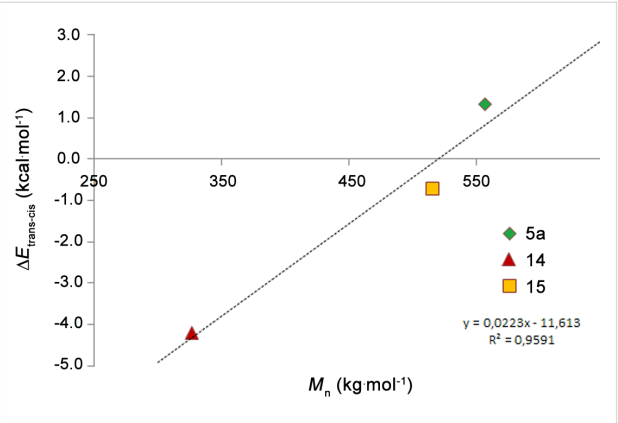

Figure 8: Number-average molecular weight (M_n) of poly-**21** prepared with initiators **5a**, **14** and **15** plotted against the theoretically determined difference of *trans–cis* energies (solvation model PCM, solvent toluene).

isomerization of *trans*-**5a** to *cis*-**5a** is a concurring reaction, thus slowing down the polymerization reaction. The reason for the unexpectedly, at first sight, delayed initiation of **14** and **15** can most probably be attributed to steric effects. It is known that a coordination at the free coordination site (*trans* to the carbene ligand) can activate the (pre-)catalyst by lowering the energy barrier $\mathbf{TS1}_{trans}$ to reach the active 14-electron species [14,56,57]. As both substituents, the CHO and the CN group, sterically shield the vacant coordination site, it is easily conceivable that such substrate-induced activation is impeded.

This effect turned out to be of particular relevance when the polymerization of dicyclopentadiene is regarded. Because polymerizations were carried out in open reaction vessels, the retro-Diels–Alder reaction of **23**, releasing volatile cyclopentadiene, is a concurring reaction and responsible for the low(er) polymer yields and pronounced endothermic signals in the DSC traces (cf. Figure 9 right) [58]. While initiator **5a** shows an appealing performance in polymerizing **23**, the electronically modified congeners **14** and **15** are not particularly interesting for this application.

Conclusion

The present work introduced two ruthenium-based olefin metathesis catalysts/initiators featuring electronically modified quinoline-based chelating carbene ligands. Their reactivity in RCM and ROMP reactions was tested and results were set in comparison to those obtained with the parent compound, bearing the unsubstituted quinoline-based chelating carbene. The entire set of compounds is very stable at high temperatures up to 140 °C in the absence of oxygen and metathesis substrates. Electronic modification of the quinoline moiety changes the position of the *trans–cis* equilibrium as shown experimentally and theoretically. At the same time, electronic modification lowers the transition state energy for the generation of the catalytically active 14-electron species and increases the energy barrier for the transformation into the corresponding *cis*-dichloro isomers. Both effects translate into an enhanced activity in RCM at 80 °C when compared to the unmodified catalyst. In particular, the position of the *trans–cis* equilibrium is the most crucial factor governing the reactivity of the complexes. While electronically modified precatalysts which exist predominantly in *trans*-dichloro configuration gave mostly RCM and minor amounts of cycloisomerization product, the unmodified congener which preferentially exists in its *cis*-dichloro isomer, shows a switched reactivity. The reactivity switch is most probably caused by different substrate-induced decomposition reactions being responsible for the occurrence of the cycloisomerization reaction, which are more important at higher temperatures of 140 °C. In ROMP, again the position of the *trans–cis* equilibrium is the most crucial factor governing the initiation efficacy. Additionally, it has been shown, that steric effects of the substitution are responsible for an altered

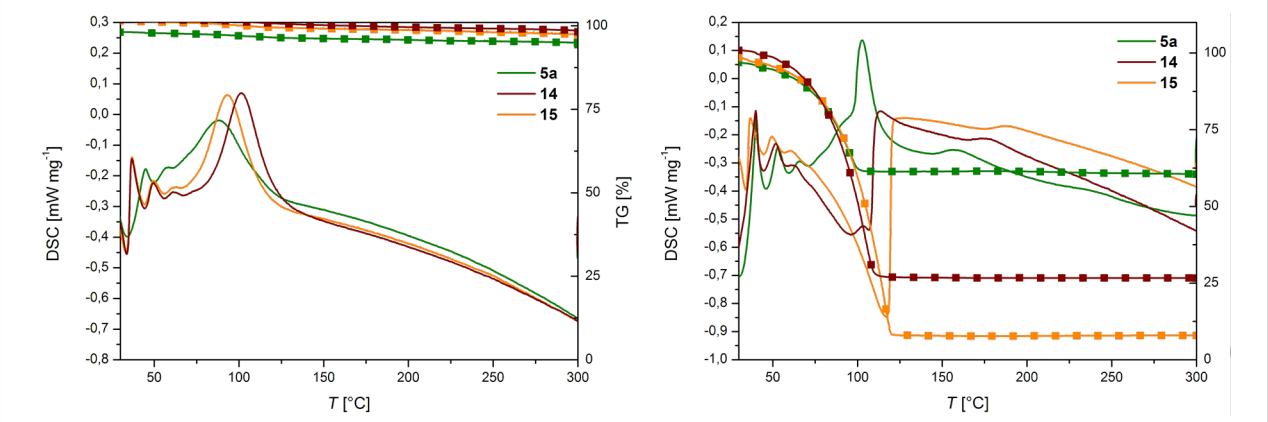

Figure 9: STA analysis of polymerization of **22** (left) and **23** (right), initiated by **5a**, **14** and **15**. Reaction conditions: [**22**]:[initiator] = 500 and [**23**]:[initiator] = 10000:1. Heating rate: 3 K/min. Big symbols: thermogravimetric analysis (TGA); no symbols: differential scanning calorimetry (DSC).

order of initiation behavior when polymerizations are conducted in bulk.

Experimental

Preparation of 14 and 15. Precursor complex **1** (0.5 mmol, 475 mg) and the respective styrene derivative (0.55 mmol) were put in a Schlenk tube under argon. Reagents were dissolved in anhydrous toluene (25 mL) and the reaction was heated at 80 °C for about an hour. Then the solvent was evaporated and the mixture was purified by flash chromatography using eluents *c*-hexane/ethyl acetate 10:1 to 1:1 v/v. The solvent was evaporated. The product was then re-dissolved in dichloromethane and cold *n*-heptane was added to yield the product **14** as dark brown crystals (0.37 mmol, 242 mg, 75%). ^{1}H NMR (CD_2Cl_2) δ 2.41 (s, 6H), 2.49 (s, 12H), 4.16 (s, 4H), 7.07 (s, 4H), 7.48–7.53 (m, 2H), 7.72 (dd, J = 0.9, 7.2 Hz, 1H), 8.24 (dd, J = 0.9, 8.3 Hz, 1H), 8.33 (d, J = 8.5 Hz, 1H), 16.95 (s, 1H) ppm; ^{13}C NMR (CD_2Cl_2) δ 19.0, 20.9, 51.8, 116.1, 117.5, 122.6, 128.1, 129.4, 129.7, 133.9, 134.0, 134.6, 136.2, 138.3, 138.9, 146.8, 155.6, 209.4, 285.5 ppm; IR (KBr) ν: 3320, 3042, 3004, 2949, 2912, 2855, 2837, 2810, 2237, 1959, 1704, 1682, 1601, 1586, 1556, 1478, 1454, 1445, 1427, 1418, 1398, 1378, 1326, 1315, 1289, 1256, 1217, 1199, 1176, 1148, 1133, 1102, 1061, 1036, 1014, 985, 966, 930, 911, 879, 848, 822, 813, 792, 777, 752, 734, 721, 701, 653, 643, 622, 580, 533, 498, 428, 415 cm^{-1}; HRMS (ESI) (*m*/*z*): [M] calcd, 644.1048; found, 644.1041.

Complex **15** was prepared analogously yielding dark brown crystals (0.43 mmol, 280 mg, 86%). ^{1}H NMR (CD_2Cl_2) δ 2.43–2.55 (m, 16H), 4.19 (s, 4H), 7.11 (s, 4H), 7.48–7.55 (m, 1H), 7.72 (dd, J = 0.9, 7.2 Hz, 1H), 7.78 (d, J = 8.5 Hz, 1H), 8.28 (dd, J = 0.9, 8.2 Hz, 1H), 8.35 (d, J = 8.3 Hz, 1H), 8.96 (d, J = 0.6, Hz, 1H), 17.11 (s, 1H) ppm; ^{13}C NMR (CD_2Cl_2) δ 19.1, 20.9, 51.6, 117.0, 122.8, 129.2, 130.8, 133.4, 134.3, 136.0, 138.9, 139.0, 145.9, 152.2, 156.3, 190.0, 210.6, 288.2 ppm; IR (KBr) ν: 3003, 2952, 2912, 2854, 2734, 2232, 1950, 1734, 1694, 1605, 1584, 1551, 1480, 1419, 1401, 1379, 1319, 1294, 1261, 1222, 1174, 1154, 1138, 1092, 1036, 987, 929, 910, 887, 846, 813, 794, 775, 732, 699, 680, 644, 591, 578, 535, 419 cm^{-1}; HRMS (ESI) (*m*/*z*): [M − 2Cl + H]$^+$ calcd, 578.1745; found, 578.1732.

Supporting Information

Supporting Information File 1

Full experimental section along with all the synthetic procedures and analytical data of the obtained compounds.
[http://www.beilstein-journals.org/bjoc/content/supplementary/1860-5397-11-158-S1.pdf]

Acknowledgements

KŻ thanks for the „Diamond Grant" research project financed from the governmental funds for science for 2012–2015. Dr. M. Kędziorek is acknowledged for providing the precursor of **5a**. EP gratefully acknowledges to "Chemical Monthly" for financial support of this work. Authors acknowledge for the WTZ PL10/2014 cooperation.

References

1. Grela, K., Ed. *Olefin Metathesis: Theory and Practice;* John Wiley & Sons, Inc.: Hoboken, 2014.
2. Bieniek, M.; Michrowska, A.; Usanov, D. L.; Grela, K. *Chem. – Eur. J.* **2008,** *14,* 806–818. doi:10.1002/chem.200701340
3. Schrock, R. R.; Hoveyda, A. H. *Angew. Chem., Int. Ed.* **2003,** *42,* 4592–4633. doi:10.1002/anie.200300576
4. Leitgeb, A.; Wappel, J.; Slugovc, C. *Polymer* **2010,** *51,* 2927–2946. doi:10.1016/j.polymer.2010.05.002
5. Vougioukalakis, G. C.; Grubbs, R. H. *Chem. Rev.* **2010,** *110,* 1746–1787. doi:10.1021/cr9002424
6. Samojłowicz, C.; Bieniek, M.; Grela, K. *Chem. Rev.* **2009,** *109,* 3708–3742. doi:10.1021/cr800524f
7. Garber, B.; Kingsbury, J. S.; Gray, B. L.; Hoveyda, A. H. *J. Am. Chem. Soc.* **2000,** *122,* 8168–8179. doi:10.1021/ja001179g
8. Vidavsky, Y.; Anaby, A.; Lemcoff, N. G. *Dalton Trans.* **2012,** *41,* 32–43. doi:10.1039/C1DT11404B
9. Ben-Asuly, A.; Tzur, E.; Diesendruck, C. E.; Sigalov, M.; Goldberg, I.; Lemcoff, N. G. *Organometallics* **2008,** *27,* 811–813. doi:10.1021/om701180z
10. Szadkowska, A.; Makal, A.; Woźniak, K.; Kadyrov, R.; Grela, K. *Organometallics* **2009,** *28,* 2693–2700. doi:10.1021/om801183g
11. Szadkowska, A.; Żukowska, K.; Pazio, A. E.; Woźniak, K.; Kadyrov, R.; Grela, K. *Organometallics* **2011,** *30,* 1130–1138. doi:10.1021/om101129b
12. van der Schaaf, P. A.; Kolly, R.; Kirner, H.-J.; Rime, F.; Mühlebach, A.; Hafner, A. *J. Organomet. Chem.* **2000,** *606,* 65–74. doi:10.1016/S0022-328X(00)00289-8
13. Szadkowska, A.; Gstrein, X.; Burtscher, D.; Jarzembska, K.; Woźniak, K.; Slugovc, C.; Grela, K. *Organometallics* **2010,** *29,* 117–124. doi:10.1021/om900857w
14. Barbasiewicz, M.; Szadkowska, A.; Bujok, R.; Grela, K. *Organometallics* **2006,** *25,* 3599–3604. doi:10.1021/om060091u
15. Peeck, L. H.; Savka, R. D.; Plenio, H. *Chem. – Eur. J.* **2012,** *18,* 12845–12853. doi:10.1002/chem.201201010
16. Diesendruck, C. E.; Tzur, E.; Ben-Asuly, A.; Goldberg, I.; Straub, B. F.; Lemcoff, N. G. *Inorg. Chem.* **2009,** *48,* 10819–10825. doi:10.1021/ic901444c
17. Żukowska, K.; Szadkowska, A.; Pazio, A. E.; Woźniak, K.; Grela, K. *Organometallics* **2012,** *31,* 462–469. doi:10.1021/om2011062
18. Hejl, A.; Day, M. W.; Grubbs, R. H. *Organometallics* **2006,** *25,* 6149–6154. doi:10.1021/om060620u
19. Slugovc, C.; Burtscher, D.; Stelzer, F.; Mereiter, K. *Organometallics* **2005,** *24,* 2255–2258. doi:10.1021/om050141f
20. De Clercq, B.; Verpoort, F. *Adv. Synth. Catal.* **2002,** *344,* 639–648.
21. Jordaan, M.; Vosloo, H. C. M. *Adv. Synth. Catal.* **2007,** *349,* 184–192. doi:10.1002/adsc.200600474
22. Slugovc, C.; Perner, B.; Stelzer, F.; Mereiter, K. *Organometallics* **2004,** *23,* 3622–3626. doi:10.1021/om049877n

23. Poater, A.; Ragone, F.; Correa, A.; Szadkowska, A.; Barbasiewicz, M.; Grela, K.; Cavallo, L. *Chem. – Eur. J.* **2010,** *16,* 14354–14364. doi:10.1002/chem.201001849
24. Pump, E.; Cavallo, L.; Slugovc, C. *Monatsh. Chem.* **2015,** *146,* 1131–1141. doi:10.1007/s00706-015-1433-8
25. Ung, T.; Hejl, A.; Grubbs, R. H.; Schrodi, Y. *Organometallics* **2004,** *23,* 5399–5401. doi:10.1021/om0493210
26. Guidone, S.; Songis, O.; Nahra, F.; Cazin, C. S. J. *ACS Catal.* **2015,** *5,* 2697–2701. doi:10.1021/acscatal.5b00197
27. Aharoni, A.; Vidavsky, Y.; Diesendruck, C. E.; Ben-Asuly, A.; Goldberg, I.; Lemcoff, N. G. *Organometallics* **2011,** *30,* 1607–1615. doi:10.1021/om1011402
28. Zaja, M.; Connon, S. J.; Dunne, A. M.; Rivard, M.; Buschmann, N.; Jiricek, J.; Blechert, S. *Tetrahedron* **2003,** *59,* 6545–6558. doi:10.1016/S0040-4020(03)01029-9
29. Michrowska, A.; Bujok, R.; Harutyunyan, S.; Sashuk, V.; Dolgonos, G.; Grela, K. *J. Am. Chem. Soc.* **2004,** *126,* 9318–9325. doi:10.1021/ja048794v
30. Pump, E.; Poater, A.; Zirngast, M.; Torvisco, A.; Fischer, R.; Cavallo, L.; Slugovc, C. *Organometallics* **2014,** *33,* 2806–2813. doi:10.1021/om500315t
31. Grela, K.; Barbasiewicz, M.; Szadkowska, A. Complexes of Ruthenium and osmium, method of production thereof and use thereof as (pre)catalysts of the metathesis reaction. WO Patent WO140954, Dec 13, 2007.
32. Puentener, K.; Scalone, M. New ruthenium complexes as catalysts for metathesis reactions. WO Patent WO2008000644, Jan 3, 2008.
33. Nelson, D. J.; Manzini, S.; Urbina-Blanco, C. A.; Nolan, S. P. *Chem. Commun.* **2014,** *50,* 10355–10375. doi:10.1039/C4CC02515F
34. Lummiss, J. A. M.; Beach, N. J.; Smith, J. C.; Fogg, D. E. *Catal. Sci. Technol.* **2012,** *2,* 1630–1632. doi:10.1039/C2CY20213A
35. Sanford, M. S.; Love, J. A.; Grubbs, R. H. *J. Am. Chem. Soc.* **2001,** *123,* 6543–6554. doi:10.1021/ja010624k
36. Hong, S. H.; Wenzel, A. G.; Salguero, T. T.; Day, M. W.; Grubbs, R. H. *J. Am. Chem. Soc.* **2007,** *129,* 7961–7968. doi:10.1021/ja0713577
37. Nelson, D. J.; Percy, J. M. *Dalton Trans.* **2014,** *43,* 4674–4679. doi:10.1039/C4DT00007B
38. Lloyd-Jones, G. C. *Org. Biomol. Chem.* **2003,** *1,* 215–236. doi:10.1039/B209175P
39. van Rensburg, W. J.; Steynberg, P. J.; Meyer, W. H.; Kirk, M. M.; Forman, G. S. *J. Am. Chem. Soc.* **2004,** *126,* 14332–14333. doi:10.1021/ja0453174
40. van Rensburg, W. J.; Steynberg, P. J.; Kirk, M. M.; Meyer, W. H.; Forman, G. S. *J. Organomet. Chem.* **2006,** *691,* 5312–5325. doi:10.1016/j.jorganchem.2006.08.075
41. Bourgeois, D.; Pancrazi, A.; Nolan, S. P.; Prunet, J. *J. Organomet. Chem.* **2002,** *643–644,* 247–252. doi:10.1016/S0022-328X(01)01269-4
42. Lehman, S. E., Jr.; Schwendeman, J. E.; O'Donnel, P. M.; Wagener, K. B. *Inorg. Chim. Acta* **2003,** *345,* 190–198. doi:10.1016/S0020-1693(02)01307-5
43. Feng, C.; Wang, X.; Wang, B.-Q.; Zhao, K.-Q.; Hu, P.; Shi, Z.-J. *Chem. Commun.* **2012,** *48,* 356–358. doi:10.1039/C1CC15835J
44. Lysenko, Z.; Maughon, B. R.; Mokhtar-Zadeh, T.; Tulchinsky, M. L. *J. Organomet. Chem.* **2006,** *691,* 5197–5203. doi:10.1016/j.jorganchem.2006.08.031
45. Monfette, S.; Eyholzer, M.; Roberge, D. M.; Fogg, D. E. *Chem. – Eur. J.* **2010,** *16,* 11720–11725. doi:10.1002/chem.201001210
46. Skowerski, K.; Czarnocki, S. J.; Knapkiewicz, P. *ChemSusChem* **2014,** *7,* 536–542. doi:10.1002/cssc.201300829
47. Stewart, I. C.; Keitz, B. K.; Kuhn, K. M.; Thomas, R. M.; Grubbs, R. H. *J. Am. Chem. Soc.* **2010,** *132,* 8534–8535. doi:10.1021/ja1029045
48. Slugovc, C.; Demel, S.; Riegler, S.; Hobisch, J.; Stelzer, F. *Macromol. Rapid Commun.* **2004,** *25,* 475–480. doi:10.1002/marc.200300196
49. Kozłowska, A.; Dranka, M.; Zachara, J.; Pump, E.; Slugovc, C.; Skowerski, K.; Grela, K. *Chem. – Eur. J.* **2014,** *20,* 14120–14125. doi:10.1002/chem.201403580
50. Urbina-Blanco, C. A.; Bantreil, X.; Wappel, J.; Schmid, T. E.; Slawin, A. M. Z.; Slugovc, C.; Cazin, C. S. J. *Organometallics* **2013,** *32,* 6240–6247. doi:10.1021/om4004362
51. Pump, E.; Fischer, R. C.; Slugovc, C. *Organometallics* **2012,** *31,* 6972–6979. doi:10.1021/om300785t
52. Urbina-Blanco, C. A.; Leitgeb, A.; Slugovc, C.; Bantreil, X.; Clavier, H.; Slawin, A. M. Z.; Nolan, S. P. *Chem. – Eur. J.* **2011,** *17,* 5045–5053. doi:10.1002/chem.201003082
53. Broggi, J.; Urbina-Blanco, C. A.; Clavier, H.; Leitgeb, A.; Slugovc, C.; Slawin, A. M. Z.; Nolan, S. P. *Chem. – Eur. J.* **2010,** *16,* 9215–9225. doi:10.1002/chem.201000659
54. Strasser, S.; Pump, E.; Fischer, R. C.; Slugovc, C. *Monatsh. Chem.* **2015,** *146,* 1143–1151. doi:10.1007/s00706-015-1484-x
55. Diesendruck, C. E.; Vidavsky, V.; Ben-Asuly, A.; Lemcoff, N. G. *J. Polym. Sci., Part A: Polym. Chem.* **2009,** *47,* 4209–4213. doi:10.1002/pola.23476
56. Żukowska, K.; Szadkowska, A.; Trzaskowski, B.; Pazio, A.; Pączek, Ł.; Woźniak, K.; Grela, K. *Organometallics* **2013,** *32,* 2192–2198. doi:10.1021/om400064c
57. Trzaskowski, B.; Grela, K. *Organometallics* **2013,** *32,* 3625–3630. doi:10.1021/om400233s
58. Leitgeb, A.; Wappel, J.; Urbina-Blanco, C. A.; Strasser, S.; Wappl, C.; Cazin, C. S. J.; Slugovc, C. *Monatsh. Chem.* **2014,** *145,* 1513–1517. doi:10.1007/s00706-014-1249-y

License and Terms

BEILSTEIN JOURNAL OF ORGANIC CHEMISTRY

Thermal properties of ruthenium alkylidene-polymerized dicyclopentadiene

Yuval Vidavsky[1], Yotam Navon[2], Yakov Ginzburg[1], Moshe Gottlieb[2] and N. Gabriel Lemcoff[*1]

Full Research Paper

Open Access

Address:
[1]Department of Chemistry, Ben-Gurion University of the Negev Beer Sheva-84105, Israel and [2]Department of Chemical Engineering, Ben-Gurion University of the Negev Beer Sheva-84105, Israel

Email:
N. Gabriel Lemcoff[*] - lemcoff@bgu.ac.il

* Corresponding author

Keywords:
glass-transition temperature; polydicyclopentadiene; ring opening metathesis polymerization; ruthenium-catalyzed olefin metathesis; thermoset polymers

Beilstein J. Org. Chem. **2015,** *11,* 1469–1474.
doi:10.3762/bjoc.11.159

Received: 22 March 2015
Accepted: 04 August 2015
Published: 21 August 2015

This article is part of the Thematic Series "Progress in metathesis chemistry II".

Guest Editor: K. Grela

Abstract

Differential scanning calorimetry (DSC) analysis of ring opening methatesis polymerization (ROMP) derived polydicyclopentadiene (PDCPD) revealed an unexpected thermal behavior. A recurring exothermic signal can be observed in the DSC analysis after an elapsed time period. This exothermic signal was found to be proportional to the resting period and was accompanied by a constant increase in the glass-transition temperature. We hypothesize that a relaxation mechanism within the cross-linked scaffold, together with a long-lived stable ruthenium alkylidene species are responsible for the observed phenomenon.

Introduction

Olefin metathesis [1-6] has advanced to become a major synthetic tool in academia [7-11] and industry [12]. Metathesis polymerization techniques [13-15], and especially ring opening metathesis polymerization (ROMP) [16,17], have had a vital role in this growth. Polydicyclopentadiene (PDCPD), probably the most widely used metathesis polymer, is formed through ROMP of mostly endo-dicyclopentadiene (DCPD, **1**) (Figure 1). The Grubbs-type ruthenium initiators, known for their high activity, stability and functional group tolerance are extensively used to promote this type of olefin metathesis reactions. For example, the Grubbs second generation catalyst **2** [18] (Figure 1), may be used to initiate ROMP reactions of suitable strained cycloolefins.

DCPD is a common byproduct in the naphtha cracking process [19] and has two carbon–carbon double bonds, which readily

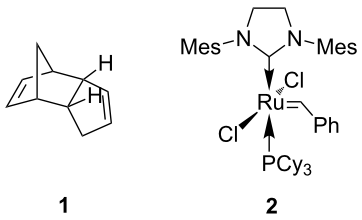

Figure 1: DCPD (**1**) and ruthenium benzylidene catalyst **2**.

undergo ROMP reactions with ruthenium alkylidenes. By adding the appropriate initiator, the highly strained and reactive norbornene double bond can be disrupted first to afford a linear polymer, followed by the ring opening of the less reactive cyclopentene double bond to effectively cross-link the chains (Scheme 1). Notably, with tungsten and molybdenum initiators the linear polymer may be isolated [20,21]; unlike the case with ruthenium initiators where only cross-linked polymers are obtained. This polyolefinic cross-linked thermoset material exhibits outstanding thermal stability [22], mechanical strength [23], fracture toughness [24] and dielectric characteristics [25]. Thanks to these properties PDCPD has become a very attractive polymer for several applications and is one of the most ubiquitous ROMP materials in industrial uses.

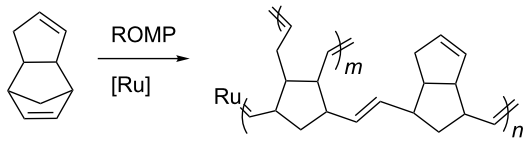

Scheme 1: ROMP of dicyclopentadiene by a ruthenium alkylidene initiator.

The relatively new PDCPD polymer has been widely explored for its thermal properties over the past decade. Cao et al. [26] reported glass-transition temperatures (T_g) as high as 165 °C and total conversions of 98.9% at polymerization temperatures of 60 °C with the Grubbs first generation catalyst. By carrying out detailed differential scanning calorimetry (DSC) analyses Kessler and Mauldin [27] demonstrated a sharp exothermic peak related to the heat of reaction and a final T_g of 164 °C at conversions of 90% right after curing. Dimonie et al. [28,29] examined the nature of the first exothermic peak of linear PDCPD using DSC and showed thermal polymerization completion after 2 h at 150 °C as the exothermic peak disappeared given these conditions. Kessler and White [30] also explored the cure kinetics of the polymer using DSC and reached a T_g of 139 °C for a "fully cured" product. In addition, Lee et al. [31] showed the absence of the exothermic peak on a second DSC scan, revealing a T_g as high as 160 °C. While literature glass-transition temperatures range from 140 to 165 °C, the polymer's thermal behavior for extended periods of time is not usually reported. Understanding this behavior is crucial for a polymer with a wide range of engineering applications in order to ensure the effectiveness and long-standing stability of the polymer. In this work we examined the thermal behavior over time of PDCPD obtained by ruthenium-induced ROMP of DCPD.

Results and Discussion

The observation of recurrent exothermic peaks in calorimetric analyses and a continuous rise in glass-transition temperature over time led us to study this phenomenon and propose a plausible mechanism for this behavior.

When a sample of PDCPD produced by ROMP of DCPD with catalyst **2** was initially subjected to a differential scanning calorimeter (DSC) run cycle, a strong exothermic peak was observed, which was at first associated with the reaction of remaining DCPD according to previous studies. Fourteen further DSC cycles were run immediately and, as expected, no exothermic peak was observed (Figure 2, top). The glass-transition temperature (T_g) signature was observed at 148 °C, with good correlation to literature values (vide supra).

As stated before, we desired to monitor the T_g over time; thus, the same sample was subjected to an additional identical DSC cycle two weeks later. To our surprise, an exothermic peak reappeared and the T_g value was recorded at 162.6 °C (Figure 2, bottom). Carrying out the measurement and the subsequent storage under nitrogen atmosphere afforded the same results. DSC analyses were then repeated with a number of polymer samples and the ‘return’ of the exothermic peak after prolonged time periods was found to be completely reproducible, a finding which led us to further investigate this phenomenon.

Thus, a set of PDCPD samples was subjected to a series of DSC heating–cooling cycles, with resting periods at room temperature between the cycles. During a period of 120 days the T_g constantly increased with every rest period until its value could not be further detected by the DSC analysis. A maximum glass-transition temperature was recorded at approximately 210 °C, which is to our knowledge the highest T_g recorded for PDCPD in the scientific literature (Figure 3).

The rise of the T_g after the rest periods was permanently accompanied by the reappearance of the exothermic peak. It was furthermore observed that the sample with the longest rest period of 16 months at room temperature showed the largest exothermic peak. The intensity of the exothermic peak was

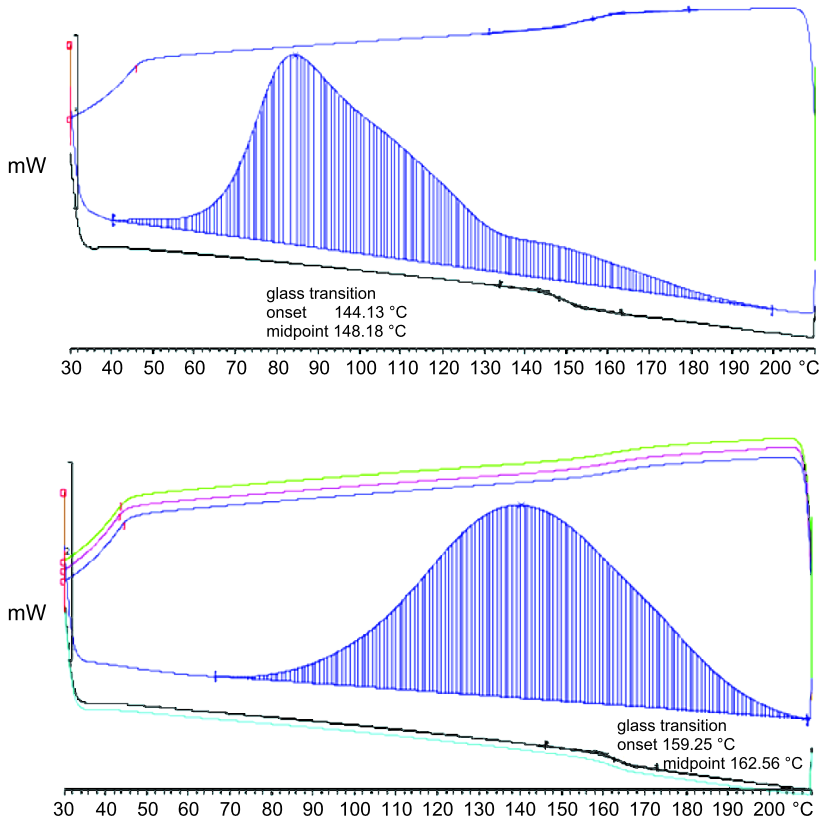

Figure 2: Top: DSC plot of PDCPD 24 hours after polymerization. Blue line: 1st heating–cooling cycle. Black line: 2nd cycle. Bottom: DSC of PDCPD sample after two weeks. Blue line shows the reappearing exothermic peak (1st cycle). The black and cyan lines show the elevation in T_g and disappearance of the exothermic peak.

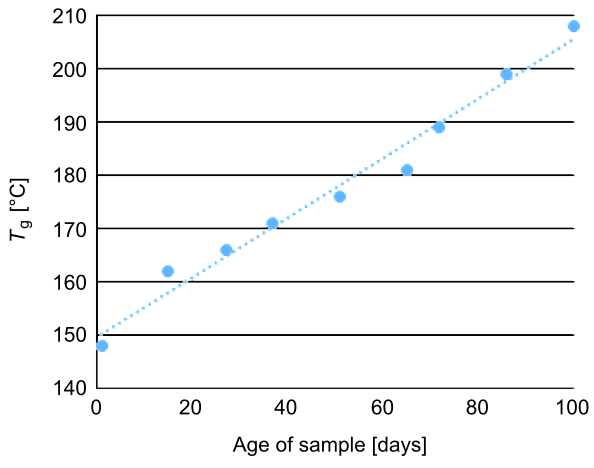

Figure 3: Change in T_g for a representative PDCPD sample as a function of time.

strongly correlated to the rest time between the analyses, where longer resting periods gave larger exothermic peaks (Figure 4) and very short time periods (such as the immediate repetition) did not afford any exothermic signal at all. For instance, a sample that was rested for 16 months without heating showed an extremely strong exothermic peak with a value of 151 J/g, even larger than the peaks observed at the first measurement.

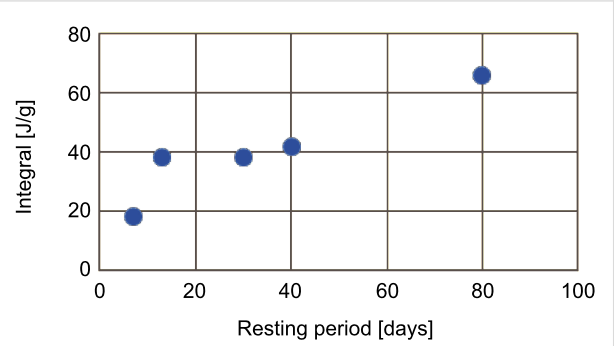

Figure 4: Intensity of exothermic peak as a function of rest time at room temperature for different samples.

A sample that was allowed equal rest periods of two weeks (Figure 5) showed very similar exothermic integrals (ca.

40 J/g), even after 90 days, except for the first two abnormally high peaks (probably due to reaction of unreacted strained cycloalkenes in the sample).

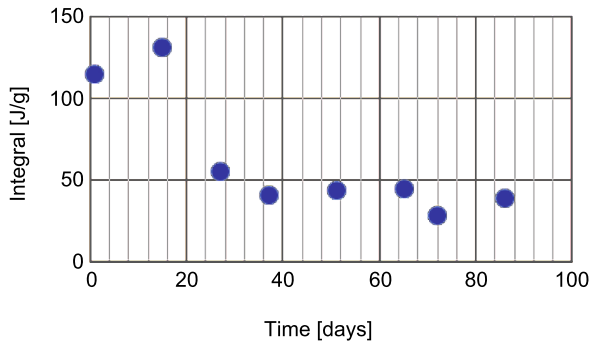

Figure 5: Peak intensity as function of age. Samples were analyzed every two weeks. The abnormal low intensity of the peak after 72 days is due to one week rest time instead of the regular two weeks rest time. The high intensity observed in the first two measurements may be attributable to further polymerization of unreacted cyclopentene bonds and free monomer.

It is important to note that the samples were always weighed between heating cycles and the weight of the crucible and polymer remained unchanged throughout the experiment. As the effect of resting time was established, we proceeded to study whether the resting temperature would influence the observed exothermic signal and the resultant T_g. Therefore, a set of samples was prepared, similar DSC cycles were run but this time, the samples were rested at different temperatures, i.e., room temperature, −5 °C, and at −196 °C (liquid nitrogen).

As shown in Figure 6, only extreme cooling using liquid nitrogen reduced the peak intensity significantly by 63%, compared to ambient temperature. Storage of the sample at −5 °C still afforded a relatively strong exothermic signal.

According to the ROMP mechanism, a ruthenium alkylidene species may remain entrapped within the PDCPD matrix. The data collected led us to assume that the exothermic peak may arise from an internal metathetic process which occurs only after the polymer microstructure equilibrates and further ruthenium–alkylidene metathesis with neighboring double bonds may be promoted. Alternatively, thermal decomposition of DCPD (or larger oligomers) to cyclopentadiene (CPD) by a retro-Diels–Alder reaction could also explain the observed phenomenon, although unlikely at room temperature. Both hypotheses were tested.

CPD is less reactive in metathesis reactions than DCPD, and will gradually dimerize at ambient conditions to give the latter. In order to estimate a possible formation of CPD as the reason

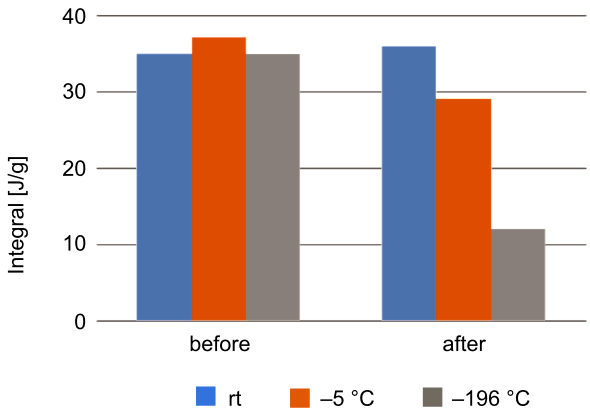

Figure 6: Resting temperature effect. Blue columns: resting at room temperature. Orange columns: resting at −5 °C. Gray columns: resting at −196 °C. Time elapsed between measurements was 1 week.

for the observed thermal behavior, a series of DCPD samples with different percentages of externally added CPD were subjected to heat–cool–rest cycles. Table 1 shows the lack of correlation between the amount of CPD in the sample and the glass-transition temperature increase. Moreover, the presence of volatile monomers such as DCPD and, even more so CPD, after heating cycles and long periods of time is highly improbable.

Table 1: T_g dependence on CPD content (%).

Entry[a]	vol % CPD	1st T_g[b]	2nd T_g[c]
1	0	148	162
2	2.5	142	158
3	10	158	165

[a]Conditions: 0.5 mg of **2** in 0.1 mL CH_2Cl_2; 10 mL of monomer/s. [b]First DSC run after 24 hours at 60 °C. [c]Second DSC run after two weeks at room temperature.

As mentioned before, we hypothesized that the exothermic signal reemerged due to secondary metathesis reactions which can occur after polymer relaxation and repositioning of the active ruthenium alkylidene within the cross-linked polymer network. To validate this assumption a sample in the DSC crucible was flooded with ethyl vinyl ether for 5 days, trying to deactivate any remaining catalytic species by formation of inert Fischer carbene [32]. A control sample was flooded with diethyl ether. To our satisfaction, in the sample treated with ethyl vinyl ether the exothermic peak was suppressed while the control experiment (with diethyl ether) behaved as indicated in previous experiments (Figure 7). These results support the theory that an olefin metathesis reaction is occurring and that it is the source of the observed exothermic peak.

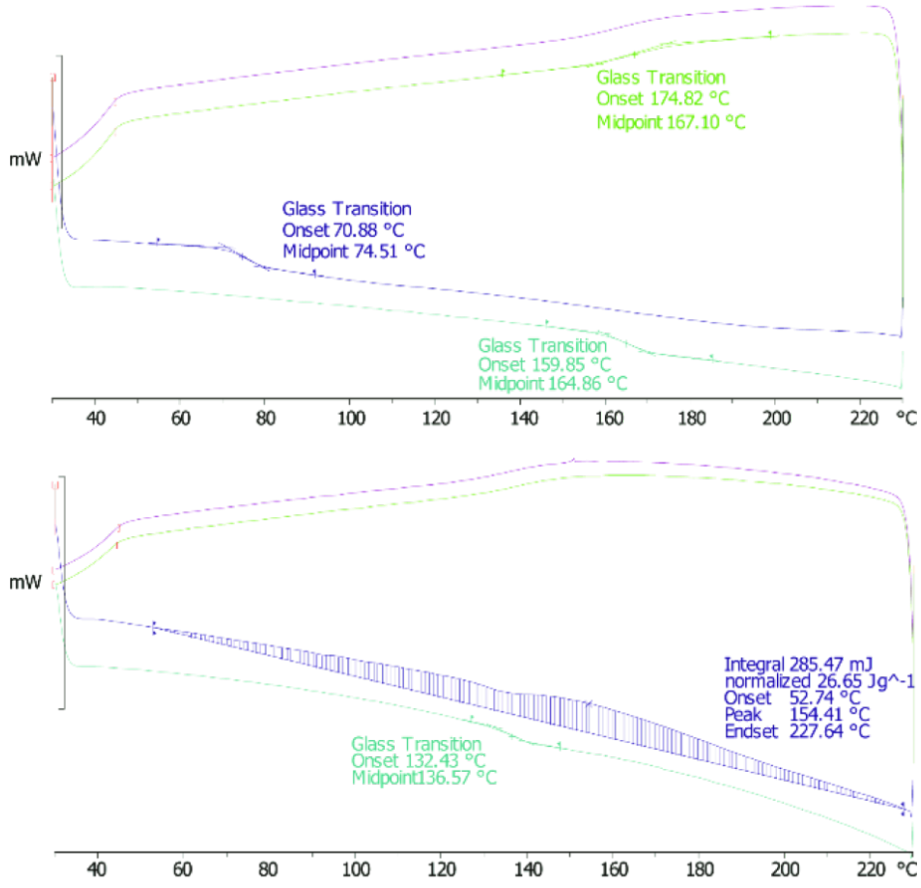

Figure 7: Top: Sample after 1 week with ethyl vinyl ether. Bottom: Sample after 1 week with diethyl ether.

Conclusion

In summary, the ruthenium-catalyzed DCPD polymerization produced a polymer with an unexpected thermal behavior over long periods of time. The DSC analysis after polymerization showed a large exothermic peak, which was initially assigned to exothermicity of ROMP of unreacted cycloalkane. However, this peak reappeared repeatedly after defined resting periods (days–weeks). Our study suggests that a relaxation process is occurring within the polymer and that a long-lived catalytic species inside the polymer may still be active after prolonged periods of time. Additionally, we showed that by repeating the heating–cooling cycles over time an unprecedented glass-transition temperature for PDCPD of 210 °C was obtained. This is to the best of our knowledge the highest T_g for PDCPD recorded so far. Ongoing efforts in the lab are geared towards further elucidating the mechanism and possible applications of these observations.

Experimental

All commercially available chemicals were of reagent grade quality and used without further purification, unless described. Differential scanning calorimetry (DSC) data was obtained using a METTLER-TOLEDO DSC 823 and results were evaluated with the STARe software. All experiments were performed with a nitrogen flow of 80 mL/min at a heating rate of 5 °C/min. Each sample was subjected to 2–3 heating–cooling cycles.

Polymerization procedures

endo-Dicyclopentadiene (10 mL, 74 mmol) and a stirring magnet were added to a 20 mL vial and kept at 40 °C in order to melt the monomer. In a separate 2 mL vial, initiator **2** (0.5 mg, 5.9×10^{-4} mmol) was dissolved in dichloromethane (100 µL). The dissolved initiator was then transferred by syringe to the vial containing the monomer upon vigorous stirring and a 10–15 µL sample was immediately placed in a DSC 40 µL aluminum crucible. Because the monomer mixture solidifies as it comes into contact with the crucible, the latter was warmed up to 40 °C to ensure a uniform coverage on the surface of the crucible. The crucible was then sealed with an aluminum cap, and stored at 60 °C for 24 hours for complete curing of the PDCPD. During resting periods the crucible was stored at room temperature under ambient conditions unless otherwise noted.

Acknowledgements

The Israel Science Foundation is gratefully acknowledged for partial financial support.

References

1. Vougioukalakis, G. C.; Grubbs, R. H. *Chem. Rev.* **2010,** *110,* 1746–1787. doi:10.1021/cr9002424
2. Samojłowicz, C.; Bieniek, M.; Grela, K. *Chem. Rev.* **2009,** *109,* 3708–3742. doi:10.1021/cr800524f
3. Boeda, F.; Clavier, H.; Nolan, S. P. *Chem. Commun.* **2008,** 2726–2740. doi:10.1039/b718287b
4. Diesendruck, C. E.; Tzur, E.; Lemcoff, N. G. *Eur. J. Inorg. Chem.* **2009,** *28,* 4185–4203. doi:10.1002/ejic.200900526
5. Monfette, S.; Fogg, D. E. *Chem. Rev.* **2009,** *109,* 3783–3816. doi:10.1021/cr800541y
6. Dunbar, M. A.; Balof, S. L.; LaBeaud, L. J.; Yu, B.; Lowe, A. B.; Valente, E. J.; Schanz, H.-J. *Chem. – Eur. J.* **2009,** *15,* 12435–12446. doi:10.1002/chem.200901013
7. Nicolaou, K. C.; Bulger, P. G.; Sarlah, D. *Angew. Chem., Int. Ed.* **2005,** *44,* 4490–4527. doi:10.1002/anie.200500369
8. Connon, S. J.; Blechert, S. *Angew. Chem., Int. Ed.* **2003,** *42,* 1900–1923. doi:10.1002/anie.200200556
9. Grubbs, R. H., Ed. *Handbook of Metathesis: Catalyst Development;* Wiley-VCH Verlag GmbH: Weinheim, 2008.
10. Giudici, R. E.; Hoveyda, A. H. *J. Am. Chem. Soc.* **2007,** *129,* 3824–3825. doi:10.1021/ja070187v
11. Michrowska, A.; Gułajski, L.; Kaczmarska, Z.; Mennecke, K.; Kirschning, A.; Grela, K. *Green Chem.* **2006,** *8,* 685–688. doi:10.1039/b605138c
12. Mol, J. C. *J. Mol. Catal. A: Chem.* **2004,** *213,* 39–45. doi:10.1016/j.molcata.2003.10.049
13. Bielawski, C. W.; Benitez, D.; Grubbs, R. H. *Science* **2002,** *297,* 2041–2044. doi:10.1126/science.1075401
14. Schwendeman, J. E.; Church, A. C.; Wagener, K. B. *Adv. Synth. Catal.* **2002,** *344,* 597–613.
15. Burtscher, D.; Lexer, C.; Mereiter, K.; Winde, R.; Karch, R.; Slugovc, C. *J. Polym. Sci., Part A-1: Polym. Chem.* **2008,** *46,* 4630–4635. doi:10.1002/pola.22763
16. Ivin, K. J.; Mol, J. C. *Olefin Metathesis and Metathesis Polymerization;* Academic Press: San Diego, 1997.
17. Sutthasupa, S.; Shiotsuki, M.; Sanda, F. *Polym. J.* **2010,** *42,* 905–915. doi:10.1038/pj.2010.94
18. Schwab, P.; Grubbs, R. H.; Ziller, J. W. *J. Am. Chem. Soc.* **1996,** *118,* 100–110. doi:10.1021/ja952676d
19. Johnson, H. F. Cyclopentadiene. U.S. Patent 2,636,054, April 21, 1953.
20. Davidson, T. A.; Wagener, K. B. *J. Mol. Catal. A: Chem.* **1998,** *133,* 67–74. doi:10.1016/S1381-1169(98)00091-0
21. Dragutan, V.; Demonceau, A.; Dragutan, I.; Finkelshtein, E. S., Eds. *Green Metathesis Chemistry;* Springer: Dordrecht, 2010. doi:10.1007/978-90-481-3433-5
22. Mühlebach, A.; van der Schaaf, P. A.; Hafner, A.; Setiabudi, F. *J. Mol. Catal. A: Chem.* **1998,** *132,* 181–188. doi:10.1016/S1381-1169(97)00241-0
23. Hine, P. J.; Leejarkpai, T.; Khosravi, E.; Duckett, R. A.; Feast, W. J. *Polymer* **2001,** *42,* 9413–9422. doi:10.1016/S0032-3861(01)00488-8
24. Jeong, W.; Kessler, M. R. *Chem. Mater.* **2008,** *20,* 7060–7068. doi:10.1021/cm8020947
25. Yin, W.; Kniajanski, S.; Amm, B. Dielectric properties of polydicyclopentadiene and polydicyclopentadiene-silica nanocomposite. In *Conference Record of the IEEE International Symposium on Electrical Insulation,* San Diego, CA, June 6–9, 2010; IEEE, 2010. doi:10.1109/ELINSL.2010.5549749
26. Yao, Z.; Zhou, L.; Dai, B.; Cao, K. *J. Appl. Polym. Sci.* **2012,** *125,* 2489–2493. doi:10.1002/app.36359
27. Mauldin, T. C.; Kessler, M. R. *J. Therm. Anal. Calorim.* **2009,** *96,* 705–713. doi:10.1007/s10973-009-0039-y
28. Dimonie, D.; Dimonie, M.; Munteanu, V.; Iovu, H.; Couve, J.; Abadie, M. J. *Polym. Degrad. Stab.* **2000,** *70,* 319–324. doi:10.1016/S0141-3910(00)00093-8
29. Dimonie, D.; Dimonie, M.; Stoica, S.; Munteanu, V.; Abadie, M. J. *Polym. Degrad. Stab.* **2000,** *67,* 167–170. doi:10.1016/S0141-3910(99)00108-1
30. Kessler, M. R.; White, S. R. *J. Polym. Sci.* **2002,** *40,* 2373–2383. doi:10.1002/pola.10317
31. Lee, J. K.; Liu, X.; Ho Yoon, S.; Kessler, M. R. *J. Polym. Sci.* **2007,** *45,* 1771–1780. doi:10.1002/polb.21089
32. Wu, Z.; Nguyen, S. T.; Grubbs, R. H.; Ziller, J. W. *J. Am. Chem. Soc.* **1995,** *117,* 5503–5511. doi:10.1021/ja00125a010

BEILSTEIN JOURNAL OF ORGANIC CHEMISTRY

Tandem cross enyne metathesis (CEYM)–intramolecular Diels–Alder reaction (IMDAR). An easy entry to linear bicyclic scaffolds

Javier Miró[1], María Sánchez-Roselló[1,2], Álvaro Sanz[1], Fernando Rabasa[1], Carlos del Pozo[*1] and Santos Fustero[*1,2]

Full Research Paper

Open Access

Address:
[1]Departamento de Química Orgánica, Universidad de Valencia, E-46100 Burjassot, Spain and [2]Laboratorio de Moléculas Orgánicas, Centro de Investigación Príncipe Felipe, E-46012 Valencia, Spain

Email:
Carlos del Pozo[*] - carlos.pozo@uv.es; Santos Fustero[*] - santos.fustero@uv.es

* Corresponding author

Keywords:
bicyclic frameworks; cross enyne metathesis; Diels–Alder reaction; tandem reaction

Beilstein J. Org. Chem. **2015,** *11,* 1486–1493.
doi:10.3762/bjoc.11.161

Received: 08 May 2015
Accepted: 06 August 2015
Published: 25 August 2015

This article is part of the Thematic Series "Progress in metathesis chemistry II".

Guest Editor: K. Grela

Abstract

A new tandem cross enyne metathesis (CEYM)–intramolecular Diels–Alder reaction (IMDAR) has been carried out. It involves conjugated ketones, esters or amides bearing a remote olefin and aromatic alkynes as the starting materials. The overall process enables the preparation of a small family of linear bicyclic scaffolds in a very simple manner with moderate to good levels of diastereoselectivity. This methodology constitutes one of the few examples that employ olefins differently than ethylene in tandem CEYM–IMDAR protocols.

Introduction

Among all metathetic processes, the enyne metathesis reaction has received significant attention as an attractive and frequently used synthetic tool in organic synthesis [1-7]. It is an atom economical process that combines alkene and alkyne moieties to generate conjugated 1,3-dienes under mild conditions. These 1,3-dienes are versatile building blocks suitable for further non-metathetic transformations, either in a step-wise or a tandem fashion. Thus, the enyne metathesis methodology has become a powerful tool for the generation of carbon–carbon bonds, expanding the utility of metathesis processes beyond olefinic substrates [8,9].

The inherent tandem nature of enyne metathesis is particularly appealing in its combination with the Diels–Alder reaction. This tandem protocol is well suited for addressing a broad range of complex molecules since multiple carbon–carbon bonds can be

generated in a single operation, therefore increasing molecular complexity in a quite simple manner [10].

While examples of ring-closing enyne metathesis (RCEYM) reactions are widespread in the literature [11], the development of the intermolecular version, i.e., the cross enyne metathesis (CEYM), lagged behind probably due to difficulties in controlling the stereoselectivity in the newly formed double bond leading to the formation of mixtures of *E* and *Z*-isomers. These inherent selectivity problems are absent when the olefin counterpart is the ethylene unit, which explains why most of the reported examples that combine a CEYM reaction with a Diels–Alder cycloaddition in a tandem manner involve the use of ethylene as the olefin partner either by employing an internal source of it or by bubbling it into the reaction mixture. This strategy allowed for the synthesis of a wide variety of natural and non-natural products in the last decade [12-22].

The use of olefins other than ethylene in CEYM-Diels–Alder tandem protocols is very scarce. The first example was reported in 2005 by combining Baylis–Hillman adducts with alkynes in the presence of second generation Hoveyda–Grubbs catalyst [23]. After the initial formation of the trienic unit, an intramolecular Diels–Alder reaction (IMDAR) rendered highly functionalized bicyclic derivatives in a very efficient manner. More recently, a multicomponent CEYM–intermolecular hetero-Diels–Alder reaction involving alkynes, ethyl glyoxalate and ethyl vinyl ether was described for the preparation of 2,3-dihydropyrans [24,25]. Additionally, a tandem CEYM–IMDAR reaction in combination with a final aromatization step was employed for the synthesis of biaryl derivatives [26]. Herein, a new example of this tandem protocol CEYM–IMDAR with alkynes and α,ω-dienes as starting materials is reported, which will give access to a new family of linear bicyclic carbo- and heterocyclic scaffolds. We envisioned that the initial CEYM would occur in the electronically neutral olefin to generate the corresponding triene intermediate, which would evolve under the reaction conditions through the cycloaddition event to render the final products (Scheme 1).

Results and Discussion

The use of 1,5-, 1,6- and 1,7-dienes in cross metathesis-type transformations is not trivial since chemoselectivity issues can arise. It is well known that electronically deficient olefins should undergo metathesis in a slow rate based on the model developed by Grubbs and coworkers that classifies olefins and predicts their reactivity in CM reactions [27]. We anticipated that, according to these studies, in substrates bearing two different olefin units one being an α,β-unsaturated moiety, the tandem CM–IMDAR protocol would initiate on the electronically neutral olefin. Furthermore, those dienes could undergo an intramolecular cyclization (RCM) promoted by the ruthenium carbene that would compete with the desired intermolecular CM process.

In order to prove our assumptions, phenylacetylene (**1a**) and conjugated ester **2a** were employed as model substrates to study the tandem protocol. The results obtained in the optimization process are summarized in Table 1.

The first attempt to carry out the projected tandem protocol was performed by heating 1.0 equiv of phenylacetylene (**1a**) and 3.0 equiv of diolefinic ester **2a** in toluene in the presence of second generation Hoveyda–Grubbs catalyst [Ru-II]. After 6 hours at 90 °C, bicyclic lactone **3a** was obtained in 25% yield (Table 1, entry 1), together with lactone **4a** (15%, arising from the ring closing metathesis (RCM) of **2a**), and unreacted **2a**. The isolated yield of **3a** was improved to 57% by increasing the reaction time to 48 hours (Table 1, entries 2 and 3). An extended reaction time (72 h) led to a drop in the final yield (Table 1, entry 4). In all cases variable amounts of **4a**, which never exceeded 15%, and unreacted **2a** were detected in the crude mixture. On the other hand, it is worth noting that although compound **4a** can be considered as a good dienophile, its inter-

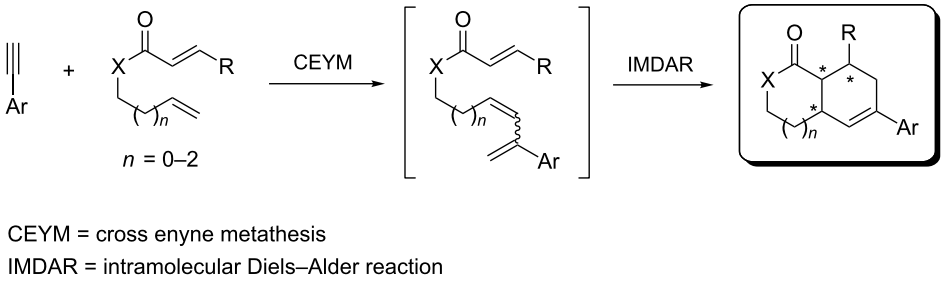

Scheme 1: Tandem cross enyne metathesis–intramolecular Diels–Alder reaction.

Table 1: Optimization of the tandem CEYM–IMDAR.

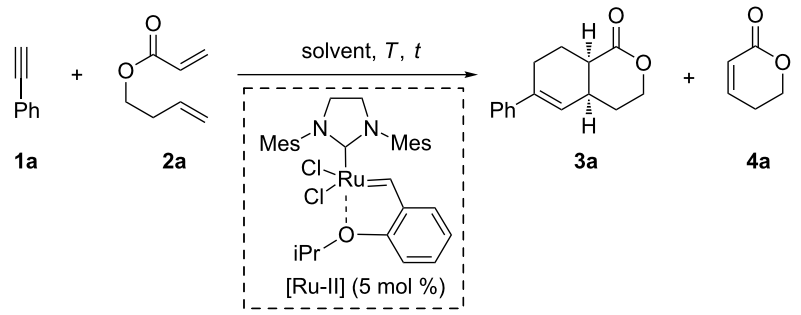

entry	solvent	*T* (°C)	**1a**:**2a**	*t* (h)	additive	% yield **3a**[a]
1	toluene	90	1:3	6	–	25
2	toluene	90	1:3	24	–	37
3	toluene	90	1:3	48	–	57
4	toluene	90	1:3	72	–	39
5	toluene	90	1:1	48	–	36
6	toluene	90	1:5	48	–	30
7	toluene	110	1:3	48	–	52
8	toluene	140	1:3	48	–	37
9	DCM	60	1:3	48	–	25
10	$C_6H_5CF_3$	90	1:3	48	–	60
11	toluene	90	1:3	48	$Ti(OiPr)_4$[b]	38
12	toluene	90	1:3	48	$BF_3{\cdot}OEt_2$[b]	15
13	toluene	90	1:3	48	thiourea[c]	49
14	toluene	90	1:3	48	BQ[b,d]	37

[a]Isolated yield after column chromatography. Variable amounts of **4a** were observed in all cases, but never exceeded 15% (based on **2a**). Some unreacted **2a** was also detected in all cases; [b]5 mol %; [c]1 mol %; [d]benzoquinone.

molecular Diels–Alder reaction with the triene intermediate formed after the initial CEYM was not observed. This fact, together with the successful formation of the desired bicycle **3a**, indicates that the CEYM between **1a** and **2a** is faster than the RCM of **2a**, and also that the intramolecular Diels–Alder process is more favoured once the triene unit is formed.

Different ratios of substrates **1a**:**2a** did not improve the efficiency of the process (Table 1, entries 5 and 6). Likewise, higher temperatures afforded comparable yields of product **3a** (Table 1, entries 7 and 8). When the reaction was performed in DCM only 25% of **3a** were isolated, while the use of trifluorotoluene as solvent afforded the best yield (60%) of the tandem process (Table 1, entries 9 and 10).

The use of Lewis acids as co-catalysts was also tested although the efficiency of the process did not improve neither with $Ti(OiPr)_4$ nor with $BF_3{\cdot}OEt_2$ (Table 1, entries 11 and 12). Alternatively, thiourea derivatives have proven to be very effective hydrogen-bonding catalysts for Diels–Alder reactions [28]. However, in our case no influence was observed when the reaction was performed in the presence of diaryl thioureas (Table 1, entry 13). Finally, the use of benzoquinone (BQ) as an additive, which has been reported to suppress the formation of byproducts in enyne metathesis protocols [29], was also unsuccessful in the present case (Table 1, entry 14).

It is noteworthy that compound **3a** was always obtained as a single diastereoisomer showing a *cis* fusion between the two cycles [30].

Next, the optimized conditions (heating at 90 °C for 48 h in the presence of Ru-II catalyst) were applied to other aromatic alkynes **1** and dienes **2**, affording a new family of linear carbocycles and heterocycles **3** in moderate yields (Table 2).

Bicyclic lactone **3a**, ketone **3b** and lactam **3c** were obtained in moderate yields following the tandem CEYM-IMDAR protocol (Table 2, entries 1–3). Comparable yields were obtained with either electron-donating or electron-withdrawing substituents in the starting alkyne **1** (Table 2, entries 4 and 5). In addition, 5- and 7-membered bicyclic lactams **3f** and **3g** were also synthe-

Table 2: Scope of the tandem CEYM-IMDAR protocol.

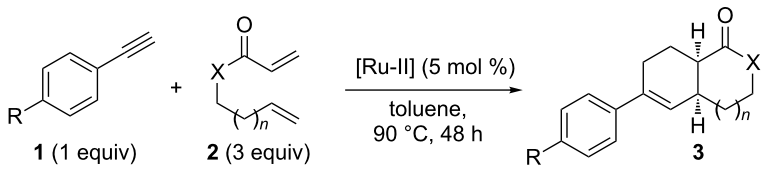

1 (1 equiv) **2** (3 equiv) **3**

entry	**1** (R)	**2**	**3** (yield)[a]
1	**1a** (H)	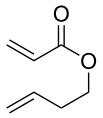 **2a**	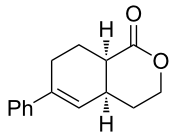 **3a** (57%)
2	**1a** (H)	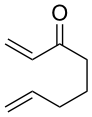 **2b**	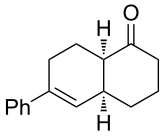 **3b** (38%)
3	**1a** (H)	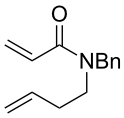 **2c**	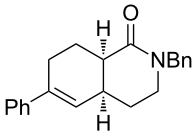 **3c** (62%)
4	**1b** (F)	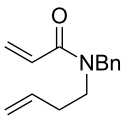 **2c**	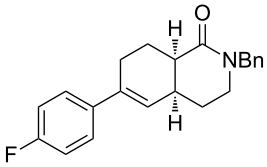 **3d** (45%)
5	**1c** (OMe)	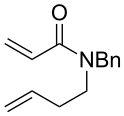 **2c**	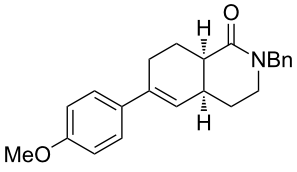 **3e** (35%)
6	**1a** (H)	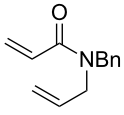 **2d**	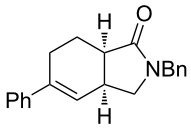 **3f** (50%)
7	**1a** (H)	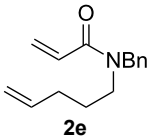 **2e**	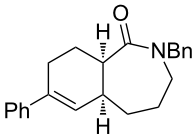 **3g** (44%)

[a]Isolated yields after column chromatography. All final products **3** were obtained as single diastereoisomers.

sized in moderate yields (Table 2, entries 6 and 7). Again, all bicycles **3** were obtained as single diastereoisomers, assuming the same *cis*-stereochemistry as in compound **3a** [30].

Although it was not possible to isolate the intermediate trienes formed after the initial CEYM under the reaction conditions, they should be formed as a mixture of *E*/*Z* diastereoisomers. We

would expect that only the *E*-isomer possesses the adequate disposition to undergo the IMDAR, while the *Z*-isomer would not cyclize. However, since this *Z*-isomer was not detected after 48 h, it was assumed that this triene intermediate decomposes under the reaction conditions or, alternatively, it undergoes an RCM to render compounds **4** (Table 1) and only the final products arising from the *E*-isomer were observed. Moreover, the IMDAR of dienes and dienophiles linked by ester or amide tethers was theoretically studied [31]. These studies indicated that *endo* geometries are favoured over *exo* ones and also that boat-like conformations are preferred over chair-like ones. These studies accurately correlated with the experimental results observed in these types of cyclizations [32-34]. The preference of the boat-like transition state was ascribed to the co-planarity of the carbonyl group during the cycloaddition, being maximized in the *E*-*endo* boat-like transition state leading to the formation of the *cis*-cycloadduct **3**-*endo* (Scheme 2).

The tandem protocol was next extended to substituted dienes **8**. These substrates were assembled by condensation of homoallyl benzylamine **7** with carboxylic acids **5** (method A) or acyl chlorides **6** (method B) under standard conditions (Scheme 3). Since the basic indole nitrogen in substrate **8f** could interfere with the ruthenium catalyst, it was *N*-methylated to render compound **8g**.

With substrates **8** in hand, they were subjected to the optimized conditions of the tandem CEYM–IMDAR protocol. The results of these tandem reactions are depicted in Table 3.

Diolefinic substrate **8a** underwent the tandem sequence in excellent yield (85%) to afford the *endo* isomer **10a**-*endo* as the major product together with a small amount of the *exo* isomer **10a**-*exo* (Table 3, entry 1). On the other hand, compound **8b** bearing a phenyl substituent at the α-olefinic carbon gave an

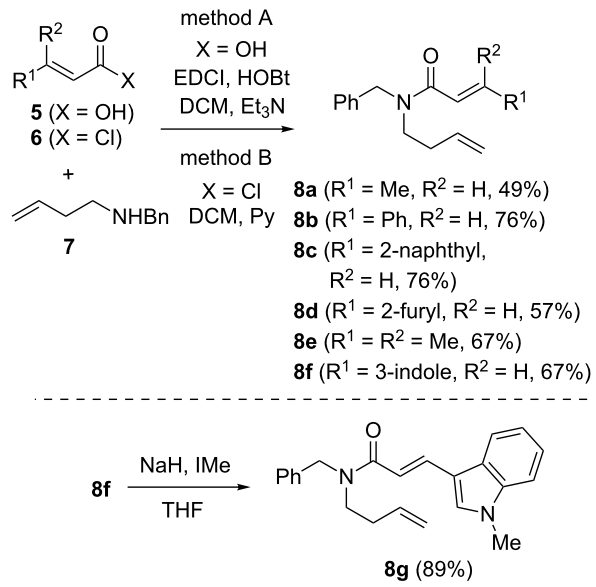

Scheme 3: Preparation of starting materials **8**.

almost equimolecular but separable mixture of bicycles **10b**-*endo* and **10b**-*exo* (78% overall yield). In this case, a small amount of triene intermediate **9b**-*cis* (15% yield) was also isolated, which was in agreement with our previous assumption that the *cis*-triene does not undergo the IMDAR.

Diolefinic amides **8c** and **8d** bearing the 2-naphthyl and 2-furyl substituents, respectively, rendered the corresponding bicyclic products **10c** and **10d** in acceptable yields (47 and 68%) and moderate diastereoselectivity (Table 3, entries 3 and 4). The use of a trisubstituted olefin as the starting material (**8e**) caused a significant drop of the final yield, probably due to steric reasons (Table 3, entry 5). Finally, the indole-containing derivative **8g**

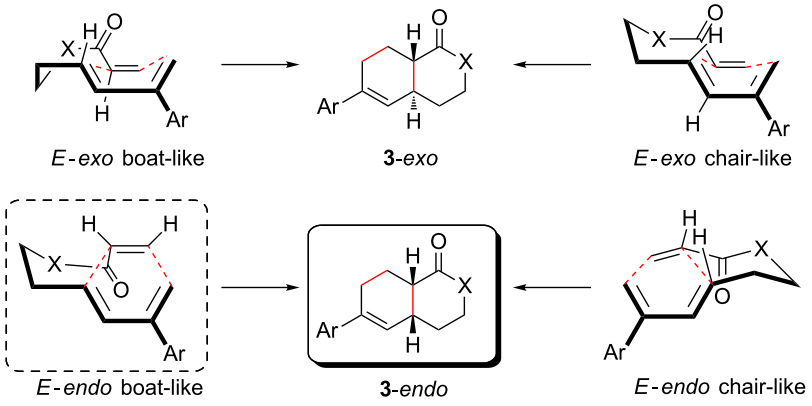

Scheme 2: Stereochemical outcome of the IMDAR.

gave an equimolecular but separable mixture of adducts **10f**-*endo* and **10f**-*exo* in moderate yield (Table 3, entry 6).

It can be assumed that in these cases, the *E*-*exo* boat-like transition state is also in operation (see Scheme 2), which gives rise to the diastereoisomeric *endo*/*exo* mixtures.

The relative stereochemistry of the final products **10** was determined on compounds **10b**-*endo* and **10b**-*exo*. After chromatographic separation, NOESY experiments indicated that **10b**-*endo* shows two nOe correlations: one between H^1 and H^2 (which indicates the *cis*-fusion of the two cycles) and another one between H^1 and the aromatic proton H^3. These two nOe

Table 3: Extending the scope of the tandem CEYM–IMDAR protocol to amides **8**.

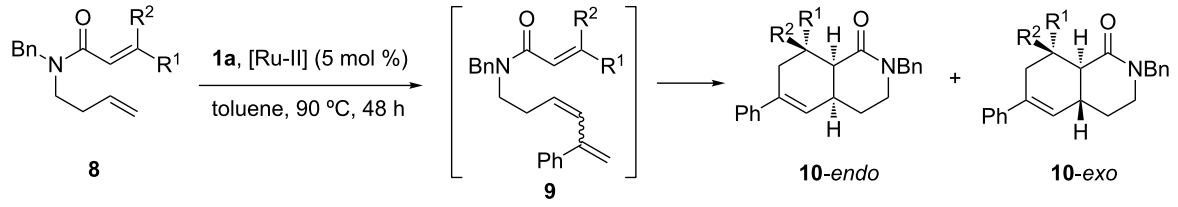

8 **9** **10**-*endo* + **10**-*exo*

entry	8	9	10	% yield **10**[a] (*endo*: *exo*)[b]
1	**8a**	–[c]	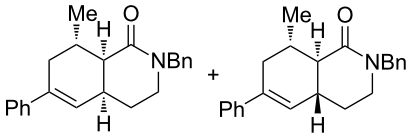 **10a**-*endo* + **10a**-*exo*	85 (93:7)
2	**8b**	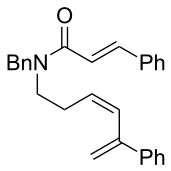 **9b**-*cis* (15%)	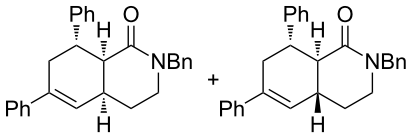 **10b**-*endo* + **10b**-*exo*	78 (53:47)
3	**8c**	–[c]	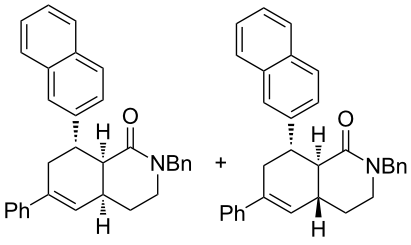 **10c**-*endo* + **10c**-*exo*	47 (66:34)
4	**8d**	–[c]	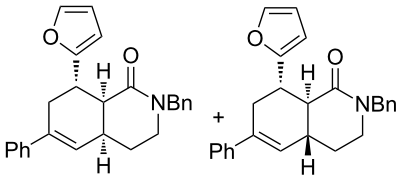 **10d**-*endo* + **10d**-*exo*	68 (72:28)
5	**8e**	–[c]	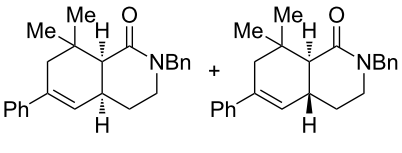 **10e**-*endo* + **10e**-*exo*	25 (77:23)

Table 3: Extending the scope of the tandem CEYM–IMDAR protocol to amides **8**. (continued)

6	**8g**	–[c]	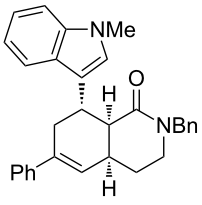 **10f**-*endo*	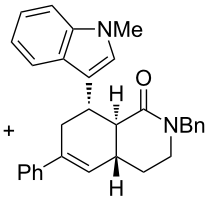 **10f**-*exo*	33 (50:50)

[a]Isolated yields after column chromatography; [b]diasteroisomeric ratio determined by ^{1}H NMR; [c]not observed;

interactions, together with the absence of a correlation between H^1 and H^4 indicated that the phenyl ring and H^1 display a *cis* relationship. Additionally, compound **10b**-*exo* only showed an nOe correlation between H^1 and H^3 (Figure 1). For the rest of compounds **10**, an analogous stereochemical outcome was assumed.

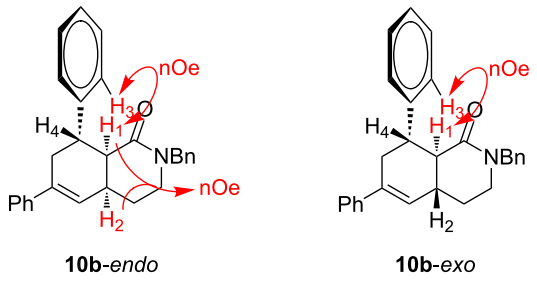

Figure 1: Determination of the relative stereochemistry on compounds **10b**.

Conclusion

In conclusion, a new tandem CEYM–IMDAR involving aromatic alkynes and dienes bearing two electronically different olefin moieties is described. Non-substituted substrates **2** are good partners in the tandem protocol affording linear bicyclic derivatives **3** as single diastereoisomers. The IMDAR takes place with complete *endo* selectivity, by means of an *endo* boat-like transition state. The use of substrates **8** with increased substitution at the β-olefinic carbon provides the formation of final products **10** as mixtures of *endo*/*exo* diastereoisomers, indicating that an *exo* boat-like transition state is also in operation in this case. It is noteworthy that this is one of the few examples of this tandem protocol that employs olefins other than ethylene.

Experimental

General procedure for the tandem protocol. A solution of Hoveyda–Grubbs 2nd generation (5 mol %), diene **2** or **8** (3.0 equiv) and alkyne **1** (0.5 mmol) in dry toluene 0.05 M was heated at 90 °C in a sealed tube. The reaction mixture was stirred at this temperature for 48 h. The solvents were then removed under reduced pressure and the crude mixture was purified by flash chromatography in *n*-hexanes/ethyl acetate.

(4a*R,8a*S**)-6-Phenyl-3,4,4a,7,8,8a-hexahydro-1*H*-isochromen-1-one (3a).** Following the general procedure described above, **3a** was obtained in 57% yield as a brown oil. ^{1}H NMR ($CDCl_3$, 300 MHz) δ 1.68–1.87 (m, 2H), 2.00–2.10 (m, 1H), 2.25–2.36 (m, 2H), 2.41–2.53 (m, 1H), 2.75–2.85 (m, 2H), 4.22 (dd, J_1 = 6.0 Hz, J_2 = 4.5 Hz, 2H), 5.81–5.83 (m, 1H), 7.13–7.29 (m, 5H); ^{13}C NMR (CDCl3, 75.5 MHz) δ 24.1, 24.7, 28.5, 32.5, 38.9, 67.3, 124.8, 125.1, 127.3, 128.3, 139.4, 141.2, 173.4; HRMS (ES): $[M + 1]^+$ calcd for $C_{15}H_{17}O_2$, 229.1223; found, 229.1233.

Supporting Information

Supporting Information File 1

Experimental and analytical data.
[http://www.beilstein-journals.org/bjoc/content/supplementary/1860-5397-11-161-S1.pdf]

Acknowledgements

We would like to thank the Spanish Ministerio de Economia y Competitividad (CTQ-2013-43310-P) and Generalitat Valenciana (GV/PrometeoII/2014/073) for their financial support. J. M., F. R. and A. S. thank the University of Valencia and the Spanish Ministerio de Economia y Competitividad for a predoctoral fellowship.

References

1. Fischmeister, C.; Bruneau, C. *Beilstein J. Org. Chem.* **2011,** *7,* 156. doi:10.3762/bjoc.7.22
2. Nolan, S. P.; Clavier, H. *Chem. Soc. Rev.* **2010,** *39,* 3305. doi:10.1039/b912410c
3. Li, J.; Lee, D. In *Handbook of Metathesis,* 2nd ed.; Grubbs, R. H.; O'Leary, D. J., Eds.; Wiley-VCH: Weinheim, 2015; pp 381 ff.

4. Diver, S. T.; Clark, J. R. *Comprehensive Organic Synthesis,* 2nd ed.; Elsevier, 2014; Vol. 5, pp 1302 ff.
5. Diver, S. T. Synthesis by Alkene Metathesis. *Science of Synthesis;* Thieme: Stuttgart, 2009; Vol. 46, pp 97 ff.
6. Mori, M. *Adv. Synth. Catal.* **2007,** *349,* 121. doi:10.1002/adsc.200600484
7. Hansen, E. C.; Lee, D. *Acc. Chem. Res.* **2006,** *39,* 509. doi:10.1021/ar050024g
8. Kotha, S.; Meshram, M.; Tiwari, A. *Chem. Soc. Rev.* **2009,** *38,* 2065. doi:10.1039/b810094m
9. Fustero, S.; Simón-Fuentes, A.; Barrio, P.; Haufe, G. *Chem. Rev.* **2015,** *115,* 871. doi:10.1021/cr500182a
10. Grubbs, R. H. *Handbook of Metathesis;* Wiley-VCH Verlag Gmbh and Co. KGaA: Weinheim, 2003; Vol. 1–3.
11. Li, J.; Lee, D. *Eur. J. Org. Chem.* **2011,** 4269. doi:10.1002/ejoc.201100438
12. Kueh, J. T. B.; Moodie, L. W. K.; Lukas, N. T.; Larsen, D. S. *Eur. J. Org. Chem.* **2015,** 1485. doi:10.1002/ejoc.201403482
13. Fustero, S.; Bello, P.; Miró, J.; Sánchez-Roselló, M.; Haufe, G.; del Pozo, C. *Beilstein J. Org. Chem.* **2013,** *9,* 2688. doi:10.3762/bjoc.9.305
14. Fustero, S.; Bello, P.; Miró, J.; Simón, A.; del Pozo, C. *Chem. – Eur. J.* **2012,** *18,* 10991. doi:10.1002/chem.201200835
15. Kotha, S.; Waghule, G. T. *J. Org. Chem.* **2012,** *77,* 6314. doi:10.1021/jo300766f
16. Kotha, S.; Goyal, D.; Thota, N.; Srinivas, V. *Eur. J. Org. Chem.* **2012,** 1843. doi:10.1002/ejoc.201101744
17. Danz, M.; Hilt, G. *Adv. Synth. Catal.* **2011,** *353,* 303. doi:10.1002/adsc.201000832
18. Subrahmanyam, A. V.; Palanichamy, K.; Kaliappan, K. P. *Chem. – Eur. J.* **2010,** *16,* 8545. doi:10.1002/chem.201000482
19. Nandurdikar, R. S.; Subrahmanyam, A. V.; Kaliappan, K. P. *Eur. J. Org. Chem.* **2010,** 2788. doi:10.1002/ejoc.201000001
20. Kotha, S.; Khedkar, P. *Eur. J. Org. Chem.* **2009,** 730. doi:10.1002/ejoc.200800924
21. Kotha, S.; Mandal, K.; Banerjee, S.; Mobin, S. M. *Eur. J. Org. Chem.* **2007,** 1244. doi:10.1002/ejoc.200600970
22. Kaliappan, K. P.; Subrahmanyam, V. *Org. Lett.* **2007,** *9,* 1121. doi:10.1021/ol0701159
23. Mix, S.; Blechert, S. *Org. Lett.* **2005,** *7,* 2015. doi:10.1021/ol050508c
24. Castagnolo, D.; Botta, L.; Botta, M. *Carbohydr. Res.* **2009,** *344,* 1285. doi:10.1016/j.carres.2009.05.007
25. Castagnolo, D.; Botta, L.; Botta, M. *Tetrahedron Lett.* **2009,** *50,* 1526. doi:10.1016/j.tetlet.2009.01.047
26. Kotha, S.; Seema, V. *Synlett* **2011,** 2329. doi:10.1055/s-0030-1260315
27. Chatterjee, A. K.; Choi, T.-L.; Sanders, D. P.; Grubbs, R. H. *J. Am. Chem. Soc.* **2003,** *125,* 11360. doi:10.1021/ja0214882
28. Clark, J. R.; French, J. M.; Jecs, E.; Diver, S. T. *Org. Lett.* **2012,** *14,* 4178. doi:10.1021/ol301846q
29. Wittkopp, A.; Schreiner, P. R. *Chem. – Eur. J.* **2003,** *9,* 407. doi:10.1002/chem.200390042
30. Saito, A.; Yanai, H.; Taguchi, T. *Tetrahedron* **2004,** *60,* 12239. doi:10.1016/j.tet.2004.10.012
31. Tantillo, D. J.; Houk, K. N.; Jung, M. E. *J. Org. Chem.* **2001,** *66,* 1938. doi:10.1021/jo001172h
32. Kim, P.; Nantz, M. H.; Kurth, M. J.; Olmstead, M. M. *Org. Lett.* **2000,** *2,* 1831. doi:10.1021/ol005886q
33. Jung, M. E.; Huang, A.; Johnson, T. W. *Org. Lett.* **2000,** *2,* 1835. doi:10.1021/ol000104e
34. White, J. D.; Demnitz, F. W. J.; Oda, H.; Hassler, C.; Snyder, J. P. *Org. Lett.* **2000,** *2,* 3313. doi:10.1021/ol000200f

License and Terms

BEILSTEIN JOURNAL OF ORGANIC CHEMISTRY

Synthesis of a tricyclic lactam via Beckmann rearrangement and ring-rearrangement metathesis as key steps

Sambasivarao Kotha*, Ongolu Ravikumar and Jadab Majhi

Full Research Paper

Open Access

Address:
Department of Chemistry, Indian Institute of Technology-Bombay, Powai, Mumbai-400 076, India, Fax: 022-25767152

Email:
Sambasivarao Kotha* - srk@chem.iitb.ac.in

* Corresponding author

Keywords:
allylation; Beckmann rearrangement; lactams; oximes; ring-rearrangement metathesis

Beilstein J. Org. Chem. **2015,** *11,* 1503–1508.
doi:10.3762/bjoc.11.163

Received: 12 June 2015
Accepted: 12 August 2015
Published: 27 August 2015

This article is part of the Thematic Series "Progress in metathesis chemistry II".

Guest Editor: K. Grela

Abstract

A tricyclic lactam is reported in a four step synthesis sequence via Beckmann rearrangement and ring-rearrangement metathesis as key steps. Here, we used a simple starting material such as dicyclopentadiene.

Introduction

The Beckmann rearrangement (BR), a well-known protocol for the conversion of ketoxime to an amide in the presence of acid was discovered in 1886. This rearrangement involves the migration of a group anti to the leaving group on the nitrogen atom. The BR has widely been used in synthetic organic chemistry, for example, a large-scale production of Nylon-6 is based on the synthesis of ε-caprolactam from cyclohexanone oxime involving the BR. The activation energy for the BR is almost the same as that of the nucleophilic substitution at sp^2 nitrogen. To synthesize various aza-arenes and cyclic imines, such as quinolines, aza-spiro compounds and dihydropyrroles, the intramolecular S_N2-type reaction at the oxime nitrogen is useful [1-6]. Here, we plan to use the BR in combination with a ring-rearrangement metathesis (RRM) [7-24] to generate lactam derivative **1**. The RRM protocol involves a tandem process with several metathetic transformations such as ring-closing metathesis (RCM) and ring-opening metathesis (ROM). The RRM has emerged as a powerful tool in organic synthesis because of its ability to transform simple starting materials into complex targets involving an ingenious design. The retrosynthetic strategy to the target molecule **1** is shown in Figure 1. RRM of the tricyclic allylated compound **2** can deliver the target lactam **1**. The key synthon **2** can be derived by allylation of lactam **3**, which in turn can be prepared via BR starting with the known enone **4** [25-27], derived from dicyclopentadiene (**5**) [28-30].

Results and Discussion

To begin with, the oxidation of dicyclopentadiene (**5**) in the presence of SeO_2 gave 1α-dicyclopentadienol (**6**), which on

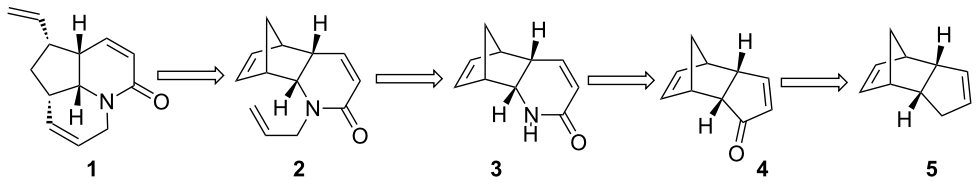

Figure 1: Retrosynthetic analysis of tricyclic amide **1**.

treatment with pyridinium chlorochromate (PCC) [31] delivered the known tricyclic enone **4**. Selective reduction of enone **4** with Zn in AcOH/EtOH under reflux conditions gave the saturated ketone **7** [32] (Scheme 1).

Later, tricyclic ketone **7** was reacted with $NH_2OH{\cdot}HCl$ in the presence of NaOAc in dry MeOH at rt to give a mixture of oximes **8a** and **8b** and this mixture was subjected to a BR under different reaction conditions, like (a) *p*-TsCl, rt, 15 h, CH_3CN (b) *p*-TsCl, reflux, 15 h, CH_3CN (c) PPA, reflux for 20 min. Surprisingly, in all these instances no rearrangement product was observed. Interestingly, when the mixture of oximes **8a** and **8b** was treated with TsCl in the presence of NaOH at rt lactams **9a** and **9b** were obtained in 66% combined yield for two steps (**9a**:**9b** = 2:1) (Scheme 2) but the products were inseparable by column chromatography. Next, we attempted to separate the mixture of these isomers (**9a** and **9b**) by selective crystallization using different solvent systems. Finally, one of the lactam derivative **9a** (δ = 3.86, dd, *J* = 5.8, 2.9 Hz, 1H) was isolated in pure form from ethanol in 20% yield over two steps.

Subsequently, we attempted to synthesize the desired lactam **9a** via Schmidt reaction or BR of the keto derivative **7** in a single step. In this regard, the tricyclic ketone **7** was treated under different reaction conditions. These include: (a) NaN_3, heat 1 day in TFA (b) NaN_3, $FeCl_3$ in DCE at rt and reflux, 1 day and (c) $TMSN_3$, $FeCl_3$ in DCE, 1 day. Surprisingly, the desired lactam **9a** was not formed. Interestingly, when the tricyclic ketone **7** was treated with hydroxylamine-*O*-sulfonic acid (NH_2OSO_3H) in glacial AcOH under reflux conditions, the lactams **9a** and **9b** were obtained in 48% yield (**9a**:**9b** = 2:1) the ratio of oximes **9a** and **9b** was calculated based on ^1H NMR spectral data (Scheme 3).

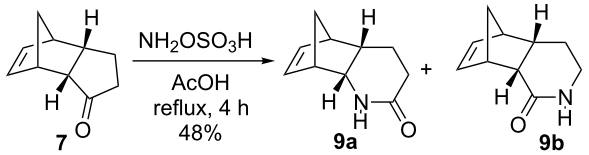

Scheme 3: Beckmann rearrangement reaction in a single step.

Having prepared the lactams **9a** and **9b**, the allylation reaction was attempted with the lactam mixture in the presence of NaH/allyl bromide in dry DMF to generate allyl derivatives **10a** and **10b** in 84% yield. Later, without separation of allyl lactams **10a** and **10b**, RRM was attempted with the lactam mixture under different catalyst conditions. For example, reaction conditions

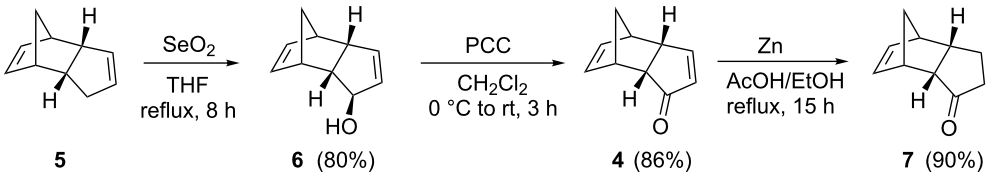

Scheme 1: Synthesis of tricyclic ketone **4**.

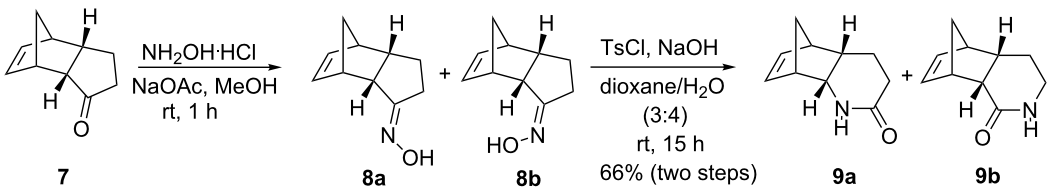

Scheme 2: Beckmann rearrangement of oximes **8a** and **8b**.

such as: (a) G-I in dry CH_2Cl_2, under ethylene atmosphere at rt; (b) G-II in dry CH_2Cl_2, under ethylene atmosphere at rt and (c) G-I and G-II in dry toluene under ethylene atmosphere did not deliver the desired RRM product **1a** (Scheme 4).

Separation of the required isomer from the mixture of oximes **8a** and **8b** or the lactams **9a** and **9b** was not possible by column chromatography because of the same R_f value of the individual compounds. Finally, isolation of the required lactam **9a** from the mixture was accomplished by using crystallization. Since this method is cumbersome, an alternate method was attempted. To this end, we changed our synthetic route and tried to use the unsaturated ketone **4** and hoped for a different outcome during the BR. In this content, oximation of the enone **4** was carried out with $NH_2OH{\cdot}HCl$ in the presence of NaOAc in dry MeOH. The stereoisomeric oximes, i.e., (*E*)-**11b** and (*Z*)-**11a** were separated by silica gel column chromatography to deliver 47% and 23% yields, respectively (Scheme 5).

When the oxime **11a** was treated with TsCl in the presence of NaOH in dioxane/H_2O (3:4 v/v) at rt lactam **12** was formed in 34% yield. However, the oxime **11b** did not give the rearranged product under the same reaction conditions, which clearly indicates that the oxime **11b** is unreactive towards BR (Scheme 6). The stereostructure of the oxime **11b** has been determined by single crystal X-ray diffraction data (Figure 2) [33].

Allylation of lactam **12** in the presence of NaH/allyl bromide in dry DMF gave the allyl derivative **2** in 80% yield. Finally, the RRM of compound **2** was accomplished with G-II catalyst in dry CH_2Cl_2, under ethylene atmosphere at rt in the presence of $Ti(OiPr)_4$ to deliver the tricyclic compound **1** in 90% yield (Scheme 7). Its structure has been established on the basis of ^1H NMR and ^{13}C NMR spectral data and further supported by HRMS data.

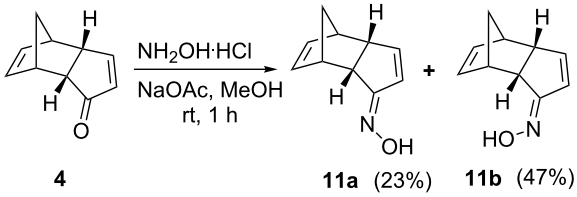

Scheme 5: Synthesis of Beckmann rearrangement precursors.

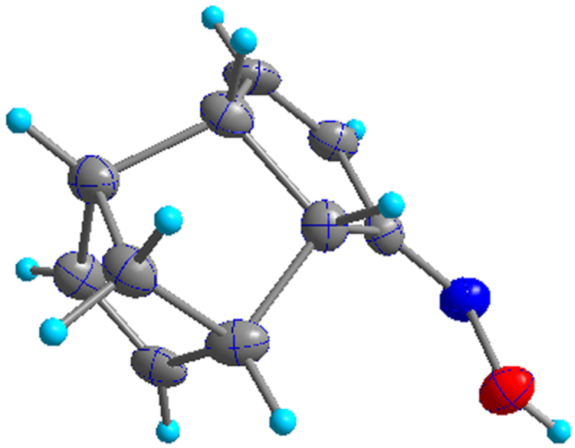

Figure 2: Molecular crystal structure of compound **11b**.

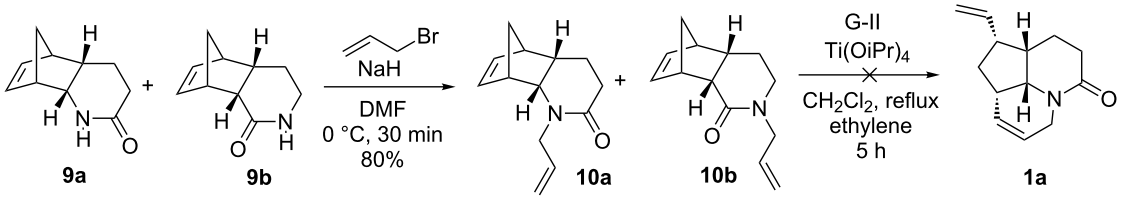

Scheme 4: Synthesis of ring-rearrangement precursors.

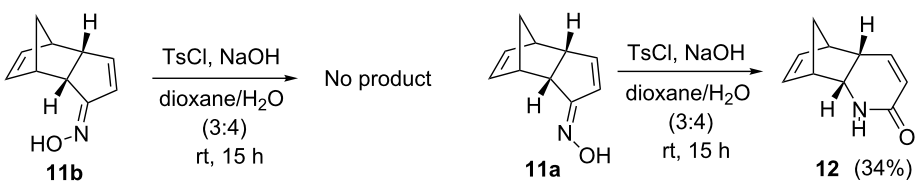

Scheme 6: Beckmann rearrangement of oxime isomers **11a** and **11b**.

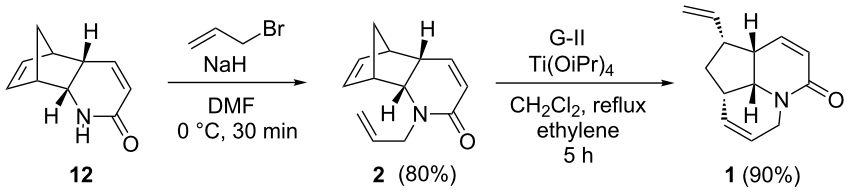

Scheme 7: Synthesis of aza tricyclic compound **1** by RRM.

Conclusion

In summary, we have demonstrated the RRM strategy with the norbornene derivative **2** to deliver the tricyclic compound **1** involving a short synthetic sequence. However, a similar compound **10a** did not deliver the RRM product. For the first time, we have demonstrated that BR in combination with RRM is a useful strategy to generate azacyclic compounds. Here we have used an inexpensive starting material such as dicyclopentadiene (**5**).

Experimental

Synthesis of compounds **9a** and **9b**

Method 1: Analogously as described in [4], a mixture of **7** (2 g, 13.51 mmol), hydroxylamine hydrochloride (1.41 g, 20.27 mmol), NaOAc (1.66 g, 20.27 mmol) and methanol (50 mL) was stirred at rt for 1 h. The residue after evaporation of the solvent was diluted with water and extracted with ether. Removal of ether furnished the crude oxime (2.4 g). *p*-Toluenesulfonyl chloride (6.15 g, 32.28 mmol) was added portion-wise over 15 min to a stirred solution of the crude oxime (2.4 g) and NaOH (2.97 g. 74.44 mmol) in 150 mL dioxane/water 3:4 at 5 °C. The mixture was stirred at rt for 15 h and dioxane was removed in vacuo. The residue was dissolved in CH_2Cl_2 and washed with brine. Removal of the solvent and column chromatography gave a mixture of amide isomers (**9a**, **9b**) (1.45 g, 66%). The amide mixture was crystalized in different solvents and finally one of isomer **9a** was isolated from ethanol 20%.

Method 2: A mixture of **7** (100 mg, 0.68 mmol) and hydroxylamine-O-sulfonic acid (113 mg, 1.0 mmol) in AcOH (5 mL) was heated at reflux conditions for 4 h under nitrogen. After completion of the reaction (TLC monitoring), the reaction mixture was basified with 3 N NaOH solution and the organic layer was extracted with CH_2Cl_2, washed with water, brine and dried by Na_2SO_4. The combined organic layer was concentrated under reduced pressure and column chromatography gave a mixture of amide isomers **9a** and **9b** (1.06 g, 48%). The amide mixture was crystalized in different solvents and finally isomer **9a** was isolated from ethanol. White solid **9a**; mp = 150–155 °C; yield 15%: R_f = 0.30 (EtOAc/pentane 1:1 v/v); IR (neat): 3195 (m), 3067 (w), 2938 (s), 2868 (m), 1674 (s), 1627 (m), 1452 (w), 1434 (w), 1410 (m), 1333 (m), 1252 (w), 1201 (m), 1031 (w), 783 (m), 541 (m) cm^{-1}; ^1H NMR (400 MHz, $CDCl_3$) δ 6.31 (s, 1H), 6.22 (dd, *J* = 5.8, 3.0 Hz, 1H), 6.10 (dd, *J* = 5.8, 3.0 Hz, 1H), 3.86, (dd, *J* = 5.8, 2.9 Hz, 1H), 2.97 (s, 1H), 2.88 (s, 2H), 2.48–2.40 (m, 1H), 2.13–2.05 (m,1H), 1.94–1.87 (m, 1H), 1.56 (dt, *J* = 8.8, 1.8 Hz, 1H), 1.42 (d, *J* = 8.8 Hz, 1H), 1.23–1.13 (m, 1H) ppm; ^{13}C NMR (100 Hz, $CDCl_3$) δ 175.5, 137.6, 134.2, 54.8, 48.0, 47.8, 46.5, 39.49, 31.4, 23.2 ppm.

Synthesis of compounds **11a** and **11b**

Analogously as described in [4], a mixture of **4** (9 g, 61.64 mmol), hydroxylamine hydrochloride (6.41 g, 92.34 mmol), NaOAc (7.58 g, 92.49 mmol) and methanol (225 mL) were stirred at rt for 1 h. The residue after evaporation of the solvent was diluted with water and extracted with diethyl ether. Removal of ether furnished the crude oxime which was purified by silica gel column chromatography by eluting appropriate mixture of ethyl acetate/petroleum ether to afford compounds **11a** (2.29 g, 23%) and **11b** (4.61 g, 47%) as colourless solids.

11a: R_f = 0.29 (EtOAc/pentane 2:8 v/v); IR (neat): 3325 (m), 3013 (m), 2400 (w), 1725 (w), 1337 (w), 1216 (m), 927 (m), 759 (s) cm^{-1}; ^1H NMR (500 MHz, $CDCl_3$) δ 9.15 (s, 1H), 6.54 (dd, *J* = 5.8, 1.3 Hz, 1H), 6.38 (dd, *J* = 5.8, 2.5 Hz, 1H), 5.97 (dd, *J* = 5.6, 2.8 Hz, 1H), 5.77 (dd, *J* = 5.6, 2.9 Hz, 1H), 3.32 (m, 1H), 3.18 (dd, *J* = 10.7, 4.5 Hz, 1H), 3.16 (s, 1H), 2.28 (s, 1H), 2.90 (s, 1H), 1.61 (d, *J* = 8.3 Hz, 1H), 1.47 (d, *J* = 8.3 Hz, 1H) ppm; ^{13}C NMR (125 Hz, $CDCl_3$) δ 165.1, 149.1, 133.3, 133.1, 126.4, 51.0, 50.5, 46.1, 45.9, 44.1 ppm; HRMS (Q-Tof) *m*/*z*: $[M + Na]^+$ calcd for $C_{10}H_{11}NNaO$, 184.0733; found, 184.0734.

11b: mp = 89–91 °C; R_f = 0.30 (EtOAc/petroleum ether 2:8 v/v); IR (neat): 3322 (m), 3020 (m), 2396 (w), 2125 (w), 1705 (m), 1217 (m), 926 (m), 759 (s) cm^{-1}; ^1H NMR (500 MHz, $CDCl_3$) δ 8.71 (s, 1H), 6.30 (dd, *J* = 5.8, 2.5 Hz, 1H), 6.00 (dd, *J* = 5.7, 1.3 Hz, 1H), 5.90 (dd, *J* = 5.6, 3.0 Hz, 1H), 5.76 (dd, *J* = 5.6, 2.9 Hz, 1H), 3.43 (s, 1H), 3.35 (dd, *J* = 6.1, 4.2 Hz, 1H),

3.30 (m, 1H), 2.90 (s, 1H), 1.64 (d, J = 8.3 Hz, 1H), 1.50 (d, J = 8.3, 1H) ppm; ^{13}C NMR (125 Hz, $CDCl_3$) δ 168.1, 147.0, 133.1, 132.9, 131.1, 51.9, 50.8, 45.1, 45.0, 44.1 ppm; HRMS (Q-Tof) m/z: [M + Na]$^+$ calcd for $C_{10}H_{11}NNaO$, 184.0733; found, 184.0737.

Synthesis of compound **12**

Analogously as described in [4], *p*-toluenesulfonyl chloride (2.36 g, 12.42 mmol) was added portionwise over 15 min to a stirred solution of oxime **11a** (1.0 g, 6.21 mmol) and NaOH (1.24 g. 31.05 mmol) in 100 mL dioxane/water 3:4 at 5 °C. The mixture was stirred at rt for 15 h and the dioxane was removed in vacuo. The residue was dissolved in CH_2Cl_2 and washed with the brine. Removal of solvent and column chromatography using an appropriate mixture of ethyl acetate/petroleum ether gave the pure lactam **12** (0.33 g, 34%) as a semi solid. IR (neat): 3020 (m), 2400 (w), 2125 (w), 1678 (w), 1422 (w), 1216 (m), 1049 (w), 1022 (w), 929 (w), 759 (s) cm^{-1}; ^{1}H NMR (500 MHz, $CDCl_3$) δ 6.36–6.34 (m, 1H), 6.15 (dd, J = 5.5, 3 Hz, 1H), 6.07 (dd, J = 5.5, 3 Hz, 1H), 5.96 (bs, 1H), 5.63 (dt, J = 8.5, 2 Hz, 1H), 4.12–4.08 (m, 1H), 3.10 (t, J = 0.5 Hz, 1H), 3.06 (d, J = 0.5 Hz, 1H), 2.99–2.95 (m, 1H), 1.44 (dt, J = 8.5, 2Hz, 1H), 1.25–1.22 (m, 1H) pmm; ^{13}C NMR (125 Hz, $CDCl_3$) δ 164.4, 142.4, 136.9, 134.5, 122.4, 54.9, 49.8, 47.8, 44.5, 39.3 ppm; HRMS (Q-Tof) m/z: [M + Na]$^+$ calcd for $C_{10}H_{11}NNaO$, 184.0733; found, 184.0733.

Synthesis of compound **2**

Analogously as described in [8], a suspension of NaH (20 mg, 0.83 mmol) in dry DMF (5mL), was added to compound **12** (70 mg, 0.43 mmol) in dry DMF (5 mL) and allyl bromide (57 mg, 0.47 mmol) at 0 °C under nitrogen and it was stirred for 20 minutes at 0 °C. After completion of the reaction (TLC monitoring) the reaction mixture was acidified with saturated ammonium chloride and extracted with ethyl acetate. The combined organic layer was washed with water and brine and then dried over sodium sulfate. Later, the organic layer was concentrated under reduced pressure and purified by silica gel column chromatography by eluting with an appropriate mixture of ethyl acetate/petroleum ether to afford compound **2** as a brown liquid (87 mg, 80%). IR (neat): 3370 (s), 2945 (m), 2832 (m), 2532 (w), 2044 (w), 1662 (w), 1450 (m), 1114 (m), 1030 (s), 770 (m) cm^{-1}; ^{1}H NMR (500 MHz, $CDCl_3$) δ 6.25–6.23 (m, 1H), 6.05–6.01 (m, 2H), 5.85–5.77 (m, 1H), 5.67 (dd, J = 10, 2 Hz, 1H), 5.26–5.22 (m, 2H), 4.47–4.46 (m, 1H), 4.02 (dd, J = 10, 3.5 Hz, 1H), 3.65–3.60 (m, 1H), 3.29 (s, 1H), 3.08 (s, 1H), 3.01–2.97 (m, 1H), 1.45 (dt, J = 9, 2 Hz, 1H), 1.21–1.24 (m, 1H) ppm; ^{13}C NMR (125 Hz, $CDCl_3$) δ 162.5, 140.1, 137.1, 133.8, 133.6, 123.1, 117.7, 59.43, 48.4, 47.4, 47.3, 44.7, 40.0 ppm; HRMS (Q-Tof) m/z: [M + Na]$^+$ calcd for $C_{13}H_{15}NNaO$, 224.1046; found, 224.1041.

Synthesis of compound **1**

Analogously as described in [8], to a stirred solution of compound **2** (20 mg, 0.099 mmol) in dry CH_2Cl_2 (20 mL) degassed with nitrogen for 10 minutes, purged with ethylene gas for 10 minutes was then added $Ti(OiPr)_4$ and Grubbs-II catalyst (8.4 mg, 10 mol %) and stirred for 5 h at reflux conditions under ethylene atmosphere. After completion of the reaction (TLC monitoring) the solvent was removed on a rotavapor under reduced pressure and purified by silica gel column chromatography by eluting with an appropriate mixture of ethyl acetate/petroleum ether to afford **1** as a brown coloured semi solid (18 mg, 90%). IR (neat): 3020 (m), 2927 (m), 2861 (m), 2396 (w), 1727 (w), 1608 (w), 1461 (w), 1216 (m), 929 (w), 762 (s) cm^{-1}; ^{1}H NMR (500 MHz, $CDCl_3$) δ 6.35–6.27 (m, 1H), 6.05–5.89 (m, 1H), 5.88–5.83 (m, 1H), 5.75–5.72 (m, 1H), 5.63 (dt, J = 16.0, 9.7 Hz, 1H), 5.02–4.91 (m, 2H), 4.64–4.57 (m, 1H), 4.07–4.03 (m , 1H), 3.50–3.42 (m, 1H), 3.19–3.14 (m, 1H), 3.12–2.94 (m, 1H), 2.62–2.55 (m, 1H), 2.21–2.03 (m, 1H), 1.62–1.53 (m, 1H) ppm; ^{13}C NMR (125 Hz, $CDCl_3$) δ 164.2, 139.6, 139.6, 125.7, 123.5, 123.2, 115.5, 59.0, 58.8, 49.1, 42.3, 40.9, 39.6 ppm; HRMS (Q-Tof) m/z: [M + Na]$^+$ calcd for $C_{13}H_{15}NNaO$, 224.1046; found, 224.1041.

Supporting Information

Supporting Information File 1

NMR spectra of synthesized compounds and X-ray data of compound **11b**.
[http://www.beilstein-journals.org/bjoc/content/supplementary/1860-5397-11-163-S1.pdf]

Acknowledgements

We thank the Department of Science and Technology (DST), New Delhi for the financial support and the Sophisticated Analytical Instrument Facility (SAIF), IIT-Bombay for recording spectral data and also thank Gaddamedi Sreevani and Darshan Mhatre for their help in collecting the X-ray data and structure refinement. S. K. thanks the Department of Science and Technology for the award of a J. C. Bose fellowship. O. R. thanks the University Grants Commission, New Delhi for the award of a research fellowship. J. M thanks DST for the award of inspire fellowship.

References

1. Beckmann, E. *Ber. Dtsch. Chem. Ges.* **1886,** *19,* 988. doi:10.1002/cber.188601901222
2. Blatt, A. H. *Chem. Rev.* **1933,** *12,* 215. doi:10.1021/cr60042a002
3. Chandrasekhar, S. The Beckmann and Related Reactions. In *Comprehensive Organic Synthesis II;* Knochel, P.; Molander, G. A., Eds.; Elsevier, 2014; Vol. 7, pp 770 ff. doi:10.1016/B978-0-08-097742-3.00730-8

4. Mehta, G.; Praveen, M. *J. Org. Chem.* **1995,** *60,* 279. doi:10.1021/jo00106a052
5. Kaur, N.; Sharma, P.; Kishore, D. *J. Chem. Pharm. Res.* **2012,** *4,* 1938.
6. Narasaka, K.; Kitamura, M. *Eur. J. Org. Chem.* **2005,** 4505. doi:10.1002/ejoc.200500389
7. Kotha, S.; Dipak, M. K. *Tetrahedron* **2012,** *68,* 397. doi:10.1016/j.tet.2011.10.018
8. Kotha, S.; Ravikumar, O. *Eur. J. Org. Chem.* **2014,** 5582. doi:10.1002/ejoc.201402273
9. Kotha, S.; Ravikumar, O. *Tetrahedron Lett.* **2014,** *55,* 5781. doi:10.1016/j.tetlet.2014.08.108
10. Zuercher, W. J.; Hashimoto, M.; Grubbs, R. H. *J. Am. Chem. Soc.* **1996,** *118,* 6634. doi:10.1021/ja9606743
11. Beligny, S.; Eibauer, S.; Maechling, S.; Blechert, S. *Angew. Chem., Int. Ed.* **2006,** *45,* 1900. doi:10.1002/anie.200503552
12. Holub, N.; Blechert, S. *Chem. – Asian J.* **2007,** *2,* 1064. doi:10.1002/asia.200700072
13. Li, J.; Lee, D. *Eur. J. Org. Chem.* **2011,** 4269. doi:10.1002/ejoc.201100438
14. Kotha, S.; Singh, K. *Eur. J. Org. Chem.* **2007,** 5909. doi:10.1002/ejoc.200700744
15. Carreras, J.; Avenoza, A.; Busto, J. H.; Peregrina, J. M. *J. Org. Chem.* **2011,** *76,* 3381. doi:10.1021/jo200321t
16. North, M.; Banti, D. *Adv. Synth. Catal.* **2002,** *344,* 694.
17. Scholl, M.; Ding, S.; Lee, C. W.; Grubbs, R. H. *Org. Lett.* **1999,** *1,* 953. doi:10.1021/ol990909q
18. Nguyen, N. N. M.; Leclère, M.; Stogaitis, N.; Fallis, A. G. *Org. Lett.* **2010,** *12,* 1684. doi:10.1021/ol100150f
19. Miege, F.; Meyer, C.; Cossy, J. *Org. Lett.* **2010,** *12,* 248. doi:10.1021/ol9025606
20. Schrock, R. R.; Hoveyda, A. H. *Angew. Chem., Int. Ed.* **2003,** *42,* 4592. doi:10.1002/anie.200300576
21. Trnka, T. M.; Grubbs, R. H. *Acc. Chem. Res.* **2001,** *34,* 18. doi:10.1021/ar000114f
22. Vincent, G.; Kouklovsky, C. *Chem. – Eur. J.* **2011,** *17,* 2972. doi:10.1002/chem.201002558
23. Gao, F.; Stamp, C. T. M.; Thoenton, P. D.; Cameron, T. S.; Doyle, L. E.; Miller, D. O.; Burnell, D. J. *Chem. Commun.* **2012,** *48,* 233. doi:10.1039/C1CC15452D
24. Malik, C. K.; Hossain, M. F.; Ghosh, S. *Tetrahedron Lett.* **2009,** *50,* 3063. doi:10.1016/j.tetlet.2009.04.033
25. Woodward, R. B.; Katz, T. J. *Tetrahedron* **1959,** *5,* 70. doi:10.1016/0040-4020(59)80072-7
26. Rosenblum, M. *J. Am. Chem. Soc.* **1957,** *79,* 3179. doi:10.1021/ja01569a050
27. Lin, H.-C.; Wu, H.-J. *J. Chin. Chem. Soc.* **2009,** *56,* 1072. doi:10.1002/jccs.200900155
28. Álvarez, C.; Peláez, R.; Medarde, M. *Tetrahedron* **2007,** *63,* 2132. doi:10.1016/j.tet.2007.01.001
29. Yamaguchi, T.; Ono, T. *Chem. Ind.* **1968,** 769.
30. Crivello, J. V.; Song, S. *Chem. Mater.* **2000,** *12,* 3674. doi:10.1021/cm000556l
31. Corey, E. J.; Suggs, W. *Tetrahedron Lett.* **1975,** *16,* 2647. doi:10.1016/S0040-4039(00)75204-X
32. Shao, C.; Yu, H.-J.; Wu, N.-Y.; Feng, C.-G.; Lin, G.-Q. *Org. Lett.* **2010,** *12,* 3820. doi:10.1021/ol101531r
33. CCDC-1403298 contains the supplementary crystallographic data for this paper. This data can be obtained free of charge from The Cambridge Crystallographic Data Centre via http://www.ccdc.cam.ac.uk/data_request/cif.

License and Terms

The definitive version of this article is the electronic one which can be found at:
doi:10.3762/bjoc.11.163

BEILSTEIN JOURNAL OF ORGANIC CHEMISTRY

Design and synthesis of hybrid cyclophanes containing thiophene and indole units via Grignard reaction, Fischer indolization and ring-closing metathesis as key steps

Sambasivarao Kotha*, Ajay Kumar Chinnam‡ and Mukesh E. Shirbhate‡

Full Research Paper

Open Access

Address:
Department of Chemistry, Indian Institute of Technology-Bombay, Powai, Mumbai-400 076, India, Fax: 022-2572 7152

Email:
Sambasivarao Kotha* - srk@chem.iitb.ac.in

* Corresponding author ‡ Equal contributors

Keywords:
cyclophane; Grignard reaction; Fischer indolization; ring-closing metathesis

Beilstein J. Org. Chem. **2015,** *11,* 1514–1519.
doi:10.3762/bjoc.11.165

Received: 01 May 2015
Accepted: 13 August 2015
Published: 31 August 2015

This article is part of the Thematic Series "Progress in metathesis chemistry II".

Guest Editor: K. Grela

Abstract

We demonstrate a new synthetic strategy to cyclophanes containing thiophene and indole moieties via Grignard addition, Fischer indolization and ring-closing metathesis as key steps.

Introduction

Modern olefin metathesis catalysts enable a late stage ring-closing step starting with bisolefinic substrates containing polar functional groups [1]. As part of a major program aimed at developing new and intricate strategies to cyclophanes [2-10], we envisioned various building blocks [11] by ring-closing metathesis (RCM) as a key step [12-25]. Cyclophanes containing different heterocyclic systems are difficult to assemble [26-31]. However, we believe that architecturally complex cyclophanes can be accessed by employing a reasonable selection of a synthetic strategy [32]. To enhance the chemical space and also the diversity of cyclophanes the development of powerful and general synthetic methods is highly desirable. Herein, we report a new approach to thiophene- and indole-containing hybrid cyclophane derivatives via Grignard addition, Fischer indolization and RCM as key steps.

Strategy

The retrosynthetic strategy to the target cyclophane **1** containing the thiophene and indole moieties is shown in Figure 1. Here, we conceived thiophene-containing diolefin **3** as a possible synthon to assemble the target molecule **1** via **2**. Route A involves an RCM of **3** followed by Fischer indolization of **2** (Figure 1). Alternatively, Fischer indolization of **3** followed by an RCM of diindole **5** can deliver target molecule **1** (Route B). The advantages of these approaches are: one can vary the length of the alkene chain during the Grignard addition, and generate

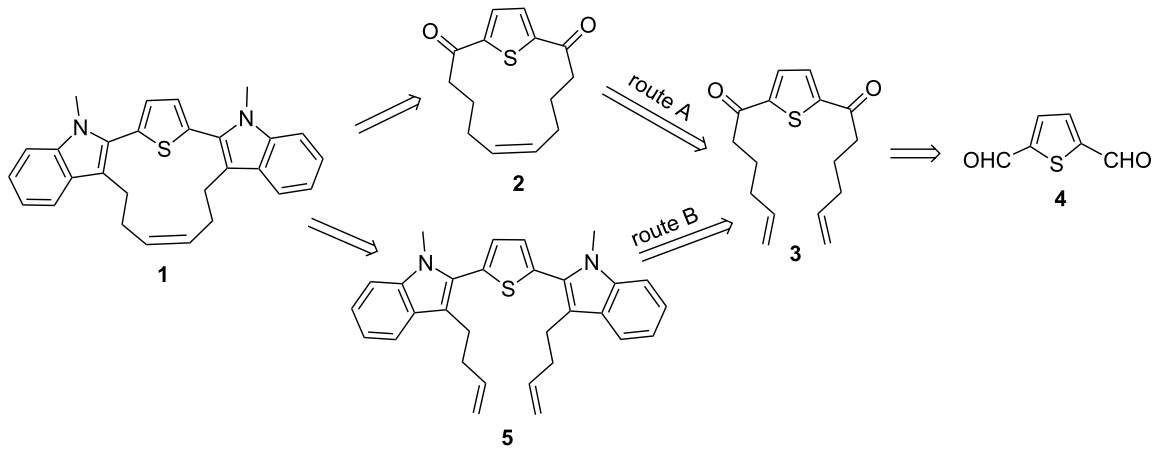

Figure 1: Retrosynthetic approach to hybrid cyclophane derivative **1**.

diverse cyclophanes of different ring size. Diverse aromatic rings can be incorporated by altering the aryl hydrazones during the Fischer indolization step. Finally, the additional double bond generated during the RCM sequence can be further manipulated synthetically.

Results and Discussions

Our synthetic approach to the hybrid cyclophane derivative **1** containing thiophene and indole units started with a Grignard addition reaction. In this context, commercially available thiophene-2,5-dicarbaldehyde (**4**) was reacted with the Grignard reagent [23] derived from 5-bromo-1-pentene to give diol **6** as a diastereomeric mixture (Scheme 1). Alternatively, the dialdehyde **4** can be prepared by using the Vilsmeier–Haack reaction starting with the thiophene [33]. Later, diol **6** was oxidized with MnO_2 [34] to deliver diketone **3**. Our attempts to realize the RCM product **2** with dione **3** via a reaction with Grubbs' catalyst failed to give the expected cyclized product. In most instances, we observed the degradation of the starting material leading to a complex mixture of products as indicated by thin-layer chromatography (TLC). It is known that sulfur can coordinate with the ruthenium catalyst and deactivate the catalytic cycle [35-37]. Therefore, the diolefin did not undergo the RCM sequence.

Next, we explored the alternative option to the target cyclophane **1** involving the bisindolization followed by RCM (Figure 1, Route B). To design aza-polyquinanes, we reported several bisindole derivatives starting with diketones under conditions of a low melting reaction mixture [38-40]. Based on this insight, diketone **3** was subjected to a double Fischer indolization with 1-methyl-1-phenylhydrazine under conditions of a low melting reaction mixture to generate the bisindole derivative **5**. It is interesting to note that conventional conditions (AcOH/HCl) for Fischer indolization were not successful with systems related to **3**. Later, the bisindole derivative **5** was subjected to RCM in the presence of Grubbs' 2nd generation catalyst to deliver the desired product **1** in good yield (Scheme 2). The sulfur atom present in the bisolefin **3** is more accessible for coordination with the Grubbs' catalyst. Whereas in case of the rigid bisindole the sulfur atom is somewhat shielded by the two bulky indole units. Therefore, the bisolefin **5** had undergone RCM easily. The structure of compound **1** has been assigned on the bases of ^{1}H and ^{13}C NMR spectra. However, the configuration of the double bond present in **1** cannot be unambiguously assigned (δ = 5.63, t, J = 5.40 Hz, 2H). The stereochemistry of the double bond was assigned based on single crystal X-ray diffraction studies and it was found to be the *cis* (Figure 2) [41].

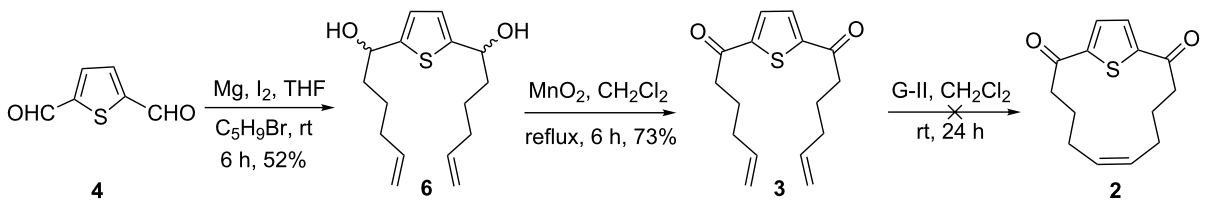

Scheme 1: Attempted synthesis of thiophenophane derivative **2**.

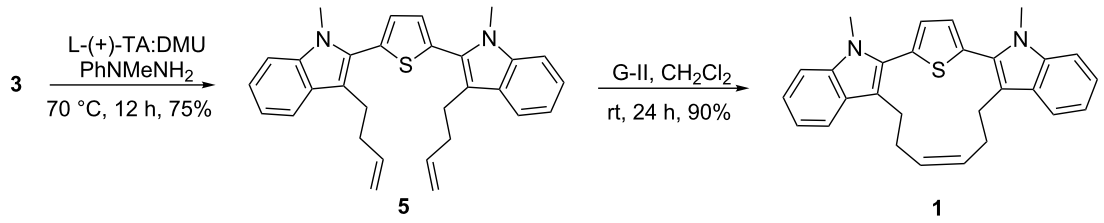

Scheme 2: Synthesis of hybrid cyclophane **1**.

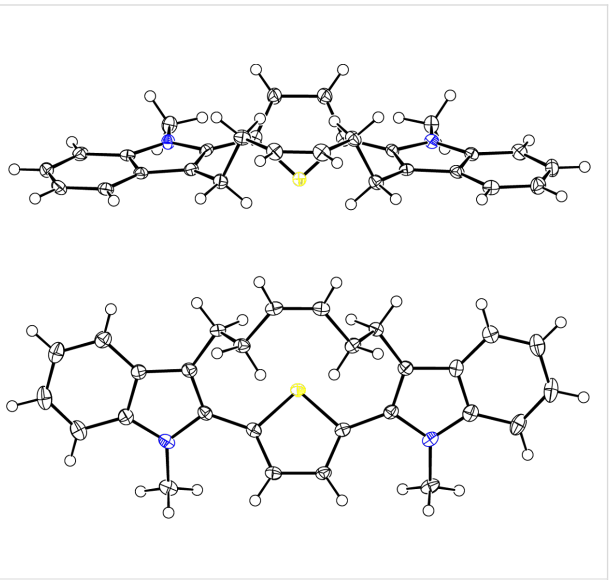

Figure 2: The molecular crystal structure of **1** with 50% probability [41].

Having, demonstrated the RCM step, next, we attempted to expand this strategy. In this regard a synthesis of a higher analogue containing seven carbon alkenyl chains was undertaken. To achieve this goal, thiophene dicarbaldehyde **4** was subjected to a Grignard addition reaction with hexenylmagnesium bromide which gave diol **6a** as a mixture of diastereomers. Further, the diol was subjected to an oxidation step in the presence of MnO_2 to generate dione **3a**. Later, RCM was attempted with various Grubbs' catalysts. However, the RCM product **2a** was not realized (Scheme 3). Under similar reaction conditions, dione **3a** was converted into the bisindole derivative **5a** by using the Fischer indolization and subsequently an RCM protocol to convert **5a** to the cyclized product **1a** (Scheme 4). Based on the structure of compound **1**, here also we anticipate the double bond stereochemistry as "*cis*".

Conclusion

We have developed a simple synthetic strategy to hybrid cyclophane derivatives **1** and **1a** containing thiophene and indole

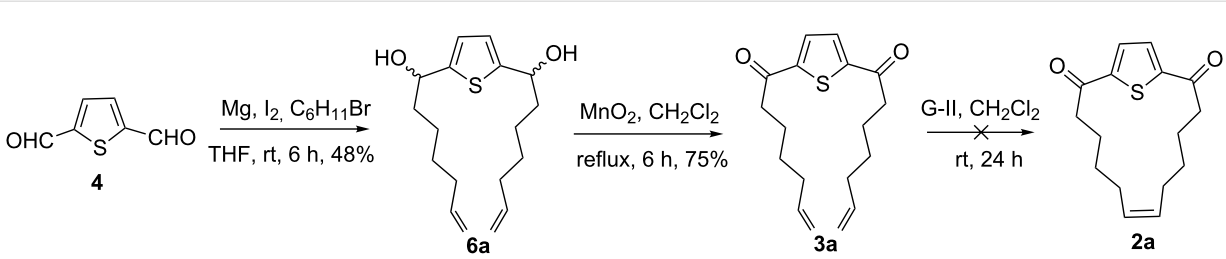

Scheme 3: Attempted synthesis of thiophenophane derivative **2a**.

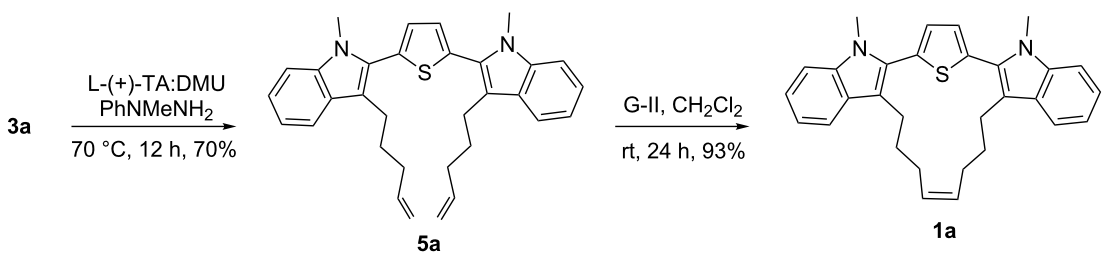

Scheme 4: Synthesis of cyclophane **1a** with a thiophene and an indole moiety.

moieties. Simple dialkene-containing thiophene derivative **3a** failed to deliver the RCM product. However, the sterically congested bisindole systems **5** and **5a** undergo RCM easily. Here, the bulky indole moieties shield the sulfur atom and prevent its coordination with the catalyst. In essence, the power of this synthetic strategy has been harnessed to realize complex cyclophanes starting with simple synthons.

Experimental

Analytical TLC was performed on (10 × 5 cm) glass plate coated with silica gel GF_{254} (containing 13% $CaSO_4$ as a binder). Visualization of the spots on the TLC plate was achieved by exposure to UV light and/or I_2 vapor. Column chromatography was performed using silica gel (100–200 mesh) and the column was usually eluted with an ethyl acetate/petroleum ether mixture (bp 60–80 °C). Melting points were recorded on a Büchi apparatus. ^{1}H NMR and ^{13}C NMR spectral data were recorded on Bruker 400 and 500 MHz spectrometers using TMS as an internal standard and $CDCl_3$ as solvent. The coupling constants (*J*) are given in hertz (Hz). Chemical shifts are expressed in parts per million (ppm) downfield from internal reference, tetramethylsilane. The standard abbreviation s, d, t, q, m, dd and td, refer to singlet, doublet, triplet, quartet, multiplet, doublet of doublet, and triplet of the doublet, respectively. Mass spectral data were recorded on a Q–TOF micromass spectrometer. For the preparation of anhydrous THF, initially it was passed through a column of activated alumina. Later, it was refluxed over and distilled from P_2O_5 and stored over sodium wire. Other reagents and solvents were purchased from commercial suppliers and used without further purification.

General procedure for the Grignard reaction

Analogously as described in [23], Mg turnings and iodine in THF were heated to reflux until the brown colour disappeared. Then, 5-bromo-1-pentene (273 mg, 1.92 mmol) was added and the reaction mixture was stirred for 30 min. Next, thiophene 2,5-dialdehyde (**4**, 100 mg, 0.71 mmol) was added and the resulting mixture was stirred and heated at reflux for 3 h. After completion of the reaction (TLC monitoring), 2 N HCl was added and reaction mixture was stirred for 30 min. The reaction mixture was diluted with EtOAc (10 mL) and H_2O (10 mL) and extracted with EtOAc. The organic layer was washed with brine, dried over Na_2SO_4, and concentrated under reduced pressure. The crude products were purified by column chromatography to obtain the diol **6** (or **6a**).

Compound 6: Semi solid, 104 mg (52%), by using the general procedure 100 mg (0.71 mmol) of thiophene-2,5-carbaldehyde **4** was reacted with 4-pentenylmagnesium bromide. IR (neat): 3943, 3677, 3601, 3050, 2923, 1261, 739 cm^{-1}; ^{1}H NMR (400 MHz, $CDCl_3$) δ 1.35–1.48 (m, 2H), 1.50–1.60 (m, 2H), 1.74–1.89 (m, 4H), 2.09 (q, *J* = 7.10 Hz, 4H), 2.59 (bs, 2H), 4.81 (t, *J* = 6.50 Hz, 2H), 4.94–5.03 (m, 4H), 5.73–5.83 (m, 2H), 6.78 (s, 2H) ppm; ^{13}C NMR (100.6 MHz, $CDCl_3$) δ 25.15, 33.53, 38.60, 70.36, 70.39, 114.93, 123.33, 138.57, 147.99; HRMS (Q-Tof) *m*/*z*: $[M + Na]^+$ calcd for $C_{16}H_{24}NaO_2S$, 303.1389; found, 303.1394.

Compound 6a: Semi solid, 107 mg (48%), by using the general procedure 100 mg (0.71 mmol) of thiophene-2,5-carbaldehyde **4** was reacted with 5-hexenylmagnesium bromide. IR (neat): 743, 1270, 2933, 3042, 3589, 3694, 3942 cm^{-1}; ^{1}H NMR (400 MHz, $CDCl_3$) δ 1.27–1.52 (m, 8H), 1.72–1.89 (m, 4H), 2.01–2.11 (m, 4H), 2.57 (bs, 2H), 4.77–4.84 (m, 2H), 4.91–5.03 (m, 4H), 5.73–5.83 (m, 2H), 6.77 (s, 2H) ppm; ^{13}C NMR (100.6 MHz, $CDCl_3$) δ 25.41, 28.74, 33.73, 39.03, 70.43, 114.58, 123.33, 138.89, 148.03 ppm; HRMS (Q-Tof) *m*/*z*: $[M + H]^+$ calcd for $C_{18}H_{29}O_2S$, 309.1888; found, 309.1959.

General procedure for the MnO_2 oxidation

To the solution of diol derivative **6** (or **6a**) (50 mg) in CH_2Cl_2 (10 mL) was added MnO_2 (4 equiv) as the oxidizing agent at rt and reaction mixture was heated at reflux overnight. After completion of the reaction (TLC monitoring), the crude reaction mixture was filtered through a Celite pad (washed with CH_2Cl_2) and concentrated under reduced pressure. The crude product was purified by column chromatography (silica gel; 5% EtOAc/petroleum ether) to give bisalkene dione derivative **3** (or **3a**).

Compound 3: Semi solid, 71 mg (73%), by using the general procedure 100 mg (0.35 mmol) of thiophene derivative **6** was oxidized with MnO_2 to deliver **3**. IR (neat): 738, 1267, 1687, 2934, 3055, 3357, 3690, 3945 cm^{-1}; ^{1}H NMR (400 MHz, $CDCl_3$) δ 1.84 (q, *J* = 7.28 Hz, 4H), 2.15 (q, *J* = 7.05 Hz, 4H), 2.93 (t, *J* = 4.12 Hz, 4H), 4.99–5.07 (m, 4H), 5.75–5.85 (m, 2H), 7.67 (s, 2H) ppm; ^{13}C NMR (100.6 MHz, $CDCl_3$) δ 23.45, 33.16, 38.86, 115.77, 131.52, 137.81, 148.82, 193.55 ppm; HRMS (Q-Tof) *m*/*z*: $[M + H]^+$ calcd for $C_{16}H_{21}O_2S$, 277.1262; found, 277.1266.

Compound 3a: Semi solid, 74 mg (75%), by using the general procedure 100 mg (0.32 mmol) of thiophene derivative **6a** was oxidized with MnO_2 to deliver **3a**. IR (neat): 740, 1270, 1685, 2939, 3051, 3361, 3689, 3950 cm^{-1}; ^{1}H NMR (400 MHz, $CDCl_3$): δ = 1.44–1.49 (m, 4H), 1.73–1.80 (m, 4H), 2.10 (q, *J* = 7.24 Hz, 4H), 2.92 (t, *J* = 7.50 Hz, 4H), 4.95–5.05 (m, 4H), 5.75–5.85 (m, 2H), 7.67 (s, 2H) ppm; ^{13}C NMR (100.6 MHz, $CDCl_3$) δ 24.05, 28.59, 33.66, 39.68, 115.03, 131.55, 138.50, 148.83, 193.68 ppm; HRMS (Q-Tof) *m*/*z*: $[M + H]^+$ calcd for $C_{18}H_{25}O_2S$, 305.1574; found, 305.1557.

General procedure for the preparation of diindole derivatives

Analogously as described in [39,40], in a typical experiment, 1.5 g of a mixture of L-(+)-tartaric acid/*N*,*N*′-dimethylurea (30:70) was heated to 70 °C to obtain a clear melt. To this melt, 2 mmol of *N*-methyl-*N*-phenylhydrazine and 1 mmol of diketone were added at 70 °C. After completion of the reaction (TLC monitoring by mini work up), the reaction mixture was quenched with water while it was still hot. The reaction mixture was cooled to rt and the solid was filtered through a sintered glass funnel and washed with water (2 × 5 mL). The crude product was dried under vacuum and then it was purified by silica gel column chromatography.

Compound 5: Pale yellow oil, 123 mg (75%), by using the general procedure 100 mg (0.36 mmol) of dione **3** was converted into diindole derivative **5**. IR (neat): 1048, 1097, 1242, 1374, 1447, 1465, 2927, 2974, 3019 cm^{-1}; ^1H NMR (500 MHz, $CDCl_3$) δ 2.49–2.51 (m, 4H), 2.99–3.04 (m, 4H), 3.80 (s, 6H), 5.00–5.13 (m, 4H), 5.92–5.98 (m, 2H), 7.20–7.24 (m, 4H), 7.32–7.36 (m, 2H), 7.39–7.41 (m, 2H), 7.70–7.73 (m, 2H) ppm; ^{13}C NMR (100.6 MHz, $CDCl_3$) δ 24.86, 31.06, 35.70, 109.65, 114.83, 115.88, 119.44, 119.53, 122.59, 127.52, 129.16, 129.72, 134.45, 137.67, 138.79 ppm; HRMS (Q-Tof) *m*/*z*: $[M + H]^+$ calcd for $C_{30}H_{31}N_2S$, 451.2208; found, 451.2212.

Compound 5a: Pale yellow oil, 110 mg (70%), by using the general procedure 100 mg (0.33 mmol) of dione **3a** was converted into bisindole derivative **5a**. IR (neat): 738, 1267, 2934, 3055, 3357, 3690, 3945 cm^{-1}; ^1H NMR (500 MHz, $CDCl_3$) δ 1.83 (t, *J* = 6.50 Hz, 4H), 2.15–2.16 (m, 4H), 2.89–2.93 (m, 4H), 3.78 (s, 6H), 4.95–5.04 (m, 4H), 5.81–5.90 (m, 2H), 7.18–7.21 (m, 4H), 7.30–7.33 (m, 2H), 7.37–7.39 (m, 2H), 7.67–7.79 (m, 2H) ppm; ^{13}C NMR (125.6 MHz, $CDCl_3$) δ 24.59, 30.69, 31.04, 33.91, 109.63, 114.67, 116.52, 119.48, 122.57, 127.62, 129.18, 129.67, 134.56, 137.70, 138.92 ppm; HRMS (Q-Tof) *m*/*z*: $[M + H]^+$ calcd for $C_{32}H_{35}N_2S$,479.2521; found, 479.2548.

General procedure for RCM reaction

Analogously as described in [42], a solution of bisindole-alkene derivative **5** (0.05 mmol) in dry CH_2Cl_2 (50 mL) was degassed with N_2 gas for 10 min. Then, Grubbs' second generation catalyst (10 mol %) was added and the reaction mixture was stirred at room temperature for 24 h. After completion of the reaction (TLC monitoring), the solvent was removed under reduced pressure and the crude product was purified by silica gel column chromatography (5% EtOAc/petroleum ether) to give the RCM compound **1** as a colourless solid.

Compound 1: White solid, 25 mg (90%), by using the general procedure 30 mg (0.06 mmol) of bisindole **5** was treated with Grubbs' second generation catalyst to deliver RCM product **1**. Mp 187–189 °C; IR (neat): 1098, 1265, 1364, 1458, 1644, 1734, 2858, 2926 cm^{-1}; ^1H NMR (400 MHz, $CDCl_3$) δ 2.09–2.15 (m, 4H), 2.96–3.01 (m, 4H), 3.92 (s, 6H), 5.63 (t, *J* = 5.40 Hz, 2H), 7.15–7.19 (m, 4H), 7.28–7.30 (m, 2H), 7.37 (d, *J* = 8.16 Hz, 2H), 7.65 (d, *J* = 7.88 Hz, 2H) ppm; ^{13}C NMR (125.6 MHz, $CDCl_3$): *δ* 26.20, 28.14, 30.80, 109.64, 115.73, 118.89, 119.65, 122.54, 127.75, 128.23, 130.16, 130.31, 134.28, 137.05 ppm; HRMS (Q-Tof) *m*/*z*: $[M + H]^+$ calcd for $C_{28}H_{27}N_2S$, 423.1895; found, 423.1893.

Compound 1a: White solid, 35 mg (93%), By using the general procedure 40 mg (0.08 mmol) of diindole **5a** was treated with Grubbs' second generation catalyst to deliver RCM product **1a**. Mp 183–185 °C; IR (neat): 1048, 1245, 1374, 1448, 1742, 1889, 2085, 2943, 2987, 3464, 3628 cm^{-1}; ^1H NMR (500 MHz, $CDCl_3$) δ 1.76–1.78 (m, 4H), 2.03 (d, *J* = 5.25 Hz, 4H), 2.96 (t, *J* = 7.80 Hz, 4H), 3.80 (s, 6H), 5.37 (s, 2H), 7.13–7.18 (m, 4H), 7.27–7.30 (m, 2H), 7.35–7.37 (m, 2H), 7.67 (d, *J* = 7.85 Hz, 2H) ppm; ^{13}C NMR (125.6 MHz, $CDCl_3$) δ 23.33, 30.45, 30.96, 31.14, 109.64, 116.79, 119.43, 122.49, 127.68, 128.95, 129.68, 130.52, 134.11, 137.58 ppm; HRMS (Q-Tof) *m*/*z*: $[M + H]^+$ calcd for $C_{30}H_{31}N_2S$, 451.2208; found, 451.2192.

Supporting Information

Supporting Information File 1

Copies of ^1H, ^{13}C NMR and HRMS spectra for all new compounds.
[http://www.beilstein-journals.org/bjoc/content/supplementary/1860-5397-11-165-S1.pdf]

Acknowledgements

We thank the Department of Science and Technology (DST), New Delhi for the financial support and Sophisticated Analytical Instrument Facility (SAIF), IIT-Bombay for recording spectral data. S. K. thanks the Department of Science and Technology for the award of a J. C. Bose fellowship. A. K. C. thanks the University Grants Commission, New Delhi for the award of a research fellowship. M. E. S. thanks the IIT-Bombay for the award of a research fellowship.

References

1. Nilewski, C.; Carreira, E. M. *Eur. J. Org. Chem.* **2012,** 1685–1698. doi:10.1002/ejoc.201101525
2. Hopf, H.; Gleiter, R. *Modern Cyclophane Chemistry;* Wiley-VCH: Weinheim, Germany, 2004.

3. Keehn, P. M.; Rosenfeld, S. M. *Cyclophanes;* Acadamic Press: New York, 1983; Vol. 2.
4. Pigge, F. C.; Ghasedi, F.; Rath, N. P. *J. Org. Chem.* **2002,** *67,* 4547–4552. doi:10.1021/jo0256181
5. Gibe, R.; Green, J. R.; Davidson, G. *Org. Lett.* **2003,** *5,* 1003–1005. doi:10.1021/ol027564n
6. Reiser, O.; König, K.; Meerholz, K.; Heinze, J.; Wellauer, T.; Gerson, F.; Frim, R.; Rabinovitz, M.; de Meijere, A. *J. Am. Chem. Soc.* **1993,** *115,* 3511–3518. doi:10.1021/ja00062a015
7. Fallis, A. G. *Synthesis* **2004,** 2249–2267. doi:10.1055/s-2004-832847
8. Frampton, M. J.; Anderson, H. L. *Angew. Chem., Int. Ed.* **2007,** *46,* 1028–1064. doi:10.1002/anie.200601780
9. Xi, H.-T.; Zhao, T.; Sun, X.-Q.; Miao, C.-B.; Zong, T.; Meng, Q. *RSC Adv.* **2013,** *3,* 691–694. doi:10.1039/c2ra22802e
10. Wex, B.; Jradi, F. M.; Patra, D.; Kaafarani, B. R. *Tetrahedron* **2010,** *66,* 8778–8784. doi:10.1016/j.tet.2010.08.073
11. Kotha, S. *Acc. Chem. Res.* **2003,** *36,* 342–351. doi:10.1021/ar020147q
12. Fürstner, A.; Stelzer, F.; Rumbo, A.; Krause, H. *Chem. – Eur. J.* **2002,** *8,* 1856–1871. doi:10.1002/1521-3765(20020415)8:8<1856::AID-CHEM1856>3.0.CO;2-R
13. Huang, M.; Song, L.; Liu, B. *Org. Lett.* **2010,** *12,* 2504–2507. doi:10.1021/ol100692x
14. Kotha, S.; Chavan, A. S.; Shaikh, M. *J. Org. Chem.* **2012,** *77,* 482–489. doi:10.1021/jo2020714
15. Alcaide, B.; Almendros, P.; Quirós, M. T.; Lázaro, C.; Torres, M. R. *J. Org. Chem.* **2014,** *79,* 6244–6255. doi:10.1021/jo500993x
16. Kotha, S.; Mandal, K. *Chem. – Asian J.* **2009,** *4,* 354–362. doi:10.1002/asia.200800244
17. Kotha, S.; Dipak, M. K. *Tetrahedron* **2012,** *68,* 397–421. doi:10.1016/j.tet.2011.10.018
18. Kotha, S.; Sreenivasachary, N.; Mohanraja, K.; Durani, S. *Bioorg. Med. Chem. Lett.* **2001,** *11,* 1421–1423. doi:10.1016/S0960-894X(01)00227-X
19. Kotha, S.; Sreenivasachary, N. *Bioorg. Med. Chem. Lett.* **1998,** *8,* 257–260. doi:10.1016/S0960-894X(98)00002-X
20. Kotha, S.; Bansal, D.; Singh, K.; Banerjee, S. *J. Organomet. Chem.* **2011,** *696,* 1856–1860. doi:10.1016/j.jorganchem.2011.02.019
21. Kotha, S.; Manivannan, E. *ARKIVOC* **2003,** No. iii, 67–76.
22. Kotha, S.; Ali, R.; Chinnam, A. K. *Tetrahedron Lett.* **2014,** *55,* 4492–4495. doi:10.1016/j.tetlet.2014.06.049
23. Kotha, S.; Waghule, G. T.; Shirbhate, M. E. *Eur. J. Org. Chem.* **2014,** 984–992. doi:10.1002/ejoc.201301493
24. Kotha, S.; Shirbhate, M. E. *Tetrahedron Lett.* **2014,** *55,* 6972–6975. doi:10.1016/j.tetlet.2014.10.092
25. Kotha, S.; Waghule, G. T. *Tetrahedron Lett.* **2014,** *55,* 4264–4268. doi:10.1016/j.tetlet.2014.05.129
26. Raatikainen, K.; Huuskonen, J.; Kolehmainen, E.; Rissanen, K. *Chem. – Eur. J.* **2008,** *14,* 3297–3305. doi:10.1002/chem.200701862
27. Rajakumar, P.; Swaroop, M. G. *Tetrahedron Lett.* **2006,** *47,* 3019–3022. doi:10.1016/j.tetlet.2006.03.013
28. Dohm, J.; Vögtle, F. *Top. Curr. Chem.* **1992,** *161,* 69–106. doi:10.1007/3-540-54348-1_8
29. Matsuoka, Y.; Ishida, Y.; Sasaki, D.; Saigo, K. *Chem. – Eur. J.* **2008,** *14,* 9215–9222. doi:10.1002/chem.200800942
30. Tanaka, K. *Synlett* **2007,** 1977–1993. doi:10.1055/s-2007-984541
31. Garrison, J. C.; Panzner, M. J.; Tessier, C. A.; Youngs, W. J. *Synlett* **2005,** 99–102. doi:10.1055/s-2004-836042
32. Deslongchamps, P. *Aldrichimica Acta* **1991,** *24,* 43–56.
33. Mikhaleva, A. I.; Ivanov, A. V.; Skital'tseva, E. V.; Ushakov, I. A.; Vasil'tsov, A. M.; Trofimov, B. A. *Synthesis* **2009,** 587–590. doi:10.1055/s-0028-1083312
34. Wei, X.; Taylor, R. J. K. *J. Org. Chem.* **2000,** *65,* 616–620. doi:10.1021/jo9913558
35. Shon, Y.-S.; Lee, T. R. *Tetrahedron Lett.* **1997,** *38,* 1283–1286. doi:10.1016/S0040-4039(97)00072-5
36. Ghosh, S.; Ghosh, S.; Sarkar, N. *J. Chem. Sci.* **2006,** *118,* 223–235.
37. Samojłowicz, C.; Grela, K. *ARKIVOC* **2011,** No. iv, 71–81.
38. Gore, S.; Baskaran, S.; König, B. *Org. Lett.* **2012,** *14,* 4568–4571. doi:10.1021/ol302034r
39. Kotha, S.; Chinnam, A. K. *Synthesis* **2014,** *46,* 301–306. doi:10.1055/s-0033-1340341
40. Kotha, S.; Chinnam, A. K. *Heterocycles* **2015,** *90,* 690–697. doi:10.3987/COM-14-S(K)35
41. CCDC 1060941 contains the supplementary crystallographic data for this paper. These data can be obtained free of charge from The Cambridge Crystallographic Data Centre via http://www.ccdc.cam.ac.uk
42. Kotha, S.; Chavan, A. S.; Dipak, M. K. *Tetrahedron* **2011,** *67,* 501–504. doi:10.1016/j.tet.2010.10.080

License and Terms

BEILSTEIN JOURNAL OF ORGANIC CHEMISTRY

Ruthenium indenylidene "1st generation" olefin metathesis catalysts containing triisopropyl phosphite

Stefano Guidone, Fady Nahra, Alexandra M. Z. Slawin and Catherine S. J. Cazin*

Full Research Paper

Open Access

Address:
EaStCHEM School of Chemistry, University of St Andrews, St Andrews, UK, KY16 9ST, UK

Email:
Catherine S. J. Cazin* - cc111@st-andrews.ac.uk

* Corresponding author

Keywords:
1st generation; indenylidene; metathesis; phosphite; ruthenium

Beilstein J. Org. Chem. **2015,** *11,* 1520–1527.
doi:10.3762/bjoc.11.166

Received: 16 June 2015
Accepted: 05 August 2015
Published: 01 September 2015

This article is part of the Thematic Series "Progress in metathesis chemistry II".

Guest Editor: K. Grela

Abstract

The reaction of triisopropyl phosphite with phosphine-based indenylidene pre-catalysts affords "1st generation" *cis*-complexes. These have been used in olefin metathesis reactions. The *cis*-Ru species exhibit noticeable differences with the *trans*-Ru parent complexes in terms of structure, thermal stability and reactivity. Experimental data underline the importance of synergistic effects between phosphites and L-type ligands.

Introduction

The olefin metathesis reaction is a powerful tool for C–C bond formation in the synthesis of highly valuable organic compounds [1-4]. Protocols involving W-, Mo- and Ru-based pre-catalysts can shorten or provide alternative synthetic pathways for the synthesis of natural products displaying complex chemical structures [5-9]. Ru-based pre-catalysts are known to be more air-, moisture- and functional-group tolerant compared to early transition metal complexes [10-13]. In general, the commonly used Ru(II)-based pre-catalysts have five ligands in the metal coordination sphere and adopt a distorted square pyramidal geometry (Figure 1).

The basic components of this structure include two L-type ligands mutually *trans* (e.g., phosphines and *N*-heterocyclic carbene) and two halides. The apex of the pyramid is occupied by an alkylidene moiety, such as a benzylidene or an indenylidene. Mixed NHC/phosphine complexes (**G-II** and **Ind-II**) known as "2nd generation" pre-catalysts generally display higher catalytic activity than "1st generation" complexes (**G-I** and **Ind-I**) containing two phosphines [14-23]. The most common phosphine, so called "throw-away ligand", is tricyclohexyl phosphine [10-23]. In other words, such phosphorus donor ligands dissociate from the metal center to afford the $14e^-$ active species [10-13,24]. In order to reduce the cost of the Ru-based pre-catalyst, our group has investigated the use of phosphites as an economical alternative to phosphines. The reaction of triisopropyl phosphite with the pyridine-containing indenylidene complex [$RuCl_2$(Ind)(SIMes)(py)] (SIMes = *N*,*N*'-

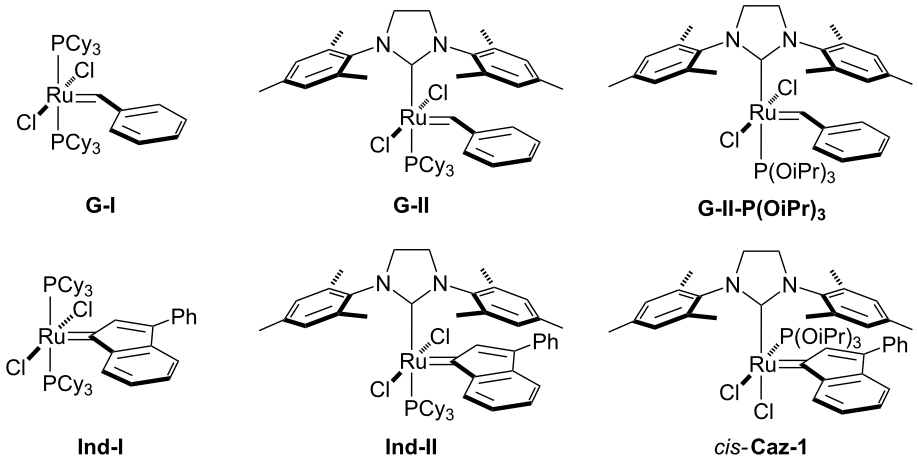

Figure 1: Examples of ruthenium complexes used in olefin metathesis reactions.

bis[2,4,6-(trimethyl)phenyl]imidazolidin-2-ylidene) afforded a Ru pre-catalyst displaying an unusual *cis*-geometry [25]. ***cis*-Caz-1**, which is more thermodynamically stable than its *trans*-isomer represents a breakthrough in catalyst-design for metathesis reactions of challenging hindered substrates (Figure 1) [25-34]. The latent behavior exhibited by ***cis*-Caz-1** can be of interest in fields such as polymer chemistry, where its thermally-switchable properties can be used to inhibit polymerization during the storage of monomer-catalyst mixtures, and/or to initiate polymerization on demand through use of a stimulus [35,36]. The use of this catalyst in the ring-closing metathesis (RCM) reaction gave excellent conversions of challenging substrates, even at low catalyst loadings. The high activity and robustness of ***cis*-Caz-1** is derived from synergistic effects between the σ-donor ligand NHC and the π-acidic triisopropyl phosphite [25,37]. Subsequently, the benzylidene analogue **G-II-P(OiPr)$_3$** was also reported. The latter displayed a typical *trans*-configuration, seen in other Ru pre-catalysts, and gave a similar catalytic activity to that of the phosphine-containing parent **G-II** [26].

Because of the recent interest in "1st generation" complexes [9,38-40], previous findings concerning "2nd generation" complexes [25-33] and the desire to further reduce catalyst cost, the aim of this contribution is to replace the phosphine ligands in **Ind-I** with the less expensive triisopropyl phosphite and to study the structural and catalytic properties of these new species.

Results and Discussion

Synthesis of [RuCl$_2$(Ind)(PCy$_3$){P(OiPr)$_3$}] (**1**)

Attempts towards the synthesis of a mixed phosphine/phosphite complex involved the reaction of **Ind-I** with a stoichiometric amount of triisopropyl phosphite. Complex **1** was isolated in analytically pure form in 85% yield, after recrystallization, using a simple ligand exchange reaction (Scheme 1).

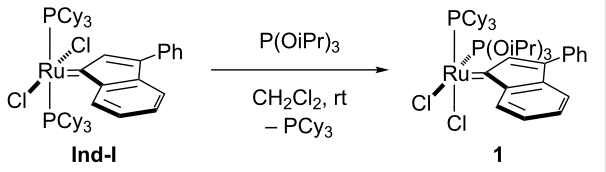

Scheme 1: Synthesis of the mixed phosphine/phosphite complex **1**.

Similarly to the mixed NHC/phosphite species **Caz-1** [25], the *cis*-geometry is the most thermodynamically stable conformation for the phosphine/phosphite complex **1**. The corresponding *trans*-isomer was not isolated due to the fast isomerization occurring under the reaction conditions, although traces of transient species were detected by ^{31}P-{^{1}H} NMR spectroscopy (see Supporting Information File 1, section 4). The ^{1}H NMR spectrum of **1** in CD_2Cl_2 showed the typical indenylidene proton system (characteristic doublet at low field, δ_H = 8.80 ppm). Coalescence of the aliphatic protons assigned to the cyclohexyl and the phosphite moieties was also observed at room temperature. These signals were resolved at a lower temperature (193 K). The ^{13}C-{^{1}H} NMR spectrum showed a doublet of doublets for the carbene carbon at δ_C = 290.3 ppm with two $^2J_{CP}$ of 12.5 and 24.5 Hz (cf., ***cis*-Caz-1**; 24.7 Hz) [25]. In the ^{31}P-{^{1}H} NMR spectrum, two doublets at 120.1 and 47.4 ppm with $^2J_{PP}$ of 37.0 Hz were observed, consistent with a *cis*-disposition of the phosphorus donor ligands. This geometry was confirmed by X-ray diffraction analysis on a single crystal (Figure 2).

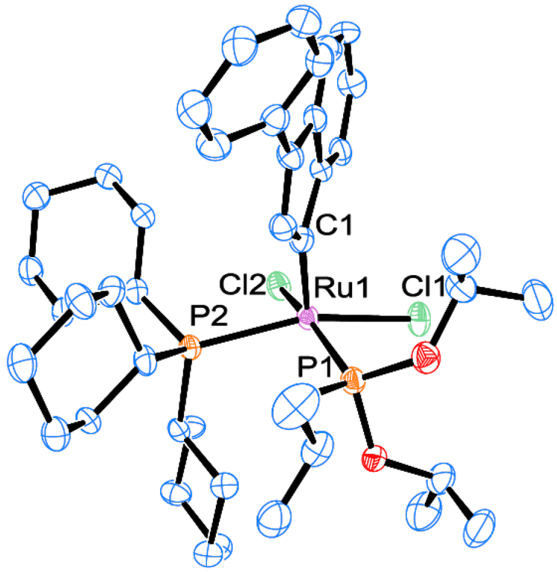

Figure 2: Molecular structure of mixed phosphine/phosphite complex **1**. Hydrogen atoms are omitted for clarity.

Synthesis of $[RuCl_2(Ind)\{P(OiPr)_3\}_2]$ (**2**)

The synthesis of the bis-phosphite species **2** was first attempted by the reaction of **Ind-I** with 2.5 equivalents of $P(OiPr)_3$. Full conversion of the starting material was observed affording complex **2** (Scheme 2). Unfortunately, all attempts to purify **2** failed due to the presence of PCy_3 decomposition products. The PPh_3 adduct **Ind-I^0** was then employed as alternative starting material for the ligand substitution reaction with the phosphite (Scheme 2) (see Supporting Information File 1, section 4). During the recrystallization from dichloromethane/pentane, compound **3** was detected as a decomposition product [41].

Due to the high solubility of this species and difficulties encountered in the purification process, product **2** was isolated with traces of compound **3** still present. In the ^{1}H NMR spectrum of **2** in CD_2Cl_2 (with **3** present), the characteristic doublet at δ_H = 8.53 ppm for the indenylidene system was observed. The ^{13}C-{^{1}H} NMR spectrum contains a doublet of doublets for the carbene carbon at δ_C = 291.1 ppm with two similar $^2J_{CP}$ of 22.0 Hz (cf. *cis*-**Caz-1**, 24.7 Hz) [25]. In the ^{31}P-{^{1}H} NMR spectrum, two singlets at δ_P = 123.0 ppm and 10.9 ppm corresponding to **2** and **3**, respectively, were detected. Fortunately, we were able to cleanly isolate **3**, which allowed its full characterization and assignment. Crystals suitable for X-ray diffraction studies were grown for both species. These studies confirmed the relative *cis*-disposition of the phosphite ligands in **2** and the structure of **3** (Figure 3).

Complexes **1** and **2** display a rare distorted *cis*-square pyramidal geometry as observed in the case of *cis*-**Caz-1** [25]. The *cis*-geometry differentiates these species from other "1st generation" complexes that display the more common *trans*-geometry [14-17]. Comparing the details of the three structures in Table 1 (entries 1 to 3), the Ru–C_{NHC} bond distances are found shorter than Ru–$P_{phosphite}$, and both of them are shorter than Ru–$P_{phosphine}$ (Ru(1)–P(2) complex **1**) [34].

From data listed in Table 1, the Ru–P bond appears stronger in the case of the Ru–phosphite than the Ru–phosphine scenario, suggesting the latter as the leaving ligand in catalysis (see Supporting Information File 1, section 5).

Catalytic activity in ring-closing metathesis (RCM)

The reactivity of the mixed phosphine/phosphite complex **1** was first evaluated in the RCM of the easily cyclized diethyl diallylmalonate (**4**) (see Supporting Information File 1, section 2). The need for thermal activation for this pre-catalyst was clearly revealed by the low catalytic activity at 30–50 °C and the high conversion observed at 80 °C in toluene (0.1 mol % of **1**, 94% conv.). Contrary to **1**, the phosphine-based **Ind-I** initiates at 30 °C exhibiting good catalytic activity and undergoes fast decomposition at higher temperature with moderate conversion (see Supporting Information File 1, section 2). This trend was further studied by profiling reactions under catalytic conditions (Figure 4).

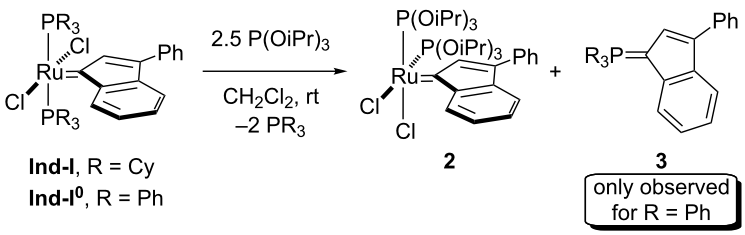

Scheme 2: Synthesis of the bis-phosphite complex **2**.

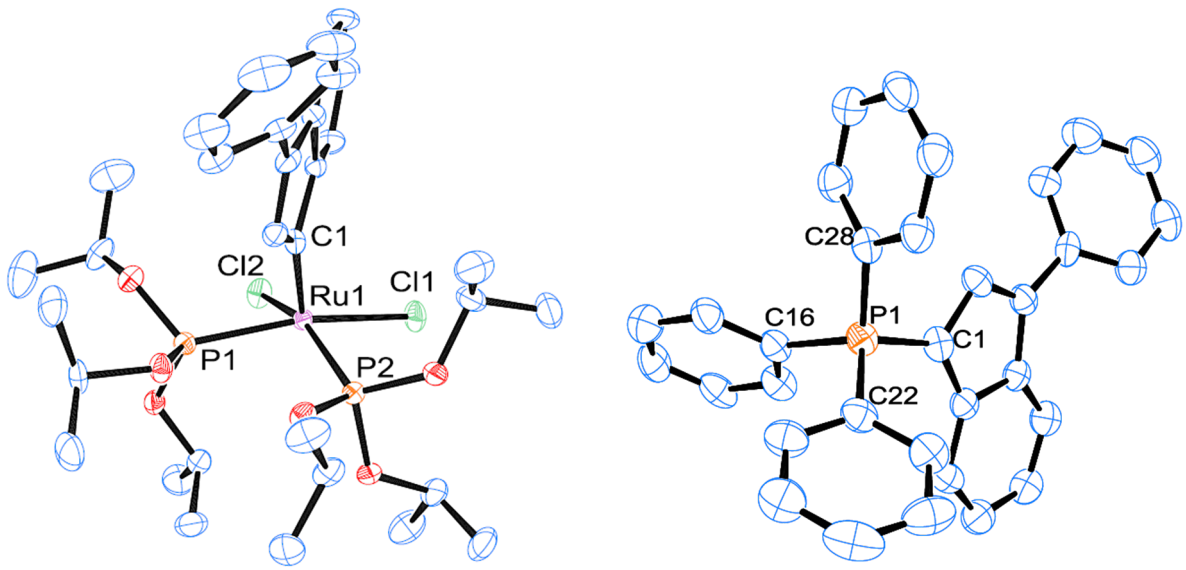

Figure 3: Molecular structure of **2** and the ylide **3**. Hydrogen atoms and solvent molecules are omitted for clarity. Selected bond distances (Å) and angles (°) (ESD) for compound **3**: P(1)–C(1), 1.713(5); P(1)–C(28), 1.795(5); P(1)–C(22), 1.805(5); P(1)–C(16), 1.811(5); C(1)–P(1)–C(28), 106.2(2); C(1)–P(1)-C(22), 113.1(3); C(28)–P(1)–C(22), 109.0(2); C(1)–P(1)–C(16), 113.3(2); C(28)–P(1)–C(16), 109.2(2); C(22)–P(1)–C(16), 105.9(2).

Table 1: Selected bond distances (Å) and angles (°) for **1**, **2** and *cis*-**Caz-1**.

Entry	Parameter	**1**	**2**	*cis*-**Caz-1**[25]
1	Ru(1)–C(1)	1.873(14)	1.869(3)	1.881(8)
2	Ru(1)–P(1)	2.239(4)	2.2300(9)	2.249(2)
3	Ru(1)–P(2)	2.387(4)	2.2663(8)	–
4	Ru(1)–C(NHC)	–	–	2.067(7)
5	Ru(1)–Cl(1)	2.398(4)	2.3999(9)	2.4036(18)
6	Ru(1)–Cl(2)	2.369(3)	2.3789(8)	2.3974(19)
7	P(1)–Ru(1)–P(2)	98.74(13)	97.34(3)	–
8	C(NHC)–Ru(1)–P(1)	–	–	100.06(19)
9	C(1)–Ru(1)–P(1)	90.2(5)	90.94(10)	90.5(2)
10	C(1)–Ru(1)–P(2)	94.3(4)	86.41(9)	–
11	C(1)–Ru(1)–C(NHC)	–	–	98.7(3)

An induction period was observed for **1** at the early stage of the catalysis, a behavior similar to *cis*-**Caz-1** [25], followed by a fast reaction with full conversion of the substrate at 80 °C in less than 50 min. These features prompted us to hypothesize an isomerization step from the *cis*-pre-catalyst **1** to the corresponding *trans* isomer as reported for *cis*-**Caz-1** (see Supporting Information File 1, section 2) [25]. Under the same conditions, instant pre-catalyst initiation and fast decomposition of the active species were observed for the phosphine-based pre-catalyst **Ind-I** (86% conversion after 30 min). When the experiment was performed at 30 °C, **Ind-I** exhibited slower conversion of the substrate, reaching complete conversion after 4 h [22]. The reaction profiles show the importance of synergistic effects in the case of the mixed phosphine/phosphite system. Complex **1** is a thermally-switchable, latent pre-catalyst displaying higher thermal stability compared to the phosphine-based **Ind-I**.

Consequently, a brief study of the scope of the reaction was investigated employing "1st generation" complexes **1** and **Ind-I** (Table 2).

The diene **6** was poorly converted by mixed $PCy_3/P(OR)_3$ complex **1**, whereas 94% conversion was obtained with **Ind-I** (Table 2, entries 1–4). In the case of tri-substituted diene **8**, a more challenging substrate compared to **6**, pre-catalyst **1** gave

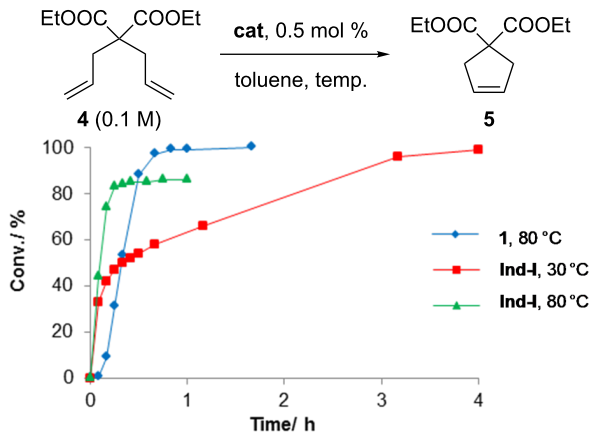

Figure 4: Reaction profiles of mixed phosphine/phosphite **1** and phosphine-based **Ind-I** in the RCM of **4** (lines are visual aids and not curve fits).

79% conversion while **Ind-I** converted 33% of the substrate at 80 °C and 53% at 30 °C (Table 2, entries 5–7). The tosylamide derivative **10** was converted into product **11** by **1** (1 mol %) with 41% conversion (Table 2, entry 8). When the loading was increased to 2 mol %, no improvement in the conversion was detected (Table 2, entry 9). A higher catalytic activity was observed for **Ind-I** with 77% conversion when using 2 mol % pre-catalyst at 30 °C (Table 2, entry 13). Complex **1** was active in the ring-closing enyne metathesis (RCEYM) with 78% conversion of substrate **12** obtained with 1 mol % catalyst loading (Table 2, entry 14). A higher conversion of compound **12** was detected with **Ind-I** (98%, Table 2, entry 15).

Conclusion

The influence of triisopropyl phosphite in Ru-based indenylidene "1st generation" complexes has been presented. The mixed phosphine/phosphite complex **1** and the bis-phosphite complex **2** adopt distorted square pyramidal geometries with the P-donor ligands mutually *cis* as the most thermodynamically stable conformation. The isolation of the corresponding *trans*-isomers was not possible due to a fast isomerization process occurring during the synthesis of the complexes. Pre-catalyst **1** was found to be active in olefin metathesis reaction showing similarities with *cis*-**Caz-1** in terms of reactivity. Both pre-catalysts need thermal activation; they display an induction period in the reaction profiling and exhibit higher thermal stability compared to their phosphine-based analogues. In terms of catalytic efficiency, **Ind-I** was found more active than **1** unless higher thermal stability is needed. Indeed, in the case of the malonate derivative **8**, pre-catalyst **1** afforded the tri-substituted ring-closed product in 71% isolated yield. The similar structural and catalytic properties observed in the mixed phosphine/phosphite complex **1** and the mixed NHC/phosphite *cis*-**Caz-1** suggest the importance of synergistic effects involving phosphites, an inexpensive alternative to phosphines for Ru-based pre-catalysts, and the L-type ligands, a concept that can be used to incite further improvements in catalyst design.

Table 2: Scope of the reaction employing **1** and **Ind-I**.[a]

Entry	Substrate	Product	Pre-catalyst (mol %)	*T* (°C)	Conv. (%)[b]
1	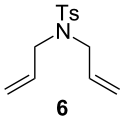		**1** (0.1)	80	<1
2			**1** (1)	80	4
3			**Ind-I** (0.1)	80	94
4	**6**	**7**	**Ind-I** (0.1)	30	94
	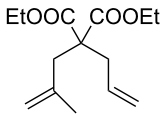	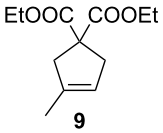			
5			**1** (1)	80	79 (71)
6			**Ind-I** (1)	80	33
7	**8**	**9**	**Ind-I** (1)	30	53
8	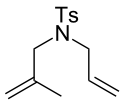	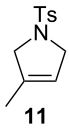	**1** (1)	80	41
9			**1** (2)	80	41
10			**Ind-I** (1)	80	22
11			**Ind-I** (1)	30	21
12			**Ind-I** (2)	80	30
13	**10**	**11**	**Ind-I** (2)	30	77
	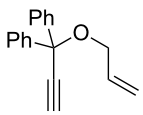	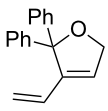			
14			**1** (1)	80	78
15	**12**	**13**	**Ind-I** (1)	30	98

[a]Reaction conditions: substrate (0.25 mmol), pre-catalyst (0.1 to 2 mol %), toluene (0.5 mL), 19 h. [b]Conversions were determined by GC analysis. Isolated yields in parentheses.

Experimental

Synthesis and characterization of [$RuCl_2$(Ind)(PCy_3){P($OiPr)_3$}] (1): Under an inert atmosphere of argon, triisopropyl phosphite (364 μL, 1.53 mmol) was added to a solution of **Ind-I** (1.414 g, 1.53 mmol) in dichloromethane (20 mL). The mixture was stirred for 24 h at room temperature and the solvent was then removed in vacuo. The crude product was recrystallized twice from dichloromethane/pentane. The solid was collected by filtration and washed with pentane (3 × 10, 2 × 15 mL). The product was obtained as a brownish red solid (1.116 g, 85%). During NMR experiments, peaks originating from the decomposition of the PCy_3 were observed. ^{1}H NMR of the mixture: (400 MHz, CD_2Cl_2) δ 1.08–1.33 (m, 6H, PCy_3), 1.11 (d, $^3J_{HH}$ = 6.3 Hz, 9H, CH-CH_3), 1.30 (d, $^3J_{HH}$ = 6.3 Hz, 9H, CH-CH_3), 1.40–1.55 (m, 9H, PCy_3), 1.60–1.85 (m, 15H, PCy_3), 2.50 (m, 3H, CH PCy_3), 4.55 (m, 3H, CH-CH_3), 6.79 (s, 1H, H^2), 7.27 (d, $^3J_{HH}$ = 7.1 Hz, 1H, H^4), 7.43 (dd, $^3J_{HH}$ = 6.7 Hz, $^3J_{HH}$ = 6.3 Hz, 1H, H^5), 7.44 (dd, $^3J_{HH}$ = 7.4 Hz, $^3J_{HH}$ = 6.3 Hz, 2H, H^{10}), 7.50 (dd, $^3J_{HH}$ = 7.4 Hz, $^3J_{HH}$ = 7.7 Hz, 1H, H^{11}), 7.53 (dd, $^3J_{HH}$ = 7.4 Hz, $^3J_{HH}$ = 7.4 Hz, 1H, H^6), 7.76 (d, $^3J_{HH}$ = 7.3 Hz, 2H, H^9), 8.80 (d, $^3J_{HH}$ = 7.3 Hz, 1H, H^7) ppm; ^{13}C-{^{1}H} NMR of the mixture (100.6 MHz, CD_2Cl_2) δ 24.3 (s, CH-$C$$H_3$), 24.5 (d, $^3J_{CP}$ = 4 Hz, CH-$C$$H_3$), 26.9 (s, CH_2 PCy_3), 28.1 (d, $^2J_{CP}$ = 11 Hz, CH_2 PCy_3), 28.4 (d, $^2J_{CP}$ = 10 Hz, CH_2 PCy_3), 30.1 (s, CH_2 PCy_3), 30.6 (s, CH_2 PCy_3), 35.3 (s, CH PCy_3), 71.4 (s, CH-CH_3), 118.4 (s, C^4), 127.0 (s, C^9), 129.6 (s, C^{10}), 129.7 (s, C^{11}), 130.2 (s, C^7), 130.3 (s, C^6), 130. 7 (s, C^5), 135.1 (s, C^8), 136.5 (s, C^3), 140.6 (s, C^{3a}), 141.3 (dd, $^3J_{CP}$ = 5.0 Hz, $^3J_{CP}$ = 14.0 Hz, C^2) 147.8 (s, C^{7a}), 290.3 (dd, $^3J_{CP}$ = 12.5 Hz, $^2J_{CP}$ = 24.5 Hz, C^1) ppm; ^{31}P-{^{1}H} NMR of the mixture (162 MHz, CD_2Cl_2) δ 120.1 (d, $^2J_{PP}$ = 37.0 Hz, PCy_3), 47.4 (d, $^2J_{PP}$ = 37.0 Hz, P($O^iPr)_3$) ppm; anal. calcd for $C_{42}H_{64}Cl_2O_3P_2Ru$: C, 59.29; H, 7.58; found: C, 59.45; H, 7.66. CCDC-889638 contains the supplementary crystallographic data for **1**. These data can be obtained free of charge from the Cambridge Crystallographic Data Centre via http://www.ccdc.cam.ac.uk/data_request/cif.

Synthesis and characterization of [$RuCl_2$(Ind){P($OiPr)_3$}$_2$] (2): Under an inert atmosphere of argon, triisopropyl phosphite (65 μL, 0.28 mmol) was added to a solution of **Ind-I^0** (0.100 g, 0.113 mmol) in dichloromethane (1.2 mL). The mixture was stirred for 24 h at room temperature and the solvent was removed in vacuo. The crude product was recrystallized from dichloromethane/pentane. The solid was collected by filtration and washed with pentane (3 × 3 mL). The product was obtained as a brownish green solid in a mixture with the phosphonium ylide **3** (0.032 g, 35%). ^{1}H NMR of the mixture (400 MHz, CD_2Cl_2) δ 1.13 (d, $^3J_{HH}$ = 6.3 Hz, 18H, CH-CH_3), 1.31 (d, $^3J_{HH}$ = 6.1 Hz, 18H, CH-CH_3), 4.53 (m, $^3J_{HH}$ = 6.3 Hz, 6H, CH-CH_3), 7.18 (s, 1H, H^2), 7.26 (d, $^3J_{HH}$ = 6.9 Hz, 1H, H^4), 7.40 (dd, $^3J_{HH}$ = 7.1 Hz, $^3J_{HH}$ = 7.1 Hz, 1H, H^5), 7.43 (dd, $^3J_{HH}$ = 7.4 Hz, $^3J_{HH}$ = 7.4 Hz, 1H, H^6), 7.46 (dd, $^3J_{HH}$ = 7.4 Hz, $^3J_{HH}$ = 7.4 Hz, 2H, H^{10}), 7.53 (dd, $^3J_{HH}$ = 7.4 Hz, $^3J_{HH}$ = 7.4 Hz, 1H, H^{11}), 7.77 (d, $^3J_{HH}$ = 7.3 Hz, 2H, H^9), 8.53 (d, $^3J_{HH}$ = 7.0 Hz, 1H, H^7) ppm; ^{13}C-{^{1}H} NMR of the mixture (100.6 MHz, CD_2Cl_2) δ 24.0 (s, CH-$C$$H_3$), 24.4 (s, CH-$C$$H_3$), 71.5 (m, CH-CH_3), 119.0 (s, C^4), 127.1 (s, C^9), 129.6 (s, C^{11}), 130.0 (s, C^{10}), 130.2 (s, C^6), 130.3 (s, C^7), 131. 2 (s, C^5), 134.8 (s, C^8), 136.8 (s, C^3), 140.3 (s, C^{3a}), 140.7 (dd, $^3J_{CP}$ = 8.5 Hz, C^2) 150.2 (s, C^{7a}), 291.1 (dd, $^2J_{CP}$ = 22.0 Hz, $^2J_{CP}$ = 22.0 Hz, C^1) ppm; ^{31}P-{^{1}H} NMR (162 MHz, CD_2Cl_2) δ 123.0 (s, P($OiPr)_3$) ppm; CCDC-889639 contains the supplementary crystallographic data for **2**. These data can be obtained free of charge from the Cambridge Crystallographic Data Centre via http://www.ccdc.cam.ac.uk/data_request/cif.

Characterization of Ph_3P(Ind) (3): Under an inert atmosphere of argon, compound **3** was obtained as a side product from the reaction of **Ind-I^0** (0.303 mg, 0.34 mmol, 1 equiv) with triisopropyl phosphite (179 μL, 0.75 mmol, 2.2 equiv) for 24 h. During recrystallization in a dichloromethane/pentane mixture, compound **3** was isolated as a yellow solid (63.4 mg, 41%). ^{1}H NMR (400 MHz; CD_2Cl_2) δ 6.73 (d, $^2J_{HP}$ = 4.9 Hz, 1H, H^2), 6.77 (dd, $^3J_{HH}$ = 7.5 Hz, $^3J_{HH}$ = 7.5 Hz, 1H, H^6), 6.89 (d, $^3J_{HH}$ = 7.9 Hz, 1H, H^7), 6.97 (dd, $^3J_{HH}$ = 7.5 Hz, $^3J_{HH}$ = 7.5 Hz, 1H, H^5), 7.08 (dd, $^3J_{HH}$ = 7.4 Hz, $^3J_{HH}$ = 7.4 Hz, 1H, H^{11}), 7.32 (dd, $^3J_{HH}$ = 7.6 Hz, $^3J_{HH}$ = 7.6 Hz, 2H, H^{10}), 7.52–7.60 (m, 6H, C_6H_5), 7.61 (d, $^3J_{HH}$ = 7.9 Hz, 2H, H^9), 7.66–7.75 (m, 9H, C_6H_5), 7.96 (d, $^3J_{HH}$ = 8.1 Hz, 1H, H^4) ppm; ^{13}C-{^{1}H} NMR (100.6 MHz; CD_2Cl_2) δ 68.5 (d, $^1J_{CP}$ = 121.6 Hz, C^1), 118.2 (s, C^5), 118.5 (s, C^6), 118.7 (s, C^7), 119.4 (s, C^4), 121.2 (d, $^3J_{CP}$ = 15.8 Hz, C^3), 123.8 (s, C^{11}), 125.6 (d, $^1J_{CP}$ = 90.3 Hz, i-C_6H_5), 127.1 (s, C^9), 127.8 (d, $^2J_{CP}$ = 16.5 Hz, C^2), 128.7 (s, C^{10}), 129.5 (d, $^3J_{CP}$ = 12.3 Hz, m-C_6H_5), 133.3 (d, $^4J_{CP}$ = 2.7 Hz, p-C_6H_5), 134.2 (d, $^2J_{CP}$ = 10.3 Hz, o-C_6H_5), 135.0 (d, $^3J_{CP}$ = 13.9 Hz, C^{3a}), 137.1 (d, $^2J_{CP}$ = 13.2 Hz, C^{7a}), 140.5 (s, C^8) ppm; ^{31}P-{^{1}H} NMR (162 MHz; CD_2Cl_2) δ 10.9 (s, Ph_3P(Ind)) ppm; HMRS (APCI): *m/z* calcd for [$C_{33}H_{25}P$ + H] 453.18; found 453.1754. CCDC-889640 contains the supplementary crystallographic data for **3**. These data can be obtained free of charge from the Cambridge Crystallographic Data Centre via http://www.ccdc.cam.ac.uk/data_request/cif.

General procedure for catalysis: Substrates **6** [42], **8** [43], **10** [42], **12** [22], were synthesized following previous reports in the literature. Compound **4** was obtained from a commercial source and its purity confirmed prior to use. ^{1}H NMR data of product **9** were compared to previously reported analyses [22].

A 5 mL screwcap-vial fitted with a septum equipped with a magnetic stirring bar was charged with the olefin (0.25 mmol)

then purged with nitrogen, closed and introduced in a glovebox. The solvent and pre-catalyst (stock solution for <1 mol %, or weighed in the vial) were added to the reaction mixture (total amount of solvent 0.5 mL). Once out of the glovebox, the reaction mixture was heated at the desired temperature and stirred for 14 or 19 hours. The reaction mixture was then analyzed by GC and/or purified by flash chromatography.

General procedure for kinetic experiments. A Schlenk flask was charged with the olefin (0.5 mmol), then closed, placed under vacuum and introduced in a glovebox. The solvent was added (5 mL) and then the pre-catalyst was weighed and charged into the Schlenk flask. Out of the glovebox, the reaction was performed at the desired temperature. Samples were taken under nitrogen flow and quenched with ethyl vinyl ether. Data were obtained by GC analysis.

Supporting Information

Crystallographic data for complexes **1**–**3** in CIF format can be obtained free of charge from the Cambridge Crystallographic Data Centre via http://www.ccdc.cam.ac.uk/data_request/cif (CCDC/889638-889640).

Supporting Information File 1

Crystallographic data for compounds **1**–**3**, NMR spectra of all the complexes, spectroscopic data.
[http://www.beilstein-journals.org/bjoc/content/supplementary/1860-5397-11-166-S1.pdf]

Supporting Information File 2

CIF file for complex **2**.
[http://www.beilstein-journals.org/bjoc/content/supplementary/1860-5397-11-166-S2.cif]

Supporting Information File 3

CIF file for complex **3**.
[http://www.beilstein-journals.org/bjoc/content/supplementary/1860-5397-11-166-S3.cif]

Supporting Information File 4

CIF file for complex **4**.
[http://www.beilstein-journals.org/bjoc/content/supplementary/1860-5397-11-166-S4.cif]

Acknowledgements

The authors gratefully acknowledge the Royal Society (University Research Fellowship to CSJC) and the EC (CP-FP 211468-2 EUMET) for funding and the EPSRC National Mass Spectrometry Service Centre Swansea University for HMRS analyses.

References

1. Hoveyda, A. H.; Zhugralin, A. R. *Nature* **2007,** *450,* 243–251. doi:10.1038/nature06351
2. Chauvin, Y. *Angew. Chem., Int. Ed.* **2006,** *45,* 3740–3747. doi:10.1002/anie.200601234
3. Schrock, R. R. *Angew. Chem., Int. Ed.* **2006,** *45,* 3748–3759. doi:10.1002/anie.200600085
4. Grubbs, R. H. *Angew. Chem., Int. Ed.* **2006,** *45,* 3760–3765. doi:10.1002/anie.200600680
5. Fürstner, A. *Angew. Chem., Int. Ed.* **2000,** *39,* 3012–3043. doi:10.1002/1521-3773(20000901)39:17<3012::AID-ANIE3012>3.0.CO;2-G
6. Buchmeiser, M. R. *Chem. Rev.* **2000,** *100,* 1565–1604. doi:10.1021/cr990248a
7. Connon, S. J.; Blechert, S. *Angew. Chem., Int. Ed.* **2003,** *42,* 1900–1923. doi:10.1002/anie.200200556
8. Grubbs, R. H.; Miller, S. J.; Fu, G. C. *Acc. Chem. Res.* **1995,** *28,* 446–452. doi:10.1021/ar00059a002
9. Nicolaou, K. C.; Bulger, P. G.; Sarlah, D. *Angew. Chem., Int. Ed.* **2005,** *44,* 4490–4527. doi:10.1002/anie.200500369
10. Trnka, T. M.; Grubbs, R. H. *Acc. Chem. Res.* **2001,** *34,* 18–29. doi:10.1021/ar000114f
11. Schrock, R. R.; Hoveyda, A. H. *Angew. Chem., Int. Ed.* **2003,** *42,* 4592–4633. doi:10.1002/anie.200300576
12. Grubbs, R. H., Ed. *Handbook of Metathesis: Catalyst Development;* Wiley-VCH: Weinheim, Germany, 2003. doi:10.1002/9783527619481
13. Grela, K., Ed. *Olefin Metathesis – Theory and Practice;* Wiley-VCH: Weinheim, Germany, 2014.
14. Nguyen, S. T.; Johnson, L. K.; Grubbs, R. H.; Ziller, J. W. *J. Am. Chem. Soc.* **1992,** *114,* 3974–3975. doi:10.1021/ja00036a053
15. Nguyen, S. T.; Grubbs, R. H.; Ziller, J. W. *J. Am. Chem. Soc.* **1993,** *115,* 9858–9859. doi:10.1021/ja00074a086
16. Schwab, P.; Grubbs, R. H.; Ziller, J. W. *J. Am. Chem. Soc.* **1996,** *118,* 100–110. doi:10.1021/ja952676d
17. Boeda, F.; Clavier, H.; Nolan, S. P. *Chem. Commun.* **2008,** 2726–2740. doi:10.1039/b718287b
18. Weskamp, T.; Kohl, F. J.; Herrmann, W. A. *J. Organomet. Chem.* **1999,** *582,* 362–365. doi:10.1016/S0022-328X(99)00163-1
19. Huang, J.; Schanz, H.-J.; Stevens, E. D.; Nolan, S. P. *Organometallics* **1999,** *18,* 5375–5380. doi:10.1021/om990788y
20. Scholl, M.; Ding, S.; Lee, C. W.; Grubbs, R. H. *Org. Lett.* **1999,** *1,* 953–956. doi:10.1021/ol990909q
21. Sanford, M. S.; Love, J. A.; Grubbs, R. H. *J. Am. Chem. Soc.* **2001,** *123,* 6543–6554. doi:10.1021/ja010624k
22. Clavier, H.; Nolan, S. P. *Chem. – Eur. J.* **2007,** *13,* 8029–8036. doi:10.1002/chem.200700256
23. Monsaert, S.; Drozdzak, R.; Dragutan, V.; Dragutan, I.; Verpoort, F. *Eur. J. Inorg. Chem.* **2008,** 432–440. doi:10.1002/ejic.200700879
24. Nelson, D. J.; Manzini, S.; Urbina-Blanco, C. A.; Nolan, S. P. *Chem. Commun.* **2014,** *50,* 10355–10375. doi:10.1039/C4CC02515F
25. Bantreil, X.; Schmid, T. E.; Randall, R. A. M.; Slawin, A. M. Z.; Cazin, C. S. J. *Chem. Commun.* **2010,** *46,* 7115–7117. doi:10.1039/c0cc02448a
26. Schmid, T. E.; Bantreil, X.; Citadelle, C. A.; Slawin, A. M. Z.; Cazin, C. S. J. *Chem. Commun.* **2011,** *47,* 7060–7062. doi:10.1039/c1cc10825e

27. Songis, O.; Slawin, A. M. Z.; Cazin, C. S. J. *Chem. Commun.* **2012,** *48,* 1266–1268. doi:10.1039/C2CC15903A
28. Bantreil, X.; Poater, A.; Urbina-Blanco, C. A.; Bidal, Y. D.; Falivene, L.; Randall, R. A. M.; Cavallo, L.; Slawin, A. M. Z.; Cazin, C. S. J. *Organometallics* **2012,** *31,* 7415–7426. doi:10.1021/om300703p
29. Urbina-Blanco, C. A.; Bantreil, X.; Wappel, J.; Schmid, T. E.; Slawin, A. M. Z.; Slugovc, C.; Cazin, C. S. J. *Organometallics* **2013,** *32,* 6240–6247. doi:10.1021/om4004362
30. Falivene, L.; Poater, A.; Cazin, C. S. J.; Slugovc, C.; Cavallo, L. *Dalton Trans.* **2013,** *42,* 7312–7317. doi:10.1039/C2DT32277C
31. Guidone, S.; Songis, O.; Nahra, F.; Cazin, C. S. J. *ACS Catal.* **2015,** *5,* 2697–2701. doi:10.1021/acscatal.5b00197
32. Guidone, S.; Songis, O.; Falivene, L.; Nahra, F.; Slawin, A. M. Z.; Jacobsen, H.; Cavallo, L.; Cazin, C. S. J. *ACS Catal.* **2015,** *5,* 3932–3939. doi:10.1021/acscatal.5b00219
33. Bantreil, X.; Cazin, C. S. J. *Monatsh. Chem.* **2015,** *146,* 1043–1052. doi:10.1007/s00706-015-1487-7
34. Cazin, C. S. J., Ed. *N-Heterocyclic Carbenes in Transition Metal Catalysis and Organocatalysis;* Catalysis by Metal Complexes, Vol. 32; Springer: New York, NY, U.S.A., 2011. doi:10.1007/978-90-481-2866-2
35. Ung, T.; Hejl, A.; Grubbs, R. H.; Schrodi, Y. *Organometallics* **2004,** *23,* 5399–5401. doi:10.1021/om0493210
36. Slugovc, C.; Burtscher, D.; Stelzer, F.; Mereiter, K. *Organometallics* **2005,** *24,* 2255–2258. doi:10.1021/om050141f
37. Ho, C.-Y.; Jamison, T. F. *Angew. Chem., Int. Ed.* **2007,** *46,* 782–785. doi:10.1002/anie.200603907
38. Wallace, D. J.; Reamer, R. A. *J. Org. Chem.* **2014,** *79,* 5644–5651. doi:10.1021/jo500815q
39. Chatterjee, S.; Guchhait, S.; Goswami, R. K. *J. Org. Chem.* **2014,** *79,* 7689–7695. doi:10.1021/jo501184t
40. Keck, C. G.; Kendall, J. L.; Caster, K. C. *Adv. Synth. Catal.* **2007,** *349,* 165–174. doi:10.1002/adsc.200600455
41. Hong, S. H.; Day, M. W.; Grubbs, R. H. *J. Am. Chem. Soc.* **2004,** *126,* 7414–7415. doi:10.1021/ja0488380
Phosphorus ylide bearing the alkylidene moiety has already been proposed.
42. Terada, Y.; Arisawa, M.; Nishida, A. *Angew. Chem., Int. Ed.* **2004,** *43,* 4063–4067. doi:10.1002/anie.200454157
43. Kirkland, T. A.; Grubbs, R. H. *J. Org. Chem.* **1997,** *62,* 7310–7318. doi:10.1021/jo970877p

License and Terms

BEILSTEIN JOURNAL OF ORGANIC CHEMISTRY

Latent ruthenium–indenylidene catalysts bearing a *N*-heterocyclic carbene and a bidentate picolinate ligand

Thibault E. Schmid[1], Florian Modicom[1], Adrien Dumas[1], Etienne Borré[1], Loic Toupet[2], Olivier Baslé[*1] and Marc Mauduit[*1]

Full Research Paper

Open Access

Address:
[1]Ecole Nationale supérieure de chimie de rennes, UMR CNRS 6226, 11 Allée de Beaulieu, 35708, Rennes, cedex 7, France and [2]Institut de Physique de Rennes, Université de Rennes 1, CNRS, UMR 6251, Rennes Cedex, France

Email:
Olivier Baslé[*] - olivier.basle@ensc-rennes.fr; Marc Mauduit[*] - marc.mauduit@enscr-rennes.fr

* Corresponding author

Keywords:
latent catalyst; olefin metathesis; picolinate ligand; ruthenium indenylidene

Beilstein J. Org. Chem. **2015,** *11,* 1541–1546.
doi:10.3762/bjoc.11.169

Received: 18 June 2015
Accepted: 11 August 2015
Published: 03 September 2015

This article is part of the Thematic Series "Progress in metathesis chemistry II". In memory of Guy Lavigne.

Guest Editor: K. Grela

Abstract

A silver-free methodology was developed for the synthesis of unprecedented *N*-heterocyclic carbene ruthenium indenylidene complexes bearing a bidentate picolinate ligand. The highly stable (SIPr)(picolinate)RuCl(indenylidene) complex **4a** (SIPr = 1,3-bis(2-6-diisopropylphenyl)imidazolidin-2-ylidene) demonstrated excellent latent behaviour in ring closing metathesis (RCM) reaction and could be activated in the presence of a Brønsted acid. The versatility of the catalyst **4a** was subsequently demonstrated in RCM, cross-metathesis (CM) and enyne metathesis reactions.

Introduction

Olefin metathesis has witnessed tremendous development in the last decades and has emerged as a powerful tool with dramatic impact on both organic chemistry and materials science [1,2]. Intensive research has notably allowed for the design of efficient ruthenium-based catalysts that exhibit improved reactivity [3-6]. On the other hand, some applications require a precatalyst that can remain inert towards substrates and only initiate in response to a specific stimulus [7]. A common strategy for the preparation of latent catalysts is to incorporate additional strongly binding chelating ligands to the ruthenium coordination sphere [8]. Thus, activation of the catalyst is made possible by liberation of coordination vacancy under specific conditions, such as elevated temperature or addition of cocatalyst. While first examples of latent catalysts were based on phosphine-containing ruthenium complexes bearing a Schiff base ligand (O–N) [9] replacement of the phosphine ligand by sterically demanding and strongly σ-donor *N*-heterocyclic carbenes (NHC) afforded catalysts with improved catalytic performance [10-12]. Among the different [N–O]-chelating ligands that have been previously considered [13-17], the pyridyl-2-

carboxylate (picolinate) ligand has demonstrated its usefulness in the preparation of efficient latent catalysts based on (NHC)Ru–alkylidene complexes [18,19]. Nevertheless, indenylidene complexes, that have notably showed an improved stability in comparison to their benzylidene counterparts [20-22], have never been considered in association with picolinic ligands for the synthesis of robust latent catalysts. Moreover, this strategy would provide an interesting alternative to indenylidene-Schiff base complexes that in most cases require toxic thallium salts for their preparation [23,24].

Here, we report the synthesis of (NHC)Ru–indenylidene complexes incorporating chelating picolinic ligands and evaluate their potential as latent catalysts in model ring closing metathesis and cross-metathesis transformations.

Results and Discussion

With the objective to develop an attractive strategy for the synthesis of indenylidene-picolinic ruthenium complexes, we initially attempted their preparation using a silver-free methodology. In fact, silver residues are known to induce ruthenium-complex decomposition, and increase purification complexity [25]. Moreover, in a previous report regarding the synthesis of a dormant ruthenium catalyst bearing a chelating carboxylate ligand, spontaneous chloride/carboxylate exchange with elimination of HCl has been established [26]. Therefore, using only CuCl as a phosphine scavenger, we investigated the picolinic acid addition using the commercially available M2 complex **1** [27], featuring the NHC SIMes (SIMes = 1,3-bis(2,4,6-trimethylphenyl)-4,5-dihydroimidazol-2-ylidene) as a precursor. To our delight, using only 1.1 equiv of 2-picolinic acid, complex **2**, resulting from the single Cl/picolinate exchange, was identified as the major product (Scheme 1). Column chromatography enabled the purification of compound **2**, which could be isolated as a mixture of isomers with 62% yield. Encouraged by these preliminary results, we considered the preparation of a SIPr-based species, which would generate complexes with a higher catalytic potential and an improved stability [6,28,29]. Gratifyingly, under the same reaction conditions, the desired complex **4a** could be isolated as a single isomer in 54% yield.

In order to improve the synthesis efficiency of the desired complex **4a**, the [(SIPr)$RuCl_2$(indenylidene)pyridine] complex **5** was used as a precursor (Scheme 2). The latter species offers both the advantages to avoid the use of phosphine scavenger and to trap the acid formed as a pyridinium chloride salt. Gratifyingly, under these modified conditions the desired complex **4a** could be prepared in a clean manner with an improved 62% isolated yield. Given the importance of the substitution pattern of the chelating [N–O] ligand, X-ray diffraction analysis unambiguously confirmed the structure of complex **4a**, which displayed a distorted square pyramidal geometry (Figure 1) [30]. The nitrogen atom of the picolinate occupied a position *trans* to the bulky NHC ligand, with the carboxylate group *cis* to the indenylidene. In order to determine the influence of the electronic parameters of the chelating pseudo-halide fragment, we proceeded to synthesize complex **4b**, featuring the 5-bromo-2-picolinate moiety. Using a similar methodology, the desired complex was obtained with 42% yield.

The activation of the new picolinic complex **4a** was initially evaluated in the presence of trifluoroacetic acid (TFA), a Brønsted acid easy to handle and to operate (Figure 2). Consistent with its stability in solution, the latent catalyst **4a** appeared totally inactive at room temperature (<1% conversion after 24 h at 297 K), while catalytic activity was observed in the RCM of

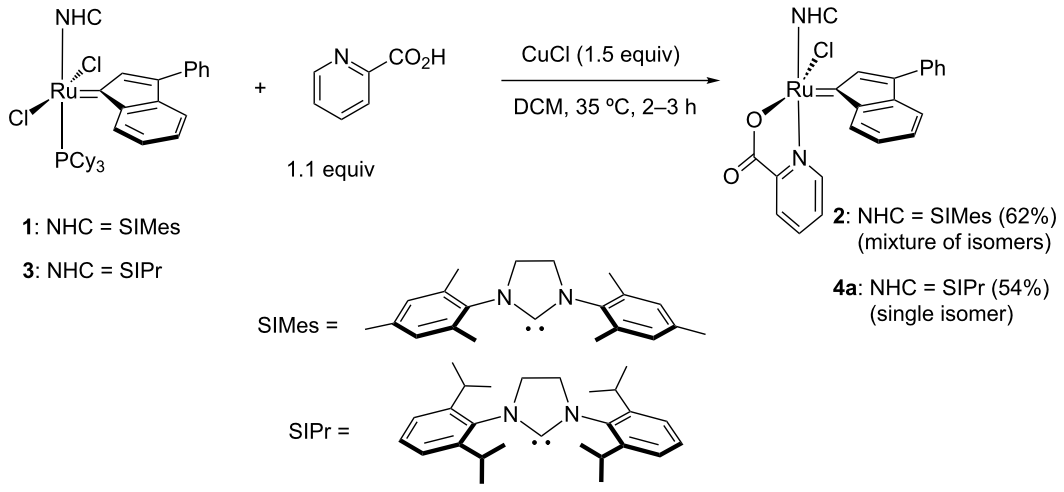

Scheme 1: Synthesis of [NHC(picolinate)RuCl(indenylidene)] complexes **2** and **4a**.

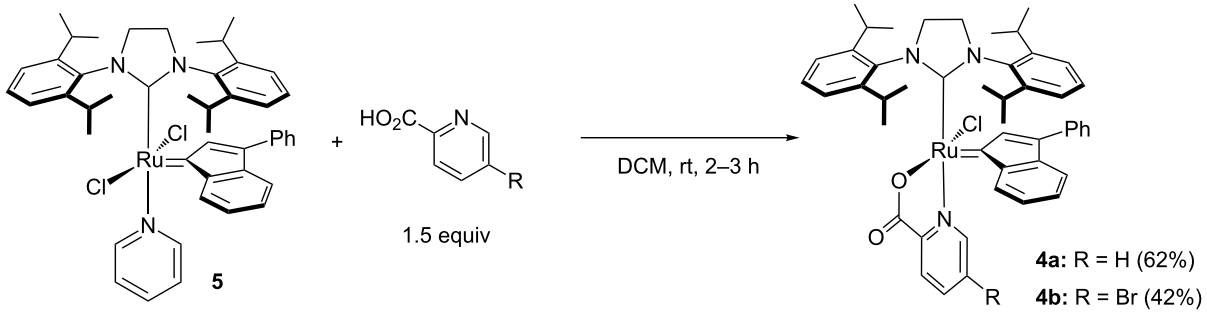

Scheme 2: Synthesis of complex **4a** and **4b** from (SIPr)(pyridine)$RuCl_2$(indenylidene) (**5**).

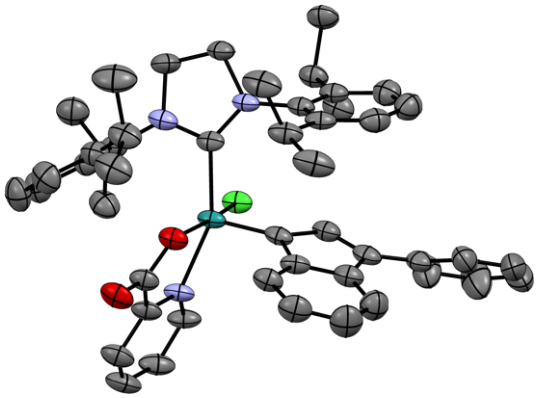

Figure 1: Solid-state structure of complex **4a** from single crystal X-ray diffraction. Hydrogens have been omitted for clarity. (N in blue, C in grey, O in red, Cl in green).

diethyl diallylmalonate (DEDAM) after addition of TFA. Several acid/catalyst ratios were investigated, and 150 equiv of TFA afforded the best catalytic performance in terms of initiation rate and conversion. In fact, both a decrease (100 equiv) and an increase (200 equiv) of this acid/catalyst ratio led to a significant deterioration of the kinetic profile.

Subsequently, the SIMes-based complex **2** and the 4-bromo-substituted complex **4b** were evaluated and compared with complex **4a** under these optimized reaction conditions (Figure 3). While in the absence of acid, **2** displayed no catalytic activity after 30 min, the complex **4b** bearing a more electron-deficient picolinate ligand demonstrated modest latency potential with 5% conversion after this period. In both cases, activation of the catalysts with 150 equiv of TFA did not provide full conversion of the benchmark substrate. Notably, despite a faster initiation rate, the SIMes-based catalyst **2**

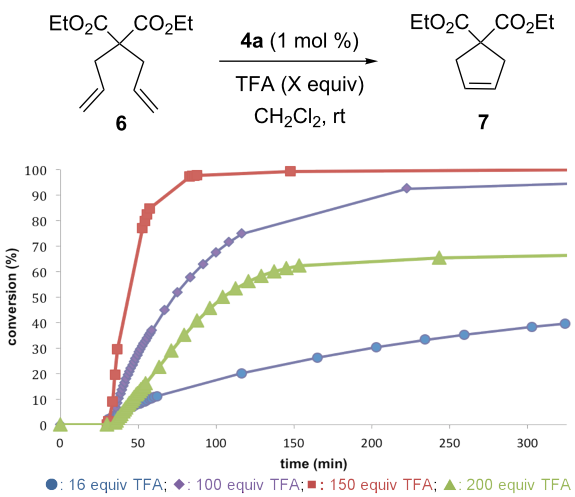

Figure 2: Olefin metathesis profiles in response to TFA equivalents.

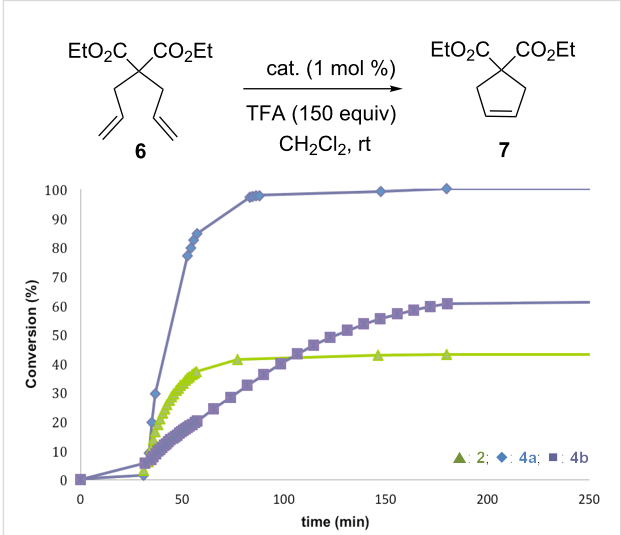

Figure 3: Comparison of olefin metathesis profiles for catalysts **2**, **4a** and **4b** after activation with 150 equiv of TFA.

afforded a lower conversion rate, that can be explained by a rapid decomposition of the corresponding active species. Therefore, the complex **4a** that displayed the best catalytic performance was selected for further investigations.

Efforts were then focused to determine the effect of different acids on the catalyst efficiency in RCM of DEDAM [31]. The replacement of TFA by a weaker acid, acetic acid afforded a lower initiation rate and a conversion of only 40% was obtained after 5 h. On the other hand, hydrochloric acid outperformed TFA to complete the reaction in 10 min, as depicted in Figure 4.

With the best conditions in hand, we then briefly investigated the scope of metathesis transformations using 1 mol % of **4a** in dichloromethane at 25 °C, using hydrochloric acid as activator (Table 1). Both substrates **6** and the tosylamine **8** were efficiently converted to the desired cyclopentene products that were isolated in 97 and 96% yields, respectively. Interestingly, the

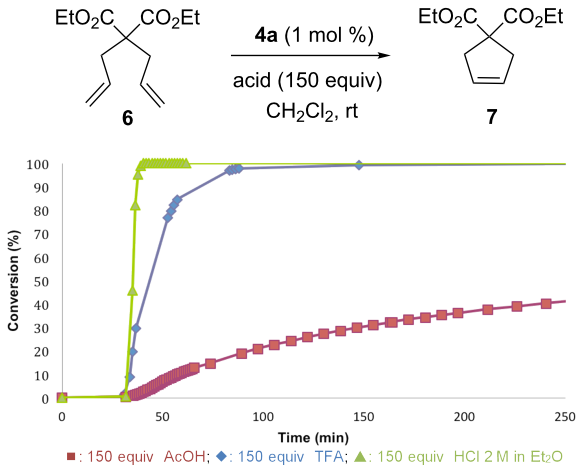

Figure 4: Influence of various acids for the activation of **4a** in the RCM of DEDAM.

Table 1: Substrate scope in RCM, CM and enyne metathesis catalyzed by **4a**[a].

Entry	Substrate	Product	Yield (%)
1	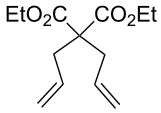 **6**	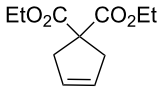 **7**	97
2	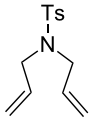 **8**	 **9**	96
3	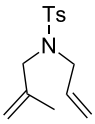 **10**	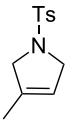 **11**	93
4	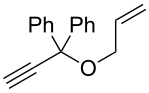 **12**	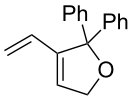 **13**	89
5	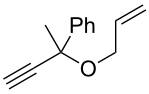 **14**	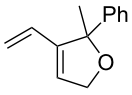 **15**	90
6	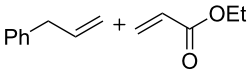 **16** + **17**	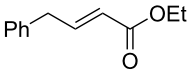 **18**	62

[a]Reaction conditions: substrate (0.238 mmol), CH_2Cl_2 (2.4 mL), **4a** (0.00238 mmol, injected from stock solution in CH_2Cl_2), HCl (0.357 mmol, injected from a 2 M solution in Et_2O), room temperature, 2 h.

more sterically-demanding diene **10** afforded the trisubstituted olefin cyclized product with high 93% isolated yield. Catalyst **4a** was also efficient regarding the cyclization of enynes **12** and **14** and the desired diene products were obtained with 89 and 90% isolated yields, respectively. Finally, the cross metathesis reaction between allylbenzene and ethyl acrylate afforded the desired internal *E*-olefin with 62% yield.

Conclusion

We described the synthesis and characterization of three novel latent 2nd generation indenylidene-based precatalysts for olefin metathesis reactions. A picolinate moiety was successfully inserted into SIMes- and SIPr-containing architectures, affording unprecedented mono-picolinate complexes. Whilst SIMes-containing species **2** was identified as a mixture of isomers with a low stability in solution, compounds **4a** and **4b**, featuring the bulkier ancillary ligand SIPr, appeared as highly stable, well-defined species. These species were shown to activate in the presence of a Brønsted acid and precatalysts **2** and **4a** showed an excellent latent behaviour. The best reaction rates were obtained in the RCM of DEDAM with complex **4a** after activation by HCl addition. The versatility of the catalyst was subsequently demonstrated in RCM, CM and enyne metathesis reactions.

Supporting Information

Supporting Information File 1

Full experimental procedures and detailed analytical data for ruthenium complexes.
[http://www.beilstein-journals.org/bjoc/content/supplementary/1860-5397-11-169-S1.pdf]

Acknowledgements

This work was supported by the Agence Nationale de la Recherche (ANR) (ANR-12-CD2I-0002 Cflow-OM), Oméga Cat System and the Association Nationale de la Recherche et la Technologie (ANRT, grant to A.D.). M.M. and O.B. thank the Centre National de la Recherche Scientifique (CNRS) and the Ecole Nationale Supérieure de Chimie de Rennes (ENSCR).

References

1. Grela, K., Ed. *Olefin Metathesis: Theory and Practice;* John Wiley & Sons: Hoboken, 2014.
2. Vougioukalakis, G. C.; Grubbs, R. H. *Chem. Rev.* **2010,** *110,* 1746–1787. doi:10.1021/cr9002424
3. Wakamatsu, H.; Blechert, S. *Angew. Chem., Int. Ed.* **2002,** *41,* 794–796. doi:10.1002/1521-3773(20020301)41:5<794::AID-ANIE794>3.0.CO;2-B
4. Grela, K.; Harutyunyan, S.; Michrowska, A. *Angew. Chem., Int. Ed.* **2002,** *41,* 4210–4212. doi:10.1002/1521-3757(20021104)114:21<4210::AID-ANGE4210>3.0.CO;2-J
5. Clavier, H.; Caijo, F.; Borré, E.; Rix, D.; Boeda, F.; Nolan, S. P.; Mauduit, M. *Eur. J. Org. Chem.* **2009,** 4254–4265. doi:10.1002/ejoc.200900407
6. Nelson, J. D.; Queval, P.; Rouen, M.; Magrez, M.; Toupet, L.; Caijo, F.; Borré, E.; Laurent, I.; Crévisy, C.; Baslé, O.; Mauduit, M.; Percy, J. M. *ACS Catal.* **2013,** *3,* 259–264. doi:10.1021/cs400013z
7. Monsaert, S.; Lozano Vila, A.; Drozdzak, R.; Van Der Voort, P.; Verpoort, F. *Chem. Soc. Rev.* **2009,** *38,* 3360–3372. doi:10.1039/b902345n
8. Morin, Y.; Gauvin, R. M. Schiff Base Catalysts and Other Related Latent Systems for Polymerization Reactions. In *Olefin Metathesis: Theory and Practice;* Grela, K., Ed.; John Wiley & Sons: Hoboken, 2014; pp 453–471.
9. Chang, S.; Jones, L.; Wang, C.; Henling, L. M.; Grubbs, R. H. *Organometallics* **1998,** *17,* 3460–3465. doi:10.1021/om970910y
10. De Clerq, B.; Verpoort, F. *Tetrahedron Lett.* **2002,** *43,* 9101–9104. doi:10.1016/S0040-4039(02)02247-5
11. De Clerq, B.; Verpoort, F. *J. Organomet. Chem.* **2003,** *672,* 11–16. doi:10.1016/S0022-328X(03)00055-X
12. Opstal, T.; Verpoort, F. *Angew. Chem., Int. Ed.* **2003,** *42,* 2876–2879. doi:10.1002/anie.200250840
13. van der Schaaf, P. A.; Mühlbach, A.; Hafner, A.; Kolly, R. Heterocyclic ligand containing ruthenium and osmium catalysts. WO Patent WO99/29701, Dec 4, 1999.
14. Denk, K.; Fridgen, J.; Hermann, W. A. *Adv. Synth. Catal.* **2002,** *344,* 666–670.
15. Jordaan, M.; Vosloo, H. C. M. *Adv. Synth. Catal.* **2007,** *349,* 184–192. doi:10.1002/adsc.200600474
And references cited therein.
16. Samec, J. S. M.; Grubbs, R. H. *Chem. Commun.* **2007,** 2826–2828. doi:10.1039/B704821A
17. Samec, J. S. M.; Grubbs, R. H. *Chem. – Eur. J.* **2008,** *14,* 2686–2692. doi:10.1002/chem.200701495
See for the reaction with tetrahydro-2-furoic acid.
18. Hahn, E. F.; Paas, M.; Fröhlich, R. *J. Organomet. Chem.* **2005,** *690,* 5816–5821. doi:10.1016/j.jorganchem.2005.07.060
19. Samec, J. S. M.; Keitz, B. K.; Grubbs, R. H. *J. Organomet. Chem.* **2010,** *695,* 1831–1837. doi:10.1016/j.jorganchem.2010.04.017
20. Clavier, H.; Nolan, S. P. *Chem. – Eur. J.* **2007,** *13,* 8029–8036. doi:10.1002/chem.200700256
21. Torborg, C.; Szczepaniak, G.; Zieliński, A.; Malińska, M.; Woźniak, K.; Grela, K. *Chem. Commun.* **2013,** *49,* 3188–3190. doi:10.1039/c2cc37514a
22. Drozdzak, R.; Nishioka, N.; Recher, G.; Verpoort, F. *Macromol. Symp.* **2010,** *293,* 1–4. doi:10.1002/masy.200900052
23. Occhipinti, G.; Jensen, V. R.; Bøjrsvik, H.-R. *J. Org. Chem.* **2007,** *72,* 3561–3564. doi:10.1021/jo070164z
See for an example with silver salts.
24. Öztürk, B. Ö.; Şehitoğlu, S. K.; Meier, M. A. R. *Eur. Polym. J.* **2015,** *62,* 116–123. doi:10.1016/j.eurpolymj.2014.11.014
See for an example with potassium salts.
25. Herbert, M. B.; Lan, Y.; Keitz, B. K.; Liu, P.; Endo, K.; Day, M. W.; Houk, K. N.; Grubbs, R. H. *J. Am. Chem. Soc.* **2012,** *134,* 7861–7866. doi:10.1021/ja301108m

26. Gawin, R.; Makal, A.; Woźniak, K.; Mauduit, M.; Grela, K. *Angew. Chem., Int. Ed.* **2007,** *46,* 7206–7209. doi:10.1002/anie.200701302
27. Umicore ruthenium-based olefin metathesis precatalysts library. http://chemistry.umicore.com/products/#tax_reactiontype_ms=Metathesis (accessed July 21, 2015).
28. Clavier, H.; Urbina-Blanco, C. A.; Nolan, S. P. *Organometallics* **2009,** *28,* 2848–2854. doi:10.1021/om900071t
29. Urbina-Blanco, C. A.; Leitgeb, A.; Slugovc, C.; Bantreil, X.; Clavier, H.; Slawin, A. M. Z.; Nolan, S. P. *Chem. – Eur. J.* **2011,** *17,* 5045–5053. doi:10.1002/chem.201003082
30. The CIF file for complex **4a** has been deposited with the CCDC, No. 1405734. Copies of the data can be obtained free of charge on applications to CCDC, 12 Union Road, Cambridge, CB2 1EZ, UK; fax: +44 1223 336 033; http://www.ccdc.cam.ac.uk; e-mail: deposit@ccdc.cam.ac.uk.
31. Keitz, B. K.; Bouffard, J.; Bertrand, G.; Grubbs, R. H. *J. Am. Chem. Soc.* **2011,** *133,* 8498–8501. doi:10.1021/ja203070r

License and Terms

BEILSTEIN JOURNAL OF ORGANIC CHEMISTRY

Grubbs–Hoveyda type catalysts bearing a dicationic *N*-heterocyclic carbene for biphasic olefin metathesis reactions in ionic liquids

Maximilian Koy[1], Hagen J. Altmann[1], Benjamin Autenrieth[1], Wolfgang Frey[2] and Michael R. Buchmeiser[*1,3]

Full Research Paper

Open Access

Address:
[1]Lehrstuhl für Makromolekulare Stoffe und Faserchemie, Institut für Polymerchemie, Universität Stuttgart, Pfaffenwaldring 55, D-70569 Stuttgart, Germany, Fax: +49 (0)711-685-64050, [2]Institut für Organische Chemie, Universität Stuttgart, Pfaffenwaldring 55, D-70569 Stuttgart, Germany and [3]Institut für Textilchemie und Chemiefaser (ITCF) Denkendorf, Körschtalstr. 26, D-73770 Denkendorf, Germany

Email:
Michael R. Buchmeiser* - michael.buchmeiser@ipoc.uni-stuttgart.de

* Corresponding author

Keywords:
biphasic catalysis; ionic initiators; recycling; ROMP; ruthenium

Beilstein J. Org. Chem. **2015,** *11,* 1632–1638.
doi:10.3762/bjoc.11.178

Received: 14 June 2015
Accepted: 25 August 2015
Published: 15 September 2015

This article is part of the Thematic Series "Progress in metathesis chemistry II".

Guest Editor: K. Grela

Abstract

The novel dicationic metathesis catalyst $[(RuCl_2(H_2ITapMe_2)(=CH–2-(2-PrO)-C_6H_4))^{2+}\ (OTf^-)_2]$ (**Ru-2**, $H_2ITapMe_2$ = 1,3-bis(2',6'-dimethyl-4'-trimethylammoniumphenyl)-4,5-dihydroimidazol-2-ylidene, OTf^- = $CF_3SO_3^-$) based on a dicationic *N*-heterocyclic carbene (NHC) ligand was prepared. The reactivity was tested in ring opening metathesis polymerization (ROMP) under biphasic conditions using a nonpolar organic solvent (toluene) and the ionic liquid (IL) 1-butyl-2,3-dimethylimidazolium tetrafluoroborate $[BDMIM^+][BF_4^-]$. The structure of **Ru-2** was confirmed by single crystal X-ray analysis.

Introduction

Ionic metathesis catalysts offer access to metathesis reactions in either aqueous solution [1-10] or under biphasic conditions [11-14]. Particularly the latter aspect is of utmost relevance in case of ionic liquids (ILs) can be used as the phase in which the catalyst is dissolved. The ionic character of both the IL and the ionic catalyst effectively block any crossover of catalyst into the second (organic) phase. This offers access to metathesis reactions in which the products have a low ruthenium contamination [11]. Equally important, reactions can be run under biphasic, continuous conditions applying supported ionic liquid phase (SILP) technology [11]. We recently reported on different Ru-based ionic metathesis catalysts that can be used for these

purposes. In these systems, the charge is either located directly at the ruthenium [11,12] or at the 1-methylpyridinium-4-carboxylate ligands that are introduced via anion metathesis [13,14]. These novel catalytic systems have successfully been used under SILP conditions [11,15]. Furthermore, they allow running ring-opening metathesis polymerization (ROMP) reactions under biphasic conditions, an approach that offers access to both ROMP-derived polymers with unprecedented low Ru contamination (typically 25–80 ppm) and to a regeneration of the initiator [14]. With all that systems at hand it also became apparent that reactivity of a certain catalyst strongly depends on the location of the charge. In principle, ionic Ru-based metathesis catalysts can also be prepared with the aid of *N*-heterocyclic carbenes (NHCs) that bear pendant ionic groups (Figure 1) [10,16-19]. We addressed that issue by preparing a novel ionic Ru-NHC-alkylidene using NHCs with ionic groups. Here we report our results.

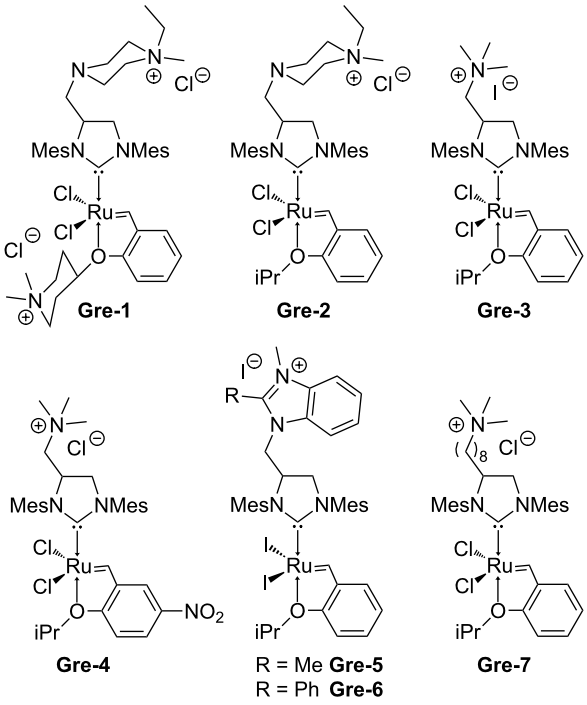

Figure 1: Catalysts synthesized by post-assembly tagging (Mes = mesitylene).

Results and Discussion

Catalyst synthesis

We were attracted by NHC ligands containing a diamino function at the aromatic ring as realized in **1** [20-22] since such ligands can be permanently quaternized to the corresponding dicationic species via double alkylation. Additionally, they remain structurally closely related to mesitylene-based NHC ligands. Attempts to synthesize ionic Ru-based olefin metathesis catalysts using imidazolinium salts bearing two quaternary ammonium groups turned out to be unsuccessful, probably due to their insolubility in common organic solvents. However, quaternization of $RuCl_2(H_2ITap)(=CH–(2-(2-PrO-C_6H_4)))$ (**Ru-1**, Scheme 1) [21] turned out to be successful.

To ensure the solubility in common organic solvents until the last step of the synthesis, the neutral precursor **Ru-1** [21] was prepared in an improved one-step synthesis in 82% yield. Quaternization using 2.05 equiv of methyl trifluoromethanesulfonate gave the dicationic ruthenium alkylidene **Ru-2** in 90% isolated yield (Scheme 1). This is to the best of our knowledge the first example of a ruthenium alkylidene bearing an NHC

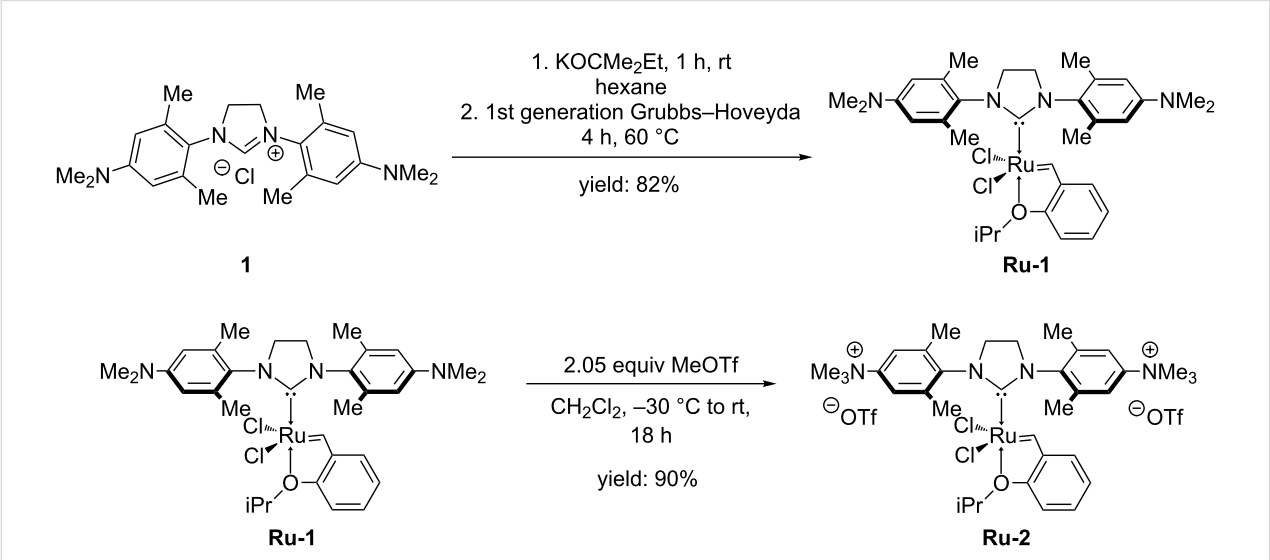

Scheme 1: Improved synthesis of **Ru-1** and quarternization with methyl trifluoromethanesulfonate to **Ru-2**.

ligand with permanent dicationic charge. Crystals of **Ru-2** suitable for single-crystal X-ray analysis were obtained from DMF/diethyl ether. Catalyst **Ru-2** crystallizes in the triclinic space group $\overline{P}-1$, a = 1398.08(6) pm, b = 1399.41(7) pm, c = 1750.26(13) pm, α = 106.079(3)°, β = 112.209(3)°, γ = 99.300(2)°, Z = 2 (Figure 2, Supporting Information File 1).

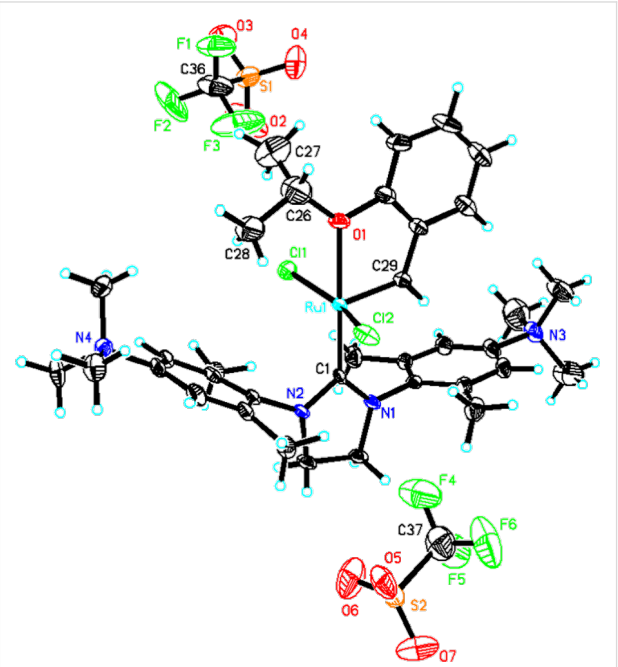

Figure 2: Single crystal X-ray structure of **Ru-2**. Co-solvent and disordered triflates have been omitted for clarity.

Selected bond lengths are summarized in Table 1. For purposes of comparison, the corresponding distances of the parent system **Ru-1** are provided, too. As can be seen, the dicationic charge does influence the binding situation in **Ru-2**, though not dramatically. Interestingly only a slight increase in the Ru–NHC bond length is observed, accompanied by a very minor decrease in the Ru–O bond. The Ru–Cl bonds remain unaffected. The most dramatic effect is observed in the Ru–alkylidene bond, which is about 9 pm longer in **Ru-2** than in **Ru-1**. This increase in the alkylidene's length points towards a substantially reduced polarization of the Ru=C bond and accounts for a reduced activity of **Ru-2** compared to standard Grubbs- and Grubbs–Hoveyda catalysts. Thus, **Ru-2** delivers only turn-over numbers well below 100 in the biphasic ring-closing metathesis (RCM) of 1,7-octadiene, diethyl diallylmalonate and *N*,*N*-diallyl *p*-toluoenesulfonamide using [BDMIM$^+$][BF$_4^-$] as IL and toluene as the organic phase (see Supporting Information File 1). It is thus also in line with the fact that Ru–alkylidenes based on electron-rich NHCs, e.g., based on tetrahydropyrimidin-2-ylidenes [23], strongly promote olefin metathesis.

Table 1: Selected bond lengths (pm) for **Ru-2** and **Ru-1** [21].

	Ru-2	Ru-1
Ru1–C1	198.2(4)	196.6(7)
Ru1–C29	182.8(4)	173.5(9)
Ru1–O1	225.2(3)	226.0(5)
Ru1–Cl1	233.89(12)	233.0(2)
Ru1–Cl2	233.50(12)	233.9(2)

Biphasic ring-opening metathesis polymerization (ROMP) reactions

To test the reactivity of **Ru-2,** various ROMP reactions were run under biphasic conditions using [BDMIM$^+$][BF$_4^-$] [24] as IL and toluene as the organic phase. The structure of monomers **M1**–**M6** that were used are shown in Figure 3 [14]. Results are summarized in Table 2. At this point it is worth stressing that the purity of the IL used is of utmost importance, the more since imidazolium-based ILs can contain substantial amounts of free base [25], which in turn can negatively affect catalyst performance.

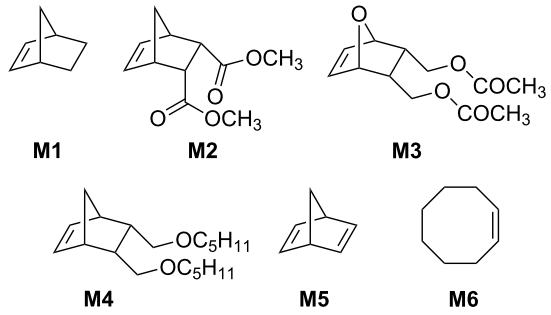

Figure 3: Monomers used for biphasic ROMP reactions.

As can be seen, **M1**–**M6** can be polymerized via ROMP under biphasic conditions in good yields, except for **M6**. This low yield is attributed to the comparable low ring strain in **M6**. Polydispersity indices (PDIs) were in the range of 1.2 to 3.8. Together with the high molecular weights, this is indicative for substantial chain transfer and potentially incomplete initiation of the Ru–alkylidene, particularly with unsubstituted norbornene (**M1**) and *cis*-cyclooctene (**M6**) but also with **M4**. However, in turn it allows for the synthesis of high molecular weight polymers. The most striking feature, however, is related to the Ru content of the resulting polymers, which were all obtained as white powders. Unlike in many other Ru–alkylidene-triggered metathesis-based polymerizations, Ru contamination was very low (<2.5 ppm) and even outrivals earlier reported systems bearing two pyridinium carboxylates by at least a factor of 10 [14]. Clearly, both the initiator and any

Table 2: ROMP reactions under biphasic conditions.[a,b]

Monomer	*T* [°C]	Time [h]	Yield [%][c]	M_{theo} [g/mol]	M_n [g/mol][d]	PDI[d]
M1	50	2	93	6,600	258,000	3.8
M2	50	2	89	14,700	94,500	2.3
M3	50	2	80	16,800	15,800	1.2
M4	50	2	86	20,600	907,000	2.8
M5	50	1	100	6,500	–[e]	–[e]
M6	70	3	36	7,700	186,000	1.50

[a]**Ru-2**, toluene, [BDMIM$^+$][BF_4^-], 50−70 °C, 1−3 h. [b]Ru content (measured by ICP–OES) was lower than the limit of detection, which allows for calculating a Ru content <2.5 ppm. [c]Determined after precipitation in methanol. [d]Measured by GPC in THF. [e]Insoluble because of crosslinking.

Ru-containing decomposition products selectively stay in the IL phase while after termination, the polymer stays selectively in the organic (toluene) phase. Notably, polymers were simply precipitated from methanol and not subjected to any further purification steps. We believe that particularly for biomedical applications such virtually Ru-free polymers will be of utmost interest.

Recycling experiments carried out with **M1** revealed that with the aid of 2-(2-PrO)-styrene, **Ru-2** could be used in three consecutive cycles (Scheme 2). Over these three cycles, the number-average molecular weight, M_n, significantly decreased while PDIs increased from 2.1 to 3.0. Again, Ru leaching into the product was below the limit of detection, i.e., <2.5 ppm. The results are summarized in Table 3.

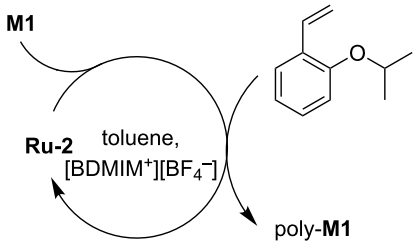

Scheme 2: Recycling of **Ru-2** for continuous ROMP reactions.

Conclusion

The first dicationic Ru–alkylidene catalyst based on an *N*-heterocyclic carbene bearing two quaternary ammonium groups, [($RuCl_2$(H_2ITapMe$_2$)(=CH–2-(2-PrO)-C_6H_4))$^{2+}$ (OTf^-)$_2$] (**Ru-2**), was prepared from the neutral precursor $RuCl_2$(H_2ITap)(=CH–2-(2-PrO)-C_6H_4)) (**Ru-1**) and methyl trifluoromethanesulfonate. Also, an improved, high-yield synthesis of **Ru-1** has been presented. **Ru-2** was tested for its reactivity in ROMP under biphasic conditions using [BDMIM$^+$][BF_4^-] as the ionic liquid and toluene as the organic solvent. While **Ru-2** showed low RCM activity, it turned out to be active in ROMP reactions of strained cyclic olefins like norbornenes, 7-oxanorbornenes, norbornadiene and *cis*-cyclooctene allowing for the synthesis of the corresponding polymers with unprecedented low metal contamination (<2.5 ppm) without any additional purification steps.

Table 3: ROMP of **M1** under biphasic conditions with recycling.[a]

Cycle	Yield [%][b]	M_n [g/mol][c]	PDI[c]
1	89	1,340,000	2.1
2	83	230,000	3.0
3	75	120,000	3.0

[a]1. **Ru-2**, **M1**, toluene, [BDMIM$^+$][BF_4^-], 50 °C, 1.5 h; 2. 2-(2-PrO)-styrene, toluene, 50 °C, 1 h; 3. **M1**, toluene, 50 °C, 1.5 h; following cycles: repeat 2 + 3; last cycle: quenched with ethyl vinyl ether. [b]Determined after precipitation in methanol. [c]Measured by GPC in THF, $M_{n,\,theor}$: 6,600 g/mol.

Experimental

General: Unless noted otherwise, all manipulations were performed in a Labmaster 130 glovebox (MBraun; Garching, Germany) or by standard Schlenk techniques under N_2 atmosphere. CH_2Cl_2 and toluene were purchased from J. T. Baker (Devender, Netherlands) and were dried by using an MBraun SPS-800 solvent purification system. Hexane was purchased from VWR and distilled from sodium/benzophenone under N_2. Starting materials were purchased from ABCR, Aldrich, Alfa Aesar, Fluka and TCI Europe and used without further purification. $KOCMe_2Et$ was purchased from Alfa Aesar as a 25 wt % solution in toluene. Toluene was co-evaporated with pentane in vacuo prior to use.

NMR spectra were recorded on a Bruker Avance III 400 spectrometer in the indicated solvent at 25 °C and are listed in parts per million downfield from tetramethylsilane as an internal standard. IR spectra were measured on a Bruker ATR/FT-IR

IFS 128. GPC measurements were carried out on a system, consisting of a Waters 515 HPLC pump, a Waters 2707 autosampler, Polypore columns (300 × 7.5 mm, Agilent technologies, Böblingen, Germany), a Waters 2489 UV–vis and a Waters 2414 refractive index detector. For calibration, polystyrene standards with 800 < M_n < 2,000,000 g/mol were used. ICP–OES measurements were carried out using a Spectro Acros device (Ametek GmbH; Meerbusch, Germany). Calibration was done with Ru standards containing 0.1, 0.5, 1.0 and 5.0 ppm. Mass spectra were recorded on a Bruker Daltonics Microtof Q mass spectrometer at the Institute of Organic Chemistry at the University of Stuttgart. 1,3-Bis(2,6-dimethyl-4-dimethylaminophenyl)-4,5-dihydroimidazol-2-ylidene (**1**) [21], 2-(2-PrO)-styrene [23,24], **M3** [26] and **M4** [27] were prepared according to the literature.

$RuCl_2(H_2ITap)(=CH\text{-}2\text{-}(2\text{-}PrO)\text{-}C_6H_4\text{-}O)$ (Ru-1) [27,28]: Inside a glovebox, **1** (281 mg, 0.70 mmol), $KOCMe_2Et$ (88 mg, 0.70 mmol) and hexane (9 mL) were added to a 50 mL Schlenk flask equipped with a magnetic stir bar. The reaction mixture was allowed to stir for 1 h at room temperature, during which time a brownish orange suspension formed. The 1st-generation Grubbs–Hoveyda catalyst (400 mg, 0.67 mmol) dissolved in hexane (6 mL) was added to the reaction mixture. The reaction mixture was removed from the glovebox and was heated to 60 °C for 4 h. The formation of a green solid was observed. After cooling to room temperature, all solids were filtered off and washed with pentane (3 × 10 mL) and diethyl ether (3 × 10 mL); then the product was redissolved in CH_2Cl_2. Purification was accomplished by chromatography using silica G60 and CH_2Cl_2/hexane. Drying in vacuo gave the product as a dark green solid (375 mg, 0.55 mmol, 82%). Analytical data were in accordance with the literature [20].

$[(RuCl_2(H_2ITapMe_2)(=CH\text{–}2\text{-}(2\text{-}PrO)\text{-}C_6H_4))^{2+}\ (OTf^-)_2]$ (Ru-2): At −30 °C, methyl trifluormethanesulfonate (99 mg, 601 µmol) dissolved in CH_2Cl_2 (3 mL) was added to **Ru-1** (200.5 mg, 293 µmol) dissolved in CH_2Cl_2 (5 mL). The mixture was stirred for 18 h at room temperature and then, CH_2Cl_2 was removed under reduced pressure. The residue was washed with CH_2Cl_2 (3 × 3 mL) and ethyl acetate (3 × 3 mL), allowing for the isolation of the target compound as a light-green solid (267 mg, 264 µmol, 90%). ^{1}H NMR (DMF-d_7) δ 16.47 (s, 1H, Ru=CH), 8.17 (s, 4H, NHC-Ar), 7.70–7.66 (m, 1H, C_6H_4), 7.20 (d, J = 8.4 Hz, 1H, C_6H_4), 7.06–7.04 (m, 1H, C_6H_4), 6.96 (t, J = 7.4 Hz, 1H, C_6H_4), 5.10 (hept, J = 7.4 Hz, 1H, O-C*H*-$(CH_3)_2$), 4.42 (s, 4H, N-CH_2), 4.00 (s, 18H, N-$(CH_3)_3$), 2.66 (s, 12H, NHC-Ar-CH_3), 1.27 (d, J = 6.1 Hz, 6H, O-CH-C*H*$_3$); ^{13}C NMR (DMF-d_7) δ 292.9 (Ru=CH), 211.6 (N-C=N), 153.5, 148.7, 145.9, 143.1, 141.2, 131.3, 123.6, 123.5, 121.8, 114.5 (C_6H_2, C_6H_4), 127.3, 124.1, 120.9, 117.7 (CF_3-SO_3^-, q, $J_{C\text{-}F}$ = 322.5 Hz), 76.4 (*C*H$(CH_3)_2$), 57.9 (N$(CH_3)_3$), 52.6, 21.9, 20.3 (CH(*C*H$_3)_2$, Ar-CH_3); ^{19}F NMR (DMF-d_7) δ −78.5; FTIR (ATR, cm^{-1}) $\tilde{\nu}$: 1589 (s), 1491 (m), 1251 (m), 1152 (m), 1114 (m), 1028 (s), 923 (m), 840 (s), 801 (s), 754 (s), 637 (s), 572 (s), 517 (s) cm^{-1}; MS (ESI) m/z: calcd. for $C_{35}H_{50}Cl_2N_4ORu$ (dication, z = 2): 357.1199, found: 357.1214; m/z calcd. for $C_{36}H_{50}F_3Cl_2N_4O_4RuS$: 863.1923, found: 863.1905. Crystals suitable for X-ray diffraction were obtained by layering diethyl ether over a solution of **Ru-2** in anhydrous DMF.

General ROMP-procedure: Ru-2 (5.6 mg, 5 µmol or 11.13 mg, 10 µmol) and $[BDMIM^+][BF_4^-]$ (400 mg) were placed inside a flame-dried Schlenk tube (25 mL) equipped with a magnetic stir bar. The reaction mixture was heated to the indicated temperature. The monomer (350 µmol or 700 µmol) and toluene (2 mL) were added to a separate flame-dried Schlenk tube. The monomer solution was added via syringe in one portion and the reaction mixture was allowed to stir at the indicated temperature for the indicated time. After cooling to room temperature, ethyl vinyl ether (1 mL) was added and the reaction mixture was allowed to stir for another 30 min. Finally, the reaction mixture was poured into methanol. The polymer was obtained as a white or off-white solid.

General ROMP-procedure with recycling: Ru-2 (11.1 mg, 10 µmol) and $[BDMIM^+][BF_4^-]$ (400 mg) were placed inside a flame-dried Schlenk tube (25 mL) equipped with a magnetic stir bar. The reaction mixture was heated to the indicated temperature. **M1** (65.9 mg, 700 µmol) and toluene (5 mL) were added to a separate flame-dried Schlenk tube. The monomer solution was added via syringe in one portion and the reaction mixture was allowed to stir at 50 °C for 1.5 h. Then a solution of 2-(2-PrO)-styrene in anhydrous toluene (1 mL, 1 M) was added. The reaction mixture was stirred at 50 °C for 1 h. The two phases were allowed to separate. The organic phase was poured into methanol. The IL phase was extracted with toluene (4 × 2 mL). The extracted organic phases were also poured into methanol. Poly-**M1** was obtained as a white solid. New **M1** was added to the IL phase and the procedure was repeated. After the last cycle, the reaction was quenched with ethyl vinyl ether (1 mL).

ICP–OES measurements: The corresponding polymer (20 mg) was added to high-pressure Teflon tubes. Digestion was performed under microwave conditions using aqua regia (10 mL). The mixture was cooled to room temperature, diluted with deionized water (approx. 40 mL), filtered and subjected to ICP–OES for Ru with λ = 240.272 nm ion line and background lines at λ_1 = 240.254 nm and λ_2 = 240.295 nm.

Poly-M1: ^{1}H NMR ($CDCl_3$) δ 5.35 (s, 1H), 5.21 (s, 1H), 2.79 (bs, 1H), 2.44 (bs, 1H), 1.88–1.79 (2bs, 3H), 1.35 (bs, 2H),

1.09–1.02 (m, 2H); ^{13}C NMR ($CDCl_3$) δ 134.1, 134.0, 133.9, 133.3, 133.2, 133.0, 43.6, 43.3, 42.9, 42.2, 41.5, 38.8, 38.6, 33.3, 33.1, 32.5, 32.4; FTIR (ATR, cm^{-1}) $\tilde{\nu}$: 2941 (s), 2863 (m), 1446 (w), 1260 (s), 1189 (w), 1081 (s), 1020 (s), 965 (s), 862 (w), 798 (s), 737 (m), 688 (w).

Poly-M2: ^{1}H NMR ($CDCl_3$) δ 5.52 (bs, 2H), 3.64–3.60 (2bs, 6H), 3.13–2.85 (4bs, 4H), 1.89 (2bs, 2H); ^{13}C NMR ($CDCl_3$) δ 172.9, 172.5, 131.9, 131.1, 130.5, 51.7, 51.6, 51.5, 51.4, 51.1, 44.5, 39.2, 38.8, 38.1; FTIR (ATR, cm^{-1}) $\tilde{\nu}$: 3020 (w), 2951 (w), 1726 (s), 1434 (m), 1386 (w), 1347 (w), 1194 (m), 1169 (m), 1153 (m), 1095 (w), 1041 (w), 978 (w), 957 (w), 807 (w), 747 (m), 666 (w), 603 (w).

Poly-M3: ^{1}H NMR ($CDCl_3$) δ 5.74 (bs, 1H), 5.56 (bs, 1H), 4.59–4.49 (2bs, 1H), 4.17–4.11 (2bs, 5H), 2.39 (bs, 2H), 2.04–2.02 (2s, 6H); ^{13}C NMR ($CDCl_3$) δ 170.8, 170.7, 133.3, 132.9, 132.4, 131.8, 81.5, 81.2, 62.0, 61.9, 61.8, 46.5, 46.2, 46.1, 45.9, 45.6, 21.0, 20.9; FTIR (ATR, cm^{-1}) $\tilde{\nu}$: 3017 (w), 2958 (w), 2902 (w), 1733 (s), 1468 (w), 1434 (w), 1389 (w), 1366 (m), 1221 (s), 1119 (w), 1030 (s), 968 (m), 834 (w), 750 (m), 667 (w), 604 (m), 506 (w), 471 (w).

Poly-M4: ^{1}H NMR ($CDCl_3$) δ 5.27–5.17 (2bs, 2H), 3.40–3.35 (2bs, 8H), 2.69 (bs, 1H), 2.32 (bs, 1H), 1.96 (bs, 3H), 1.55 (bs, 4H), 1.32–1.13 (2bs, 10H), 0.90 (bs, 6H); ^{13}C NMR ($CDCl_3$) δ 134.0, 133.8, 71.3, 71.2, 70.8, 70.6, 48.1, 47.8, 47.6, 47.0, 45.6, 45.3, 41.2, 40.1, 29.7, 28.7, 22.7, 14.2; FTIR (ATR, cm^{-1}) $\tilde{\nu}$: 3005 (w), 2919 (s), 2850 (s), 1465 (m), 1438 (w), 1261 (w), 1091 (w), 1071 (w), 1026 (w), 965 (s), 805 (w), 720 (w).

Poly-M6: ^{1}H NMR ($CDCl_3$) δ 5.43–5.31 (m, 2H), 2.02–1.97 (m, 4H), 1.33–1.29 (bs, 8H); ^{13}C NMR ($CDCl_3$) δ 130.5, 130.0, 32.8, 29.9, 29.8, 29.4, 29.3, 29.2, 27.4; FTIR (ATR, cm^{-1}) $\tilde{\nu}$: 2954 (m), 2929 (m), 2853 (m), 1795 (w), 1482 (w), 1465 (w), 1367 (w), 1104 (s), 1066 (m), 1010 (w), 966 (w), 741 (m).

Supporting Information

Supporting Information File 1

Analytical data for **Ru-2**, the polymers prepared, details on the single crystal X-ray structural analysis of **Ru-2**, results for biphasic RCM.
[http://www.beilstein-journals.org/bjoc/content/supplementary/1860-5397-11-178-S1.pdf]

Acknowledgements

Financial support provided by the Deutsche Forschungsgemeinschaft (DFG, grant no. BU 2174/8-1) is gratefully acknowledged.

References

1. Gallivan, J. P.; Jordan, J. P.; Grubbs, R. H. *Tetrahedron Lett.* **2005,** *46,* 2577–2580. doi:10.1016/j.tetlet.2005.02.096
2. Hong, S. H.; Grubbs, R. H. *J. Am. Chem. Soc.* **2006,** *128,* 3508–3509. doi:10.1021/ja058451c
3. Jordan, J. P.; Grubbs, R. H. *Angew. Chem., Int. Ed.* **2007,** *119,* 5244–5247. doi:10.1002/ange.200701258
4. Kirkland, T. A.; Lynn, D. M.; Grubbs, R. H. *J. Org. Chem.* **1998,** *63,* 9904–9909. doi:10.1021/jo981678o
5. Lynn, D. M.; Mohr, B.; Grubbs, R. H. *J. Am. Chem. Soc.* **1998,** *120,* 1627–1628. doi:10.1021/ja9736323
6. Lynn, D. M.; Mohr, B.; Grubbs, R. H. *Polym. Prepr. (Am. Chem. Soc., Div. Polym. Chem.)* **1998,** *39,* 278–279.
7. Lynn, D. M.; Mohr, B.; Grubbs, R. H.; Henling, L. M.; Day, M. W. *J. Am. Chem. Soc.* **2000,** *122,* 6601–6609. doi:10.1021/ja0003167
8. Mohr, B.; Lynn, D. M.; Grubbs, R. H. *Organometallics* **1996,** *15,* 4317–4325. doi:10.1021/om9603373
9. Wagaman, M. W.; Grubbs, R. H. *Macromolecules* **1997,** *30,* 3978–3985. doi:10.1021/ma9701595
10. Klučiar, M.; Grela, K.; Mauduit, M. *Dalton Trans.* **2013,** *42,* 7354–7358. doi:10.1039/c2dt32856a
11. Autenrieth, B.; Frey, W.; Buchmeiser, M. R. *Chem. – Eur. J.* **2012,** *18,* 14069–14078. doi:10.1002/chem.201201199
12. Autenrieth, B.; Anderson, E. B.; Wang, D.; Buchmeiser, M. R. *Macromol. Chem. Phys.* **2013,** *214,* 33–40. doi:10.1002/macp.201200544
13. Autenrieth, B.; Willig, F.; Pursley, D.; Naumann, S.; Buchmeiser, M. R. *ChemCatChem* **2013,** *5,* 3033–3040. doi:10.1002/cctc.201300199
14. Ferraz, C. P.; Autenrieth, B.; Frey, W.; Buchmeiser, M. R. *ChemCatChem* **2014,** *6,* 191–198. doi:10.1002/cctc.201300751
15. Zhao, J.; Wang, D.; Autenrieth, B.; Buchmeiser, M. R. *Macromol. Rapid Commun.* **2015,** *36,* 190–194. doi:10.1002/marc.201400413
16. Skowerski, K.; Szczepaniak, G.; Wierzbicka, C.; Gułajski, Ł.; Bieniek, M.; Grela, K. *Catal. Sci. Technol.* **2012,** *2,* 2424–2427. doi:10.1039/c2cy20320k
17. Skowerski, K.; Wierzbicka, C.; Szczepaniak, G.; Gułajski, L.; Bienieka, M.; Grela, K. *Green Chem.* **2012,** *14,* 3264–3268. doi:10.1039/c2gc36015b
18. Szczepaniak, G.; Kosiński, K.; Grela, K. *Green Chem.* **2014,** *16,* 4474–4492. doi:10.1039/C4GC00705K
19. Kośnik, W.; Grela, K. *Dalton Trans.* **2013,** *42,* 7463–7467. doi:10.1039/C3DT33010A
20. Leuthäußer, S.; Schwarz, D.; Plenio, H. *Chem. – Eur. J.* **2007,** *13,* 7195–7209. doi:10.1002/chem.200700228
21. Balof, S. L.; P'Pool, S. J.; Berger, N. J.; Valente, E. J.; Shiller, A. M.; Schanz, H.-J. *Dalton Trans.* **2008,** 5791–5799. doi:10.1039/B809793C
22. Balof, S. L.; Yu, B.; Lowe, A. B.; Ling, Y.; Zhang, Y.; Schanz, H.-J. *Eur. J. Inorg. Chem.* **2009,** 1717–1722. doi:10.1002/ejic.200801145
23. Krause, J. O.; Wurst, K.; Nuyken, O.; Buchmeiser, M. R. *Chem. – Eur. J.* **2004,** *10,* 777–784. doi:10.1002/chem.200305031
24. Vygodskii, Y. S.; Shaplov, A. S.; Lozinskaya, E. I.; Filippov, O. A.; Shubina, E. A.; Bandari, R.; Buchmeiser, M. R. *Macromolecules* **2006,** *39,* 7821–7830. doi:10.1021/ma061456p
25. Aitken, B. S.; Lee, M.; Hunley, M. T.; Gibson, H. W.; Wagener, K. B. *Macromolecules* **2010,** *43,* 1699–1701. doi:10.1021/ma9024174
26. Takao, K.-i.; Yasui, H.; Yamamoto, S.; Sasaki, D.; Kawasaki, S.; Watanabe, G.; Tadano, K.-i. *J. Org. Chem.* **2004,** *69,* 8789–8795. doi:10.1021/jo048566j

27. Endo, K.; Grubbs, R. H. *J. Am. Chem. Soc.* **2011,** *133,* 8525–8527. doi:10.1021/ja202818v
28. Jafarpour, L.; Hillier, A. C.; Nolan, S. P. *Organometallics* **2002,** *21,* 442–444. doi:10.1021/om0109511

License and Terms

BEILSTEIN JOURNAL OF ORGANIC CHEMISTRY

Design and synthesis of propellane derivatives and oxa-bowls via ring-rearrangement metathesis as a key step

Sambasivarao Kotha*§ and Rama Gunta

Full Research Paper

Open Access

Address:
Department of Chemistry, Indian Institute of Technology-Bombay, Powai, Mumbai-400 076, India

Email:
Sambasivarao Kotha* - srk@chem.iitb.ac.in

* Corresponding author
§ Fax: 022-25767152

Keywords:
allylation; propellane derivatives; quinones; ring-rearrangement metathesis

Beilstein J. Org. Chem. **2015,** *11,* 1727–1731.
doi:10.3762/bjoc.11.188

Received: 15 June 2015
Accepted: 10 September 2015
Published: 24 September 2015

This article is part of the Thematic Series "Progress in metathesis chemistry II".

Guest Editor: K. Grela

Abstract

Various intricate propellane derivatives and oxa-bowls have been synthesized via a ring-rearrangement metathesis (RRM) as a key step starting from readily accessible starting materials such as *p*-benzoquinone, 1,4-naphthoquinone and 1,4-anthraquinone.

Introduction

The synthesis of complex target structures requires bond-disconnection analysis of the target molecule, eventually to arrive at simple starting materials by working in an opposite direction to a chemical synthesis. The 'retrosynthetic analysis' was first introduced by E. J. Corey and defined as "*it is a problem solving technique for transforming the structure of a synthetic target molecule to a sequence of progressively simpler structures along a pathway which ultimately leads to a simple or commercially available starting materials for a chemical synthesis*" [1] . Generally, this type of retrosynthetic analysis has been used to design [2-6] the target molecule. However, a "transformation-based" retrosynthetic approach is rarely used. In the transformation-based strategy the target and precursor compounds are related by a rearrangement as the key transformation. The advantages of the rearrangement-based strategy are: the target molecule can be assembled from less obvious and more accessible precursors. Several C–C bonds are formed in a simple manner by taking advantage of the key rearrangement and the overall synthetic economy of the process can be enhanced. One can design unprecedented synthetic routes to complex targets [7] through the rearrangement-based approach. In this regard, the ring-rearrangement metathesis (RRM) [8-12] is useful and moreover, the stereochemical information can be transferred from the starting material to the final product during the RRM. In continuation of our interest to design novel molecules via metathesis [13-20] we conceived a new and simple route to propellane derivatives and oxa-bowls [21-26]. This strategy starts from simple starting materials and involves a Diels–Alder (DA) reaction [27,28] and RRM as the key steps.

Results and Discussion

Strategy

The retrosynthetic strategy to diverse propellane derivatives and oxa-bowls is shown in Figure 1. Oxa-bowl **1** can be synthesized from the tetracyclic compound **2** using RRM, which could be obtained from the known DA adduct **3** by O-allylation. On the other hand, the propellane derivative **7** may be synthesized from the tetraallyl compound **6** by a RRM sequence. Further, the tetraallyl compound **6** can be assembled from the C-allyl derivative **4** via reduction followed by O-allylation. The C-allyl derivative **4** may be obtained from the known DA adduct **3** by a C-allylation sequence which in turn could be prepared by the DA reaction of the corresponding 1,4-quinones (*p*-benzoquinone, 1,4-naphthoquinone or 1,4-anthraquinone) with a freshly cracked cyclopentadiene.

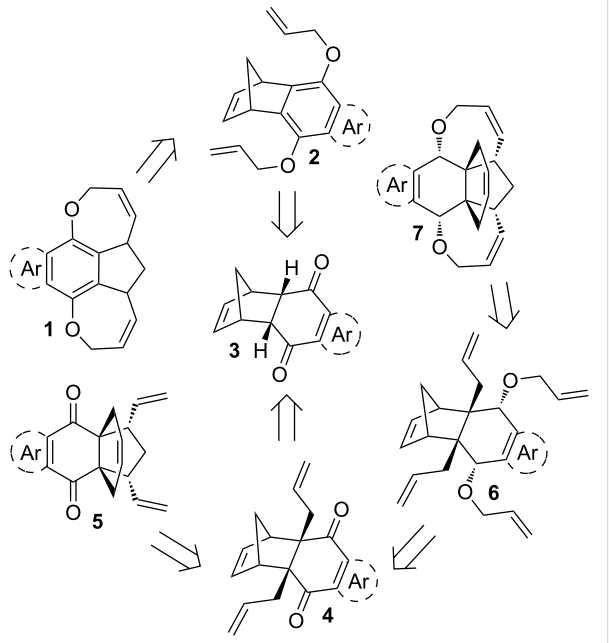

Figure 1: RRM route to propellane derivatives and oxa-bowls.

To realize the synthetic strategy (Figure 1) to various propellane derivatives [29-31] and oxa-bowls, we commenced with the preparation of a known DA adduct **3a** [32]. Subsequent allylation of **3a** with allyl bromide in the presence of NaH delivered the aromatized compound **2a** in 42% yield. Then, the tricyclic compound **2a** was subjected to RRM with Grubbs 1st generation (G-I) catalyst in the presence of ethylene to furnish the tetracyclic compound **1a** in 75% yield (Scheme 1). The structures of compounds **2a** and **1a** have been confirmed on the basis of ^{1}H, ^{13}C NMR and DEPT-135 spectral data and further supported by HRMS data.

To expand the strategy, another DA adduct **3b** was prepared from the commercially available 1,4-naphthoquinone and freshly cracked cyclopentadiene by following the literature procedure [33]. Allylation of adduct **3b** under similar reaction conditions as described above gave O-allylated compound **2b** and C-allylated compound **4a** in 70% and 28% yields, respectively. Then, treatment of the O-allyl compound **2b** with G-I catalyst in the presence of ethylene at room temperature (rt) produced the RRM product, a pentacyclic oxa-bowl **1b** in 90% yield. When the C-allyl compound **4a** was treated with G-II catalyst in CH_2Cl_2 at rt or in refluxing toluene, the propellane derivative **5a** was obtained in 69% yield (Scheme 2). The structures of the new compounds **2b**, **4a**, **1b** and **5a** have been established on the basis of ^{1}H and ^{13}C NMR spectral data and further supported by HRMS data.

Next, another DA adduct **3c** was prepared from readily available starting materials. In this regard, 1,4-anthraquinone was prepared from quinizarin (1,4-dihydroxyanthraquinone) by using the literature procedure [34] and the known DA adduct **3c** was obtained by a cycloaddition reaction [35] of 1,4-anthraquinone and cyclopentadiene.

Again, allylation of the DA adduct **3c** with allyl bromide in the presence of NaH afforded the O-allylated compound **2c** in 41% and the C-allylated compound **4b** in 7% yield. Compound **2c** was further subjected to RRM with G-I catalyst in the presence of ethylene to deliver the hexacyclic oxa-bowl **1c** in quantitative yield (Scheme 3).

Having the C-allylated DA adducts **4a**,**b** in hand, compound **4a** was reduced with diisobutylaluminium hydride (DIBAL-H) at

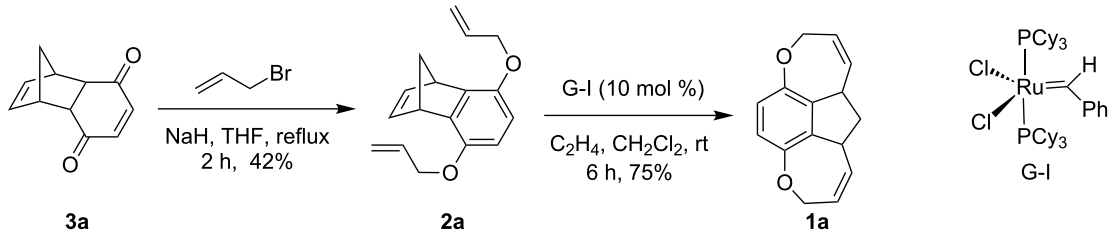

Scheme 1: Synthesis of the oxa-bowl **1a** via RRM.

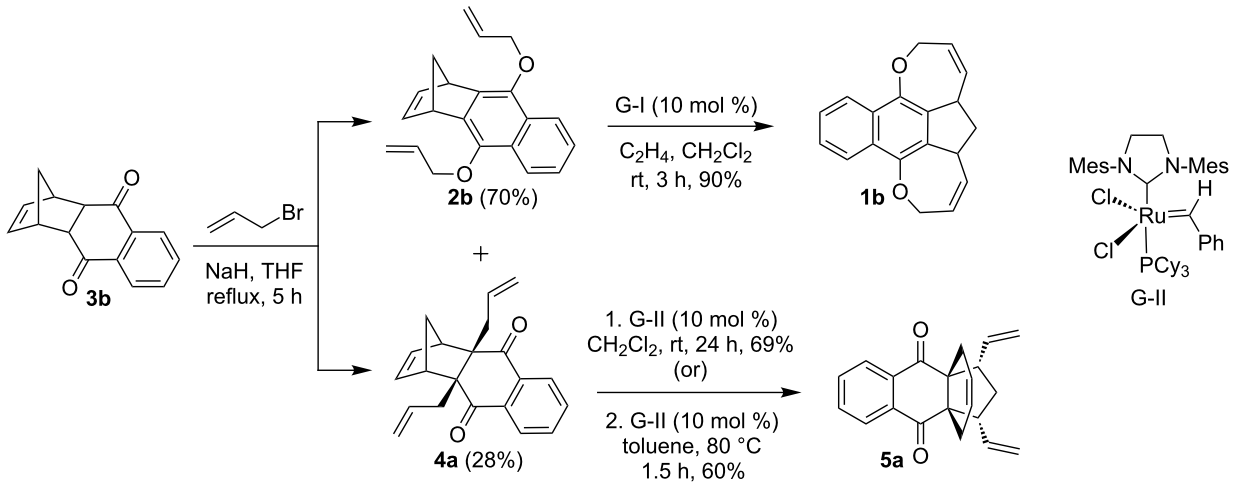

Scheme 2: Synthesis of RRM products **1b** and **5a** starting from DA adduct **3b**.

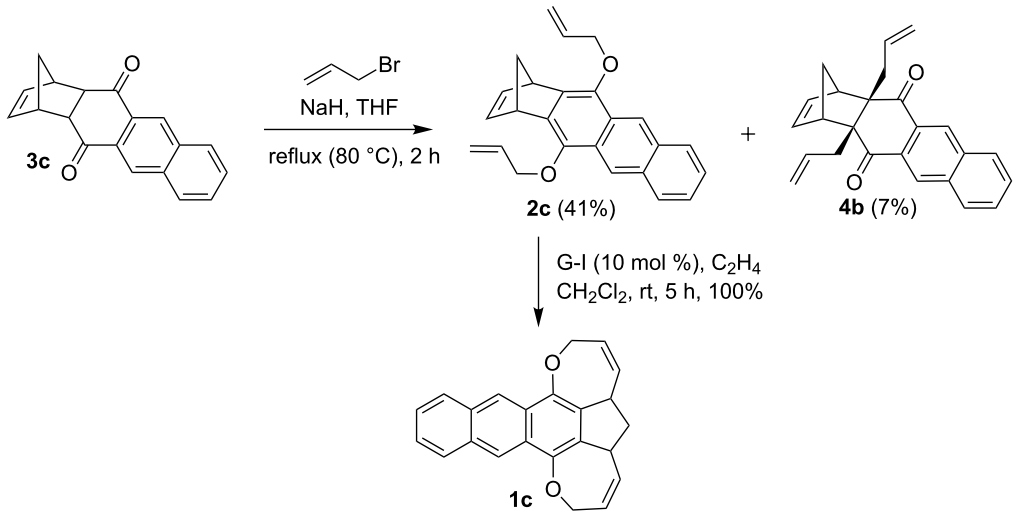

Scheme 3: Synthesis of the hexacyclic compound **1c** using RRM.

−74 °C to furnish diol **8a** in 81% yield along with a minor amount of compound **9** (8%). The formation of compound **9** may be explained on the basis of a retro-DA reaction [36] followed by reduction and elimination. In the same way, reduction of C-allyl compound **4b** under similar reaction conditions gave diol **8b** in 88% yield.

In the next step, diols **8a,b** were O-allylated with allyl bromide in the presence of NaH to furnish the desired RRM precursors **6a**,**b** in 67% and 79% yields respectively (Scheme 4).

Finally, the tetraallyl derivatives **6a**,**b** were subjected to RRM with G-I catalyst in the presence of ethylene at rt to produce the corresponding propellane/oxa-bowl hybrids **7a**,**b** in 71% and 97% yields, respectively. The new compounds **2c**, **4b**, **1c**, **8a**,**b**, **9**, **6a**,**b** and **7a**,**b** have been fully characterized by using spectroscopic techniques (^{1}H, ^{13}C NMR and DEPT-135) and HRMS data.

Conclusion

We have successfully synthesized diverse heterocycles **1a–c** in a simple manner starting from the known DA adducts **3a–c**, including the propellane/oxa-bowl hybrids **7a**,**b** and propellane derivative **5a**. Interestingly, the structurally complex propellane/oxa-bowl hybrids **7a**,**b** were obtained through a four step synthetic sequence starting from simple DA adducts **3b**,**c**, which are otherwise difficult to synthesize following conventional retrosynthetic routes. This methodology can easily be extended

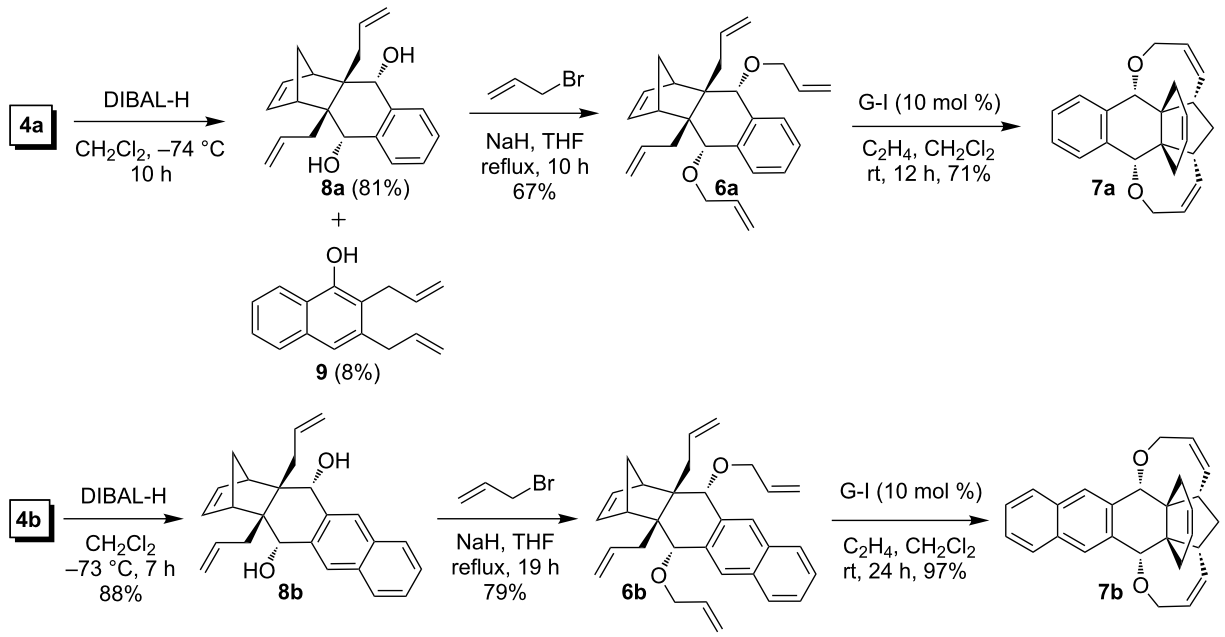

Scheme 4: Synthesis of the propellane/oxa-bowl hybrids **7a**,**b** via RRM.

for diversity-oriented synthesis [37] by employing different dienes and dienophiles during the DA reaction sequence.

Supporting Information

Supporting Information File 1

Detailed experimental procedures, characterization data and copies of ^{1}H and ^{13}C NMR for all new compounds.
[http://www.beilstein-journals.org/bjoc/content/supplementary/1860-5397-11-188-S1.pdf]

Acknowledgements

We thank the Department of Science and Technology (DST), New Delhi for the financial support and the Sophisticated Analytical Instrument Facility (SAIF), IIT-Bombay for recording spectral data. S.K. thanks the Department of Science and Technology for the award of a J. C. Bose fellowship. R.G. thanks the University Grants Commission (UGC), New Delhi for the award of a research fellowship.

References

1. Corey, E. J.; Cheng, X.-M. *The Logic of Chemical Synthesis;* John Wiley & Sons: New York, 1989.
2. Hanessian, S.; Giroux, S.; Merner, B. L. *Design and Strategy in Organic Synthesis;* Wiley-VCH: Weinheim, 2013.
3. Wyatt, P.; Warren, S. *Organic Synthesis: Strategy and Control;* John Wiley & Sons: Sussex, 2013.
4. Smit, W. A.; Bochkov, A. F.; Caple, R. *Organic Synthesis: The Science Behind the Art;* Royal Society of Chemistry: Cambridge, 1998. doi:10.1039/9781847551573
5. Hopf, H. *Classics in Hydrocarbon Chemistry;* Wiley-VCH: Weinheim, 2000.
6. Hudlicky, T.; Reed, J. W. *The Way of Synthesis: Evolution of Design and Methods for Natural Products;* Wiley-VCH: Weinheim, 2007.
7. Nicolaou, K. C.; Sorensen, E. J. *Classics in Total Synthesis: Targets, Strategies, Methods;* Wiley-VCH: Weinheim, 1996.
8. Holub, N.; Blechert, S. *Chem. – Asian J.* **2007,** *2,* 1064–1082. doi:10.1002/asia.200700072
And references cited therein.
9. Schmidt, B.; Krehl, S. Domino and Other Olefin Metathesis Reaction Sequences. In *Olefin Metathesis: Theory and Practice, Part I;* Grela, K., Ed.; John Wiley & Sons: Hoboken, New Jersey, 2014.
10. Nolan, S. P.; Clavier, H. *Chem. Soc. Rev.* **2010,** *39,* 3305–3316. doi:10.1039/B912410c
11. Kotha, S.; Ravikumar, O. *Eur. J. Org. Chem.* **2014,** 5582–5590. doi:10.1002/ejoc.201402273
12. Kotha, S.; Gunta, R. *Beilstein J. Org. Chem.* **2015,** *11,* 1373–1378. doi:10.3762/bjoc.11.148
13. Grubbs, R. H.; O'Leary, D. J., Eds. *Handbook of Metathesis,* 2nd ed.; Wiley-VCH: Weinheim, 2015; Vol. 2.
14. Kotha, S.; Misra, S.; Sreevani, G.; Babu, B. V. *Curr. Org. Chem.* **2013,** *17,* 2776–2795. doi:10.2174/13852728113179990118
15. Kotha, S.; Dipak, M. K. *Tetrahedron* **2012,** *68,* 397–421. doi:10.1016/j.tet.2011.10.018
16. Kotha, S.; Krishna, N. G.; Halder, S.; Misra, S. *Org. Biomol. Chem.* **2011,** *9,* 5597–5624. doi:10.1039/c1ob05413a
17. Kotha, S.; Meshram, M.; Tiwari, A. *Chem. Soc. Rev.* **2009,** *38,* 2065–2092. doi:10.1039/B810094m
18. Kotha, S.; Lahiri, K. *Synlett* **2007,** 2767–2784. doi:10.1055/s-2007-990954

19. Kotha, S.; Sreenivasachary, N. *Indian J. Chem., Sect. B* **2001,** *40,* 763–780.
20. Kotha, S.; Mandal, K. *Tetrahedron Lett.* **2004,** *45,* 1391–1394. doi:10.1016/j.tetlet.2003.12.075
21. Kotha, S.; Chinnam, A. K. *Synthesis* **2014,** *46,* 301–306. doi:10.1055/s-0033-1340341
22. Kotha, S.; Chinnam, A. K.; Tiwari, A. *Beilstein J. Org. Chem.* **2013,** *9,* 2709–2714. doi:10.3762/bjoc.9.307
23. Kotha, S.; Chavan, A. S.; Dipak, M. K. *Tetrahedron* **2011,** *67,* 501–504. doi:10.1016/j.tet.2010.10.080
24. Kotha, S.; Dipak, M. K. *Chem. – Eur. J.* **2006,** *12,* 4446–4450. doi:10.1002/chem.200501366
25. Gharpure, S. J.; Porwal, S. K. *Org. Prep. Proced. Int.* **2013,** *45,* 81–153. doi:10.1080/00304948.2013.764782
And references cited therein.
26. Kotha, S.; Ravikumar, O. *Tetrahedron Lett.* **2014,** *55,* 5781–5784. doi:10.1016/j.tetlet.2014.08.108
27. Kotha, S.; Chavan, A. S.; Goyal, D. *ACS Comb. Sci.* **2015,** *17,* 253–302. doi:10.1021/co500146u
28. Kotha, S.; Brahmachary, E.; Sreenivasachary, N. *Tetrahedron Lett.* **1998,** *39,* 4095–4098. doi:10.1016/S0040-4039(98)00562-0
29. Ginsburg, D. *Propellanes: Structure and Reactions;* Verlag Chemie: Weinheim, 1975.
30. Ginsburg, D. *Propellanes: Structure and Reactions: Sequel I;* Technion: Haifa, 1981.
31. Ginsburg, D. *Propellanes: Structure and Reactions: Sequel II;* Technion: Haifa, 1985.
32. Mal, D.; Ray, S. *Eur. J. Org. Chem.* **2008,** 3014–3020. doi:10.1002/ejoc.200800218
33. Valderrama, J. A.; Espinoza, O.; González, M. F.; Tapia, R. A.; Rodríguez, J. A.; Theoduloz, C.; Schmeda-Hirschmann, G. *Tetrahedron* **2006,** *62,* 2631–2638. doi:10.1016/j.tet.2005.12.038
And references cited therein.
34. Hua, D. H.; Tamura, M.; Huang, X.; Stephany, H. A.; Helfrich, B. A.; Perchellet, E. M.; Sperfslage, B. J.; Perchellet, J.-P.; Jiang, S.; Kyle, D. E.; Chiang, P. K. *J. Org. Chem.* **2002,** *67,* 2907–2912. doi:10.1021/jo010958s
35. Patney, H. K.; Paddon-Row, M. N. *Synthesis* **1986,** 326–328. doi:10.1055/s-1986-31602
36. Kotha, S.; Banerjee, S. *RSC Adv.* **2013,** *3,* 7642–7666. doi:10.1039/C3ra22762f
37. Trabocchi, A. *Diversity-Oriented Synthesis: Basics and Applications in Organic Synthesis, Drug Discovery, and Chemical Biology;* John Wiley & Sons: Hoboken, 2013.

License and Terms

BEILSTEIN JOURNAL OF ORGANIC CHEMISTRY

A comprehensive study of olefin metathesis catalyzed by Ru-based catalysts

Albert Poater*[1] and Luigi Cavallo*[2]

Full Research Paper

Open Access

Address:
[1]Institut de Química Computacional i Catàlisi and Departament de Química, Universitat de Girona, Campus Montilivi, 17071 Girona, Catalonia, Spain and [2]KAUST Catalysis Center, Physical Sciences and Engineering Division, King Abdullah University of Science and Technology, Thuwal 23955-6900, Saudi Arabia

Email:
Albert Poater* - albert.poater@udg.edu; Luigi Cavallo* - luigi.cavallo@kaust.edu.sa

* Corresponding author

Keywords:
cis; density functional theory (DFT); N-heterocyclic carbene; olefin metathesis; ruthenium

Beilstein J. Org. Chem. **2015,** *11,* 1767–1780.
doi:10.3762/bjoc.11.192

Received: 29 June 2015
Accepted: 04 September 2015
Published: 29 September 2015

This article is part of the Thematic Series "Progress in metathesis chemistry II".

Guest Editor: K. Grela

Abstract

During a Ru-catalyzed reaction of an olefin with an alkylidene moiety that leads to a metallacycle intermediate, the cis insertion of the olefin can occur from two different directions, namely side and bottom with respect to the phosphine or N-heterocyclic ligand (NHC), depending on the first or second generation Grubbs catalyst. Here, DFT calculations unravel to which extent the bottom coordination of olefins with respect is favored over the side coordination through screening a wide range of catalysts, including first and second generation Grubbs catalysts as well as the subsequent Hoveyda derivatives. The equilibrium between bottom and side coordination is influenced by sterics, electronics, and polarity of the solvent. The side attack is favored for sterically less demanding NHC and/or alkylidene ligands. Moreover the generation of a 14-electron species is also discussed, with either pyridine or phosphine ligands to dissociate.

Introduction

Organic synthesis is based on reactions that drive the formation of carbon–carbon bonds [1]. Olefin metathesis represents a metal-catalyzed redistribution of carbon–carbon double bonds [2-6] and provides a route to unsaturated molecules that are often challenging or impossible to prepare by any other means. Furthermore, the area of ruthenium-catalyzed olefin metathesis reactions is an outstanding field for the synthesis of C–C double bonds [7-9]. After the discovery of well-defined Ru-based (pre)catalysts, such as $(PCy_3)_2Cl_2Ru{=}CHPh$ [10], first by Grubbs and co-workers the range of these catalysts was broadened because of their tolerancy towards heteroatom ligands and the possibility to work under mild conditions.

The next step was the substitution of one phosphine group by an N-heterocyclic carbene, NHC, which strongly increases the activity [11-15]. And, furthermore, a detailed comprehensive

analysis of the chemical mechanics of these Grubbs catalysts was required. Once a better understanding of the performance of such catalysts was achieved, a rational design of new more active catalysts was envisaged [16-19]. Despite experimental [20-24] and theoretical [8,9,25,26] insights during the last two decades, demonstrating the mechanism in Scheme 1, there are still missing parts in the understanding. Anyway, it is also confirmed that the first steps go through a dissociative mechanism instead of an associative, i.e., the entering olefin arrives after the extraction of two pyridine groups. Most of studies are related to phosphine groups instead of pyridine groups, but the function of both chemical groups is the same.

The release of a pyridine or phosphine group generates a 14-electron (14e) species, which binds to an olefin, coordinated cis to the alkylidene. The exchange of the leaving group by an olefin is found to be mainly dissociative [4,27-29], towards the associative or the concerted mechanisms [30]. The next metallacycle intermediate is due to the reaction of the olefin with the alkylidene moiety. Nevertheless in the cis insertion of the olefin, this olefin can enter from two different directions, side and bottom, displayed in Scheme 2. Regarding this cis insertion of the olefin, even though most papers favor the side insertion of the olefin (see Scheme 2) over the bottom insertion [31], both pathways might exist depending on the ligands and type of olefin. Since the year 2000 many papers try to unravel the preference for the bottom attack and how to favor the cis one [8,32-34], with an open debate still for the(NHC)Ru-based catalysts [35-38]. The postulated binding of the substrate can be preferentially trans to the NHC ligand (bottom path in Scheme 2) or cis to this ligand with the simultaneous shift of an halogen group to a trans position (side path in Scheme 2).

Bearing the general acceptance [39-45] that olefin metathesis with Ru-catalysts starts from a bottom-bound olefin complex because of energetics, i.e., reporting higher energies for the possible side-bound olefin complexes, Piers and co-workers demonstrated the bottom-bound geometry for a Ru-cyclobutane model compound by NMR data [46]. However, Grubbs and co-workers supported the side-bound pathway [47]. And this sort of discrepancy is displayed in Scheme 3, where the same catalyst shows two conformations, **a** and **b**, bottom and side, respectively. Next, by means of DFT calculations Goddard and

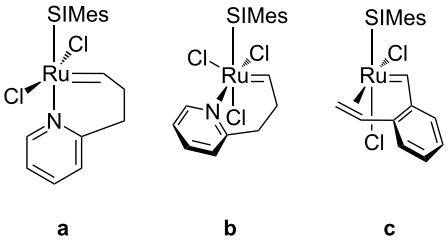

Scheme 3: Ruthenium catalysts, bottom-bound (**a**) or side-bound (**b** and **c**).

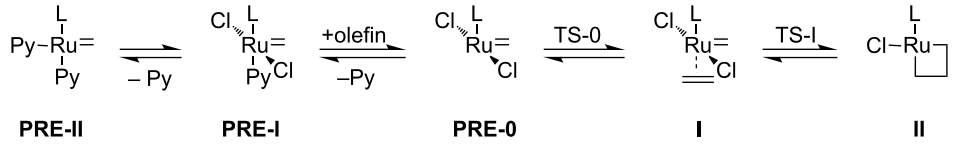

Scheme 1: Mechanism of the olefin metathesis.

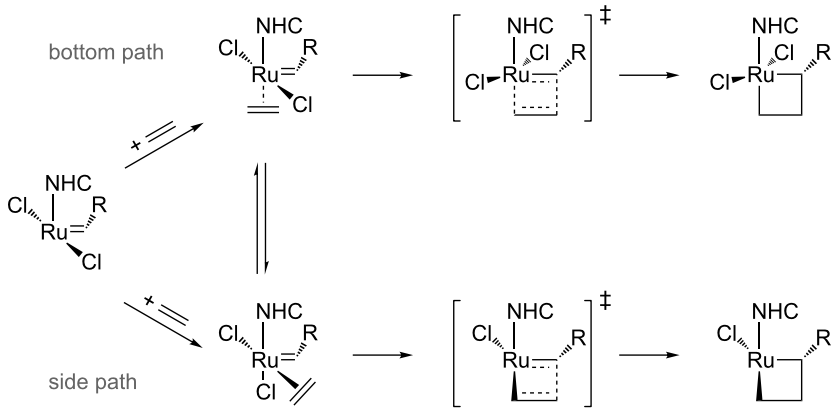

Scheme 2: Possible side or bottom mechanism of the insertion of the olefin.

co-workers indicated clearly that solvent effects were of paramount relevance to the relatively high stability of **b** [48], while in the gas phase structure **a** was much favored [13]. Moreover, Grubbs and co-workers reported the X-ray structure of the model compound **c**, which clearly indicates that the olefin is side-bound to Ru [49].

Next, Correa and Cavallo discussed about the feasibility of the side conformation for the classical olefin metathesis catalysts **7**, **16**, and **19** displayed in Scheme 4 [8], concluding that the bottom/side equilibrium is based on a delicate balance between electronic, steric, and solvent effects. Particularly sterically demanding substituents of the NHC and bulky olefins clearly favor the side reaction pathway. Moreover this study corroborated the validity of BP86 for these second generation Grubbs catalysts and the conclusion was that any generalization could be done about the side/bottom stability of the coordination intermediate, as well as it is not possible for the first Grubbs catalysts [9]. Overall, the inclusion of a polar solvent and the absence of strong steric effects, i.e., with less bulky ligands (less than SIMes) and/or substrates [50,51], favored the side-bound structures over the bottom-bound ones as suggested by Goddard and Grubbs, respectively [16-18]. This is a possible explanation of why there is experimental evidence for some structures with side confirmation. On the other hand, complex **19** is an example of an asymmetric catalyst, suggesting that the NHC ligand is the source of asymmetry [52].

In this paper we contribute in the understanding of the side- and bottom-bound coordination intermediates and the stability of the corresponding transition states as well as the relative stability of the next metallacycle formed for (NHC)Ru(X)$_2$ catalysts through a DFT approach with the BP86 functional. The comparison with the first generation Grubbs catalysts with a phosphine group instead of an NHC and the game based on the possible electronic and steric possibilities of the NHC will center our interests. All studied systems are displayed in Scheme 4. System **7** has been thoroughly studied because of its simplicity, playing especially with the NHC ligand, replacing one or both mesityl groups by CH_3, CF_3, *t*-Bu, H, F, and combinations between them to also observe the effects of an asymmetric NHC ligand. Furthermore this system **7** was also taken to discuss about the evolution of the precatalysts, **PRE-II**, **PRE-I** and **PRE-0** (see Scheme 1). This can corroborate the dissociative mechanism of the entering olefin, a step which has been taken into account. Then complex **15** reveals a more representative substrate, and is useful to focus on the study of steric effects of the substrate, reinforced the steric hindrance aspect replacing one or both mesityl groups of NHC ligand by methyl groups. Bearing the asymmetric catalysts **17**–**19**, particularly complex **19** can be compared to **16** but introducing asymmetry [17,53]. Then complexes **1** and **14** are representative of the first generation Grubbs catalysts. Finally, several systems are displayed to get insight into the typical properties of free halogen catalysts [54,55].

Computational details

The density functional calculations were performed on all the systems at the GGA level with the Gaussian03 set of programs [56]. Two popular functionals, B3LYP and BP86, were considered. B3LYP calculations utilize Becke's three parameter hybrid exchange functional together with the correlation functional of Lee, Yang and Parr [57-59]. For BP86 calculations, gradient corrections were taken from the work of Becke and Perdew [60-62]. The electronic configuration of the molecular systems was described by the standard SVP basis set, i.e., the split-valence basis set with polarization functions of Ahlrichs and co-worker, for H, C, N, P, O, S, F, Cl and Br [63]. For Ru and I we used the small-core, quasi-relativistic Stuttgart/Dresden effective core potential (standard SDD basis set in Gaussian03) basis set, with an associated (8s7p6d)/[6s5p3d] valence basis set contracted according to a (311111/22111/411) scheme [64-66].

The geometry optimizations were performed without symmetry constraints, and the nature of the extrema was checked by analytical frequency calculations. Furthermore, all extrema were confirmed by calculation of the intrinsic reaction paths. The energies discussed throughout the text contain ZPE corrections. Solvent effects including contributions of non-electrostatic terms have been estimated in single point calculations on the gas phase optimized structures, based on the polarizable continuous solvation model PCM using CH_2Cl_2 as a solvent [67]. The cavity is created via a series of overlapping spheres.

For the sake of clarity we did not change the functional for the solvent calculations, despite knowing that the dispersion interactions can occur [68-73]. However, here we consider that the qualitative comparison between the set of studied catalysts and even the quantitative trends (side/bottom) should not be affected by this omission.

Results and Discussion

In this section we first discuss the structure and energetics of the key steps of metallacycle formation, starting with dissociation of the leaving L ligand, pyridine in this manuscript, from precatalysts **1**–**13**, and moving to coordination of the C=C double bond of ethene in systems **1**–**13**, or of the C=C bond tethered to the Ru atom in systems **14**–**19**. Then, we will discuss structure and energetics of the four-center transition state for metallacycle formation, and finally structure and energetics of the metallacycle. In all cases, we assumed the naked 14e species as zero of energy.

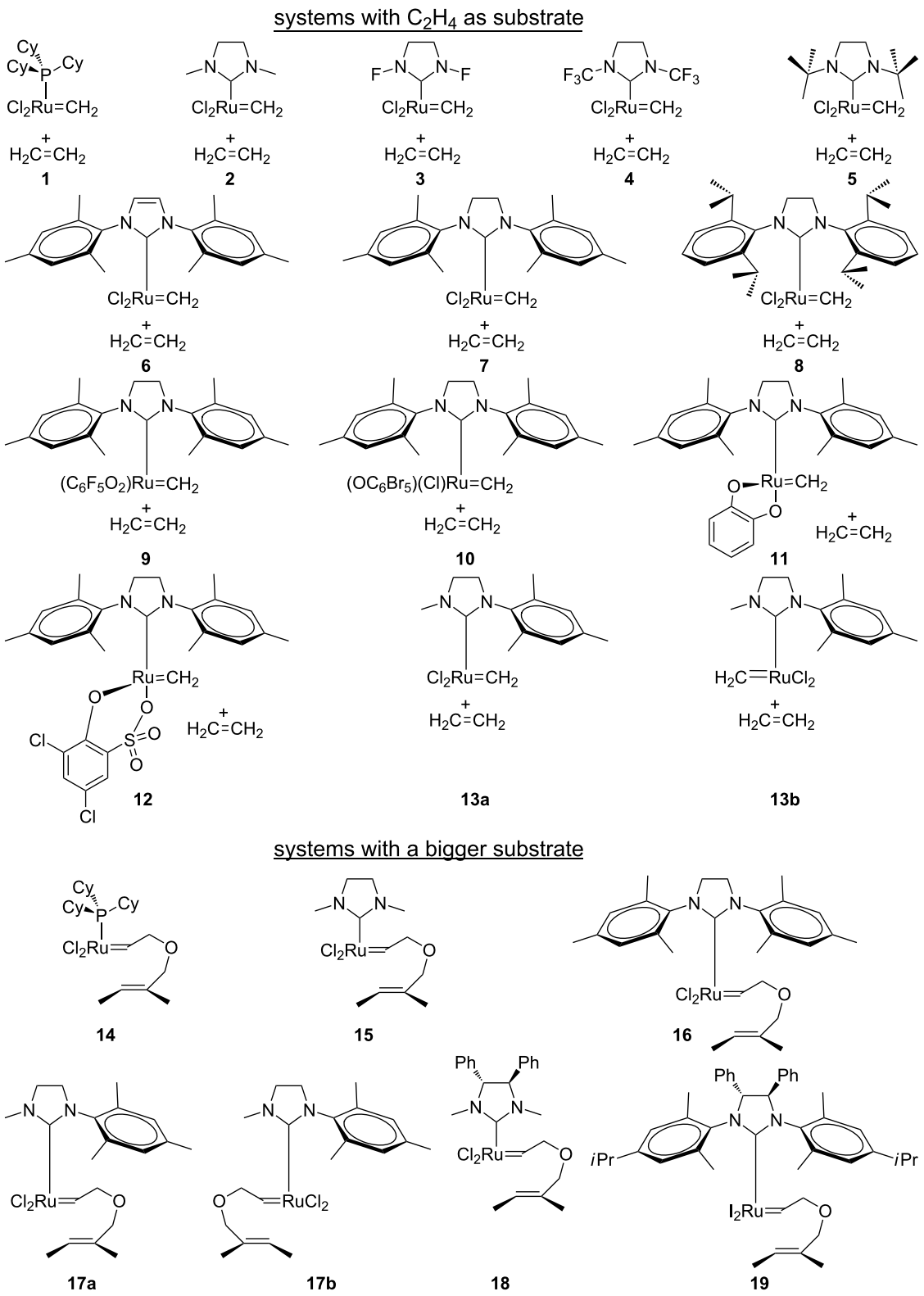

Scheme 4: Studied systems.

Structure of the naked 14e species. According to all the calculations reported so far, the naked 14e species is very unstable. The dissociation of PR_3 or pyridine ligands is highly endothermic, approximately 15–20 kcal/mol even if solvent effects with implicit methods are considered. An unfavorable entropic term of roughly 8–10 kcal/mol would reduce this internal binding energy to free energies of binding around 5–12 kcal/mol [13].

According to simple Boltzmann statistics, these energetics implies that the fraction of the naked 14e species in solution at 25 °C should be in the range of 10^{-11} to 10^{-13} of the total precatalyst. Even considering an overestimation of PR_3 or pyridine binding by roughly 5 kcal/mol, an error that would be quite large for this kind of calculations, still the fraction of the active species should be in the range of 10^{-6} to 10^{-11}. Considering that the precatalyst concentration is usually in the order of 10^{-1} to 10^{-3} M, this means that the concentration of the real 14e catalyst should be roughly in the range of 10^{-7} to 10^{-13}. These numbers suggest that it is very unlikely that the naked 14e species is the "real" active species, and that probably some other species is indeed coordinated to the Ru atom in place of the pyridine or phosphine to first dissociate.

Pyridine and phosphine binding. The binding energy of the first (trans to the PR_3 or NHC ligand) and of the second (trans to the ylidene group) pyridine ligands to the naked 14e species of **1**–**19** are reported in the 2nd and 3rd column of Table 1. These values indicate that the first pyridine is bonded quite strongly to the Ru atom. Indeed, it is competitive with PCy_3 binding in the prototype 1st and 2nd generation systems based on **1** and **7** [74-76]. In precatalysts **1**–**7** the binding energy of the first pyridine is roughly 20 kcal/mol, with a small effect of the ligand bulkiness, which only changes for system **8** bearing more sterically demanding isopropyl groups, displaying a value of 15.0 kcal/mol. The pseudo-halide systems, instead, show a remarkably different behavior. The pyridine is quite weakly bound to **9**, E_1 = 14.3 kcal/mol, and this binding energy decreases to 7.7 kcal/mol only in **10**. Differently, the pyridine is bound very strongly to the Ru atom, by more than 30 kcal/mol, in systems **11** and **12**. Of course, the pyridine is coordinated trans to the NHC ligand in **9** and **10**, whereas it is cis coordinated in **11** and **12**. Considering the pseudo-halide family, our results are in qualitative agreement with the experimental finding of Fogg and co-workers that systems **11** and **12** have to be thermally activated [19], while system **10** is even more active than the prototype 2nd generation system **7**. Finally, the C_1-symmetric system **13** shows E_1 values which are substantially independent from the specific geometry; i.e., whether the methylidene group is on the side of the mesityl or of the methyl group of the NHC ligand, species, **13a** and **13b**, respectively.

Table 1: Binding energy, in kcal/mol, of the first, E_1, and of the second, E_2, pyridine/PMe_3 molecule to the naked 14e species **1**–**13**.

system	pyridine			PMe_3		
	E_1	E_2	$E_1 + E_2$	E_1	E_2	$E_1 + E_2$
1	20.3	2.5	22.8	27.3	5.1	32.4
2	18.3	9.6	27.9	26.8	9.1	35.9
3	21.0	7.7	30.7	25.5	13.2	38.7
4	19.9	0.2	20.1	29.3	−5.4	23.9
5	21.7	−15.4	6.3	32.8	—	—
6	20.7	7.5	28.2	28.5	−4.4	26.1
7	19.7	6.8	26.5	27.7	3.6	24.1
8	15.0	−6.0	21.0	23.6	−4.6	19.0
9	14.3	0.6	14.9	17.9	3.6	21.5
10	7.7	−5.0	2.7	11.9	—	—
11	33.2	−2.9	30.3	41.1	—	—
12	35.6	—	—	45.7	—	—
13a	21.1	5.8	26.9	28.9	5.0	33.9
13b	13.5	6.1	19.6	17.9	4.9	22.8
14	8.7	7.3	16.0	17.9	−2.8	15.1
15	11.1	12.6	23.7	19.5	11.9	31.4
16	11.5	7.8	19.3	20.8	—	—
17a	10.4	5.3	15.7	18.5	4.1	22.6
17b	10.3	8.6	18.9	19.2	0.0	19.2
18	2.2	5.4	7.6	5.1	9.5	14.6
19	13.0	−1.5	11.5	19.8	—	—

Table 1 also includes corresponding values for the phosphine dissociation, PMe_3 for this analysis. The trend is the same as the one explained above for the pyridine dissociation. But quantitatively the phosphine dissociation is more expensive.

The double coordination of pyridine or trimethylphosphine is not possible for all systems. Systems **5**, **10**, **11**, **12**, **16**, and **19** do not accept the second phosphine group because of steric hindrances. We must point out that for system **12** when bonding one Py or PMe_3 moiety the octahedral environment around the metal is already obtained. Furthermore there are some other systems that exhibit a negative value for E_2, i.e., no stability for the octahedral structure. This instability is related to the elongation of the Ru–P bond distance cis to the NHC ligand. Indeed in all systems the Ru–P bond is much shorter for the phosphine placed trans to the NHC (around 2.45 Å), compared with the Ru–P bond distance cis to the NHC (around 2.60 Å). However for some systems this distance is too long to be more stable than the monophosphine complex. Thus, when this bond distance is over 2.65 Å the bisphosphine precatalyst structure is not stable.

Substrate coordination. The coordination energy of the C=C double bond of the substrate to the Ru atom of the various 14e species are reported in the 3rd column of Table 2, while in the 4th column the coordination energy of the cis isomer relative to

the trans isomer is reported. We focus first on C_2H_4 coordination to the symmetric precatalysts **1**–**8**. For these systems we considered both trans and cis coordination of C_2H_4 to the PR_3 or NHC ligand, denoted as "T" and "C" in Table 2. In agreement with experimental findings on related systems, we found that cis coordination of the substrate is preferred. This preference is influenced by the bulkiness of the NHC ligand, and is smaller for larger N-substituents. Indeed, the calculated energy difference between the cis and trans geometries in the coordination intermediates of **2**–**5**, ΔE of 4th column in Table 2, follows a clear trend with the bulkiness of the N-substituents, F < Me < CF_3 < *t*-Bu, ΔE = −8.0 < −5.2 < −3.4 < −2.1 kcal/mol, respectively.

Steric effects have little influence on the absolute C_2H_4 binding energy, *E* of 3rd column in Table 2, since rather similar values are calculated for **2** and **5** (−18.6 and −19.1 kcal/mol, respectively). Differently, electronic effects influence the ability of the Ru atom to capture C_2H_4, particularly in the trans isomer. For example, the electron withdrawing F substituents in **3** results in a trans C_2H_4 coordination energy of only 6.6 kcal/mol, whereas in the sterically similar system **2** the trans C_2H_4 coordination energy is 13.4 kcal/mol. The highest coordination energies are calculated for **2** and **5**, which present electron donating substituents, whereas systems **6** and **7**, with aromatic N-substituents, lie in between. This suggests that electron donating N-substituents increase electron density at the carbene

Table 2: Energies (*E*) in kcal/mol, of the coordination intermediates, transition states and metallacycles with respect to the 14e species and the uncoordinated C=C double bond. For each system, the energies of both isomers with the C=C trans or cis to the NHC ligand are reported. For each species, Δ*E* is the energy difference between the cis and the trans isomer, labeled as C and T, respectively.

system	geometry	I		TS		II	
		E	Δ*E*	*E*	Δ*E*	*E*	Δ*E*
1 P	T	−10.0	0	−4.2	0	−19.6	0
	C	−11.3	−1.3	−6.6	−2.4	−19.8	-0.2
2 Me	T	−13.4	0	−9.5	0	−25.7	0
	C	−18.6	−5.2	−10.2	−0.7	−23.4	2.3
3 F	T	−6.6	0	−5.7	0	−17.8	0
	C	−14.6	−8.0	−10.4	−4.7	−23.2	−5.4
4 CF_3	T	−11.9	0	−10.9	0	−23.6	0
	C	−15.3	−3.4	−8.7	2.2	−22.5	1.1
5 *t*-Bu	T	−17.0	0	−13.1	0	−30.2	0
	C	−19.1	−2.1	−5.6	7.5	−18.0	12.2
6 IMes	T	−15.5	0	−11.4	0	−25.2	0
	C	−13.6	1.9	−7.8	3.6	−20.8	4.4
7 SIMes	T	−11.8	0	−10.1	0	−25.0	0
	C	−14.7	−2.9	−6.2	3.9	−19.0	6.0
8 SIPr	T	−9.9	0	−7.2	0	−21.9	0
	C	−14.7	−4.8	−6.9	0.3	−19.5	2.4
9 FgF5	T	−7.8	0	−6.7	0	−14.2	0
	C	−16.3	−8.5	−9.7	−3.0	−20.2	−6.0
10 FgBr	T	1.1	0	0.6	0	−9.1	0
	C1	−9.7	−10.8	−0.9	−1.5	−11.4	−2.3
	C2	−5.7	−6.8	0.6	0.0	−15.0	−5.9
11 FgO	T	3.1	0	3.2	0	−20.6	0
	C	−33.5	−36.6	−24.0	−27.1	−39.1	−18.5
12 FgS	C (S_1)	−27.5	0	−21.9	0	−35.6	0
	C(S_2)	−34.3	−6.8	−26.6	−4.7	−37.6	−2.0
	C(O)	−29.4	−1.9	−18.7	−2.8	−37.5	−1.9
13a C1	T	−14.6	0	−13.0	0	−26.3	0
	C	−19.7	−5.1	−9.5	3.5	−23.9	2.4
13b C1	T	−8.8	0	−4.9	0	−22.4	0
	C	−12.7	−3.9	−4.8	0.1	−20.1	2.3
14 PR_3	T	4.5	0	19.0	0	7.7	0
	C-re	9.7	5.2	20.2	1.2	15.9	8.2
	C-si	14.4	9.9	20.7	1.7	17.1	9.4

Table 2: Energies (*E*) in kcal/mol, of the coordination intermediates, transition states and metallacycles with respect to the 14e species and the uncoordinated C=C double bond. For each system, the energies of both isomers with the C=C trans or cis to the NHC ligand are reported. For each species, Δ*E* is the energy difference between the cis and the trans isomer, labeled as C and T, respectively. (continued)

15 Me	T	0.1	0	1.0	0	−3.3	0
	C-re	−5.9	−6.0	4.0	3.0	−1.8	2.5
	C-si	−8.1	−8.2	4.5	3.5	2.2	5.5
16 Mes	T	−1.8	0	0.6	0	−2.7	0
	C-re	−1.5	0.3	12.6	12.0	8.4	11.1
	C-si	2.4	4.2	19.9	19.3	12.1	14.8
17a C1	T	0.0	0	2.7	0	−0.2	0
	C-re	−4.6	−4.6	11.2	8.5	7.4	7.6
	C-si	−0.8	−0.8	12.8	10.1	5.5	5.7
17b C1	T	−0.1	0	0.5	0	−4.7	0
	C-re	−2.1	−2.0	2.4	1.9	−3.8	0.9
	C-si	−2.4	−2.3	6.8	6.3	7.4	12.1
18 Me1	T	1.3	0	2.1	0	−2.7	0
	C-re	−2.7	−4.0	6.9	4.8	0.9	3.6
	C-si	−7.7	−9.0	13.2	11.1	7.3	10.0
19 Pr1	T	−0.7	0	0.7	0	−4.2	0
	C-re	−0.9	−0.2	14.7	14.0	11.8	16.0
	C-si	−2.8	−2.1	16.7	16.0	12.9	17.1

C atom of the NHC, which results in a higher electron density on the σ contribution of the HOMO of the NHC. When 1st and 2nd generation catalysts are compared, system **1**, with the PCy_3 ligand, behaves rather similary to the 2nd generation catalyst **7**, with a SIMes NHC ligand.

Substitution of the Cl ligands of **7** with the far bulkier $O(C_6F_5)$ ligands, such as in **9**, increases the preference for cis C_2H_4 coordination from 2.9 to 8.5 kcal/mol, while the absolute C_2H_4 binding energy in the cis isomer increases from 14.7 to 16.3 kcal/mol. Interestingly, in the naked 14e species one of the F atoms of the $O(C_6F_5)$ ligands is engaged in a Ru···F interaction trans to the NHC, which makes the bottom pathway for the entering olefin more difficult, see Figure 1. This kind of Ru···F interactions was first reported by Grubbs and co-workers [77,78]. Finally, replacing just one Cl atom of **7** with a C_6Br_5

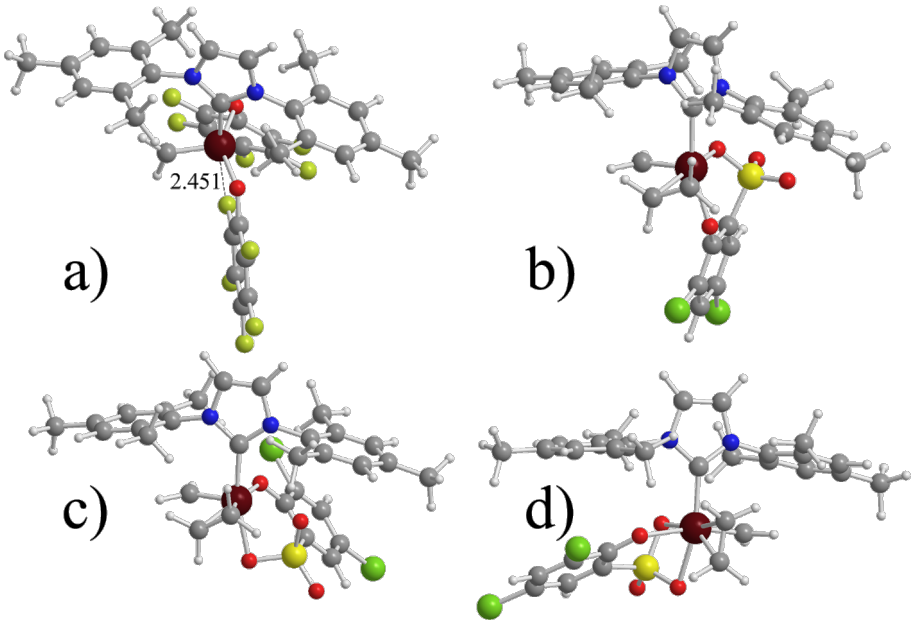

Figure 1: a) Naked 14e species for system **9** (distance in Å). b) trans (T); c) cis(S) (C(S)); and d) cis(O) (C(O)) C_2H_4 coordinated species for **12**.

ring, such as in **9**, results again in a preferred cis coordination, and the most stable isomer presents the Cl atom cis to the SIMes ligand.

Moving to the pseudo-halide systems with a chelating ligand, the most striking difference is in the absolute C_2H_4 coordination energy, roughly 30 kcal/mol, which is about 15 kcal/mol better than in the non-chelating ligands. The chelating ligand has a minor effect on the cis/trans preference for **12**, whereas for **11** trans coordination of C_2H_4 is not favored. This is easily explained by considering that the 5-membered ring formed through chelation of the cresol group to Ru makes a trans O–Ru–O disposition geometrically difficult, whereas the 6-membered ring formed by chelation of the sulfoxide ligand in **12** allows for a trans O–Ru–O geometry with little steric strain. **12** presents three cis isomers, denoted as C(S_1), C(S_2), and C(O) in Table 2, which correspond to have the phenolic or the sulfonic O atom trans to the NHC ligand (see Figure 1). Our calculations indicate a preference for the C(S_2) isomer, which is 4.9 and 6.8 kcal/mol more stable than the C(O) and the C(S_1) isomers, respectively. The preference for the C(S_2) isomer can be explained by the weaker donicity of the sulphonic O atom with respect to the phenolic O atom, which results in a softer ligand trans to the SIMes ligand.

Focusing on system **13**, bearing a C_1-symmetric ligand, we found that the cis coordination still is favored, and the most stable structure corresponds to **13a**, which presents the methylidene moiety on the side of the mesityl N-substituent, while isomer **13b**, which presents the methylidene moiety on the side of the Me N-substituent is 7.0 kcal/mol higher in energy. The structure of the two cis coordination intermediates clearly indicates that the C_2H_4 molecule nicely avoids steric repulsion with the NHC ligand in **13a**, whereas it experiences repulsive interaction with the methyl on the NHC ligand in **13b** (see Figure 2).

Moving to substrates bulkier than C_2H_4, systems **14**–**19**, the cis geometry is favored only in the systems that present small methyl N-substituents, i.e., **15**, **17a** and **18**. This indicates that bulkier substrates can be accommodated in the cis position with difficulty. Furthermore, in almost all the cases coordination of the C=C double bond, either in the cis or trans position, is disfavored (positive *E* values in the 3rd column of Table 2). This striking difference relative to C_2H_4 coordination, which is always favored (negative *E* values in the 3rd column of Table 2), is due to the coordination of the O atom of the substrate in **14**–**19**. In other words, with a heteroatom containing substrate the heteroatom can coordinate to the Ru center, as in the Hoveyda-type precatalysts [6], maybe stabilizing the active species, see Figure 3a. In any case, coordination of the C=C double bond requires displacement of the coordinated O atom, and it is likely that the terminal C=C double bond of complex substrates will be dangling, which is in agreement with the NMR experiments of Piers and co-workers on strictly related systems [13]. Focusing on a selection between the two prochiral faces of the C=C bond in **14**–**19**, we always found that coordination takes places in the face that presents the two methyl groups pointing away from the NHC ligand. Of course, this results in reduced steric interactions with the NHC ligand.

In the trans geometries, instead, the C=C double bond of C_2H_4 is nearly perpendicular to the Ru–methylidene bond, whereas in the bigger substrate the tether forces the coordinated C=C bond to be almost aligned with the Ru–alkylidene bond. However, the molecular dynamics simulations (vide infra) clearly indicate that in the trans geometries the C_2H_4 molecule can freely rotate around the coordination axis to the Ru center. Finally, the Ru–C bond distances are roughly the same (2.20–2.25 Å) in the case of C_2H_4 coordination, whereas in the case of the bigger substrate the coordination of the olefin is highly asymmetric, with the internal C roughly 2.50–2.60 Å away from the Ru atom.

Transition state for metallacycle formation. The energy of the various transition states for metallacycle formation with respect to the uncoordinated C=C double bond are reported in

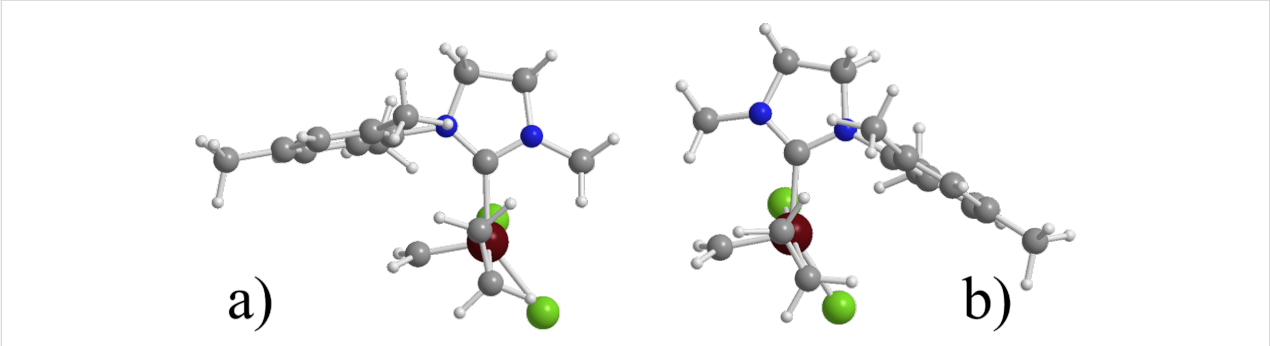

Figure 2: Coordinated species for species a) **13a** and b) **13b**.

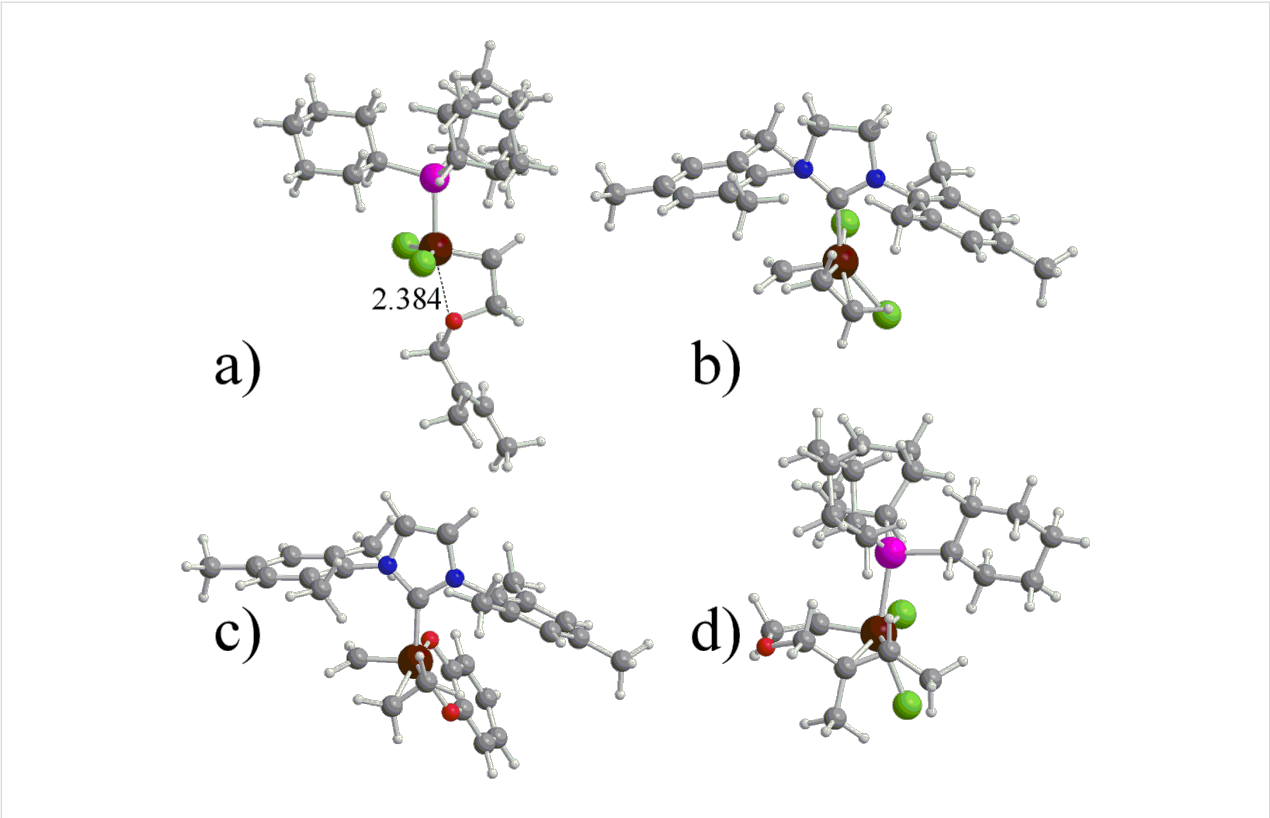

Figure 3: Naked 14e species for system **14** with the O atom of the substrate coordinated to the Ru center (distance in Å), part a; and representative coordination geometries for systems **7**, **11** and **14** with a cis coordinated C_2H_4 molecule, parts b–d.

the 5th column of Table 2, while in the 6th column it is reported the energy of the cis transition states with respect to the trans transition state. The numbers reported clearly indicate that at the transition state the bulkiness of the N-substituents plays a more remarkable role. Indeed, while cis C_2H_4 coordination is favored for all the systems we considered, the cis transition state is favored only for some systems. Specifically, for the 1st generation system **1**, for symmetric NHC systems with small N-substituents, such as **3**, for all the pseudo-halide systems, and for system **13**, with a C_1-symmetric NHC ligand. Differently, for non pseudo-halide NHC systems with N-substituents bulkier than Me, such as **4**, **5**, **6**, and **7**, the trans transition state is clearly favored. The increased role of steric effects can be clearly understood if we consider that at the transition state the C=C double bond must be placed almost parallel to the Ru=CH_2 bond, which results in increased steric repulsion with the NHC ligand, whereas in the coordination intermediates the C=C double bond is almost perpendicular to the Ru=CH_2 bond, to occupy the free space above the NHC ring, between the N-substituents. The pseudo-halide systems, where the cis coordination is strongly favored, prefer the cis geometry also in the transition state. Finally, for system **9** the Ru···F interaction is preserved, see Figure 4. A similar interaction is also retained in the trans transition state, see again Figure 4.

In the case of systems **14–19**, with the bulkier substrate, the trans transition state is clearly favored for all the systems. Also for those that present rather stable cis geometry at the level of the coordination intermediate, such as system **15**. As already indicated, this is due to the steric pressure of the PCy_3 or NHC ligands on the bulkier substrate. Interestingly, in all the systems considered the energy barrier for metallacyle formation, that is the energy difference between the transition states and the coordination intermediates, is quite small, always below 10 kcal except for system **14**, and usually below 5 kcal/mol. This indicates that all these systems should be highly active, which unfortunately is not the case. This fact suggests that the origin of the remarkably different catalytic activity shown by these systems lays somewhere else.

Metallacycle. The energy of the various metallacycles with respect to the uncoordinated C=C double bond are reported in the 5th column of Table 2, while in the 6th column the energy of the cis metallacycle with respect to the trans metallacycle is reported. Beside a few cases, the general trend is that ongoing from the coordination intermediates, to the transition states and finally to the metallacycles, there is an energetic shift towards the trans geometry. In fact, besides the pseudo-halide systems, which strongly favor the cis isomer, the cis metallacycle is

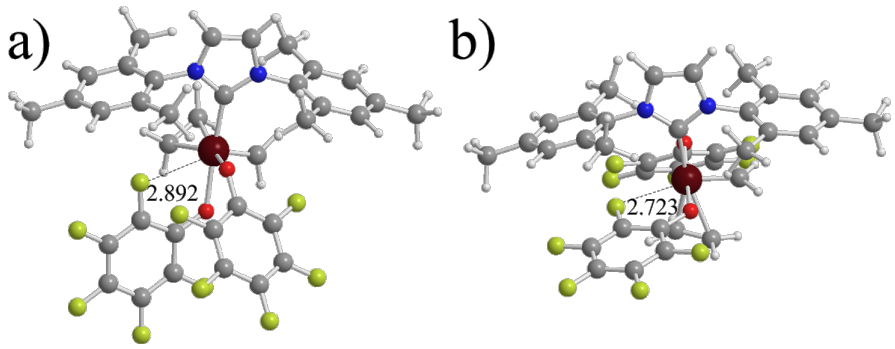

Figure 4: System **9** with a Ru···F interaction in the cis and trans geometries, parts a and b, respectively (distance in Å).

favored only for system **3**, with the small F substituents. The stability of the metallacycles relative to the coordination intermediates is strongly influenced by the nature of the substrate. In fact, with C_2H_4 as the substrate, systems **1**–**13**, the metallacycle is roughly 10 kcal/mol lower in energy with respect to the coordination intermediates, which suggests that the resting state is the Ru–metallacycle species. This is in agreement with the NMR experiments of Piers and co-workers that found the Ru–metallacycle as the most abundant species in the ethene exchange metathesis promoted by system **7** [32,79]. Differently, with the bigger substrate the metallacycle is of comparable stability or slightly higher in energy with respect to the coordination intermediate, also in agreement with the data of Piers and coworkers [33].

Structurally, the Ru–C(metallacycle) bonds in **1**, **2**, **3** and **7** are rather similar, around 1.97–1.98 Å, see Figure 5a, while in **5** they are remarkably longer with 2.01 Å, probably due to the steric pressure of the *t*-Bu N-substituents. In all the cases the C–C bonds of the Ru–cyclobutane are around 1.58–1.59 Å. Differently, in the presence of the bigger substrate the metallacycle is quite asymmetric, see Figure 5b. The C–C length of the former C=C double bond is quite shorter, around 1.57 Å in **14** and **16**, than the C–C bond just formed, which is around 1.65–1.66 Å. This finding is in good agreement with the NMR experiments by Piers and co-workers [33].

After this reporting on the energetic and structure of each intermediate separately, we combine this information into the energy profile that connects the naked 14e precatalysts and the uncoordinated substrate with the metallacycles. For reasons of simplicity, we selected the most representative cases, which we believe are the 1st and 2nd generation systems with PCy_3 and SIMes as ligands, both for the small substrate C_2H_4, systems **1** and **7**, and the bigger substrate, systems **14** and **16**. In the case of C_2H_4 as substrate, coordination of the olefin is clearly favored both for the 1st and 2nd generation systems **1** and **7**, see Figure 6 and Figure 7, although it is clear that the 2nd generation catalysts coordinate to the substrate somewhat better. With the more complex substrate C=C binding has to compete with the O binding, which substantially results in no energy gain for the C=C coordination. Moving to the transition states for metallacycle formation requires climbing the rather low energy barrier of 4.7 and 1.7 kcal/mol for **1** and **7**, respectively, and in both cases the transition state is lower in energy than the naked 14e precatalyst, by 6.6 and 10.1 kcal/mol, respectively. This indicates that metallacycle formation is favored with respect to C_2H_4 dissociation. Finally, both transition states collapse into very stable metallacycles. However, beside an overall similarity there is the sharp difference that in **1** the cis path is favored, whereas in **7** the trans path is favored. Furthermore, the energy gain associated with metallacycle formation is quite higher in the 2nd generation catalyst rather than for the 1st

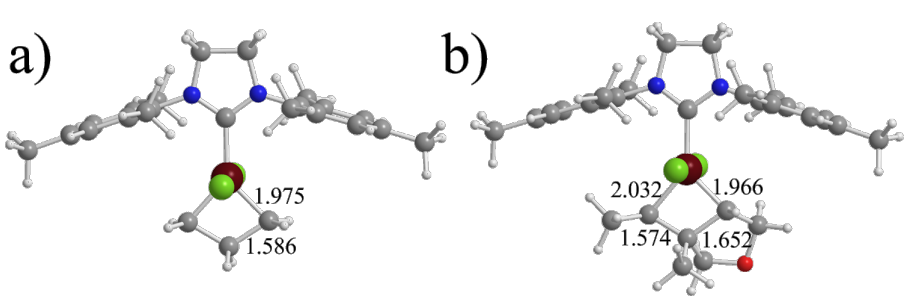

Figure 5: Representative geometries of the metallacycles **7** and **15**, parts a and b, respectively (distance in Å).

generation catalyst. Moving to the same catalysts with the bigger substrate, systems **14** and **16**, metallacycle formation is an overall uphill path. Coordination of the terminal C=C double bond with respect to coordination of the O heteroatom is disfavored by 4.5 kcal/mol in **14** and favored by 1.8 kcal/mol in **16**, respectively. The transition states are 20.2 and 19.9 kcal/mol higher in energy with respect to the 14e species, and the metallacycles are 7.7 kcal/mol above and 12.1 kcal/mol above the 14e species.

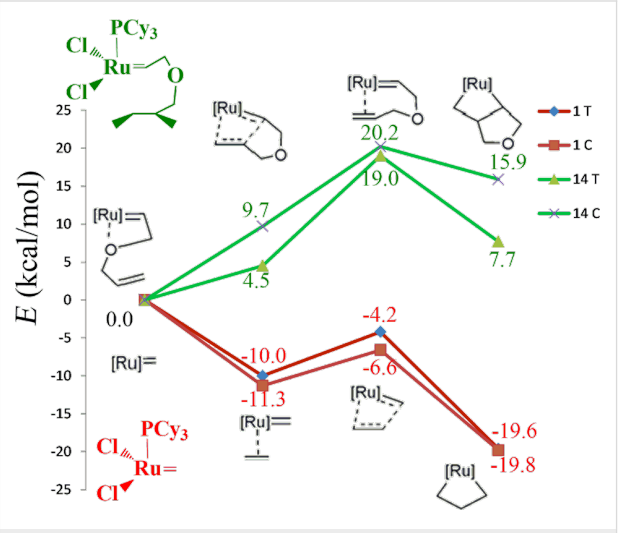

Figure 6: Energy profiles for systems **1** and **14**.

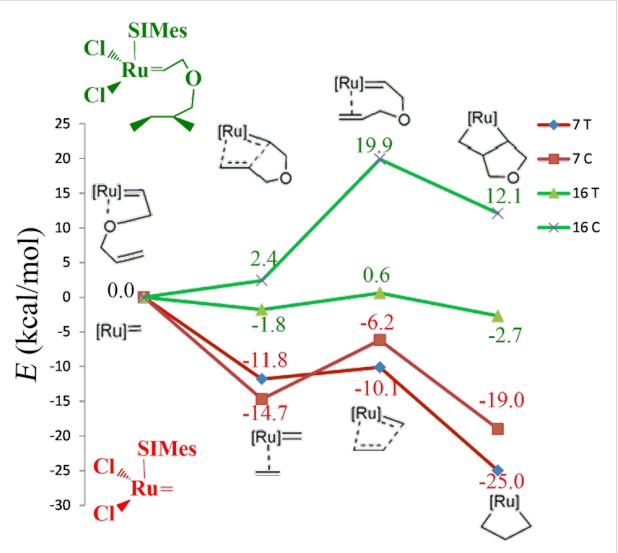

Figure 7: Energy profiles for systems **7** and **16**.

To better understand the different stability of the metallacycle relative to the coordination intermediate of the 1st and 2nd generation catalysts we investigated the thermodynamics of the reaction shown in Figure 8. E_1 is the energy gain associated to metallacycle formation, already discussed, while E_2 is the energy loss due to the hypothetical release of cyclopropane from the Ru–metallacycle species. The larger E_1 and E_2 values for the 2nd generation system **7** clearly indicate that the Ru–C σ-bonds are stronger in the presence of an NHC ligand. The origin of this difference is in the better ability of the NHC ligand to donate electron density to the Ru center, which formally is in the high formal oxidation state of +4 in the metallacycle.

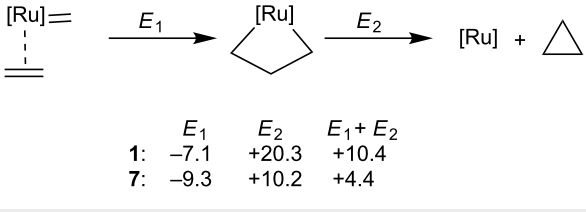

Figure 8: Metallocycle and cyclopropane formation energy profile (energies in kcal/mol).

Conclusion

After discussing a wide range of representative systems of second generation Grubbs catalysts the conclusion is that any compound sterically demanding either through the alkylidene group or the olefin or even the NHC ligand means a stabilization of the bottom-bound isomer with respect to the side-bound. However, with the simplest olefin and alkylidene groups this less favored isomer plays a key role, especially if taking into account the solvent effect. Therefore, calculations indicate that the preferred reaction pathway is an equilibrium described by steric, electronic, and solvent effects. In spite of the expectation that the hydrogen atom is the less sterically demanding it can produce H–H repulsion with the alkylidene group, which the mesityl or even the methyl groups do not. And comparing these last two complexes the possible H–H repulsions are possible when there is a methyl group in the NHC ligand, but never in the case of mesityl groups. Therefore, for the latter substituent, any H–H repulsion is avoided, and there are favorable C–H interactions even though the mesityl group is sterically more demanding. When including *t*-Bu in the NHC ligand the effect of a high sterically demanding group is present, and for this compound no side-bound isomers occurs.

The differentiation between the power of the three effects, steric, electronic and solvent, has turned out be a hazard to make predictions difficult. However the CF_3 groups have become key to explain the electronic effects, as well as the *t*-Bu for steric effects. Steric effects owing to interaction between bulky NHC ligands [16] and bulky substrates make the bottom reaction pathway more likely surpassing the other effects. Finally the solvent effect helps the stabilization of the side-

bound isomer, but at a higher degree for the high sterically demanding complexes. As already stated by Goddard, polar solvents favor the side reaction pathway or at least reduce the electronic preference for the bottom reaction pathway [13]. Therefore, bearing less sterically demanding substrates and/or ligands, the side reaction pathway, as suggested by Grubbs and co-workers [12,14], might be competitive.

Even though over the last three decades thousands of papers have presented and described the olefin metathesis catalysis, neither a general catalyst for any metathesis reaction has been found [80-82], nor are perfect rules available to predict the behavior of a given catalyst [83-92], although great efforts in characterizing the decomposition reactions [93-97], to validate computational protocols [37,45,68,98-102], and in the experimental synthesis and characterization [33,103] have been taken. Thus, this study provides valuable insight and yields at least a general recipe to obtain a side attack of the olefin towards the NHC ligand.

Acknowledgements

A.P. thanks the Spanish MINECO for a project CTQ2014-59832-JIN, and European Commission for a Career Integration Grant (CIG09-GA-2011-293900).

References

1. Trnka, T. M.; Grubbs, R. H. *Acc. Chem. Res.* **2001,** *34,* 18–29. doi:10.1021/ar000114f
2. Chauvin, Y. *Angew. Chem., Int. Ed.* **2006,** *45,* 3740–3747. doi:10.1002/anie.200601234
3. Grubbs, R. H. *Angew. Chem., Int. Ed.* **2006,** *45,* 3760–3765. doi:10.1002/anie.200600680
4. Schrock, R. R. *Angew. Chem., Int. Ed.* **2006,** *45,* 3748–3759. doi:10.1002/anie.200600085
5. Hérisson, P. J.-L.; Chauvin, Y. *Makromol. Chem.* **1971,** *141,* 161–176. doi:10.1002/macp.1971.021410112
6. Fustero, S.; Bello, P.; Miró, J.; Sánchez-Roselló, M.; Haufe, G.; del Pozo, C. *Beilstein J. Org. Chem.* **2013,** *9,* 2688–2695. doi:10.3762/bjoc.9.305
7. Yuan, W.; Wei, Y.; Shi, M. *ChemistryOpen* **2013,** *2,* 63–68. doi:10.1002/open.201300002
8. Perfetto, A.; Costabile, C.; Longo, P.; Bertolasi, V.; Grisi, F. *Chem. – Eur. J.* **2013,** *19,* 10492–10496. doi:10.1002/chem.201301540
9. Perfetto, A.; Costabile, C.; Longo, P.; Grisi, F. *Organometallics* **2014,** *33,* 2747–2759. doi:10.1021/om5001452
10. Nguyen, S. T.; Grubbs, R. H.; Ziller, J. W. *J. Am. Chem. Soc.* **1993,** *115,* 9858–9859. doi:10.1021/ja00074a086
11. Scholl, M.; Ding, S.; Lee, C. W.; Grubbs, R. H. *Org. Lett.* **1999,** *1,* 953–956. doi:10.1021/ol990909q
12. Huang, J.; Stevens, E. D.; Nolan, S. P.; Peterson, J. L. *J. Am. Chem. Soc.* **1999,** *121,* 2674–2678. doi:10.1021/ja9831352
13. Weskamp, T.; Kohl, F. J.; Hieringer, W.; Gleich, D.; Herrmann, W. A. *Angew. Chem., Int. Ed.* **1999,** *38,* 2416–2419. doi:10.1002/(SICI)1521-3773(19990816)38:16<2416::AID-ANIE2416>3.0.CO;2-#
14. Bielawski, C. W.; Grubbs, R. H. *Angew. Chem., Int. Ed.* **2000,** *39,* 2903–2906. doi:10.1002/1521-3773(20000818)39:16<2903::AID-ANIE2903>3.0.CO;2-Q
15. Samojłowicz, C.; Bieniek, M.; Grela, K. *Chem. Rev.* **2009,** *109,* 3708–3742. doi:10.1021/cr800524f
16. Hoveyda, A. H.; Schrock, R. R. *Chem. – Eur. J.* **2001,** *7,* 945–950. doi:10.1002/1521-3765(20010302)7:5<945::AID-CHEM945>3.0.CO;2-3
17. Schrock, R. R.; Hoveyda, A. H. *Angew. Chem., Int. Ed.* **2003,** *42,* 4592–4633. doi:10.1002/anie.200300576
18. Fürstner, A. *Angew. Chem., Int. Ed.* **2000,** *39,* 3012–3043. doi:10.1002/1521-3773(20000901)39:17<3012::AID-ANIE3012>3.0.CO;2-G
19. Grubbs, R. H., Ed. *Handbook of Olefin Metathesis;* Wiley-VCH: Weinheim, Germany, 2003. doi:10.1002/9783527619481
20. Dias, E. L.; Nguyen, S. T.; Grubbs, R. H. *J. Am. Chem. Soc.* **1997,** *119,* 3887–3897. doi:10.1021/ja963136z
21. Ulman, M.; Grubbs, R. H. *Organometallics* **1998,** *17,* 2484–2489. doi:10.1021/om9710172
22. Adlhart, C.; Hinderling, C.; Baumann, H.; Chen, P. *J. Am. Chem. Soc.* **2000,** *122,* 8204–8214. doi:10.1021/ja9938231
23. Adlhart, C.; Volland, M. A. O.; Hofmann, P.; Chen, P. *Helv. Chim. Acta* **2000,** *83,* 3306–3311. doi:10.1002/1522-2675(20001220)83:12<3306::AID-HLCA3306>3.0.CO;2-7
24. Adlhart, C.; Chen, P. *Helv. Chim. Acta* **2000,** *83,* 2192–2196. doi:10.1002/1522-2675(20000906)83:9<2192::AID-HLCA2192>3.0.CO;2-G
25. Aagaard, O. M.; Meier, R. J.; Buda, F. *J. Am. Chem. Soc.* **1998,** *120,* 7174–7182. doi:10.1021/ja974131k
26. Cavallo, L. *J. Am. Chem. Soc.* **2002,** *124,* 8965–8973. doi:10.1021/ja016772s
27. Tallarico, J. A.; Bonitatebus, P. J., Jr.; Snapper, M. L. *J. Am. Chem. Soc.* **1997,** *119,* 7157–7158. doi:10.1021/ja971285r
28. Chen, P. *Angew. Chem., Int. Ed.* **2003,** *42,* 2832–2847. doi:10.1002/anie.200200560
29. Correa, A.; Cavallo, A. *J. Am. Chem. Soc.* **2006,** *128,* 13352–13353. doi:10.1021/ja064924j
30. Urbina-Blanco, C. A.; Poater, A.; Lebl, T.; Manzini, S.; Slawin, A. M. Z.; Cavallo, L.; Nolan, S. P. *J. Am. Chem. Soc.* **2013,** *135,* 7073–7079. doi:10.1021/ja402700p
31. Poater, A.; Ragone, F.; Correa, A.; Szadkowska, A.; Barbasiewicz, M.; Grela, K.; Cavallo, L. *Chem. – Eur. J.* **2010,** *16,* 14354–14364. doi:10.1002/chem.201001849
32. Romero, P. E.; Piers, W. E. *J. Am. Chem. Soc.* **2007,** *129,* 1698–1704. doi:10.1021/ja0675245
33. Pump, E.; Poater, A.; Zirngast, M.; Torvisco, A.; Fischer, R.; Cavallo, L.; Slugovc, C. *Organometallics* **2014,** *33,* 2806–2813. doi:10.1021/om500315t
34. Poater, A.; Correa, A.; Pump, E.; Cavallo, L. *Chem. Heterocycl. Compd.* **2014,** *50,* 389–395. doi:10.1007/s10593-014-1491-6
35. Benitez, D.; Tkatchouk, E.; Goddard, W. A., III. *Chem. Commun.* **2008,** *46,* 6194–6196. doi:10.1039/b815665d

36. Vidavsky, Y.; Anaby, A.; Lemcoff, N. G. *Dalton Trans.* **2012,** *41,* 32–43. doi:10.1039/C1DT11404B
37. Urbina-Blanco, C. A.; Bantreil, X.; Wappel, J.; Schmid, T. E.; Slawin, A. M. Z.; Slugovc, C.; Cazin, C. S. J. *Organometallics* **2013,** *32,* 6240–6247. doi:10.1021/om4004362
38. Schmid, T. E.; Bantreil, X.; Citadelle, C. A.; Slawin, A. M. Z.; Cazin, C. S. J. *Chem. Commun.* **2011,** *47,* 7060–7062. doi:10.1039/c1cc10825e
39. Costabile, C.; Cavallo, L. *J. Am. Chem. Soc.* **2004,** *126,* 9592–9600. doi:10.1021/ja0484303
40. Adlhart, C.; Chen, P. *J. Am. Chem. Soc.* **2004,** *126,* 3496–3510. doi:10.1021/ja0305757
41. Adlhart, C.; Chen, P. *Angew. Chem., Int. Ed.* **2002,** *41,* 4484–4487. doi:10.1002/1521-3773(20021202)41:23<4484::AID-ANIE4484>3.0.CO;2-Q
42. Vyboishchikov, S. F.; Bühl, M.; Thiel, W. *Chem. – Eur. J.* **2002,** *8,* 3962–3975. doi:10.1002/1521-3765(20020902)8:17<3962::AID-CHEM3962>3.0.CO;2-X
43. Fomine, S.; Martinez Vargas, S.; Tlenkopatchev, M. A. *Organometallics* **2003,** *22,* 93–99. doi:10.1021/om020581w
44. Suresh, C. H.; Koga, N. *Organometallics* **2004,** *23,* 76–80. doi:10.1021/om034011n
45. Occhipinti, G.; Bjørsvik, H.-R.; Jensen, V. R. *J. Am. Chem. Soc.* **2006,** *128,* 6952–6954. doi:10.1021/ja060832i
46. Romero, P. E.; Piers, W. E. *J. Am. Chem. Soc.* **2005,** *127,* 5032–5033. doi:10.1021/ja042259d
47. Ung, T.; Hejl, A.; Grubbs, R. H.; Schrodi, Y. *Organometallics* **2004,** *23,* 5399–5401. doi:10.1021/om0493210
48. Benitez, D.; Goddard, W. A., III. *J. Am. Chem. Soc.* **2005,** *127,* 12218–12219. doi:10.1021/ja051796a
49. Anderson, D. R.; Hickstein, D. D.; O'Leary, D. J.; Grubbs, R. H. *J. Am. Chem. Soc.* **2006,** *128,* 8386–8387. doi:10.1021/ja0618090
50. Dorta, R.; Stevens, E. D.; Scott, N. M.; Costabile, C.; Cavallo, L.; Hoff, C. D.; Nolan, S. P. *J. Am. Chem. Soc.* **2005,** *127,* 2485–2495. doi:10.1021/ja0438821
51. Viciu, M. S.; Navarro, O.; Germaneau, R. F.; Kelly, R. A., III; Sommer, W.; Marion, N.; Stevens, E. D.; Cavallo, L.; Nolan, S. P. *Organometallics* **2004,** *23,* 1629–1635. doi:10.1021/om034319e
52. Seiders, T. J.; Ward, D. W.; Grubbs, R. H. *Org. Lett.* **2001,** *3,* 3225–3228. doi:10.1021/ol0165692
53. Funk, T. W.; Berlin, J. M.; Grubbs, R. H. *J. Am. Chem. Soc.* **2006,** *128,* 1840–1846. doi:10.1021/ja055994d
54. Monfette, S.; Fogg, D. E. *Organometallics* **2006,** *25,* 1940–1944. doi:10.1021/om050952j
55. Conrad, J. C.; Parnas, H. H.; Snelgrove, J. L.; Fogg, D. E. *J. Am. Chem. Soc.* **2005,** *127,* 11882–11883. doi:10.1021/ja042736s
56. *Gaussian 03,* Version B.1; Gaussian, Inc.: Pittsburgh, PA, U.S.A., 2003.
57. Becke, A. D. *J. Chem. Phys.* **1993,** *98,* 5648–5651. doi:10.1063/1.464913
58. Stephens, P. J.; Devlin, F. J.; Chabalowski, C. F.; Frisch, M. J. *J. Phys. Chem.* **1994,** *98,* 11623–11627. doi:10.1021/j100096a001
59. Lee, C.; Yang, W.; Parr, R. G. *Phys. Rev. B* **1988,** *37,* 785–789. doi:10.1103/PhysRevB.37.785
60. Becke, A. D. *Phys. Rev. A* **1988,** *38,* 3098–3100. doi:10.1103/PhysRevA.38.3098
61. Perdew, J. P. *Phys. Rev. B* **1986,** *33,* 8822–8824. doi:10.1103/PhysRevB.33.8822
62. Perdew, J. P. *Phys. Rev. B* **1986,** *34,* 7406. doi:10.1103/PhysRevB.34.7406
63. Schäfer, A.; Horn, H.; Ahlrichs, R. *J. Chem. Phys.* **1992,** *97,* 2571–2577. doi:10.1063/1.463096
64. Häusermann, U.; Dolg, M.; Stoll, H.; Preuss, H.; Schwerdtfeger, P.; Pitzer, R. M. *Mol. Phys.* **1993,** *78,* 1211–1224. doi:10.1080/00268979300100801
65. Küchle, W.; Dolg, M.; Stoll, H.; Preuss, H. *J. Chem. Phys.* **1994,** *100,* 7535–7542. doi:10.1063/1.466847
66. Leininger, T.; Nicklass, A.; Stoll, H.; Dolg, M.; Schwerdtfeger, P. *J. Chem. Phys.* **1996,** *105,* 1052–1059. doi:10.1063/1.471950
67. Barone, V.; Cossi, M. *J. Phys. Chem. A* **1998,** *102,* 1995–2001. doi:10.1021/jp9716997
68. Zhao, Y.; Truhlar, D. G. *Org. Lett.* **2007,** *9,* 1967–1970. doi:10.1021/ol0705548
69. Pandian, S.; Hillier, I. H.; Vincent, M. A.; Burton, N. A.; Ashworth, I. W.; Nelson, D. J.; Percy, J. M.; Rinaudo, G. *Chem. Phys. Lett.* **2009,** *476,* 37–40. doi:10.1016/j.cplett.2009.06.021
70. Minenkov, Y.; Occhipinti, G.; Heyndrickx, W.; Jensen, V. R. *Eur. J. Inorg. Chem.* **2012,** *2012,* 1507–1516. doi:10.1002/ejic.201100932
71. Fey, N.; Ridgway, B. M.; Jover, J.; McMullin, C. L.; Harvey, J. N. *Dalton Trans.* **2011,** *40,* 11184–11191. doi:10.1039/c1dt10909j
72. Pump, E.; Slugovc, C.; Cavallo, L.; Poater, A. *Organometallics* **2015,** *34,* 3107–3111. doi:10.1021/om501246q
73. Poater, A.; Pump, E.; Vummaleti, S. V. C.; Cavallo, L. *J. Chem. Theory Comput.* **2014,** *10,* 4442–4448. doi:10.1021/ct5003863
74. Credendino, R.; Poater, A.; Ragone, F.; Cavallo, L. *Catal. Sci. Technol.* **2011,** *1,* 1287–1297. doi:10.1039/c1cy00052g
75. Poater, A.; Ragone, F.; Correa, A.; Cavallo, L. *Dalton Trans.* **2011,** *40,* 11066–11069. doi:10.1039/c1dt10959f
76. Manzini, S.; Urbina-Blanco, C. A.; Nelson, D. J.; Poater, A.; Lebl, T.; Meiries, S.; Slawin, A. M. Z.; Falivene, L.; Cavallo, L.; Nolan, S. P. *J. Organomet. Chem.* **2015,** *780,* 43–48. doi:10.1016/j.jorganchem.2014.12.040
77. Vougioukalakis, G. C.; Grubbs, R. H. *Chem. Rev.* **2010,** *110,* 1746–1787. doi:10.1021/cr9002424
78. Schwab, P.; Grubbs, R. H.; Ziller, J. W. *J. Am. Chem. Soc.* **1996,** *118,* 100–110. doi:10.1021/ja952676d
79. van der Eide, E. F.; Piers, W. E. *Nat. Chem.* **2010,** *2,* 571–576. doi:10.1038/nchem.653
80. Falivene, L.; Poater, A.; Cazin, C. S. J.; Slugovc, C.; Cavallo, L. *Dalton Trans.* **2013,** *42,* 7312–7317. doi:10.1039/C2DT32277C
81. Leitgeb, A.; Abbas, M.; Fischer, R. C.; Poater, A.; Cavallo, L.; Slugovc, C. *Catal. Sci. Technol.* **2012,** *2,* 1640–1643. doi:10.1039/c2cy20311a
82. Bantreil, X.; Poater, A.; Urbina-Blanco, C. A.; Bidal, Y. D.; Falivene, L.; Randall, R. A. M.; Cavallo, L.; Slawin, A. M. Z.; Cazin, C. S. *Organometallics* **2012,** *31,* 7415–7426. doi:10.1021/om300703p
83. Szczepaniak, G.; Kosinski, K.; Grela, K. *Green Chem.* **2014,** *16,* 4474–4492. doi:10.1039/C4GC00705K
84. Minenkov, Y.; Singstad, A.; Occhipinti, G.; Jensen, V. R. *Dalton Trans.* **2012,** *41,* 5526–5541. doi:10.1039/c2dt12232d
85. Minenkov, Y.; Occhipinti, G.; Heyndrickx, W.; Jensen, V. R. *Eur. J. Inorg. Chem.* **2012,** *2012,* 1507–1516. doi:10.1002/ejic.201100932
86. Minenkov, Y.; Occhipinti, G.; Jensen, V. R. *Organometallics* **2013,** *32,* 2099–2111. doi:10.1021/om301192a

87. Paredes-Gil, K.; Solans-Monfort, X.; Rodriguez-Santiago, L.; Sodupe, M.; Jaque, P. *Organometallics* **2014,** *33,* 6065–6075. doi:10.1021/om500718a
88. Poater, A.; Pump, E.; Vummaleti, S. V. C.; Cavallo, L. *Chem. Phys. Lett.* **2014,** *610–611,* 29–32. doi:10.1016/j.cplett.2014.06.063
89. Poater, A.; Vummaleti, S. V. C.; Pump, E.; Cavallo, L. *Dalton Trans.* **2014,** *43,* 11216–11220. doi:10.1039/c4dt00325j
90. Poater, A.; Credendino, R.; Slugovc, C.; Cavallo, L. *Dalton Trans.* **2013,** *42,* 7271–7275. doi:10.1039/c3dt32884h
91. Poater, A.; Falivene, L.; Urbina-Blanco, C. A.; Manzini, S.; Nolan, S. P.; Cavallo, L. *Dalton Trans.* **2013,** *42,* 7433–7439. doi:10.1039/c3dt32980a
92. Nuñez-Zarur, F.; Solans-Monfort, X.; Rodríguez-Santiago, L.; Sodupe, M. *Organometallics* **2012,** *31,* 4203–4215. doi:10.1021/om300150d
93. Poater, A.; Cavallo, L. *J. Mol. Catal. A: Chem.* **2010,** *324,* 75–79. doi:10.1016/j.molcata.2010.02.023
94. Poater, A.; Bahri-Lalehac, N.; Cavallo, L. *Chem. Commun.* **2011,** *47,* 6674–6676. doi:10.1039/c1cc11594d
95. Manzini, S.; Poater, A.; Nelson, D. J.; Cavallo, L.; Nolan, S. P. *Chem. Sci.* **2014,** *5,* 180–188. doi:10.1039/C3SC52612G
96. Manzini, S.; Poater, A.; Nelson, D. J.; Cavallo, L.; Slawin, A. M. Z.; Nolan, S. P. *Angew. Chem., Int. Ed.* **2014,** *53,* 8995–8999. doi:10.1002/anie.201403770
97. Manzini, S.; Nelson, D. J.; Lebl, T.; Poater, A.; Cavallo, L.; Slawin, A. M. Z.; Nolan, S. P. *Chem. Commun.* **2014,** *50,* 2205–2207. doi:10.1039/c3cc49481k
98. Kulkarni, A. D.; Truhlar, D. G. *J. Chem. Theory Comput.* **2011,** *7,* 2325–2332. doi:10.1021/ct200188n
99. Zhao, Y.; Truhlar, D. G. *J. Chem. Theory Comput.* **2009,** *5,* 324–333. doi:10.1021/ct800386d
100. Zhao, Y.; Truhlar, D. G. *Chem. Phys. Lett.* **2011,** *502,* 1–13. doi:10.1016/j.cplett.2010.11.060
101. Zhao, Y.; Truhlar, D. G. *Acc. Chem. Res.* **2008,** *41,* 157–167. doi:10.1021/ar700111a
102. Tsipis, A. C.; Orpen, A. G.; Harvey, J. N. *Dalton Trans.* **2005,** 2849–2858. doi:10.1039/b506929g
103. Bantreil, X.; Nolan, S. P. *Nat. Protoc.* **2011,** *6,* 69–77. doi:10.1038/nprot.2010.177

License and Terms

BEILSTEIN JOURNAL OF ORGANIC CHEMISTRY

Cross-metathesis of polynorbornene with polyoctenamer: a kinetic study

Yulia I. Denisova[1], Maria L. Gringolts[1], Alexander S. Peregudov[2], Liya B. Krentsel[1], Ekaterina A. Litmanovich[3], Arkadiy D. Litmanovich[1], Eugene Sh. Finkelshtein[1] and Yaroslav V. Kudryavtsev[*1]

Full Research Paper

Open Access

Address:
[1]Topchiev Institute of Petrochemical Synthesis, Russian Academy of Sciences, Leninsky prosp. 29, 119991 Moscow, Russia, [2]Nesmeyanov Institute of Organoelement Compounds, Russian Academy of Sciences, Vavilova str. 28, 119991 Moscow, Russia and [3]Chemistry Department, Moscow State University, Leninskie gory 1, build. 3, 119991 Moscow, Russia

Email:
Yaroslav V. Kudryavtsev[*] - yar@ips.ac.ru

* Corresponding author

Keywords:
cross-metathesis; 1st generation Grubbs' catalyst; interchange reactions; kinetics; multiblock copolymer

Beilstein J. Org. Chem. **2015,** *11,* 1796–1808.
doi:10.3762/bjoc.11.195

Received: 15 June 2015
Accepted: 10 September 2015
Published: 01 October 2015

This article is part of the Thematic Series "Progress in metathesis chemistry II".

Guest Editor: K. Grela

Abstract

The cross-metathesis of polynorbornene and polyoctenamer in *d*-chloroform mediated by the 1st generation Grubbs' catalyst $Cl_2(PCy_3)_2Ru{=}CHPh$ is studied by monitoring the kinetics of carbene transformation and evolution of the dyad composition of polymer chains with in situ ^1H and ex situ ^{13}C NMR spectroscopy. The results are interpreted in terms of a simple kinetic two-stage model. At the first stage of the reaction all Ru-benzylidene carbenes are transformed into Ru-polyoctenamers within an hour, while the polymer molar mass is considerably decreased. The second stage actually including interpolymeric reactions proceeds much slower and takes one day or more to achieve a random copolymer of norbornene and cyclooctene. Its rate is limited by the interaction of polyoctenamer-bound carbenes with polynorbornene units, which is hampered, presumably due to steric reasons. Polynorbornene-bound carbenes are detected in very low concentrations throughout the whole process thus indicating their higher reactivity, as compared with the polyoctenamer-bound ones. Macroscopic homogeneity of the reacting media is proved by dynamic light scattering from solutions containing the polymer mixture and its components. In general, the studied process can be considered as a new way to unsaturated multiblock statistical copolymers. Their structure can be controlled by the amount of catalyst, mixture composition, and reaction time. It is remarkable that this goal can be achieved with a catalyst that is not suitable for ring-opening metathesis copolymerization of norbornene and *cis*-cyclooctene because of their substantially different monomer reactivities.

Introduction

A desired sequence of monomer units in a polymer chain can be achieved not only in the course of polymerization but also through chemical modification of macromolecules [1]. In particular, main-chain polyesters and polyamides are capable of cross-reactions (also known as interchange reactions) characterized by the rearrangement of macromolecular backbones via

break up and the formation of new C–O and C–N bonds [2]. Such reactions are extensively used in practice for combining the functionality and the processability of different polymers in one material [3]. A more recent line of research is associated with dynamic covalent polymers containing alkoxyamine, imine, disulfide, and other easily cleavable moieties in their backbone [4,5]. It aims at stimuli-responsive, intelligent polymeric materials, the structure and properties of which can be precisely controlled by adjusting temperature, pH or by introducing low molecular additives.

Much less is known about the possibility of monomer unit reshuffling in unsaturated carbon-chain polymers, such as polydienes, which constitute a core of commercially available elastomers. As soon as the olefin metathesis was discovered, it became possible to think on the implementation of cross-reactions between C=C bonds in polymers. Until recently the studies were focused on the intramolecular reactions [6,7] and polymer degradation by interaction with olefins [8,9], whereas the interchain cross-metathesis was merely an idea for many years [10]. Only recently a few publications appeared that demonstrated the possibility of using the Grubbs' Ru catalysts to make polybutadiene networks malleable [11] and self-healing [12] and to marry chain-growth 1,4-polybutadiene with step-growth unsaturated polyesters [13,14]. Hydrogenation of the reaction product led to saturated ethylene/ester copolymers with a multiblock chain structure predefined at the cross-metathesis stage [14].

In our previous communication [15] we reported the obtaining of a copolymer of norbornene (NB) and *cis*-cyclooctene (COE) by the cross-metathesis of polynorbornene (poly(1,3-cyclopentylenevinylene), PNB) with polyoctenamer (poly(1-octenylene), PCOE). It is noteworthy that the reaction is readily mediated by the 1st generation Grubbs' catalyst $Cl_2(PCy_3)_2Ru{=}CHPh$ (Gr-1), which is not suitable for metathesis ring-opening copolymerization of NB and COE. Our approach makes it possible to synthesize statistical multiblock NB-COE copolymers containing up to 50% of alternating dyads. By adjusting the conditions of the cross-metathesis between PNB and PCOE, such as the polymer/catalyst ratio, PNB/PCOE ratio and their molecular masses, reaction time, etc., one can obtain NB-COE copolymers with the mean block lengths varying from 200 to 2 units.

It is noteworthy that PNB and PCOE are commonly synthesized by ring-opening metathesis polymerization (ROMP). PNB is a well-known commercial product available under the trademark Norsorex® [8,16], which is mainly used as a solidifier of oil and solvent for the complete absorption of oil or other hydrocarbons. PCOE, known as Vestenamer® [17], is a semi-crystalline rubber applied as a polymer processing aid for extrusion, injection molding etc. Though easily homopolymerized, NB and COE hardly enter metathesis copolymerization [18,19] because of the much higher activity of NB possessing a considerably more strained bicyclic structure, which gets opened during ROMP [8,20]. To solve this problem, two approaches were elaborated in the literature. One approach utilizes a specially designed catalyst that facilitates the formation of a highly alternating NB-COE copolymer [21-25]. The other approach is associated with a reduction of the polymerization activity of NB through introducing substituents into its molecule [26-28]. Therefore, the cross-metathesis of PCOE and PNB can be considered as a novel way to statistical NB-COE copolymers.

In the present article we try to gain more insight into this reaction by undertaking a kinetic study. We begin with discussing the choice of the reaction media and solution properties of PCOE, PNB, and their mixture in $CHCl_3$ studied by light scattering. Then we describe use of the in situ ^{1}H NMR spectroscopy for monitoring the separate reactions between Gr-1 and PCOE and between Gr-1 and PNB in $CDCl_3$. This technique is widely applied for investigating ROMP in the presence of well-defined catalysts since it allows quantitative determination of the active complex type and conversion during the reaction [29-31]. By fitting the experimental data with a simple kinetic model we estimate and compare the formation and decay rates of Ru–carbene complexes bound to PCOE and PNB. Then we proceed to the investigation of PCOE/PNB/Gr-1 mixtures, where we combine in situ ^{1}H NMR measurements of the concentrations of Ru–carbene complexes with ex situ ^{13}C NMR measurements of alternating dyad content in the NB-COE copolymer. Such dyads are formed via the reactions of PNB-bound carbenes with COE units and, vice versa, of PCOE-bound carbenes with NB units. The above kinetic model for the separate reactions of PCOE and PNB with Gr-1 is extended, which makes it possible to outline the scenario of the cross-metathesis of those polymers in the presence of the Gr-1 catalyst.

Results and Discussion

The initial homopolymers, PCOE and PNB, were synthesized by the ROMP of COE and NB, respectively, using Gr-1 under the conditions that prevent the formation of cyclooligomers (at a high monomer concentration). As known from the literature [29], Gr-1 cannot initiate a living process of COE and NB so that the obtained polymers are rather polydisperse because of back-biting and chain-transfer reactions (the molar-mass dispersity $Đ$ is close to 2 for PCOE and to 3 for PNB). For more details on the polymer synthesis and characterization, see the Experimental section.

Light-scattering studies on PCOE and PNB solutions

First of all, it was important to find a suitable solvent that provides homogeneity of the reaction media. Chloroform ($CHCl_3$ or $CDCl_3$) was chosen as the best solvent for PCOE/PNB mixtures compared with toluene, THF, CH_2Cl_2, and PhCl. Since we are interested in the cross-metathesis, the polymer concentration in solution should be as high as possible to minimize the impact of intrachain reactions [7]. At the same time increasing polymer concentration can lead to polymer/solvent and (in mixtures) polymer/polymer phase separation. We addressed this issue with the light scattering measurements on PCOE (M_n = 140000 g/mol, $Đ$ = 1.9), PNB (M_n = 80000 g/mol, $Đ$ = 2.8), and PCOE/PNB solutions in $CHCl_3$.

For both polymers, only one relaxation mode was observed. The mean hydrodynamic radius $\overline{R}_h$ calculated from its relaxation rate was independent of the light scattering angle (Figure 1a). This proves the diffusive nature of the concentration relaxation processes in the studied solutions. Therefore, the concentration dependence of $\overline{R}_h$ was measured at a maximum available angle of θ = 150°, where the contribution of dust particles to scattering is minimized. As seen from Figure 1b, PNB demonstrated the typical concentration behavior for a polymer in good solvent [32]. In the dilute regime (c < 0.01 g/mL) $\overline{R}_h$ = 14 nm characterizes the mean size of a polymer coil. At higher concentrations macromolecules overlap and their self-diffusion is replaced with a faster cooperative diffusion. In that case $\overline{R}_h$ slowly decreases with c corresponding to a distance at which hydrodynamic interactions are screened out. For the PCOE solution Figure 1b displays a quite different concentration dependence of $\overline{R}_h$. In the dilute regime flexible PCOE macromolecules form very compact coils of 4 nm size, which are much smaller than those of rigid PNB chains of nearly the same M_w. At c = 0.03 g/mL $\overline{R}_h$ is abruptly increased, thus indicating the aggregation of PCOE chains into particles of 25 nm mean size. At even higher concentrations, DLS measurements with PCOE are impossible since the solution is not filterable through a 220 nm porosity membrane. Taking into account that the melting temperature of PCOE is about 45 °C, we can relate aggregation in the PCOE solutions at 25 °C to the onset of crystallization. In any case, it makes no sense to carry out metathesis reactions at a PCOE concentration higher than 0.03 g/mL.

DLS experiments on the PCOE/PNB mixtures were conducted at the equal component concentrations taken to be 0.015 and 0.03 g/mL. Figure 2 compares the normalized hydrodynamic radius distributions in the separate components and in their mixture. It is seen that the (mixture) red and (PNB) green curves in Figure 2a almost coincide, which means that the concentration relaxation at lower concentrations is controlled by larger PNB particles (at the concentration of 0.015 g/mL they may be still identified with the individual macromolecules). In the more concentrated solution (Figure 2b) PCOE particles grow (see also Figure 1b), thereby increasing the mean hydrodynamic radius of the PCOE/PNB mixture to 25 nm. It is important that in the both cases the mixture displays a unimodal distribution indicating that no polymer/polymer segregation takes place.

The data of static scattering shown in Table 1 corroborate this conclusion because the mean intensity of light scattered by the mixture with the total polymer concentration of 0.06 g/mL appear, on the one hand, approximately equal to the sum of intensities produced by the solutions of the pure components of that mixture and, on the other hand, nearly twice as much as the intensity of light scattered by the mixture with the total concentration of 0.03 g/mL. Thus, PCOE/PNB solutions in $CHCl_3$ with the concentration of each component close to 0.03 g/mL can be considered as suitable objects for studying cross-metathesis reactions.

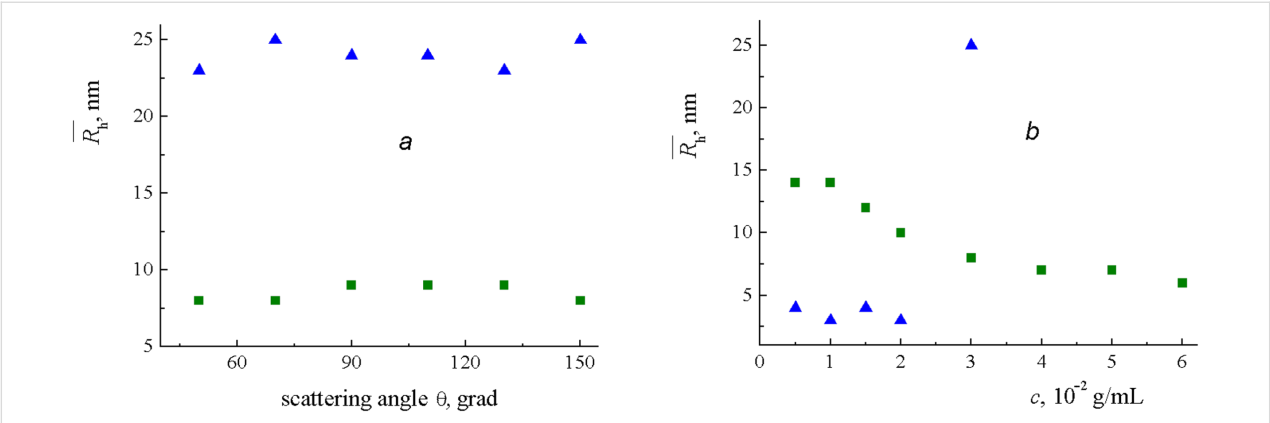

Figure 1: Dependences of the (blue) PCOE and (green) PNB mean hydrodynamic radius $\overline{R}_h$ in $CHCl_3$ on the (a) light scattering angle θ at c = 0.03 g/mL and (b) concentration c at θ = 150° found by DLS at 25 °C.

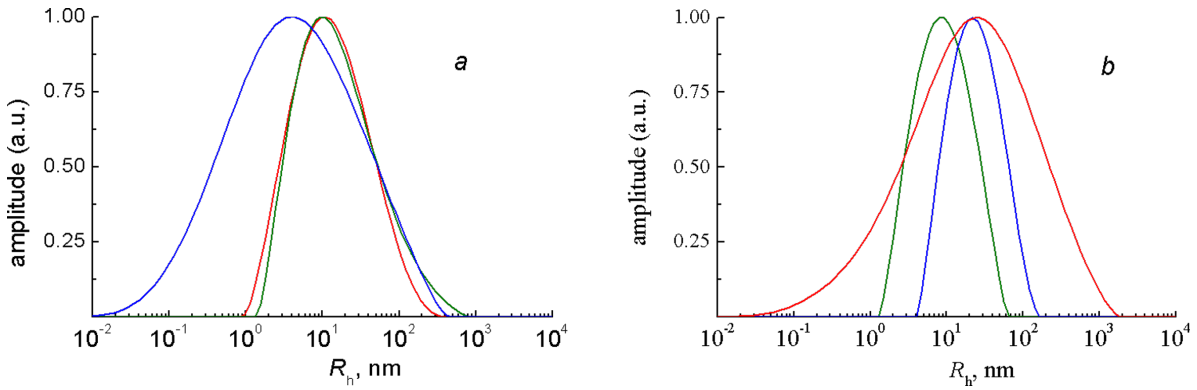

Figure 2: Hydrodynamic radius distributions (normalized by their maximum values) in the $CHCl_3$ solutions of (blue) PCOE, (green) PNB, and (red) their mixture at the concentration of (a) 0.015 g/mL and (b) 0.03 g/mL of each of the polymers measured by DLS at θ = 150° and 25 °C.

Table 1: Static scattering intensity from different $CHCl_3$ solutions:

Solute	Polymer concentration, g/mL	Scattering intensity, counts s^{-1}
PCOE	0.03	1940
PNB	0.03	3170
PCOE/PNB	0.03	2590
PCOE/PNB	0.06	5070

Interaction of the Gr-1 catalyst with PCOE and PNB

Dissolving Gr-1 in $CDCl_3$ results in the formation of a product, which we call a primary [Ru]=CHPh carbene. Its ^{1}H NMR spectrum is characterized by a peak at 20.0 ppm. Figure 3 demonstrates that in the absence of polymers a 0.03 M solution of Gr-1 in $CDCl_3$ is practically stable at 20–25 °C during one day, which is a characteristic timescale in our further experiments. The decrease in the primary carbene concentration c_0 does not exceed 3%, being within the accuracy of the NMR method. Thus we can neglect the decay of primary carbenes due to the reasons other than their interaction with macromolecules.

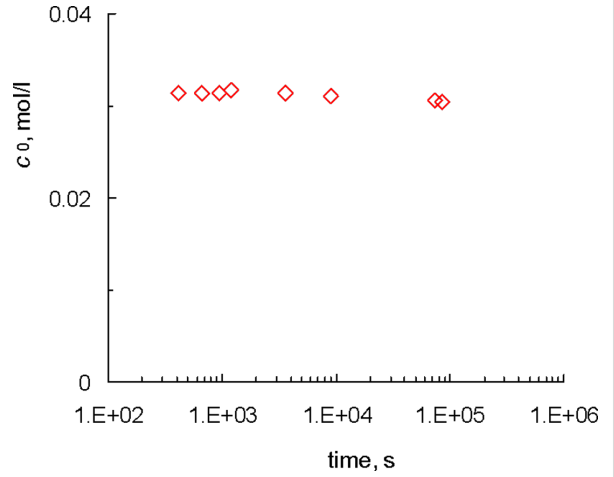

Figure 3: Stability of the primary carbene [Ru]=CHPh in the pure solvent ($CDCl_3$).

Interaction of PCOE (M_n = 120000 g/mol, $Đ$ = 1.8) with Gr-1 was studied in $CDCl_3$ at the initial polymer/catalyst concentration ratio of 20:1. Note that the initial catalyst concentration found by in situ NMR was somewhat lower in all our experiments and these effective values were used in the kinetic calculations. Along with the singlet at 20.0 ppm the ^{1}H NMR spectrum showed a new peak at 19.3 ppm, which grew rapidly to 40% of the initial primary carbene within 5 min of the reaction. According to the accepted mechanism of olefin metathesis mediated by Gr-1 [30], this signal can be attributed to a new, secondary carbene ([Ru]=PCOE) formed via break up of a PCOE chain attacked by a primary carbene, as shown in Scheme 1. The mixture viscosity was considerably reduced at the early stage of the reaction (10–20 min) indicating a decrease in the molar mass of PCOE due to its interaction with Gr-1.

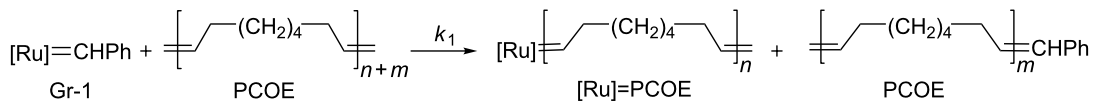

Scheme 1: Formation of polyoctenamer-bound carbene by the interaction of Gr-1 with PCOE.

Looking ahead, we note that similar effects were observed for PNB and PCOE/PNB solutions interacting with this catalyst.

After 1 h the primary carbene signal almost disappeared, while that of the [Ru]=PCOE carbene reached its maximum, kept constant for a couple of hours, and then began to decline very slowly, while the molar mass of the system remained approximately constant after an initial drop. The dependences of the (c_0) [Ru]=CHPh and (c_1) [Ru]=PCOE carbene concentrations, normalized by the initial value $c_0(t = 0) = c_{in}$, on time are shown as points in Figure 4a. The observed fast transformation of the primary carbenes into the secondary ones followed by the slow decay of the latter can be described in terms of a simple kinetic model.

Let us introduce the rate constants k_1 and k_{1d} characterizing two mentioned processes. The first of them is a reversible reaction but this can be neglected due to a considerable excess of the polymer with respect to the catalyst (the repeating unit concentration c_p = 0.532 mol/L >> c_{in} = 0.0213 mol/L). According to the literature data [30], the carbene decay can proceed either as a first-order or second-order reaction. The latter option implies coupling of two polymer chains through the reaction between their end groups, which would lead to an increase in the average molar mass of the polymer. Monitoring the molar mass distribution by GPC does not reveal such effect, therefore, the decay of [Ru]=PCOE carbenes can be described as a first-order reaction with the rate proportional to the carbene concentration. Thus, the concentrations of the primary and secondary carbenes are described by the following equations

$$\begin{cases} dc_0/dt = -k_1 c_p c_0 \\ dc_1/dt = k_1 c_p c_0 - k_{1d} c_1 \end{cases} \quad (1)$$

with the initial conditions $c_0(t = 0) = c_{in}$, $c_1(t = 0) = 0$.

At a constant polymer concentration c_p = const, the solution of Equation 1 reads

$$\begin{aligned} c_0(t) &= c_{in} \exp(-k_1 c_p t) \\ c_1(t) &= \frac{k_1 c_p c_{in}}{k_1 c_p - k_{1d}} \left(\exp(-k_{1d} t) - \exp(-k_1 c_p t) \right) \end{aligned} \quad (2)$$

Since [Ru]=CHPh carbenes are completely converted into [Ru]=PCOE ones long before the carbene decay becomes noticeable, then $k_1 c_p >> k_{1d}$ and, therefore, these constants can be found separately by representing the early and late kinetic data in the semi-logarithmic coordinates of Figure 4b and Figure 4c. These plots are obviously linear that yields $k_1 c_p = 1.65 \times 10^{-3}$ s^{-1} (so that $k_1 = 3.1 \times 10^{-3}$ L mol^{-1} s^{-1}) and $k_{1d} = 2.6 \times 10^{-6}$ s^{-1}. Red and blue lines in Figure 4a correspond to the $c_0(t)/c_{in}$ and $c_1(t)/c_{in}$ dependences calculated from Equation 2 with the above found values of k_1 and k_{1d}. Close

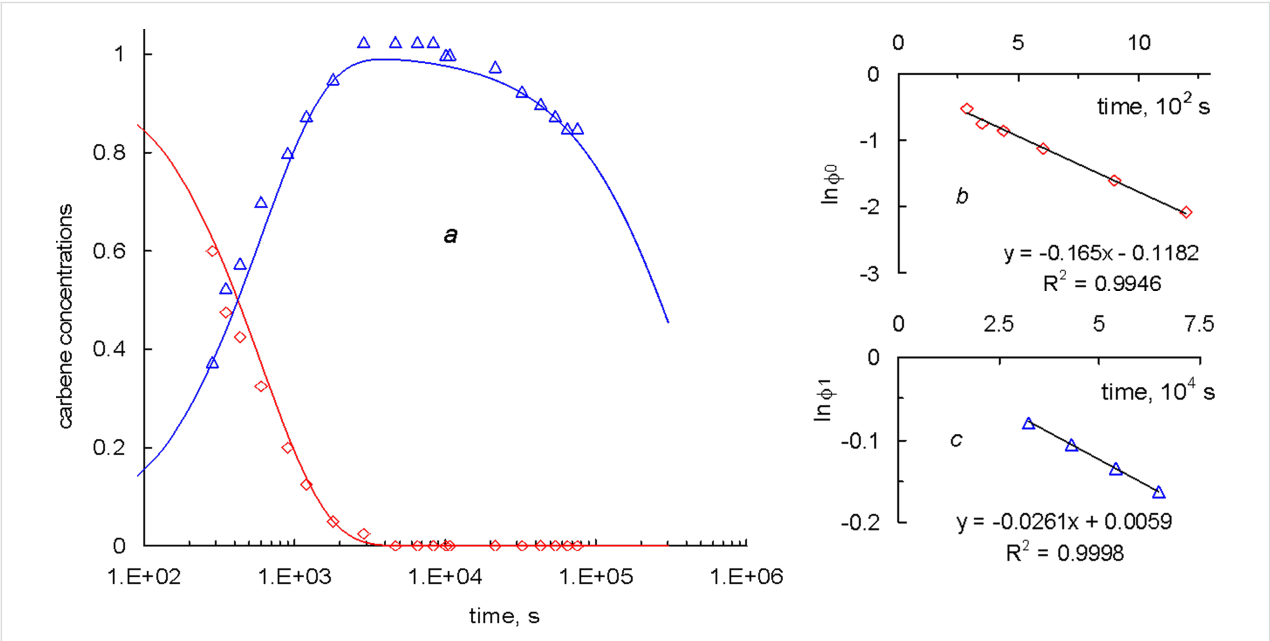

Figure 4: (a) Dependences of the normalized (red) [Ru]=CHPh and (blue) [Ru]=PCOE carbene concentrations on time: (points) experimental data, (curves) calculations according to Equation 2 with the rate constants $k_1 = 3.1 \times 10^{-3}$ L mol^{-1} s^{-1} and $k_{1d} = 2.6 \times 10^{-6}$ s^{-1} found from the (b) early and (c) late kinetic stages of the reaction.

fitting of the experimental data corroborates the consistency of our kinetic approach.

Interaction of PNB (M_n = 60000 g/mol, $Đ$ = 2.6) with Gr-1 was studied in a similar way. In that case new resonances in the ^{1}H NMR spectrum (18.82, 18.83, 18.94 ppm) appeared only after several minutes of the reaction. It can be identified as a secondary [Ru]=PNB carbene formed via cleavage of a PNB chain under the action of a primary carbene, as shown in Scheme 2.

After 1 h only about 20% of the primary carbenes were transformed into secondary ones. The concentration of [Ru]=PNB carbenes reached its maximum at ca. 11 h from the outset of the reaction and immediately began to decline. The dependences of the (c_0) [Ru]=CHPh and (c_2) [Ru]=PNB carbene concentrations, normalized by the initial value $c_0(t = 0) = c_{in}$, on time are shown as points in Figure 5. The peak value of c_2 constitutes only 40% of c_{in}, which means that the processes of the secondary carbene formation and decay cannot be separated in the time scale of our experiment.

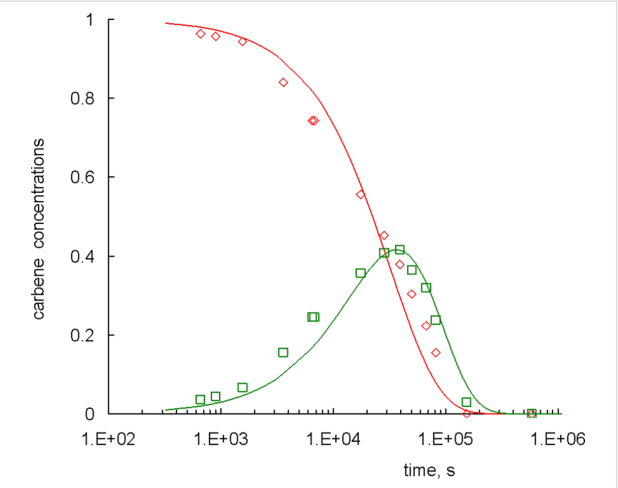

Figure 5: (a) Dependences of the normalized (red) [Ru]=CHPh and (green) [Ru]=PNB carbene concentrations on time: (points) experimental data, (curves) calculations according to Equation 3 with the rate constants k_2 = 5.4 × 10^{-5} L mol^{-1} s^{-1} and k_{2d} = 2.4 × 10^{-5} s^{-1}.

Nevertheless, we tried to describe the experimental data with the model introduced above. A solution of the kinetic equations for this case is given by the expressions

$$c_0(t) = c_{in}\exp(-k_2 c_p t)$$
$$c_2(t) = \frac{k_2 c_p c_{in}}{k_2 c_p - k_{2d}}\left(\exp(-k_{2d}t) - \exp(-k_2 c_p t)\right) \quad (3)$$

that are similar to Equation 2 up to replacing k_1 with k_2, k_{1d} with k_{2d}, and c_1 with c_2, c_p = 0.575 mol/L.

The rate constant k_2 was found by fitting the whole $c_0(t)$ curve to the experimental data, whereas for k_{2d} we focused on the position and value of the maximum of the $c_2(t)$ curve. As seen from Figure 5, the agreement between the model and experiment is not as good as for PCOE even for the best fit (k_2 = 5.4 × 10^{-5} L mol^{-1} s^{-1}, k_{2d} = 2.4 × 10^{-5} s^{-1}). The reason of this discrepancy is not clear taking into account a very standard dynamical behavior of PNB solutions in the DLS experiments reported above. We supposed that it could be correlated with a high viscosity of the PNB solution at early stages of the reaction, which was decreased rather slowly due to lower activity of the primary carbene, as compared with the PCOE case. However, when we synthesized PNB (M_n = 28000 g/mol, $Đ$ = 2.8) of nearly half the molar mass of the first sample, the two-constant kinetic model gave approximately the same performance.

In any case we can firmly conclude that $k_1 >> k_2$. In other words, the Gr-1 catalyst bounds to PCOE chains much more easily than to PNB ones. We can speculate that this property is correlated with the volume of groups surrounding double C=C bonds, i.e., it is sterically caused by more bulky groups in PNB chains that effectively hinder the attack of Gr-1. At the same time, we find that $k_{1d} << k_{2d}$, which means that [Ru]=PNB carbenes are considerably less stable than [Ru]=PCOE ones, which are in turn inferior to the primary [Ru]=CHPh carbenes in the absence of polymers. With that notion we turn to studying chemical transformations in a PCOE/PNB mixture in the presence of Gr-1 catalyst.

Cross-metathesis in the mixture of PCOE and PNB

Interaction of PCOE (M_n = 142000 g/mol, $Đ$ = 1.9), PNB (M_n = 60000 g/mol, $Đ$ = 2.6), and Gr-1 was studied in $CDCl_3$ solution at the initial concentration ratio [PCOE]/[PNB]:[Gr-1] = 10:10:1 (mol/mol). The chosen total

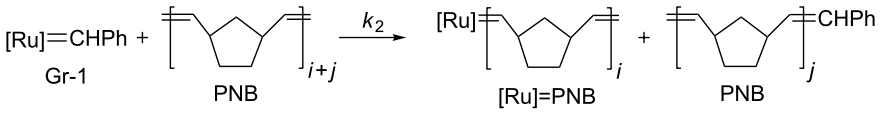

Scheme 2: Formation of polynorbornene-bound carbene by the interaction of Gr-1 with PNB.

polymer concentration of 4–6% (wt/v) was a compromise between being well above the crossover concentration in order to study the law of mass action kinetics and restricting aggregation of PCOE chains detected by DLS. We supposed that, apart from the reactions of polymer carbenes formation shown in Scheme 1 and Scheme 2 above and their decay, the cross-metathesis reactions could take place as depicted in Scheme 3.

However, two orders of magnitude difference in the activity of Gr-1 with respect to PCOE and PNB left little chance to observe the formation of [Ru]=PNB carbenes in the equimolar mixture. In situ experiments on a 600 MHz NMR spectrometer allowed detecting this secondary carbene at 18.82–18.94 ppm, but its concentration throughout the reaction was indeed very low, as shown by the green squares in Figure 6. One could guess that if [Ru]=PCOE were the only active polymer carbene, then the extent of the cross-metathesis would be very low and the fraction of alternating NB-COE dyads in a copolymer product would be limited by the initial catalyst/polymer concentration ratio of 1/20. Nevertheless, ex situ ^{13}C NMR experiments demonstrated that the alternating dyads shown with the full purple circles in Figure 6 not only appeared but gradually became to prevail in the NB-COE copolymer.

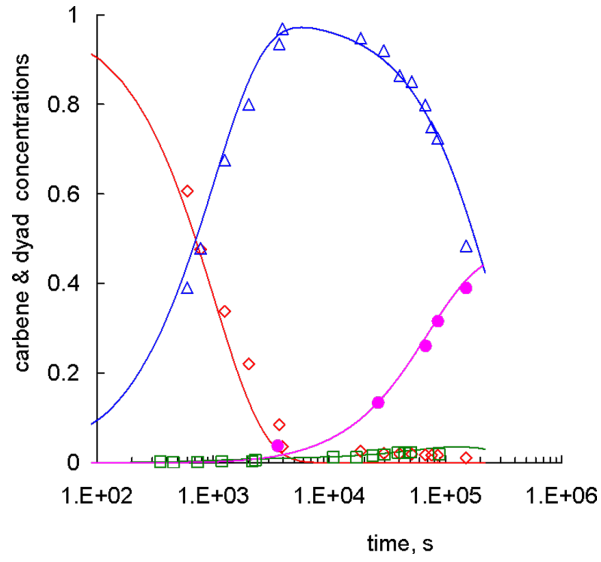

Figure 6: Dependences of the normalized (red) primary, (blue) PCOE, and (green) PNB carbene concentrations and (purple) the fraction of alternating NB-COE dyads on time: (points) experimental data, (curves) calculations according to Equation 4 with the rate constants k_1 = 3.1 × 10^{-3} L mol^{-1} s^{-1}, k_2 = 0, k_{1d} = 2.6 × 10^{-6} s^{-1}, k_{2d} = 2.4 × 10^{-5} s^{-1}, k_{211} = 2.2 × 10^{-2} L mol^{-1} s^{-1}, k_{122} = k_{211}/100, k_{212} = k_{112} = $(k_{211}k_{122})^{1/2}$.

This fact can be understood if we assume that the concentration of [Ru]=PNB carbenes is low because they actively react with PCOE (the second direct reaction of Scheme 3), being an important intermediate in the cross-metathesis between PCOE and PNB. Indeed, the reactants here are a [Ru]=PNB carbene that decays faster than a [Ru]=PCOE one and a PCOE chain that is attacked by Gr-1 easier than a PNB one. Therefore, it will be not surprising if this reaction is characterized by the highest reaction rate of four elementary processes depicted in Scheme 3.

The kinetic equations describing reactions in the mixture under study are written down in Equation 4.

In Equation 4 c_0, c_1, c_2 are the concentrations (mol/L) of [Ru]=CHPh, [Ru]=PCOE, and [Ru]=PNB carbenes, respective-

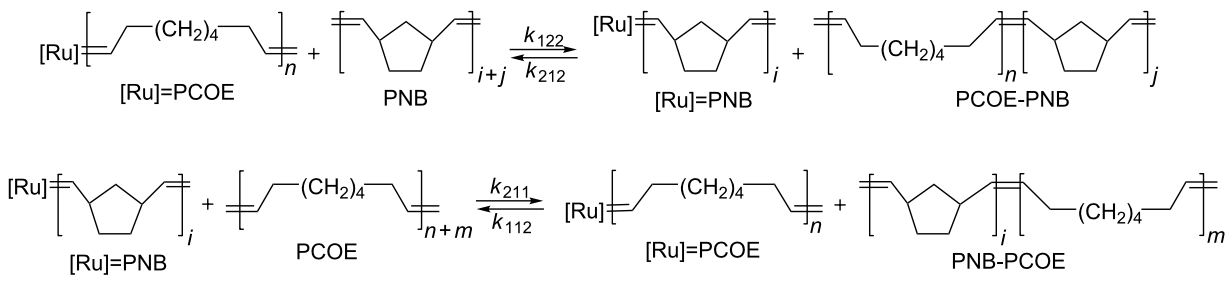

Scheme 3: Elementary cross-metathesis reactions in the mixture of PCOE with PNB.

$$\begin{cases} dc_0/dt = -(k_1\phi c_p + k_2(1-\phi)c_p)c_0 \\ dc_1/dt = k_1\phi c_p c_0 - k_{122}c_1c_p(1-\phi-\phi_{12}) + k_{212}c_2c_p\phi_{12} + k_{211}c_2c_p(\phi-\phi_{12}) - k_{112}c_1c_p\phi_{12} - k_{1d}c_1 \\ dc_2/dt = k_2(1-\phi)c_p c_0 + k_{122}c_1c_p(1-\phi-\phi_{12}) - k_{212}c_2c_p\phi_{12} - k_{211}c_2c_p(\phi-\phi_{12}) + k_{112}c_1c_p\phi_{12} - k_{2d}c_2 \\ 2d\phi_{12}/dt = k_{122}c_1c_p(1-\phi-\phi_{12}) - k_{212}c_2c_p\phi_{12} + k_{211}c_2c_p(\phi-\phi_{12}) - k_{112}c_1c_p\phi_{12} \end{cases} \quad (4)$$

ly; ϕ and $2\phi_{12}$ are the molar fractions of PCOE units (which is constant) and alternating (COE-NB and NB-COE) dyads. Note that Equation 4 implies that the law of mass action is valid and does not discriminate between interchain and intrachain reactions. The initial conditions for it read

$$c_0(t=0) = c_{in}, c_1(t=0) = c_1(t=0) = \phi_{12}(t=0) = 0 \quad (5)$$

where the initial carbene concentration c_{in} = 0.0266 mol/L is again assumed to be much less than the total polymer concentration c_p = 0.586 mol/L.

Values of the rate constants k_1, k_2, k_{1d}, and k_{2d} can be taken from the above considerations of PCOE – Gr-1 ($k_1 = 3.1 \times 10^{-3}$ L mol^{-1} s^{-1} and $k_{1d} = 2.6 \times 10^{-6}$ s^{-1}) and PNB – Gr-1 ($k_2 = 5.4 \times 10^{-5}$ L mol^{-1} s^{-1} and $k_{2d} = 2.4 \times 10^{-5}$ s^{-1}) reactions. Looking ahead, we should note that nothing is changed if we just put k_2 to zero, which means that [Ru]=PNB carbenes are formed via the cross-metathesis reaction rather than by the direct transformation of primary [Ru]=CHPh carbenes.

There are still four rate constants (k_{122}, k_{212}, k_{211}, and k_{112}, where the first index denotes the type of an interacting polymer-bound carbene and the last two indices designate the type of a dyad containing a reacting C=C bond) unknown and only one "new" $\phi_{12}(t)$ function available for fitting. Therefore we will search for the highest rate constant k_{211} that describes the attack of a [Ru]=PNB carbene onto a PCOE chain, as discussed above. We also assume that the rate constant k_{122} responsible for the interaction of a [Ru]=PCOE carbene with a PNB chain is a hundred times smaller than k_{211}, by analogy with ca. hundred times smaller reaction rate of Gr-1 with PNB than that of Gr-1 with PCOE. In this manner we take into account the difference in the local environment of C=C bonds in PNB and PCOE. The remaining two constants describing the interaction of [Ru]=PCOE and [Ru]=PNB carbenes with NB-COE heterodyads are taken to be equal to each other and to the geometric mean of k_{122} and k_{211}: $k_{212} = k_{112} = (k_{211}k_{122})^{1/2}$, since a C=C bond in a NB-COE dyad should be more accessible than in a NB-NB dyad but less than in a COE-COE dyad.

With these assumptions made, we achieved a good agreement between the dependences $c_0(t)/c_{in}$, $c_1(t)/c_{in}$, $c_1(t)/c_{in}$, and $2\phi_{12}(t)$ calculated for $k_{211} = 2.2 \times 10^{-2}$ L mol^{-1} s^{-1} and the corresponding experimental NMR data plotted in Figure 6. Qualitatively, it means that the cleavage of a polymeric double C=C bond is about an order of magnitude more probable in the reaction with a polymer-bound Ru-carbene than with a [Ru]=CHPh carbene. Further kinetic studies on that issue are needed to get quantitative results.

Before concluding this paper we would like to briefly discuss the role of the polymer/catalyst initial ratio and of the polymer mixture composition. The former parameter determines the final molar mass of the NB-COE copolymer. However, if we consider the dependence of the NB-COE dyad fraction on time (Figure 7), both parameters appear not so important at the early stage. Now it is clear that this stage is associated with the formation of polymer carbenes rather than with the cross-metathesis itself. Later on, the content of alternating dyads grows predictably slower for the system with a lower catalyst loading (cf. the red and blue curves) and for the compositionally asymmetric mixture (cf. the red and purple curves). Note that these experiments were carried out under constant mixing of the reaction media [15], which was impossible for in situ experiments.

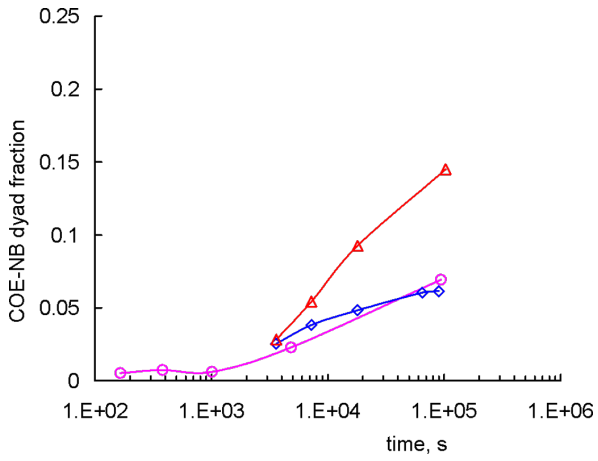

Figure 7: The kinetics of NB-COE dyads formation under mixing conditions for the systems with (red) $c_{in}/c_p = 1.0 \times 10^{-2}$, [COE]/[NB] = 0.54/0.46; (blue) $c_{in}/c_p = 3.4 \times 10^{-3}$, [COE]/[NB] = 0.53/0.47; (purple) $c_{in}/c_p = 1.0 \times 10^{-2}$, [COE]/[NB] = 0.69/0.31. The curves are only for eye guidance.

Conclusion

The kinetic data analysis undertaken in the present study makes it possible to outline the cross-metathesis scenario for the mixtures of PCOE and PNB in the presence of the Gr-1 catalyst. Contrary to the situation with a corresponding monomer mixture, where this catalyst first initiates vigorous polymerization of norbornene and only then polymerizes cyclooctene, in the polymer system it first interacts with PCOE and approximately in an hour all Ru-carbenes become bound to PCOE chains. This stage is also characterized by a marked decrease in the average molar mass of the mixture. Then, the cross-metathesis actually starts and it takes about a day to obtain a statistical NB-COE copolymer under chosen conditions, while its molar mass is kept nearly constant. The process is controlled by the slowest elementary reaction, which is the interaction between a

[Ru]=PCOE carbene and a double C=C bond in a PNB chain. We suppose that this reaction can be sterically hindered by the bulky structure of a norbornene monomer unit. During the cross-metathesis, [Ru]=PNB carbenes exist at a low concentration but their presence is crucial for the course of the whole process. For developing the cross-metathesis as a new method of obtaining unsaturated statistical copolymers, especially promising for the comonomers with considerably different polymerization rates, it would be interesting to also try a one-pot process, in which case the reaction starts with a monomeric mixture of COE and NB. This could eliminate tedious procedures of homopolymer isolation and purification and allow increasing the concentration of the reacting solution.

Experimental

Chemicals

All manipulations involving air- and moisture-sensitive compounds were carried out in oven-dried glassware using dry solvents and standard Schlenk and vacuum-line techniques under argon atmosphere. Monomers, norbornene (Acros Organics) and *cis*-cyclooctene (Aldrich), were dried over sodium, distilled, and stored under argon. The 1st generation Grubbs' catalyst $Cl_2(PCy_3)_2Ru$=CHPh (Aldrich) was used without further purification as 0.007–0.077 M solutions in toluene or $CHCl_3$. All other reagents and solvents were purchased from Aldrich and used as received or purified according to standard procedures.

Instrumentation

Nuclear magnetic resonance measurements were carried out at room temperature using a Bruker Avance™ 600 NMR spectrometer operating at 600.22 MHz (^{1}H NMR) and 150.93 MHz (^{13}C NMR); $CDCl_3$ (Aldrich) was used as solvent. Chemical shifts δ were reported in parts per million relative to the residual $CHCl_3$ signal as an internal reference standard. Differential scanning calorimetry (DSC) thermograms were recorded on a Mettler TA 4000 system at a rate of 10 °C/min under argon flow of 70 mL/min in the range from −100 °C to 100 °C. The molar mass of the polymers was determined by GPC on a Waters high pressure chromatograph equipped with a refractometric detector and Microgel mix 1–5 μm 300 × 7.8 mm Waters Styragel HR 5E column, with toluene for PNB and NB-COE copolymers and tetrahydrofurane for PCOE as a solvent, the flow rate of 1 mL/min, sample volume of 100 μL, and sample concentration of 1 mg/mL. The molar mass and its dispersity ($Đ$) were calculated by a standard procedure relative to polystyrene standards. Light scattering was studied on a Photocor Complex goniometer equipped with a HeNe laser (a wavelength of λ = 633 nm, an intensity of 25 mW) as a light source. The scattering angle θ was varied in the range 30–150°. In static experiments, the total scattering intensity was measured. In dynamic experiments, the time cross-correlation function g_2 of the scattered-light intensity fluctuations was determined with a 288-channel Photocor-FC correlator board and treated with the Alango DynaLS software through the inverse Laplace transform method to yield the hydrodynamic radius distributions. Prior to measurements, the solutions in $CHCl_3$ were filtered through a polytetrafluoroethylene membrane with the pore diameter of 0.22 μm.

Polymer synthesis (typical)

Polyoctenamer (PCOE): C*is*-cyclooctene (3.58 g, 32.6 mmol) was added to the 1st generation Grubbs' catalyst (38.3 mg, 0.0465 mmol) solution in CH_2Cl_2 (12.2 mL) prepared in a round-bottom glass flask (50 mL) equipped with a magnetic stirrer under inert atmosphere at 20 °C. The polymerization was stopped by the addition of 0.3 mL of ethyl vinyl ether after 2 h. The polymers were precipitated in a 0.1% acetone solution of an antioxidant 2,2'-methylenebis(6-*tert*-butyl-4-methylphenol) (**1**), decanted, washed with several portions of the same solution, and dried under reduced pressure at room temperature until constant mass. The yield was 2.72 g (76%). Polymer (1 g) was dissolved in 0.4% THF solution of HCl (30 mL), stirred for 4 h and precipitated in a 0.1% ethanol solution of an antioxidant **1**, decanted, washed with several portions of the same solution, and dried under reduced pressure at room temperature until constant mass. Immediately before the cross-metathesis, 0.9 M polymer solution in $CHCl_3$ was passed through a column with SiO_2 (SiO_2/PCOE 8:1, w/w) and precipitated in ethanol, decanted, washed with several portions of ethanol, and dried under reduced pressure at room temperature until constant mass. M_n = 120000 g/mol, $Đ$ = 1.8, T_g = −79 °C, T_m = 44 °C, *trans*-68%.

Polynorbornene (PNB): 4.0 mL of a 3.2 M solution of norbornene (1.21 g, 13 mmol) in toluene was added to the 1st generation Grubbs' catalyst (43 mg, 0.052 mmol) solution in toluene (12.3 mL) prepared as described above at 20 °C. The polymerization was stopped by the addition of 0.4 mL of ethyl vinyl ether after 1 h. The polymers were precipitated in a 0.1% ethanol solution of antioxidant **1**, decanted, washed with several portions of the same solution, and dried under reduced pressure. The polymer was twice reprecipitated in ethanol from toluene solution and dried under reduced pressure at room temperature until constant mass. The yield was 1.20 g (99%). PNB was purified with HCl solution in THF and column chromatography (SiO_2) as described above. M_n = 60000 g/mol, $Đ$ = 2.6, T_g = 39 °C, *trans*-88%.

Other thermal characteristics as well as the NMR spectra details of the synthesized PCOE and PNB and NB-COE copolymers are given in our previous paper [15].

Monitoring Gr-1 – polymer interaction

PCOE (44.4 mg, 0.35 mmol) and $CDCl_3$ (0.46 mL) were placed into a Young's NMR tube under Ar atmosphere for 24 h with periodic mixing until a homogenous polymer solution was obtained. The mixture was degassed three times by using the freeze-pump-thaw technique before the 0.08 M separately prepared solution of Gr-1 in $CDCl_3$ (0.25 mL, 16.4 mg, 0.0199 mmol) was added to the frozen polymer solution. The mixture was melted, mixed, and immediately put into the NMR spectrometer at 20 °C. A typical ^{1}H NMR spectrum is shown in Figure 8.

PNB (33 mg, 0.35 mmol) and $CDCl_3$ (0.35 mL) were placed into a Young's NMR tube under Ar atmosphere for 24 h with periodic mixing until homogenous polymer solution was obtained. The mixture was degassed three times by using the freeze–pump–thaw technique before the 0.08 M separately prepared solution of Gr-1 in $CDCl_3$ (0.22 mL, 14.4 mg, 0.0176 mmol) was added to the frozen polymer solution. The mixture was melted, mixed, and immediately put into the NMR spectrometer at 20 °C. A typical 1H NMR spectrum is shown in Figure 9. After a reaction time of 24 h, the molar mass of PNB dropped to M_n = 11200 g/mol, $Đ$ = 1.8.

Monitoring the cross-metathesis

In situ ^{1}H NMR: PNB (26 mg, 0.25 mmol), PCOE (22 mg, 0.25 mmol), and $CDCl_3$ (0.38 mL) were placed into a Young's NMR tube in Ar atmosphere for 24 h with periodic mixing until homogenous polymer solution was obtained. The mixture was degassed three times using the freeze–pump–thaw technique before the 0.063 M separately prepared solution of Gr-1 in $CDCl_3$ (0.37 mL, 20 mg, 0.023 mmol) was added to the frozen polymer solution. The mixture was melted, mixed, and immediately put into the NMR spectrometer at 20 °C. A typical ^{1}H NMR spectrum is shown in Figure 10. After 24 h of the reaction, an amorphous NB-COE copolymer of M_n = 7000 g/mol, $Đ$=1.6, T_g = −53 °C was formed.

Ex situ ^{13}C NMR: PNB (156 mg, 1.68 mmol) and PCOE (182 mg, 1.68 mmol) were dissolved in $CHCl_3$ (3 mL) in a round-bottom glass flask (25 mL) under inert atmosphere at 20 °C. Then a 0.031 M solution of Gr-1 (2.16 mL, 142.3 mg, 0.173 mmol) in $CHCl_3$ was added. Samples for NMR analyses were obtained by adding an aliquot (0.9 mL) of the reaction mixture to 0.2 mL of ethyl vinyl ether, stirred for 30–40 min at ambient temperature, and concentrated in vacuum, after that

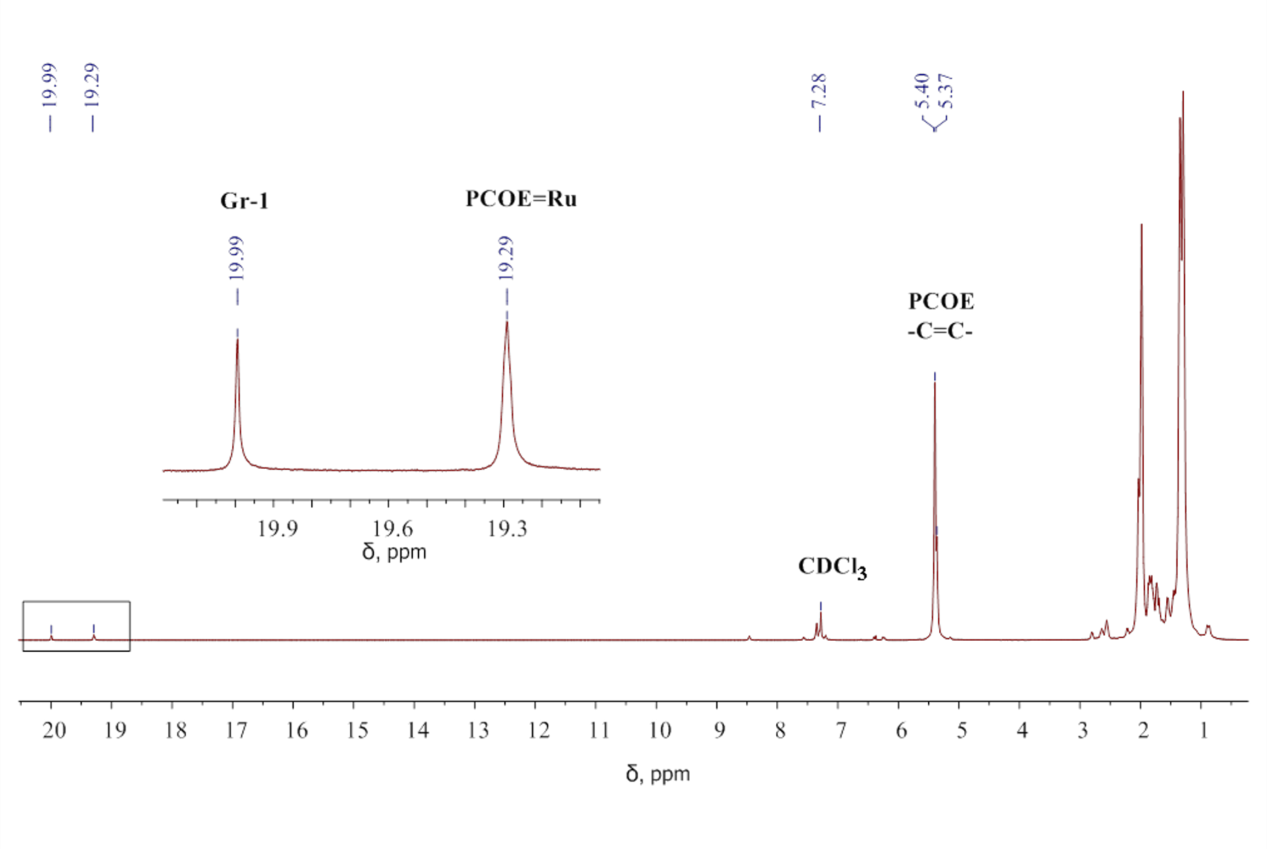

Figure 8: The ^{1}H NMR spectrum recorded after 10 min of the reaction between PCOE and Gr-1 at the initial concentration ratio of 20:1 mol/mol in $CDCl_3$. Carbene signals (19.99 ppm for [Ru]=CHPh and 19.29 ppm for [Ru]=PCOE) are enlarged in the inset.

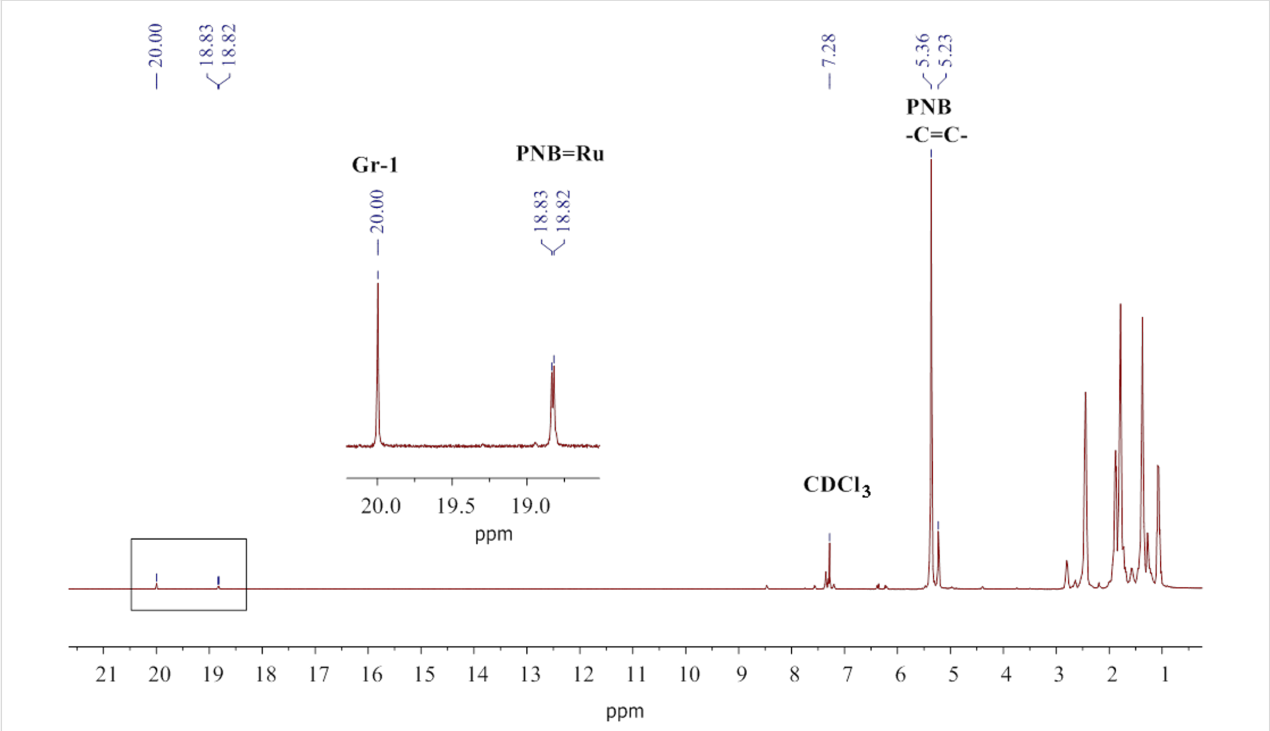

Figure 9: The ^{1}H NMR spectrum recorded after 653 min of the reaction between PNB and Gr-1 at the initial concentration ratio of 20:1 mol/mol in $CDCl_3$. The carbene signals (20.00 ppm for [Ru]=CHPh and 18.82, 18,83, 18.94 ppm for [Ru]=PNB) are enlarged in the inset.

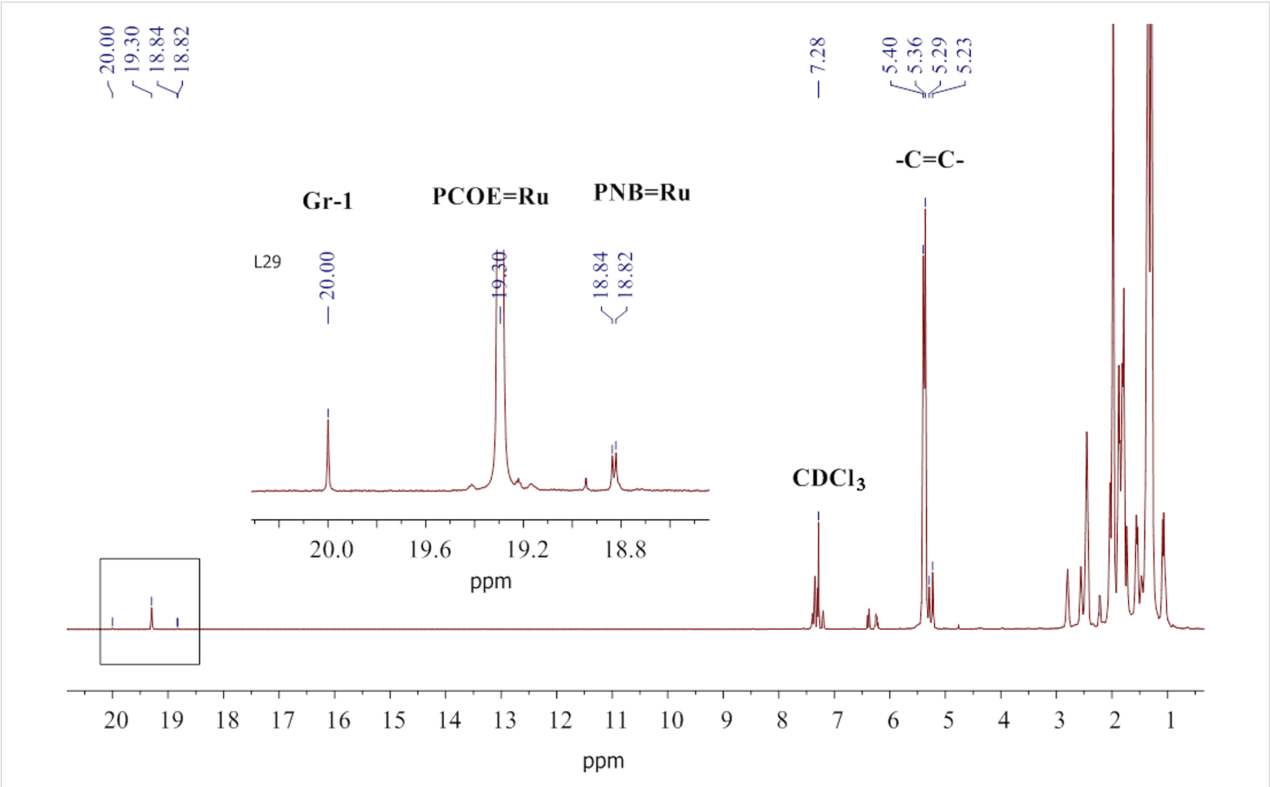

Figure 10: The ^{1}H NMR spectrum recorded after 24 h of the reaction between PCOE, PNB, and Gr-1 at the initial concentration ratio of 10:10:1 mol/mol in $CDCl_3$. The carbene signals (20.00 ppm for [Ru]=CHPh, 19.30 for [Ru]=PCOE, and 18.82, 18.83, 18.94 ppm for [Ru]=PNB) are enlarged in the inset.

$CDCl_3$ was added. For DSC and GPC measurements, the copolymers were precipitated in ethanol and dried as described above. A typical ^{13}C NMR spectrum is shown in Figure 11.

Acknowledgements

The authors are thankful to M. Yu. Gorshkova and to G. A. Shandryuk (Topchiev Institute of Petrochemical Synthesis RAS) for performing the GPC and DSC measurements, respectively. The work was partially supported by the Russian Foundation for Basic Research (Project 14-03-00665). Yu. I. D. is also grateful to the RF Presidential grant for young scientists (MK-7525.2015.3)

References

1. Platé, N. A.; Litmanovich, N. A.; Noah, O. V. *Macromolecular Reactions;* Wiley: New York, NY, U.S.A., 1995.
2. Litmanovich, A. D.; Platé, N. A.; Kudryavtsev, Y. V. *Prog. Polym. Sci.* **2002,** *27,* 915–970. doi:10.1016/S0079-6700(02)00003-5
3. Fakirov, S., Ed. *Transreactions in Condensation Polymers;* Wiley: Weinheim, Germany, 1999.
4. Maeda, T.; Otsuka, H.; Takahara, A. *Prog. Polym. Sci.* **2009,** *34,* 581–604. doi:10.1016/j.progpolymsci.2009.03.001
5. Ayres, N.; Weck, M. *Polym. Chem.* **2012,** *3,* 3019–3190. doi:10.1039/c2py90036j
6. Bertrand, A.; Hillmyer, M. A. *J. Am. Chem. Soc.* **2013,** *135,* 10918–10921. doi:10.1021/ja4050532
7. Monfette, S.; Fogg, D. E. *Chem. Rev.* **2009,** *109,* 3783–3816. doi:10.1021/cr800541y
8. Ivin, K. J.; Mol, J. C. *Olefin Metathesis and Metathesis Polymerization;* Academic Press: London, United Kingdom, 1997.
9. Gutiérrez, S.; Tlenkopatchev, M. A. *Rev. Latinoam. Metal Mat.* **2009,** *S1,* 1463–1467.
10. Streck, R. *J. Mol. Catal.* **1982,** *15,* 3–19. doi:10.1016/0304-5102(82)80001-1
11. Lu, Y.-X.; Tournilhac, F.; Leibler, L.; Guan, Z. *J. Am. Chem. Soc.* **2012,** *134,* 8424–8427. doi:10.1021/ja303356z
12. Lu, Y.-X.; Guan, Z. *J. Am. Chem. Soc.* **2012,** *134,* 14226–14231. doi:10.1021/ja306287s
13. Otsuka, H.; Muta, T.; Sakada, M.; Maeda, T.; Takahara, A. *Chem. Commun.* **2009,** *9,* 1073–1075. doi:10.1039/b818014h
14. Maeda, T.; Kamimura, S.; Ohishi, T.; Takahara, A.; Otsuka, H. *Polymer* **2014,** *55,* 6245–6251. doi:10.1016/j.polymer.2014.10.001
15. Gringolts, M. L.; Denisova, Yu. I.; Shandryuk, G. A.; Krentsel, L. B.; Litmanovich, A. D.; Finkelshtein, E. S.; Kudryavtsev, Y. V. *RSC Adv.* **2015,** *5,* 316–319. doi:10.1039/C4RA12001A
16. Norsorex® APX. Technical product bulletin # M-30. http://www2.epa.gov/emergency-response/norsorexr-apx (accessed June 6, 2015).

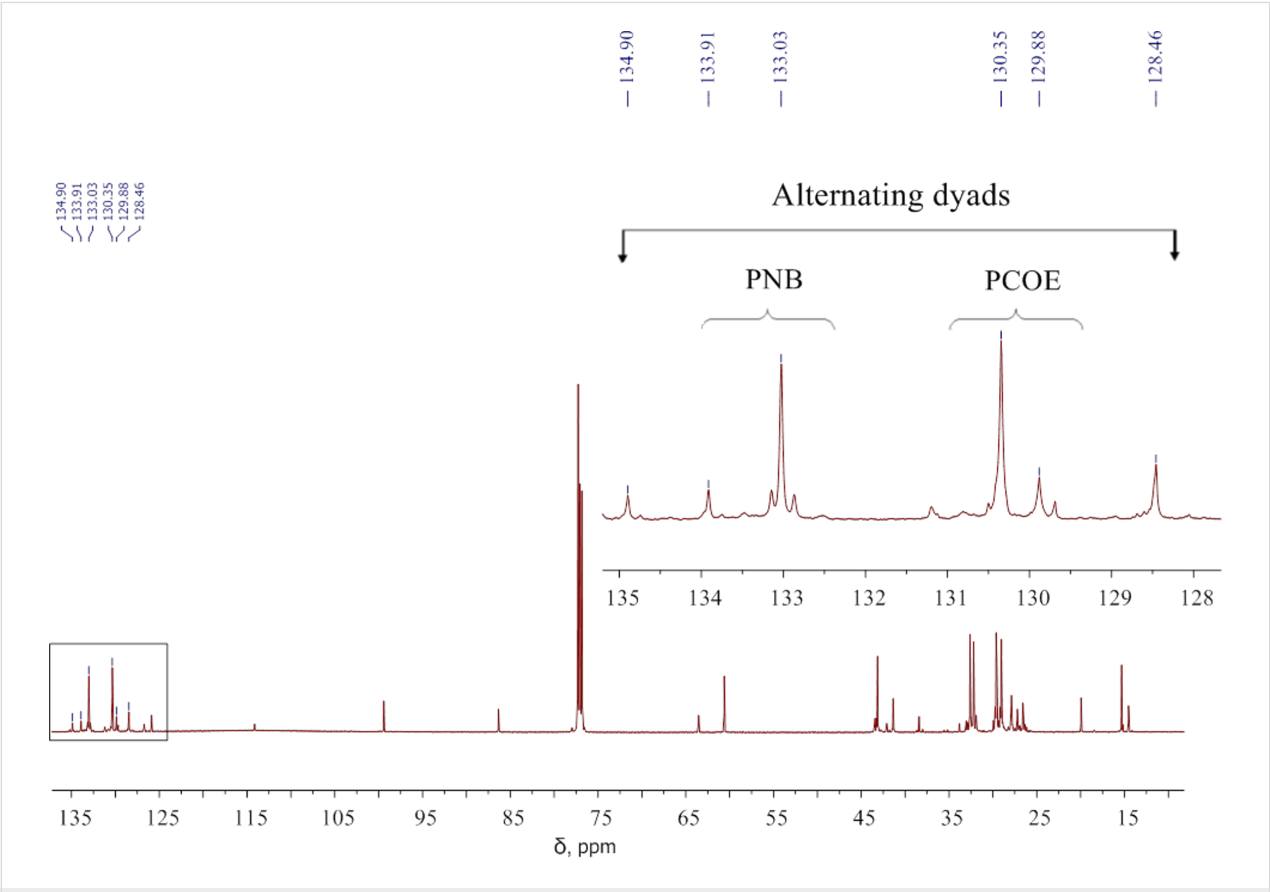

Figure 11: The ^{13}C NMR spectrum recorded after 8 h of the reaction between PCOE, PNB, and Gr-1 at the initial concentration ratio of 10:10:1 mol/mol in $CDCl_3$. The region of C=C signals including those from alternating NB-COE dyads (128.5, 134.90 m ppm) is enlarged in the inset.

17. Evonik Industries, Products & Solutions. Vestenamer®. http://corporate.evonik.com/en/products/search-products/pages/product-details.aspx?pid=10076 (accessed June 6, 2015).
18. Naofumi, N.; Genzo, K.; Akinori, T. *Polymer* **2006,** *47,* 6081–6090. doi:10.1016/j.polymer.2006.06.015
19. Bornand, M.; Chen, P. *Angew. Chem., Int. Ed.* **2005,** *44,* 7909–7911. doi:10.1002/anie.200502606
20. von R. Schleyer, P.; Williams, J. E.; Blanchard, K. R. *J. Am. Chem. Soc.* **1970,** *92,* 2377–2386. doi:10.1021/ja00711a030
21. Bornand, M.; Torker, S.; Chen, P. *Organometallics* **2007,** *26,* 3585–3596. doi:10.1021/om700321a
22. Torker, S.; Müller, A.; Sigrist, R.; Chen, P. *Organometallics* **2010,** *29,* 2735–2751. doi:10.1021/om100185g
23. Vehlow, K.; Wang, D.; Buchmeiser, M. R.; Blechert, S. *Angew. Chem., Int. Ed.* **2008,** *47,* 2615–2618. doi:10.1002/anie.200704822
24. Lichtenheldt, M.; Wang, D.; Vehlow, K.; Reinhardt, I.; Kühnel, C.; Decker, U.; Blechert, S.; Buchmeiser, M. R. *Chem. – Eur. J.* **2009,** *15,* 9451–9457. doi:10.1002/chem.200900384
25. Buchmeiser, M. R.; Ahmad, I.; Gurram, V.; Santhosh Kumar, P. *Macromolecules* **2011,** *44,* 4098–4106. doi:10.1021/ma200995m
26. Ilker, M. F.; Coughlin, E. B. *Macromolecules* **2002,** *35,* 54–58. doi:10.1021/ma011394x
27. Romulus, J.; Patel, S.; Weck, M. *Macromolecules* **2012,** *45,* 70–77. doi:10.1021/ma201812x
28. Daeffler, C. S.; Grubbs, R. H. *Macromolecules* **2013,** *46,* 3288–3292. doi:10.1021/ma400141c
29. Schwab, P.; Grubbs, R. H.; Ziller, J. W. *J. Am. Chem. Soc.* **1996,** *118,* 100–110. doi:10.1021/ja952676d
30. Grubbs, R. H., Ed. *Handbook of Metathesis;* Wiley-VCH: Weinheim, Germany, 2003. doi:10.1002/9783527619481
31. Gringolts, M. L.; Bermeshev, M. V.; Rogan, Yu. V.; Moskvicheva, M. V.; Filatova, M. P.; Finkelshtein, E. S.; Bondarenko, G. N. *Silicon* **2015,** *7,* 107–115. doi:10.1007/s12633-014-9238-7
32. Doi, M.; Edwards, S. F. *The Theory of Polymer Dynamics;* Clarendon Press: Oxford, United Kingdom, 1986.

License and Terms

BEILSTEIN JOURNAL OF ORGANIC CHEMISTRY

Nitro-Grela-type complexes containing iodides – robust and selective catalysts for olefin metathesis under challenging conditions

Andrzej Tracz[1,2], Mateusz Matczak[1], Katarzyna Urbaniak[1] and Krzysztof Skowerski[*1]

Full Research Paper

Open Access

Address:
[1]Apeiron Synthesis SA, Duńska 9, 54-427 Wrocław, Poland and [2]Department of Bioorganic Chemistry, Faculty of Chemistry, Wroclaw University of Technology, Wybrzeże Wyspańskiego 27, 50-370 Wrocław, Poland

Email:
Krzysztof Skowerski[*] - krzysztof.skowerski@apeiron-synthesis.com

* Corresponding author

Keywords:
green solvents; macrocyclization; metathesis; ruthenium

Beilstein J. Org. Chem. **2015,** *11,* 1823–1832.
doi:10.3762/bjoc.11.198

Received: 01 July 2015
Accepted: 10 September 2015
Published: 06 October 2015

This article is part of the Thematic Series "Progress in metathesis chemistry II".

Associate Editor: I. Marek

Abstract

Iodide-containing nitro-Grela-type catalysts have been synthesized and applied to ring closing metathesis (RCM) and cross metathesis (CM) reactions. These new catalysts have exhibited improved efficiency in the transformation of sterically, non-demanding alkenes. Additional steric hindrance in the vicinity of ruthenium related to the presence of iodides ensures enhanced catalyst stability. The benefits are most apparent under challenging conditions, such as very low reaction concentrations, protic solvents or with the occurrence of impurities.

Introduction

Olefin metathesis (OM) is a mild and versatile catalytic method which allows the formation of carbon–carbon double bonds [1]. Understanding the key events in ruthenium-catalyzed olefin metathesis [2] and developing efficient and selective catalysts [3] provides opportunities for industrial applications of this technology. In many cases, however, the achievement of high turn over numbers (TONs) requires tedious purification of starting materials and solvents. New catalysts with increased efficiency and selectivity, especially under challenging conditions, are therefore of high interest. Currently, the second generation Hoveyda-type catalysts, such as **HII** [4], **A** [5], **B** [6], and **C** [7] are considered to be the most versatile tool for OM (Figure 1).

Modifications of ligands permanently bound to the ruthenium center appear to be the most efficient methods for altering the catalyst properties. Great improvement of catalyst efficiency in the transformation of sterically non-demanding alkenes have been achieved by the replacement of the classical SIMes ligand with the bulkier SIPr ligand (Scheme 1) [8,9]. Metathesis catalysts with even larger NHC ligands have also been reported, but their syntheses require additional steps because the necessary

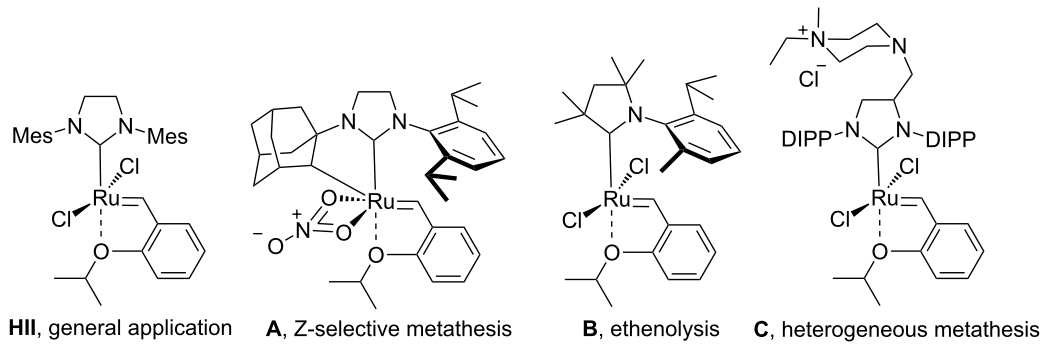

Figure 1: The diversity of Hoveyda-type complexes (Mes – 2,4,6-trimethylphenyl, DIPP – 2,6-diisopropylphenyl).

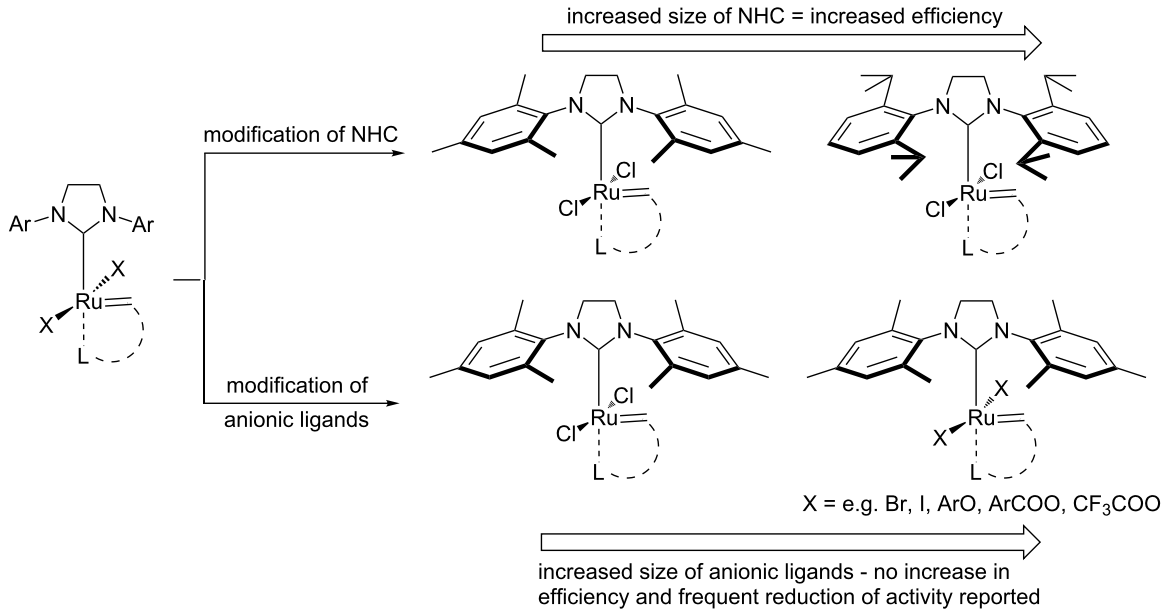

Scheme 1: Modifications of the 2nd generation alkylidene complexes.

anilines – the starting materials for the preparation of NHCs precursors – are not commercially available [10,11]. Up until now, there had been no disclosures of increased catalyst efficiency caused by the exchange of chlorides with larger anionic ligands. Grubbs et al. showed that the exchange of chlorides for bromides or iodides in the second generation Grubbs' catalysts facilitated the initiation, but reduced the propagation rate and eventually provided no overall improvement [12]. More recently Slugovc et al. synthesized bromo- and iodo- analogues of **HII,** but no improvement was noted [13-15]. Moreover, the presence of iodide ligands reduced initiation rates for Hoveyda second generation complex bearing iodides (**HII-I2**) in ring-closing metathesis (RCM). Similarly, Schrodi and colleagues did not find any advantages for halide exchanged Hoveyda-type complexes in cross metathesis of methyl oleate with ethylene [16]. Complexes containing iodide lead to products of asymmetric OM with better enantio- and diastereoselectivity, but this came at the price of lower activity [17]. In the past few years the replacement of chloride ligands created the first *Z*-selective catalysts [18-21]. Their efficiency, however, is noticeably lower than that observed for classical complexes. The second generation indenylidene catalysts with phosphite ligand (frequently reported as "Cazin-type catalysts") bearing mixed chloride–fluoride or difluoride anionic ligands were also reported very recently [22]. The former catalyst exhibited thermal stability and efficiency comparable with the original complex having two chlorides, while the difluoride catalyst showed low catalytic activity. Finally, alternative anionic

ligands have been used in order to heterogenize catalysts, which resulted in the formation of materials with reduced activity and efficiency [23,24].

It is well recognized that the benzylidene ligand structure strongly influences initiation rates for Hoveyda-type catalysts [25]. As a consequence of the "boomerang effect", which was recently strongly supported by Fogg et al. [26], the benzylidene ligand also most likely affects propagation rates.

In our search for active, more robust and selective catalysts, we synthesized iodide-containing nitro-Grela type catalysts. A synergistic effect of the ligands was sought: the nitro-substituted benzylidene ligand was expected to ensure fast initiation, while the bulky iodides were anticipated to provide additional stabilization of the active species.

Results and Discussion

The new iodide-containing catalysts, **nG-I2** and **nG-SIPr-I2,** were prepared with a 93% yield from commercially available complexes, **nG** and **nG-SIPr**, and with the use of potassium iodide as the iodide anions source (Scheme 2). In the synthesis of both catalysts, the isolated material contained 99% of the expected diiodo catalyst and 1% of the "mixed halogen" complex, which was identified by field desorption mass spectrometry (FD–MS) and quantified by ^{1}H NMR.

In order to determine the differences in the initiation rate between the new and parent complexes, we ran the RCM of diethyl diallylmalonate (DEDAM) in toluene (C^0_{DEDAM} 0.2 M) at a relatively low temperature (18 °C) with only 0.15 mol % of the catalyst (Figure 2). The **nG-I2** catalyst initiated slightly more slowly than the parent **nG**, but was more stable and after 1 h gave greater than a 10% better conversion of the substrate as indicated in Figure 2. The catalytic performance of **nG-I2** was almost identical to that observed for **nG-SIPr**, suggesting that the exchange of chloride with iodide can – at least for some substrates – provide similar catalyst stabilization as the introduction of a bulky NHC ligand. In the case of the most sterically crowded **nG-SIPr-I2**, initiation was delayed, but a very fast reaction propagation was observed. This catalyst was the most stable and efficient among all tested complexes.

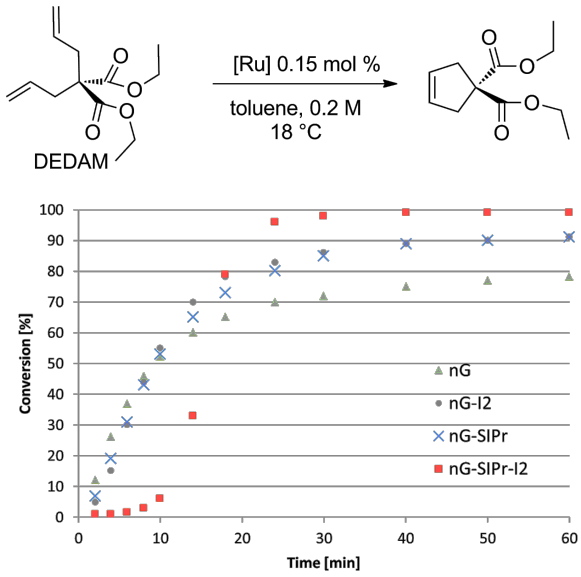

Figure 2: Reaction profiles for RCM of DEDAM; toluene, 0.2 M, 18 °C, [Ru] 0.15 mol %; conversion determined by GC.

To gain more information about the scope of application of the obtained catalysts, we carried out a set of standard RCM and CM transformations (Table 1 and Table 2). The reactions were performed in dry, degassed toluene, at 70 °C with varied catalyst loadings to demonstrate differences in their efficiencies.

The efficiency pattern observed in RCM of DEDAM was confirmed in the synthesis of five- to seven-membered, disubstituted heterocycles (Table 1, entries 1–3). Both **nG-I2** and **nG-SIPr-I2** proved to be sensitive to the steric bulk in close proximity to the double bond. Thus, RCM with substrate **7** having one double bond terminally substituted with the phenyl

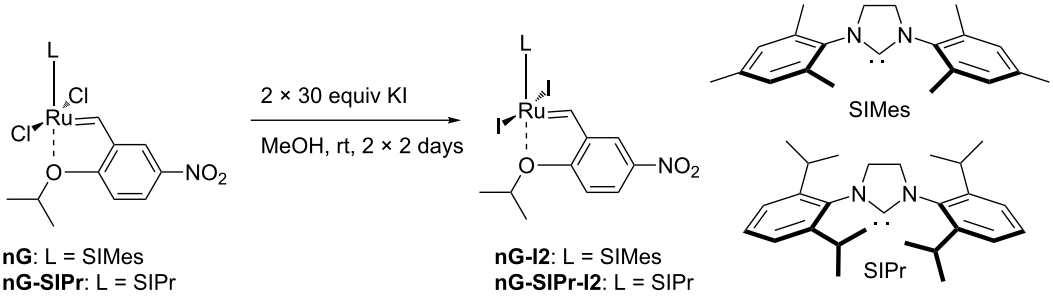

Scheme 2: Synthesis of iodide-containing nitro-Grela type catalysts.

Table 1: Results of RCM reactions.[a]

Entry	Substrate	Product	Catalyst (mol %)	GC Conversion [%]
1	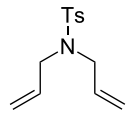 **1**	 **2**	**nG** (0.0025)	32
			nG-I2 (0.0025)	72
			nG-SIPr (0.0025)	85
			nG-SIPr-I2 (0.0025)	95
2	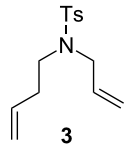 **3**	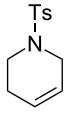 **4**	**nG** (0.003)	67
			nG-I2 (0.003)	91
			nG-SIPr (0.003)	90
			nG-SIPr-I2 (0.003)	97
3	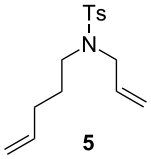 **5**	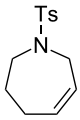 **6**	**nG** (0.0075)	57
			nG-I2 (0.0075)	87
			nG-SIPr (0.0075)	86
			nG-SIPr-I2 (0.0075)	94
4	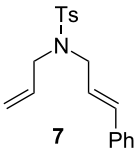 **7**	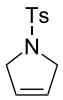 **2**	**nG** (0.015)	89
			nG-I2 (0.015)	82
			nG-SIPr (0.015)	95
			nG-SIPr-I2 (0.015)	47
5	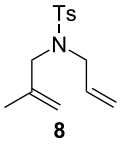 **8**	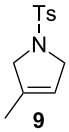 **9**	**nG** (0.05)	93
			nG-I2 (0.05)	79
			nG-SIPr (0.05)	99
			nG-SIPr-I2 (0.05)	75
6	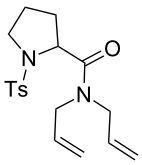 **10**	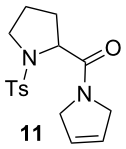 **11**	**nG** (0.04)	80
			nG-I2 (0.04)	94
			nG-SIPr (0.04)	99
			nG-SIPr-I2 (0.04)	94

[a]Toluene, 0.2 M, 70 °C, 2 h.

ring as well as the formation of the trisubstituted heterocycle **9** proceeded better with chloride-containing catalysts. When proline derivative **10** was used, the diiodo catalysts performed better than **nG** but slightly worse than **nG-SIPr**.

As outlined in Table 2, all tested catalysts were similarly effective in CM of methyl undecenoate **12** with *cis*-1,4-diacetoxy-2-butene (**13**), but parent dichloro complexes provided smaller quantities of dimerization product of **12**. In CM of **12** with electron deficient methyl acrylate **15**, diiodo derivatives were significantly less efficient and provided much more dimer of **12**. Apparently **nG-I2** and **nG-SIPr-I2** can perform noticeably better than parent dichloro complexes only in metathesis of sterically non-demanding substrates. With this knowledge, we decided to test their applicability under conditions which require high stability of the active species. Macrocyclization of dienes having low effective molarity provides access to a number of valuable musk-like compounds [27,28]. This type of transformation must be carried out at a very low concentration (usually <10 mM) in order to avoid formation of oligomeric/polymeric byproducts. Moreover, high temperature is required to complete the reaction in an acceptably short time. Therefore, a very stable and efficient catalyst is required to perform macrocyclization at reasonable loadings. The additional challenge related to high dilutions is the efficient removal of ethylene, which can be especially difficult on a large scale. Accordingly, the optimal catalyst for macrocyclization should form stable active species (usually ruthenium methylidenes), but it should also exhibit high preference of productive metathesis over unproductive metathesis.

Table 2: Results of CM reactions.[a]

Entry	Substrates	Product	Catalyst (mol %)	GC Yield (selectivity) [%]	*E*/*Z*
1[b]	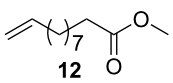 **12** 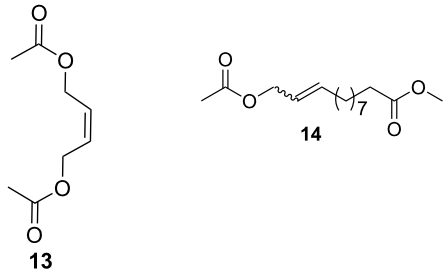 **13**	**14**	**nG** (0.4)	84 (99)	6/1
			nG-I2 (0.4)	88 (96)	4.8/1
			nG-SIPr (0.4)	88 (98)	5/1
			nG-SIPr-I2 (0.4)	84 (90)	3/1
2[c]	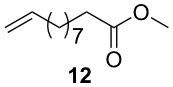 **12** 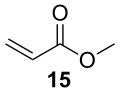 **15**	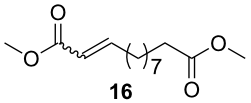 **16**	**nG** (0.5)	98 (>99)	19/1
			nG-I2 (0.5)	74 (88)	9/1
			nG-SIPr (0.5)	98 (>99)	9/1
					9/1
			nG-SIPr-I2 (0.5)	30 (44)	

[a]Toluene, 0.2 M, 70 °C, 2 h; [b]3 equiv of **13**; [c]3 equiv of **15**.

Experiments with ethylene

To gain more information about the behavior of tested catalysts in the presence of ethylene, we performed two experiments. In the first test, 100 ppm of each catalyst was stirred for 45 minutes at 25 °C in an ethylene atmosphere [29,30]. During that period, ruthenium methylidenes were generated and involved in the unproductive metathesis of ethylene (Figure 3). Subsequently, the atmosphere was changed to argon and the substrate **1** (C^0_1 0.05 M) was added. To our surprise, ethylene pre-treatment had the strongest negative effect on the most sterically crowded **nG-SIPr-I2**, which in our initial tests showed the highest efficiency in RCM of **1**. In contrast, **nG-I2** turned out to be the least sensitive to ethylene. Both dichloro complexes showed similar levels of stability. These results suggest that most stable ruthenium methylidenes were generated from **nG-I2**.

Next, the RCM of **1** was carried out under ethylene atmosphere which increases the probability of unproductive events (Figure 4). In this setup, the efficiency of catalysts decreased in the following order: **nG-I2** = **nG-SIPr-I2** > **nG-SIPr** > **nG**. Good conversion obtained with **nG-SIPr-I2** indicated high preference of this catalyst toward productive RCM over non-productive metathesis. This observation partially explains the high efficiency of this catalyst obtained in RCM of **1** under conventional conditions. On the other hand, fast initiation of **nG-SIPr-I2** under ethylene suggests that in the first catalytic turn-over, the small molecule of ethylene is coordinated to the ruthenium generating highly active methylidene species.

Macrocyclization reactions

As model substrates for macrocyclization we choose esters **17** and **18** which are metathesized to the 16- and 14- membered lactones. The RCM was run in toluene, at 70 °C and at 5 mM concentration; the catalysts were added in 10 portions with 7 minutes intervals. The 16-membered lactone **19** was synthesized with the catalyst loading of 0.3 mol % (Table 3, entries 1–4). The highest yield (91%) along with good selectivity (93%) was obtained with **nG-I2** while only a 54% yield and rather poor selectivity (70%) was observed for **nG.** Low selectivity of the reaction promoted by **nG** was the result of the formation of 13% of GC-observable byproducts (originated from double bond isomerization and ring contraction) as well as 10% of oligomeric/polymeric byproducts. The **nG-SIPr-I2** was more efficient than **nG-SIPr**, but the difference was not as striking in this pair (85% and 69% of yield, respectively). The same efficiency profile was observed in the synthesis of 14-membered **20**, which was carried out with the catalyst loading of 0.2 mol % (Table 3, entries 9–12). In this transformation each catalyst formed significant amounts of oligomeric/polymeric byproducts. Interestingly, we noticed a strong dependence of the catalyst efficiency on the argon flow over the reaction mixture which indicates the high importance of the ethylene removal in this type of RCM. The high stability of ruthenium

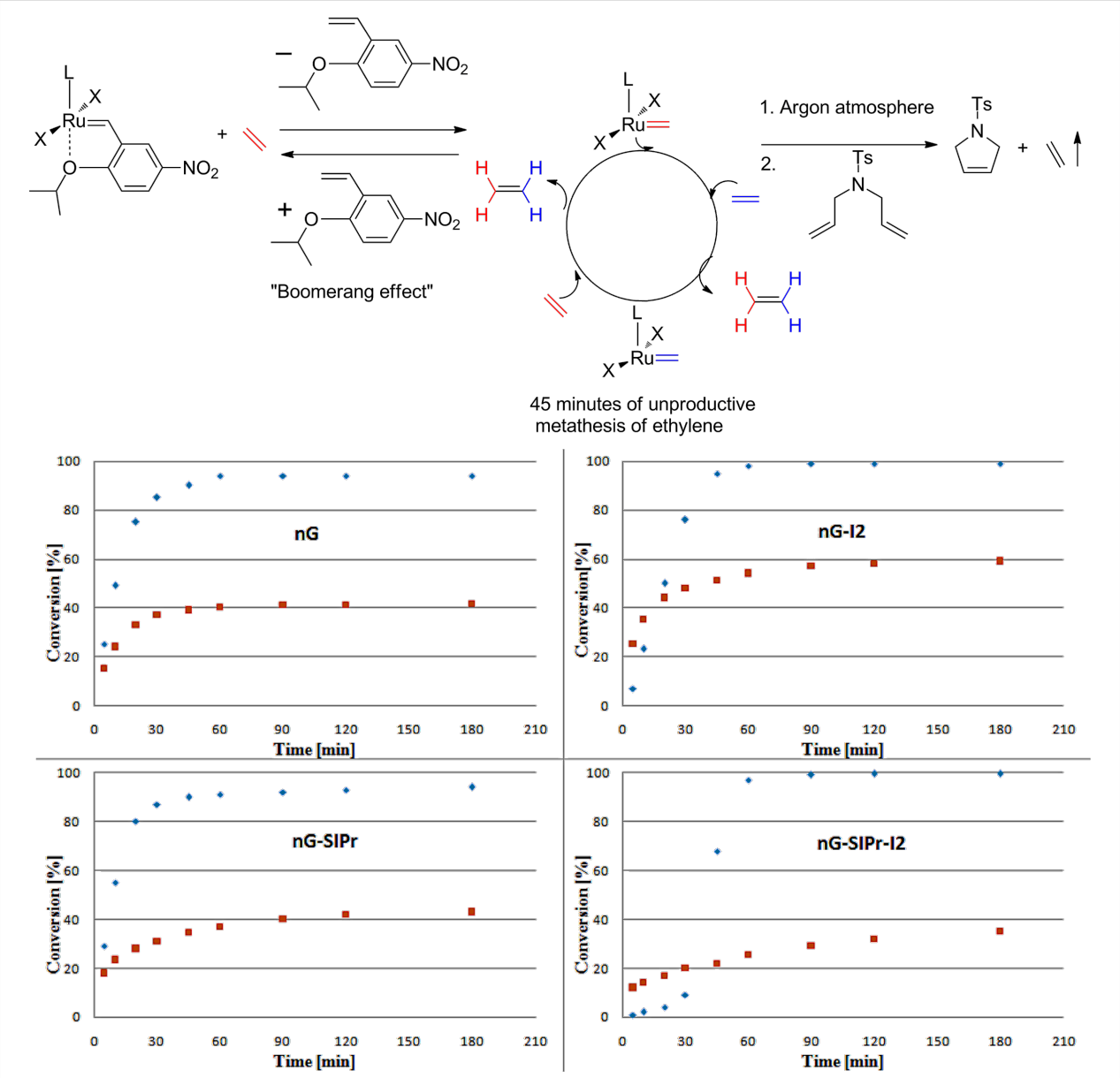

Figure 3: RCM of **1** (toluene, 0.05 M, 25 °C, [Ru] 0.01 mol %); blue diamonds – original (pre)catalysts; red squares – complexes pretreated with ethylene for 45 minutes.

methylidenes generated from **nG-I2** proved to be of great importance when macrocyclizations were run without active removal of ethylene (no flow of argon over the reaction mixture). In these conditions, which simulate the difficult removal of ethylene on large scale processes, **nG-I2** delivered expected products with fair yields (77% and 57% of **19** and **20**, respectively) while other catalysts demonstrated less than a 10% yield.

Metathesis in ACS-grade and "green" solvents

Our continuous interest in the development of more sustainable, environmentally and user-friendly olefin metathesis has recently inspired us to test a range of commercially available, classical ruthenium initiators in ACS grade solvents under air [31]. For this study we choose substrate **1**, which is highly prone to non-metathesis reactions, namely isomerization and cycloisomerization. The result we found is that esters constitute exeptionally good solvents for RCM and CM. Conversely, application of ACS grade alcohols, ethers and toluene in many cases dramatically reduced catalyst efficiency and selectivity. It was particularly noticeable in isopropanol, in which only Hoveyda–Grubbs type complexes bearing a SIPr ligand provided expected products with 80–88% yields (0.25 mol % of catalyst, 40 or 70 °C). The catalysts containing a less sterically crowded SIMEs ligand

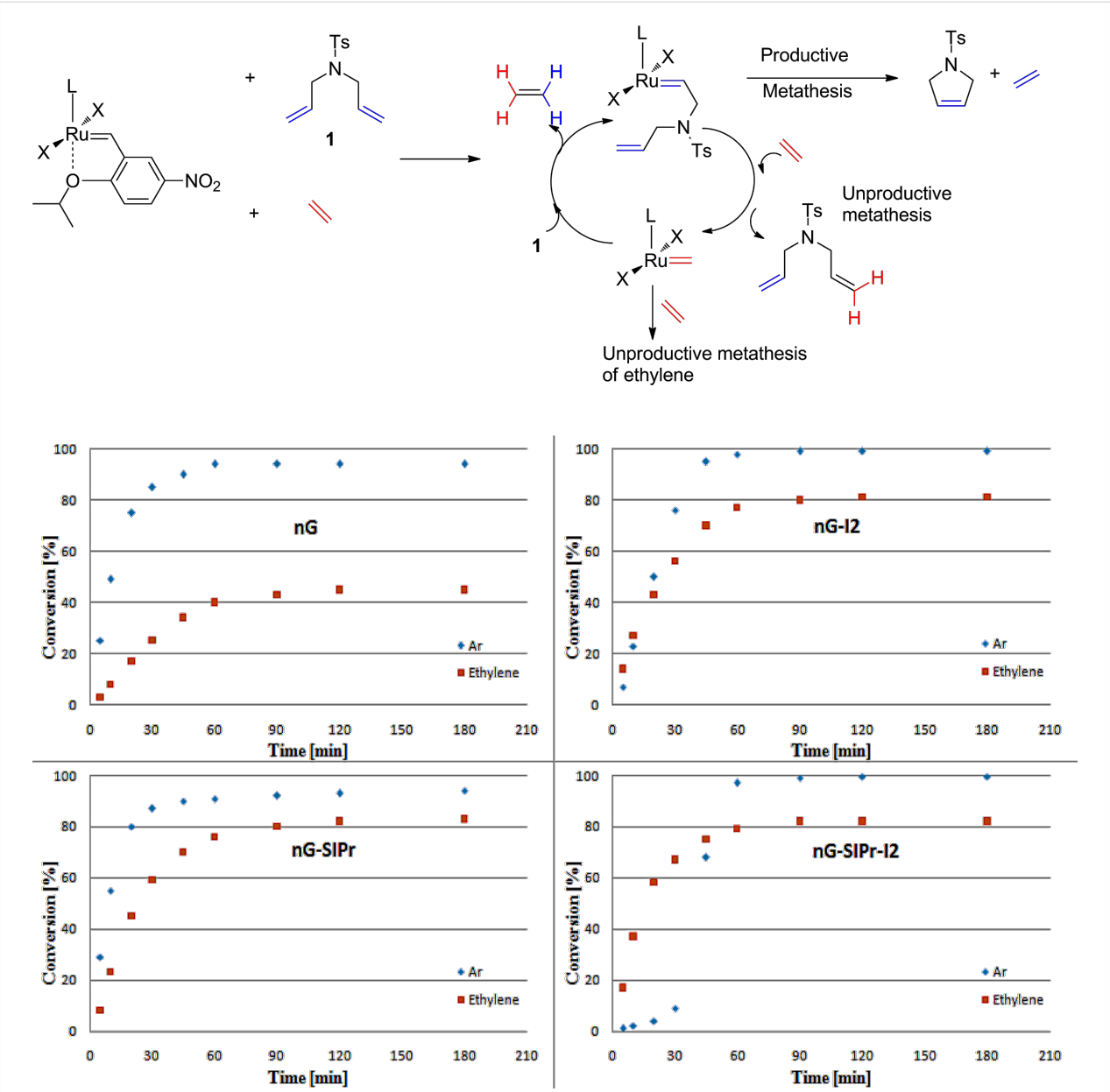

Figure 4: RCM of **1** (toluene, 0.05 M, 25 °C, [Ru] 0.01 mol %): top – productive RCM and possible non-productive events; bottom – reaction profiles of tested catalysts (blue diamonds – reaction under Ar, red squares – reaction under ethylene).

delivered **2** with poor yield, usually accompanied by significant amounts of byproducts **21** and **22**. This demonstrates that large substituents in *N*-heterocyclic ligands (NHC) not only increased efficiency of Hoveyda-type catalysts, but also to some extent prevented formation of ruthenium species active in non-metathetical transformations.

We decided to check whether additional steric restraints around the ruthenium center caused by iodides [32] can stabilize catalysts during OM in ACS grade solvents under air. RCM of **1** carried out in toluene was accomplished by **nG** with only 54% yield and 89% selectivity (Table 4). This reduced efficiency and selectivity observed in ACS grade toluene is most probably related to the small amounts of basic amines present in this solvent [33,34]. As anticipated, **nG-SIPR** performed better, giving 92% of product and 8% of isomers. We were pleased to see that **nG-I2** and **nG-SIPr-I2** provided over 99% of the expected product. As observed previously, **nG** exhibited very low activity in 2-MeTHF while **nG-SIPR** gave 90% of **2** which was, however, accompanied by 10% of isomers. The yield (96–97%) and the selectivity (98%) for both iodide analogues were noticeably better. The advantage of sterically crowded

Table 3: Results of the macrocyclization reactions.

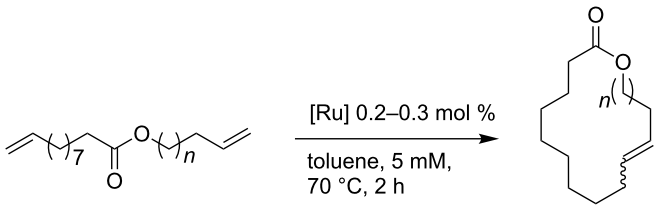

17: *n* = 3
18: *n* = 1

19: *n* = 3
20: *n* = 1

Entry	*n*	Conditions	Catalyst (mol %)	GC Conversion (selectivity) [%]	GC Yield [%] (*E*/*Z*)
1	3	active removal of ethylene	**nG** (0.3)	77 (70)	54 (2.9/1)
2			**nG-I2** (0.3)	98 (93)	91 (3.1/1)
3			**nG-SIPr** (0.3)	77 (90)	69 (2.5/1)
4			**nG-SIPr-I2** (0.3)	90 (94)	85 (2.3/1)
5	3	no active removal of ethylene	**nG** (0.3)	5 (80)	4
6			**nG-I2** (0.3)	87 (89)	77 (2.7/1)
7			**nG-SIPr** (0.3)	8 (88)	7
8			**nG-SIPr-I2** (0.3)	7 (100)	7
9	1	active removal of ethylene	**nG** (0.2)	72 (62)	45 (8/1)
10			**nG-I2** (0.2)	99 (82)	81 (8/1)
11			**nG-SIPr** (0.2)	97 (68)	66 (9/1)
12			**nG-SIPr-I2** (0.2)	98 (73)	72 (6/1)
13	1	no active removal of ethylene	**nG** (0.2)	8 (62)	5
14			**nG-I2** (0.2)	68 (84)	57 (5/1)
15			**nG-SIPr** (0.2)	5 (60)	3
16			**nG-SIPr-I2** (0.2)	6 (50)	3

Table 4: RCM of **1** in ACS-grade solvents under air.[a]

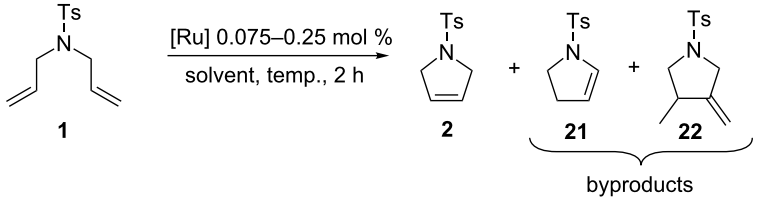

1

2

21

22

Catalyst	GC Yield (selectivity) [%]			
	toluene[b]	2-MeTHF[c]	iPrOH[d]	MeOH[e]
nG	54 (89)	28 (97)	21 (72)	14 (88)
nG-I2	>99	97 (98)	84 (99)	47 (98)
nG-SIPr	92 (92)	90 (90)	77 (82)	46 (87)
nG-SIPr-I2	99 (99)	96 (98)	94 (97)	94 (95)

[a]Reactions carried out in non-degassed, non-distilled ACS grade solvents under air; [b][Ru] 0.1 mol %, 70 °C; [c][Ru] 0.25 mol %, 40 °C; [d][Ru] 0.075 mol %, 70 °C; [e][Ru] 0.25 mol %, 40 °C.

catalysts was even more pronounced when reactions were carried out in alcohols. In iPrOH 0.075 mol % of **nG** gave only 21% of **2** with 72% selectivity; **nG-SIPr** was much more efficient (77% of yield), but the selectivity was limited (82%). In contrast **nG-I2** delivered 84% of the product with 99% selectivity, and **nG-SIPr-I2** yielded 94% of **2** with 97% selectivity.

Noteworthy is that **nG-SIPr-I2** was the only catalyst able to efficiently promote RCM of **1** in methanol.

To further differentiate the tested catalysts, we performed RCM of DEDAM, which required an even higher stability of the active species. In this transformation, **nG** failed to give substantial amounts of the product in any solvent (Table 5). Interestingly, **nG-SIPr** exhibited very low efficiency in 2-MeTHF, but in other solvents ensured better yields than **nG-I2**. Regardless, the solvent applied, **nG-SIPr-I2**, was the most efficient catalyst.

Table 5: RCM of DEDAM in ACS-grade solvents under air.[a]

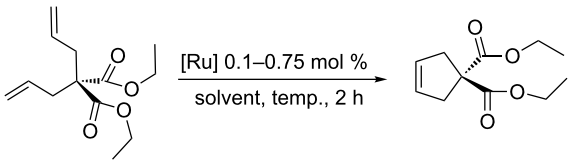

Catalyst	GC Yield [%]			
	toluene[b]	2-MeTHF[c]	iPrOH[d]	MeOH[e]
nG	33	31	15	9
nG-I2	77	98	76	31
nG-SIPr	96	25	87	43
nG-SIPr-I2	98	100	99	64

[a]Reactions carried out in non-degassed, non-distilled ACS grade solvents under air; [b][Ru] 0.1 mol %, 70 °C; [c][Ru] 0.25 mol %, 40 °C; [d][Ru] 0.25 mol %, 70 °C; [e][Ru] 0.75 mol %, 40 °C.

In our final experiment we performed self metathesis of *tert*-butyldimethylsilyl (TBS)-protected 5-hexen-1-ol without any additives that are known to prevent double bond isomerization [35]. As expected, SM turned out to be much more challenging than RCM reactions in terms of the catalyst efficiency and selectivity (Table 6). With 1 mol % of **nG** only a minor amount of **24** was observed in toluene and no catalytic activity was noted in 2-MeTHF. **nG-SIPr** performed better in these solvents, but iodide catalysts were twice as efficient and in addition, were noticeably more selective. In alcohols 2.5 mol % of **nG** or **nG-SIPr** delivered from 9 to 19% of **24** with dramatically low selectivity in the range of 25–47%. Application of **nG-I2** or **nG-SIPr-I2** resulted in the formation of 48–72% of the expected product with fair selectivity (83–91%).

Conclusion

The iodide-containing nitro-Grela analogues exhibit improved efficiency in RCM and CM of sterically non-demanding substrates. Additional steric hindrance in the metal center proximity caused by iodides makes the 14-electron species less sensitive to small impurities, coordinative solvents (e.g., 2-MeTHF) and protic solvents. These factors lead in some cases, to dramatic improvement in the reaction(s) yield and selectivity. Increased stability of the ruthenium methylidenes generated from **nG-I2** makes this catalyst especially suitable for macrocyclization of dienes with low effective molarity.

Supporting Information

Supporting Information File 1

Experimental and spectral data for **nG-I2**, **nG-SIPr-I2** and the test reactions.
[http://www.beilstein-journals.org/bjoc/content/supplementary/1860-5397-11-198-S1.pdf]

References

1. Grela, K. *Olefin Metathesis Theory and Practice;* Wiley: Hoboken, 2014.
2. Nelson, D. J.; Manzini, S.; Urbina-Blanco, C. A.; Nolan, S. P. *Chem. Commun.* **2014,** *50,* 10355–10375. doi:10.1039/C4CC02515F

Table 6: CM of TBS protected 5-hexen-1-ol in ACS-grade solvents under air.[a]

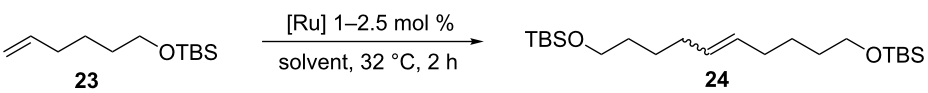

23 **24**

Catalyst	GC Yield (selectivity) [%]			
	toluene[b]	2-MeTHF[b]	iPrOH[c]	MeOH[c]
nG	13 (87)	0	19 (27)	19 (25)
nG-I2	70 (99)	67 (97)	72 (91)	48 (83)
nG-SIPr	38 (93)	33 (87)	15 (25)	9 (47)
nG-SIPr-I2	67 (97)	57 (95)	65 (86)	65 (86)

[a]Reactions carried out in non-degassed, non-distilled ACS grade solvents under air; [b][Ru] 1 mol %; [c][Ru] 2.5 mol %.

3. Grubbs, R. H.; Wenzel, A. G. *Handbook of Metathesis,* 2nd ed.; Wiley-VCH: Weinheim, 2015; Vol. 1. doi:10.1002/9783527674107
4. Garber, S. B.; Kingsbury, J. S.; Gray, B. L.; Hoveyda, A. H. *J. Am. Chem. Soc.* **2000,** *122,* 8168–8179. doi:10.1021/ja001179g
5. Rosebrugh, L. E.; Herbert, M. B.; Marx, V. M.; Keitz, B. K.; Grubbs, R. H. *J. Am. Chem. Soc.* **2013,** *135,* 1276–1279. doi:10.1021/ja311916m
6. Marx, V. M.; Sullivan, A. H.; Melaimi, M.; Virgil, S. C.; Keitz, B. K.; Weinberger, D. S.; Bertrand, G.; Grubbs, R. H. *Angew. Chem., Int. Ed.* **2015,** *54,* 1919–1923. doi:10.1002/anie.201410797
7. Skowerski, K.; Pastva, J.; Czarnocki, S. J.; Janoscova, J. *Org. Process Res. Dev.* **2015,** *19,* 872–877. doi:10.1021/acs.oprd.5b00132
8. Nelson, D. J.; Queval, P.; Rouen, M.; Magrez, M.; Toupet, L.; Caijo, F.; Borré, E.; Laurent, I.; Crévisy, C.; Baslé, O.; Mauduit, M.; Percy, J. M. *ACS Catal.* **2013,** *3,* 259–264. doi:10.1021/cs400013z
9. Urbina-Blanco, C. A.; Leitgeb, A.; Slugovc, C.; Bantreil, X.; Clavier, H.; Slawin, A. M. Z.; Nolan, S. P. *Chem. – Eur. J.* **2011,** *17,* 5045–5053. doi:10.1002/chem.201003082
10. Gatti, M.; Vieille-Petit, L.; Luan, X.; Mariz, R.; Drinkel, E.; Linden, A.; Dorta, R. *J. Am. Chem. Soc.* **2009,** *131,* 9498–9499. doi:10.1021/ja903554v
11. Manzini, S.; Urbina-Blanco, C. A.; Slawin, A. M. Z.; Nolan, S. P. *Organometallics* **2012,** *31,* 6514–6517. doi:10.1021/om300719t
12. Sanford, M. S.; Love, J. A.; Grubbs, R. H. *J. Am. Chem. Soc.* **2001,** *123,* 6543–6554. doi:10.1021/ja010624k
13. Wappel, J.; Urbina-Blanco, C. A.; Abbas, M.; Albering, J. H.; Saf, R.; Nolan, S. P.; Slugovc, C. *Beilstein J. Org. Chem.* **2010,** *6,* 1091–1098. doi:10.3762/bjoc.6.125
14. Abbas, M.; Wappel, J.; Slugovc, C. *Macromol. Symp.* **2012,** *311,* 122–125. doi:10.1002/masy.201000095
15. Abbas, M.; Slugovc, C. *Tetrahedron Lett.* **2011,** *52,* 2560–2562. doi:10.1016/j.tetlet.2011.03.038
16. Schrodi, Y.; Ung, T.; Vargas, A.; Mkrtumyan, G.; Lee, C. W.; Champagne, T. M.; Pederson, R. L.; Hong, S. H. *Clean: Soil, Air, Water* **2008,** *36,* 669–673. doi:10.1002/clen.200800088
17. Gillingham, D. G.; Kataoka, O.; Garber, S. B.; Hoveyda, A. H. *J. Am. Chem. Soc.* **2004,** *126,* 12288–12290. doi:10.1021/ja0458672
18. Koh, M. J.; Khan, R. K. M.; Torker, S.; Hoveyda, A. H. *Angew. Chem., Int. Ed.* **2014,** *53,* 1968–1972. doi:10.1002/anie.201309430
19. Endo, K.; Grubbs, R. H. *J. Am. Chem. Soc.* **2011,** *133,* 8525–8527. doi:10.1021/ja202818v
20. Teo, P.; Grubbs, R. H. *Organometallics* **2010,** *29,* 6045–6050. doi:10.1021/om1007924
21. Occhipinti, G.; Hansen, F. R.; Törnroos, K. W.; Jensen, V. R. *J. Am. Chem. Soc.* **2013,** *135,* 3331–3334. doi:10.1021/ja311505v
22. Guidone, S.; Songis, O.; Falivene, L.; Nahra, F.; Slawin, A. M. Z.; Jacobsen, H.; Cavallo, L.; Cazin, C. S. J. *ACS Catal.* **2015,** *5,* 3932–3939. doi:10.1021/acscatal.5b00219
23. Marciniec, B.; Rogalski, S.; Potrzebowski, M. J.; Pietraszuk, C. *ChemCatChem* **2011,** *3,* 904–910. doi:10.1002/cctc.201000376
24. Bek, D.; Gawin, R.; Grela, K.; Balcar, H. *Catal. Commun.* **2012,** *21,* 42–45. doi:10.1016/j.catcom.2012.01.020
25. Thiel, V.; Wannowius, K.-J.; Wolff, C.; Thiele, C. M.; Plenio, H. *Chem. – Eur. J.* **2013,** *19,* 16403–16414. doi:10.1002/chem.201204150
26. Bates, J. M.; Lummiss, J. A. M.; Bailey, G. A.; Fogg, D. E. *ACS Catal.* **2014,** *4,* 2387–2394. doi:10.1021/cs500539m
27. Hamasaki, R.; Funakoshi, S.; Misaki, T.; Tanabe, Y. *Tetrahedron* **2000,** *56,* 7423–7425. doi:10.1016/S0040-4020(00)00654-2
28. Fürstner, A.; Thiel, O. R.; Ackermann, L. *Org. Lett.* **2001,** *3,* 449–451. doi:10.1021/ol0069554
29. Lysenko, Z.; Maughon, B. R.; Mokhtar-Zadeh, T.; Tulchinsky, M. L. *J. Organomet. Chem.* **2006,** *691,* 5197–5203. doi:10.1016/j.jorganchem.2006.08.031
30. Skowerski, K.; Pastva, J.; Czarnocki, S. J.; Janoscocva, J. *Org. Process Res. Dev.* **2015,** *19,* 872–877. doi:10.1021/acs.oprd.5b00132
31. Skowerski, K.; Białecki, J.; Tracz, A.; Olszewski, T. K. *Green Chem.* **2014,** *16,* 1125–1130. doi:10.1039/C3GC41943F
32. The ionic radii of chloride and iodide are 167 pm and 206 pm, respectively; the covalent radii of chlorine and iodine are 99 pm and 133 pm, respectively.
33. Nicola, T.; Brenner, M.; Donsbach, K.; Kreye, P. *Org. Process Res. Dev.* **2005,** *9,* 513–515. doi:10.1021/op0580015
34. Ireland, B. J.; Dobigny, B. T.; Fogg, D. E. *ACS Catal.* **2015,** *5,* 4690–4698. doi:10.1021/acscatal.5b00813
35. Hong, S. H.; Sanders, D. P.; Lee, C. W.; Grubbs, R. H. *J. Am. Chem. Soc.* **2005,** *127,* 17160–17161. doi:10.1021/ja052939w

License and Terms

BEILSTEIN JOURNAL OF ORGANIC CHEMISTRY

Recent applications of ring-rearrangement metathesis in organic synthesis

Sambasivarao Kotha*[1], Milind Meshram[1], Priti Khedkar[2], Shaibal Banerjee[3] and Deepak Deodhar[1]

Review

Open Access

Address:
[1]Department of Chemistry, Indian Institute of Technology Bombay, Powai, Mumbai-400 076, India. Fax: (+91)-22-2572-3480 2576 7152; Phone: (+91)-22-2576-7160, [2]Department of Chemistry, Guru Nanak Khalsa College of Arts, Science & Commerce, Matunga, Mumbai–400 019, India and [3]Department of Applied Chemistry, Defence Institute of Advanced Technology (DU), Girinagar, Pune–411025, Pune, India

Email:
Sambasivarao Kotha* - srk@chem.iitb.ac.in

* Corresponding author

Keywords:
Diels–Alder chemistry; green chemistry; natural products; olefin metathesis; polycycles; ring-rearrangement metathesis

Beilstein J. Org. Chem. **2015,** *11,* 1833–1864.
doi:10.3762/bjoc.11.199

Received: 13 June 2015
Accepted: 17 September 2015
Published: 07 October 2015

This article is part of the Thematic Series "Progress in metathesis chemistry II".

Guest Editor: K. Grela

Abstract

Ring-rearrangement metathesis (RRM) involves multiple metathesis processes such as ring-opening metathesis (ROM)/ring-closing metathesis (RCM) in a one-pot operation to generate complex targets. RRM delivers complex frameworks that are difficult to assemble by conventional methods. The noteworthy point about this type of protocol is multi-bond formation and it is an atom economic process. In this review, we have covered literature that appeared during the last seven years (2008–2014).

Introduction

Transition metal–carbene complexes (Figure 1) introduced during the last two decades have changed the landscape of organic synthesis. Armed with these advances, olefin metathesis has become a staple in retrosynthesis. Metathesis protocols such as ring-closing metathesis (RCM), cross-metathesis (CM), and enyne metathesis (EM) have gained popularity in the synthesis of complex molecules. Ring-rearrangement metathesis (RRM) involves a tandem process, where the ring-opening metathesis (ROM) and the RCM sequence occur in tandem to generate complex end products (Figure 2). Several demanding structures related to natural products and non-natural products were synthesized by RRM. However, a limited number of papers appeared dealing with RRM due to the complexity involved in designing the required precursors suitable for RRM. There are several factors which facilitates the RRM. Among them, the release of ring strain is the main driving force. For example, with bicyclo[2.2.1]heptene systems, RRM produce less strained end products. A general mechanism for the RRM process is shown in Figure 3 [1,2]. During RRM the stereochemical information is transformed from the substrate to the product. Interestingly, RRM is applicable to mono- and polycyclic systems of varying ring sizes. The outcome of the RRM process depends

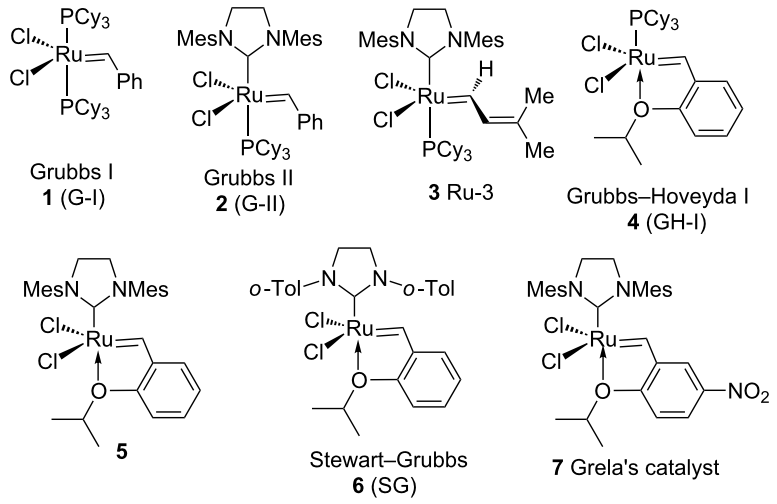

Figure 1: Ruthenium alkylidene catalysts used in RRM processes.

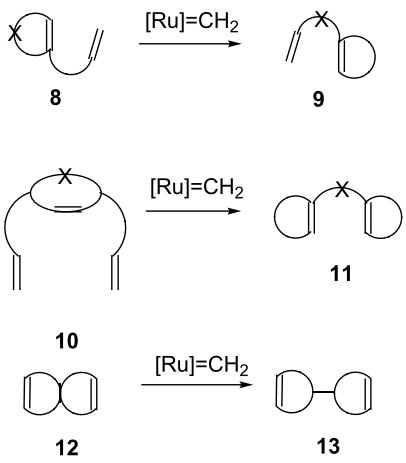

Figure 2: General representation of various RRM processes.

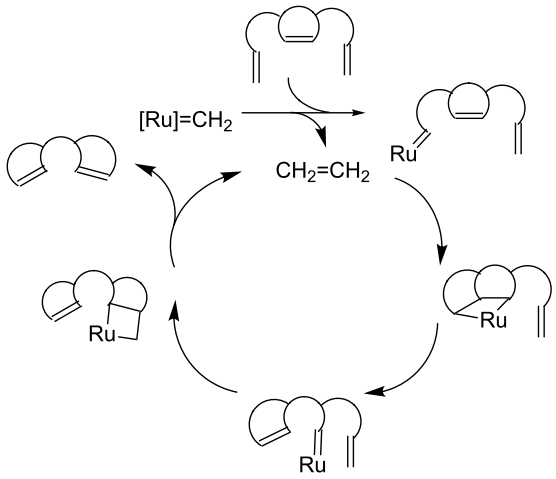

Figure 3: A general mechanism for RRM process.

on the selection of the protecting groups, reaction conditions, and electronic properties of substrates involved. Oligomerization is a common side reaction in the RRM and external olefins such as ethylene prevents unwanted oligomerization processes. For earlier work related to the RRM readers may refer to excellent reviews available in the literature [3-6].

Review

Cyclopropene systems

Cyclopropene derivatives are highly strained systems and they are ideal candidates for the RRM process. In this context, Zhu and Shi [7] have reported the ring-closing enyne metathesis (RCEM) of small-rings such as cyclopropenes by employing the Grubbs' first-generation (G-I) catalyst. They have reported a new tandem ROM–RCM–CM sequence starting with 1,6-cyclopropenynes **16** with a wide variety of substituted olefins. To this end, the required building block **16** has been prepared with the aid of a carbene insertion reaction. Further, this cyclopropene system **16** was subjected to RRM in the presence of catalyst **1** to generate 3-pyrroline derivatives **18a,b** using simple starting materials in a single step (Scheme 1).

A wide range of heterocycles have been assembled by RRM. When a substituted cyclopropene such as **19** (or **20**) was treated with catalyst **2** in the presence of ethylene (**24**) the required heterocycle **22** (or **23**) was obtained in moderate to good yield (Scheme 2) [8]. Allyl ethers **25a**,**b** and **26a**,**b** were reacted with catalyst **2** to deliver the corresponding dihydrofurans (**27a**,**b** and **28a**,**b**) in excellent yields (82–92%). Involvement of acrylates **29a**,**b** delivered lactones **30a**,**b** in moderate yields (**30a** 41%,

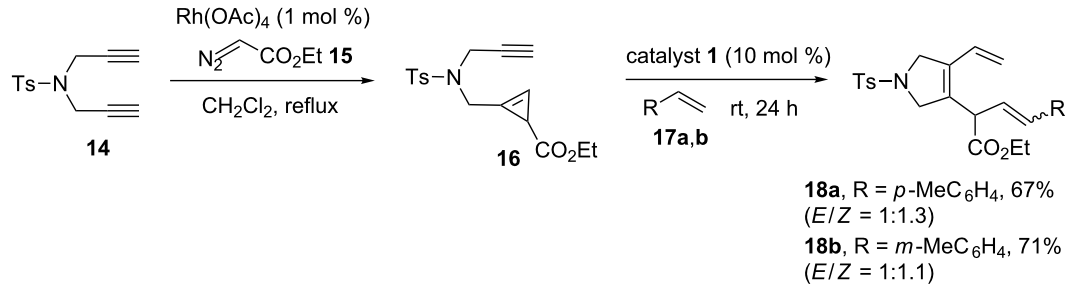

Scheme 1: RRM of cyclopropene systems.

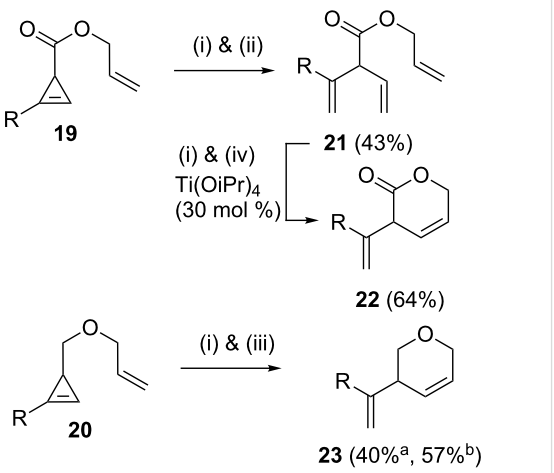

Scheme 2: RRM of cyclopropene with catalyst **2**. (i) catalyst **2** (2.5 mol %), ethylene (**24**, 1 atm), (ii) toluene (*c* = 0.02 M), reflux, (iii) CH_2Cl_2 (*c* = 0.02 M), reflux, (iv) C_6H_6 (*c* = 0.01 M), reflux. (a) without ethylene (**24**); (b) with ethylene (**24**).

30b 50%) upon treatment with catalyst **2** in dichloromethane at reflux conditions. However, **29a** generated lactone **30a** in 65% yield when the metathesis was performed using Grela's catalyst **7**. Pyrrolines were produced in excellent yields by RRM of sulfonamides **31a**,**b** using the catalyst **2** under dichloromethane reflux conditions (**32a** 99%, **32b** 70%) (Scheme 3). Five-membered heterocycles such as **34** and a seven membered heterocycle **35** in 40:60 ratio (97%) were formed by RRM of cyclopropenylcarbinyl ether **33** with catalyst **2** (Scheme 4).

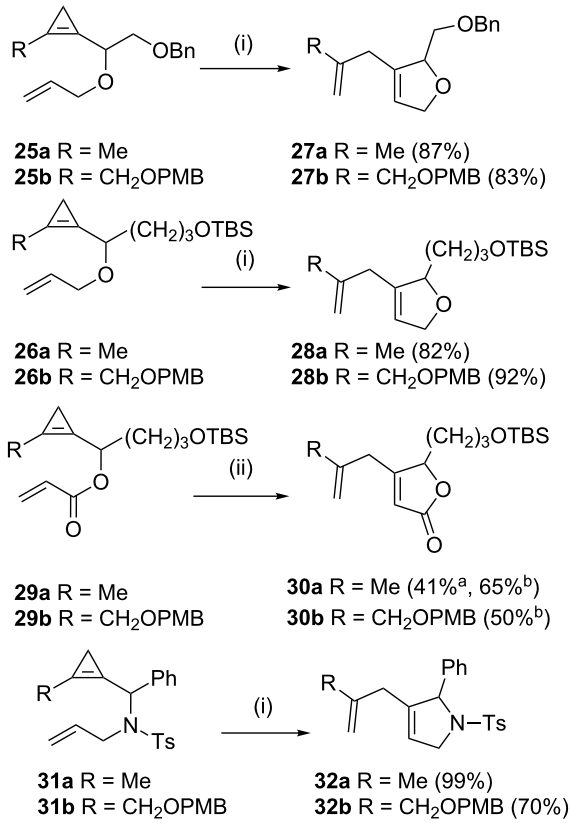

Scheme 3: RRM of various cyclopropene derivatives with catalyst **2**. (i) catalyst **2** (2.5 mol %), CH_2Cl_2 (*c* = 0.1 M), reflux, (ii) (a) catalyst **2** (2.5 mol %), toluene (*c* = 0.1 M), reflux, (b) catalyst **7**, toluene (*c* = 0.1 M), reflux.

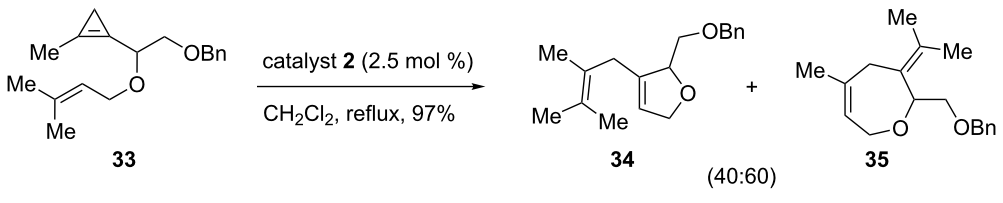

Scheme 4: RRM of substituted cyclopropene system with catalyst **2**.

Cyclobutene systems

Cyclobutene is also highly strained and prone to RRM very easily. Maougal and co-workers synthesized 3,3'-bipiperidine and 3,3'-bis(1,2,3,6-tetrahydropyridine) systems through a RRM sequence [9]. In this context, they have identified compound **38** as the key starting synthone, easily prepared from **36** via an *N*-allylation sequence. Next, diallyl compound **38** was treated with catalyst **2** to deliver the expected bipiperidine derivative **39** in 60% yield. Further, this protocol has been extended to various oxygenated systems (Scheme 5).

Snapper and White [10] have reported a new and efficient method to various medium size bicyclic systems. Here, the RRM strategy has been employed with catalyst **2** starting with various cyclobutene systems containing an alkene tether (e.g., **40**, **42**, and **44**) to generate bicyclic systems such as **41**, **43**, and **45** (Scheme 6).

The erythrina alkaloids are known to exhibit sedative, hypotensive and neuromuscular activity. This alkaloid skeleton consists of a tetracyclic spiroamine framework and synthetic chemists consider it as a challenging target. Simpkins and co-workers [11] have used the RRM sequence tactically to assemble the erythrina skeleton. To this end, they have identified cyclobutene derivative **48** as a useful synthone for RRM. The cyclobutene derivative **46** has been extended via Grignard addition followed by cyclization reaction. Later, cyclobutene derivative **48** was treated with catalyst **1** in the presence of ethylene (**24**) under high dilution conditions to deliver the tetracyclic compound **49** in 62% yield (Scheme 7).

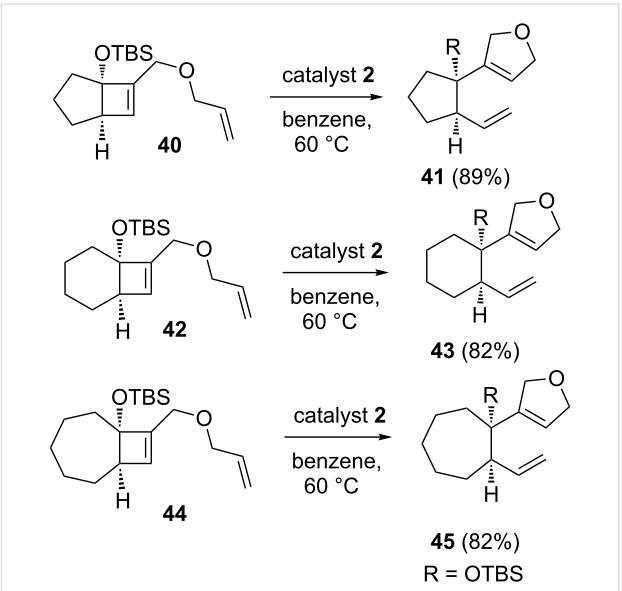

Scheme 6: RRM approach to various bicyclic compounds.

To assemble 5-F_2-isoprostanes, lipid oxidation metabolites, various functionalized cyclobutene derivatives were subjected to a RRM sequence [12]. Cyclobutene derivative **50** in the presence of the catalyst **1** delivered lactone **51** as a mixture of isomers (3:1) in 37% yield. When the substrate was modified as in **52**, the RCM product was not formed; however, compound **52** gave the ring-opened product with ethylene (**24**) in low yield. Further, the ROM homodimer was obtained in 17% yield in the presence of ethylene (**24**) with the aid of catalyst **4** (Scheme 8).

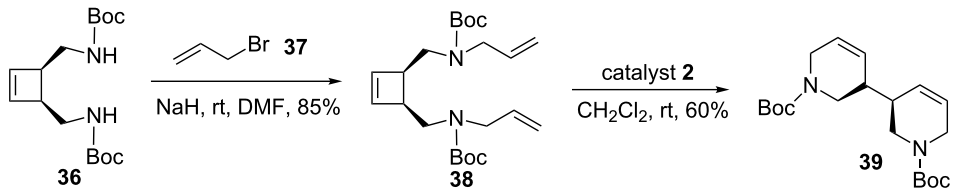

Scheme 5: RRM of cyclobutene system with catalyst **2**.

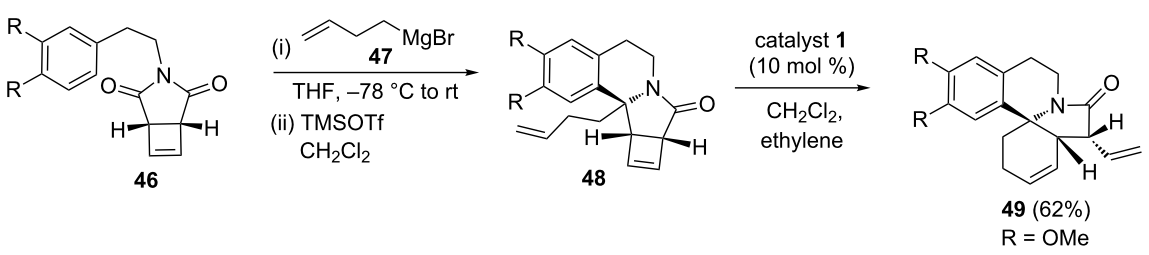

Scheme 7: RRM approach to erythrina alkaloid framework.

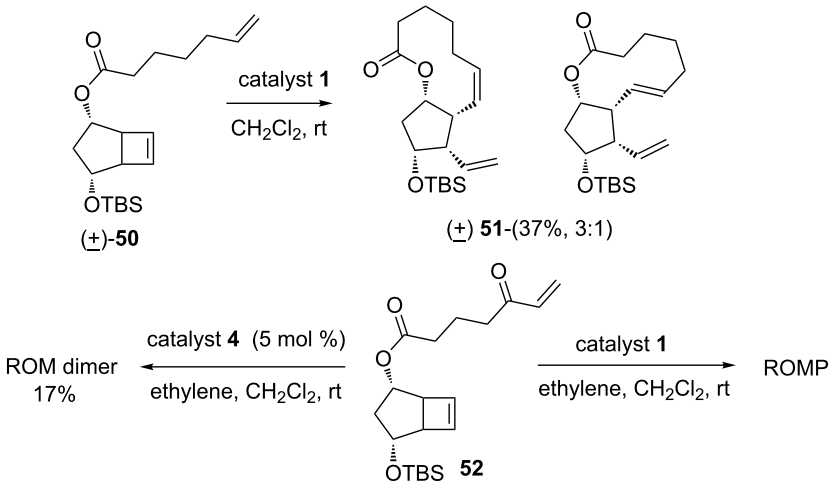

Scheme 8: ROM–RCM sequence to lactone derivatives.

Pattenden and co-workers [13] have described a novel synthesis of (+)-*Z*-deoxypukalide using substituted butenolide intermediate **58**. Interestingly, it was synthesized starting with cyclobutene ester **55** involving ROM–RCM and CM protocols. In this regard, the cyclobutene ester was subjected to a ROM–RCM and CM protocol under conditions with catalyst **2** in the presence of 2-methylpropenol **57** to afford the required butenolide intermediate **58** in 57% yield (Scheme 9).

An asymmetric synthesis of humulanolides is achieved by a RRM approach. In this context, Li and co-workers [14] prepared the key precursor **60** in five steps from commercially available starting material **59**. Later, the cyclobutene derivative **60** was treated with catalyst **5** under toluene reflux conditions to give the expected RRM cascade product, i.e., asteriscunolide D (**61**) in 36% yield along with the dimer **62** (7%). Interestingly, they also found asteriscunolide D as a useful synthone for the synthesis of asteriscunolides A−C (Scheme 10).

In several instances RRM has proved to be a useful strategy for the construction of 12- to 16-membered macrolides [15]. In this regard, ester **65** was prepared from the corresponding allylic alcohol **63** by esterification with the anhydride **64** derived from cyclobutene. Later, the ester **65**, on treatment with the catalyst **1** under toluene reflux conditions followed by treatment with the catalyst **2** furnished the macrolide-butenolides **66** in 42–48% yields via RRM with *E*-selectivity at the macrocyclic double bond. Along similar lines, compound **65f** was treated with cata-

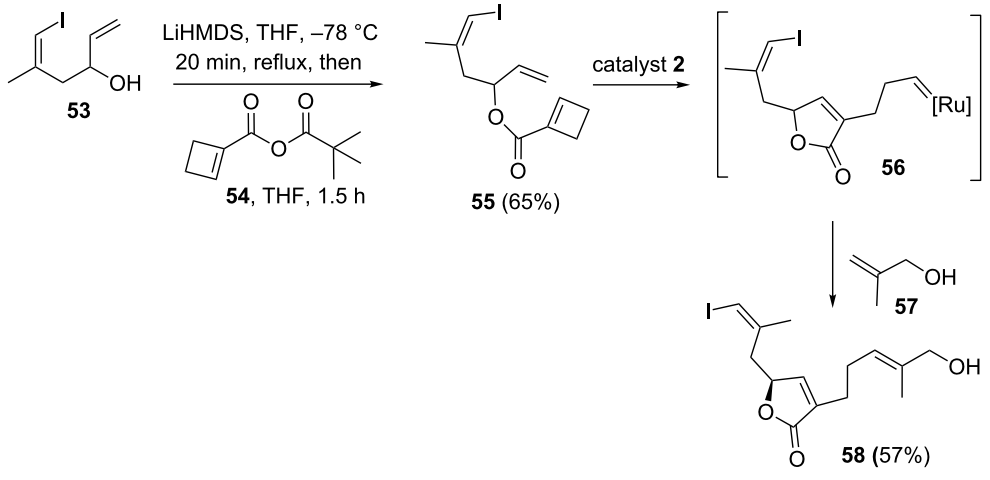

Scheme 9: RRM protocol towards the synthesis of lactone derivative **58**.

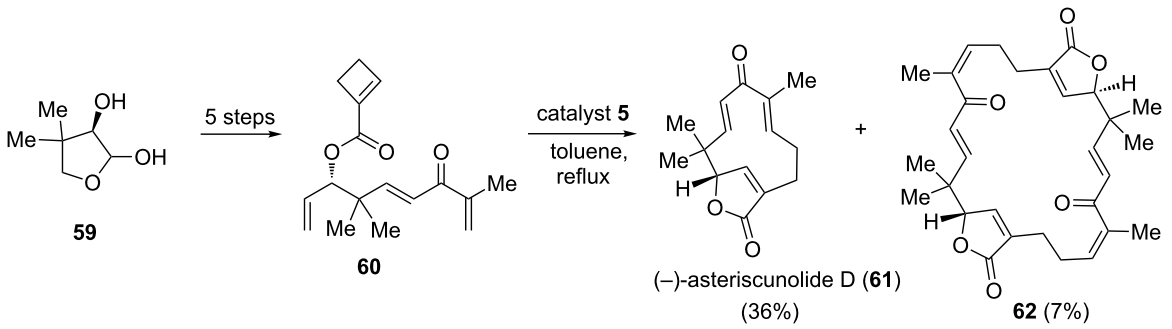

Scheme 10: RRM protocol towards the asymmetric synthesis of asteriscunolide D (**61**).

lyst **1** in refluxing toluene followed by treatment with catalyst **2** to deliver desmethylmanshurolide **67** in 44% yield (Scheme 11).

Cyclopentene systems

In RRM with cyclopentene systems, the release of ring strain is a less important contributor to the driving force of the reaction.

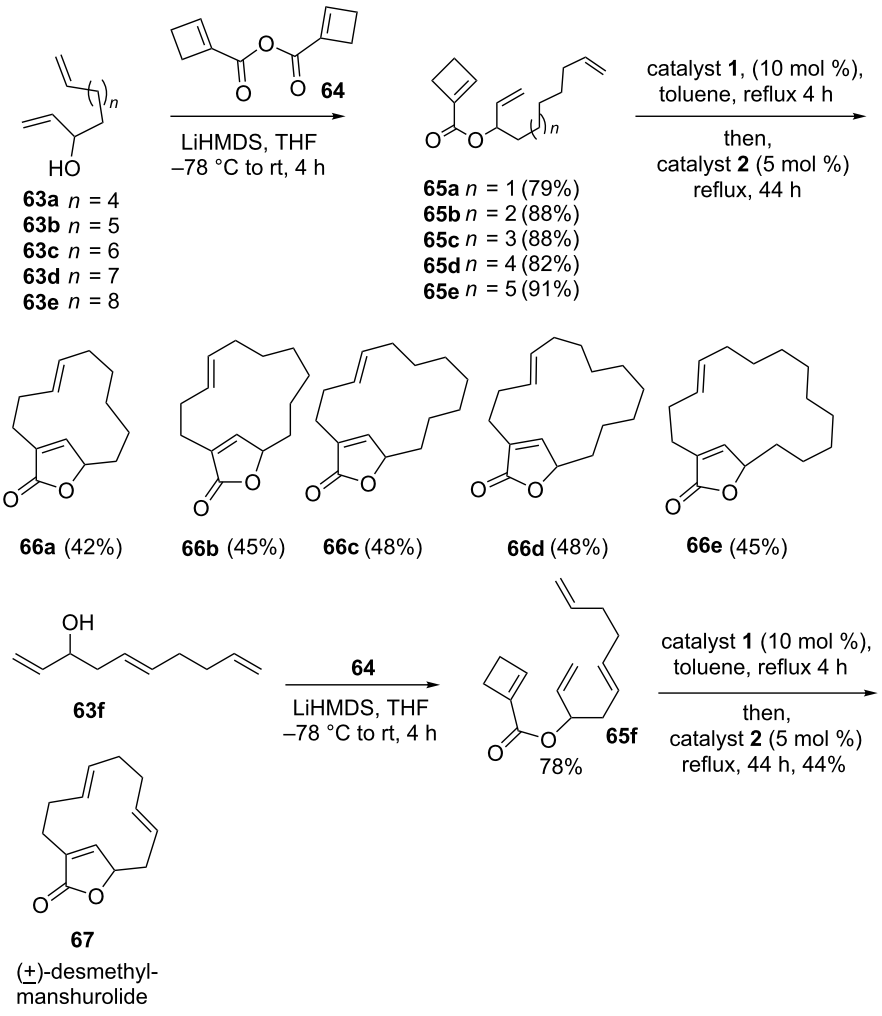

Scheme 11: RRM strategy towards the synthesis of various macrolide rings.

However, unfavorable interaction of vicinal or proximal substituents may be minimized in the rearranged product. In this context, Blechert and co-workers [16] demonstrated the first enantioselective total syntheses of virgidivarine and virgiboidine by employing an intramolecular ene–ene–yne domino RRM protocol in combination with an oxidative C–C bond cleavage. This protocol opens-up new opportunities for the construction of intricate dipiperidine-based targets in a stereoselective manner (Scheme 12).

Lee and Li [17] disclosed a highly distereoselective RRM approach starting with cyclopentene derivatives. In this regard, the cyclopentene derivative **72** was treated with the catalyst **2** in the presence of ethylene (**24**) to generate the required cyclohexene-based product **73**. The total synthesis of spiropiperidine alkaloid nitramine was proved to be efficient by this methodology (Scheme 13).

In 2004, Ni and Ma [18] have described the synthesis of bicyclic compounds **75** and **76** by adopting a metathesis protocol with catalysts **1** and **2** in good yields, but the product ratio is catalyst-dependent. In this context, when the cyclopentene derivative **74** gave **75** and **76** (1:5, 75%) with catalyst **1**; whereas, the catalyst **2** produced **75** and **76** in 85% yield (12:1). Here, they have shown the thermodynamically favored RRM leads to the formation of **75**, while kinetically favored RCM gave the product **76** (Scheme 14).

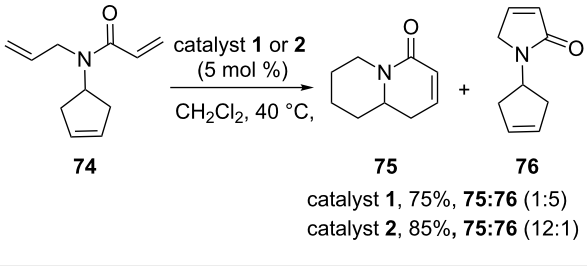

Scheme 14: RRM of cyclopentene system **74**.

Cyclohexene systems

Banti and co-workers have reported a tandem metathesis sequence with the aid of catalysts **1** and **2** starting with cyclohexene and norbornene systems containing allylamino moieties [19]. When the reaction was carried out in the presence of catalyst **2**; RRM product **79** was observed in 29% yield along with the RCM product **78** in 71% (Scheme 15).

Burnell and co-workers [20] have demonstrated the RRM of unsaturated spirocycles with two alkenyl chains by employing catalyst **2** to generate a unsaturated spiro-fused tricyclic system. In this context, the compounds **80** and **81** were subjected to RRM with catalyst **2** to furnish exclusively fused tricyclic systems **83a** and **83b** in 85% and 61% yields, respectively. Substitution on the cyclohexene system as in compound **82** did not deliver the RRM product (Scheme 16).

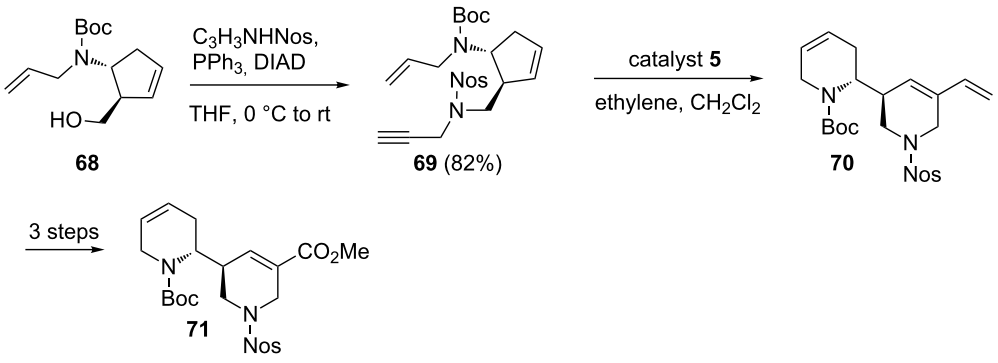

Scheme 12: RRM protocol to dipiperidine system.

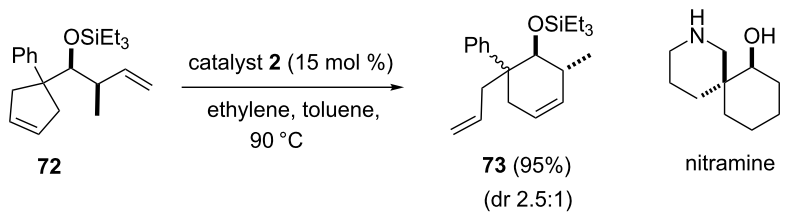

Scheme 13: RRM of cyclopentene system to generate the cyclohexene systems.

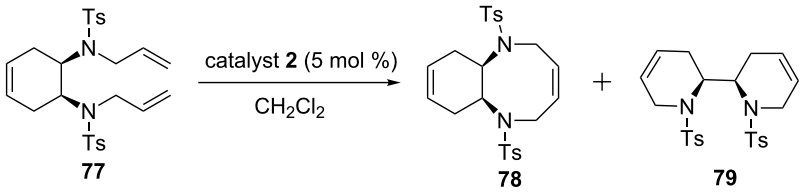

entry	catalyst (5 mol %)	yields (%) 78	79	77
1.	catalyst **1**, N_2	100	0	0
2.	catalyst **1**, **24**	83	0	17
3.	catalyst **2**, N_2	71	29	0
4.	catalyst **2**, **24**	21	9	70

Scheme 15: RRM approach to compound **79**.

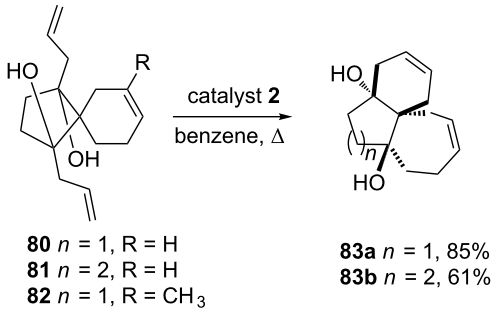

80 *n* = 1, R = H
81 *n* = 2, R = H
82 *n* = 1, R = CH_3

83a *n* = 1, 85%
83b *n* = 2, 61%

Scheme 16: RRM approach to spirocycles.

Pyran systems

Donnard and co-workers [21] have accomplished a RRM approach for assembling complex heterocycles by employing simple starting materials. They have studied the RRM of dihydropyrans and dihydrofurans and this approach was found to be useful for the synthesis of non-classical saccharides. The synthesis of unusual di- or trisaccharides and related systems are also accessible by this approach. The required building block **85** has been prepared from compound **84** by allylation with allyl bromide (**37**). Later, the pyran derivative **85** was treated with catalyst **2** to generate the bicyclic system **86** (73%) (Scheme 17).

They also demonstrated a RCM–ROM–RCM cascade using a strain-free allyl heterocycle as useful starting material [22]. The required building blocks such as **90a–c** were prepared from compound **87**. Later, treatment of **90b** with catalyst **2** gave the expected RRM product **91b** (83%), whereas compound **90a** gave the rearranged product **91a** in 8% yield. On the other hand, when compound **90c** was reacted with catalyst **2** the rearranged product was not formed. Here, they have demonstrated that the success of the reaction depends on electronic and stereochemical factors. Moreover, the synthesis of unusual polydeoxydisaccharides could be achieved starting with these simple starting materials. Similarly, **93** has been obtained by the RRM of compound **92** (Scheme 18).

Eustache and co-workers [23] have reported a novel ROM–RCM–ROM–RCM cascade involving a simple heterocycle as a useful precursor for the RRM protocol. To this end, the required precursor **96** was synthesized from **94** in two steps. Next, **96** was treated with catalyst **2** to generate the expected RRM product **97** in 68% yield. Further, this approach is useful

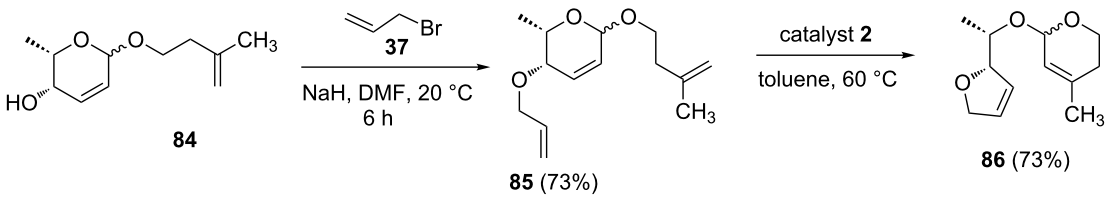

Scheme 17: RRM approach to bicyclic dihydropyrans.

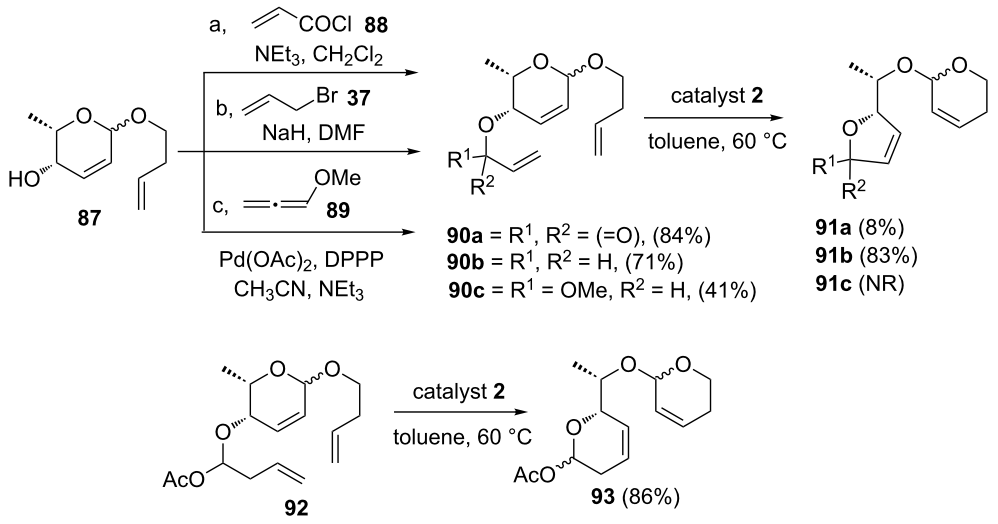

Scheme 18: RCM–ROM–RCM cascade using non strained alkenyl heterocycles.

for the preparation of polyunsaturated trisaccharides (Scheme 19).

Mori and co-workers [24] have used the RRM protocol starting with enyne **98** using catalyst **2** in the presence of ethylene (**24**) to generate the dimerized 16-membered ring product **101** in 57% yield, which was generated by a RRM–dimerization sequence and its monomer **100** in 14% yield along with **99** in 26% yield (Scheme 20).

Bicyclo[2.2.1]heptene derivatives

Holtsclaw and Koreeda [25] have explored a chemoselective RRM of the enone containing norbornene system such as **102**. To this end, the spironorbornene **102** was subjected to a RRM sequence under the influence of catalyst **1** to deliver the RRM product **103** and the RCM product **104** in a 99:1 ratio. When norbornene derivative **102** was treated with catalyst **2** tricyclic compound **103** and spironorbornene derivative **104** were obtained in a 22:78 ratio (Scheme 21).

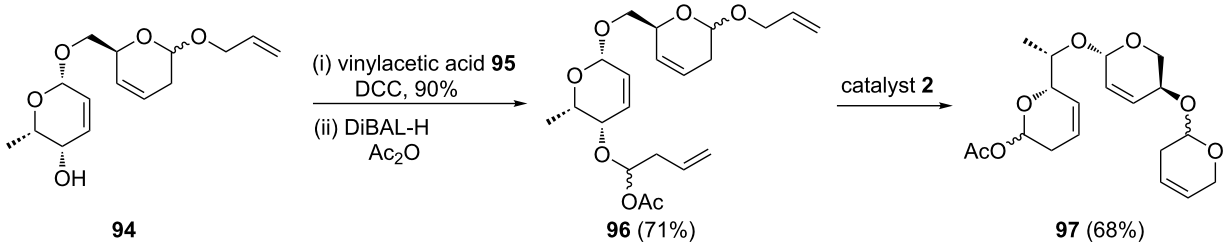

Scheme 19: First ROM–RCM–ROM–RCM cascade for the synthesis of trisaccharide **97**.

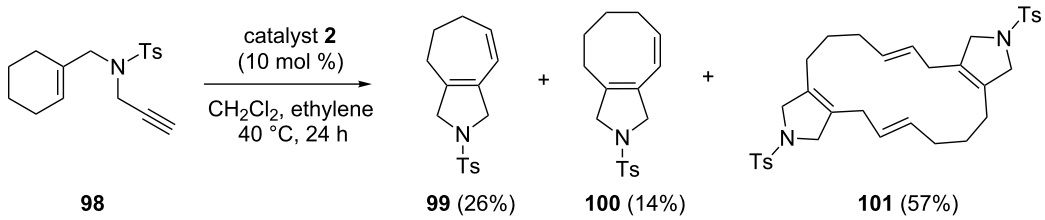

Scheme 20: RRM of cyclohexene system.

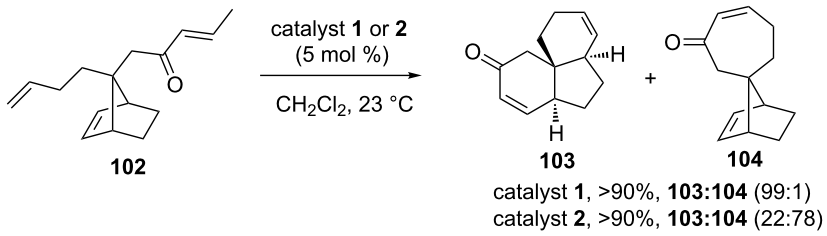

Scheme 21: RRM approach to tricyclic spirosystem.

Aubé and co-workers [26] have accomplished the asymmetric synthesis of the dendrobatid alkaloid 251F by employing a RRM as the key step. The required building block **108a** has been synthesized from enone **107** via a RRM protocol. When enone **107** was exposed to catalyst **1** in the presence of ethylene (**24**) the RRM product **108a** was obtained in 93% yield. Further, this bicyclic building block **108a** has been successfully utilized in the synthesis of the dendrobatid alkaloid 251F (Scheme 22).

Phillips and Henderson [27] have demonstrated the synthesis of aburatubolactam A (**113**) by using a tandem ROM–RCM sequence as the key step. To this end, the required key building block, the bicyclo[3.3.0]octene ring system **108b** has been synthesized by a RRM sequence via catalyst **1** starting with the functionalized bicyclo[2.2.1]heptene system **107**. Thus, the Diels–Alder (DA) reaction of ketone **109** with cyclopentadiene (**111**) in the presence of MacMillans catalyst **110** gave bicyclic ketone **112** in 65% yield. Then, ketone **112** was transformed into enone **107** in 80% yield by adopting the known oxidation protocol. Later, enone **107** was treated with catalyst **1** under ethylene (**24**) atmosphere to deliver the required bicyclo[3.3.0]octane derivative **108b** in 90% yield (Scheme 23).

Shibatomi and co-workers have reported an enantioselective DA reaction of β-fluoromethylacrylate under the influence of the chiral Lewis acid-activated catalyst, oxazaborolidine to

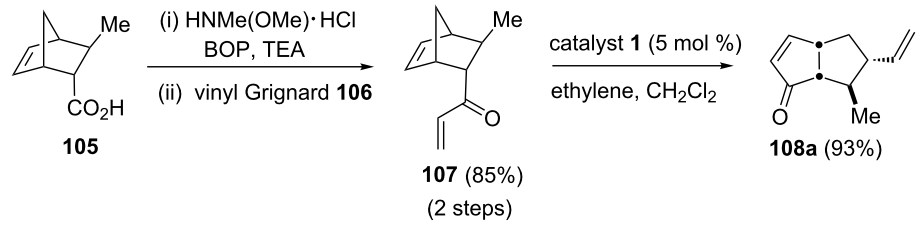

Scheme 22: RRM approach to bicyclic building block **108a**.

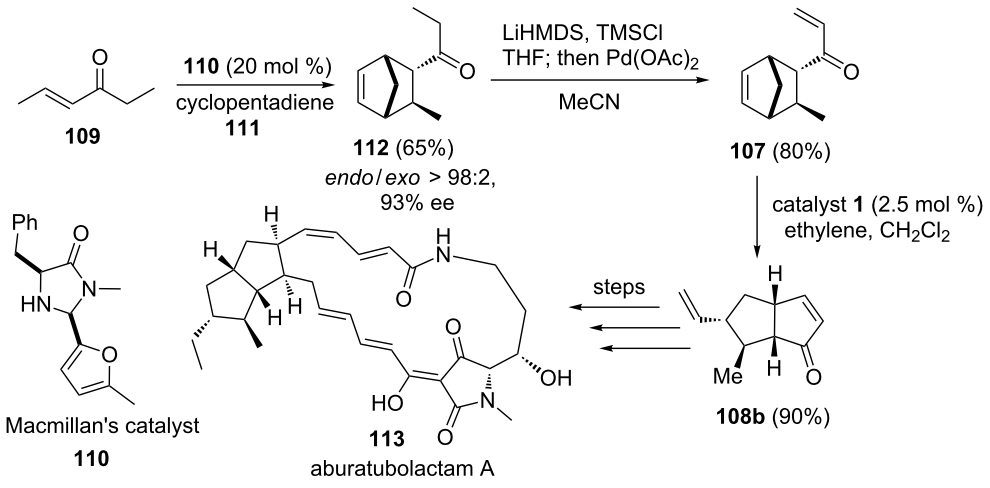

Scheme 23: ROM–RCM protocol for the synthesis of the bicyclo[3.3.0]octene system.

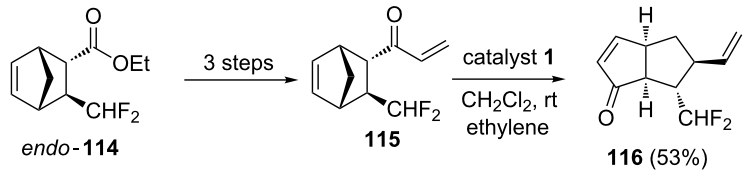

Scheme 24: RRM protocol to bicyclic enone.

generate the difluoromethylated cycloaddition *endo*-product **114** (99% ee). Further, it was used to prepare the required enone **115**. Later, enone **115** was subjected to a RRM protocol by employing catalyst **1** in the presence of ethylene (**24**) to generate the bicyclic enone **116** in 53% yield (Scheme 24) [28].

In 2005, Funel and Prunet have disclosed the synthesis of fused tricyclic systems by employing a RRM protocol [29]. For example, the bicyclic system **117** was treated with catalyst **2** to generate the rearranged tricyclic system **118**. This strategy has been extended with higher analogues (Scheme 25).

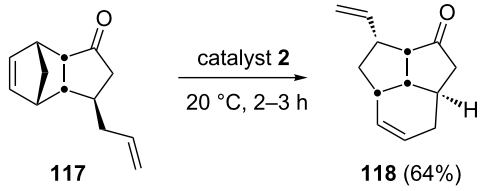

Scheme 25: RRM protocol toward the synthesis of the tricyclic system **118**.

Kotha and Ravikumar [30] have utilized the RRM and the enyne RRM to generate various polycyclic scaffolds. In this context, enones, such as **121a** and **121b** were assembled easily from dicyclopentadiene derivative **119**. Later, these componds were subjected to a RRM to generate the tricyclic enones **122a** and **122b**, respectively. To this end, compound **121a** was treated with catalyst **2** under ethylene (**24**) atmosphere to deliver the tricyclic enone **122a** in 75% yield. Similarly, the tricyclic compound **122b** (50%) was obtained under the influence of catalyst **5** in the presence of ethylene (**24**, Scheme 26).

Along similar lines, the oxa analog **125** was obtained by RRM of **124** using catalyst **1** under ethylene (**24**) atmosphere. Interestingly, the diene building block **128**, produced by employing an enyne-ring rearrangement metathesis (ERRM) sequence, was subjected to a DA reaction in refluxing toluene with various dienophiles such as dimethyl acetylenedicarboxylate (DMAD, **129)** to generate the tetracyclic system **130** (Scheme 27).

To design synthetically challenging oxa-bowls, Kotha and Ravikumar [31] have utilized the RRM and ERRM of extended norbornene systems. The key building blocks such as **133** and **134** were prepared from a readily available DA adduct **131** derived from cyclopentadiene (**111**) and 1,4-benzoquinone. The diol **132** was produced by reduction of **131** in an efficient manner. To this end, the bis-*O*-allylated compound **133** was prepared by an allylation sequence using allyl bromide (**37**) in

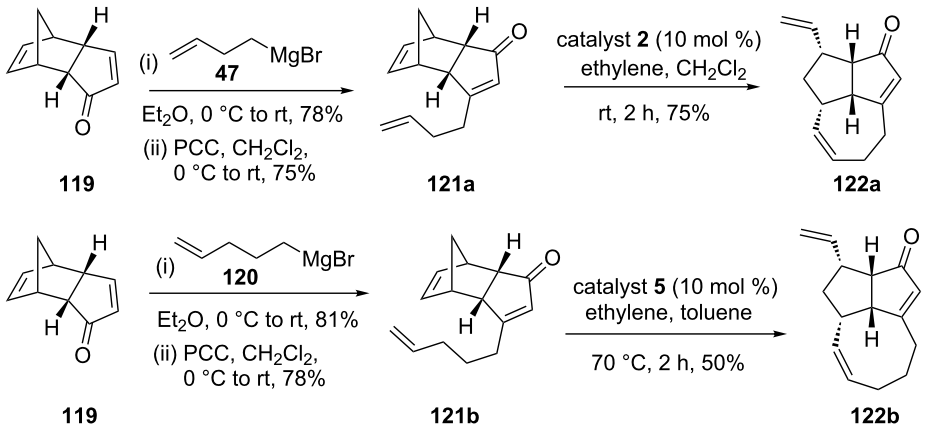

Scheme 26: RRM approach toward the synthesis of the tricyclic enones **122a** and **122b**.

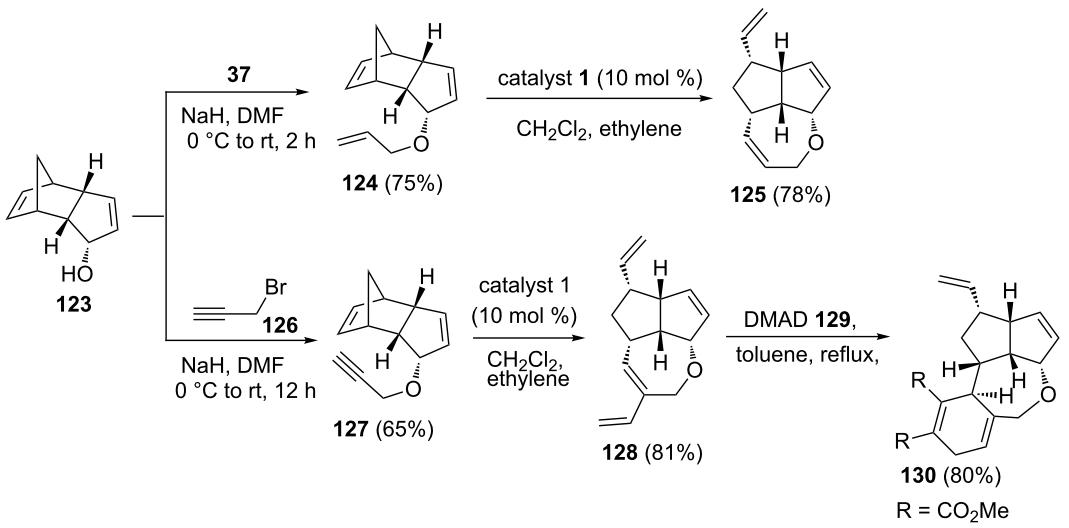

Scheme 27: Synthesis of tricyclic and tetracyclic systems via RRM protocol.

the presence of NaH starting with the diol **132**, whereas compound **134** was derived via bis-*O*-propargylation of compound **132** using propargyl bromide (**126**) under similar reaction conditions. Later, these compounds (**133** and **134**) were subjected to RRM and ERRM protocols under the influence of catalyst **1** in the presence of ethylene (**24**) to generate the tetracyclic systems **135** (100%) and **136** (76%), respectively. Moreover, this strategy can easily be extended to other complex systems (Scheme 28).

Banti and co-workers have described a RRM with catalysts **1** and **2** by using an aminopropargylated norbornene system as a starting material [19]. In this reaction, three possible products were observed by employing either catalyst **1** or **2**. The norbornene derivative **137** was subjected to a RRM protocol under the influence of catalyst **1** in the presence of ethylene (**24**) to obtain the expected product **138** in 41% yield (Table 1, entry 1) along with the *cis*- and *trans*-monocyclized products **139** and **140**. Further, NMR spectroscopic studies showed the presence of products **139** and **140** as a mixture of isomers, and it was difficult to purify this mixture by conventional separation techniques (Scheme 29).

Recently, Kotha and Gunta have reported a RRM to generate various polycyclic compounds using catalysts **1** and **2** [32]. The tetraallyl derivative, prepared from **142** by an allylation protocol, was subjected to a RRM sequence in the presence of the catalyst **1** to produce propellane derivative **144** containing

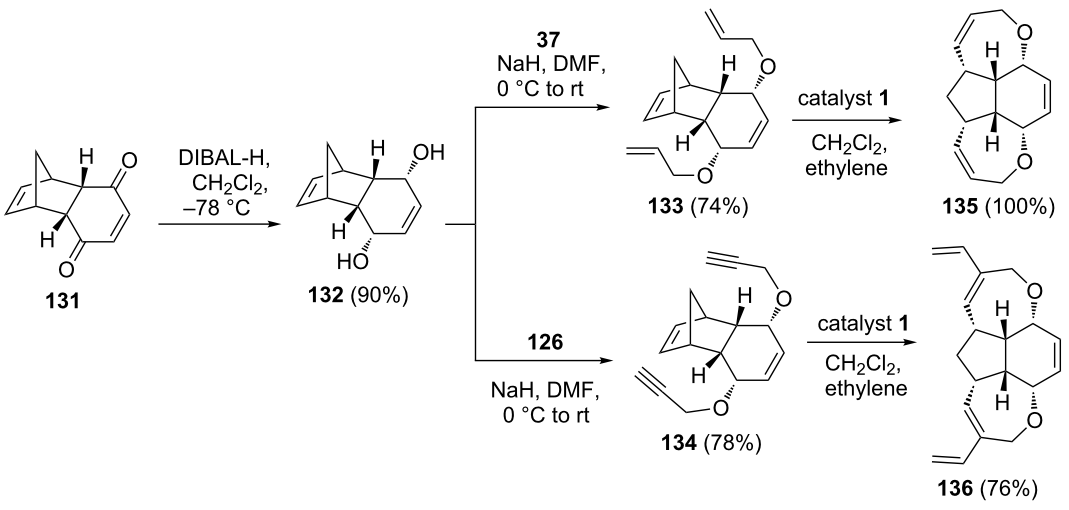

Scheme 28: RRM protocol towards the synthesis of tetracyclic systems.

Table 1: RRM of propargylamino derivative.

Entry	Cat (mol %)	Solvent	*T* (°C)	time (h)	Conv.	**138** (yield %)
1	**1** (5)	CH_2Cl_2	25	6	100	41
2	**1** (5)	CH_2Cl_2	25	16	100	43
3	**1** (5) + **2** (5)	CH_2Cl_2	25	24	100	37
4	**2** (5)	toluene	60	24	0	0

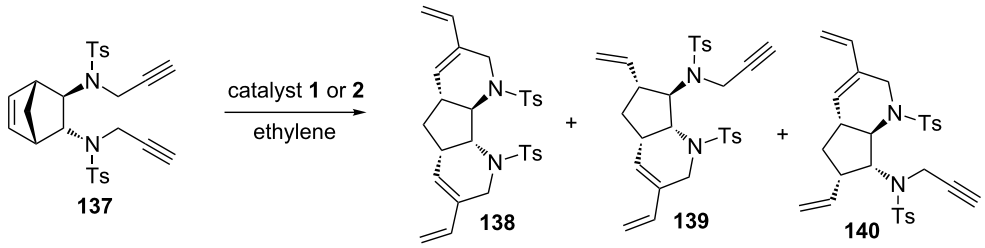

Scheme 29: RRM of the propargylamino[2.2.1] system.

an oxa-bowl moiety. In another sequence [33], the alkenylation of sulfone **145** gave the dialkenylated product **147** in 21% yield along with the monoalkenylated product. Later, the dialkenylated compound **147** was treated with catalyst **2** to give the tetracyclic compound **148** in 97% yield (Scheme 30).

Along similar lines, Kotha and co-workers [34] prepared *N*-allylated compounds and subjected them to a RRM to produce the tricyclic aza compound **152** in an excellent yield. The required synthone **151** was prepared by employing a Beckman rearrangement followed by a *N*-allylation sequence. Later, it was reacted with catalyst **2** in the presence of ethylene (**24**) to deliver the expected tricyclic product **152** in 90% yield (Scheme 31).

Ghosh and Maity [35,36] reported a stereoselective route to functionalized tricyclic system present in umbellactal (**153**) via a RRM protocol starting with intricate norbornene derivatives.

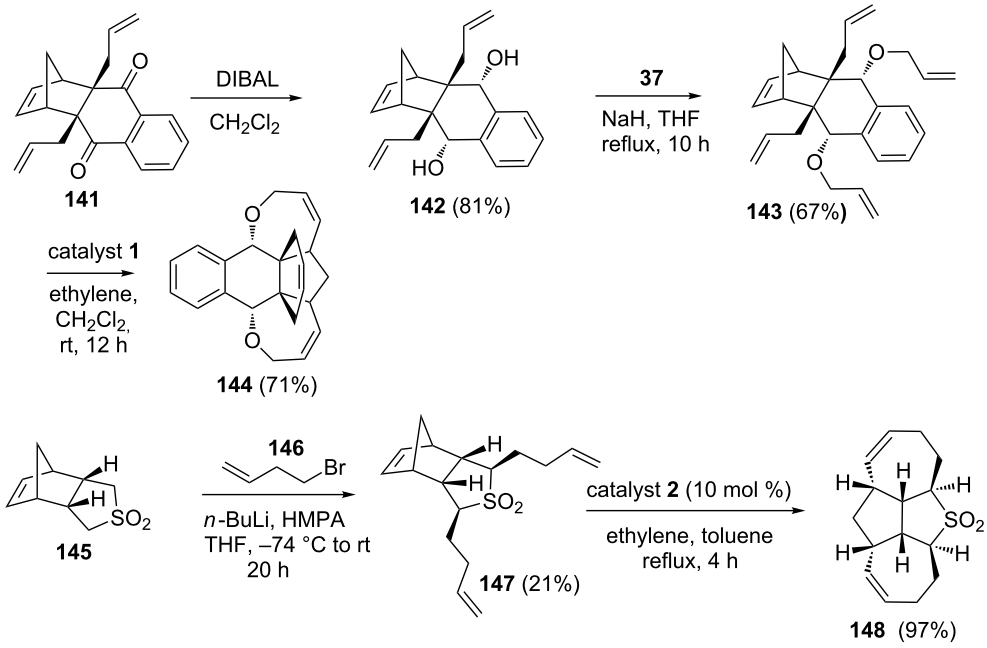

Scheme 30: RRM of highly decorated bicyclo[2.2.1] systems.

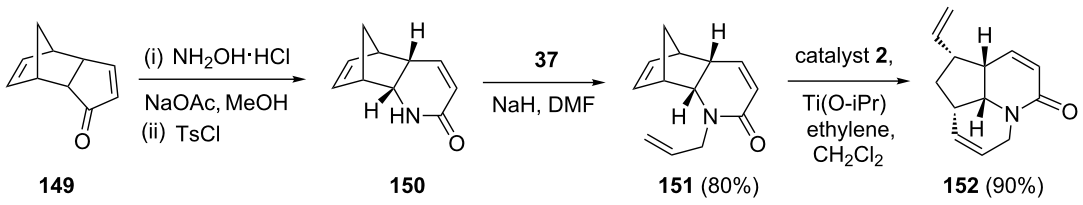

Scheme 31: RRM protocol towards fused tricyclic compounds.

The tricyclic anhydride **154** was reduced to lactone **155** using sodium borohydride and then it was monoallylated to deliver an inseparable mixture of products **156** and **157** in 85% combined yield. Later, the mixture (**156** and **157**) was subjected to a RRM protocol under the influence of the catalyst **1** in the presence of ethylene (**24**) to yield a mixture (4:1) of tricyclic lactones **158** and **159** (70% yield). Next, the major product **158** was converted into **159** by isomerization via DBU in 82% yield. The *cis*-lactone **159** was found to be a core structural unit present in umbellactal (Scheme 32).

Ghosh and co-workers also reported [37] a short and efficient approach to a highly functionalized lactarane skeleton using RRM with appropriate norbornene systems. The strategy starts with the aldol condensation of aldehyde **160** with ester **161** in the presence of LDA to generate the required building block **162** in 78% yield. Later, the norbornene derivative **162** was subjected to a RRM sequence under the influence of the catalyst **1** in the presence of ethylene (**24**) to produce the rearranged product **163** in 65% yield (Scheme 33).

Ghosh and co-workers have described an efficient route for the synthesis of the fused tricyclic system found in caribenol A by employing a RRM approach [38]. The steps employed here involve: a sequential aldol condensation of dihydrocarvone with norbornene 2-carboxaldehyde followed by a ROM–RCM of the resulting aldol product. The norbornene derivative **164** was subjected to a RRM using the catalyst **1** to produce the ROM product **165** exclusively. The ring-closure of the resulting ROM product **165** under the influence of the catalyst **2** led to the formation of the dimeric product. Alternatively, RCM of **165** under the influence of catalyst **5** generated the required tricyclic compound **166** in 45% yield (epimeric mixture at C-5). Interestingly, this tricyclic system was found as a core structural unit present in caribenol A (Scheme 34).

In another instance, they [39] achieved an efficient synthesis of the functionalized tricyclic ring system **171** in the context of the synthesis of the nonterpenoids schintrilactones A and B by a RRM approach of alkenylated norbornene derivative **170**. They also reported an impressive set of example with complex

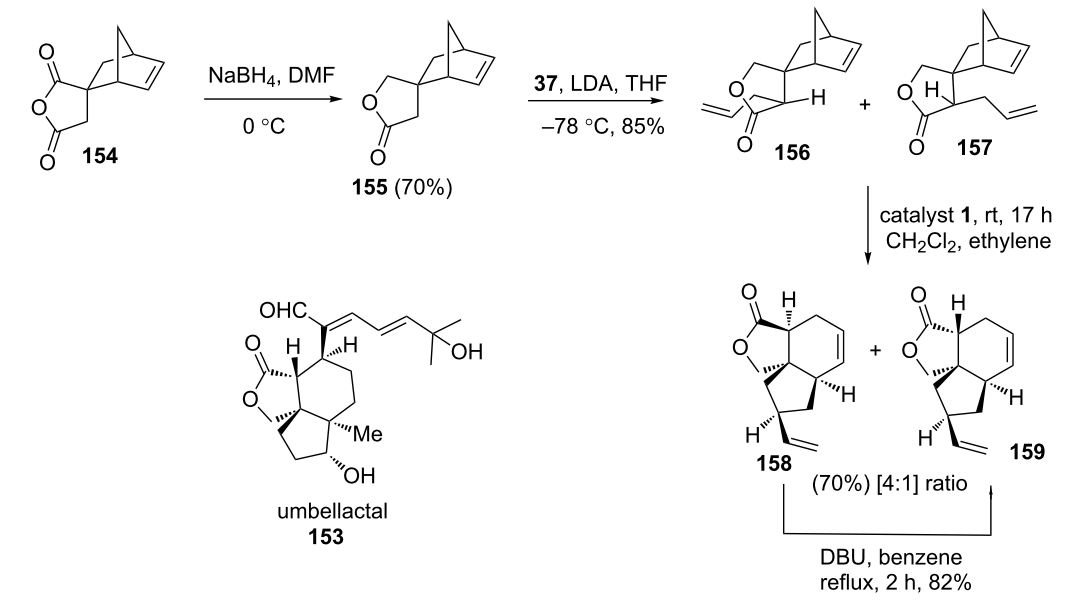

Scheme 32: RRM protocol to functionalized tricyclic systems.

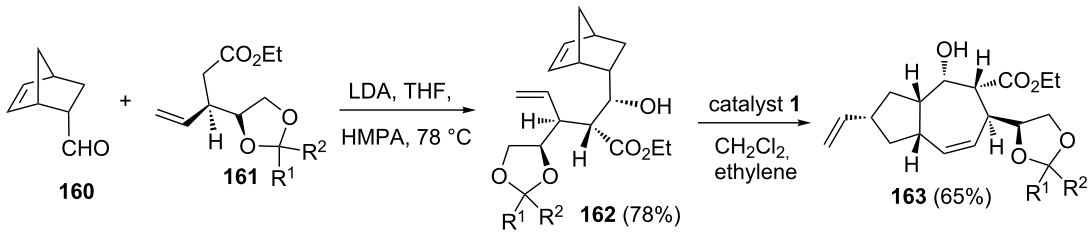

Scheme 33: RRM approach to functionalized polycyclic systems.

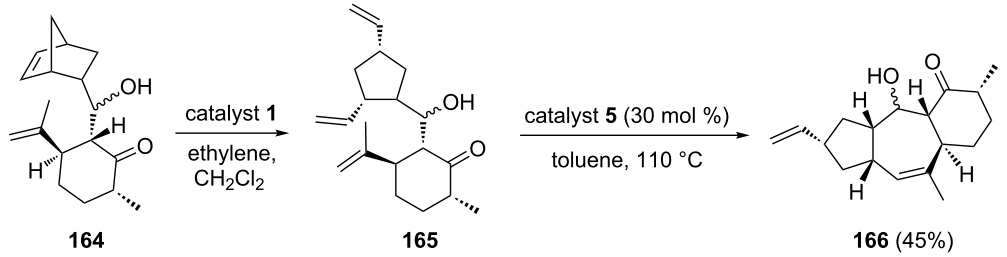

Scheme 34: Sequential RRM approach to functionalized tricyclic ring system **166**.

norbornene systems. The required synthone **170**, suitable for RRM, has been prepared from **167** in three steps. Later, compound **170** was treated with catalyst **2** in the presence of ethylene (**24**) to generate the desired tricyclic ring system **171** (94%), which is found to be a core structure of schintrilactones A and B (Scheme 35).

In 2012, Ghosh's group [40] demonstrated a RRM approach towards the synthesis of a 7/5 fused system by using a bicyclo[2.2.1]heptene derivative via a sequential RRM approach. Moreover, they have studied the feasibility of a RRM protocol starting with highly substituted bicyclo[2.2.1]heptene and bicyclo[2.2.2]octene systems. Here, the silyl ether **172** was treated with catalyst **1** to give the ring-opened product **174**. Next, the triene **174** was subjected to a RCM protocol in the presence of catalyst **2** to furnish the tricyclic product **176**. Along similar lines, methyl substituted norbornene derivative **173** was treated with catalyst **1** in the presence of ethylene (**24**) to generate the ROM product **175**, which was further subjected to a RCM using catalyst **2** to deliver the expected tricyclic system **177** (7/5 fused system) (Scheme 36).

A synthesis of fused medium-sized rings has been reported by Ghosh and co-workers [41] via a sequential diastereoselective DA reaction and a RRM protocol. A variety of sugar-based norbornene derivatives provide an entry to various functionalized bicyclic sugar derivatives containing 7–9 membered rings. To this end, compounds **178** and **181** were subjected to a ROM sequence with catalyst **1** in the presence of ethylene (**24**) followed by treatment with catalyst **2** under the same reaction conditions to give the RRM products **180** and **183**, respectively, derived from the ROM products. Here, the

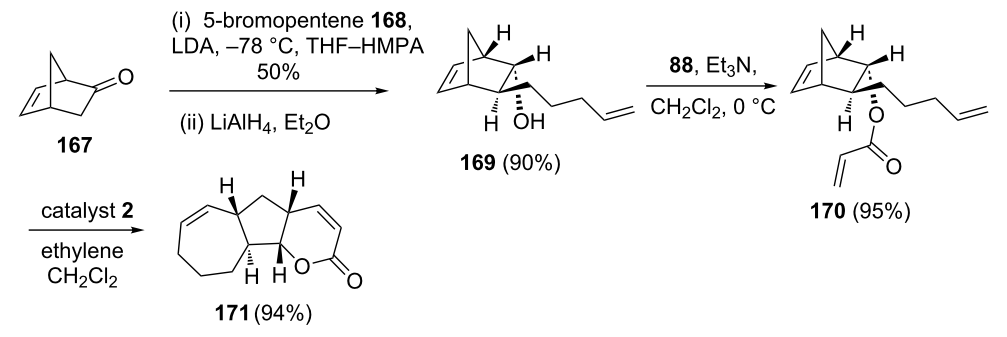

Scheme 35: RRM protocol to functionalized CDE tricyclic ring system of schintrilactones A and B.

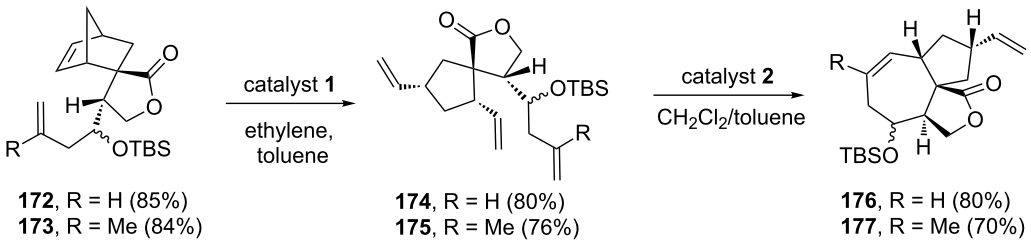

172, R = H (85%)
173, R = Me (84%)

174, R = H (80%)
175, R = Me (76%)

176, R = H (80%)
177, R = Me (70%)

Scheme 36: Sequential RRM approach to 7/5 fused bicyclic systems.

norbornene derivatives **178a**,**b**,**d** and **181a**,**c**,**d** furnished the RRM products **180a**,**b**,**d** and **183a**,**c**,**d**, respectively. As expected, when the compounds **178c** and **181b** were subjected to metathesis under the influence of the catalyst **1**, the RRM products (**180c** and **183b**) were obtained respectively (Scheme 37).

Along similar lines, compound **185** was reacted with cyclopentadiene in a DA fashion to deliver an inseparable mixture of adducts **186** and **187**. Later, the ROM–RCM of this mixture of norbornene derivatives, gave the *cis-syn-cis* and *cis-anti-cis* 5-7-6 tricyclic systems **188** (60%) and **189** (26%), respectively, via the RRM approach (Scheme 38).

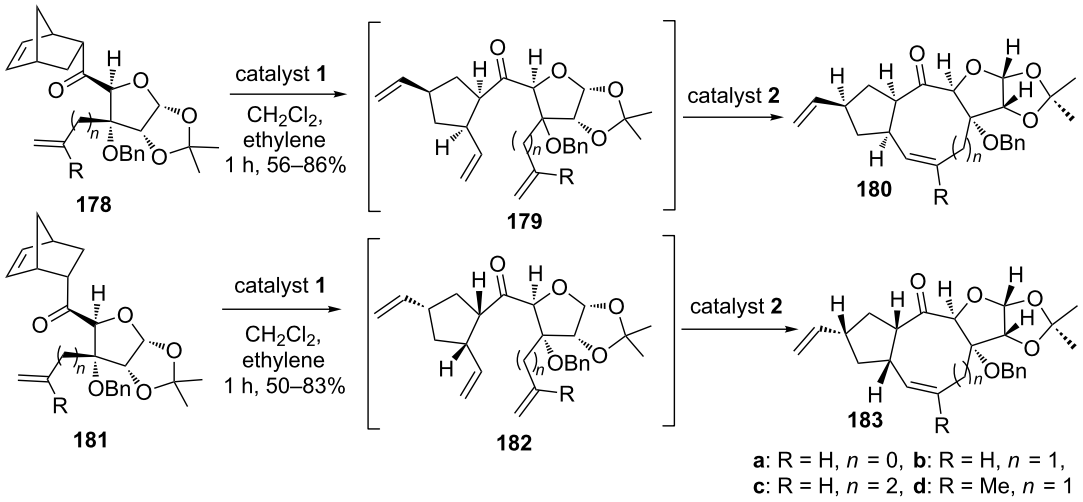

178 **179** **180**

181 **182** **183**

a: R = H, *n* = 0, **b**: R = H, *n* = 1,
c: R = H, *n* = 2, **d**: R = Me, *n* = 1

Scheme 37: Sequential ROM-RCM protocol for the synthesis of bicyclic sugar derivatives.

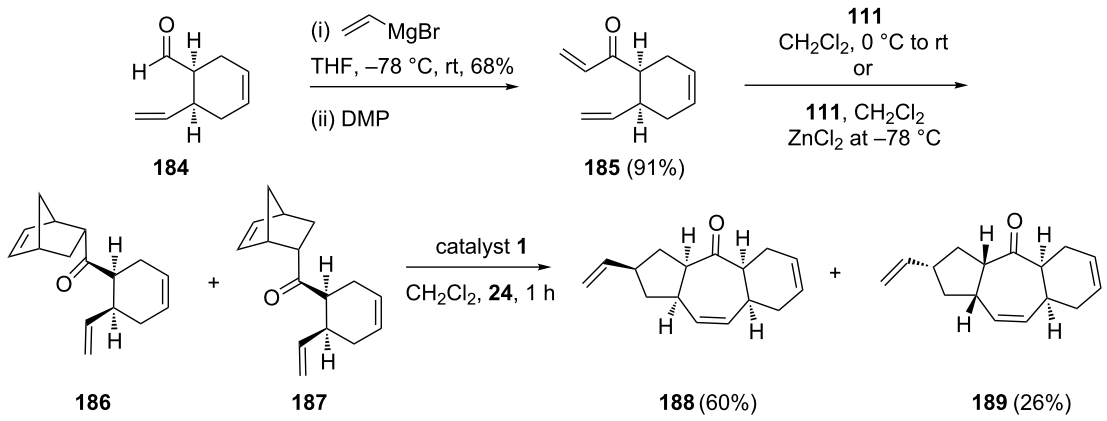

184 **185** (91%)

186 **187** **188** (60%) **189** (26%)

Scheme 38: ROM–RCM sequence of the norbornene derivatives **186** and **187**.

Ghosh's group [42] disclosed an elegant approach to a highly functionalized bridged tricyclic system by employing a RRM approach involving catalyst **1**. The required synthone **192** has been prepared from the allyl substituted norbornene derivative **190** in three-steps. Later, the keto derivative **192** was subjected to a RRM sequence via catalyst **1** to generate the bridged tricyclic system **193** in 40% yield (Scheme 39).

A novel approach to highly functionalized tricyclic systems such as **197** and **198** has been reported via a RRM protocol. In this context, the *endo*-aldehyde **160** was identified as a starting material in the synthetic sequence and it was transformed into enone **194** by treatment of vinyl Grignard **106** followed by Jones oxidation. Later, enone **194** was subjected to a DA reaction in the presence of cyclopentadiene (**111**) to deliver an inseparable mixture of cycloadducts **195** (*endo,endo*) and **196** (*exo,exo*) in a 1:2 ratio. Then, treatment of the cycloadducts **195** and **196** separately with catalyst **1** in the presence of ethylene (**24**) furnished the tricyclic compounds **197** (23%) and **198** (45%), respectively (Scheme 40). Analogously, they have also achieved the synthesis of angularly annelated carbocycles by employing the RRM protocol starting with appropriate norbornene derivatives [43].

Recently, Kotha and Ravikumar [44] have found a new route to various polycyclic compounds by employing the DA reaction and the RRM protocol as key steps. To this end, the key building block **202** has been prepared from **199** via Grignard addition followed by *O*-allylation. The double DA adduct **199** has been derived from cyclopentadiene and 1,4-benzoquinone. Next, compound **202** was exposed to catalyst **2** in the presence of ethylene (**24**) to generate the expected hexacyclic system **203** (70%) containing 10 stereogenic centres (Scheme 41).

Sakurai and co-workers have successfully established an enantioselective synthesis of the C_3-symmetric chiral trimethylsumanene through a Pd-catalyzed cyclotrimerization and the RRM protocol as key steps [45]. Here compound **207** reacted with catalyst **1** in the presence of ethylene (**24**) to deliver a mixture of ring-opened products. A sequential treatment with catalyst **2** resulted in a ring-closing product to deliver the expected hexahydrotrimethylsumanene **208** in 24% yield. When the tris-

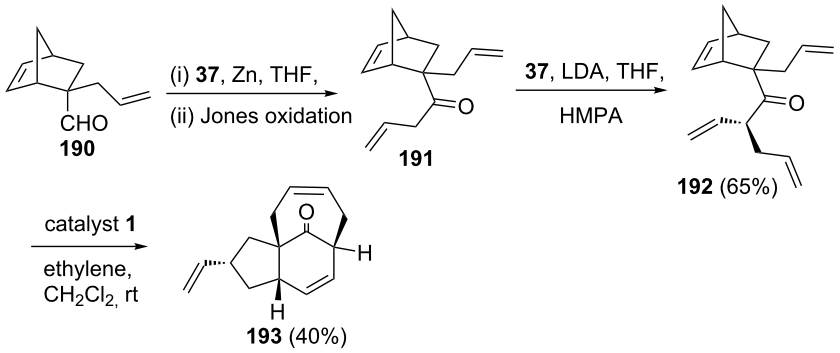

Scheme 39: RRM approach toward highly functionalized bridge tricyclic system.

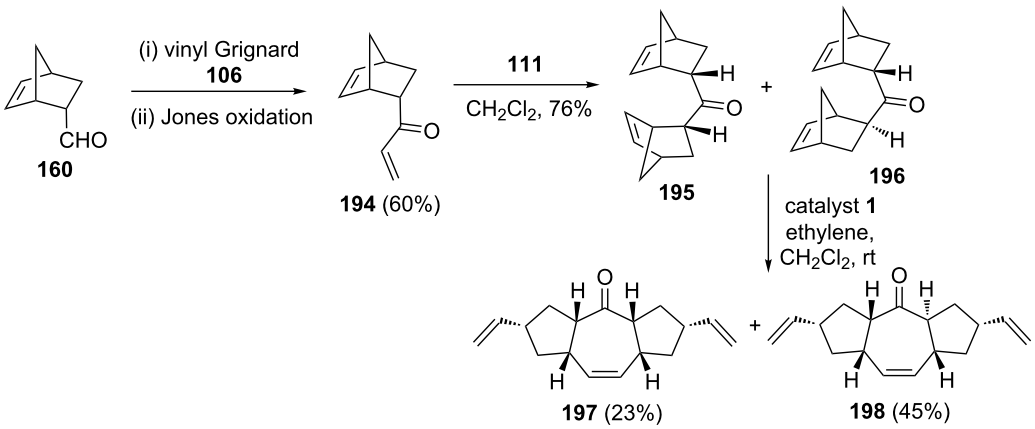

Scheme 40: RRM approach toward highly functionalized tricyclic systems.

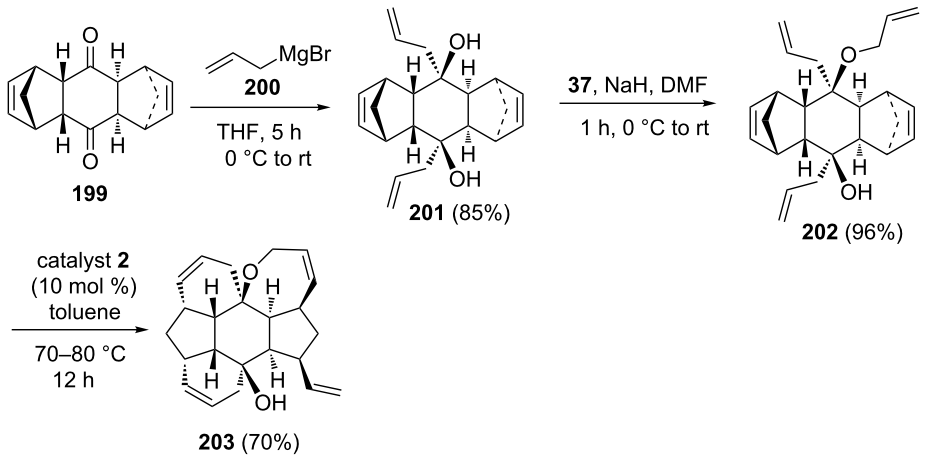

Scheme 41: Synthesis of hexacyclic compound **203** by RRM approach.

norbornene derivative **207** was treated with catalyst **2** in the presence of (*Z*)-oct-4-ene the required RRM product **208** was formed in 26% yield. Later, the expected chiral buckybowl **209** was assembled via aromatization of **208** in the presence of DDQ (Scheme 42).

Design of intricate polyquinanes has been considered as a challenging task for synthetic chemists. To this end, Fallis and co-workers [46] have demonstrated an intramolecular Diels–Alder (IMDA) reaction followed by a RCM–ROM–CM cascade was found to be useful to assemble a linear triquinane framework. Microwave assisted IMDA reaction of cyclopentadiene derivative **210** performed in chlorobenzene at 201 °C under 310 psi pressure gave the required DA adduct **211**. Later, the cycloadduct **211** was reacted with the catalyst **1** in the presence ethylene (**24**) to generate a linear *cis*-*anti*-*cis* triquinane derivative **212** (Scheme 43).

In search of new antibacterial drugs, Spring and co-workers [47] have designed a diversity-oriented approach to structurally diverse small molecules starting with solid-supported phosphonate **213**. In this regard, they have shown the use of a RRM protocol to prepare the bicyclic product **218** as well as tricyclic product **217**. To this end, the phosphonate ester **213** reacted with a wide variety of aldehydes **214** such as aryl, heteroaryl, and alkyl, etc. to produce α,β-unsaturated acylimidazolidinones **215**. Next, the Evan's asymmetric DA methodology involving a [4 + 2] cycloaddition of chiral bis(oxazoline) in the presence of $Cu(OTf)_2$ was employed to furnish the required norbornene system **216**. Later, it was converted into a lactam and then

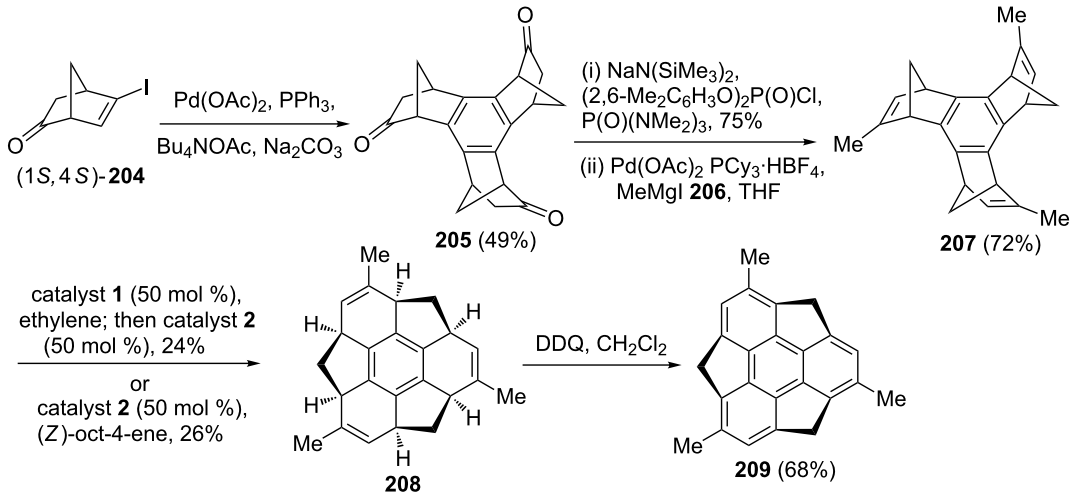

Scheme 42: RRM approach toward C_3-symmetric chiral trimethylsumanene **209**.

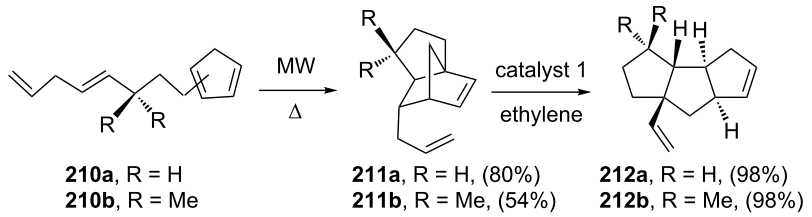

Scheme 43: Triquinane synthesis via IMDA reaction and RRM protocol.

subjected to a RRM sequence with catalyst **2** in the presence of ethylene (**24**) to furnish the tricyclic product **217** as well as bicyclic product **218** (Scheme 44).

The bicyclo[3.3.0]octene system represent a core structural unit present in several natural products. Kimber and co-workers [48] have utilized a RRM approach to generate *cis*-fused bicyclo[3.3.0]octene derivatives. In this regard, various norbornenyl derivatives **219**, **221**, **223** and **225** were subjected to RRM by treatment with catalyst **2** in the presence of ethylene (**24**) to generate various bicyclo[3.3.0]octene derivatives such as **220**, **222**, **224**, and **226** with high regioselectivity. The thermodynamic stability of the product is anticipated to play an important role in the observed regioselectivity of these transformations (Scheme 45).

In the course of the asymmetric synthesis of (−)-isoschizogamine, a bicyclic lactone **230** has been identified as a key building block. To this end, Fukuyama and co-workers [49] have used the RRM to generate the required building block **230**. In this reaction, the required norbornene derivative **228** was prepared from epoxide **227** in two steps and later it was treated with the more reactive catalyst **6** in the presence of 1,6-heptadiene (**229**) to generate the required bicyclic lactone **230** (73%). In this process, 1,6-heptadiene (**229**) helps to enhance the rate of the reaction and to improve the yield. However, when the bicyclic system **228** was treated with catalyst **5** in refluxing benzene lactone **230** was obtained in 24% yield (Scheme 46).

Azanorbornene systems

7-Azanorbornene derivatives have been used to generate a wide variety of heterocyclic compounds via the RRM approach [50]. To this end, the azanorbornene derivative **231** was treated with catalyst **2** in the presence of ethylene (**24**) to produce the heterospiro system **234** (91%). Alternatively, a ROM–RCM–CM sequence was employed under similar reaction conditions in the presence of methyl acrylate (**232**) as a CM partner. The tandem metathesis product **233** was obtained in 68% yield along with the ROM–RCM product **234** in 18% yield (Scheme 47).

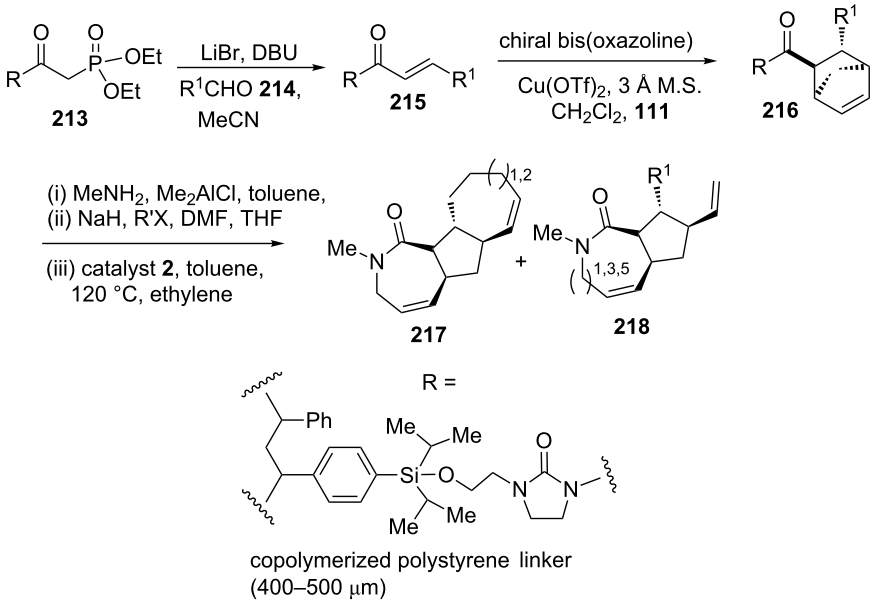

Scheme 44: RRM approach to polycyclic compounds.

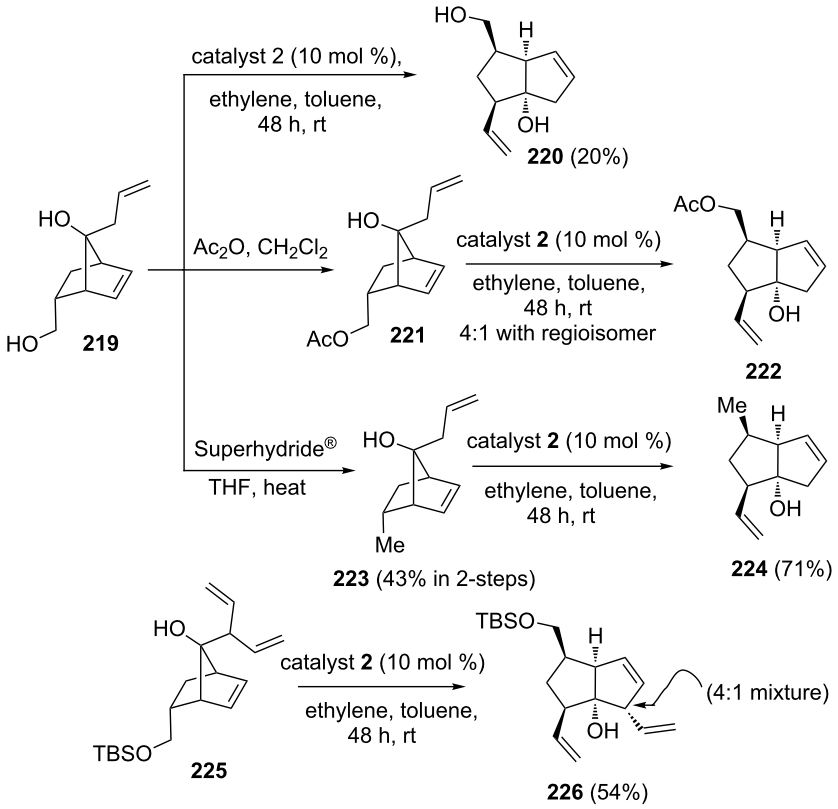

Scheme 45: RRM strategy toward *cis*-fused bicyclo[3.3.0]carbocycles.

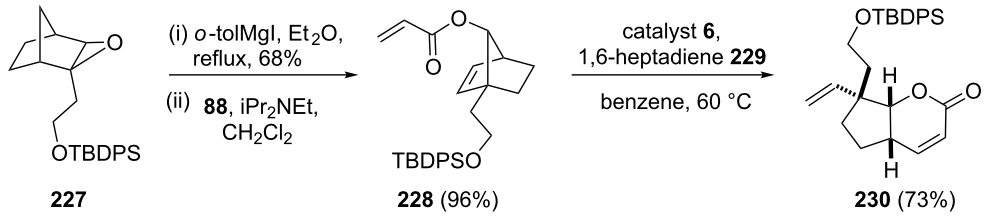

Scheme 46: RRM protocol towards the synthesis of bicyclic lactone **230**.

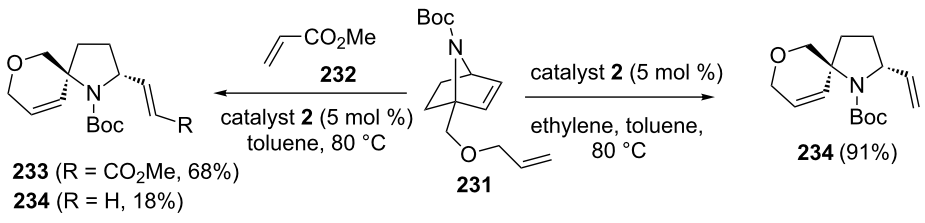

Scheme 47: RRM approach to spiro heterocyclic compounds.

Later, 7-azanorbornene **235** has been used in RRM. To this end, compound **235** was subjected to a RRM under the influence of catalyst **3** to deliver the spiro heterocyclic compound **236** (41%). Similarly, compound **237** was treated with catalyst **2** under the same reaction conditions to produce the spiro heterocycle **238** (91%) (Scheme 48).

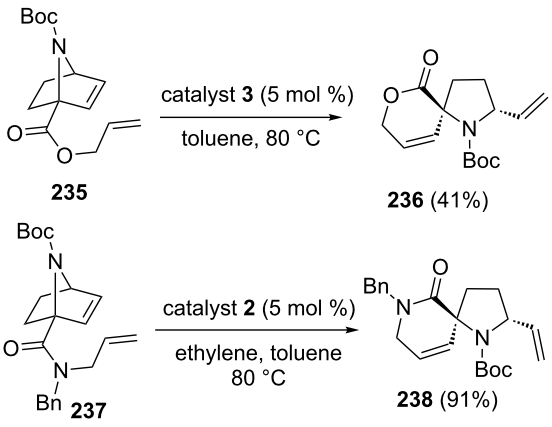

Scheme 48: RRM approach to spiro heterocyclic compounds.

The RRM strategy has provided an easy access to a variety of 1-azabicyclo[*n*.3.0]alkenones. For example, when 7-azanorbornene derivative **239** was subjected to a ROM–RCM sequence by treatment with catalyst **2** in toluene in the presence of ethylene (**24**) delivered the pyrrolizidine system **240** in 63% yield [51]. The regioselective formation of **240** may be attributed to the facile formation of a Ru–carbene intermediate where the metal participates on the side opposite to that of the methyl ester and thereby minimizing the steric crowding between ruthenium and carbonyl oxygen of an ester functionality (Scheme 49). Homologous starting material **242** underwent a RRM with catalyst **2** in the presence of ethylene (**24**) at 80 °C to produce indolizidine-based compound **243** in 63% yield. Under similar reaction conditions, the azabicyclic system **244** generated pyrrolo[1,2-*a*]azepine derivative **245**. When the RRM protocol was applied to compounds **246a–c** with different bridgehead substituents, they also generated the corresponding pyrrolo[1,2-*a*]azepine derivatives **247a–c** in good yields with a high degree of regioselectivity (Scheme 50).

Treatment of ether-bridged triene **248** with catalyst **2** in chloroform at 50 °C generated the spiroannulated pyrrolidine **249** in 68% yield. However, when the reaction was performed in toluene at 80 °C, the isomeric tricyclic compound **250** was afforded in 34% yield and tricyclic derivative **249** was obtained in 37% yield (Scheme 51).

Rainier's group [52] has successfully demonstrated the synthesis of various perhydroindolines by adopting a ROM–RCM cascade using catalyst **2** starting with 7-azanorbornene derivative **251**. In this context, RRM precursors such as **252** and **253** were obtained from **251** by detosylation sequence. Later, they were subjected to a RRM protocol under the influence of catalyst **2** in the presence of ethylene (**24**) to generate the expected rearranged products **254** and **255**, respectively (Scheme 52).

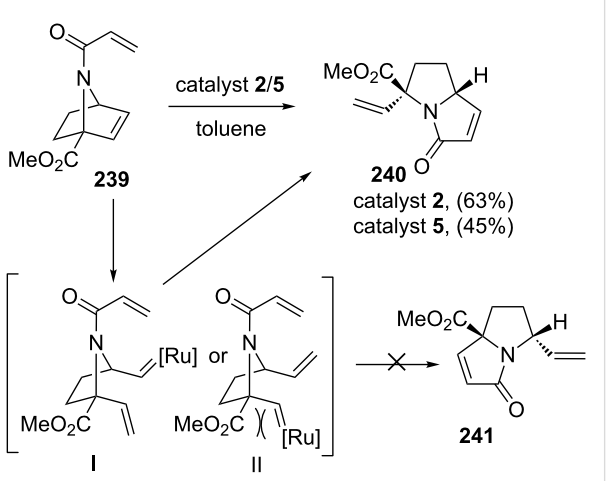

Scheme 49: RRM approach to regioselective pyrrolizidine system **240**.

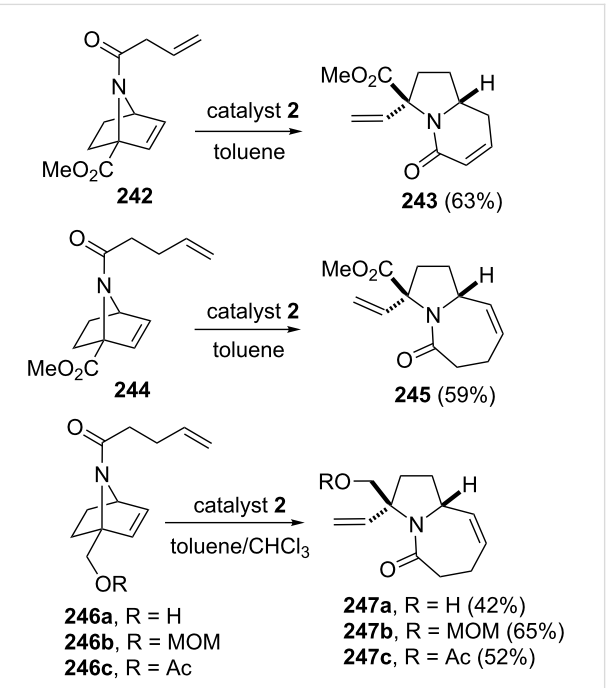

Scheme 50: RRM approach to functionalized bicyclic derivatives.

Oxanorbornene systems

Lee and co-workers [53] have successfully constructed a fused bis(oxacyclic) system useful towards the formal total synthesis of dysiherbaine and neodysiherbaine via the RRM protocol. To this end, the oxabicyclo[2.2.1]hept-5-ene **256** was subjected to a RRM cascade with catalyst **2** in dichloromethane to produce pyran derivative **257** in 84% yield, which serves as a core structural unit of disyherbaine. Highly functionalized pyran derivative **259** was obtained by the reaction of **256** with catalyst **5** in the presence of vinyl acetate (**258**) (Scheme 53).

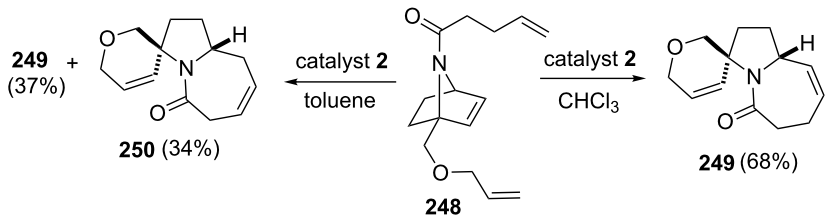

Scheme 51: RRM approach to tricyclic derivatives **249** and **250**.

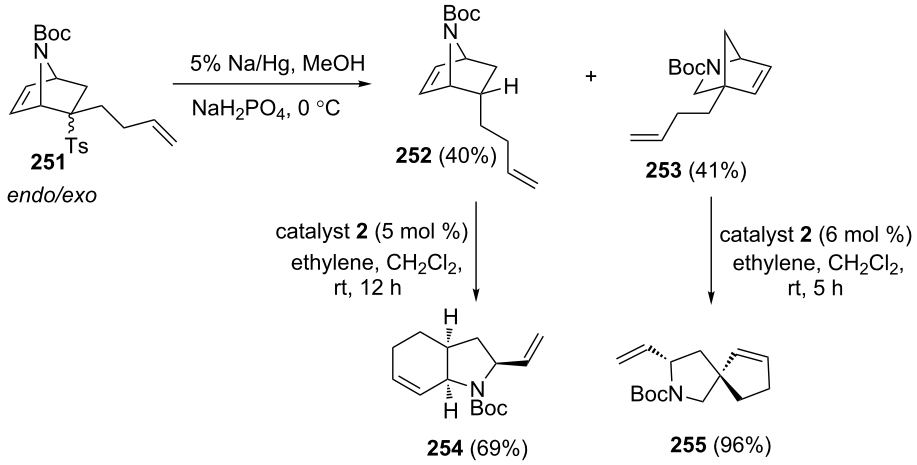

Scheme 52: RRM approach to perhydroindoline derivative and spiro system.

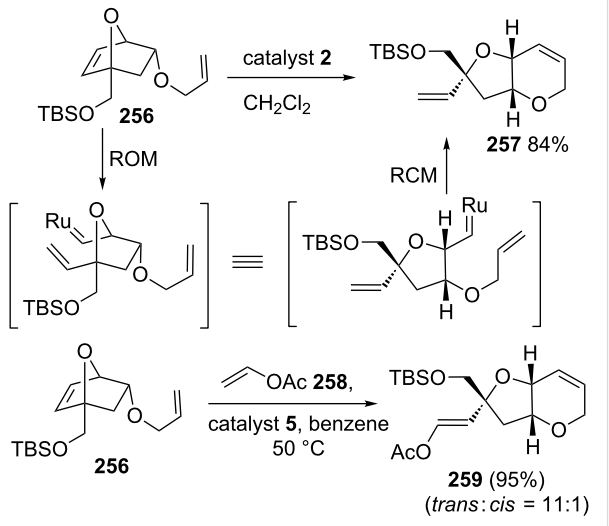

Scheme 53: RRM approach to bicyclic pyran derivatives.

The RRM approach is useful to design diverse analogs of the marine toxin dysiherbaine, which displays antagonistic activity on ionotropic glutamate receptors from oxanorbornenes [54]. The report reveals the regiochemical directing effect of the exocyclic amidocarbonyl group in a ROM sequence of norbornenes. When the 7-oxanorbornene **260** containing an exocyclic amidocarbonyl moiety was subjected to a metathesis reaction using catalyst **5** in the presence of vinyl acetate (**258**) at room temperature, the required RRM product **261** was generated in 87% yield with high regio- (>99%) and good stereoselectivity (*E*/*Z* = 13:1). Next, tricyclic compound **263** was generated in quantitative yield when the oxanorbornene derivative **262** was subjected to a metathesis with catalyst **5** in the presence of vinyl acetate (**258**) at room temperature. On the other hand, when the norbornene derivative **264** without the *N*-benzylaminocarbonyl side chain was subjected to a metathesis under similar reaction conditions a mixture of four products (30:28:6:1) was obtained in 31% combined yield (Scheme 54).

Phelligridin G, a natural product isolated from the fruiting body of *P. igniarius,* is a well-known anticancer agent. To assemble the spiro-fused furanone core of phelligridin G, Wright and Cooper [55] have used a RRM process as a key step. Wittig olefination of furylbenzaldehyde derivative **265** using methyltriphenylphosphonium bromide in the presence of *n*-BuLi provided styrylfuran **270** in 72% yield. The DA reaction of styrene derivative **270** with DMAD **129** at 40 °C yielded oxabridged compound **268**. Another route to **268** involves a DA reaction of **265** with DMAD at 55 °C for longer reaction time

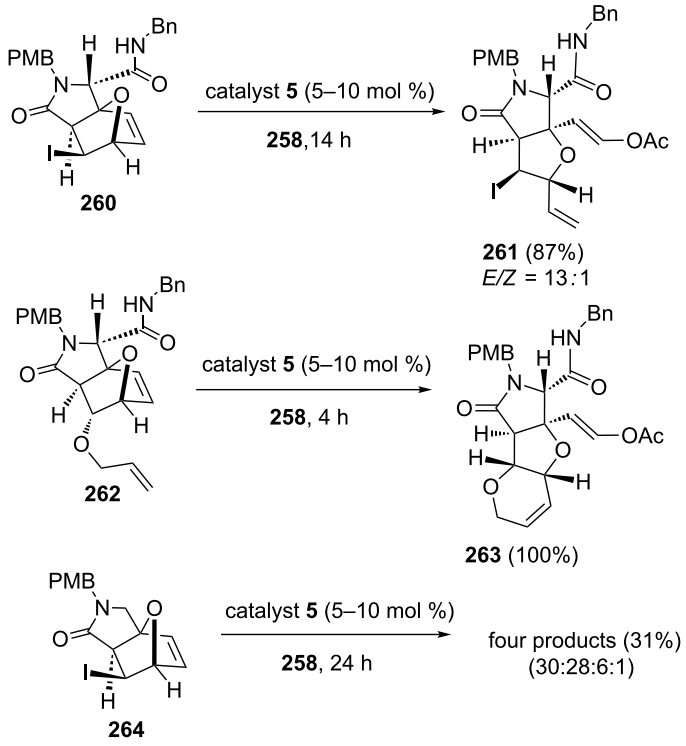

Scheme 54: RRM of various functionalized oxanorbornene systems.

(3 days) and sequential Wittig olefination. The spiro compound **269** was obtained from oxabicyclo adduct **268** by a domino metathesis sequence in the presence of catalyst **2**. Moreover, compound **269** was obtained as a single diastereomer and constitutes the core structure of phelligridin G (Scheme 55).

In 2009, Hanson's group reported [56] the synthesis of skeletally diverse bi-, and tricyclic sultam derivatives (sulfonamide analogs) using norbornenyl sultam **272** as a core unit assembled by an intramolecular Diels–Alder (IMDA) reaction via a domino ROM–RCM–CM cascade. Diversity has been incorporated by using various cross-metathesis partners (Scheme 56).

Basso and co-workers [57] have demonstrated a tandem Ugi–ROM–RCM protocol towards the synthesis of the 2-aza-7-oxabicyclo[4.3.0]nonane framework by employing catalyst **2**.

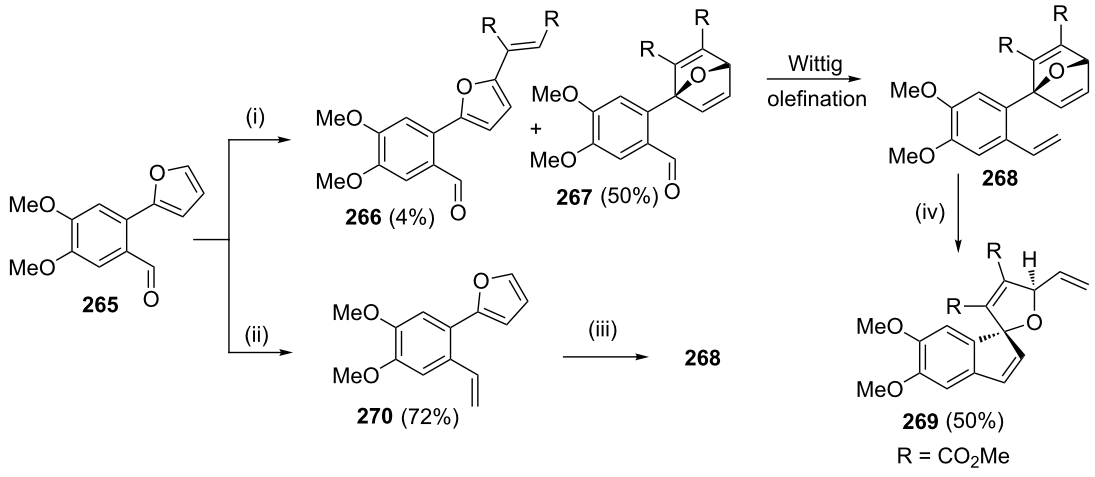

Scheme 55: RRM to assemble the spiro fused-furanone core unit. (i) **129**, benzene, 55 °C, 3 days; (ii) $Ph_3P{=}CH_2Br$, *n*-BuLi, THF, 0 °C; (iii) **129**, benzene, 40 °C, 24 h; (iv) catalyst **2** (10 mol %), CH_2Cl_2, 35 °C.

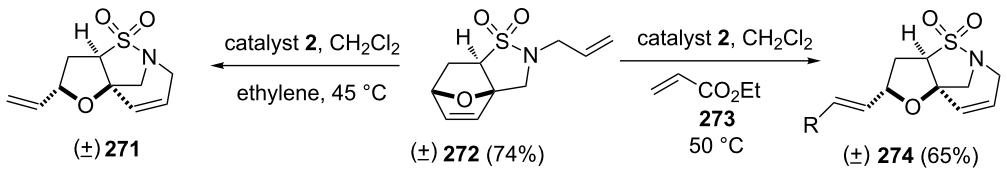

Scheme 56: RRM protocol to norbornenyl sultam systems.

They begin the synthesis with *N*-allyl-3-*endo*-amino-7-oxabicyclo[2.2.1]hept-5-ene-2-*exo*-carboxylic acid (**277**) and it was used in an Ugi 5-centre-4-component reaction (U-5C-4CR) with a wide variety of aldehydes and isocyanides. Subsequently, the products obtained (e.g., **278**) were subjected to a RRM protocol with catalyst **2** to generate the required 2-aza-7-oxabicyclo systems such as **279** (Scheme 57). The advantage of this approach is to provide a simple and short synthetic route to complex polycycles containing the 2-aza-7-oxabicyclo[4.3.0]nonane framework.

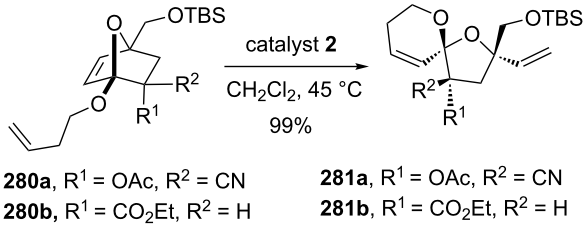

Scheme 58: Synthesis of spiroketal systems via RRM protocol.

Blanchard and co-workers [58] have reported a novel protocol for the synthesis of spiro- and dispiroketals. The required oxabicyclic derivatives such as **280** were synthesized using α-alkoxyfurans by employing [4 + 2] and/or [4 + 3] cycloaddition reactions. Further, they used a RRM protocol in the presence of catalyst **2** to generate the spiroketal derivative **281** (Scheme 58).

Ikoma and co-workers [59] have reported a short synthetic sequence to *cis*-fused heterocycles by employing the 7-oxanorbornene system **282**. In this regard, compound **282** has been prepared by an intramolecular DA reaction as a key step and later, it was subjected to a RRM with catalyst **5** in the presence of ethylene (**24**) to generate the *cis*-fused heterotricyclic system **283** (Scheme 59).

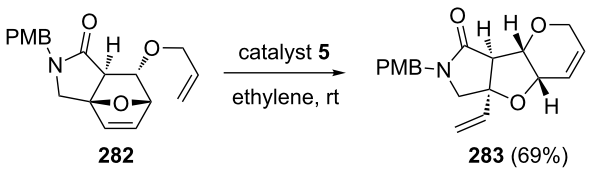

Scheme 59: RRM approach to *cis*-fused heterotricyclic system.

Quinn and co-workers [60] have demonstrated a simple approach to the synthesis of 2,6-dioxabicyclo[3.3.0]octenes **286** starting with the vinyl ether **284** derived from endo-7-oxanorbornene-2-ol by employing a tandem RRM–CM protocol (Scheme 60).

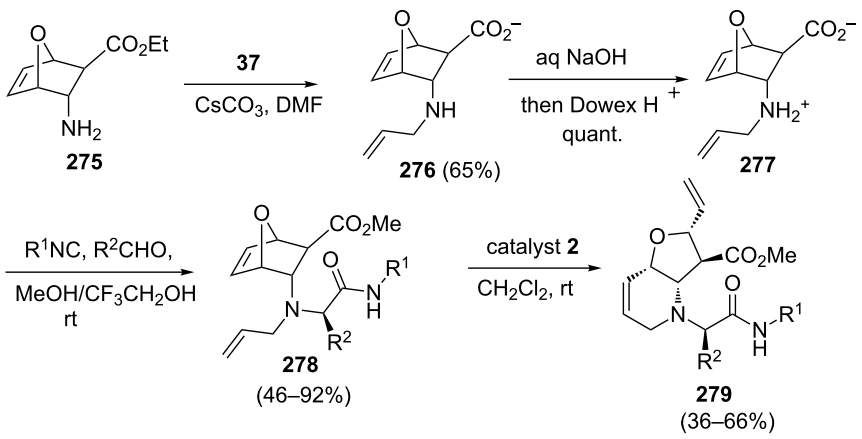

Scheme 57: Ugi-RRM protocol for the synthesis of 2-aza-7-oxabicyclo system.

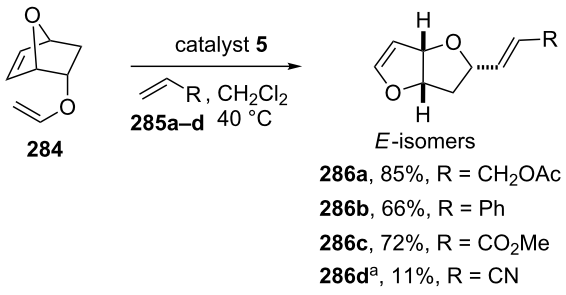

Scheme 60: RRM protocol to functionalized bicyclic systems.

Norbornene systems containing two heteroatoms

Kouklovsky and Vincent have disclosed the RRM of nitroso Diels–Alder (NDA) adducts with a variety of alkenes under microwave or conventional heating conditions by employing catalyst **2** or catalyst **5** to generate various bicyclic compounds [61]. In this regard, compound **287** was subjected to a RRM cascade by employing catalyst **2** in the presence of but-3-en-1-ol (**288**) under optimized reaction conditions (MW, toluene, 80 °C) and the expected tandem metathesis product **289b** was obtained along with the ROM–RCM product **289a**. These compounds are useful synthones for the alkaloids synthesis (Scheme 61). In another instance, they also studied the efficiency of this method by isolating the RCM product of the ROM–CM byproduct **290**, which was recovered in the ROM–RCM–CM cascade (Scheme 62).

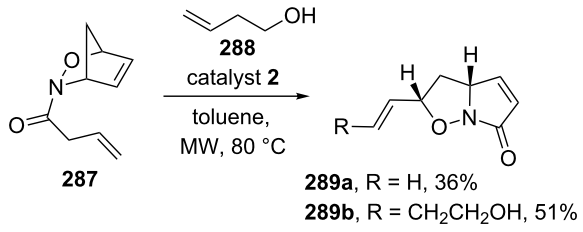

Scheme 61: ROM/RCM/CM cascade to generate bicyclic scaffolds.

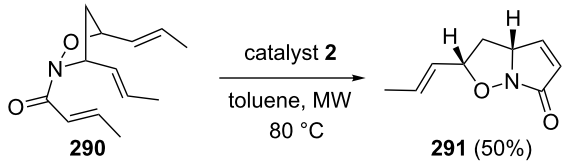

Scheme 62: RCM of ROM/CM product.

Kouklovsky and co-workers [62] have described a stereoselective synthesis of 2-(2-hydroxyalkyl)piperidine alkaloids by employing a RRM of NDA adduct **293**. The required building block **293** has been prepared via NDA reaction of compound **292** and cyclopentadiene (**111**). Later, the DA adduct was subjected to a RRM under the influence of catalyst **2** in the presence of but-2-ene (**294**) to generate the bicyclic isoxazolidine derivative **295**. By keeping the bicyclic isoxazolidine ring system intact, this protocol opened an efficient strategy for the formal synthesis of porantheridine and a total synthesis of andrachcinidine (Scheme 63).

They also reported the formal synthesis of (±)-porantheridine (**301**) and total synthesis of (±)-8-epihalosaline (**300**) via a sequential NDA reaction and a RRM [63]. The bicyclic compound **299** was identified as a key building block for the synthesis of 8-epihalosaline (**300**) and porantheridine (**301**). To this end, but-3-enoic acid (**296**) was converted to the required compound **297**, which on subjection to NDA in the presence of cyclopentadiene (**111**) furnished the desired cycloadduct **298** (61% overall yield). Later, it was subjected to the RRM cascade under the influence of catalyst **2** in the presence of **294** to obtain the desired precursor **299** (75% yield, Scheme 64).

Bicyclo[2.2.2]octene systems

Ghosh and co-workers [40] demonstrated that a RRM approach generates the decalin system **304** rather than the expected 7/6

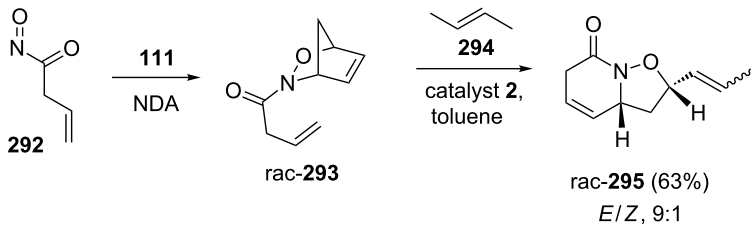

Scheme 63: RRM protocol to bicyclic isoxazolidine ring system.

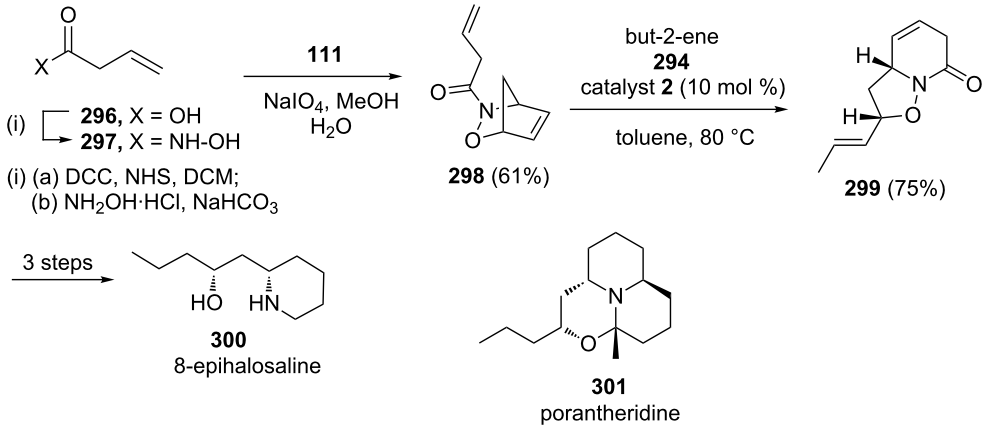

Scheme 64: RRM approach toward the total synthesis of (±)-8-epihalosaline (**300**).

fused bicyclic system **305**. The decalin system has been generated via ROM–RCM starting with bicyclo[2.2.2]octene derivative **303**. In this context, compound **302** was initially reacted with catalyst **1** in the presence of ethylene (**24**) to give **303**. Further, treatment with catalyst **2** gave the decalin derivative **304** rather than expected compound **305**. However, the metathesis of compound **306**, prepared by an independent route produced the expected RCM product **305** in 70% yield (Scheme 65).

Kimber and co-workers [64] have described the synthesis of various carbocylic scaffolds by utilizing the RRM protocol involving catalyst **2**. They identified the bicyclo[2.2.2]oct-2-en-7-one (**307**) as the key building block, which was transformed into a mixture of alcohols such as *syn*-**309a** and *anti*-**309b** in 53% and 24% yield, respectively as a separable diastereomeric mixture (dr, 2:1 ratio). To this end, the *syn*-product **309a** effectively gave the RRM product **310** related to the bicyclo[3.3.1] system with catalyst **2** in the presence of ethylene (**24**). Alternatively, the *anti*-product **309b** gave the corresponding *trans*-fused [4.3.0]nonene derivative **311** in 24% yield (Scheme 66).

Liao and co-workers [65] have employed the RRM protocol with the DA adduct derived from masked *o*-benzoquinones (MOBs). Here, they demonstrated an efficient RRM protocol for the synthesis of *cis*-hydrindenols starting with a readily available starting material such as 2-methoxyphenols. To this end, 2-allylbicyclo[2.2.2]octenol derivative **313** was identified as a key building block in the synthetic sequence, which was prepared from bicyclic system **312** in two steps. When the bicyclic compound **313** (*endo* isomer) was subjected to a RRM sequence with catalyst **2** in the presence of ethylene (**24**) at room temperature the desired *cis*-hydrindenols **315a** (95%), **315b** (95%) were obtained in excellent yield (Scheme 67).

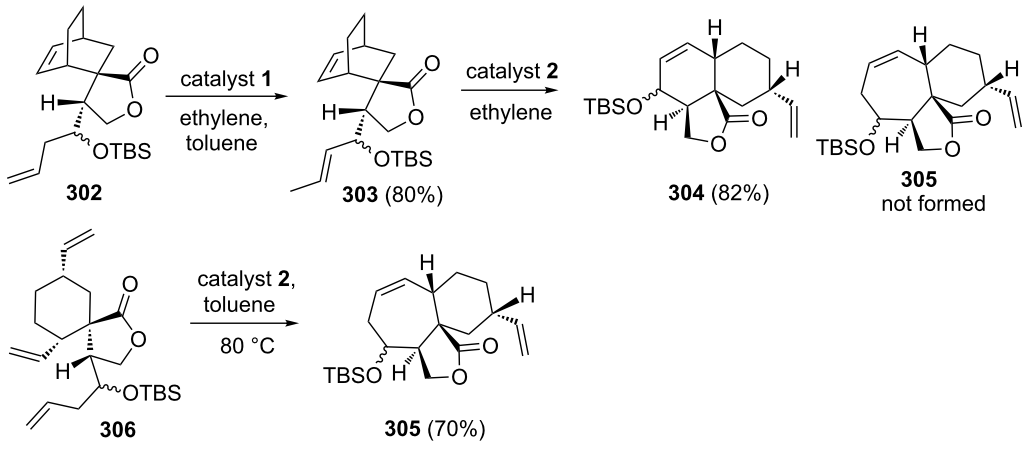

Scheme 65: Sequential RRM approach to decalin **304** and 7/6 fused **305** systems.

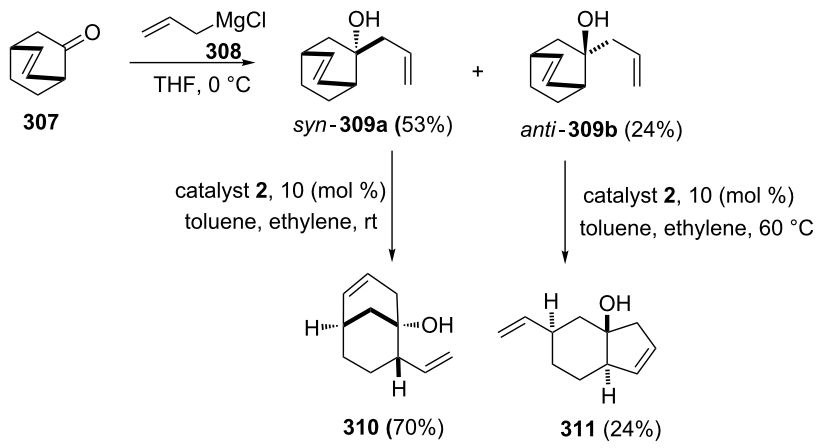

Scheme 66: RRM protocol to various fused carbocyclic derivatives.

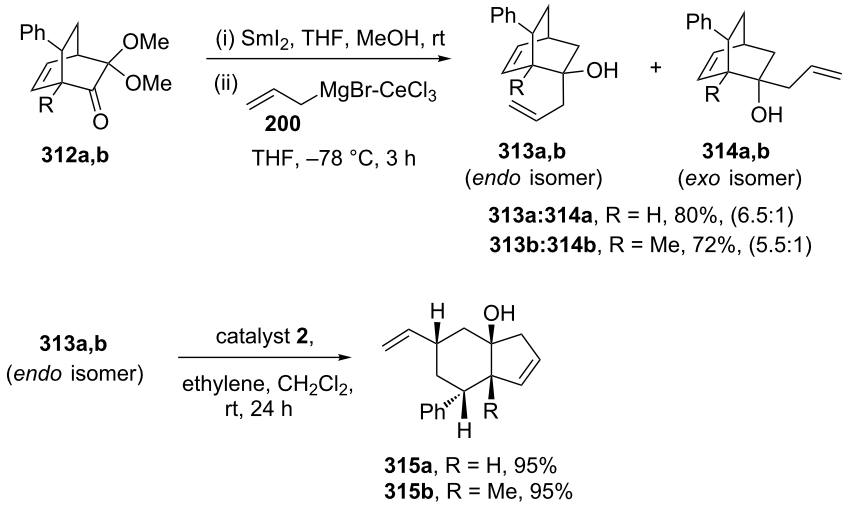

Scheme 67: RRM to *cis*-hydrindenol derivatives.

They have also shown that the RRM protocol is applicable with 2-allylbicyclo[2.2.2]octenol derivative **316**. The building block **316** required for this purpose has been generated via the DA reaction as a key step starting with 2-methoxyphenol. Later, compound **316** was subjected to a RRM under the influence of catalyst **2** in the presence of ethylene (**24**) to deliver the expected rearranged product **317** (Scheme 68).

Vanderwal and co-workers [66] described the synthesis of polycyclic lactams obtained by arene/allene cycloaddition, discovered by Himbert and Henn were found to undergo a RRM in a facile manner in the presence of catalyst **6** to produce complex polycyclic lactams. In this regard, the required building block **319** was obtained from compound **318** by cycloaddition reaction. A variety of complex molecular frames were accessed via the RRM sequence under the influence of catalyst **6** in toluene at 50–100 °C in the presence of **24**. The procedure is suitable for the preparation of diverse polycyclic lactams with a variety of substitution patterns (Scheme 69).

Kotha and Ravikumar [44] have successfully executed the RRM protocol for the synthesis of condensed polycyclic systems. To this end, bicyclo[2.2.2]octene derivative **321** has been identified as a key starting material. The required key building block **323** has been prepared from the known bis-DA adduct **321** [67] via allyl Grignard addition followed by *O*-allylation sequence.

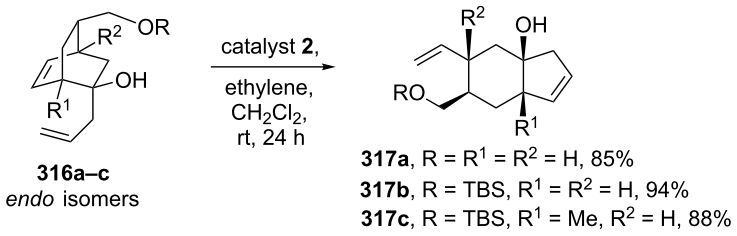

Scheme 68: RRM protocol towards the *cis*-hydrindenol derivatives.

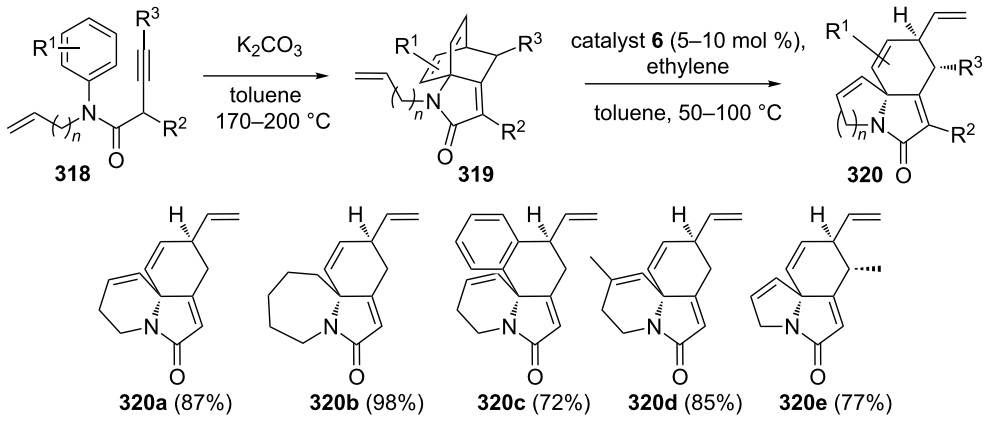

Scheme 69: RRM approach toward the synthesis of diversed polycyclic lactams.

The starting cycloadduct **321** was obtained by the double DA reaction between 1,3-cyclohexadiene and 1,4-benzoquinone. Further, treatment of **323** with catalyst **2** in the presence of titanium isopropoxide furnished the expected RRM product **324** in 92% yield (Scheme 70).

Bicyclo[2.2.2]octene systems containing nitrogen

To design lycopodium alkaloids, Barbe and co-workers [68] have used RRM judiciously. The required precursor **326** suitable for RRM has been prepared from pyridine (**325**) in four

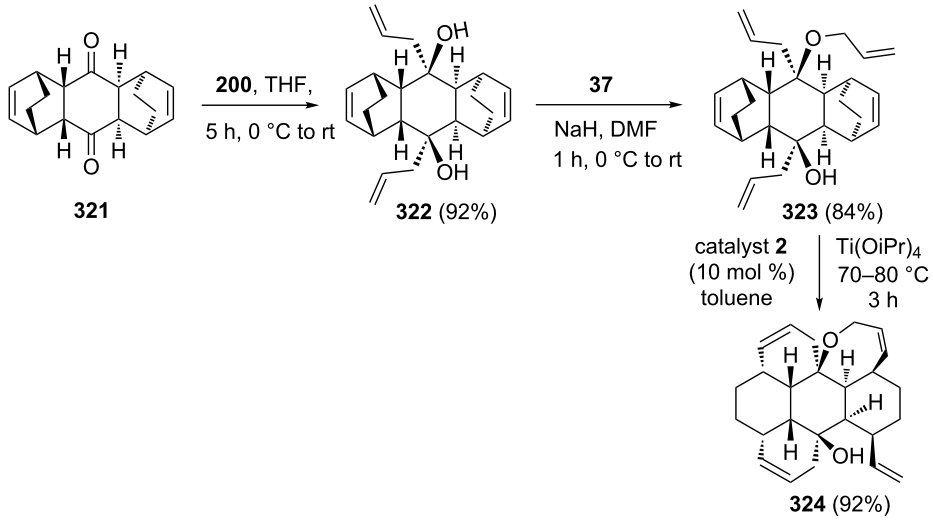

Scheme 70: RRM approach towards synthesis of hexacyclic compound **324**.

steps on gram scale. Later, the azabicyclic system was reacted with catalyst **2** to generate the desired hydroquinoline derivative **327** in 81% yield. Further, they have used the bicyclic compound **327** as a key building block in the total synthesis of (+)-luciduline (Scheme 71).

Lepadins are natural products consisting of *cis*-fused decahydroquinoline subunits and they display cytotoxic activity against many human cancer cell lines. The total synthesis of (+)-lepadin B developed by Charette and Barbe [69] utilized a RCM–ROM as key step. In this regard the azabicyclic system **329** (obtained from pyridine (**325**)) was subjected to a RRM sequence by employing catalyst **2** at 80 °C in toluene to furnish the rearranged product **330** (79%). Further, the building block **330** was used in the stereoselective total synthesis of lepadin B (Scheme 72).

Bicyco[3.2.1]octene derivatives

Norhalichondrin B is a marine polyether belonging to the halichondrin family and its macrolactone analog has displayed anticancer activity. Phillips and co-workers [70] have described a total synthesis of norhalichondrin B in 37 steps from β-furylethanol. Interesting feature of this synthetic sequence is the tactical utilization of tandem ROM–RCM protocol towards the synthesis of the key intermediate **335**. In this reaction, the required RRM precursor **333** was obtained from diazo ester **331** in five steps. Further, the RRM of **333** with catalyst **2** furnished the required pyran derivative **334** (71%). Next, the fused ether **334** was transformed into the desired intermediate **335** in eight steps, which is a key intermediate required for the synthesis of norhalichondrin B (Scheme 73).

To expand the scope of the RRM methodology, Wright and Cooper [55] reported the synthesis of a highly functionalized pyran system by employing a RRM as a key step. To this end, 2-phenylfuran derivatives **265** and **270** were reacted with tetrachlorocyclopropene (TCCP, **336**) followed by olefination to result the required oxabicyclo[3.2.1]octene derivative **338**. Later, the RRM of the styrene derivative **338** with catalyst **2** delivered a highly-functionalized spiro-pyran derivative **339** in 48% yield (Scheme 74).

The Dysiherbaine and acetogenin groups of natural products have been synthesized by the RRM approach. In this regard, secondary alcohol derivatives related to 8-oxabicyclo[3.2.1]octenes such as **341a,b**,**c** were used as potential precursors for the synthesis of a variety of cyclic polyethers [71]. Allylation of **340a–c** using sodium hydride and allyl bromide (**37**) in the presence of a phase-transfer catalyst such as tetrabutylammonium iodide generated bicyclic compounds **341a–c**. The RRM of these ether derivatives **341a–c** was performed under ethylene (**24**) atmosphere with catalyst **5** to generate the dihydrofuran derivatives **342a–c**. When compounds **340d**, **340e** and **340f** were subjected to a metathesis protocol by treatment with catalyst **2** under ethylene (**24**) atmosphere in the presence of 1,4-benzoquinone, *cis*-fused hexahy-

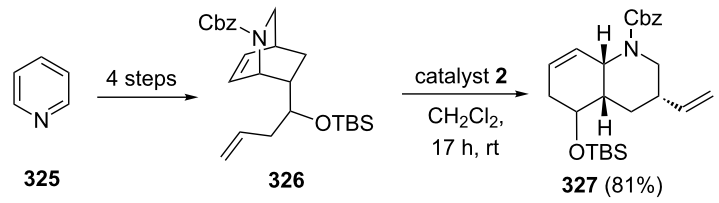

Scheme 71: RRM protocol to generate luciduline precursor **327** with catalyst **2**.

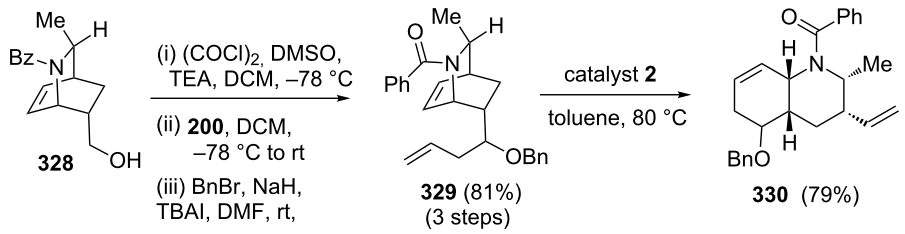

Scheme 72: RRM protocol to key building block **330**.

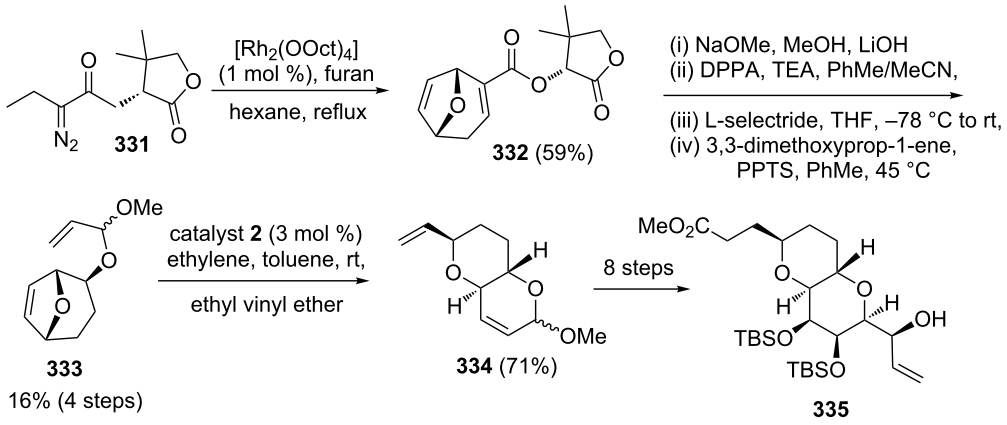

Scheme 73: RRM approach towards the synthesis of key intermediate **335**.

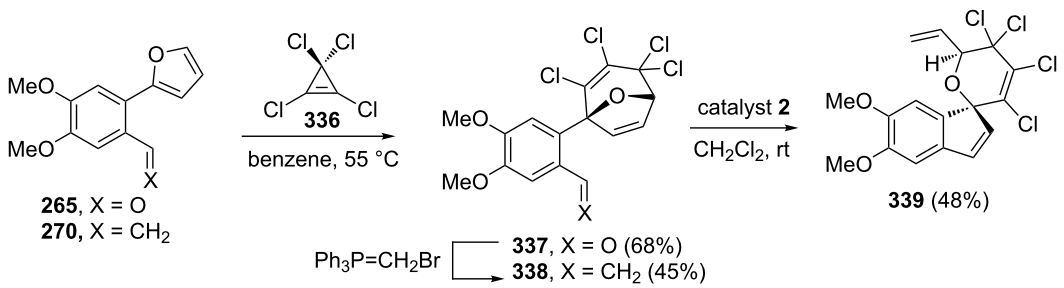

Scheme 74: RRM protocol to highly functionalized spiro-pyran system **339**.

drofuro[3,2-*b*]pyran core containing compounds **343d**, **343e** and **343f** were obtained via RRM in good yields (50–75%) (Scheme 75).

Conclusion

RRM involving ROM–RCM under the influence of various Ru–carbene complexes in one-pot sequence generate various

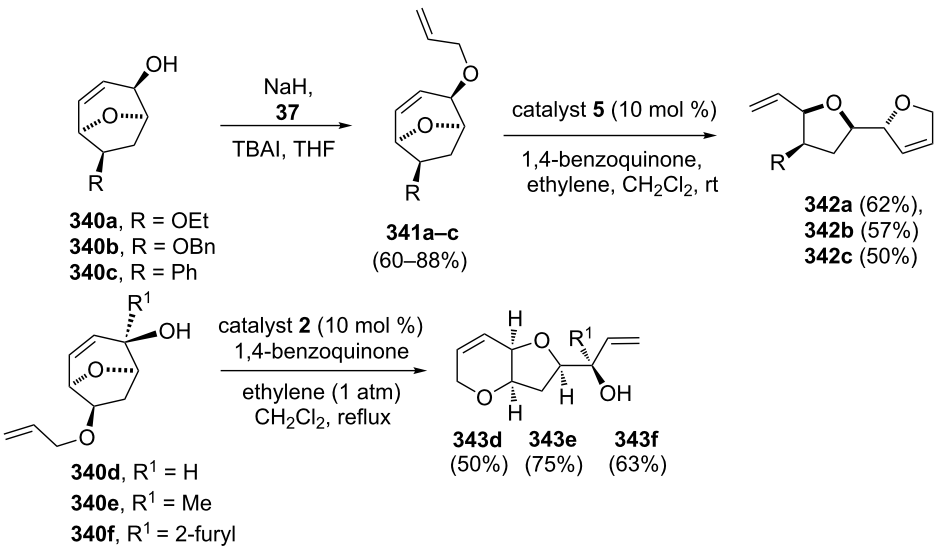

Scheme 75: RRM to various bicyclic polyether derivatives.

complex targets. It is an atom economic process producing a wide range of polycyclic compounds containing highly demanding structures efficiently. Starting with relatively simple substrates, the final compounds obtained by the RRM process are generally difficult to synthesize by conventional synthetic routes. Various examples described here have clearly established the power and scope of this methodology. We believe that an increasing number of natural as well as non-natural products of high structural complexity have assembled by the RRM process and this activity will continue with more vigour in the future.

Acknowledgements

We thank CSIR and the Department of Science and Technology (DST), New Delhi for the financial support. SK thanks DST for the award of a J. C. Bose fellowship. PK thanks DST for Fast Track Research Grant.

References

1. Zuercher, W. J.; Hashimoto, M.; Grubbs, R. H. *J. Am. Chem. Soc.* **1996,** *118,* 6634–6640. doi:10.1021/ja9606743
2. Harrity, J. P. A.; Visser, M. S.; Gleason, J. D.; Hoveyda, A. H. *J. Am. Chem. Soc.* **1997,** *119,* 1488–1489. doi:10.1021/ja9636597
3. Holub, N.; Blechert, S. *Chem. – Asian J.* **2007,** *2,* 1064–1082. doi:10.1002/asia.200700072
4. Nolan, S. P.; Clavier, H. *Chem. Soc. Rev.* **2010,** *39,* 3305–3316. doi:10.1039/b912410c
5. Schmidt, B.; Krehl, S. Domino and Other Olefin Metathesis Reaction Sequences. In *Olefin Metathesis: Theory and Practice;* Grela, K., Ed.; John Wiley & Sons: Hoboken, 2014; pp 187–232.
6. Grubbs, R. H.; O'Leary, D. J. *Handbook of Metathesis,* 2nd ed.; *Applications in Organic Synthesis*, Vol. 2; Wiley-VCH: Weinheim, Germany, 2015.
7. Zhu, Z.-B.; Shi, M. *Org. Lett.* **2010,** *12,* 4462–4465. doi:10.1021/ol101455c
8. Miege, F.; Meyer, C.; Cossy, J. *Org. Lett.* **2010,** *12,* 248–251. doi:10.1021/ol9025606
9. Maougal, E.; Dalençon, S.; Pearson-Long, M. S. M.; Mathé-Allainmat, M.; Lebreton, J.; Legoupy, S. *Synthesis* **2014,** *46,* 3268–3272. doi:10.1055/s-0034-1378663
10. White, B. H.; Snapper, M. L. *J. Am. Chem. Soc.* **2003,** *125,* 14901–14904. doi:10.1021/ja037656n
11. Zhang, F.; Simpkins, N. S.; Blake, A. J. *Org. Biomol. Chem.* **2009,** *7,* 1963–1979. doi:10.1039/b900189A
12. Pandya, B. A.; Snapper, M. L. *J. Org. Chem.* **2008,** *73,* 3754–3758. doi:10.1021/jo702702s
13. Tang, B.; Bray, C. D.; Pattenden, G.; Rogers, J. *Tetrahedron* **2010,** *66,* 2492–2500. doi:10.1016/j.tet.2010.01.059
14. Han, J.-c.; Li, F.; Li, C.-c. *J. Am. Chem. Soc.* **2014,** *136,* 13610–13613. doi:10.1021/ja5084927
15. Halle, M. B.; Fernandes, R. A. *RSC Adv.* **2014,** *4,* 63342–63348. doi:10.1039/C4RA10937F
16. Kress, S.; Weckesser, J.; Schulz, S. R.; Blechert, S. *Eur. J. Org. Chem.* **2013,** 1346–1355. doi:10.1002/ejoc.201201516
17. Li, J.; Lee, D. *Chem. Sci.* **2012,** *3,* 3296–3301. doi:10.1039/C2SC20812A
18. Ma, S.; Ni, B. *Chem. – Eur. J.* **2004,** *10,* 3286–3300. doi:10.1002/chem.200305581
19. Groaz, E.; Banti, D.; North, M. *Tetrahedron* **2008,** *64,* 204–218. doi:10.1016/j.tet.2007.10.076
20. Gao, F.; Stamp, C. T. M.; Thornton, P. D.; Cameron, T. S.; Doyle, L. E.; Miller, D. O.; Burnell, D. J. *Chem. Commun.* **2012,** *48,* 233–235. doi:10.1039/C1CC15452D
21. Donnard, M.; Tschamber, T.; Le Nouën, D.; Desrat, S.; Hinsinger, K.; Eustache, J. *Tetrahedron* **2011,** *67,* 339–357. doi:10.1016/j.tet.2010.11.036
22. Donnard, M.; Tschamber, T.; Desrat, S.; Hinsinger, K.; Eustache, J. *Tetrahedron Lett.* **2008,** *49,* 1192–1195. doi:10.1016/j.tetlet.2007.12.047
23. Donnard, M.; Tschamber, T.; Eustache, J. *Tetrahedron Lett.* **2008,** *49,* 7325–7327. doi:10.1016/j.tetlet.2008.10.048
24. Mori, M.; Kuzuba, Y.; Kitamura, T.; Sato, Y. *Org. Lett.* **2002,** *4,* 3855–3858. doi:10.1021/ol026696d
25. Holtsclaw, J.; Koreeda, M. *Org. Lett.* **2004,** *6,* 3719–3722. doi:10.1021/ol048650l
26. Wrobleski, A.; Sahasrabudhe, K.; Aubé, J. *J. Am. Chem. Soc.* **2002,** *124,* 9974–9975. doi:10.1021/ja027113y
27. Henderson, J. A.; Phillips, A. J. *Angew. Chem., Int. Ed.* **2008,** *47,* 8499–8501. doi:10.1002/anie.200803593
28. Shibatomi, K.; Kobayashi, F.; Narayama, A.; Fujisawa, I.; Iwasa, S. *Chem. Commun.* **2012,** *48,* 413–415. doi:10.1039/C1CC15889A
29. Funel, J.-A.; Prunet, J. *Synlett* **2005,** 235–238. doi:10.1055/s-2004-837200
30. Kotha, S.; Ravikumar, O. *Eur. J. Org. Chem.* **2014,** 5582–5590. doi:10.1002/ejoc.201402273
31. Kotha, S.; Ravikumar, O. *Tetrahedron Lett.* **2014,** *55,* 5781–5784. doi:10.1016/j.tetlet.2014.08.108
32. Kotha, S.; Gunta, R. *Beilstein J. Org. Chem.* **2015,** *11,* 1727–1731. doi:10.3762/bjoc.11.188
33. Kotha, S.; Gunta, R. *Beilstein J. Org. Chem.* **2015,** *11,* 1373–1378. doi:10.3762/bjoc.11.148
34. Kotha, S.; Ravikumar, O.; Majhi, J. *Beilstein J. Org. Chem.* **2015,** *11,* 1503–1508. doi:10.3762/bjoc.11.163
35. Maity, S.; Ghosh, S. *Tetrahedron Lett.* **2008,** *49,* 1133–1136. doi:10.1016/j.tetlet.2007.12.064
36. Maity, S.; Ghosh, S. *Tetrahedron* **2009,** *65,* 9202–9210. doi:10.1016/j.tet.2009.09.029
37. Mondal, S.; Malik, C. K.; Ghosh, S. *Tetrahedron Lett.* **2008,** *49,* 5649–5651. doi:10.1016/j.tetlet.2008.07.083
38. Mondal, S.; Yadav, R. N.; Ghosh, S. *Tetrahedron Lett.* **2009,** *50,* 5277–5279. doi:10.1016/j.tetlet.2009.07.012
39. Matcha, K.; Maity, S.; Malik, C. K.; Ghosh, S. *Tetrahedron Lett.* **2010,** *51,* 2754–2757. doi:10.1016/j.tetlet.2010.03.074
40. Bose, S.; Ghosh, M.; Ghosh, S. *J. Org. Chem.* **2012,** *77,* 6345–6350. doi:10.1021/jo300945b
41. Malik, C. K.; Yadav, R. N.; Drew, M. G. B.; Ghosh, S. *J. Org. Chem.* **2009,** *74,* 1957–1963. doi:10.1021/jo802077t
42. Malik, C. K.; Ghosh, S. *Org. Lett.* **2007,** *9,* 2537–2540. doi:10.1021/ol070906a
43. Datta, R.; Bose, S.; Viththlbhai, P. B.; Ghosh, S. *Tetrahedron Lett.* **2014,** *55,* 3538–3540. doi:10.1016/j.tetlet.2014.04.091
44. Kotha, S.; Ravikumar, O. *Beilstein J. Org. Chem.* **2015,** *11,* 1259–1264. doi:10.3762/bjoc.11.140
45. Higashibayashi, S.; Tsuruoka, R.; Soujanya, Y.; Purushotham, U.; Sastry, G. N.; Seki, S.; Ishikawa, T.; Toyota, S.; Sakurai, H. *Bull. Chem. Soc. Jpn.* **2012,** *85,* 450–467. doi:10.1246/bcsj.20110286

46. Nguyen, N. N. M.; Leclere, M.; Stogaitis, N.; Fallis, A. G. *Org. Lett.* **2010,** *12,* 1684–1687. doi:10.1021/ol100150f
47. Thomas, G. L.; Spandl, R. J.; Glansdorp, F. G.; Welch, M.; Bender, A.; Cockfield, J.; Lindsay, J. A.; Bryant, C.; Brown, D. F. J.; Loiseleur, O.; Rudyk, H.; Ladlow, M.; Spring, D. R. *Angew. Chem., Int. Ed.* **2008,** *47,* 2808–2812. doi:10.1002/anie.200705415
48. Standen, P. E.; Dodia, D.; Elsegood, M. R. J.; Teat, S. J.; Kimber, M. C. *Org. Biomol. Chem.* **2012,** *10,* 8669–8676. doi:10.1039/c2ob26784e
49. Miura, Y.; Hayashi, N.; Yokoshima, S.; Fukuyama, T. *J. Am. Chem. Soc.* **2012,** *134,* 11995–11997. doi:10.1021/ja305856q
50. Carreras, J.; Avenoza, A.; Busto, J. H.; Peregrina, J. M. *J. Org. Chem.* **2011,** *76,* 3381–3391. doi:10.1021/jo200321t
51. Rojas, V.; Carreras, J.; Avenoza, A.; Busto, J. H.; Peregrina, J. M. *Eur. J. Org. Chem.* **2013,** 3817–3824. doi:10.1002/ejoc.201300126
52. Liu, Z.; Rainier, J. D. *Org. Lett.* **2006,** *8,* 459–462. doi:10.1021/ol052741g
53. Lee, H.-Y.; Lee, S.-S.; Kim, H. S.; Lee, K. M. *Eur. J. Org. Chem.* **2012,** 4192–4199. doi:10.1002/ejoc.201200439
54. Ikoma, M.; Oikawa, M.; Gill, M. B.; Swanson, G. T.; Sakai, R.; Shimamoto, K.; Sasaki, M. *Eur. J. Org. Chem.* **2008,** 5215–5220. doi:10.1002/ejoc.200800704
55. Cooper, H. D.; Wright, D. L. *Molecules* **2013,** *18,* 2438–2448. doi:10.3390/molecules18022438
56. Jeon, K. O.; Rayabarapu, D.; Rolfe, A.; Volp, K.; Omar, I.; Hanson, P. R. *Tetrahedron* **2009,** *65,* 4992–5000. doi:10.1016/j.tet.2009.03.080
57. Sonaglia, L.; Banfi, L.; Riva, R.; Basso, A. *Tetrahedron Lett.* **2012,** *53,* 6516–6518. doi:10.1016/j.tetlet.2012.09.076
58. Mandel, J.; Dubois, N.; Neuburger, M.; Blanchard, N. *Chem. Commun.* **2011,** *47,* 10284–10286. doi:10.1039/C1CC14329H
59. Ikoma, M.; Oikawa, M.; Sasaki, M. *Tetrahedron* **2008,** *64,* 2740–2749. doi:10.1016/j.tet.2008.01.067
60. Quinn, K. J.; Curto, J. M.; Faherty, E. E.; Cammarano, C. M. *Tetrahedron Lett.* **2008,** *49,* 5238–5240. doi:10.1016/j.tetlet.2008.06.115
61. Vincent, G.; Kouklovsky, C. *Chem. – Eur. J.* **2011,** *17,* 2972–2980. doi:10.1002/chem.201002558
62. Vincent, G.; Karila, D.; Khalil, G.; Sancibrao, P.; Gori, D.; Kouklovsky, C. *Chem. – Eur. J.* **2013,** *19,* 9358–9365. doi:10.1002/chem.201300836
63. Sancibrao, P.; Karila, D.; Kouklovsky, C.; Vincent, G. *J. Org. Chem.* **2010,** *75,* 4333–4336. doi:10.1021/jo100768d
64. Standen, P. E.; Kimber, M. C. *Tetrahedron Lett.* **2013,** *54,* 4098–4101. doi:10.1016/j.tetlet.2013.05.112
65. Tsao, K.-W.; Devendar, B.; Liao, C.-C. *Tetrahedron Lett.* **2013,** *54,* 3055–3059. doi:10.1016/j.tetlet.2013.03.142
66. Lam, J. K.; Schmidt, Y.; Vanderwal, C. D. *Org. Lett.* **2012,** *14,* 5566–5569. doi:10.1021/ol302680m
67. Valiulin, R. A.; Arisco, T. M.; Kutateladze, A. G. *Org. Lett.* **2010,** *12,* 3398–3401. doi:10.1021/ol101297b
68. Barbe, G.; Fiset, D.; Charette, A. B. *J. Org. Chem.* **2011,** *76,* 5354–5362. doi:10.1021/jo200745n
69. Barbe, G.; Charette, A. B. *J. Am. Chem. Soc.* **2008,** *130,* 13873–13875. doi:10.1021/ja8068215
70. Jackson, K. L.; Henderson, J. A.; Motoyoshi, H.; Phillips, A. J. *Angew. Chem., Int. Ed.* **2009,** *48,* 2346–2350. doi:10.1002/anie.200806111
71. Escavabaja, P.; Viala, J.; Coquerel, Y.; Rodriguez, J. *Adv. Synth. Catal.* **2012,** *354,* 3200–3204. doi:10.1002/adsc.201200665

License and Terms

BEILSTEIN JOURNAL OF ORGANIC CHEMISTRY

Cross metathesis of unsaturated epoxides for the synthesis of polyfunctional building blocks

Meriem K. Abderrezak[1,2], Kristýna Šichová[2,3], Nancy Dominguez-Boblett[2,4], Antoine Dupé[2], Zahia Kabouche[1], Christian Bruneau[2] and Cédric Fischmeister[*2]

Full Research Paper

Open Access

Address:
[1]Université Frères Mentouri Constantine, Department of Chemistry, Laboratory of Therapeutic Substances Obtention (LOST), Chaabet Ersas Campus, 25000 Constantine, Algeria, [2]UMR6226 CNRS, Institut des Sciences Chimiques de Rennes, Université de Rennes 1, Organometallics: Materials and Catalysis, Centre for Catalysis and Green Chemistry, Campus de Beaulieu, 35042 Rennes Cedex, France, [3]Charles University in Prague, Faculty of Science, Department of Physical and Macromolecular Chemistry, Hlavova 2030, CZ-128 40 Prague, Czech Republic and [4]Faculty of Chemistry, University of Seville, E-41012 Seville, Spain

Email:
Cédric Fischmeister[*] - cedric.fischmeister@univ-rennes1.fr

* Corresponding author

Keywords:
cross metathesis; epoxide; ruthenium catalysts; tandem reactions

Beilstein J. Org. Chem. **2015,** *11,* 1876–1880.
doi:10.3762/bjoc.11.201

Received: 03 July 2015
Accepted: 15 September 2015
Published: 08 October 2015

This article is part of the Thematic Series "Progress in metathesis chemistry II".

Guest Editor: K. Grela

Abstract

The cross metathesis of 1,2-epoxy-5-hexene (**1**) with methyl acrylate and acrylonitrile was investigated as an entry to the synthesis of polyfunctional compounds. The resulting cross metathesis products were hydrogenated in a tandem fashion employing the residual ruthenium from the metathesis step as the hydrogenation catalyst. Interestingly, the epoxide ring remained unreactive toward this hydrogenation method. The saturated compound resulting from the cross metathesis of **1** with methyl acrylate was transformed by means of nucleophilic ring-opening of the epoxide to furnish a diol, an alkoxy alcohol and an amino alcohol in high yields.

Introduction

Catalytic carbon–carbon double bond transformations by olefin metathesis have significantly impacted organic and polymer synthesis over the last two decades [1-3]. If early works focused on ring-closing metathesis and ring-opening metathesis polymerization, progresses in catalysts performances [4,5] and selectivity have enabled the achievement of more challenging transformations such as cross metathesis reactions [6], stereoselective transformations [7] including the selective synthesis of *Z*-olefins [8-11]. Recently, the cross metathesis of renewable compounds with electron-deficient olefins was developed as a straightforward way for the synthesis of difunctional compounds suitable for polymer syntheses [12,13], fine chemicals [14-17], or as key synthetic tool in multistep syntheses of complex molecules [18-21]. Cross metathesis with functional

olefins is of great interest as it offers the possibility for post-transformation of the functional group. For example we have shown that cross metathesis with acrylonitrile run in a tandem fashion with hydrogenation delivered amine derivatives [22] whereas the tandem cross metathesis/hydrogenation with acrolein delivered the corresponding alcohols [23,24]. Nice examples of cross metathesis/non-metathesis sequences have also been reported by Andrade in 2011 [25].

In this article we present our results aimed at extending the scope of sequential transformations including cross metathesis to the synthesis of trifunctional compounds. Several examples involving the cross metathesis of a commercially available epoxide-containing olefin with methyl acrylate and acrylonitrile and their subsequent transformations leading to multifunctional building blocks are reported.

Results and Discussion

Cross metathesis reactions involving electron-deficient olefins are generally challenging transformations as they are substrate-dependent and therefore require optimization of experimental parameters. For instance, while cross metathesis with methyl acrylate turns out to be a rather straightforward transformation, cross metatheses with acrylonitrile, acrylamides or acrolein are much more demanding transformations [13,14,24]. We have investigated the reactivity of 1,2-epoxy-5-hexene (**1**) with methyl acrylate and acrylonitrile and further exploited the versatility of the epoxide ring to prepare trifunctional molecules by ring opening of the epoxide. To date, **1** has been scarcely used in olefin cross metathesis transformations. In some examples, Grela used **1** as a test substrate to evaluate the efficiency of new catalysts [26], and Cossy prepared vinyl functionalized oxazoles [27]. To our knowledge, the cross metathesis of **1** with electron-deficient olefins has not been reported. The cross metathesis of **1** with methyl acrylate was thus investigated under various conditions of solvents, catalysts and concentration (Scheme 1). As required in cross metathesis reactions of electron-deficient olefins, an excess of methyl acrylate was employed and a temperature of 80 °C was necessary to ensure high conversion. Reactions were carried out in dimethyl carbonate (DMC), a solvent compatible with ruthenium olefin metathesis catalysts [28] while being much greener than toluene or dichloromethane commonly used in such reactions [29]. Based on our previous results and observations in various cross metathesis reactions, the phosphine-free Hoveyda type second generation Zhan catalyst-1B [30] was selected to conduct this transformation. A recent study by Fogg rationalized the superiority of the Hoveyda catalyst vs the Grubbs catalyst in cross metathesis with acrylates showing that the phosphine could interact with the electron-deficient olefin leading to catalyst decomposition [31].

As observed by us and other groups in cross metathesis involving different substrates, double bond migration side-reactions took place during this transformation. This side reaction could be circumvented using benzoquinone [32] as an additive to decrease the extent of double-bond migration. As depicted in Table 1 (entries 1–4), 10 mol % of benzoquinone were necessary to ensure a limited amount (<10%) of side products resulting from double-bond migration. However, addition of benzoquinone resulted in slower reaction hence a catalyst loading of 2 mol % was necessary to restore full conversion within 2 h (Table 1, entry 4). In this case the product was isolated by distillation [33] in 69% yield as the sole *E*-isomer [34]. The transformation was sensitive to the concentration of the reagents and required a concentration of 0.5 M to operate with full conversion. This characteristic was previously observed in cross metathesis of fatty acid methyl esters with methyl acrylate [13]. Finally, neither toluene as solvent nor Hoveyda 2nd generation catalyst have led to improvements of the reaction performances (Table 1, entries 7 and 8).

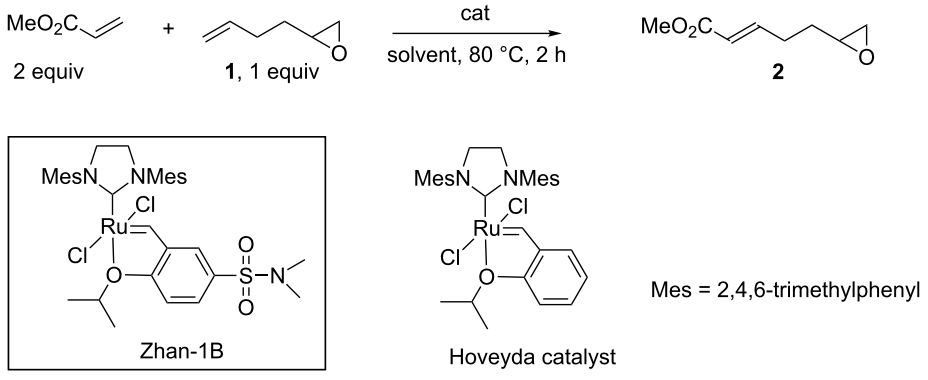

Scheme 1: Cross metathesis of **1** with methyl acrylate.

Table 1: Cross metathesis of **1** with methyl acrylate[a].

Entry	[**1**] (mol·L^{-1})	Cat. loading (mol %)	BQ[b] (mol %)	Conv. (%)[c] (yield %)[d]	% isom.[e]
1	0.5	1	5	100	13
2	0.5	2	5	100	15 (18)[f]
3	0.5	1	10	95	7.6
4	0.5	2	10	100 (69)	7
5	0.25	2	10	95	8
6	1	2	10	100	10
7[g]	0.5	2	10	100	8
8[h]	0.5	2	10	90	11

[a]0.11 mL of **1** (1 mmol), 0.18 mL of methyl acrylate (2 mmol), BQ, DMC, catalyst, 2 h; [b]benzoquinone; [c]determined by gas chromatography using dodecane as internal standard; [d]isolated yield; [e]determined by gas chromatography as ratio of ((isomerisation products)/(isomerisation products + **2**)) × 100; [f]reaction performed without benzoquinone; [g]in toluene; [h]Hoveyda 2nd gen. catalyst.

Similarly, the cross metathesis of **1** with acrylonitrile was conducted to furnish the bifunctional derivative **3** in 71% yield as a mixture of stereoisomers. In that case, high conversions and yields could only be obtained by means of slow addition of the catalyst and high dilution (Scheme 2) [13]. As we already observed, [13,14,22] together with other groups, [35,36] in various cross metathesis reactions involving acrylonitrile, the cross metathesis product **3** was obtained as a mixture of *E* (minor) and *Z* (major) stereoisomers.

With these two compounds in hands, we turned our attention to their post-metathesis transformations. First, we looked at the hydrogenation of the carbon–carbon double bond in compounds **2** and **3**. Typically, there are several ways to perform the hydrogenation of a carbon–carbon double bond resulting from a cross metathesis reaction. A possibility consists in the Pd/C catalyzed hydrogenation of the isolated product. This method presents the advantage of being effective at room temperature under a low hydrogen pressure [37,38]. However, such hydrogenations are in general carried out on purified products but more importantly in the present case, such conditions may result in the carbon–carbon double bond hydrogenation accompanied by ring opening of the epoxide leading to a mixture of primary and secondary alcohols [39]. A second and more straightforward method consists in the tandem metathesis/hydrogenation reaction where the residual ruthenium species arising from the metathesis step serve as the hydrogenation catalyst [13,22-24,40]. In general, this protocol requires higher temperature and pressure but it does not need additional costly catalyst and it can be performed without isolation of the intermediate olefin hence saving time and energy-consuming work-up procedures [41]. To the best of our knowledge, such a tandem procedure has not been applied to an epoxide containing olefin. Compound **2** was prepared as described here above (Scheme 1) and the reaction mixture was directly transferred into a high pressure reactor without any work-up. Remarkably, following the hydrogenation step carried out under 20 bar of hydrogen at 50 °C, the ^{1}H NMR of the crude reaction mixture revealed the presence of the epoxide moiety without any traces of alcohol. This tandem procedure delivered the saturated compound **4** in a satisfactory 53% yield for two steps (Scheme 3). The tandem cross metathesis of **1** with acrylonitrile followed by hydrogenation of the intermediate compound **3** was conducted similarly. In this case a higher hydrogen pressure (45 bar) was necessary to reduce the carbon–carbon double bond. Nevertheless, under these conditions, the epoxide-containing product **5** was isolated in a satisfactory 46% yield for two steps without any traces of alcohol detected in the crude ^{1}H NMR of the reaction.

With this protocol secured, we turned our attention to the synthesis of useful polyfunctional building blocks. Thus far, the post-transformation of the electron- deficient olefin cross

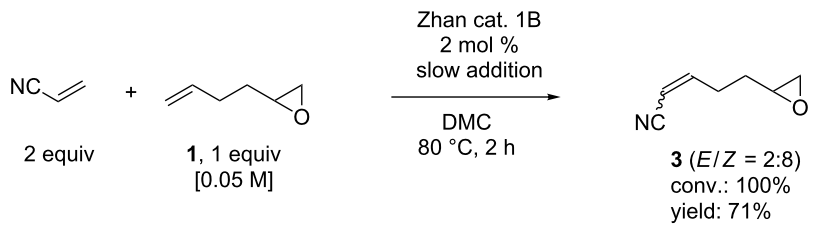

Scheme 2: Cross metathesis of **1** with acrylonitrile.

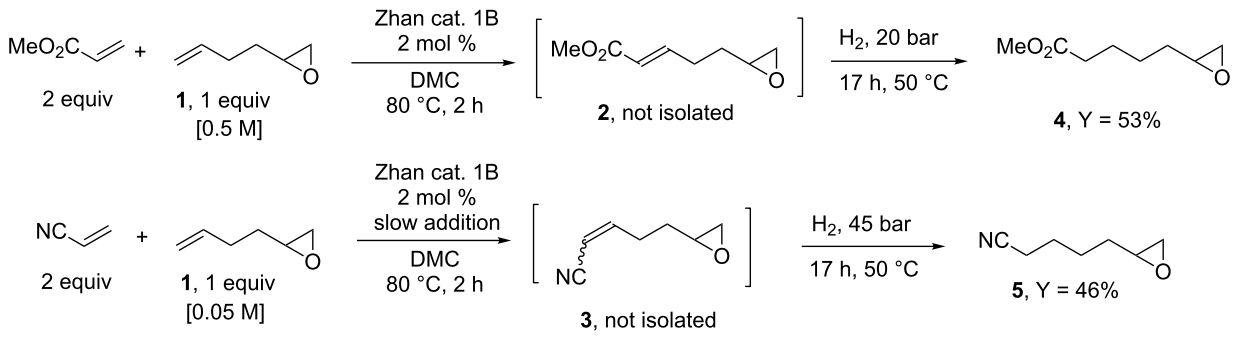

Scheme 3: Tandem cross metathesis/hydrogenation.

metathesis partner has received attention for the synthesis of polymer precursors. For instance, we have reported the reduction of the nitrile functional group into primary amine [22] and the reduction of the formyl group into alcohol [23,24]. Herein, we focused on the post-transformation of **4** by ring-opening of the epoxide moiety. The diol **6**, methoxy alcohol **7** and amino alcohol **8** were thus prepared by reacting **4** with water, sodium methoxide and aniline, respectively (Scheme 4). The synthesis of **6** proceeded cleanly and did not require any purification procedure (see Supporting Information File 1). Similarly, the synthesis of **7** proceeded cleanly and delivered a single regioisomer **7** in quantitative yield. Finally, the amino alcohol **8** was also obtained as a single regioisomer in 61% yield (Scheme 4).

Conclusion

We have shown through selected examples that cross metathesis of an epoxide containing olefin with electron-deficient olefins constitutes a versatile entry towards trifunctional building blocks by ring-opening of the epoxide. We have shown that the tandem cross metathesis/C=C hydrogenation yielded the hydrogenated compound without altering the epoxide moiety that was further efficiently transformed into a 1,2-diol, a 1,2-alkoxy alcohol and a 1,2-amino alcohol. This strategy opens the way for numerous potential transformations involving the epoxide but also the functional group of the electron-deficient olefin. In particular, lactones should be accessible by intramolecular *trans*-esterification from **6**, **7** and **8**, as well as cyclic amines by intramolecular cyclization involving primary amine resulting from hydrogenation of the nitrile functionality in **5**. All these aspects will be further developed in our group.

Supporting Information

Supporting Information File 1

Full experimental details and characterizations.
[http://www.beilstein-journals.org/bjoc/content/supplementary/1860-5397-11-201-S1.pdf]

Acknowledgements

The authors are grateful to the Region Bretagne and ADEME for a Ph.D. grant to A. D. and to MESRS (Algeria) for a grant to M. K. A. We also acknowledge the European Erasmus+ programme for grants to K. S. and N. D.-B.

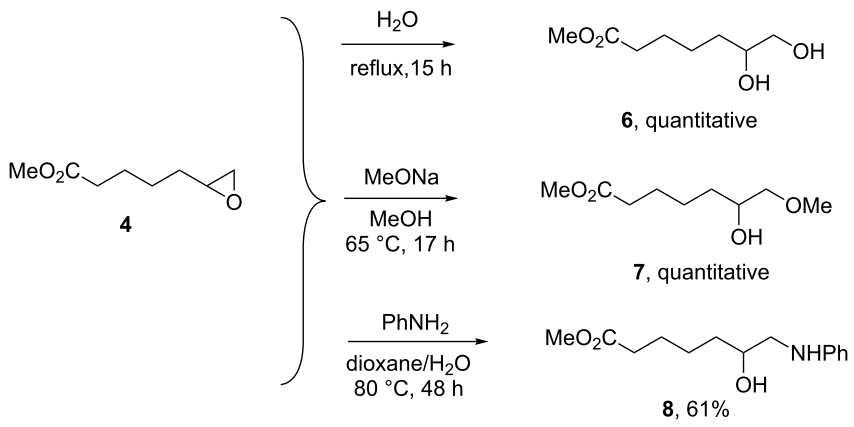

Scheme 4: Trifunctional compounds obtained by ring-opening of epoxide **4**.

References

1. Grubbs, R. H.; Wenzel, A. G.; O'Leary, D. J.; Khosravi, E., Eds. *Handbook of metathesis;* Wiley-VCH: Weinheim, Germany, 2015; Vol. 1–3. doi:10.1002/9783527674107
2. Grela, K., Ed. *Olefin Metathesis, Theory and Practice;* John Wiley & Sons, Inc.: Hoboken, NJ, U.S.A., 2014.
3. Mutlu, H.; Montero de Espinosa, L.; Meier, M. A. R. *Chem. Soc. Rev.* **2011,** *40,* 1404–1445. doi:10.1039/B924852H
4. Vougioukalakis, G. C.; Grubbs, R. H. *Chem. Rev.* **2010,** *110,* 1746–1787. doi:10.1021/cr9002424
5. Samojłowicz, C.; Bieniek, M.; Grela, K. *Chem. Rev.* **2009,** *109,* 3708–3742. doi:10.1021/cr800524f
6. Connon, S. J.; Blechert, S. *Angew. Chem., Int. Ed.* **2003,** *42,* 1900–1923. doi:10.1002/anie.200200556
7. Hoveyda, A. H.; Malcolmson, S. J.; Meek, S. J.; Zhugralin, A. R. *Angew. Chem., Int. Ed.* **2010,** *49,* 34–44. doi:10.1002/anie.200904491
8. Shahane, S.; Bruneau, C.; Fischmeister, C. *ChemCatChem* **2013,** *5,* 3436–3459. doi:10.1002/cctc.201300688
9. Fürstner, A. *Science* **2013,** *341,* No. 1229713. doi:10.1126/science.1229713
10. Herbert, M. B.; Grubbs, R. H. *Angew. Chem., Int. Ed.* **2015,** *54,* 5018–5024. doi:10.1002/anie.201411588
11. Ibrahem, I.; Yu, M.; Schrock, R. R.; Hoveyda, A. H. *J. Am. Chem. Soc.* **2009,** *131,* 3844–3845. doi:10.1021/ja900097n
12. Rybak, A.; Meier, M. A. R. *Green Chem.* **2007,** *9,* 1356–1361. doi:10.1039/b712293d
13. Miao, X.; Malacea, R.; Fischmeister, C.; Bruneau, C.; Dixneuf, P. H. *Green Chem.* **2011,** *13,* 2911–2919. doi:10.1039/c1gc15569e
14. Bilel, H.; Hamdi, N.; Zagrouba, F.; Fischmeister, C.; Bruneau, C. *RSC Adv.* **2012,** *2,* 9584–9589. doi:10.1039/c2ra21638h
15. Lummiss, J. A. M.; Oliveira, K. C.; Pranckevicius, A. M. T.; Santos, A. G.; dos Santos, E. N.; Fogg, D. E. *J. Am. Chem. Soc.* **2012,** *134,* 18889–18891. doi:10.1021/ja310054d
16. Borré, E.; Dinh, T. H.; Caijo, F.; Crévisy, C.; Mauduit, M. *Synthesis* **2011,** 2125–2130. doi:10.1055/s-0030-1260605
17. Bilel, H.; Hamdi, N.; Zagrouba, F.; Fischmeister, C.; Bruneau, C. *Green Chem.* **2011,** *13,* 1448–1452. doi:10.1039/c1gc15024c
18. Prunet, J. *Curr. Top. Med. Chem.* **2005,** *5,* 1559–1577. doi:10.2174/156802605775009801
19. Commandeur, M.; Commandeur, C.; Cossy, J. *Org. Lett.* **2011,** *13,* 6018–6021. doi:10.1021/ol202483u
20. Hume, P. A.; Sperry, J.; Brimble, M. A. *Org. Biomol. Chem.* **2011,** *9,* 5423–5430. doi:10.1039/c1ob05595j
21. Wang, S.-Y.; Song, P.; Chan, L.-Y.; Loh, T.-P. *Org. Lett.* **2010,** *12,* 5166–5169. doi:10.1021/ol102177j
22. Miao, X.; Fischmeister, C.; Bruneau, C.; Dixneuf, P. H.; Dubois, J.-L.; Couturier, J.-L. *ChemSusChem* **2012,** *5,* 1410–1414. doi:10.1002/cssc.201200086
23. Miao, X.; Malacea, R.; Fischmeister, C.; Bruneau, C.; Dixneuf, P. H. *ChemSusChem* **2009,** *2,* 542–545. doi:10.1002/cssc.200900028
24. Bonin, H.; Keraani, A.; Dubois, J.-L.; Brandhorst, M.; Fischmeister, C.; Bruneau, C. *Eur. J. Lipid Sci. Technol.* **2015,** *117,* 209–216. doi:10.1002/ejlt.201400362
25. Sirasani, G.; Paul, T.; Andrade, R. B. *Tetrahedron* **2011,** *67,* 2197–2205. doi:10.1016/j.tet.2011.01.080
26. Kirschning, A.; Gułajski, Ł.; Mennecke, K.; Meyer, A.; Busch, T.; Grela, K. *Synlett* **2008,** *17,* 2692–2696. doi:10.1055/s-0028-1083512
27. Hoffman, T. J.; Rigby, J. H.; Arseniyadis, S.; Cossy, J. *J. Org. Chem.* **2008,** *73,* 2400–2403. doi:10.1021/jo702305g
28. Miao, X.; Fischmeister, C.; Bruneau, C.; Dixneuf, P. H. *ChemSusChem* **2008,** *1,* 813–816. doi:10.1002/cssc.200800074
29. Henderson, R. K.; Jiménez-González, C.; Constable, D. J. C.; Alston, S. R.; Inglis, G. G. A.; Fisher, G.; Sherwood, J.; Binks, S. P.; Curzons, A. D. *Green Chem.* **2011,** *13,* 854–862. doi:10.1039/c0gc00918k
30. Zhan, Z.-Y. Ruthenium complex ligand, ruthenium complex and the use of the complex as a catalyst in olefin metathesis reactions, Priority 04/07/2005. CN 2005180379.
31. Bailey, G. A.; Fogg, D. E. *J. Am. Chem. Soc.* **2015,** *137,* 7318–7321. doi:10.1021/jacs.5b04524
32. Hong, S. H.; Sanders, D. P.; Lee, C. W.; Grubbs, R. H. *J. Am. Chem. Soc.* **2005,** *127,* 17160–17161. doi:10.1021/ja052939w
33. Purification by column chromatography on silica gel resulted in very poor yields likely due to epoxide decomposition.
34. In some cases, up to 5% *Z*-isomer was detected by ^{1}H NMR.
35. Zhang, W.; Zhang, R.; He, R. *Tetrahedron Lett.* **2007,** *48,* 4203–4207. doi:10.1016/j.tetlet.2007.04.065
36. Bieniek, M.; Bujok, R.; Cabaj, M.; Lugan, N.; Lavigne, G.; Arlt, D.; Grela, K. *J. Am. Chem. Soc.* **2006,** *128,* 13652–13653. doi:10.1021/ja063186w
37. Aihara, K.; Komiya, C.; Shikenaga, A.; Inokuma, T.; Takahashi, D.; Otaka, A. *Org. Lett.* **2014,** *17,* 696–699. doi:10.1021/ol503718j
38. Yadav, J. S.; Vishnu Murthy, P. *Synthesis* **2011,** *13,* 2117–2124. doi:10.1055/s-0030-1260058
39. Sajiki, H.; Hattori, K.; Hirota, K. *Chem. – Eur. J.* **2000,** *6,* 2200–2204. doi:10.1002/1521-3765(20000616)6:12<2200::AID-CHEM2200>3.0.CO;2-3
40. Fürstner, A.; Leitner, A. *Angew. Chem., Int. Ed.* **2003,** *42,* 308–311. doi:10.1002/anie.200390103
    See for an early example.
41. Zieliński, G. K.; Samojłowicz, C.; Wdowik, T.; Grela, K. *Org. Biomol. Chem.* **2015,** *13,* 2684–2688. doi:10.1039/C4OB02480J
    Recent report of metathesis/hydrogenation under milder transfer hydrogenation conditions.

License and Terms

BEILSTEIN JOURNAL OF ORGANIC CHEMISTRY

Profluorescent substrates for the screening of olefin metathesis catalysts

Raphael Reuter and Thomas R. Ward*

Full Research Paper

Open Access

Address:
Department of Chemistry, University of Basel, Spitalstrasse 51, CH-4056 Basel, Switzerland

Email:
Thomas R. Ward* - thomas.ward@unibas.ch

* Corresponding author

Keywords:
fluorescence; microplate screening; ring closing metathesis

Beilstein J. Org. Chem. **2015,** *11,* 1886–1892.
doi:10.3762/bjoc.11.203

Received: 18 June 2015
Accepted: 15 September 2015
Published: 12 October 2015

This article is part of the Thematic Series "Progress in metathesis chemistry II".

Guest Editor: K. Grela

Abstract

Herein we report on a 96-well plate assay based on the fluorescence resulting from the ring-closing metathesis of two profluorophoric substrates. To demonstrate the validity of the approach, four commercially available ruthenium-metathesis catalysts were evaluated in six different solvents. The results from the fluorescent assay agree well with HPLC conversions, validating the usefulness of the approach.

Introduction

Since its discovery in the 1950s, olefin metathesis has developed into one of the most powerful catalytic reactions both in research as well as in industrial applications [1-3]. This is mostly due to its excellent chemoselectivity, tolerance of many functional groups and its atom economy [4]. Chemists treasure its extraordinary versatility. From the production of polymers [5,6] and petrochemicals to the synthesis of complex natural products [7], olefin metathesis has been established as a useful tool for solving numerous synthetic challenges. In more recent applications, metathesis has also been used in chemical biology, either in the form of an artificial metalloenzyme [8-10] or for the post-translational modification of proteins [11]. To address these various challenges, a vast number of carbene complexes based on different transition metals have been prepared and tailored towards specific applications [12]. With the ultimate aim of identifying new olefin metathesis catalysts using high-throughput screening, we set out to develop and evaluate olefinic substrates amenable to a 96-well plate screening format.

Results and Discussion

A quick and highly sensitive analytical method that is suitable for the fast detection and quantification of small quantities of a product is fluorescence spectroscopy. In particular, biological applications heavily rely on fluorescence-based visualization techniques [13]. For this purpose, a large variety of fluorescent

probes have been developed that react to different chemical stimuli [14]. Although previous work on the development of fluorescent olefin metathesis catalysts [15,16] exists, to our knowledge, the concept of fluorescent probes based on ring-closing metathesis is new and could be of value to chemical biologists. Since microplates are a very common and practical tool for biological applications, we developed a screening assay in 96-well plate format to quickly evaluate the reaction kinetics of different commercially available metathesis catalysts. Since fluorescence spectroscopy is a highly sensitive technique, we aimed at using a low catalyst concentration (e.g., 100 µM) in a small reaction volume (150 µL). With this format, only 1 mg of catalyst is required to perform fifty to a hundred kinetic experiments.

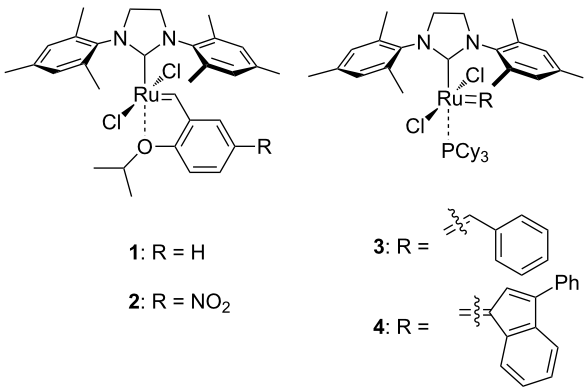

Figure 1: Catalysts **1–4** tested for the metathesis of profluorescent substrates.

For this proof-of-principle study, we selected four commercially available, second generation-type catalysts **1–4** (Figure 1). These catalysts were mainly chosen because of their high stability towards both air and moisture. Catalysts **1** and **2** are the phosphine-free Grubbs–Hoveyda and Grela-type catalysts bearing different isopropoxystyrene ligands. Catalysts **3** and **4** are phosphine-containing Grubbs-type catalysts with either a benzylidene ligand or an indenylidene ligand.

As a model reaction, we selected ring-closing metathesis and developed two profluorescent substrates that yield a fluorescent product upon ring-closing metathesis (Scheme 1). Substrate **5** consists of a fluorescent 5-methoxynaphthalene-1-sulfonamide moiety that is connected by an internal double bond to a 2,4-dinitroaniline core, acting as a fluorescence quencher [17]. Both the sulfonamide of the fluorophore and the aniline group of the quencher bear another allyl group. Upon relay ring-closing metathesis, the fluorophore and quencher are disconnected resulting in the fluorescent product **7**. A similar linker concept has previously been implemented for a solid-phase linker in the synthesis of oligosaccharides [18,19]. The second profluorescent molecule selected was diolefin **8**, which yields fluorescent 7-hydroxycoumarin (umbelliferone) (**9**) upon ring-closing metathesis. The synthesis of coumarin derivatives using this approach was described in previous publications [20,21]. By introducing an electron donor in the 7-position, a fluorescent product is obtained upon ring-closing metathesis [22].

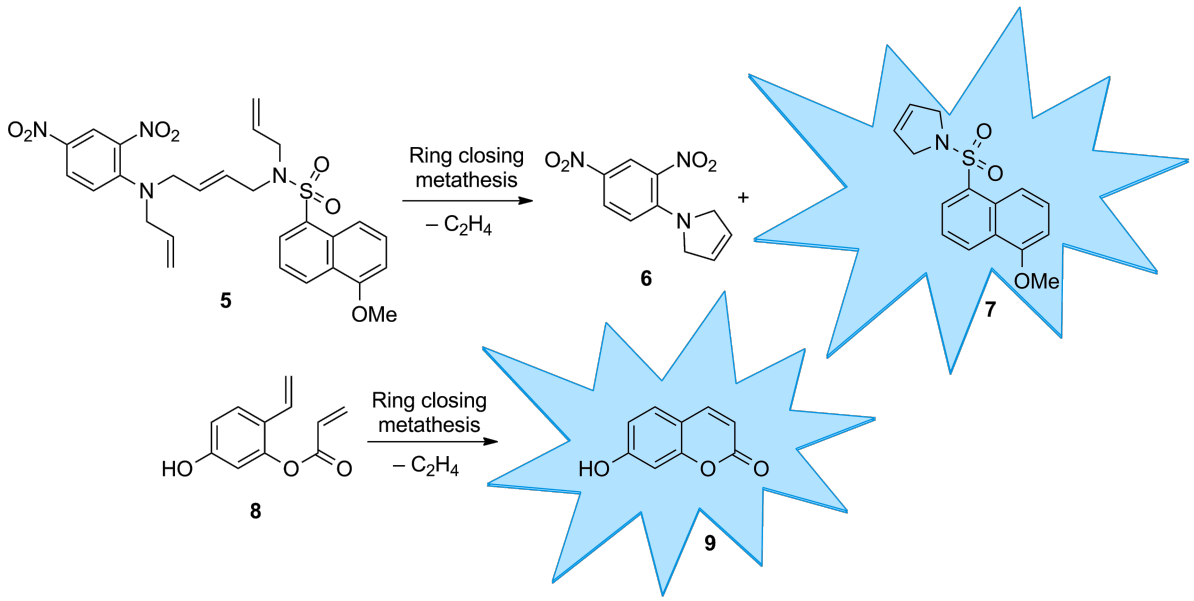

Scheme 1: Two profluorescent substrates yielding fluorescent products upon ring-closing metathesis.

Synthesis of the profluorescent substrates

The synthesis of profluorescent substrate **8** leading to umbelliferone after ring-closing metathesis was carried out according to a published, four-step procedure starting from 2,4-dihydroxybenzaldehyde (**10**) with an overall yield of 50% [23,24]. The synthesis of the fluorophore–quencher substrate **5** was achieved relying on two converging synthons (Scheme 2). The fluorophore part of the molecule was synthesized starting from sodium 5-methoxynaphthalene-1-sulfonate (**11**), which was prepared according to a known procedure [25]. It was then transformed to the corresponding allyl sulfonamide **12** by reacting the corresponding acid chloride with allylamine. The quencher part of the molecule was prepared from commercial 1-fluoro-2,4-dinitrobenzene (**13**). Following an alkylation step with allyl bromide, it was reacted with an excess of (*E*)-1,4-dibromobut-2-ene to selectively afford the mono alkylated product. A strong base (e.g., NaH) was crucial to achieve complete deprotonation of the highly deactivated aniline [26]. The fluorophore and quencher parts were finally connected in high yield relying on a nucleophilic substitution.

Ring-closing metathesis of substrates

With the aim of miniaturizing and automatizing the screening effort for the identification of ring-closing metathesis catalysts, a 96-well plate format screening was developed, relying on a total volume of 150 µL per experiment and 100 µM catalyst in the presence of 10 mM substrate. To demonstrate the versatility of the method, the kinetics of the ring-closing metathesis with umbelliferone precursor **8** were determined with different catalysts **1**–**4** (Figure 2). It is known that acryloyl ester substrates are poor substrates which typically give low yields with 1st generation precatalysts [27]. As the reactions were performed in air and with very small volumes, high boiling solvents with different structural features were selected. From the screening, the following features were apparent:

1. Grubbs–Hoveyda and Grela catalysts **1** and **2** perform better for substrate **8** in most solvents.
2. For solvents that contain a carbonyl or carboxyl function (i.e., 2-methylpentanone and γ-butyrolactone), the Grubbs 2nd generation catalyst **3** performs best.
3. In all cases, the initial ring-closing metathesis rates are highest with precatalyst **2**.

The same experiments were conducted with the fluorophore–quencher substrate **5** (Figure 3). In this case, the concentration of the substrate was reduced to 1 mM to miminize intermolecular quenching of fluorophore **7** by dinitroaniline **6**.

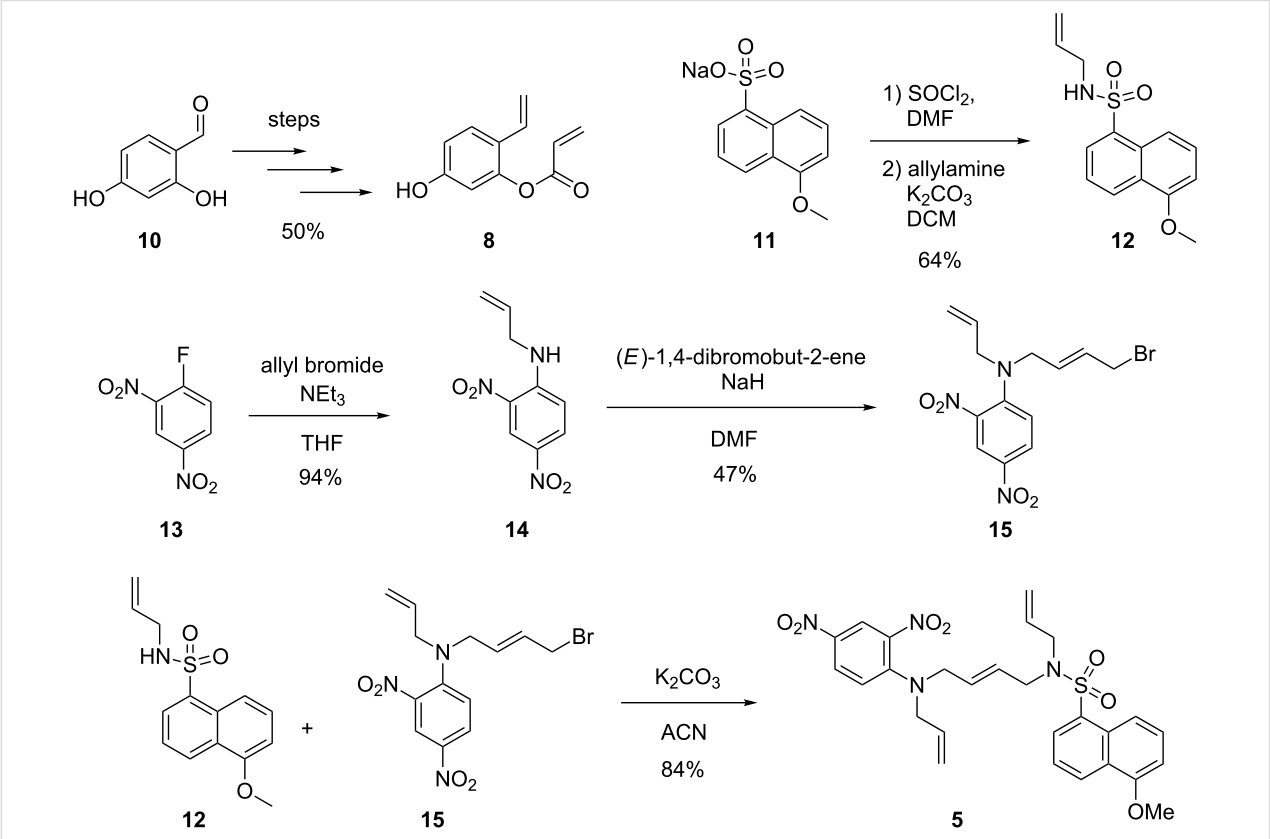

Scheme 2: Synthesis of the two profluorescent substrates amenable to ring-closing metathesis.

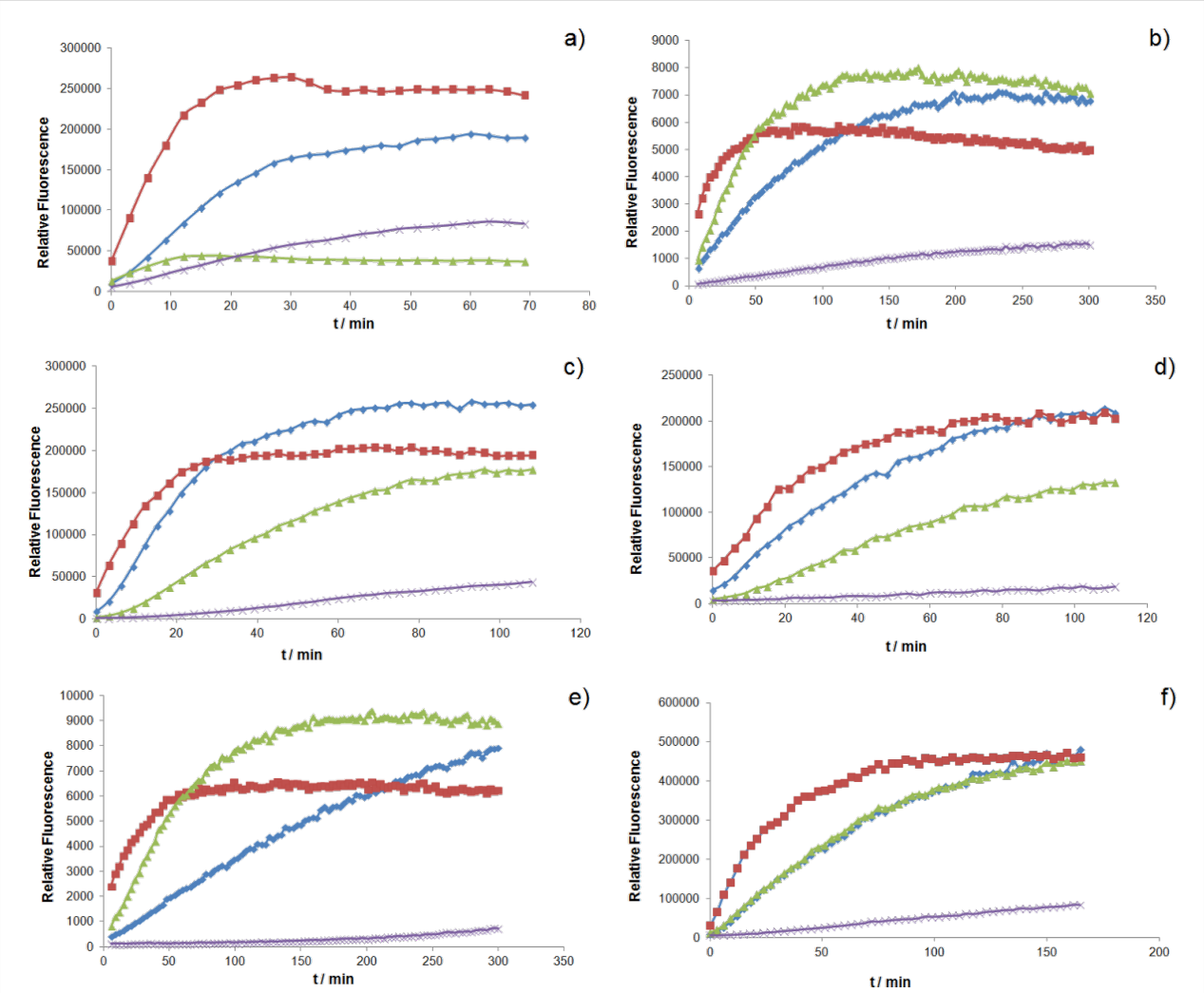

Figure 2: Fluorescence evolution resulting from closing metathesis of umbelliferone precursor **8** ($\lambda_{excitation}$ = 350 nm and $\lambda_{emission}$ = 380 nm). Different catalysts **1**–**4** (**1**: blue; **2**: red; **3**: green; **4**: purple) were screened in different solvents (a: acetic acid; b: 2-methylpentanone; c: toluene; d: *o*-xylene; e: γ-butyrolactone; f: anisole).

The following observations can be made:

1. Generally, a higher activity is observed for the Grubbs 2nd generation catalyst **3** as compared to the umbelliferone substrate **8**. The only exception is when acetic acid is used as the solvent.
2. The catalyst **4**, being nearly inactive for the electron-poor substrate **8**, showed increased activity for substrate **5**, especially in acetic acid.
3. Surprisingly, catalyst **1** was (one of) the worst performing for this bulky substrate.

To validate the kinetics determined by fluorescence, the reaction progress was monitored by HPLC for umbelliferone precursor **8** in acetic acid (Figure 4). Gratifyingly, both the fluorescence and HPLC techniques result in very similar trends.

Conclusion

In summary, two profluorescent substrates, **5** and **8**, were prepared and fully characterized. Upon ring-closing metathesis, they produce a fluorescent signal thus allowing a straightforward screening in a 96-well plate format. The validity of the approach was demonstrated by screening four commercially available catalysts **1**–**4** in different solvents. Comparison between the kinetics determined by HPLC and fluorescence showed good agreement. These profluorescent substrates could be prototypes for more complex structures that could find applications in ring-closing metathesis for biological applications by fluorescence microscopy.

Experimental

General Methods: The ^{1}H and ^{13}C NMR spectra were recorded on Bruker 400 MHz and 500 MHz spectrometers. The

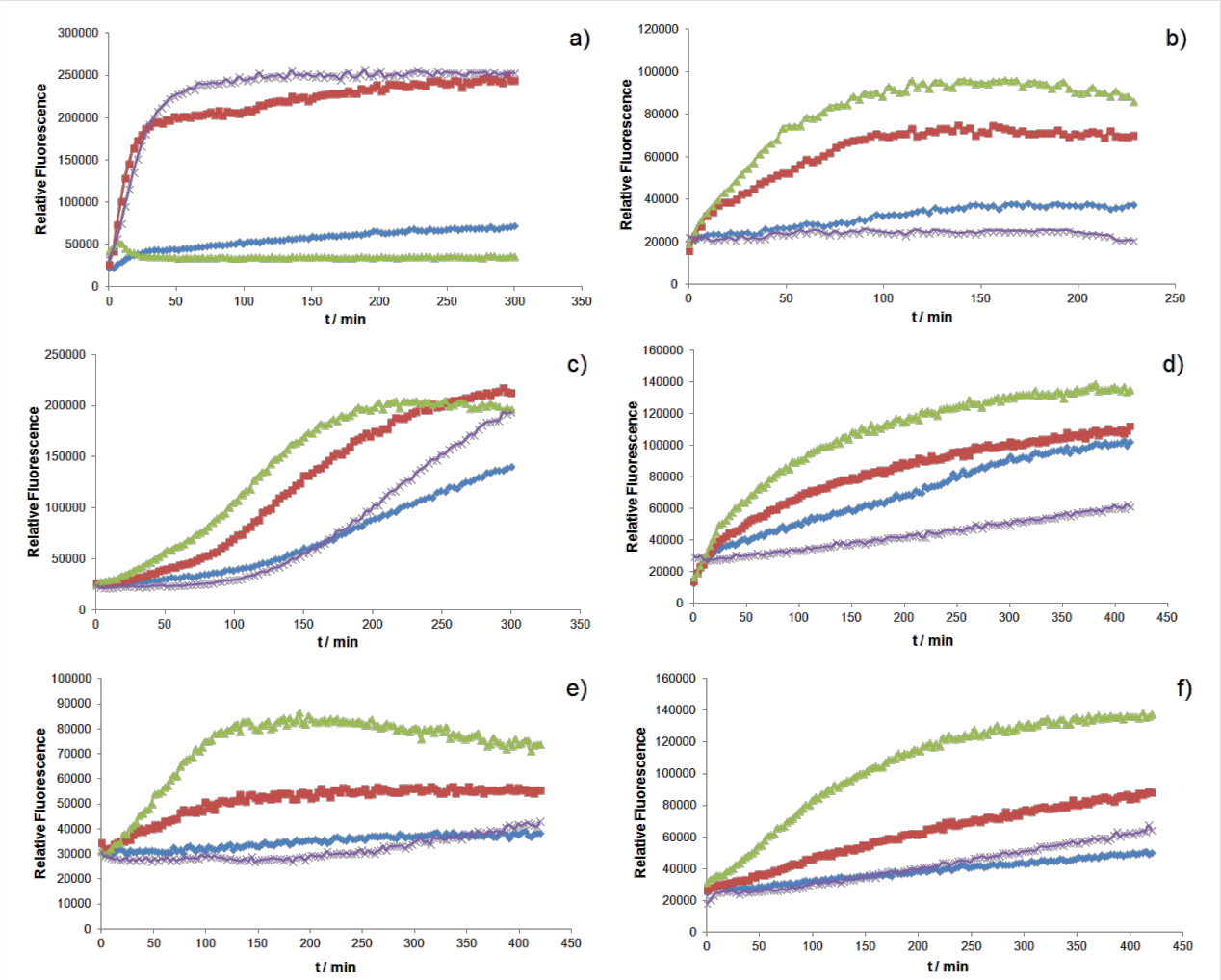

Figure 3: Fluorescence evolution resulting from closing metathesis of fluorescence–quencher substrate **5** ($\lambda_{excitation}$ = 320 nm and $\lambda_{emission}$ = 400 nm). Different catalysts **1**–**4** (**1**: blue; **2**: red, **3**: green, **4**: purple) were screened in different solvents (a: acetic acid; b: 2-methylpentanone; c: toluene; d: *o*-xylene; e: γ-butyrolactone; f: anisole).

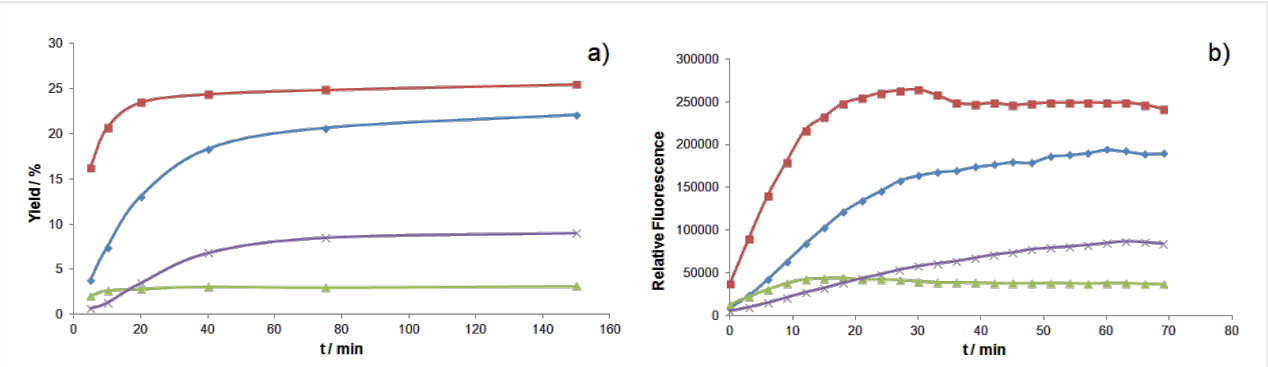

Figure 4: Comparison of kinetics measured by HPLC a) and by a plate reader b) for the ring-closing metathesis of **8** in acetic acid.

chemical shifts are reported in ppm (parts per million). Electrospray ionization mass spectra (ESIMS) were recorded on a Bruker FTMS 4.7T bioAPEX II spectrometer. HRMS was measured on a Bruker maXis 4G QTOF-ESI spectrometer. HPLC was conducted on a Waters Acquity H-Class Bio UPLC device, using a BEH C-18 reversed-phase column. Starting ma-

terials and reagents were purchased from commercial sources and used without further purification. HPLC grade solvents were used if not mentioned otherwise. For the fluorescence measurements, a TECAN Infinite M1000 platereader was used.

***N*-Allyl-5-methoxynaphthalene-1-sulfonamide (12).** To a DMF solution (30 mL) of sodium 5-methoxynaphthalene-1-sulfonate (**11**, 1.30 g, 5.00 mmol, 1.00 equiv), cooled on an ice bath, thionyl chloride (1.09 mL, 15.0 mmol, 3.00 equiv) was added dropwise. After the complete addition, the ice bath was removed and the reaction was stirred at rt for 3 h. Then, it was poured onto 300 mL of ice water and extracted with ethyl acetate (3 × 100 mL). The combined extracts were dried over $MgSO_4$ and the solvent was removed at reduced pressure. The residual oil was taken up into DCM (100 mL). Allylamine was slowly added to the solution, while stirring. After complete addition, the reaction mixture was allowed to stir overnight. The solvent was removed under vacuum and the residue was purified by flash column chromatography (silica gel, cyclohexane/EtOAc 1:1) to obtain a colourless solid (893 mg, 64%). ^{1}H NMR (400 MHz, $CDCl_3$) δ 8.46 (d, $^3J_{HH}$ = 8.4 Hz, 1H), 8.22 (d, $^3J_{HH}$ = 8.7 Hz, 1H), 8.15 (s, 1H), 8.14 (d, $^3J_{HH}$ = 7.3 Hz, 1H), 7.66–7.58 (m, 2H), 7.13 (d, $^3J_{HH}$ = 7.6 Hz, 1H), 5.56 (ddt, $^3J_{HH}$ = 17.1 Hz, $^3J_{HH}$ = 10.3 Hz, $^3J_{HH}$ = 5.5 Hz, 1H), 5.05 (ddt, $^3J_{HH}$ = 17.1 Hz, $^2J_{HH}$ = 1.7 Hz, $^4J_{HH}$ = 1.7 Hz, 1H), 4.91 (ddt, $^3J_{HH}$ = 10.3 Hz, $^2J_{HH}$ = 1.5 Hz, $^4J_{HH}$ = 1.5 Hz, 1H), 4.01 (s, 3H), 3.45 (d, $^3J_{HH}$ = 5.5 Hz); ^{13}C NMR (100 MHz, $CDCl_3$) δ 155.1, 135.6, 134.2, 128.8, 128.6, 128.3, 126.9, 125.7, 123.8, 116.8, 116.2, 105.4, 55.9, 44.8; HRMS [ESI(+)–TOF] *m*/*z*: $[M + H]^+$ calcd for $C_{14}H_{16}NO_3S$, 278.0851; found, 278.0845; Elemental analysis: anal. calcd for $C_{14}H_{15}NO_3S$: C, 60.63; H, 5.45; N, 5.05; found: C, 60.48; H, 5.58; N, 5.25.

***N*-Allyl-2,4-dinitroaniline (14).** A flask was charged with 2,4-dinitrofluorobenzene (**13**, 854 mg, 4.59 mmol, 1.00 equiv) and THF (10 mL). First, triethylamine (710 µL, 5.05 mmol, 1.10 equiv) and then allylamine (378 µL, 5.05 mmol, 1.10 equiv) was added and the mixture was stirred for 2 h at rt until the TLC showed complete consumption. The solvent was removed under reduced pressure and the residue was purified by flash chromatography (silica gel, cyclohexane/EtOAc 3:1) to obtain 960 mg of a yellow solid (94%). ^{1}H NMR (400 MHz, $CDCl_3$) δ 9.15 (d, $^4J_{HH}$ = 2.7 Hz, 1H), 8.69 (bs, 1H), 8.27 (dd, $^3J_{HH}$ = 9.5 Hz, $^4J_{HH}$ = 2.7 Hz, 1H), 6.92 (d, $^3J_{HH}$ = 9.5 Hz, 1H), 5.96 (ddt, $^3J_{HH}$ = 17.3 Hz, $^3J_{HH}$ = 10.2 Hz, $^3J_{HH}$ = 5.1 Hz, 1H), 5.39–5.30 (m, 1H), 4.13–4.08 (m, 1H); ^{13}C NMR (100 MHz, $CDCl_3$) δ 148.3, 136.4, 131.6, 130.6, 130.3, 124.2, 118.3, 114.3, 45.7; HRMS [ESI(+)–TOF] *m*/*z*: $[M + H]^+$calcd for $C_9H_{10}N_3O_4$, 224.0671; found, 224.0663. Elemental analysis: anal. calcd for $C_9H_9N_3O_4$: C, 48.43; H, 4.06; N, 18.83; found: C, 48.26; H, 4.15; N, 19.08.

(*E*)-*N*-Allyl-*N*-(4-bromobut-2-en-1-yl)-2,4-dinitroaniline (15). To a solution of *N*-allyl-2,4-dinitroaniline (**14**, 400 mg, 1.79 mmol, 1.00 equiv) in dry DMF (7 mL), NaH (60% in mineral oil, 143 mg, 3.58 mmol, 2.00 equiv) and (*E*)-1,4-dibromobut-2-ene (1.53 g, 7.16 mmol, 4.00 equiv) were added. The mixture was stirred at 70 °C for 16 h. The mixture was diluted with EtOAc (50 mL), washed with water (2 × 50 mL) and dried over $MgSO_4$. The solvent was removed under vacuum and the residue was purified by flash column chromatography (silica gel, cyclohexane/EtOAc 5:1) to obtain 300 mg of red oil (47%). ^{1}H NMR (400 MHz, $CDCl_3$) δ 8.66 (d, $^4J_{HH}$ = 2.7 Hz, 1H), 8.21 (dd, $^3J_{HH}$ = 9.4 Hz, $^4J_{HH}$ = 2.7 Hz, 1H), 7.09 (d, $^3J_{HH}$ = 9.4 Hz, 1H), 5.99–5.87 (m, 1H), 5.86–5.70 (m, 2H), 5.33 (d, $^3J_{HH}$ = 10.3 Hz, 1H), 5.28 (d, $^3J_{HH}$ = 17.2 Hz, 1H), 3.86–3.90 (m, 6H); ^{13}C NMR (100 MHz, $CDCl_3$) δ 148.1, 137.9, 137.7, 131.8, 131.3, 128.4, 127.7, 123.7, 120.1, 119.4, 54.6, 53.2, 31.0; HRMS [ESI(+)–TOF] *m*/*z*: $[M + H]^+$ calcd for $C_{13}H_{15}BrN_3O_4$, 356.0246; found, 356.0239.

Substrate 5. A round bottom flask was charged with *N*-allyl-5-methoxynaphthalene-1-sulfonamide (**12**, 449 mg, 1.62 mmol, 1.00 equiv), (*E*)-*N*-allyl-*N*-(4-bromobut-2-en-1-yl)-2,4-dinitroaniline (**15**, 610 mg, 1.71 mmol, 1.06 equiv), K_2CO_3 (672 mg, 4.86 mmol, 3.00 equiv) and acetonitrile (20 mL). The mixture was stirred at 70 °C overnight and filtered. The filtrate was concentrated at reduced pressure and the residue was purified by flash column chromatography (silica gel, cyclohexane/EtOAc 3:1) to obtain 750 mg of an orange semi-solid (84%). ^{1}H NMR (400 MHz, $CDCl_3$) δ 8.60 (d, $^4J_{HH}$ = 2.7 Hz, 1H), 8.52 (d, $^3J_{HH}$ = 8.4 Hz, 1H), 8.26 (dd, $^3J_{HH}$ = 7.4 Hz, $^4J_{HH}$ = 1.3 Hz, 1H), 8.14–8.08 (m, 2H), 7.55–7.46 (m, 2H), 6.94–6.86 (m, 2H), 5.72–5.34 (m, 4H), 5.26 (d, $^3J_{HH}$ = 10.3 Hz, 1H), 5.17 (d, $^3J_{HH}$ = 17.1 Hz, 1H), 5.14–5.05 (m, 2H), 4.03 (s, 3H), 3.86 (dd, $^3J_{HH}$ = 17.7 Hz, $^3J_{HH}$ = 6.1 Hz, 4H), 3.74 (dd, $^3J_{HH}$ = 17.8 Hz, $^3J_{HH}$ = 5.3 Hz, 4H); ^{13}C NMR (100 MHz, $CDCl_3$) δ 155.8, 147.9, 137.6, 137.4, 134.3, 132.7, 131.4, 130.8, 129.9, 129.5, 128.41, 128.39, 127.61, 127.55, 126.7, 123.6, 123.3, 120.0, 119.3, 119.1, 116.8, 104.8, 55.7, 54.5, 53.2, 49.1, 47.1; HRMS [ESI(+)–TOF]: $[M + H]^+$ calcd for $C_{27}H_{29}N_4O_7S$, 553.1757; found, 553.1756; Elemental analysis: anal. calcd for $C_{27}H_{28}N_4O_7S$: C, 58.69; H, 5.11; N, 10.14; found: C, 58.83; H, 5.45; N, 10.15.

Ring-closing metathesis in 96-well plates: To each well, 142 µL of the selected solvent (cooled at 5 °C to minimize evaporation) was pipetted. Then, 5 µL of a 3 mM precatalyst stock solution was added. Finally, 3 µL of the substrate stock solution was added (for the coumarin substrate **8** a 1 M stock solution was used, for the fluorophore quencher substrate **5**, a 50 mM stock solution was used). The plate was then sealed with transparent plastic foil and analyzed using a fluorescence plate

reader at 27 °C, in 3 min measuring intervals with shaking between the measurements (substrate **5**: $\lambda_{excitation}$ = 320 nm; $\lambda_{emission}$ = 400 nm; substrate **8**: $\lambda_{excitation}$ = 350 nm; $\lambda_{emission}$ = 380 nm).

Supporting Information

Supporting Information File 1

NMR spectra of synthesized compounds.
[http://www.beilstein-journals.org/bjoc/content/supplementary/1860-5397-11-203-S1.pdf]

Acknowledgements

The authors thank The Seventh Framework Programme Project METACODE (KBBE, ''Code-engineered new-to-nature microbial cell factories for novel and safety enhanced bioproduction'') for financial support.

References

1. Trnka, T. M.; Grubbs, R. H. *Acc. Chem. Res.* **2001,** *34,* 18. doi:10.1021/ar000114f
2. Grubbs, R. H., Ed. *Handbook of Metathesis;* Wiley-VCH: Weinheim, Germany, 2003; Vol. 1–3. doi:10.1002/9783527619481
3. Hoveyda, A. H.; Zhugralin, A. R. *Nature* **2007,** *450,* 243. doi:10.1038/nature06351
4. Bruneau, C.; Fischmeister, C. Olefin Metathesis in Green Organic Solvents and without Solvent. In *Olefin Metathesis: Theory and Practice;* Grela, K., Ed.; John Wiley & Sons, Inc.: Hoboken, NJ, U.S.A., 2014; pp 523–535. doi:10.1002/9781118711613.ch22
5. Schrock, R. R. *Acc. Chem. Res.* **1990,** *23,* 158. doi:10.1021/ar00173a007
6. Leitgeb, A.; Wappel, J.; Slugovc, C. *Polymer* **2010,** *51,* 2927. doi:10.1016/j.polymer.2010.05.002
7. Gradillas, A.; Pérez-Castells, J. *Angew. Chem., Int. Ed.* **2006,** *45,* 6086. doi:10.1002/anie.200600641
8. Lo, C.; Ringenberg, M. R.; Gnandt, D.; Wilson, Y.; Ward, T. R. *Chem. Commun.* **2011,** *47,* 12065. doi:10.1039/c1cc15004a
9. Mayer, C.; Gillingham, D. G.; Ward, T. R.; Hilvert, D. *Chem. Commun.* **2011,** *47,* 12068. doi:10.1039/c1cc15005g
10. Philippart, F.; Arlt, M.; Gotzen, S.; Tenne, S.-J.; Bocola, M.; Chen, H.-H.; Zhu, L.; Schwaneberg, U.; Okuda, J. *Chem. – Eur. J.* **2013,** *19,* 13865. doi:10.1002/chem.201301515
11. Lin, Y. A.; Chalker, J. M.; Floyd, N.; Bernardes, G. J. L.; Davis, B. G. *J. Am. Chem. Soc.* **2008,** *130,* 9642. doi:10.1021/ja8026168
12. Vougioukalakis, G. C.; Grubbs, R. H. *Chem. Rev.* **2010,** *110,* 1746. doi:10.1021/cr9002424
13. Toomre, D.; Bewersdorf, J. *Annu. Rev. Cell Dev. Biol.* **2010,** *26,* 285. doi:10.1146/annurev-cellbio-100109-104048
14. Yin, J.; Hu, Y.; Yoon, J. *Chem. Soc. Rev.* **2015,** *44,* 4619. doi:10.1039/C4CS00275J
15. Godoy, J.; García-López, V.; Wang, L.-Y.; Rondeau-Gagné, S.; Link, S.; Martí, A. A.; Tour, J. M. *Tetrahedron* **2015,** *71,* 5965. doi:10.1016/j.tet.2015.04.027
16. Vorfalt, T.; Wannowius, K. J.; Thiel, V.; Plenio, H. *Chem. – Eur. J.* **2010,** *16,* 12312. doi:10.1002/chem.201001832
17. Agudelo-Morales, C. E.; Silva, O. F.; Galian, R. E.; Pérez-Prieto, J. *ChemPhysChem* **2012,** *13,* 4195. doi:10.1002/cphc.201200637
18. Timmer, M. S. M.; Codée, J. D. C.; Overkleeft, H. S.; van Boom, J. H.; van der Marel, G. A. *Synlett* **2004,** *12,* 2155. doi:10.1055/s-2004-831301
19. de Jong, A. R.; Volbeda, A. G.; Hagen, B.; van den Elst, H.; Overkleeft, H. S.; van der Marel, G. A.; Codée, J. D. C. *Eur. J. Org. Chem.* **2013,** 6644. doi:10.1002/ejoc.201301055
20. Chatterjee, A. K.; Toste, F. D.; Goldberg, S. D.; Grubbs, R. H. *Pure Appl. Chem.* **2003,** *75,* 421–425. doi:10.1351/pac200375040421
21. Nguyen Van, T.; Debenedetti, S.; De Kimpe, N. *Tetrahedron Lett.* **2003,** *44,* 4199. doi:10.1016/S0040-4039(03)00902-X
22. Xie, L.; Chen, Y.; Wu, W.; Guo, H.; Zhao, J.; Yu, X. *Dyes Pigm.* **2012,** *92,* 1361. doi:10.1016/j.dyepig.2011.09.023
23. Kapeller, D. C.; Bräse, S. *ACS Comb. Sci.* **2011,** *13,* 554. doi:10.1021/co200107s
24. Kajetanowicz, A.; Chatterjee, A.; Reuter, R.; Ward, T. R. *Catal. Lett.* **2013,** *144,* 373. doi:10.1007/s10562-013-1179-z
25. Ogilvie, W.; Deziel, R.; O'Meara, J.; Simoneau, B. Non-Nucleoside Reverse Transcriptase Inhibitors. WO03011862 A1, Feb 13, 2003.
26. Yang, Y.; Babiak, P.; Reymond, J.-L. *Org. Biomol. Chem.* **2006,** *4,* 1746. doi:10.1039/b601151a
27. Schmidt, B.; Krehl, S. *Chem. Commun.* **2011,** *47,* 5879. doi:10.1039/c1cc11347j

License and Terms

BEILSTEIN JOURNAL OF ORGANIC CHEMISTRY

Stereochemistry of ring-opening/cross metathesis reactions of *exo*- and *endo*-7-oxabicyclo[2.2.1]hept-5-ene-2-carbonitriles with allyl alcohol and allyl acetate

Piotr Wałejko*, Michał Dąbrowski, Lech Szczepaniak, Jacek W. Morzycki and Stanisław Witkowski

Full Research Paper

Open Access

Address:
Institute of Chemistry, University of Białystok, ul. Ciołkowskiego 1K, 15-245 Białystok, Poland

Email:
Piotr Wałejko* - pwalejko@uwb.edu.pl

* Corresponding author

Keywords:
Grubbs' catalysts; metathesis; ROCM; ROMP; Z-selectivity

Beilstein J. Org. Chem. **2015,** *11,* 1893–1901.
doi:10.3762/bjoc.11.204

Received: 06 June 2015
Accepted: 23 September 2015
Published: 13 October 2015

This article is part of the Thematic Series "Progress in metathesis chemistry II".

Guest Editor: K. Grela

Abstract

The ROCM reactions of *exo*- and *endo*-2-cyano-7-oxanorbornenes with allyl alcohol or allyl acetate promoted by different ruthenium alkylidene catalysts were studied. The stereochemical outcome of the reactions was established. The issues concerning chemo- (ROCM vs ROMP), regio- (1-2- vs 1-3-product formation), and stereo- (*E*/*Z* isomerism) selectivity of reactions under various conditions are discussed. Surprisingly good yields of the ROCM products were obtained under neat conditions.

Introduction

Substituted tetrahydrofurans are a common motif found in many biologically active natural products [1,2], e.g., annonaceous acetogenins [3,4], lignans [5,6], iso- and neurofurans [7,8], as well as macrodiolides [9]. These substances exhibit a diverse biological activities including antitumor, antimicrobial, etc. [10-12].

Stereoselective construction of substituted tetrahydrofurans is still a challenging task in natural product synthesis [13-17]. One of the most promising approaches to solve this problem seemed to be the metathetic opening of substituted 7-oxanorbornenes, which was first developed by Blechert and co-workers [18,19]. They started with the ring-opening of strained alkenes (mostly 7-oxanorbornene) followed by cross metathesis with a cross partner (e.g., propene) to give the respective ring-opening cross metathesis (ROCM) products. Preliminary analysis suggested that these transformations lead mainly to incorporation of two molecules of a coupling partner, if present in excess, into

tetrahydrofurans to give a product of type B. Blechert has reported that the incorporation of only one unit of a terminal alkene (Scheme 1; products A) was also possible using only a slight excess of a terminal alkene [19]. Arjona et al. have noticed that when 7-oxanorbornenes bearing a bulky C2-substituent are used in ROCM, products of type A are formed in higher yields and with good regioselectivities [20]. Treatment of 2-acetoxy-7-oxanorbornene (Scheme 1; FG = OAc) with allyl acetate in the presence of **[Ru]1** (Figure 1) catalyst afforded mainly the product A of a 1–3 type (75% yield, 1-3:1-2 = 4:1), while the 2-hydroxy derivative (FG = OH) provided an equimolar ratio of both type A products. The authors have suggested that the observed regioselectivity comes from steric effects that favour formation of 1-3 over 1-2 metallacycles in the former case (see [20]).

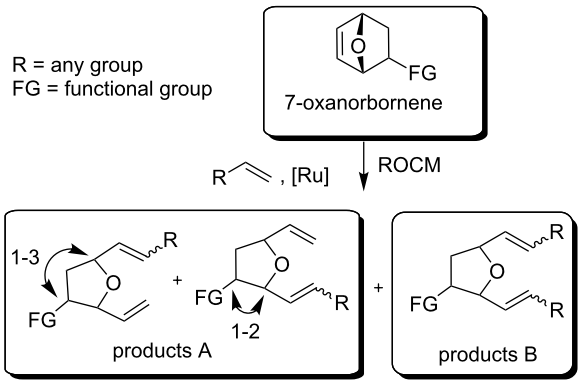

Scheme 1: ROCM reactions of 7-oxanorbornene.

The completely regioselective ROCM of 2-tosyl (FG = Ts) substituted 7-oxanorbornene was reported by Rainier [21]. The *endo* substrate gave only the regioisomer of a 1-2 type (*E*/*Z*, 1:1), whereas the *exo* substrate yielded a mixture of products of types 1-2 and 1-3 (9:1; *E*/*Z* 0.9:1).

Arjona, Blechert and others have suggested that a competing ring-opening metathesis polymerization (ROMP) can be minimized by carrying out the reaction in high dilution. Furthermore good yields of ROCM products can be obtained only when an 1.5-fold excess of a cross olefin is used [14,19,20].

Results and Discussion

Now, we wish to report our preliminary results of ROCM reactions of *exo*- and *endo*-7-oxabicyclo[2.2.1]hept-5-en-2-carbonitrile (**1** and **2,** respectively) with allyl acetate (**3**) or allyl alcohol (**4**) catalyzed by several commercially available ruthenium catalysts (**[Ru]1–6**, Figure 1). To the best of our knowledge there is no example of a ROCM reaction of 7-oxanorbornene bearing the –CN substituent with olefins. However, Arjona and co-workers described closely related transformation of 7-oxanorbornenes (bearing carbonyl, OH and ether substituents [20]) but any detailed information about the influence of the reaction conditions on the product ratio 1-2 vs 1-3 and geometry *Z*/*E* was reported. It should be emphasized that in the presence of a nitrile group an efficient metathetic transformation is difficult to carry out due to a competitive complexation of Ru by the nitrile group [22]. The influence of the reaction conditions on the distribution of the type A products and their *E*/*Z*

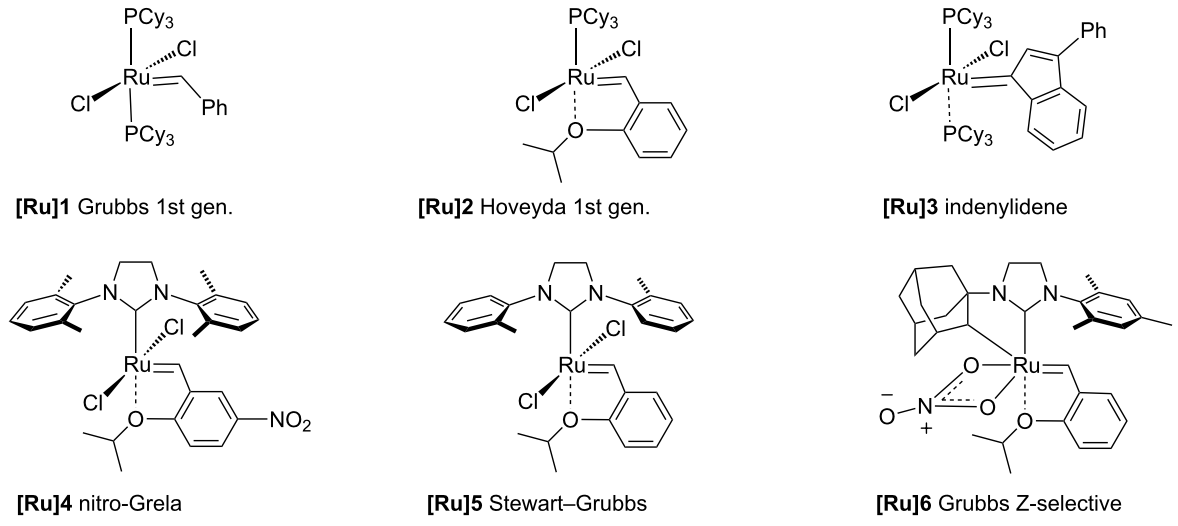

Figure 1: Chemical structures of catalysts **[Ru]1–6** used in this work.

stereochemistry was studied. Our results seem to be in some contradiction to the commonly accepted opinion that ROCM reactions should be carried out in high dilution to avoid polymerization. It was found that ROCM reactions proceed quite efficiently even under neat conditions. Furthermore, less complex mixtures of products were formed and they were easier to separate from the ROMP products.

7-Oxanorbornenes **1** and **2** were treated with olefin **3** or **4** in the presence of ruthenium catalysts **[Ru]1–6** (Figure 1) to afford mixtures of tetrahydrofurans **5**–**12** (Scheme 2). The mixtures were carefully separated using PTLC techniques. The pure samples of compound **6*E***, **7*Z***, **8*Z***, **8*E***, **10*E*** and **12*Z*** were isolated and characterized spectroscopically (^{1}H and ^{13}C NMR, GC–MS).

Two types of the regioisomeric products of type A should be taken into consideration (Scheme 1). The distinguishing of 1-2 from 1-3 isomers was done by analysis of coupling constants $^3J_{H,H}$ or $^3J_{C,H}$ in 2D NMR (DQF and HMBC) experiments, respectively. The *E*/*Z* geometry of the double bonds were determined on the basis of $^3J_{CH=CH}$ constants from an ^{1}H experiment recorded with ^{1}H-homodecoupling or with *J*-resolved techniques [23]. The compounds **6*E*** and **10*E*** were deacetylated (MeOH/KCN) [24] to give **8*E*** and **12*E***. The samples **7*Z***, **8*Z***, **8*E***, and **12*Z*** were subjected to acetylation (Py/Ac_2O) to give **5*Z***, **6*Z***, **6*E*** and **10*Z***, respectively. The acetates were directly characterized by GC–MS. Based on retention indices and literature data (MS spectra identity of *E*/*Z* isomers) [25], the identification of all ROCM components of the aforementioned mixtures was performed.

The results of these experiments are given in Table 1 and Table 2. The collected data show that the reactions in diluted solutions (Table 1, entries 1, 7, 10, and 13) led mainly to ROMP products, whereas ROCM products were formed in lower yields. However, according to literature data, the formation of a ROMP product can be minimized by carrying out the reactions in high dilution [18,20,21]. In our case, the experiments carried out in more concentrated solutions (Table 1, entries 3, 4, 8 and 12) gave substantially higher yields of ROCM products. Our results seem to be in contradiction to those reported by Blechert [15] and Arjona [20]. Satisfactory results were obtained even when the reactions were carried out under neat conditions (Table 1, entries 5, 6, 9, and 12). Furthermore, the resulted mixtures were easier to work-up and to separate from ROMP oligomers by simple filtration (see Figure 2).

A different isomeric products distribution was observed in the mixtures of type A products (1-2 and 1-3). In reactions of *exo*-

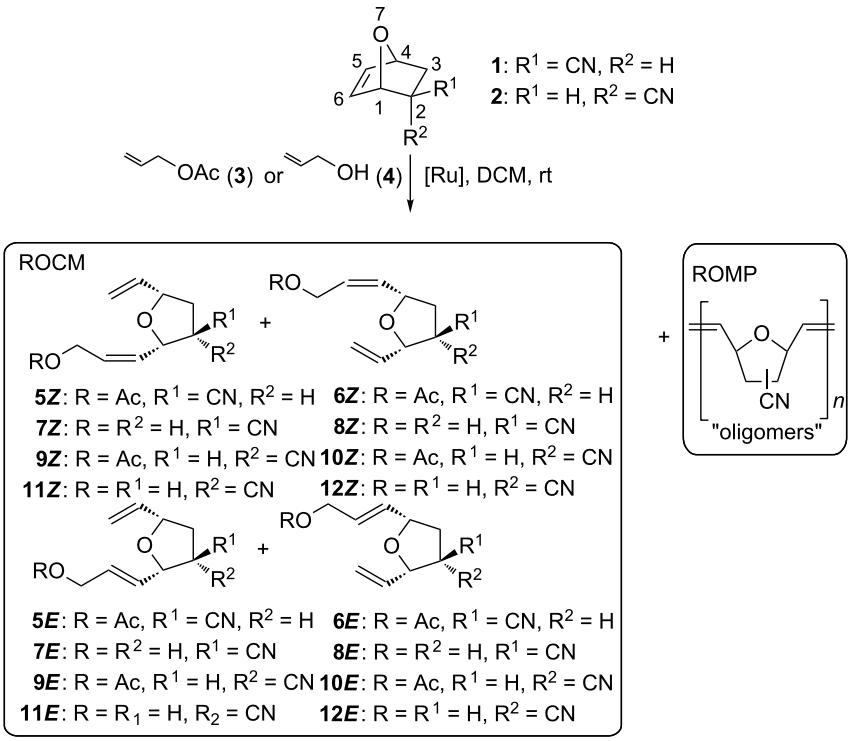

Scheme 2: Metathesis products of *exo*- and *endo*-7-oxabicyclo[2.2.1]hept-5-en-2-carbonitriles (**1** and **2**) with allyl acetate (**3**) or allyl alcohol (**4**).

Table 1: Results of ROCM reactions of nitriles **1** and **2** with olefins **3** and **4**.

reagents/conditions				products/ratio[a]						
entry	alkenes	molar ratio[b]	conc.[c] (mol/L)	total yield (%)	**5*Z*** (1630)[d]	**5*E*** (1654)[d]	*E*/*Z*	**6*Z*** (1637)[d]	**6*E*** (1667)[d]	*E*/*Z*	*1-2*/*1-3* (**5**:**6**)
1	**1**+**3**	1:1	0.023	30 (67)[e]	23	11	32:68	45	21	32:68	34:66
2	**1**+**3**	1:1	0.115	33 (45)[e]	22	10	31:69	46	22	32:68	32:68
3	**1**+**3**	1:1	0.575	57 (33)[e]	21	12	36:64	45	22	33:67	33:67
4	**1**+**3**	1:10	0.115	67 (21)[e]	23	12	34:66	44	20	31:69	35:65
5	**1**+**3**	1:10	neat	65	23	10	30:70	46	21	31:69	33:67
6	**1**+**3**	1:20	neat	58	24	10	29:71	46	20	30:70	34:66
					7*Z* (1503)[d]	**7*E*** (1548)[d]	*E*/*Z*	**8*Z*** (1528)[d]	**8*E*** (1551)[d]	*E*/*Z*	1-2/1-3 (**7**:**8**)
7	**1**+**4**	1:1	0.023	59	22	21	49:51	26	31	54:46	43:57
8	**1**+**4**	1:1	0.115	65	21	20	49:51	31	28	47:53	41:59
9	**1**+**4**	1:10	neat	56	19	19	50:50	33	29	47:53	38:62
					9*Z* (1676)[d]	**9*E*** (1713)[d]	*E*/*Z*	**10*Z*** (1712)[d]	**10*E*** (1738)[d]	*E*/*Z*	1-2/1-3 (**9**:**10**)
10	**2**+**3**	1:1	0.023	35 (40)[e]	17	5	23:77	52	26	33:67	22:78
11	**2**+**3**	1:1	0.115	38 (37)[e]	14	5	26:74	52	28	35:65	19:81
12	**2**+**3**	1:10	0.115	70 (25)[e]	10	5	33:67	57	28	33:67	15:85
					11*Z* (1575)[d]	**11*E*** (1583)[d]	*E*/*Z*	**12*Z*** (1602)[d]	**12*E*** (1614)[d]	*E*/*Z*	1-2/1-3 (**11**:**12**)
13	**2**+**4**	1:1	0.023	36	21	10	32:68	38	31	45:55	31:69
14	**2**+**4**	1:1	0.115	38	13	8	38:62	48	31	39:61	21:79
15	**2**+**4**	1:10	neat	46	20	17	46:54	32	30	48:52	37:63

[a]Conditions: **[Ru]1**, 5 mol %, DCM, rt, 18–24 h; percentage contents of products in mixtures based on the intensity of GC–MS signals; [b]molar ratio of 7-oxanorbornene **1** or **2** to the olefin; [c]concentration of **1** or **2** in DCM (mol/L); [d]the retention indices; [e]isolated yield of ROMP products (*n* = 2–9).

Table 2: Influence of the catalyst on ROCM product distribution (reaction of **1** with **3**)[a].

entry	catalyst	products/ratio[b]						
		5*Z*	**5*E***	***E*/*Z***	**6*Z***	**6*E***	***E*/*Z***	1-2/1-3 (**5**:**6**)
1	**[Ru]1**	23	12	34:66	44	20	31:69	35:65
2	**[Ru]2**	20	14	41:59	44	23	34:66	34:66
3	**[Ru]3**	20	13	39:61	45	22	33:67	33:67
4	**[Ru]4**	20	17	46:54	37	26	41:59	37:63
5	**[Ru]5**	13	25	66:34	24	37	61:39	38:62
6	**[Ru]6**	24	11	31:69	55	10	15:85	35:65

[a]Conditions: 1 equiv of **1**, 10 equiv of allyl acetate (**3**), 5 mol % of catalyst **[Ru]1–6**, rt, 18–24 h (0.115 M of **1** in DCM); [b]percentage contents of products in the mixtures based on the intensity of GC–MS signals.

and *endo*-norbornene **1** and **2**, with the acetate **3**, approximately a two-fold excess of the 1-3 *Z* isomers was formed, and the least abundant product among the four diastereoisomers was the 1-2 *E* isomer (5–12% relative yield; see Table 1). In reactions of **1** with **4** the amount of each product in the mixture (Table 1, entry 8) was in the range of 20% to 31%. However, the total ratio of 1-2 vs 1-3 products in most experiments was the same (ca. 1:2), except entries 10, 11, 12, and 14, where the portion of the 1-3 regioisomers was higher (in entry 11 even 1:4). According to Arjona et al. [20] the observed regioselectivity comes from the

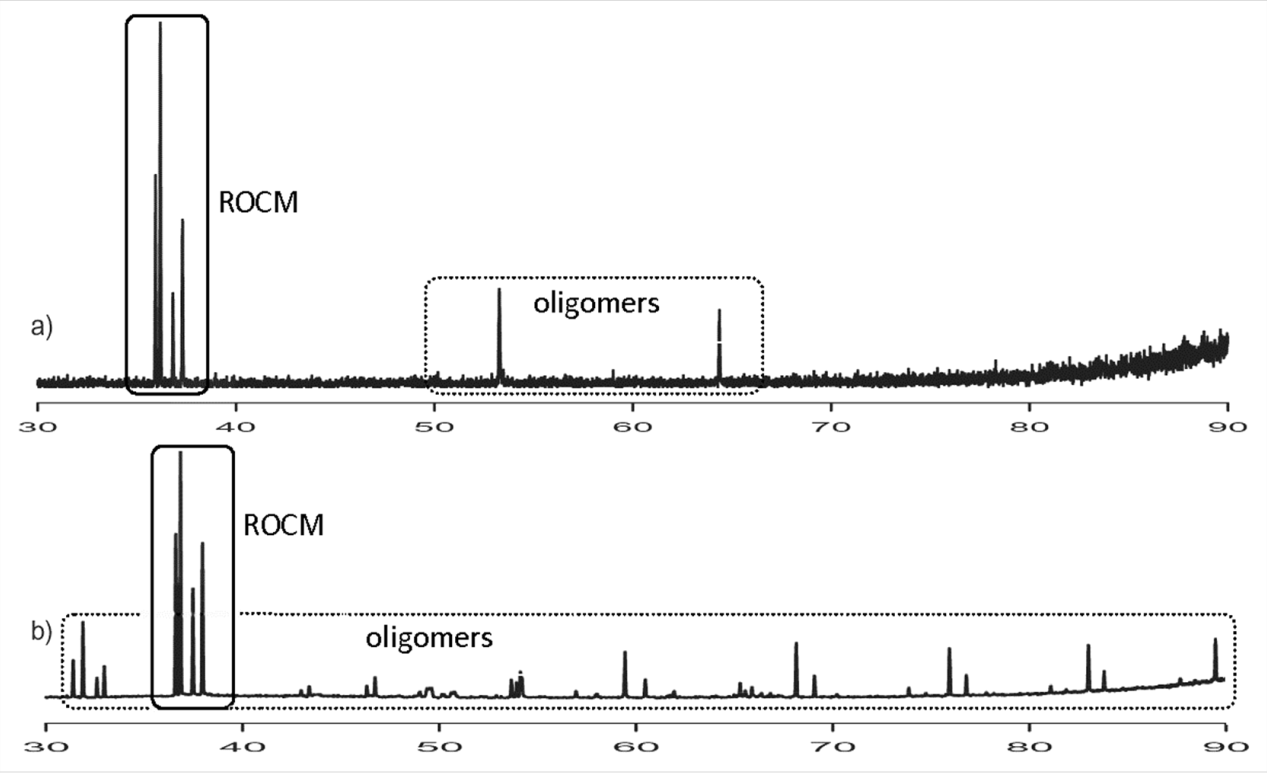

Figure 2: Representative GC chromatograms recorded from crude reaction mixtures described in Table 1: a) entry 1 and b) entry 5.

steric hindrance of the –CN group, however, some electronic effects in 7-oxanorbornene should be also taken into consideration. Unexpectedly, the *Z*-selectivity predominated in most reactions catalyzed by **[Ru]1** (see Table 1, entries 1–6, 10–15, and Table 2, entries 1–4). A two-fold excess of the *Z* isomer was observed in both groups of products (1-2 and 1-3). While the reaction of *endo*-nitrile **2** with alcohol **4** proceeded with lower *Z*/*E* selectivity (1.5:1) (Table 1, entries 13–15), the *exo*-isomer **1** reacted without any stereoselectivity (Table 1, entries 7–9).

It is worth to note that the reactions of nitriles **1** and **2** promoted by the Grubbs *Z*-selective catalyst **[Ru]6** (Table 2, entry 6) in anhydrous THF provided a fraction of ROCM products only in 14% yield (by GC – complete substrate conversion) with regioselectivity similar to that observed for the Grubbs I catalyst (**[Ru]1**) (Table 2, entry 1). In general the more reactive catalysts, namely Grubbs II and Hoveyda–Grubbs II, favored the formation of ROMP products. A different distribution of *E*/*Z*-isomers was observed in the reaction of substrate **1** with alcohol **3** in the presence of the Steward–Grubbs (**[Ru]5**) catalyst (Table 2, entry 5). The *E*-isomers of both products **5** and **6** prevailed, while the 1-2 vs 1-3 ratio was almost the same as those in other experiments. It should be noted that less sterically demanding *o*-tolyl-N-substituents in NHC-ligands provide more space around the ruthenium center.

In general, ROCM reactions are most successful when highly strained substrates are used. Furthermore, this transformation should be considered as a two-step reaction where the ring-opening metathesis (ROM) is the initial step followed by a CM. It is well known that oxanorbornenes (e.g., **1** and **2**) are generally excellent substrates for ROCM reactions [14]. The cycloaddition of the ruthenium carbene **[Ru]** to a cyclic alkene **1** or **2** affords a metallacyclobutane of the 1-2 or 1-3 type (Scheme 3). Accordingly to Arjona et al. [20] a preference of the 1-3 structures over 1-2 arises from the steric interaction between the metal–ligand moiety and the substituent at position C-2 of 7-oxanorbornene. However, an influence of the electron density of the C=C bond in the starting material, as well as its complexation effects, cannot be ruled out. In reactions of **1** (*exo*) the observed 1-2/1-3 ratio varied from 1:1.4 in to 1:2, while **2** (*endo*) gave a much higher content of the 1-3 isomer, from 1:3.5 to 1:5.6. The *endo*-face metallacyclobutane was proposed as a main intermediate [26]. Decomposition of the 1-2 and 1-3 intermediates leads to ring-opened alkylidenes **A**, which can react further in two different ways, depending on the reaction speed ratio of **A** with the strained substrate **1** or **2** (ROMP) and with the terminal olefin **3** or **4** (ROCM). This step seems to be crucial for the selectivity of the ROCM, which competes with the ROMP metathesis. It is worth to note that the reaction of **A** in diluted solutions (0.023 mol/L) with the starting olefin was faster than that with the terminal olefin. As a consequence the

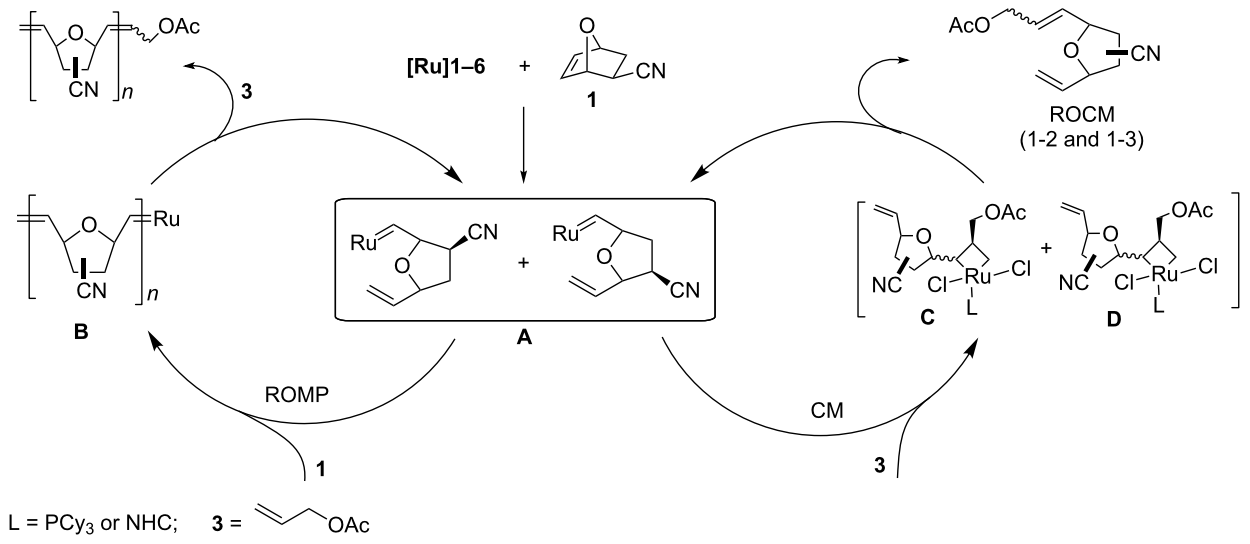

Scheme 3: The plausible mechanism of the formation of ROCM and ROMP products from *exo*- or *endo*-7-oxabicyclo[2.2.1]hept-5-ene-2-carbonitriles **1** or **2**. For simplicity of the scheme, the reaction of only *exo*-stereoisomer **1** as a substrate is presented.

ROMP products prevailed. On the other hand the formation of polymeric products **B** may be suppressed by using the olefinic cross partner in excess and increasing concentration of reagents (the best results were obtained in the neat experiments). It should be noted that a different *E*/*Z* selectivity was observed for experiments with **[Ru]1–4** compared to that of **[Ru]5**. In our opinion, the likely explanation of this fact is a different interaction between ligand moiety and the two substituents connected to metallacyclobutane intermediates (Scheme 3, **C** or **D**). According to Fortman and Nolan [27] the di-*N*,*N*'-*o*-tolyl substituted NHC ligand in **[Ru]5** exerts a smaller steric effect than the -PCy_3 residue in **[Ru]1–4**. Furthermore, the bulky phosphine ligand (PCy_3) expands away from the transition metal center (coordination sphere), while the *N*,*N*'-*o*-tolyl substituent attached to the central imidazole ring penetrates the coordination sphere. Connon and Blechert [15] suggested that a difference in energy between metallacyclobutane intermediates influences stereochemistry of metathetic products. In our case, more bulky catalysts (**[Ru]1–4**) prefer formation of *Z*-isomers in excess because the intermediate **C** is less strained than **D**. On the other hand, an interaction of less bulky *o*-tolyl ligands with the ruthenium core in **[Ru]5** causes an opposite selectivity (*E* preference). One can assume that the observed change in the *E*/*Z* selectivity resulted from chelating and electronic effects in postulated intermediates **C** and **D**. It is clear, that the *E*/*Z* selectivity depends on the catalyst applied, while the regioselectivity is largely substrate-dependent. The application of the ROCM products in the synthesis of natural products will be reported in due course.

Conclusion

The ROCM reactions of 2-cyano-7-oxanorbornenes with allyl alcohol and allyl acetate may be partially stereocontrolled by a proper choice of the reaction catalyst. However, the regioselectivity largely depends on the starting material structures. Unexpectedly, the chemoselectivity of the ROCM product formation in competition with the undesired ROMP reaction may be improved by using neat reaction conditions.

Experimental

A mixture of **1** and **2** (1.6:1) is readily available from the Diels–Alder reaction of furan and acrylonitrile according to the literature procedure [28,29]. The pure isomers were isolated by column chromatography. The ^{1}H and ^{13}C NMR spectra were identical with those described in the literature [30,31]. Compounds **5**–**12** were numerated based on auto name option in ChemBioDraw v. 13.0 (Figure 3).

^{1}H and ^{13}C NMR spectra for $CDCl_3$ solutions were obtained using a Bruker Avance II spectrometer (400 and 100 MHz, respectively). Chemical shifts (δ) are reported in ppm downfield from TMS. The assignment of chemical shifts in solution was supported by 2D NMR experiments (DFQ, HSQC and HMBC). GC–MS was carried out on an Agilent Technologies HP 6890 N gas chromatograph with mass selective detector MSD 5973 (Agilent Technologies, USA). The device was fitted with a ZB-5MSi fused silica column (30 m × 0.25 mm i.d., 0.25 μm film thickness), with electronic pressure control and split/splitless injector. Helium flow rate through the column was

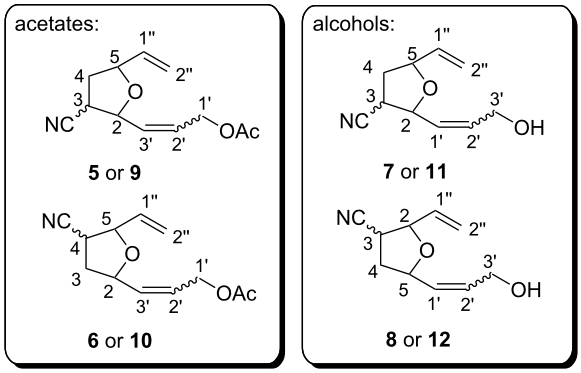

Figure 3: Numbering of carbon atoms in cross metathesis products.

1 mL/min in a constant flow mode. The injector worked at 250 °C in split (1:50) mode. The initial column temperature was 50 °C rising to 340 °C at 3 °C/min and the higher temperature was maintained for 15 min. The MS detector acquisition parameters were as follows: transfer line temperature equalled to 280 °C, MS Source temperature to 230 °C and MS Quad temperature to 150 °C. The EIMS spectra were obtained at 70 eV of ionization energy. The MS detector was set to scan 40–600 a.m.u. After integration, the fraction of each component in the total ion current was calculated. Retention indices (RI) were calculated according to the formula proposed by van Den Dool and Kratz [25] with *n*-alkanes as references substances. RI values for phases type DB-5 and MS spectra for derivatives **5**–**12**, realized at an ionization energy of 70 eV are shown in Supporting Information File 1.

General ROCM procedure

To a mixture of norbornene **1** or **2** and alkene (for details see Table 1 and Table 2) in anhydrous DCM a solution of catalyst **[Ru]1–6** (5 mol %) in DCM was added to obtain a final concentration of **1** or **2** in CH_2Cl_2 (0.023, 0.115 or 0.575 mol/L). For neat experiments (Table 1, entries 5, 6, 9 and 15) solid catalyst was used. The resulting mixture was stirred overnight at rt, then 0.5 mL of vinyl ethyl ether was added, and the reaction mixture was stirred for 10 min. The solvent was removed under reduced pressure and then the residue was redissolved in DCM and filtered through a pad of Celite. The crude reaction mixtures were purified by MPLC and PTLC chromatography. The structures of isolated compounds were determined by ^{1}H and ^{13}C NMR.

(*E*)-3'-(4-Cyano-5-vinyltetrahydrofuran-2-yl)allyl acetate (6*E*). ^{1}H NMR ($CDCl_3$, δ, ppm) 5.85–5.72 (m, 3H, H-3', 2', 1"), 5.51, 5.47, 5.34, 5.31 (4 x ~s, 2H, H-2"), 4.60–4.56 (m, 3H, H-2 and 1'), 4.43 (dd, $^3J_{H,H}$ = 6.72 and 7.40 Hz, 1H, H-5), 2.83–2.77 (m, 1H, H-4), 2.46–2.39 (m, 1H, H-3*eq*), 2.16–2.08 (m, 1H, H-3*ax*), 2.07 (s, 1H, CH_3); ^{13}C NMR ($CDCl_3$, δ, ppm) 170.5 (C=O), 134.5 (1'), 132.2 (2'), 127.2 (1"), 119.4 (CN), 119.1 (2") 83.1 (5) 78.5 (2), 63.7 (1'), 36.2 (3), 34.2 (4), 20.8 (CH_3); DQF COSY ($CDCl_3$) H-4 and H-3*ax*, H-4 and H-3*eq*, H-5 and H-4, H-3 and H-2; HMBC ($CDCl_3$) H-2" and C-5, H-5 and C-2", H-2 and C-3', H-2 and C-2'; RI: 1667 (t_R = 37.34 min); TOF MS ES$^+$: 244 $[M + Na]^+$; HRMS *m*/*z*: $[M + Na]^+$ calcd for $C_{12}H_{15}NO_3Na$: 244.0944; found: 244.0943.

5-((*E*)-3'-Hydroxyprop-1'-en-1'-yl)-2-vinyltetrahydrofuran-3-carbonitrile (8*E*). ^{1}H NMR ($CDCl_3$, δ, ppm) 5.98–5.83 (m, 2H, H-1" and 2'), 5.77–5.72 (m, 2H, H-1'), 5.51, 5.47, 5.34, 5.31 (4 x ~s, 2H, H-2"), 4.63–4.56 (m, 1H, H-5), 4.47–4.43 (m, 1H, H-2), 4.20–4.19 (m, 2H, H-3'), 2.86–2.80 (m, 1H, H-3), 2.45–2.40 (m, 1H, H-4*eq*), 2.16–2.12 (m, 1H, H-4*ax*); ^{13}C NMR (CDCl3, δ, ppm) 134.6 (1'), 132.7 (1"), 129.1 (2'), 119.5 (CN), 119.1 (2"), 83.1 (2), 78.9 (5), 62.56 (3'), 36.3 (4), 34.3 (3); DQF COSY ($CDCl_3$) H-3 and H-4*ax*, H-3 and H-4*eq*, H-3 and H-2, H-5 and H-4, H-5 and H-1'Hz. *J*-resolved; ^{1}H NMR ($CDCl_3$) $^3J_{H1',H2'}$ = 16 Hz; RI: 1551 (t_R = 33.49 min); TOF MS ES$^+$: 202 $[M + Na]^+$; HRMS *m*/*z*: $[M + Na]^+$ calcd for $C_{12}H_{15}NO_3Na$ 202.0844; found: 202.0848.

5-((*Z*)-3'-Hydroxyprop-1'-en-1'-yl)-2-vinyltetrahydrofuran-3-carbonitrile (8*Z*). ^{1}H NMR ($CDCl_3$, δ, ppm) 5.86–5.77 (m, 3H, H-1', 2' and 1"), 5.51, 5.46, 5.34, 5.31 (4 x ~s, 2H, H-2"), 4.91–4.80 (m, 1H, H-2), 4.46–4.43 (m, 1H, H-5), 4.31–4.23 (m, 2H, H-3'), 2.85–2.80 (m, 1H, H-3), 2.48–2.42 (m, 1H, H-4*eq*), 2.18–2.10 (m, 1H, H-4*ax*); ^{13}C NMR ($CDCl_3$, δ, ppm) 134.5, 133.0, 130.2 (1', 1", 2'), 119.5 (CN), 119.1 (2"), 83.2, 74.8 (2 and 5), 58.8 (3'), 36.8 (4), 34.5 (3); *J*-resolved ^{1}H NMR ($CDCl_3$) $^3J_{H1',H2'}$ = 10 Hz; RI: 1529 (t_R = 32.59 min); TOF MS ES$^+$ *m*/*z*: $[M + Na]^+$ 179, found 202; HRMS *m*/*z*: $[M + Na]^+$ calcd. for $C_{12}H_{15}NNaO_3$ 202.0844; found: 202.0849.

2-((*Z*)-3'-Hydroxyprop-1'-en-1'-yl)-5-vinyltetrahydrofuran-3-carbonitrile (7*Z*). ^{1}H NMR ($CDCl_3$, δ, ppm) 5.95–5.79 (m, 2H, H-1", 2'), 5.60–5.55 (m, 1H, H-1'), 5.36, 5.32, 5.24, 5.21 (4 x ~s, 2H, H-2"), 4.87–4.80 (m, 1H, H-2), 4.59–4.51 (m, 1H, H-5), 3.36–3.30 (m, 1H, H-3'), 2.79–2.77 (m, 2H, H-3), 2.49–2.42 (m, 1H, H-4*eq*), 2.18–2.14 (m, 1H, H-4*ax*); ^{13}C NMR ($CDCl_3$, δ, ppm) 136.4 (1'), 134.7 (1"), 128 (2'), 119.5 (CN), 117.4 (2"), 79.8, 78.2 (2 and 5), 58.8 (2'), 36.3 (4), 34.6 (3); DQF COSY ($CDCl_3$) H-3 and H-4*ax*, H-3 and H-4*eq*, H-5 and H-4, H-5 and H-1", H-2 and H-1'; *J*-resolved ^{1}H NMR ($CDCl_3$) $^3J_{H1',H2'}$ = 11 Hz; RI: 1504 (t_R = 31.62 min); TOF MS ES$^+$: *m*/*z* 202 $[M + Na]^+$; HRMS *m*/*z*: $[M + Na]^+$ calcd for $C_{12}H_{15}NO_3Na$ 202.0844; found: 202.0849.

(*E*)-3-(4-Cyano-5-vinyltetrahydrofuran-2-yl)allyl acetate (10*E*). ^{1}H NMR ($CDCl_3$, δ, ppm) 6.10–6.00 (m, 1H, H-1"),

6.01–5.87 (m, 2H, H-3' 2'), 5.51, 5.47, 5.44, 5.41 (4 x ~s, 2H, H-2"), 4.65–4.59 (m, 2H, H-1'), 4.47–4.42 (m, 1H, H-2 and 5), 3.29–3.24 (m, 1H, H-4), 2.59–2.53 (m, 1H, H-3*eq*), 2.52–2.05 (m, 1H, H-3*ax*), 2.09 (s, 3H, CH_3); ^{13}C NMR ($CDCl_3$, δ, ppm) 170.6 (C=O), 133.7, 132.3, 127.5 (3', 1", 2'), 117.7 (CN), 119.9 (2"), 80.2, 74.7 (2 and 5), 63.7 (1'), 36.7 (3), 34.4 (4), 20.8 (CH_3); DQF COSY ($CDCl_3$): H-3 and H-2, H-4 and H-5, H-1" and H-2", H-5 and H-1", H-2 and H-3'; *J*-resolved ^{1}H NMR ($CDCl_3$) $^3J_{H1',H2'}$ = 15–16 Hz; RI: 1738 (t_R = 39.85 min); TOF MS ES$^+$ *m/z* [M + Na]$^+$ 244; HRMS *m/z*: [M + Na]$^+$ calcd. for $C_{12}H_{15}NO_3Na$ 244.0949; found: 244.0942.

5-((*E*)-3'-Hydroxyprop-1'-en-1'-yl)-2-vinyltetrahydrofuran-3-carbonitrile (12*Z*). ^{1}H NMR ($CDCl_3$, δ, ppm): 6.10–6.00 (m, 1H, H-1"), 6.01–5.87 (m, 2H, H-1' 2'), 5.51, 5.47, 5.44, 5.41 (4 x ~s, 2H, H-2"), 4.85–4.79 (m, 1H, H-2), 4.47–4.42 (m, 1H, H-5), 4.31–4.20 (m, 2H, H-3'), 3.29–3.24 (m, 1H, H-4), 2.59–2.53 (m, 1H, H-3*eq*), 2.52–2.05 (m, 1H, H-3*ax*), 2.09 (s, 3H, CH_3); ^{13}C NMR ($CDCl_3$, δ, ppm) 170.6 (C=O), 133.6 (1"), 132.6 (2'), 130.9 (3'), 120.0 (2"), 118.9 (CN), 80.2 (5), 58.8 (1'), 37.3 (3), 34.5 (4); DQF COSY ($CDCl_3$) H-3 and H-2, H-4 and H-5, H-1" and H-2", H-2 and H-3', H-5 and H-1" Hz; *J*-resolved; ^{1}H NMR ($CDCl_3$) $^3J_{H1',H2'}$ = 11 Hz. RI: 1583 (t_R = 34.92 min); TOF MS ES$^+$ *m/z* [M + Na]$^+$ 202; HRMS *m/z*: [M + Na]$^+$ calcd for $C_{12}H_{15}NO_3Na$ 202.0844; found: 202.0850.

Supporting Information

Supporting Information File 1

MS spectra and retention indices of all compounds **5**–**12**.
[http://www.beilstein-journals.org/bjoc/content/supplementary/1860-5397-11-204-S1.pdf]

Acknowledgements

The authors acknowledge financial support from the Polish National Science Centre (UMO-2011/02/A/ST5/00459). The authors thank Dr Leszek Siergiejczyk for recording the NMR spectra.

References

1. Wolfe, J. P.; Hay, M. B. *Tetrahedron* **2007,** *63,* 261–290. doi:10.1016/j.tet.2006.08.105
2. Faul, M. M.; Huff, B. E. *Chem. Rev.* **2000,** *100,* 2407–2474. doi:10.1021/cr940210s
3. Bermejo, A.; Figadère, B.; Zafra-Polo, M.-C.; Barrachina, I.; Estornell, E.; Cortes, D. *Nat. Prod. Rep.* **2005,** *22,* 269–303. doi:10.1039/b500186m
4. Ramu, E.; Bhaskar, G.; Rao, B. V.; Ramanjaneyulu, G. S. *Tetrahedron Lett.* **2006,** *47,* 3401–3403. doi:10.1016/j.tetlet.2006.03.080
5. Saleem, M.; Kim, H. J.; Ali, M. S.; Lee, Y. S. *Nat. Prod. Rep.* **2005,** *22,* 696–716. doi:10.1039/B514045P
6. Hirao, H.; Yamauchi, S.; Ishibashi, F.; Ishibashi, F. *Biosci., Biotechnol., Biochem.* **2007,** *71,* 741–745. doi:10.1271/bbb.60575
7. Fessel, J. P.; Porter, N. A.; Moore, K. P.; Sheller, J. R.; Roberts, L. J. *Proc. Natl. Acad. Sci. U. S. A.* **2002,** *99,* 16713–16718. doi:10.1073/pnas.252649099
8. Song, W.-L.; Lawson, J. A.; Reilly, D.; Rokach, J.; Chang, C.-T.; Giasson, B.; FitzGerald, G. A. *J. Biol. Chem.* **2008,** *283,* 6–16. doi:10.1074/jbc.M706124200
9. Kang, E. J.; Lee, E. *Chem. Rev.* **2005,** *105,* 4348–4378. doi:10.1021/cr040629a
10. Oikawa, M.; Ikoma, M.; Sasaki, M.; Gill, M. B.; Swanson, G. T.; Shimamoto, K.; Sakai, R. *Eur. J. Org. Chem.* **2009,** 5531–5548. doi:10.1002/ejoc.200900580
11. Benjamin, N. M.; Martin, S. F. *Org. Lett.* **2011,** *13,* 450–453. doi:10.1021/ol102798f
12. Akiyama, K.; Yamauchi, S.; Nakato, T.; Maruyama, M.; Sugahara, T.; Kishida, T. A. *Biosci., Biotechnol., Biochem.* **2007,** *71,* 1028–1035. doi:10.1271/bbb.60696
13. Kress, S.; Blechert, S. *Chem. Soc. Rev.* **2012,** *41,* 4389–4408. doi:10.1039/C2CS15348C
14. Holub, N.; Blechert, S. *Chem. – Asian J.* **2007,** *2,* 1064–1082. doi:10.1002/asia.200700072
15. Connon, S. J.; Blechert, S. *Angew. Chem., Int. Ed.* **2003,** *42,* 1900–1923. doi:10.1002/anie.200200556
16. Aljarilla, A.; Murcia, M. C.; Csákÿ, A. G.; Plumet, J. *Eur. J. Org. Chem.* **2009,** 822–832. doi:10.1002/ejoc.200800936
17. Arjona, O.; Csákÿ, A. G.; Plumet, J. *Eur. J. Org. Chem.* **2003,** *2003,* 611–622. doi:10.1002/ejoc.200390100
18. Schneider, M. F.; Blechert, S. *Angew. Chem., Int. Ed. Engl.* **1996,** *35,* 411–412. doi:10.1002/anie.199604111
19. Schneider, M. F.; Lucas, N.; Velder, J.; Blechert, S. *Angew. Chem., Int. Ed. Engl.* **1997,** *36,* 257–259. doi:10.1002/anie.199702571
20. Arjona, O.; Csákÿ, A. G.; Murcia, M. C.; Plumet, J. *J. Org. Chem.* **1999,** *64,* 9739–9741. doi:10.1021/jo9913053
21. Liu, Z.; Rainier, J. D. *Org. Lett.* **2005,** *7,* 131–133. doi:10.1021/ol047808z
22. Voigtritter, K.; Ghorai, S.; Lipshutz, B. H. *J. Org. Chem.* **2011,** *76,* 4697–4702. doi:10.1021/jo200360s
23. Venkata, C.; Forster, M. J.; Howe, P. W. A.; Steinbeck, C. *PLoS One* **2014,** *9 (11),* e111576. doi:10.1371/journal.pone.0111576
24. Herzig, J.; Nudelman, A. *Carbohydr. Res.* **1986,** *153,* 162–167. doi:10.1016/S0008-6215(00)90208-8
25. van Den Dool, H.; Kratz, P. D. *J. Chromatogr. A* **1963,** *11,* 463–471. doi:10.1016/S0021-9673(01)80947-X
26. Holtsclaw, J.; Koreeda, M. *Org. Lett.* **2004,** *6,* 3719–3722. doi:10.1021/ol048650l
27. Fortman, G. C.; Nolan, S. P. *Chem. Soc. Rev.* **2011,** *40,* 5151–5169. doi:10.1039/C1CS15088J
28. Brion, F. *Tetrahedron Lett.* **1982,** *23,* 5299–5302. doi:10.1016/S0040-4039(00)85823-2
29. Vieira, E.; Vogel, P. *Helv. Chim. Acta* **1983,** *66,* 1865–1871. doi:10.1002/hlca.19830660627
30. Chau, C. W.; Fawcett, A. H.; Mulemwa, J. N.; Tan, C. E. *Polymer* **1985,** *26,* 1268–1276. doi:10.1016/0032-3861(85)90265-4

31. Morton, C. J. H.; Gilmour, R.; Smith, D. M.; Lightfoot, P.; Slawin, A. M. Z.; MacLean, E. J. *Tetrahedron* **2002,** *58,* 5547–5565. doi:10.1016/S0040-4020(02)00443-X

BEILSTEIN JOURNAL OF ORGANIC CHEMISTRY

New aryloxybenzylidene ruthenium chelates – synthesis, reactivity and catalytic performance in ROMP

Patrycja Żak, Szymon Rogalski, Mariusz Majchrzak, Maciej Kubicki and Cezary Pietraszuk*

Full Research Paper

Open Access

Address:
Adam Mickiewicz University in Poznań, Faculty of Chemistry, Umultowska 89b, 61-614 Poznań, Poland

Email:
Cezary Pietraszuk* - pietrasz@amu.edu.pl

* Corresponding author

Keywords:
chemoactivation; latent catalysts; metathesis; ROMP; ruthenium

Beilstein J. Org. Chem. **2015,** *11,* 1910–1916.
doi:10.3762/bjoc.11.206

Received: 21 July 2015
Accepted: 21 September 2015
Published: 14 October 2015

This article is part of the Thematic Series "Progress in metathesis chemistry II".

Guest Editor: K. Grela

Abstract

New phenoxybenzylidene ruthenium chelates were synthesised from the second generation Grubbs catalysts bearing a triphenylphosphine ligand (or its para-substituted analogues) by metathesis exchange with substituted 2-vinylphenols. The complexes behave like a latent catalyst and are characterized by an improved catalytic behaviour as compared to that of the known analogues, i.e., they exhibit high catalytic inactivity in their dormant forms and a profound increase in activity after activation with HCl. The strong electronic influence of substituents in the chelating ligand on the catalytic activity was demonstrated. The catalytic properties were tested in ROMP of cyclooctadien (COD) and a single selected norbornene derivative.

Introduction

Olefin metathesis is nowadays one of the most important methods for the formation of carbon–carbon bonds in organic and polymer chemistry [1,2]. The availability of well-defined ruthenium-based catalysts, showing a number of desirable features such as tolerance of functional groups, moisture and air, has significantly expanded the scope and application of this process regardless of dynamic advancement in the development of ruthenium-based metathesis catalysts. Continuous efforts have been aimed at the search for new catalysts characterized by improved stability and catalytic performance. One of the current challenges is the development of catalysts allowing control of initiation for some metathesis polymerisation processes. For such applications a variety of latent catalysts have been reported which permit control of initiation and efficient propagation of the reaction [3-5].

Among numerous examples of latent catalysts, the complexes representing the structural motif illustrated in Figure 1 have

been relative poorly investigated. Known examples include benzylidenecarboxylate (Figure 2a) [6] and nitronate complexes (Figure 2b) [7] as well as amidobenzylidene ruthenium chelates (Figure 2c–e) that we have disclosed in cooperation with the Grela group [8].

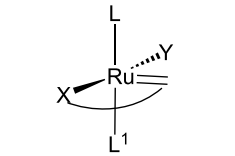

L, L^1 = PCy_3, NHC
X, Y = anionic ligands

Figure 1: Coordination motif of latent catalyst of olefin metathesis in which alkylidene ligand is bound to the heteroatom X, acting as an anionic ligand.

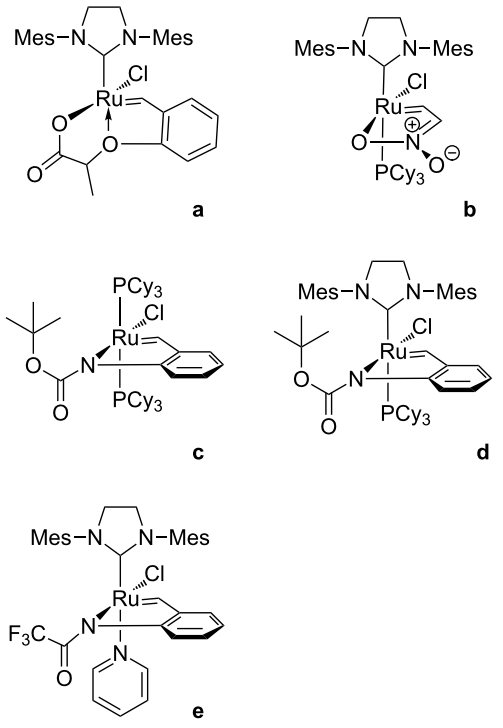

Figure 2: Known latent catalysts of olefin metathesis in which alkylidene ligands are bound to a heteroatom, acting as an anionic ligand.

Recently we have reported a study on aryloxybenzylidene ruthenium chelates (**1a–d** Figure 3) [9]. Similar complexes have also been independently studied by Skowerski and Grela [10].

Phenoxybenzylidene complexes have been demonstrated to behave like latent catalysts in common testing reactions involving ring opening metathesis polymerisation (ROMP)

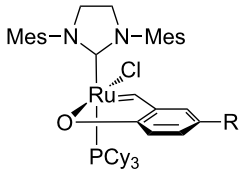

R = H (**1a**), Me (**1b**), NO_2 (**1c**), Cl (**1d**)

Figure 3: Selected, known aryloxybenzylidene chelates [9,10].

of COD, norbornene derivative and dicyclopentadiene as well as cross metathesis (CM) of allylbenzene with *Z*-1,4-(diacetoxy)but-2-ene [9,10]. Although catalysts **1a–d** are characterized by a number of advantages, they are not free from some weaknesses. They showed in some reactions a non-negligible catalytic activity in the absence of activators [9,10] and an instability of the activated forms. Herein, searching for improved latent catalysts that are less reactive in dormant form and highly active in the presence of an chemical activator, we report the synthesis and catalytic performance of new phenoxybenzylidene ruthenium chelates modified by introduction of electron donating and electron withdrawing substituents at the benzylidene ligand in para position to the coordinating oxygen and bearing instead of a strong sigma-donor ligand – tricyclohexylphosphine a weaker sigma-donor – a triphenylphosphine ligand or its derivatives. The catalytic performance of the synthesized complexes were tested in ROMP of COD and a single selected norbornene derivative.

Results and Discussion

Synthesis

Complexes containing triphenylphosphine ligands and substituted triphenylphosphine ligands were isolated in high yields (95–98%) according to the methodology described by Grubbs (Scheme 1) [11]. However, in our hands to get complete transformation 5 equiv of phosphine had to be used.

In a next step the complexes (**4**–**6**) were subjected to metathesis exchange reaction with 2-(prop-1-enyl)phenol (Scheme 2). The reaction was performed in the presence of an equimolar amount of the corresponding phosphine in order to bind the HCl liberated during the reaction, which resulted in a significant increase in the reaction yield. Complexes **8**–**10** were easily isolated by precipitation with methanol or hexane from concentrated solution in methylene chloride (isolated yields = 86–90%). ^{1}H NMR spectra confirmed the formation of new alkylidene complexes.

Complexes **13** and **14** were prepared by using a similar methodology. Complex **4** was subjected to a metathesis exchange with a slight excess of the appropriate 2-vinylphenol in the presence

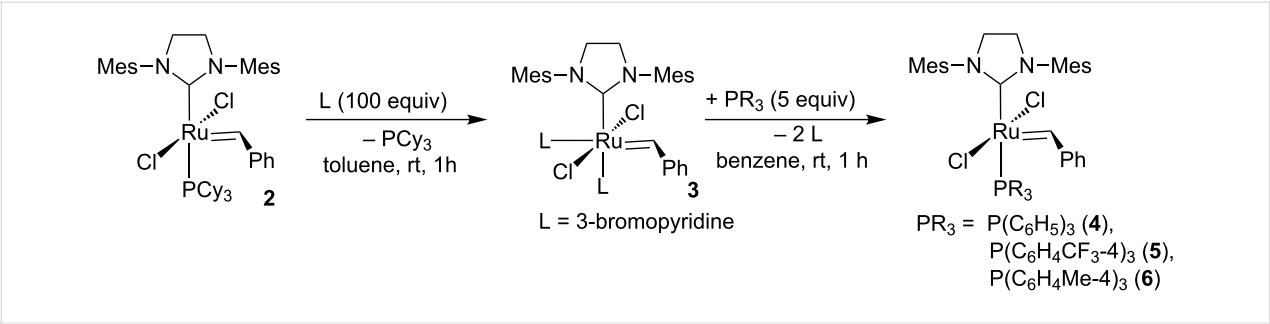

Scheme 1: Synthesis of catalyst precursors **4–6** [11].

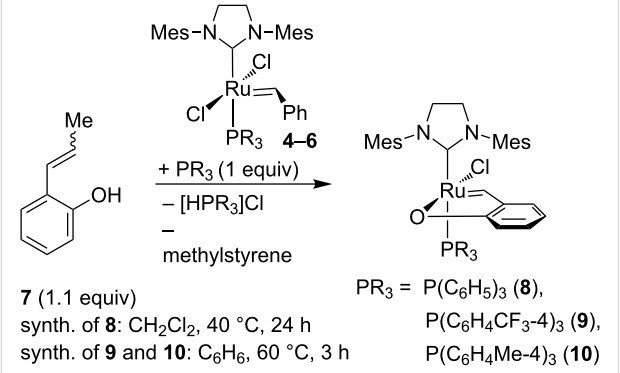

Scheme 2: Synthesis of catalysts **8–10**.

of triphenylphosphine (Scheme 3). Complexes were obtained with isolated yields of 90% (complex **13**) and 92% (complex **14**).

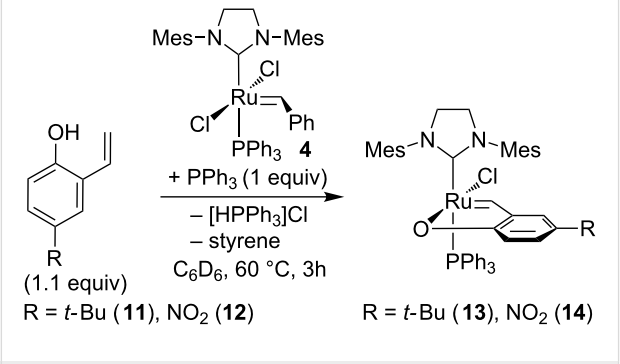

Scheme 3: Synthesis of catalysts **13** and **14**.

Catalytic activity

The obtained complexes were tested in the ring opening metathesis polymerisation (ROMP) of cyclooctadiene. First, the impact of a phosphine ligand on the catalytic activity was investigated. Preliminary tests performed showed, as expected, that in the absence of the activator complexes **1a** and **8–10** were completely inactive (CH_2Cl_2, 40 °C, 0.5 M, 0.1 mol % of catalyst). Under the same conditions, in the presence of 2 equivalents of HCl (used in the form of 2.0 M solution in diethyl ether) as an activating agent, complex **1a** was capable for providing a complete conversion after a few minutes of the reaction. Preliminary tests to optimize the concentration of the catalyst showed that complex **1a** in the presence of an activator retained high catalytic activity in the test reaction already at a concentration of 0.005 mol % (relative to the monomer). The reaction profiles for the catalysts **1a** and **8–10**, both in the dormant form and in the presence of an activator are shown in Figure 4. The results confirm the total lack of activity of complexes in their dormant forms and show a dramatic increase in catalytic activity in the presence of 2 equiv of HCl as an activator. The chart illustrates an insignificant effect of the properties of the phosphine ligand on the catalytic activity of the complexes. The order of increasing activities of the activated species, i.e., **8** (PPh_3) < **10** $P(C_6H_4Me\text{-}4)_3$ < **1a** (PCy_3) < **9** $P(C_6H_4CF_3\text{-}4)_3$ does not correlate with decreasing σ-donor

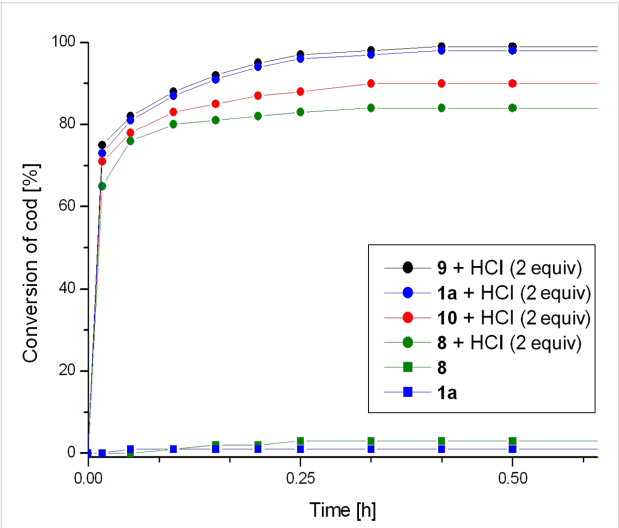

Figure 4: ROMP of COD. Conditions: CH_2Cl_2, 40 °C, 0.5 M, [COD]:[Ru] = 20000; For clarity, only two representative profiles for non-activated catalysts were presented.

ability of the phosphine ligands (represented by Hammet constant) [12,13]. The highest activity was indeed observed for complex **9** containing the weakest σ-donor and potentially most easily dissociating ligand $P(C_6H_4CF_3\text{-}4)_3$. However, the lowest activity was found for complex **8** containing triphenylphosphine which is characterised by lower σ-strength than a tris(*p*-tolyl)phosphine present in catalyst **10** and tricyclohexylphosphine present in the very active catalyst **1a**. The increase in activity could be correlated to some extent with growing basicity of the phosphine ligand. More basic phosphine more readily reacted with the activator (HCl) leading to a faster increase in the concentration of the phosphine-free form of the catalyst (Figure 4).

The influence of electronic properties of substituents placed in the aromatic ring of the chelating ligand, in para position to the oxygen covalently bound to the ruthenium atom, was examined by comparing the activity of complexes **8**, **13** and **14**. Complexes **13** and **14**, when used without any activating additives, showed no catalytic activity under the reaction conditions. However, in the presence of two equivalents of HCl, the effect of the electronic properties of the above substituents was significant. Comparison of the activities of catalysts **8**, **13** and **14** in their dormant forms and in the presence of an activator is shown in Figure 5. The highest activity was observed for catalyst **13** containing an electron donating *tert*-butyl group at the aromatic ring. In the presence of this catalyst, the addition of the activator resulted in a dramatic increase in catalytic activity, so that complete conversion was observed after a few minutes of the reaction course. On the other hand, the lowest activity was observed for complex **14** containing a strongly electron withdrawing nitro group. In the presence of this catalyst, after 1 h of the reaction only about 17% conversion took place. A similar impact of substituents was observed for complexes **1a–c** [9]. A reasonable explanation of the activating influence of electron donating groups is an increase in electron density on the chelating oxygen atom generated by a positive inductive effect, which facilitates the protonolysis of the Ru–O bond. The strongly electron withdrawing nitro group present in complex **14** caused reduction of the electron density on the oxygen atom and consequently its lower susceptibility to protonolysis which has been earlier proved to be necessary for the catalyst activation [9].

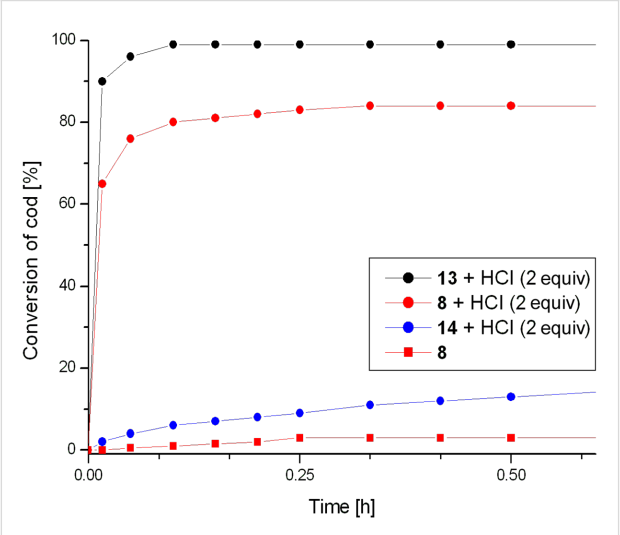

Figure 5: ROMP of cod. Conditions: CH_2Cl_2, 40 °C, 0.5 M, [cod]:[Ru] = 20000; For clarity only representative profile for non-activated catalyst is presented.

The catalytic performance of phenoxybenzylidene ruthenium chelates **1a**, **8**, **13** and **14** was also checked in ROMP of a single selected norbornene derivative **15** (Scheme 4). The reaction progress was monitored by ^{1}H NMR spectroscopy.

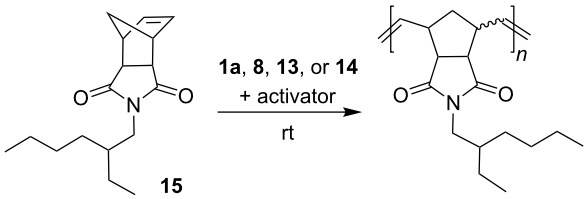

Scheme 4: ROMP of monomer **15**.

Inactivated catalyst **1a** does not exhibit catalytic activity in ROMP of **15** performed at room temperature (23 °C). When HCl is added, the activity of complex **1a** increases, but after 2 h of the reaction course only about 30% monomer conversion was observed. At 40 °C, complex **1a** used without an activator remained inactive, but the addition of HCl led to complete monomer conversion within 2 h (Figure 6). In a separate experiment performed at room temperature the activated complex **1a** gave 90% monomer conversion within 2 h, by using a monomer to catalyst ratio as high as 2000.

Preliminary studies of ROMP of monomer **15** in the presence of activated complexes **8**, **13** and **14** revealed their significantly higher catalytic activity than that of activated complex **1a**; that is why a further study of ROMP was performed at room temperature. In the absence of an activator, the reaction over all these complexes gave only trace monomer conversion (Figure 7). After the activation with 2 equiv HCl, complete monomer conversion was observed to occur within 30 min in the presence of catalyst **8** and within 20 min for catalyst **13**. Complex **14** exhibits significantly lower activity. After 1 h only 22% conversion was noted and complete monomer consumption required 24 h of the reaction course.

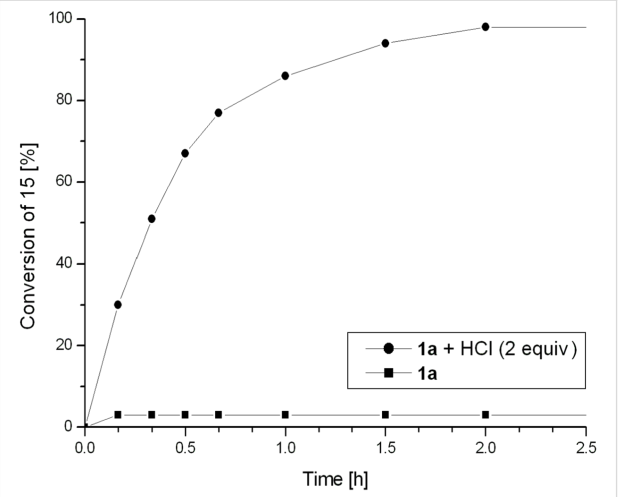

Figure 6: ROMP of monomer **15**. Conditions: $CDCl_3$, 40 °C, 0.08 M, [**15**]:[Ru] = 200.

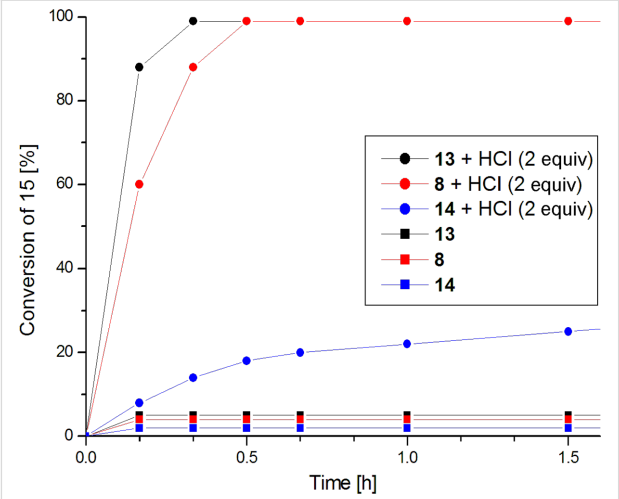

Figure 7: ROMP of monomer **15**. Conditions: $CDCl_3$, 23 °C, 0.08 M, [**15**]:[Ru] = 200.

Activation process study

Our earlier studies of the activation of complex **1a** with an ethereal solution of HCl have proved that the chelate ring opening by cleavage of the Ru–O bond is necessary for getting the catalytically active form of this complex [9]. On the other hand, the studies of the effect of CuCl, acting as a phosphine scavenger, on the activity of complex **1a** in ROMP of COD revealed a small activating effect [9]. An analogous study performed for ROMP of COD catalysed with complex **8** did not confirm the activating impact of CuCl. Complex **8** used alone or in the presence of 2–5 equiv of CuCl was totally inactive. In order to elucidate the possible transformations taking place in the system phenoxybenzylidene chelate/CuCl, a benzene solution of complex **8** was heated with 1 equiv of CuCl at 60 °C. After 24 h of the reaction course, the formation of a green precipitate was observed. X-ray diffraction analysis of single crystals obtained by slow evaporation of the post-reaction mixture revealed the formation of dimeric complex **16**, in which the phenoxybenzylidene ring was conserved (Figure 8), which points to the reaction proceeding according to Scheme 5.

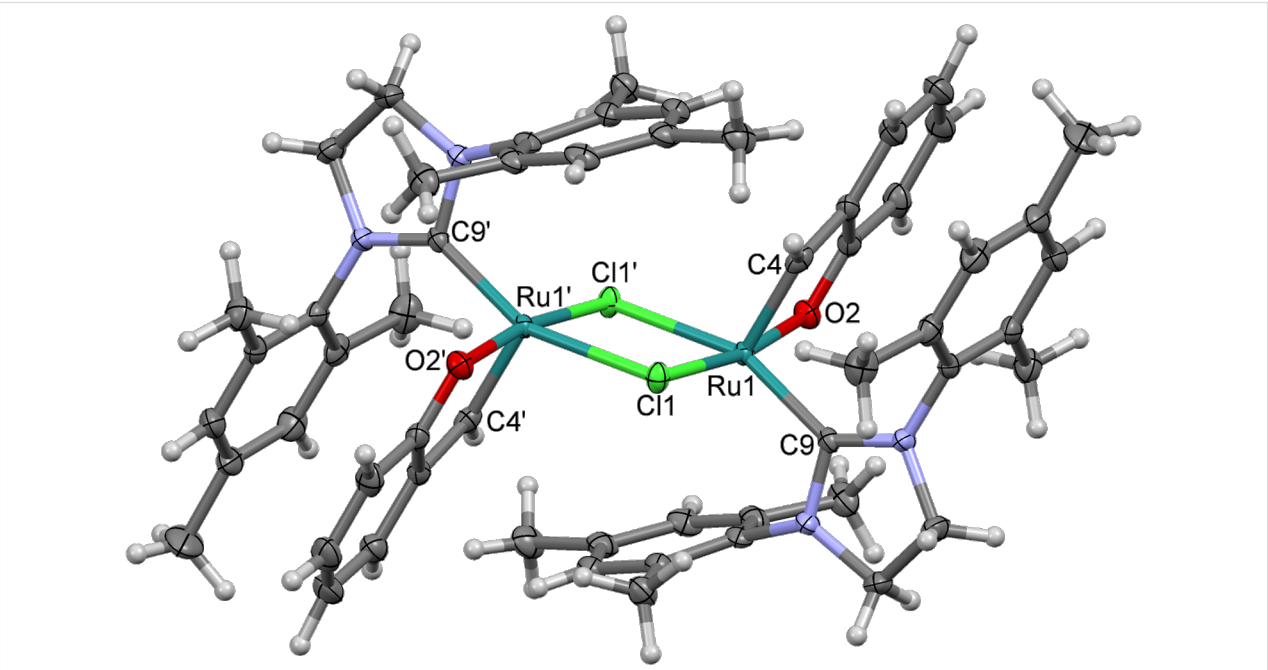

Figure 8: A perspective view of complex **16**, the ellipsoids are drawn at the 50% probability level. Hydrogen atoms are drawn as spheres of arbitrary radii.

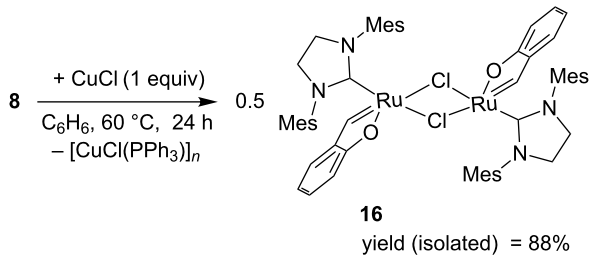

Scheme 5: Formation of phosphine free dimeric complex in the presence of CuCl.

Similar transformation was observed with the use of complex **1a** as a starting compound [9]. The reaction was particularly effective in benzene because of poor solubility of the dimer in this solvent.

As it is common for ruthenium–alkylidene complexes active in metathesis, the coordination of the Ru atom might be described as a distorted tetragonal pyramid, with the carbon atom double-bonded to Ru (C4) in the apex of the pyramid. The distortions in the dimer are more pronounced than in the similar mononuclear complex **1a** (see supplemetara data of [9]), but still four base atoms; two chlorines, carbon C9 and oxygen O2 are planar within ca. 0.22 Å, Ru lies also quite well within this plane (0.17Å), and only the C4 atom is by 1.99 Å distant from the plane. The Ru–C line makes an angle of ca. 8.6° with the normal to the mean basal plane. The double-bond Ru1–C4 (1.841(3) Å) is significantly shorter than the formally single Ru–C9 bond of 1.974(2) Å. Probably due to the steric requirements, Ru–Cl distances in the dimer are longer than in mononuclear complex **1a** (2.4145(5) and 2.42775(5) Å, as compared to 2.3827(4)), while the other bonds are slightly (Ru=C: 1.841(3) vs 1.8499(18) Å, Ru–O: 2.0720(16) vs 2.0936(12) or significantly (Ru–O: 1.974(2) vs 2.0720(16)) shorter. Complex **16** showed no catalytic activity in the ROMP of COD under the conditions used (CH_2Cl_2, 40 °C, 0.5 M, 0.005–0.1 mol % relative to the monomer). The observed catalytic inactivity was found not to be a consequence of conservation of chelating phenoxybenzylidene ring in the dimer structure but results from the fast decomposition of complex **16** in solution, leading to the loss of alkylidene moiety. However, when a suspension of dimer **16** in CH_2Cl_2 was treated with an equimolar amount of triphenylphosphine formation of complex **8** with an almost quantitative yield was observed. A similar reaction was observed when strongly nucleophilic PCy_3 was used (Scheme 6). The reaction can be successfully used as an alternative method for the synthesis of a variety of phenoxybenzylidene chelates (see Experimental).

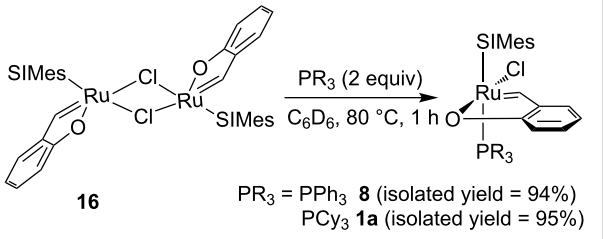

Scheme 6: Synthesis of complexes **1a** and **8** starting from dimer **16**.

According to the earlier described activation mechanism [9], the reaction of phenoxybenzylidene chelates with 1 equiv of HCl leads to protonation of the oxygen atom in the Ru–O bond, which results in the breaking of the bond and introduction of a chloride anion into the coordination sphere of ruthenium. Exposition of complex **8** to one equivalent of HCl brought a change in the solution colour from green to light-green. The fine-crystalline light-green precipitate was isolated from the post-reaction mixture by precipitation with hexane with 95% isolated yield. The precipitate was stable as solid and sufficiently stable in a CD_2Cl_2 solution to permit recording of its ^1H and ^{31}P NMR spectra. On the basis of the data obtained the reaction was proposed to proceed according to Scheme 7. However, it was impossible to identify in the ^1H NMR spectrum the signal that could be assigned to the hydroxy group. It is most probably a consequence of high lability of this proton and its suitability for exchange with deuterium coming from the NMR solvent (CD_2Cl_2) as it was observed for activated complex **1a** [9].

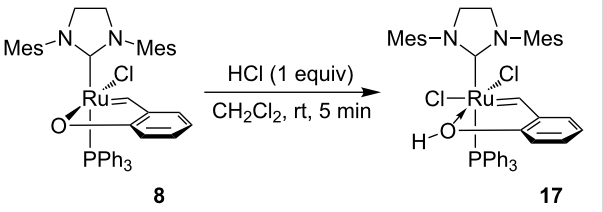

Scheme 7: Activation of complex **8** with one equivalent of HCl.

Complex **17** was proved to exhibit high catalytic activity in ROMP of the monomers tested. In ROMP of COD (CH_2Cl_2, 40 °C, 0.5 M, [COD]: [Ru] = 20000) it permits obtaining complete conversion after 10 min of the reaction course. Performed tests of ROMP of monomer **15** showed complete conversion within 15 min ($CDCl_3$, 23 °C, 0.08 M, [**15**]:[Ru] = 200) and within 1 h when using monomer to catalyst ratio equal to 2000.

Conclusion

Ruthenium–benzylidene complexes bearing a triphenylphosphine ligand or its para-substituted analogues undergo

metathetic exchange with 2-(prop-1-enyl)phenol or substituted 2-vinylphenols to form phenoxybenzylidene ruthenium chelates. These complexes in the phenoxide form exhibit nearly no activity in ROMP of COD and an exemplary norbornene derivative. However, they can be easily activated by addition of an ethereal solution of HCl. The catalytic activity in their active forms was found to be related to the basicity and nucleophilicity of the phosphine ligands. A strong electronic influence of the substituent in the ring of the phenoxybenzylidene ligand, in para position towards the oxygen atom, on the catalytic activity of the active form of the complexes was found. The presence of an electron-donating *tert*-butyl substituent gave a significant increase in the complex activity, while in the presence of a strongly electron-accepting nitro group the strong opposite effect was observed. When compared to the earlier described analogous complexes, the new phenoxybenzylidene chelates exhibit profound catalytic inactivity in their dormant forms and an improved catalytic activity (after activation) in ROMP of tested monomers.

Experimental

See Supporting Information File 1 for full experimental data including general methods and chemicals, syntheses and characterization of complexes, procedures of catalytic tests and X-ray analysis.

Supporting Information

Supporting Information File 1

General methods and chemicals, syntheses and characterization of complexes **8**–**10**, **13**, **14**, **16** and **17**, procedures of catalytic tests and X-ray analysis.
[http://www.beilstein-journals.org/bjoc/content/supplementary/1860-5397-11-206-S1.pdf]

Acknowledgements

Financial support from the National Science Centre (Poland), (project No. UMO-2011/03/B/ST5/01047) is gratefully acknowledged.

References

1. Grela, K., Ed. *Olefin Metathesis. Theory and Practice;* Wiley: Hoboken, 2014. doi:10.1002/9781118711613
2. Grubbs, R. H.; Wenzel, A. G.; O'Leary, D. J.; Khosravi, E., Eds. *Handbook of Metathesis;* Wiley-VCH: Weinheim, 2015. doi:10.1002/9783527674107
3. Vidavsky, Y.; Anaby, A.; Lemcoff, N. G. *Dalton Trans.* **2012,** *41,* 32–43. doi:10.1039/C1DT11404B
4. Szadkowska, A.; Grela, K. *Curr. Org. Chem.* **2008,** *12,* 1631–1647. doi:10.2174/138527208786786264
5. Monsaert, S.; Lozano Vila, A.; Drozdzak, R.; Van Der Voort, P.; Verpoort, F. *Chem. Soc. Rev.* **2009,** *38,* 3360–3372. doi:10.1039/b902345n
6. Gawin, R.; Makal, A.; Woźniak, K.; Mauduit, M.; Grela, K. *Angew. Chem., Int. Ed.* **2007,** *46,* 7206–7209. doi:10.1002/anie.200701302
Angew. Chem. **2007,** *119,* 7344–7347. doi:10.1002/ange.200701302
7. Wdowik, T.; Samojłowicz, C.; Jawiczuk, M.; Malińska, M.; Woźniak, K.; Grela, K. *Chem. Commun.* **2013,** *49,* 674–676. doi:10.1039/C2CC37385H
8. Pietraszuk, C.; Rogalski, S.; Powała, B.; Miętkiewski, M.; Kubicki, M.; Spólnik, G.; Danikiewicz, W.; Woźniak, K.; Pazio, A.; Szadkowska, A.; Kozłowska, A.; Grela, K. *Chem. – Eur. J.* **2012,** *18,* 6465–6469. doi:10.1002/chem.201103973
9. Żak, P.; Rogalski, S.; Przybylski, P.; Kubicki, M.; Pietraszuk, C. *Eur. J. Inorg. Chem.* **2014,** 1131–1136. doi:10.1002/ejic.201301208
10. Kozłowska, A.; Dranka, M.; Zachara, J.; Pump, E.; Slugovc, C.; Skowerski, K.; Grela, K. *Chem. – Eur. J.* **2014,** *20,* 14120–14125. doi:10.1002/chem.201403580
11. Sanford, M. S.; Love, J. A.; Grubbs, R. H. *Organometallics* **2001,** *20,* 5314–5318. doi:10.1021/om010599r
12. Love, J. A.; Sanford, M. S.; Day, M. W.; Grubbs, R. H. *J. Am. Chem. Soc.* **2003,** *125,* 10103–10109. doi:10.1021/ja027472t
13. Ewing, D. F. In *Correlation Analysis in Chemistry;* Chapman, N. B.; Shorter, J., Eds.; Plenum: New York, 1978; pp 357–396. doi:10.1007/978-1-4615-8831-3_8

License and Terms

BEILSTEIN JOURNAL OF ORGANIC CHEMISTRY

Hexacoordinate Ru-based olefin metathesis catalysts with pH-responsive N-heterocyclic carbene (NHC) and N-donor ligands for ROMP reactions in non-aqueous, aqueous and emulsion conditions

Shawna L. Balof[1], K. Owen Nix[2], Matthew S. Olliff[2], Sarah E. Roessler[2], Arpita Saha[2], Kevin B. Müller[3], Ulrich Behrens[4], Edward J. Valente[5] and Hans-Jörg Schanz[*2]

Full Research Paper

Open Access

Address:
[1]Department of Chemistry & Biochemistry, The University of Southern Mississippi, 118 College Drive, Hattiesburg, MS 39406-5043, USA, [2]Department of Chemistry, Georgia Southern University, 521 College of Education Drive, Statesboro, GA 30458-8064, USA, [3]BASF SE, G-PM/PD - F206, 67056 Ludwigshafen, Germany, [4]BASF SE, Basic Chemicals Research, GCB/C – M313, 67056 Ludwigshafen, Germany and [5]Department of Chemistry, University of Portland, 5000 N. Willamette Blvd., Portland, OR 97203, USA

Email:
Hans-Jörg Schanz[*] - hschanz@georgiasouthern.edu

* Corresponding author

Keywords:
activation; aqueous catalysis; emulsion; olefin metathesis; polymerization; ruthenium

Beilstein J. Org. Chem. **2015,** *11,* 1960–1972.
doi:10.3762/bjoc.11.212

Received: 15 June 2015
Accepted: 24 September 2015
Published: 21 October 2015

This article is part of the Thematic Series "Progress in metathesis chemistry II".

Guest Editor: K. Grela

Abstract

Three new ruthenium alkylidene complexes (PCy_3)Cl_2(H_2ITap)Ru=CHSPh (**9**), (DMAP)$_2Cl_2$(H_2ITap)Ru=CHPh (**11**) and (DMAP)$_2Cl_2$(H_2ITap)Ru=CHSPh (**12**) have been synthesized bearing the pH-responsive H_2ITap ligand (H_2ITap = 1,3-bis(2',6'-dimethyl-4'-dimethylaminophenyl)-4,5-dihydroimidazol-2-ylidene). Catalysts **11** and **12** are additionally ligated by two pH-responsive DMAP ligands. The crystal structure was solved for complex **12** by X-ray diffraction. In organic, neutral solution, the catalysts are capable of performing standard ring-opening metathesis polymerization (ROMP) and ring closing metathesis (RCM) reactions with standard substrates. The ROMP with complex **11** is accelerated in the presence of two equiv of H_3PO_4, but is reduced as soon as the acid amount increased. The metathesis of phenylthiomethylidene catalysts **9** and **12** is sluggish at room temperature, but their ROMP can be dramatically accelerated at 60 °C. Complexes **11** and **12** are soluble in aqueous acid. They display the ability to perform RCM of diallylmalonic acid (DAMA), however, their conversions are very low amounting only to few turnovers before decomposition. However, both catalysts exhibit outstanding performance in the ROMP of dicyclopentadiene (DCPD) and mixtures of DCPD with cyclooctene (COE) in acidic aqueous microemulsion. With loadings as low as 180 ppm, the catalysts afforded mostly quantitative conversions of these monomers while maintaining the size and shape of the droplets throughout the polymerization process. Furthermore, the coagulate content for all experiments stayed <2%. This represents an unprecedented efficiency in emulsion ROMP based on hydrophilic ruthenium alkylidene complexes.

Introduction

The vast application spectrum of Ru-based olefin metathesis has provided a powerful synthetic tool for the organic [1-3] and polymer chemist [4-8] alike. The catalysts' high tolerance towards functional groups, air and moisture makes them attractive to be used in combination of a wide range of substrates and solvents [9-12]. Over the past decade, Ru–alkylidene based olefin metathesis in aqueous media has become increasingly important [13]. Benefits such as the non-hazardous, vastly abundant and commercially highly attractive of water coupled with a high heat capacity make organic transformations using hydrophilic catalyst in aqueous media very attractive [14-18]. These benefits, coupled with potential applications in biological media [19], have led to the development of various water-soluble catalyst designs [20,21]. Such catalysts contain hydrophilic phosphine ligands [22-25], NHC ligands [26-29], N-donor ligands [30], alkylidene moieties [31-33] or combinations of these structural features [34-37]. Another recent development in homogeneous catalysis, and olefin metathesis in particular, have become switchable catalysts or systems where the activity can be controlled by external stimuli [38-44]. In metathesis, pH is a very straightforward stimulus that can fulfill two independent functions for catalysts bearing pH-responsive ligands resulting in metathesis activation [45-53] and/or solubilization [31,32] in aqueous media.

One of the most intriguing applications of water-soluble metathesis catalysts is the production of latexes via ring-opening metathesis polymerization (ROMP) in emulsion. However, to date very few reports have successfully employed well-defined, hydrophilic Ru–alkylidene catalysts in combination with a hydrophobic monomer in emulsion. The first emulsion ROMP was reported in the early 2000's when Claverie et al. used 1st generation Grubbs-type catalysts [24] **1** and **2** (Figure 1, approx. 400 ppm catalyst loading) to effectively polymerize norbornene (NBE) at 80 °C in microemulsion (91% conversion) [54]. The same conditions failed to polymerize significant amounts of the far less reactive monomers cyclooctene (COE) or cyclooctadiene (COD) with yields below 10%. Later, Heroguez et al. synthesized the 1st generation Grubbs-type macroinitiator **3** which accomplished near quantitative conversions with NBE and as high as 90% conversion with COE and COD using 500 ppm catalyst loading in microemulsion [55]. However, these high conversions were accompanied by flocculation of the polymers. Just recently, Maier et al. reported pH-responsive catalyst **4** which accomplished up to 95% ROMP conversion with 0.2% catalyst loading in microemulsion after the addition of HCl [56]. Interestingly, increased acid addition resulted in an increased molecular weight control of the emulsion ROMP process. To date, no hydrophilic catalyst has been reported to be employed for emulsion ROMP bearing an NHC ligand. This may a consequence of the low accessibility of these catalysts and one of the reasons for the relatively low observed activities knowing that the NHC ligand dramatically increases the propagation rates of the

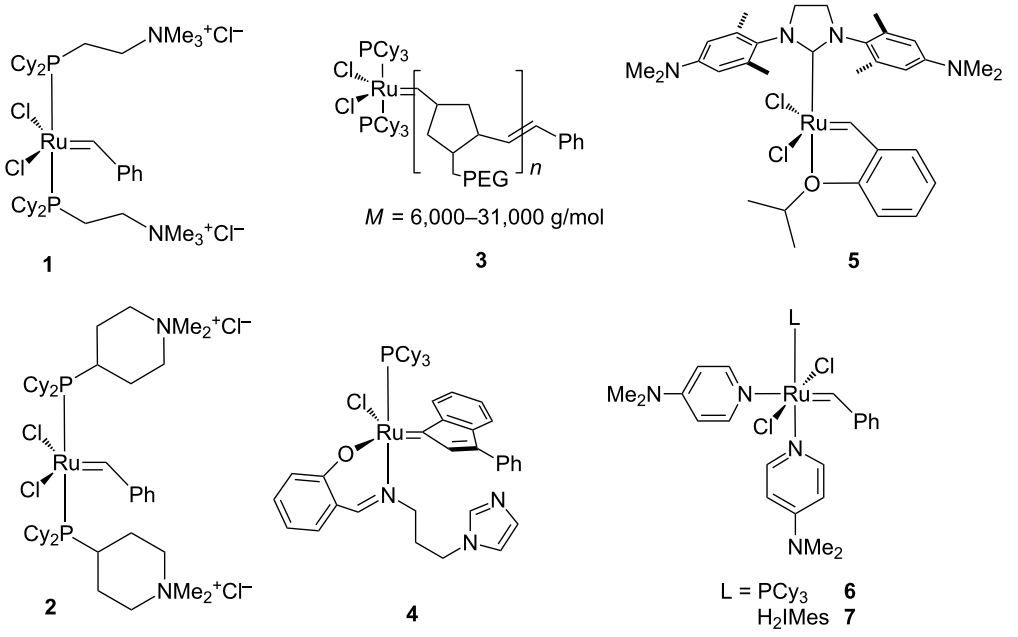

Figure 1: Hydrophilic and/or pH-responsive Ru–alkylidene complexes **1–7** for olefin metathesis.

metathesis reaction [57]. The higher accessibility of water-insoluble catalysts has resulted in an increased investigation of water-insoluble Ru–alkylidene complexes for emulsion ROMP in aqueous media. Slugovc et al. reported the ROMP of dicyclopentadiene (DCPD) in a "high internal phase emulsion" (HIPE) of the monomer in water [58]. Stable latexes have been produced by use of organic-soluble catalysts in micro or miniemulsions [59,60]. Although, this technique has been more successfully applied for a variety of ROMP substrates and allowed the use of more metathesis-active NHC-bearing catalysts, the protocols required to emulsify the catalyst and monomer separately in significant amounts of an organic cosolvent. From a practical and environmental standpoint, the use of hydrophilic complexes for emulsion ROMP eliminating or reducing the need for high amounts of organic cosolvents seems advantageous. In this light it is desirable to develop water-soluble catalyst systems which can perform the task with high activity, substrate range and sufficient hydrolytic stability to access a variety of novel ROMP latexes. We now wish to report the synthesis of two new pH-responsive, Ru-based olefin metathesis catalysts, their ROMP and ring closing metathesis (RCM) activities in organic and aqueous solvents, as well as their use in the first near-quantitative ROMP procedure in microemulsion to produce stable latexes from DCPD and DCPD/COE mixtures.

Results and Discussion

Catalyst syntheses

We have previously reported olefin metathesis catalyst **5** bearing the pH-responsive H_2ITap [1,3-bis(*N*',*N*',2',6'-tetramethylaminophenyl)-4,5-dihydroimidazol-2-ylidene] ligand containing two NMe_2 groups [61]. The addition of HCl to complex **5** results in the protonation of the amino groups to produce a water-soluble dicationic complex. Although the protonation of the ancillary NMe_2 groups was demonstrated to cause a reduced ROMP propagation rate compared the neutral catalyst [62], we hypothesized that a catalyst based on this NHC-motif could still be superior in activity to phosphine-containing catalysts **1**–**4** in an emulsion ROMP process. It should be noted that olefin metathesis catalysts bearing a similar ligand with NEt_2 groups instead of the NMe_2 groups of the H_2ITap ligand have been developed simultaneously in Plenio's laboratories [63].

We anticipated that a variety of Ru-based olefin metathesis catalysts with an H_2ITap ligand should be accessible quite straightforwardly to be used in emulsion ROMP. For this purpose, we synthesized 2nd generation Grubbs-type catalyst **9** from ruthenium phenylthiomethylidene complex **8** in a modified ligand exchange procedure (Scheme 1), which is somewhat analogous to the most common literature procedure [61,64]. The ROMP and RCM performance of Fischer-carbene complexes such as **9** are often sluggish and often do not result in high conversions [65,66]. However, these complexes are thermally very inert and economically viable options to other commercially available olefin metathesis catalyst. Furthermore, their use at elevated temperatures may be feasible or even advantageous over their more reactive counterparts. Since catalyst **9** is not very soluble in aqueous HCl despite double protonation we replaced the hydrophobic PCy_3 ligand with two 4-dimethylaminopyridine (DMAP) ligands. This was demonstrated to significantly improve the complex solubility in acidic aqueous media [32]. We have also demonstrated before that acid addition to $(DMAP)_2$Ru–alkylidene complexes **6** and **7** resulted in fast protonation of the N-donor ligand and thus resulting in fast, irreversible and generally complete metathesis initiation [45,46]. For most ROMP processes, this is desirable as a fast initiation typically affords high ROMP activity with low catalyst loadings [57,67]. Hence, hexacoordinate complexes **11** and **12** were also synthesized from their precursor complexes **9** and **10** [61] by ligand exchange according to Scheme 2. These complexes now contain pH-responsive groups at the H_2ITap ligand to afford solubility in aqueous acid and at the N-donor ligand which affords rapid metathesis initiation. It should be noted that Plenio et al. also reported a Ru–benzylidene complex similar to catalysts **11** and **12** bearing the NEt_2-analogue to the H_2ITap ligand and two pyridine ligands instead

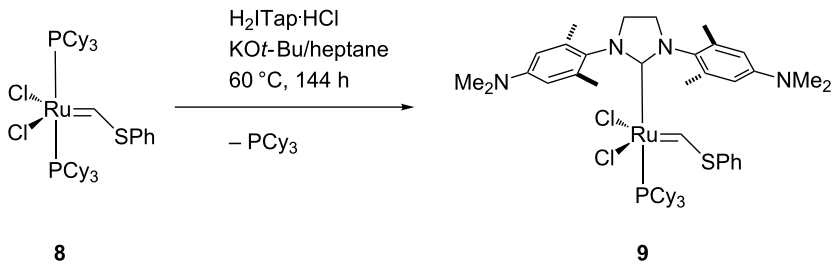

8 **9**

Scheme 1: Synthesis of 2nd Grubbs-type generation complex **9**.

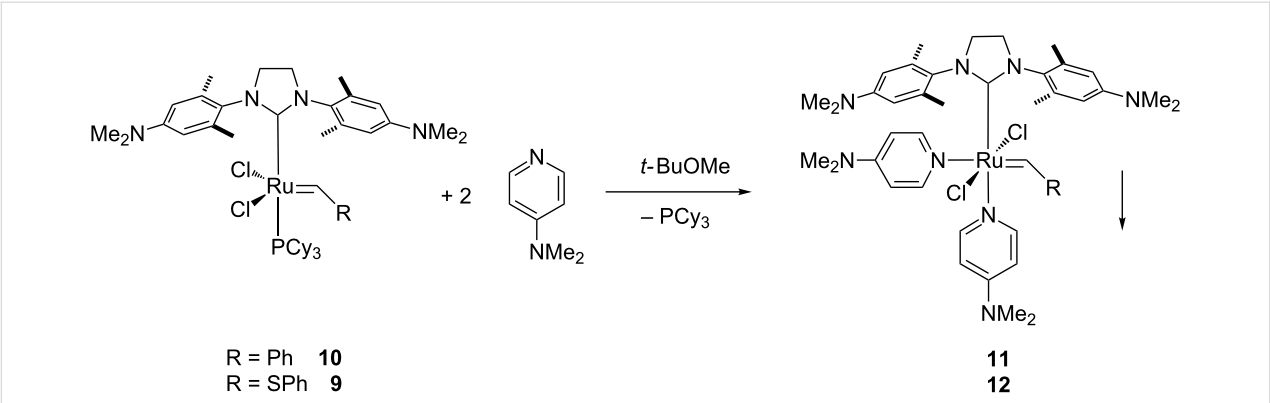

Scheme 2: Synthesis of hexacoordinate, pH-responsive complexes **11** and **12**.

of DMAP. The pH-responsive nature of this complex caused a change in the *E*/*Z*-selectivities of ROMP reactions upon acid addition but the catalyst was not tested for aqueous or emulsion ROMP [68].

Crystal structure analysis of complex **12**

Crystals of complex **12** suitable for X-ray diffraction were obtained via layer diffusion of heptane into a concentrated THF solution (Figure 2). Hexacoordinated complex **12** adopts the expected distorted octahedral coordination sphere around the Ru center with *trans* chloride and *cis* DMAP ligands. In comparison to complex **13** [46], the only other $(DMAP)_2Cl_2Ru$–alkylidene complex bearing an NHC ligand for which a crystal structure was solved, all metal ligand bond distances are very similar (within 2 pm) with the exception of one Ru–N distance to the DMAP ligand *trans* to the NHC ligand (Table 1). In complex **12** this distance is shorter by >0.04 Å. This may be a result of the bridging S-atom in the alkylidene moiety which increases the distance of the phenyl ring to the metal center and the surrounding ligands. Hence, a reduced steric repulsion of this phenyl ring on the geometry around the metal could result, in particular the sterically close N-donor ligand. This can also be seen in the cis C=Ru–N angle which is smaller by almost 2° allowing a closer proximity of these two moieties.

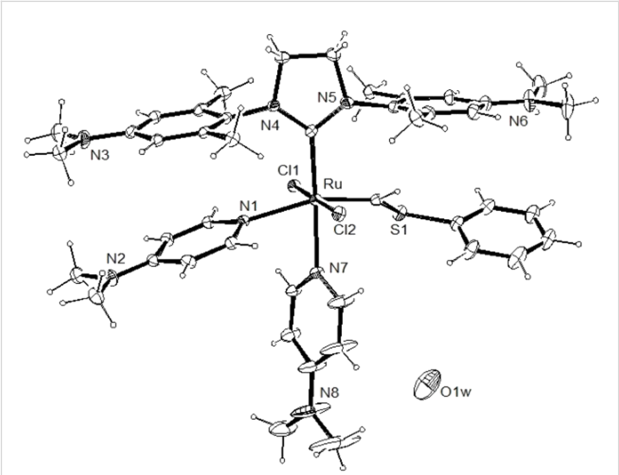

Figure 2: ORTEP diagram for $H_2ITap(DMAP)_2Cl_2Ru$=CH-SPh (**12**). The positions of the hydrogen atoms were calculated. The unit cell contains a molecule of cocrystallized water. The hydrogen atoms of the water molecule were omitted from the structure due to thermal uncertainty.

Catalytic experiments

We investigated the catalyst activity of novel complexes **9**, **11** and **12** in the ROMP of cyclooctene (COE, [Ru] = 0.5 mM, 0.5 mol % catalyst loading) and the ring-closing metathesis (RCM) of diethyl diallylmalonate (DEDAM, [Ru] = 1.0 mM, 1% (n/n) catalyst loading) in neutral organic media (Table 2). The ROMP reaction with catalyst **11** in benzene-d_6 accomplished 93% conversion of COE within 19 min which is similar in the performance to its previously reported counterpart **13**. Interestingly, the same reaction is accelerated and yields near quantitative (97%) conversion in 15 min in the presence of 2 equiv H_3PO_4 as a result of the protonation of the DMAP ligands and hence, fast and complete initiation. The addition of more acid (4 equiv H_3PO_4) results in a reduction of the activity (41% in 30 min). This may be due to significant protonation of the H_2ITap ligand which was shown to have an adverse effect on the metathesis propagation of these complexes [61,62]. By contrast, complex **12** exhibited much lower activity as expected. The ROMP of COE in $CDCl_3$ at ambient temperature only affords 3.9% conversion in 60 min. $CDCl_3$ was used owing to the low complex solubility in benzene-d_6 and it should be noted that complex **12** is stable for several hours at ambient temperature (<2% decomposition in 2 h) in this solvent. Heating the reaction to 60 °C increases the catalyst activity (36% conversion in 60 min), however, the reaction does not reach completion likely owing to catalyst degradation. In contrast to com-

Table 1: Selected bond lengths (Å) and angles (°) for complexes **12** and **13** [46].

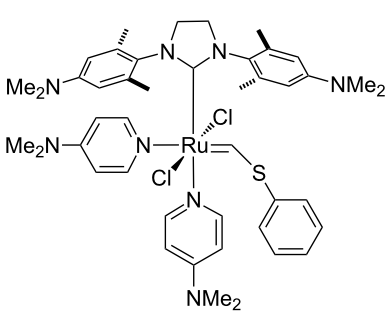

12

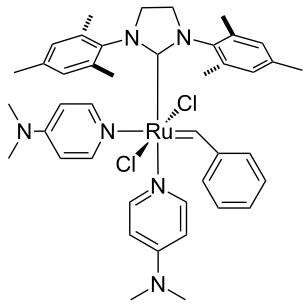

13

	12	**13**		**12**	**13**
Ru=C	1.874(5)	1.873(2)	Ru–C	2.057(4)	2.051(2)
Ru–N	2.201(4) 2.289(4)	2.1933(16) 2.3309(17)	Ru–Cl	2.4091(11) 2.4202(11)	2.3847(5) 2.4372(5)
C=Ru–C	96.22(17)	95.00(9)	Cl–Ru–Cl	179.25(4)	177.54(2)
C=Ru–N	176.86(13) 86.32(12)	176.64(7) 88.29(8)	C–Ru–N	163.28(15) 99.66(15)	162.41(8) 97.01(7)
C=Ru–Cl	93.02(14) 86.33(12)	90.47(6) 85.43(7)	C–Ru–Cl	92.42(12) 87.58(12)	88.29(8) 89.07(5)

Table 2: ROMP and RCM reactions with catalysts **8–10** in C_6D_6 ([Ru] = 0.5 mM for 0.5 mol %, 1.0 mM for 1 mol % loading).

catalyst	catalyst loading (%)	substrate	product	equiv H_3PO_4	time (min)	temperature (°C)	conversion (%)
9	0.5	 COE	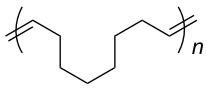	0	60	20	0.8
9				0	24	60	96
11				0	19	20	93
11				2	15	20	97
11				4	30	20	41[a]
12[b]				0	60	20	3.9
12[b]				0	30	60	32
12[b]				0	60	60	36[a]
12[b]				2	60	20	0.9[a]
9	1.0	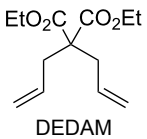 DEDAM	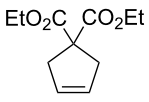	0	60	20	2.3
9				0	30	60	81
11				0	30	20	7.2
11				2	30	20	47[a]
11				4	30	20	14[a]
12[b]				0	60	20	1.2
12[b]				0	30	60	50
12[b]				0	180	60	61[a]

[a]No significant conversion after that time period due to catalyst precipitation or decomposition; [b]in $CDCl_3$.

plex **11**, the addition of 2 equiv of acid proved counter-effective for complex **12** (0.9% conversion in 60 min). It appears that the fast and complete dissociation of the DMAP ligand with this catalyst is not synonymous with the metathesis initiation. This means, while an activated species is formed, other processes, including decomposition are faster than metathesis resulting in minimal portion of complex **12** affording ROMP. 2nd generation Grubbs-type catalyst **9** by contrast exhibited a pronounced

acceleration in the ROMP of COE when heated. The reaction at ambient temperature did not afford noticeable amounts of product (<1% conversion) in 60 min, however, at 60 °C, the conversion reached 96% in less than half the time period. The low metathesis activity of Fischer-type Ru–alkylidenes at room temperature is well-documented [66]. The observed acceleration with heat indicates a significant latency for this complex based on slow metathesis initiation. Neither complexes **11** or **12** performed efficiently in the RCM of DEDAM due to rapid degradation of the catalyst. Whereas catalyst **11** levels off at 7.2% conversion after 30 min at room temperature, catalyst **12** needed to be heated to 60 °C to be activated, and no further conversion was monitored after 60 min (57%). It is likely that the observed low catalyst stability observed for the reactions with complex **11** in benzene solution is based on the rapid degradation of the corresponding $(DMAP)_2Ru{=}CH_2$ intermediate. Such a labile methylidene intermediate is not produced in the ROMP reactions making it the much more effective process. Catalyst **12** produces the very same intermediate, however, the RCM and ROMP reactions both exhibited rapid catalyst decomposition. It appears likely that other degradation mechanisms possibly influenced by the chlorinated solvent ($CDCl_3$) are also involved. Therefore it was not surprising that DMAP-free complex **9** performed quite efficiently in the RCM of DEDAM, more so than complexes **11** and **12**. While at room temperature, the slow metathesis initiation of complex **9** limited the conversion rates dramatically (2% after 60 min), at 60 °C, 90% conversion of DEDAM were monitored in 60 min resulting in a performance much more similar to other 2nd generation Grubbs-type catalysts [61,69].

In contrast to complex **9**, complexes **11** and **12** are completely soluble in aqueous acid. Similar to complex **5**, no noticeable aqueous ROMP was accomplished but the RCM of diallylmalonic acid (DAMA) afforded somewhat low conversions (Table 3) inferior to complex **5**. Based on the observed reactivity trend from the previous kinetic experiments, it is not surprising that benzylidene complex **11** exhibited a superior performance in aqueous HCl where complex **12** failed to produce noticeable amounts of ring-closed product. Interestingly however, when the aqueous solvent is changed to 0.1 m H_3PO_4, complex **12** exhibited a similar performance to catalyst **11**. In fact, this is the only time catalyst **12** exhibited an appreciable metathesis reaction in an acidic medium.

Emulsion ROMP

Based on their solubility in aqueous acid, we were investigating the suitability of catalysts **11** and **12** for the ROMP of DCPD and a DCPD/COE mixture (49:51 mol/mol) in microemulsion to give polydicyclopentadiene (PDCPD) or a statistical copolymer of DCPD and COE (Scheme 3). A 0.1 M HCl_{aq} catalyst solution was added to an emulsion of the monomer containing *n*-hexadecane (5% by mass) to improve the monomer liquidity and polyethylene glycol (PEG) based Emulgin® B3 as surfactant which was previously vigorously stirred for 1 h and then further emulsified using a sonication probe for another 5 min establishing the microemulsion. The emulsion polymerization reactions were conducted at less favorable conditions than those with all previous hydrophilic catalysts. The two different temperatures (35 °C and 55 °C or 65 °C) are significantly lower than 80 °C, which has been commonly used with previous hydrophilic catalysts [54-56]. Furthermore, DCPD and COE exhibit a much lower ROMP activity than NBE, the monomer of choice for previous applications. Finally, catalyst loadings of 180–200 ppm were used which is the lowest reported thus far for any emulsion ROMP reaction. With exception of ROMP of DCPD/COE with catalyst **12** at 35 °C, all reactions proceeded to near-quantitative degree as their determined solid contents often times exceeded the theoretical value derived from the amounts of monomer and surfactant added. This indicates that the catalysts have sufficient activity and thermal stability under the chosen conditions to promote complete ROMP of DCPD and the DCPD/COE monomer mixture.

After the reaction, the latex was filtered (20 mm filter) and the coagulated contents were determined. The z-average droplet diameter was measured via autosizer and a small sample was

Table 3: RCM of diallylmalonic acid (DAMA) in 0.1 M aqueous acid ([Ru] = 2.0 mM, 4 mol % catalyst loading).

catalyst	substrate	product	acid	time (min)	temperature (°C)	conversion (%)
5[a]	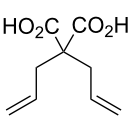 DAMA	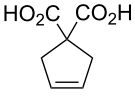	HCl	30	50	44[b]
11			HCl	30	50	25[b]
11			H_3PO_4	30	50	8.7
12			HCl	60	50	n.o.
12			H_3PO_4	60	50	10.3[b]

[a]See [61]; [b]no further conversion after this time period.

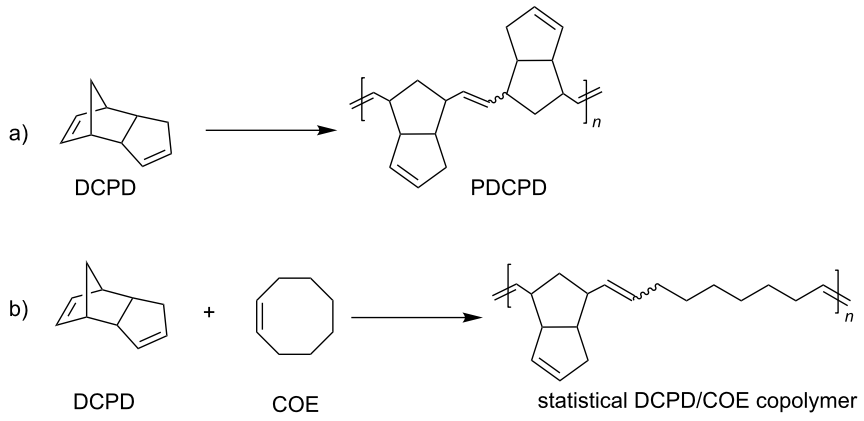

Scheme 3: ROMP reactions conducted under microemulsion conditions.

removed to determine the solid content in the moisture meter. The obtained latexes were relatively stable and could be stored without flocculation. Most reactions provided levels of <1% coagulate versus the dispersed polymer in the latex. In fact, catalyst **12** at 35 °C produced very low levels of coagulum (0.1%) for both reactions. At the higher temperatures, the coagulation increased but the levels always stayed <2%. The average latex particle diameters range from 255 nm to 315 nm using the same concentration of surfactant throughout the series of experiments. The final average droplet diameter deviated less than 3% from the initial droplet size before polymerization where determined. Therefore, the size of the latex particles is somewhat controllable. It should be noted that DCPD contains two reactive double bonds in the monomer structure. When both undergo metathesis in a ROMP reaction, particularly at elevated temperatures, then the PDCPD material is crosslinked [70]. With respect to the latexes synthesized in this project, the presence or the degree of crosslinking in the material has not been determined. The results of the emulsion ROMP experiments are summarized in Table 4.

Evidently, NHC-ligated catalysts **11** and **12** exhibit a much elevated activity under microemulsion conditions in comparison to their water-soluble predecessors **1**–**3** [8,11,12]. At first glance, these high turnover numbers are in stark contrast to the observed low metathesis activity of catalysts **11** and particularly **12** in homogeneous acidic aqueous solution. Based on the low catalyst loadings used in the experiments, their metathesis activity appears to be increased by several orders of magnitude by comparison, meaning the reaction environment must have changed from aqueous to organic. This means, the ROMP reaction is most likely occurring within the micelles. About the nature of the catalytic Ru species can only be speculated at this point. It seems likely that the aqueous acid has completely protonated the pH-responsive ligands to produce water-soluble complexes **14** and **15** (Scheme 4). The protonation of the H_2ITap ligand with aqueous DCl has been demonstrated to be effective, if not quantitative, for complex **5** [61]. The partial or complete removal of donor ligands from Ru–alkylidene complexes with strong aqueous acids has also been shown before which then resulted in catalytic species with higher metathesis

Table 4: Emulsion ROMP of DCPD (Ru/monomer = 1:5.0 × 10^4) and DCPD/COE (49:51 (mol/mol) – Ru/monomer = 1:5.6 × 10^4) mixtures with catalysts **11** and **12** after 120 min reaction time.

catalyst (in 0.012 M HCl)	temperature (°C)	monomer	catalyst loading (ppm)	conversion[a] (%)	coagulate (%)	av. particle diameter (nm)
11	35	DCPD	200	>99	0.4	269
11	55	DCPD		>99	1.0	278
12	35	DCPD		99	0.1	315
12	65	DCPD		>99	0.9	265
11	35	DCPD/COE 1:1	180	>99	0.4	270
11	65	DCPD/COE 1:1		>99	1.5	264
12	35	DCPD/COE 1:1		92	0.1	255
12	65	DCPD/COE 1:1		>99	1.6	290

[a]Conversion determined by weight analysis of non-volatile material left after drying.

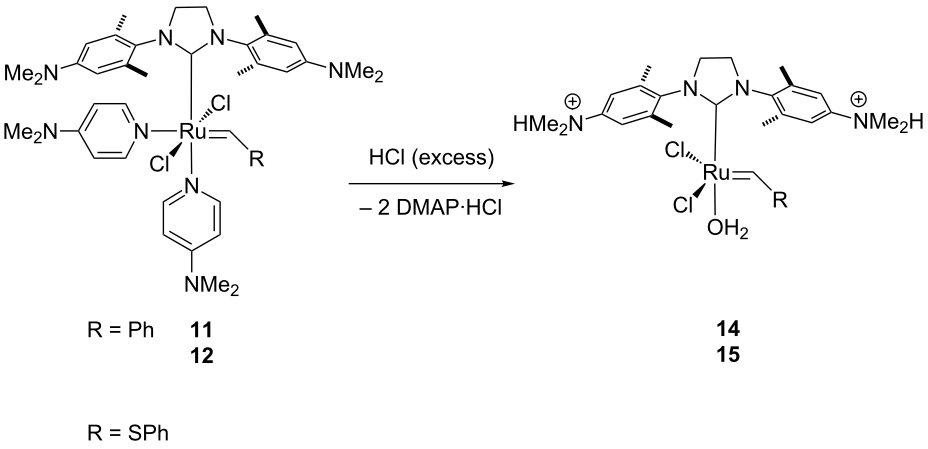

Scheme 4: Proposed formation of catalytic species **14** and **15** under emulsion ROMP conditions.

activity [23,45,46]. In these cases, the empty coordination site was proposed to be occupied by a weak O-donor ligand, i.e., a water molecule which also resulted in a significant stabilization of these activated species from thermal degradation. Since lowering the degree of protonation in H_2ITap ligated Ru–alkylidene complexes has been demonstrated to improve the catalytic activity [62], it cannot be ruled out that the ROMP active species in the micelle may be partially or even completely deprotonated. Also, in the micelle, the H_2O concentration is significantly reduced which could be another reason that a solvent-based inhibition as observed in aqueous media is minimal at best. With regard to the stability of Ru–alkylidene complexes **14** and **15**, they should exhibit much lower thermal stability due to high initiation rates [57]. However, the ability to quantitatively convert the monomers indicates that species **14** and **15** either are stabilized in the aqueous solvent, i.e., via H_2O donation, or the species rapidly migrate into the monomer droplets where they are protected by the monomer as seen previously [58].

A film was produced from the COE/DCPD latex from the ROMP reaction with catalyst **12** at 65 °C. The film was dried at room temperature and cut using a Cryo-Microtome. After the procedure, the spherical particles maintain their size and shape in the film as shown in the atom force microscope (AFM) image (Figure 3).

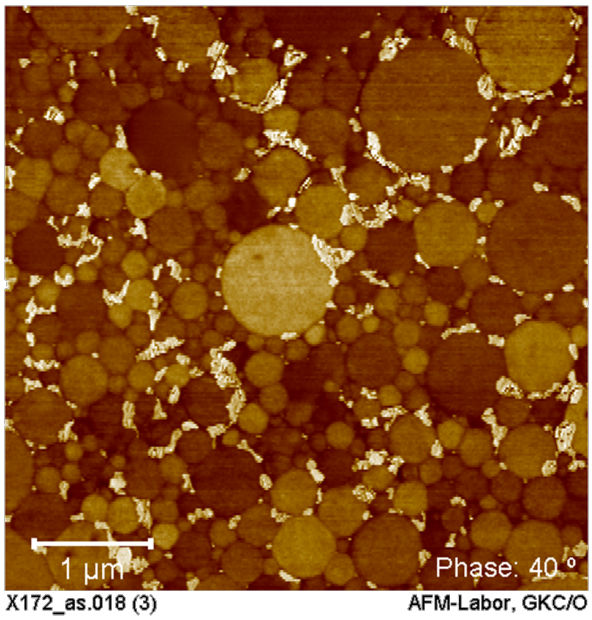

Figure 3: AFM image produced from COE/DCPD latex film. Measurement: AFM tapping at room temperature, material contrast using Phase Imaging.

Conclusion

In conclusion, the three new olefin metathesis catalysts **9**, **11** and **12** bearing the pH-responsive H_2ITap ligand were synthesized and tested in RCM and ROMP reactions. Complex **12** was characterized via X-ray diffraction. While in homogeneous organic or aqueous solution, the 2nd generation Grubbs-type catalyst **9** containing a Fischer-type phenylthiomethylidene group exhibited significant latency but proved to be a proficient ROMP and RCM catalyst at elevated temperatures. Catalyst **11** exhibited the typical high ROMP activity for a third-generation Grubbs-type catalyst in benzene. The ROMP reaction could even be strongly accelerated when two equivalents of a strong acid were added to the catalyst. However, in RCM reactions or in acidic aqueous media, catalyst **11** suffered from rapid degradation. By contrast, catalysts **12** exhibited relatively low conversions for all metathesis reactions in homogeneous solution due to slow metathesis initiation and/or rapid catalyst degradation. However, both catalysts **11** and **12** proved to be extremely

capable of ROMP in microemulsion of DCPD and COE. The (co)polymers were formed in near-quantitative yields with catalyst loadings as low as 180 ppm while forming stable latexes with minimal coagulation (0.1–1.6%). The latex particles maintain their size (between 255 and 315 nm) and shape throughout the polymerization and the processing into the film. This is the first time that hydrophilic, NHC-ligated olefin metathesis catalysts were used in emulsion ROMP. Catalysts **11** and **12** demonstrated a superior ability for this process by using the lowest ever catalyst loading for two monomers with significantly lower ROMP activity than the typically used NBE monomer at moderate temperatures while routinely affording near-quantitative conversions. Further investigations of the emulsion ROMP process with respect to the nature of catalytic species in the micelle and the properties of the resulting latexes and materials are currently under way.

Experimental

General procedures

All experiments with organometallic compounds were performed under a dry nitrogen atmosphere using standard Schlenk techniques or in an MBraun drybox (O_2 < 2 ppm). NMR spectra were recorded with a Varian Inova instrument (300.1 MHz for ^{1}H, 75.9 MHz for ^{13}C, and 121.4 MHz for ^{31}P) and an Agilent 400 MHz MR system (400.0 MHz for ^{1}H, 100.6 MHz for ^{13}C, and 162.9 MHz for ^{31}P). ^{1}H and ^{13}C NMR spectra were referenced to the residual solvent, ^{31}P NMR spectra were referenced using H_3PO_4 (δ = 0 ppm) as external standard. The crystallographic properties and data were collected using Mo Kα radiation and the charge-coupled area detector (CCD) detector on an Oxford Diffraction Systems Gemini S diffractometer. The solid contents of latexes were determined using a Mettler Toledo HR73 moisture meter. The droplet diameter was determined using an Autosizer IIC from Malvern Instruments.

Materials and methods. *n*-Heptane, THF, CH_2Cl_2 and *t*-BuOMe were dried by passage through solvent purification (MBraun-Auto-SPS). C_6D_6 and $CDCl_3$ were degassed prior to use. 2-PrOH was used without further purification. Complex **8** was donated by BASF SE and used as delivered. Other chemicals and reagents were purchased from commercial sources, and they were degassed and stored in the dry-box when directly used in combination with organometallic complexes, and otherwise were used without further purification. H_2ITap·HCl, complex **8**, as well as DEDAM and DAMA were synthesized according to literature procedures [61,71].

Synthesis of (1,3-bis(2',6'-dimethyl-4'-dimethylaminophenyl)-2-dihydroimidazolidinylidene)dichloro(phenylthiomethylene)(tricyclohexylphosphine)ruthenium(II) (PCy_3)Cl_2(H_2ITap)Ru=CHSPh (9): H_2ITap·HCl (567 mg, 1.41 mmol) and KO*t*-Bu (180 mg, 1.61 mmol) were heated to 80 °C in heptane (120 mL) for 90 min. After the slurry cooled to room temperature, (PCy_3)$_2Cl_2$Ru=CHSPh (**8**, 969 mg, 1.13 mmol) was added and the mixture was stirred at 60 °C for 144 h. The solvent was then removed under reduced pressure and 2-PrOH/water (3:1 v/v) was added (70 mL) and the slurry was sonicated at 30 °C for 60 min. The mixture was filtered in air, the residue was washed once with 2-PrOH (20 mL), and then the residue was dried in the vacuum oven at 60 °C for 4 h. The residue still contained significant amounts of the starting complex (on average approx. 30%). Cyclohexane (80 mL) was added to the dry residue (666 mg) under inert gas and sonicated at 30 °C for 60 min. The slurry was filtered in air, the residue was washed with cyclohexane (2 × 15 mL) and then dried in the vacuum oven at 60 °C for 2 h to give compound **9** (378 mg, 0.40 mmol, 36%) in >99% purity. ^{1}H NMR (300.1 MHz, C_6D_6, 20 °C) δ 17.99 (s, Ru=*CH*), 7.23 (d, $^3J[^1H^1H]$ = 7.2 Hz, 2H), 6.97 (t, $^3J[^1H^1H]$ = 8.4 Hz, 1H), 6.89 (m, 2H, =CH-C_6H_5), 6.51 (s, 2H), 6.14 (s, 2H, 2 × C_6H_2), 3.36 (m, 4H, CH_2-CH_2), 2.90 (s, 6H), 2.76 (s, 6H, 2 × N(CH_3)$_2$), 2.61 (s, 6H), 2.29 (s, 6H, 2 × C_6H_2(CH_3)$_2$), 2.57 (br, m, 3H), 1.88 (br, m, 6H), 1.65 (br, m, 6H), 1.55 (br, m, 3H), 1.45–1.02 (br, m, 18H, PCy_3); ^{13}C {^{1}H} NMR (75.9 MHz, C_6D_6, 20 °C) δ 272.5 (br, Ru=*C*H), 219.7 (d, $^2J[^{31}P^{13}C]$ = 81.1 Hz, N-*C*-N), 150.9, 149.9, 142.2, 140.8, 139.0, 129.7, 129.0, 126.8, 125.9, 125.8, 113.0, 112.3 (s, aryl-*C*), 52.7, 52.5 (s, N-CH_2-CH_2-N), 40.4, 40.0 (N-CH_3), 21.4, 20.4 (C_6H_2(CH_3)$_2$), 32.8 (d, $^1J[^{31}P^{13}C]$ = 14.9 Hz), 30.0 (s), 28.5 (d, $^2J[^{31}P^{13}C]$ = 10.1 Hz), 27.2 (s, PCy_3); ^{31}P {^{1}H} NMR (121.4 MHz, C_6D_6, 20 °C) δ 23.4 (s); Anal. calcd for $C_{44}H_{58}Cl_2N_8Ru$: C, 60.68; H, 6.71; N, 12.87; found: C, 60.21; H, 6.77, N, 12.27.

Recovery of bis(tricyclohexylphosphine)dichloro(phenylthiomethylene)ruthenium(II) (PCy_3)$_2Cl_2$Ru=CHSPh (8). The cyclohexane filtrate and washes were combined and dried under reduced pressure. Acetone (30 mL) was added to the remaining solid and the slurry was sonicated for 30 min at 30 °C. The mixture is filtered in air and the residue was washed with acetone (2 × 15 mL). Then the filter residue was dried in the vacuum oven at 60 °C for 2 h to recover 301 mg of material (approx. 31%). The ^{1}H NMR analysis showed that the residue was only composed of compound **8** (96%) and compound **9** (4%). The recovered catalyst was mixed with **9** in later synthesis reactions to synthesize **9**.

Synthesis of benzylidene(1,3-bis(2',6'-dimethyl-4'-dimethylaminophenyl)-2-dihydroimidazolidinylidene)bis(4-dimethylaminopyridine)dichlororuthenium(II) (DMAP)$_2Cl_2$(H_2ITap)Ru=CHPh (11): 4-Dimethylaminopyridine (DMAP, 315 mg, 2.58 mmol) was added to a slurry of

(PCy_3)Cl_2(H_2ITap)Ru=CHPh (**10**, 987 mg, 1.09 mmol) in *tert*-butyl methyl ether (50 mL) and the solution was stirred at room temperature for 16 h. The bright green precipitate was filtered in air, washed once with a 1 mM solution of DMAP in *tert*-butyl methyl ether (20 mL) and the residue was dried in the vacuum oven at 60 °C for 2 h to give compound **11** (844 mg, 0.968 mmol, 89%). ^{1}H NMR (300.1 MHz, C_6D_6, 20 °C) δ 19.80 (s, Ru=*CH*), 8.54 (d, $^3J[^1H^1H]$ = 6.4 Hz, 2H), 8.18 (d, $^3J[^1H^1H]$ = 7.0 Hz, 2H), 6.07 (d, $^3J[^1H^1H]$ = 7.0 Hz, 2H), 5.44 (d, $^3J[^1H^1H]$ = 6.4 Hz, 2H, 2 × C_5NH_4), 8.29 (d, $^3J[^1H^1H]$ = 7.6 Hz, 2H), 7.24 (t, $^3J[^1H^1H]$ = 7.4 Hz, 1H), 7.02 (d, $^3J[^1H^1H]$ = 7.6 Hz, 2H, C_6H_5), 6.63 (s, 2H), 6.35 (s, 2H, 2 × C_6H_2), 3.59 (m, 2H), 3.48 (m, 2H, CH_2-CH_2), 3.03 (s, 6H), 2.63 (s, 6H), 2.59 (s, 6H), 2.55 (s, 6H, 4 × N(CH_3)$_2$), 2.20 (s, 6H), 1.80 (s, 6H, 2 × C_6H_2(CH_3)$_2$; ^{13}C {^{1}H} NMR (75.9 MHz, C_6D_6, 20 °C) δ 310.2 (=*CH*), 221.6 (N-*C*-N), 154.1, 153.9, 152.9, 152.5, 150.9, 141.2, 139.0, 127.8, 131.3, 130.9, 129.3, 113.5, 113.0, 107.0, 106.6 (aryl-*C*), 52.3, 51.5 (N-CH_2-CH_2-N), 40.9, 40.7, 38.6 (br), 38.2 (N-CH_3), 22.1 (br), 19.9 (C_6H_2(CH_3)$_2$); Anal. calcd for $C_{48}H_{72}Cl_2N_4PRuS$: C, 61.32; H, 7.54; N, 5.96, found: C, 61.40; H, 7.64, N, 5.93.

Synthesis of (1,3-bis(2',6'-dimethyl-4'-dimethylaminophenyl)-2-dihydroimidazolidinylidene)bis(4-dimethylaminopyridine)dichloro(phenylthiomethylene)ruthenium(II) (DMAP)$_2$Cl$_2$(H_2ITap)Ru=CHSPh (12): 4-Dimethylaminopyridine (DMAP, 412 mg, 3.38 mmol) was added to a slurry of (PCy_3)Cl_2(H_2ITap)Ru=CHSPh (**9**, 1.237 g, 1.32 mmol) in *tert*-butyl methyl ether (80 mL) and the solution was stirred for 16 h at 50 °C. The grayish-green precipitate was filtered in air, washed once with a 1 mM solution of DMAP in *tert*-butyl methyl ether (20 mL) and the residue was dried in the vacuum oven at 60 °C for 2 h to give compound **12** (1.110 g, 1.23 mmol, 93%).

NMR specroscopic analysis of (1,3-bis(2',6'-dimethyl-4'-dimethylaminophenyl)-2-dihydroimidazolidinylidene)bis(4-dimethylaminopyrine)dichloro(phenylthiomethylene)ruthenium(II) (DMAP)$_2$Cl$_2$(H_2ITap)Ru=CHSPh (12): Complex **12** has been found to be low-soluble in a variety of organic solvents including benzene, ether, THF and acetone. Chlorinated solvents such as CH_2Cl_2 and $CHCl_3$ dramatically improve the complex solubility but have shown to result in significant degradation over a period of several hours. An NMR sample of complex **12** in $CDCl_3$ exhibited approx. 10% decomposition over a 24 h period at room temperature as observed by ^{1}H NMR spectroscopy. Both, ^{1}H NMR and ^{13}C NMR spectra, exhibit broadened signals at room temperature due to dynamic processes. ^{1}H NMR (400.1 MHz, $CDCl_3$, 20 °C) δ 17.33 (s, 1H, Ru=*CH*), 8.22 (br, 2H), 7.73 (br, 2H), 6.56 (br, 2H), 6.49 (br, 2H, 2 × C_5NH_4), 6.20 (br, 2H), 6.15 (s, 2H, 2 × C_6H_2), 7.23–7.05 (m, 5H, S-C_6H_5), 4.10 (m, 2H), 3.96 (m, 2H, CH_2-CH_2), 3.11 (s, 6H), 2.95 (s, 6H), 2.89 (s, 6H), 2.69 (s, 6H, 4 × N(CH_3)$_2$), 2.60 (s, 6H), 2.40 (s, 6H, 2 × C_6H_2(CH_3)$_2$); ^{13}C {^{1}H} NMR (75.9 MHz, $CDCl_3$, 20 °C) δ 287.1 (br, Ru=*C*H), 220.7 (N-*C*-N), 153.8 (br), 153.5 (br), 145.0, 148.9, 148.3 (br), 142.3 (br), 138.4, 128.1, 126.8, 125.9, 112.0, 111.2, 106.2 (2 signals, aryl-*C*), 52.0, 51.2 (br, N-CH_2-CH_2-N), 40.4, 39.8, 38.9 (2 signals, N-CH_3), 20.6 (br), 19.4 (C_6H_2(CH_3)$_2$). Cooling a solution of complex **12** in $CDCl_3$ to −20 °C allowed the observation of two isomers which are in a dynamic equilibrium at room temperature. A detailed analysis of the two isomers is beyond the scope of this manuscript. ^{1}H NMR (400.1 MHz, $CDCl_3$, −20 °C): δ 17.36, 17.28 (s, Ru=C*H*), 8.48, 8.16, 7.96, 7.62, 6.63, 6.54, 5.96, 5.93 (br, 4 × C_5NH_4), 6.23, 6.14, 6.04 (4 × C_6H_2), 7.23–7.05 (S-C_6H_5), 4.16, 4.01, 3.81 (2 × CH_2-CH_2), 3.15, 2.97, 2.90 (2 signals), 2.84, 2.73, 2.70, 2.59, 2.57, 2.47 (2 signals), 2.39 (8 × N(CH_3)$_2$ and 2 × C_6H_2(CH_3)$_2$); ^{13}C {^{1}H} NMR (75.9 MHz, $CDCl_3$, 20 °C): δ 287.7, 287.4 (Ru=*C*H), 220.0 (N-*C*-N), 155.6, 152.6, 151.9, 150.3, 149.6, 149.5, 148.8, 148.1, 143.4, 141.2, 138.6, 138.2, 137.8, 131.1 129.7, 128.0 (2 signals), 127.3, 126.9, 126.3, 126.0, 125.1, 123.4, 111.7, 111.2, 110.8 106.6, 106.4, 105.5 (2 signals, aryl-*C*), 52.2, 52.0, 51.7, 50.5 (N-CH_2-CH_2-N), 40.6, 40.2, 40.0, 39.7, 39.1, 38.8 (2 signals, N-CH_3), 20.9, 19.8, 19.1 (C_6H_2(CH_3)$_2$); Anal. calcd for $C_{44}H_{58}Cl_2N_8RuS$: C, 58.52; H, 6.47; N, 12.41; found: C, 58.26; H, 6.49, N, 11.74.

Crystal structure determination of complex 12. Crystals suitable for X-ray diffraction were obtained by layer diffusion of heptane into a THF solution of complex **12** at ambient temperatures over a period of 3 d to yield dark brown prisms. The crystals do not survive away from their solvent for any appreciable period at all, and disintegrate fairly soon after removal from the solvent. A small specimen (0.25 × 0.33 × 0.38 mm) was wedged at the top of a 0.3 mm glass capillary tube while in contact with a small amount of its solvent. The capillary tube was truncated to isolate the sample, sealed with epoxy, and mounted on a pin; the pin was placed on a goniometer head. The crystallographic properties and data were collected using Mo Kα radiation and the charge-coupled area detector (CCD) detector on an Oxford Diffraction Systems Gemini S diffractometer at 300(1) K. A preliminary set of cell constants was calculated from reflections observed on three sets of 5 frames which were oriented approximately in mutually orthogonal directions of reciprocal space. Data collection was carried out using Mo Kα radiation (graphite monochromator) with 8 runs consisting of 511 frames with a frame time of 45.0 s and a crystal-to-CCD distance of 50.000 mm. The runs were collected by omega scans of 1.0 degree width, and at detector position of 28.484, −30.203 degrees in 2θ. The intensity data were corrected for absorption with an analytical correction. Final cell

constants were calculated from 5404 stronger reflections from the actual data collection after integration. See Supporting Information File 1 for crystal and refinement information.

General procedure for ROMP of COE. Analogous to the procedure described in [35], COE (7.2 µL, 60 µmol) was added via a microliter syringe through a septum to a stock solution of the catalyst (in C_6D_6 for **9** and **11**, $CDCl_3$ for **12** – 0.5 mM, 0.60 mL, 0.3 µmol) in an NMR tube. The monomer conversion was monitored at 20 °C via ^{1}H NMR spectroscopy by integration of the sufficiently separated multiplet signals at δ 5.51 ppm (m, monomer =C*H*-) and 5.46 ppm (m, polymer, =C*H*-).

General procedure for RCM of diethyl diallylmalonate (DEDAM). Analogous to the procedure described in [72], DEDAM (14.6 µL, 60 µmol) was added via microliter syringe through a septum to a stock solution of the catalyst (in C_6D_6 for **9** and **11**, $CDCl_3$ for **12** – 1.0 mM, 0.60 mL, 0.6 µmol) in a NMR tube. The substrate conversion was monitored at 20 °C via ^{1}H NMR spectroscopy by integration of the sufficiently separated multiplet signals at δ 2.78 ppm (m, allyl-CH_2, DEDAM) and 3.13 ppm (m, ring-CH_2, cyclopentene derivative).

General procedure for the RCM of diallylmalonic acid (DAMA). Analogous to the procedure described in [72], the catalyst (8 µmol) and DAM (36.8 mg, 0.20 mmol) were dissolved in the 0.1 M HCl_{aq} (2.0 mL) under inert gas conditions and the solution was heated to 50 °C under stirring. An aliquot (0.3 mL) was taken after 30 min and 60 min, quenched with ethyl vinyl ether, dried under vacuum, and the monomer conversion was monitored via ^{1}H NMR spectroscopy (300.1 MHz, 20 °C, D_2O) by integration of the signals δ 2.58 (DAMA-CH_2) and δ 2.98 ppm (cyclopentene-CH_2). The aliquots taken after 60 min indicated the same conversion level as those taken after 30 min.

General procedure for the preparation of the polymer dispersions using DCPD or DCPD/COE mixtures with complexes 11 and 12. A mixture of 73.1 g of water, 8.3 g of a 10% (by strength) solution of PEG-30 cetyl stearyl ether (Emulgin® B3) as charge-neutral surfactant, 0.75 g of *n*-hexadecane and 15.3 g (116 mmol) DCPD or 8.40 g (63.5 mmol) DCPD + 7.2 g COE (65.3 mmol) was stirred vigorously for 1 h under a nitrogen atmosphere before it was further homogenized using an ultrasonic probe for 5 min. Then a solution of catalyst (20.1 mg (**11**) or 20.6 mg (**12**), 0.023 mmol) in 13.6 g of 0.1 M aqueous HCl was added dropwise to the resulting microemulsion under constant stirring over a period of 1 min. The reaction mixture was stirred then at the reaction temperature (35 °C, 55 °C, 65 °C) for 2 h. After that time, the emulsion was pressed through a 20 µm pore filter and an aliquot of approx. 0.8 g was taken from the emulsion for solid residue analysis.

Crystallographic data: Crystallographic data for structure **12** has been deposited with the Cambridge Crystallographic Data Centre (CCDC 1404596). Copies of the data can be obtained, free of charge, on application to the Director, CCDC, 12 Union Road, Cambridge CB2 1EZ, United Kingdom (Fax: 44-1223-336033 or e-mail: deposit@ccdc.cam.ac.uk).

Supporting Information

Supporting Information File 1

Crystallographic data of compound **12**.
[http://www.beilstein-journals.org/bjoc/content/supplementary/1860-5397-11-212-S1.pdf]

Supporting Information File 2

^{1}H, ^{13}C and ^{31}P NMR spectra of the synthesized Ru-complexes **9**, **11** and **12** as well as kinetic experimental data.
[http://www.beilstein-journals.org/bjoc/content/supplementary/1860-5397-11-212-S2.pdf]

Acknowledgements

This work was supported the Georgia Southern University (SEED funding for HJS) and by BASF SE. SLB would like to thank the Trent Lott National Center for the Innovation Award. EJV gratefully acknowledges NSF MRI-0618148 for crystallographic resources.

References

1. Fogg, D. E.; Conrad, J. C. *Curr. Org. Chem.* **2006,** *10,* 185–202. doi:10.2174/138527206775192942
2. Chatterjee, A. K.; Choi, T.-L.; Sanders, D. P.; Grubbs, R. H. *J. Am. Chem. Soc.* **2003,** *125,* 11360–11370. doi:10.1021/ja0214882
3. Wright, D. L. *Curr. Org. Chem.* **1999,** *3,* 211–240.
4. Nuyken, O.; Schneider, M.; Frenzel, U. Metathesis Polymerization. In *Encyclopedia Of Polymer Science and Technology;* Lyon, A.; Serpe, S., Eds.; Wiley-VCH: Weinheim, 2012. doi:10.1002/0471440264.pst195
5. Leitgelb, A.; Wappel, J.; Slugovc, C. *Polymer* **2010,** *51,* 2927–2946. doi:10.1016/j.polymer.2010.05.002
6. Bielawski, C. W.; Grubbs, R. H. *Prog. Polym. Sci.* **2007,** *32,* 1–29. doi:10.1016/j.progpolymsci.2006.08.006
7. Baughman, T. W.; Wagener, K. B. *Adv. Polym. Sci.* **2005,** *176,* 1–42. doi:10.1007/b101318
8. Trimmel, G.; Riegler, S.; Fuchs, G.; Slugovc, C.; Stelzer, F. *Adv. Polym. Sci.* **2005,** *176,* 43–87. doi:10.1007/b101317
9. Gułajski, Ł.; Michrowska, A. M.; Narożnik, J.; Kaczmarska, Z.; Rupnicki, L.; Grela, K. *ChemSusChem* **2008,** *1,* 103–109. doi:10.1002/cssc.200700111

10. Nguyen, S. T.; Johnson, L. K.; Grubbs, R. H.; Ziller, J. W. *J. Am. Chem. Soc.* **1992,** *114,* 3974–3975. doi:10.1021/ja00036a053
11. Vougiokalakis, G. C.; Grubbs, R. H. *Chem. Rev.* **2010,** *110,* 1746–1787. doi:10.1021/cr9002424
12. Anderson, E. B.; Buchmeiser, M. R. *Synlett* **2012,** *23,* 185–207. doi:10.1055/s-0031-1290120
13. Tomasek, J.; Schatz, J. *Green Chem.* **2013,** *15,* 2317–2338. doi:10.1039/c3gc41042k
14. Mecking, S.; Held, A.; Bauers, F. M. *Angew. Chem., Int. Ed.* **2002,** *41,* 544–561. doi:10.1002/1521-3773(20020215)41:4<544::AID-ANIE544>3.0.CO;2-U
15. Fuhrmann, H.; Dwars, T.; Oehme, G. *Chem. Unserer Zeit* **2003,** *37,* 40–50. doi:10.1002/ciuz.200390004
16. Pinault, N.; Bruce, D. W. *Coord. Chem. Rev.* **2003,** *241,* 1–25. doi:10.1016/S0010-8545(02)00306-5
17. Shaughnessy, K. H. *Chem. Rev.* **2009,** *109,* 643–710. doi:10.1021/cr800403r
18. Schaper, L.-A.; Hock, S. J.; Herrmann, W. A.; Kühn, F. E. *Angew. Chem., Int. Ed.* **2013,** *52,* 270–289. doi:10.1002/anie.201205119
19. Binder, J. B.; Raines, R. T. *Curr. Opin. Chem. Biol.* **2008,** *12,* 767–773. doi:10.1016/j.cbpa.2008.09.022
20. Zaman, S.; Curnow, O. J.; Abell, A. D. *Aust. J. Chem.* **2009,** *62,* 91–100. doi:10.1071/CH08470
21. Burtscher, D.; Grela, K. *Angew. Chem., Int. Ed.* **2009,** *48,* 442–454. doi:10.1002/anie.200801451
22. Lynn, D. M.; Mohr, B.; Grubbs, R. H.; Henling, L. M.; Day, M. W. *J. Am. Chem. Soc.* **2000,** *122,* 6601–6609. doi:10.1021/ja0003167
23. Lynn, D. M.; Mohr, B.; Grubbs, R. H. *J. Am. Chem. Soc.* **1998,** *120,* 1627–1628. doi:10.1021/ja9736323
24. Mohr, B.; Lynn, D. M.; Grubbs, R. H. *Organometallics* **1996,** *15,* 4317–4325. doi:10.1021/om9603373
25. Saoud, M.; Romerosa, A.; Peruzzini, M. *Organometallics* **2000,** *19,* 4005–4007. doi:10.1021/om000507i
26. Gallivan, J. P.; Jordan, J. P.; Grubbs, R. H. *Tetrahedron Lett.* **2005,** *46,* 2577–2580. doi:10.1016/j.tetlet.2005.02.096
27. Hong, S. H.; Grubbs, R. H. *J. Am. Chem. Soc.* **2006,** *128,* 3508–3509. doi:10.1021/ja058451c
28. Skowerski, K.; Szczepaniak, G.; Wierzbicka, C.; Gułajski, Ł.; Bieniek, M.; Grela, K. *Catal. Sci. Technol.* **2012,** *2,* 2424–2427. doi:10.1039/c2cy20320k
29. Lo, C.; Ringenberg, M. R.; Gnandt, D.; Wilson, Y.; Ward, T. R. *Chem. Commun.* **2011,** *47,* 12065–12067. doi:10.1039/c1cc15004a
30. Samanta, D.; Kratz, K.; Zhang, X.; Emrick, T. *Macromolecules* **2008,** *41,* 530–532. doi:10.1021/ma7019732
31. Roberts, A. N.; Cochran, A. C.; Rankin, D. A.; Lowe, A. B.; Schanz, H.-J. *Organometallics* **2007,** *26,* 6515–6518. doi:10.1021/om700887t
32. Dunbar, M. A.; Balof, S. L.; Roberts, A. N.; Valente, E. J.; Schanz, H.-J. *Organometallics* **2011,** *30,* 199–203. doi:10.1021/om100633f
33. Michrowska, A.; Gułajski, Ł.; Karczmarska, Z.; Mennecke, K.; Kirschning, A.; Grela, K. *Green Chem.* **2006,** *8,* 685–688. doi:10.1039/b605138c
34. Binder, J. B.; Guzei, A. I.; Raines, R. T. *Adv. Synth. Catal.* **2007,** *349,* 395–404. doi:10.1002/adsc.200600264
35. Rix, D.; Clavier, H.; Coutard, Y.; Gulajski, L.; Grela, K.; Mauduit, M. *J. Organomet. Chem.* **2006,** *691,* 5397–5405. doi:10.1016/j.jorganchem.2006.07.042
36. Rix, D.; Caïjo, F.; Laurent, L.; Gulajski, L.; Grela, K.; Mauduit, M. *Chem. Commun.* **2007,** 3771–3773. doi:10.1039/B705451C
37. Jordan, J. P.; Grubbs, R. H. *Angew. Chem., Int. Ed.* **2007,** *46,* 5152–5155. doi:10.1002/anie.200701258
38. Leibfarth, F. A.; Mattson, K. M.; Fors, B. P.; Collins, H. A.; Hawker, C. J. *Angew. Chem., Int. Ed.* **2013,** *52,* 199–210. doi:10.1002/anie.201206476
39. Naumann, S.; Buchmeiser, M. R. *Macromol. Rapid Commun.* **2014,** *35,* 682–701. doi:10.1002/marc.201300898
40. Monsaert, S.; Lozano Vila, A.; Drozdzak, R.; Van der Voort, P.; Verpoort, F. *Chem. Soc. Rev.* **2009,** *38,* 3360–3372. doi:10.1039/b902345n
41. Szadkowska, A.; Grela, K. *Curr. Org. Chem.* **2008,** *12,* 1631–1647. doi:10.2174/138527208786786264
42. Vidavsky, Y.; Anaby, A.; Lemcoff, N. G. *Dalton Trans.* **2012,** *41,* 32–43. doi:10.1039/C1DT11404B
43. Schanz, H.-J. *Curr. Org. Chem.* **2013,** *17,* 2575–2591. doi:10.2174/13852728113179990110
44. Wang, D.; Wurst, K.; Knolle, W.; Decker, U.; Prager, L.; Naumov, S.; Buchmeiser, M. R. *Angew. Chem., Int. Ed.* **2008,** *47,* 3267–3270. doi:10.1002/anie.200705220
45. P'Pool, S. J.; Schanz, H.-J. *J. Am. Chem. Soc.* **2007,** *129,* 14200–14212. doi:10.1021/ja071938w
46. Dunbar, M. A.; Balof, S. L.; LaBeaud, L. J.; Yu, B.; Lowe, A. B.; Valente, E. J.; Schanz, H.-J. *Chem. – Eur. J.* **2009,** *15,* 12435–12446. doi:10.1002/chem.200901013
47. Hahn, F. E.; Paas, M.; Fröhlich, R. *J. Organomet. Chem.* **2005,** *690,* 5816–5821. doi:10.1016/j.jorganchem.2005.07.060
48. Samec, J. S. M.; Keitz, B. K.; Grubbs, R. H. *J. Organomet. Chem.* **2010,** *695,* 1831–1837. doi:10.1016/j.jorganchem.2010.04.017
49. Bienik, M.; Bujok, R.; Cabaj, M.; Lugan, N.; Lavigne, G.; Arlt, D.; Grela, K. *J. Am. Chem. Soc.* **2006,** *128,* 13652–13653. doi:10.1021/ja063186w
50. Gawin, R.; Makal, A.; Woźniak, K.; Mauduit, M.; Grela, K. *Angew. Chem., Int. Ed.* **2007,** *46,* 7206–7209. doi:10.1002/anie.200701302
51. Pietraszuk, C.; Rogalski, S.; Powała, B.; Miętkiewski, M.; Kubicki, M.; Spólnik, G.; Danikiewicz, W.; Woźniak, K.; Pazio, A.; Szadkowska, A.; Kozłowska, A.; Grela, K. *Chem. – Eur. J.* **2012,** *18,* 6465–6469. doi:10.1002/chem.201103973
52. Monsaert, S.; Ledoux, N.; Drozdzak, R.; Verpoort, F. *J. Polym. Sci., Part A: Polym. Chem.* **2010,** *48,* 302–310. doi:10.1002/pola.23784
53. Rouen, M.; Queval, P.; Falivene, L.; Allard, J.; Toupet, L.; Crévisy, C.; Caijo, F.; Baslé, O.; Cavallo, L.; Mauduit, M. *Chem. – Eur. J.* **2014,** *20,* 13716–13721. doi:10.1002/chem.201403934
54. Claverie, J. P.; Viala, S.; Maurel, V.; Novat, C. *Macromolecules* **2001,** *34,* 382–388. doi:10.1021/ma001570m
55. Quémener, D.; Héroguez, V.; Gnanou, Y. *Macromolecules* **2005,** *38,* 7977–7982. doi:10.1021/ma051027b
56. Öztürk, B. Ö.; Şehitoğlu, S. K.; Meier, M. A. R. *Eur. Polym. J.* **2015,** *62,* 116–123. doi:10.1016/j.eurpolymj.2014.11.014
57. Sanford, M. S.; Love, J. L.; Grubbs, R. H. *J. Am. Chem. Soc.* **2001,** *123,* 6543–6554. doi:10.1021/ja010624k
58. Kovačič, S.; Krajnc, P.; Slugovc, C. *Chem. Commun.* **2010,** *46,* 7504–7506. doi:10.1039/c0cc02610g
59. Quémener, D.; Héroguez, V.; Gnanou, Y. *J. Polym. Sci., Part A: Polym. Chem.* **2006,** *44,* 2784–2793. doi:10.1002/pola.21370

60. Quémener, D.; Chemtob, A.; Héroguez, V.; Gnanou, Y. *Polymer* **2005,** *46,* 1067–1075. doi:10.1016/j.polymer.2004.11.096
61. Balof, S. L.; P'Pool, S. J.; Berger, N. J.; Valente, E. J.; Schiller, A. M.; Schanz, H.-J. *Dalton Trans.* **2008,** 5791–5799. doi:10.1039/b809793c
62. Balof, S. L.; Yu, B.; Lowe, A. B.; Ling, Y.; Zhang, Y.; Schanz, H.-J. *Eur. J. Inorg. Chem.* **2009,** 1717–1722. doi:10.1002/ejic.200801145
63. Leuthäußer, S.; Schmidts, V.; Thiele, C. M.; Plenio, H. *Chem. – Eur. J.* **2008,** *14,* 5465–5481. doi:10.1002/chem.200800139
64. Trnka, T. M.; Morgan, J. P.; Sanford, M. S.; Wilhelm, T. E.; Scholl, M.; Choi, T.-L.; Ding, S.; Day, M. W.; Grubbs, R. H. *J. Am. Chem. Soc.* **2003,** *125,* 2546–2558. doi:10.1021/ja021146w
65. van der Schaaf, P. A.; Kolly, R.; Kirner, H.-J.; Rime, F.; Mühlebach, A.; Hafner, A. *J. Organomet. Chem.* **2000,** *606,* 65–74. doi:10.1016/S0022-328X(00)00289-8
66. Wallace, D. J. *Adv. Synth. Catal.* **2009,** *351,* 2277–2282. doi:10.1002/adsc.200900301
67. Dias, E. L.; Nguyen, S. T.; Grubbs, R. H. *J. Am. Chem. Soc.* **1997,** *119,* 3887–3897. doi:10.1021/ja963136z
68. Peeck, L. H.; Leuthäusser, S.; Plenio, H. *Organometallics* **2010,** *29,* 4339–4345. doi:10.1021/om100628f
69. Ritter, T.; Hejl, A.; Wenzel, A. G.; Funk, T. W.; Grubbs, R. H. *Organometallics* **2006,** *25,* 5740–5745. doi:10.1021/om060520o
70. Davidson, T. A.; Wagener, K. B.; Priddy, D. B. *Macromolecules* **1996,** *29,* 786–788. doi:10.1021/ma950852x
71. Van Ornum, S. G.; Cook, J. M. *Tetrahedron Lett.* **1996,** *37,* 7185–7188. doi:10.1016/0040-4039(96)01634-6
72. Hudson, D. M.; Valente, E. J.; Schachner, J.; Limbach, M.; Müller, K.; Schanz, H.-J. *ChemCatChem* **2011,** *3,* 297–301. doi:10.1002/cctc.201000368

License and Terms

BEILSTEIN JOURNAL OF ORGANIC CHEMISTRY

Olefin metathesis in air

Lorenzo Piola[1], Fady Nahra[1] and Steven P. Nolan[*2]

Review

Open Access

Address:
[1]EaStCHEM, School of Chemistry, University of St Andrews, St Andrews, KY16 9ST, UK and [2]Chemistry Department, College of Science, King Saud University, Riyadh 11451, Saudi Arabia

Email:
Steven P. Nolan[*] - stevenpnolan@gmail.com

* Corresponding author

Keywords:
air stability; catalysis; olefin metathesis; RCM; ROMP; ruthenium

Beilstein J. Org. Chem. **2015,** *11,* 2038–2056.
doi:10.3762/bjoc.11.221

Received: 21 July 2015
Accepted: 13 October 2015
Published: 30 October 2015

This article is part of the Thematic Series "Progress in metathesis chemistry II".

Guest Editor: K. Grela

Abstract

Since the discovery and now widespread use of olefin metathesis, the evolution of metathesis catalysts towards air stability has become an area of significant interest. In this fascinating area of study, beginning with early systems making use of high oxidation state early transition metal centers that required strict exclusion of water and air, advances have been made to render catalysts more stable and yet more functional group tolerant. This review summarizes the major developments concerning catalytic systems directed towards water and air tolerance.

Introduction

Transition metal-catalyzed alkene metathesis [1-10], which involves a fragment exchange between alkenes, is nowadays one of the most used strategies for the formation of carbon–carbon bonds. This area of study began with a “black box” approach for catalysts formation in polymerization of olefins. In recent years, metathesis-type reactions have emerged as universal strategies, employed in many fields of organic chemistry: from polymer chemistry [11-18] to natural product [19-21] and fine chemical syntheses [3,22-25]. Its importance led to the 2005 Nobel Prize in chemistry being awarded to Yves Chauvin, Richard Schrock and Robert Grubbs, who developed and studied this reaction [26]. Its wide adoption in organic reactions, where the use of inert and dry conditions are not always desirable, has led to efforts to develop new catalytic systems that enable this transformation in the presence of air and water [27]. However, this field of research has suffered a slow growth and only recently, an increasing number of research groups have started to seriously focus on testing metathesis catalysts in the presence of air and water. This is a way to gauge catalyst stability but also to potentially bring operational simplicity to this now widespead assembly strategy.

In this review, we summarize improvements associated with the stability of well-defined metathesis homogeneous systems

towards the presence of air and water in the alkene metathesis and hopefully raise the awareness of the significant tolerance of standard metathesis catalysts to these conditions.

Review

Well-defined ruthenium catalysts

Although well-defined early transition metal-based catalysts formed the basis of early metathesis reactions and can be thought of as the forefathers of modern metathesis catalysts [27-30], these all showed poor tolerance towards air and water, because of their high oxophilicity [3,8,9,16,27]. To date, there are no examples of their use in the presence of air.

To overcome the sensitivity problems exhibited by early transition-based catalysts, late transition metals, which do not exhibit high oxophilicity, appeared as the most promising candidates for reactions performed in air.

Indeed in 1988, Grubbs and Novak reported that not only ruthenium was an interesting candidate for olefin metathesis, but also that reactions were successfully conducted in water [31,32]. They discovered that $Ru(H_2O)_6(tos)_2$ could polymerize 7-oxanorbonene **1** in water under air (Scheme 1).

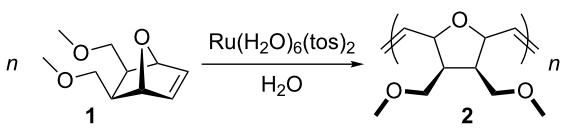

Scheme 1: Polymerization of 7-oxanorbornene in water.

In 1991, Marciniec and Pietraszuck reported the catalytic activity of $RuCl_2(PPh_3)_3$ in the self-metathesis of silicon-contaning olefins. The reactions were performed with 1 mol % of Ru at 150 °C in air, under solvent-free conditions for several days, to afford 1,2-bis(silyl)ethenes in moderate to good yields [33]. Reactions without oxygen showed no conversion, highlighting the important role that the latter plays in the activation of the catalyst.

In 1992, Grubbs and co-workers synthesized the first well-defined ruthenium(II) complex (**5**, Scheme 2) bearing a carbene moiety, able to perform ring-opening metathesis polymerization (ROMP) reactions of low-strained olefins [34,35] and ring-closing metathesis (RCM) reactions of functionalized dienes [36]. In the solid state, this complex was reported to be indefinitely stable under inert atmosphere whereas it could survive for only several minutes in air. In solution, it was stable in several degassed organic solvents, even in the presence of water or HCl [35].

Exchanging PPh_3 with PCy_3 increased significantly the activity of the catalyst **6** (Scheme 2), which then was capable of polymerizing unstrained cyclic olefins and to perform reactions with acyclic olefins [37]. Subsequent variations showed that larger and more basic phosphine ligands led to improved activity, and that an order of activity could be established as $PCy_3 > P(iPr)_3 >> PPh_3$. Reactions had to be performed in degassed and distilled solvents under N_2 atmosphere to obtain maximum yields.

Grubbs' 1st generation catalyst

To overcome the aforementioned difficulties, Grubbs and co-workers synthesized, what has become known as the Grubbs' 1st generation catalyst (**9**, Scheme 3). The reaction of $RuCl_2(PPh_3)_{3\text{-}4}$ (**3**) with phenyldiazomethane (**7**), followed by a phosphine exchange reaction, afforded complex **9** in high yields. Complex **9** has become the most used metathesis cata-

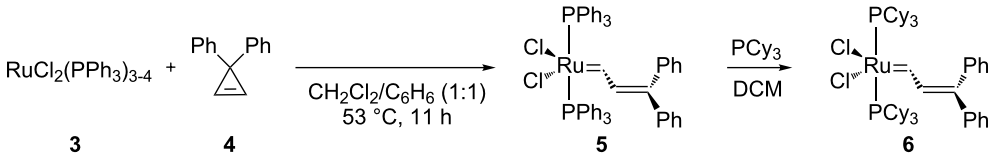

Scheme 2: Synthesis of the first well-defined ruthenium carbene.

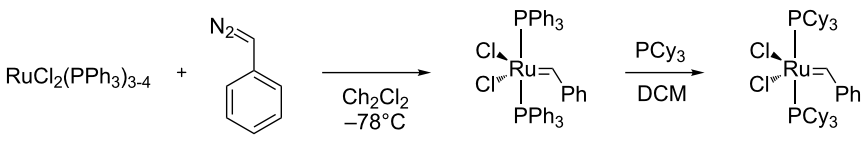

Scheme 3: Synthesis of Grubbs' 1st generation catalyst.

lyst, because of its good activity, relatively good stability to air (storage of **9** has been recommended to be performed under anaerobic conditions and lower temperatures), compatibility with a large variety of functional groups [36,38] and because of its feasible large-scale production. So far, the use of this catalyst in air has not been reported.

2nd generation catalyst

The synthesis of heteroleptic complexes, bearing one *N*-heterocyclic carbene (NHC) (**16–19**, Figure 1) and one phosphine as ligands, represented the second crucial turning point in this chemistry. Following Herrmann's report on bis-NHC ruthenium complexes (**10–15**) and their low activity [39], independently and simultaneously the groups of Nolan (**14**) [40,41], Grubbs (**15**) [42-45] and Hermann [46-48] reported on the synthesis of this family of complexes. The combination of a labile phosphine group with a non-labile NHC ligand provided a significant improvement in terms of reactivity and stability. The bulky NHC provides steric protection to the metal center and its σ-donating ability stabilizes both the pre-catalyst and the catalytically operating intermediate [49]. The most active being complex **15**, bearing SIMes (1,3-bis(2,4,6-trimethylphenyl)-4,5-dihydroimidazol-2-ylidene, **17**) as ligand, is known nowadays as the Grubbs' 2nd generation catalyst. The increased stability of **17** is due to the unsaturated backbone of the NHC; the steric bulkiness on the metal center is improved and the σ-donating ability is increased compared to other NHCs.

These were the first ruthenium-based catalysts able to perform RCM reactions of tri- and tetrasubstituted olefins [42,46], cross-metathesis (CM) to afford trisubstituted olefins [44] and CM and RCM reactions of electron-withdrawing substituted olefins [45]. In comparison to the 1st generation, they show a generally higher stability towards thermal degradation [41-43,49,50]. To date, only one example is reported where catalyst **15** is used in air (see following section).

Hoveyda–Grubbs catalyst

The next notable evolution in terms of higher catalyst stability came from the Hoveyda group in 1999 [51]. While performing metathesis in the presence of isopropoxystyrene (**20**, Scheme 4), they noticed that the reaction proceeded very slowly. They postulated that the isopropoxystyrene formed a Ru-chelate complex in situ, which would be more stable than the precatalyst used in the reaction; therefore reducing the rate of the subsequent steps. Upon synthesis and evaluation of this new Ru-chelate complex (**21**, Scheme 4), they noted its astonishing stability. It could be recycled after reaction via column chromatography and it could be kept in undistilled $CDCl_3$ for 2 weeks without any noticeable decomposition [51]. The isopropoxy group stabilized the complex by chelating the Ru moiety. Decomplexation of the latter allowed the approach of the olefinic substrate. Once the reaction reached completion and the starting materials depleted, the isopropoxy group coordinated back to the Ru center, allowing for the recycling of the catalyst. However, it should be mentioned that this increased stability diminished the activity of **21** when compared to **15** [52].

In 2000, Dowden [53] and co-workers reported the use of a polystyrene-supported ruthenium complex **24** (Scheme 5); a variation of the Hoveyda–Grubbs catalyst. It could be reused up to 5 times without loss of activity and without the use of a stabilizer. The catalysts were stored and used in air with non degassed DCM, providing average to good yields, with a catalyst loading of 5 mol % (Figure 2).

As complex **21**, the efficiency of **24** is limited to terminal alkenes [54], and performs poorly in CM reactions. Soon after,

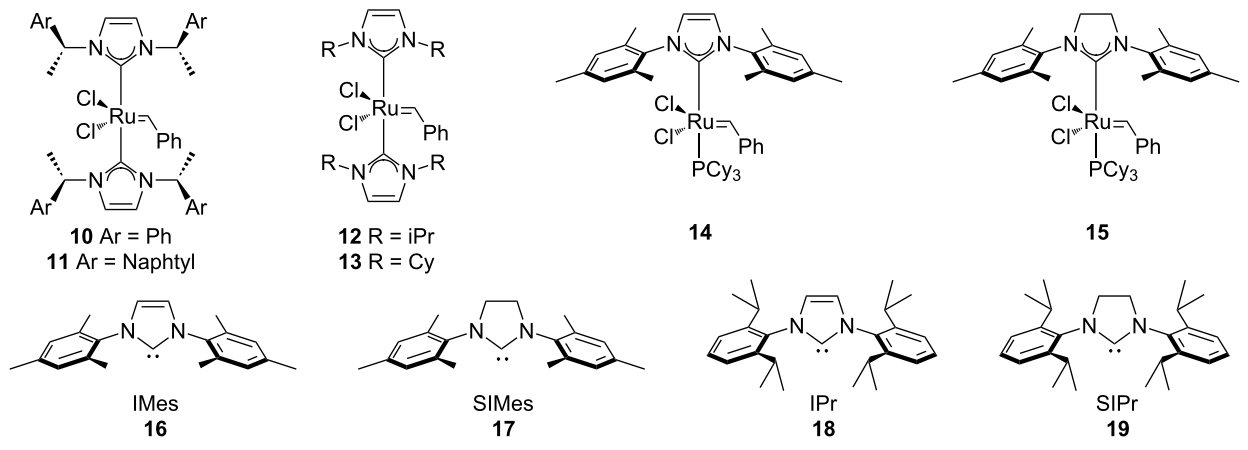

Figure 1: NHC-Ruthenium complexes and widely used NHC carbenes.

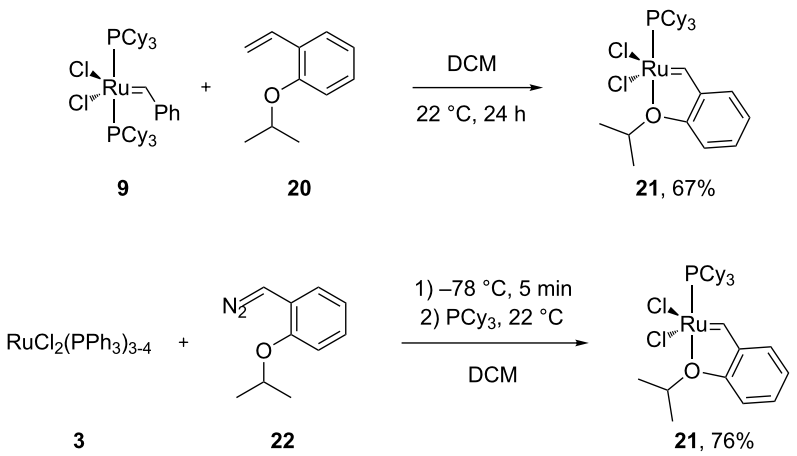

Scheme 4: Access to **21** from the Grubbs' 1st generation catalyst and its one-pot synthesis.

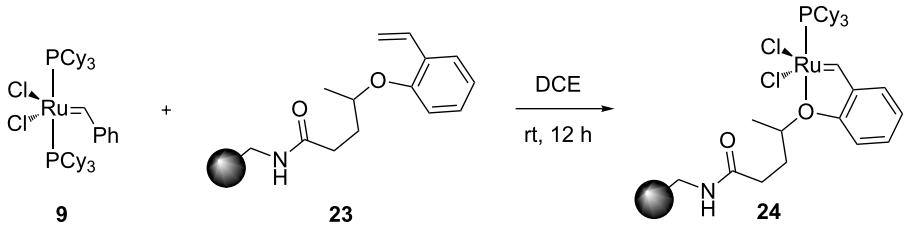

Scheme 5: Synthesis of supported Hoveyda-type catalyst.

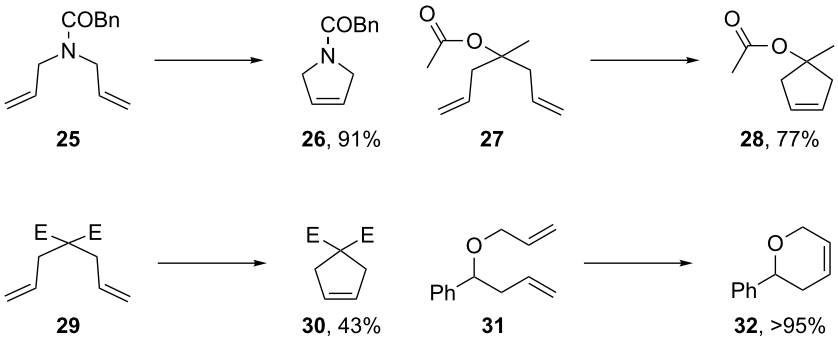

Figure 2: Scope of RCM reactions with supported Hoveyda-type catalyst. Reaction conditions: **24** (5 mol %), nondegassed DCM, rt, 3 h, in air. Conversions determined by ^{1}H NMR. E = COOEt.

in 2000, the Hoveyda–Grubbs 2nd generation catalyst was reported (**33**), simultaneously, by Hoveyda (Scheme 6, entry 1) [54] and Blechert (Scheme 6, entry 2) [55] bearing a SIMes ligand instead of the phosphine.

Complex **33** was able to perform RCM of trisubstitued olefins and CM in high efficiency, and retained the properties of stability and recyclability.

In 2002, Hoveyda et al. reported the Hoveyda–Grubbs' 2nd generation type catalyst **36** (Figure 3) [56]: Complex **36**, bearing an unsymmetrical and chiral NHC, was active in the asymmetric ring-opening cross-metathesis (RO/CM) in air using undistilled solvents, and yielded products with high enantiomeric excess (ee). The results where comparable to previously reported results for molybdenum-catalyzed systems [57], although the latter was used under inert conditions.

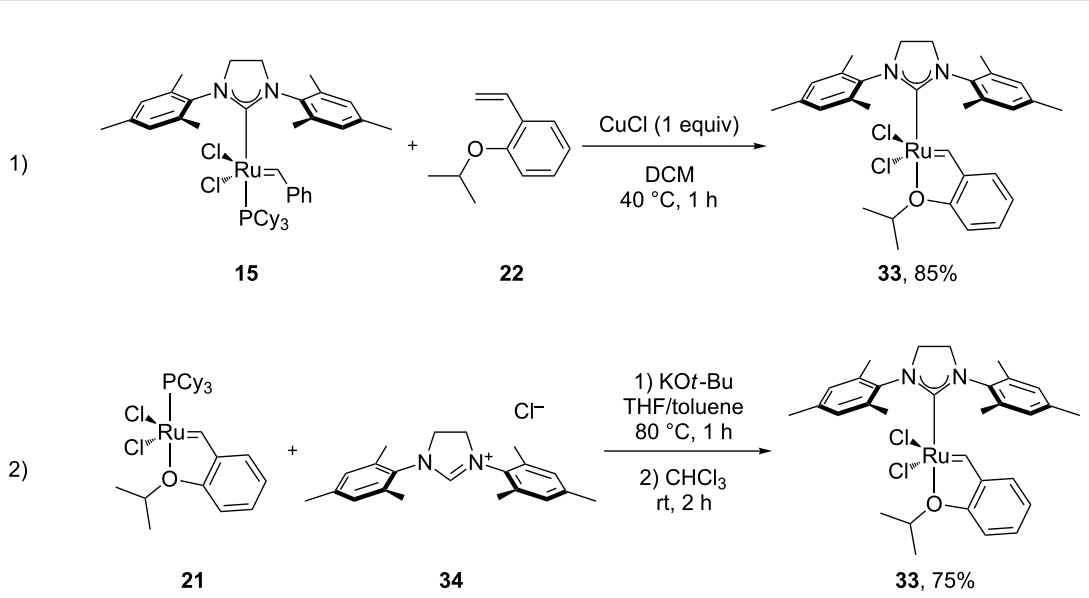

Scheme 6: Synthesis of **33** by Hoveyda and Blechert.

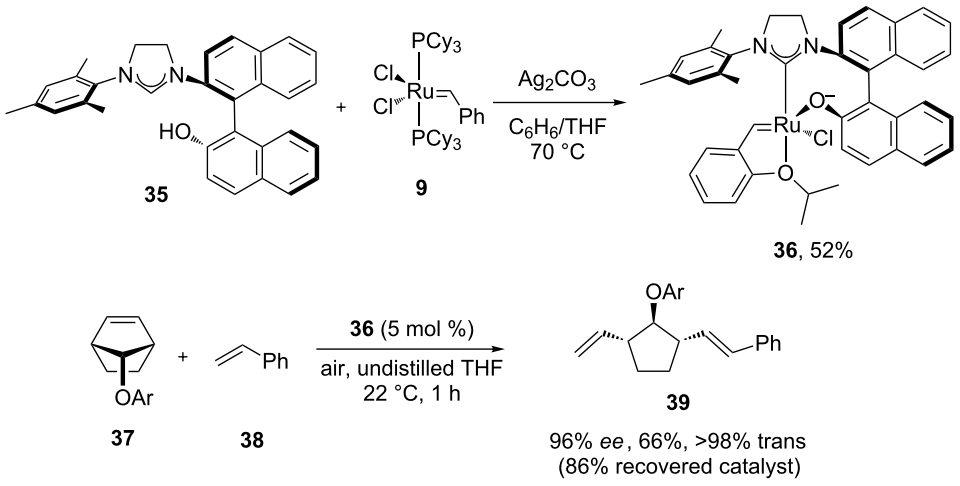

Figure 3: Synthesis of chiral Hoveyda–Grubbs type catalyst and its use in RO/CM.

In 2003, Blechert et al. reported the first systematic example of olefin metathesis in air [58]. Grubbs' 2nd generation catalyst **15** was compared to an *m*-isopropoxy-substituted Hoveyda–Grubbs' 2nd generation catalyst **41** (Scheme 7), using MeOH, water and DMF as solvents. Catalyst **41** bore two isopropoxy groups; the first one presented as a chelating group for the ruthenium center and the second one increased the solubility of the complex in alcohol solvents and DMF.

RCM reactions led to high conversions with all the solvents used, employing 5 mol % of **41** (Figure 4 and Table 1). It should be noted that catalyst **15** gave lower conversions when the water ratio was increased but it remained compatible with air.

The CM reaction, which is known to be a most difficult reaction, gave only low yield, while the ROM/CM reaction gave a much higher yield (Figure 5). It should be noted that long reaction times were needed as well as high catalyst loadings (5 mol %) in these transformations.

In 2004, the Grela group presented some variations of the Hoveyda–Grubbs catalyst **21** [52,59,60]. They reported some modifications to the isopropoxystyrene group; a nitro group

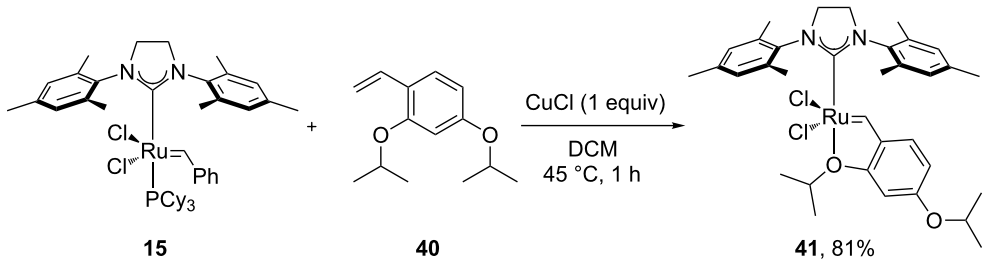

Scheme 7: Synthesis of **41**.

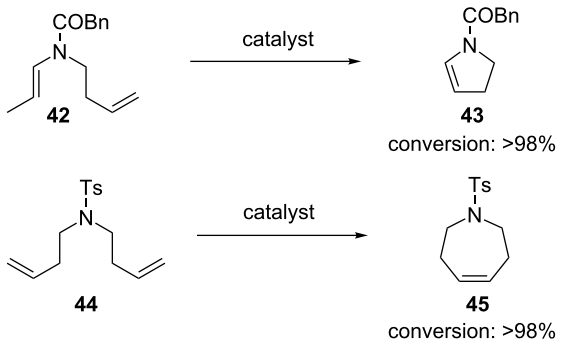

Figure 4: RCM reactions in air using **41** as catalyst. Reaction conditions: **41** (5 mol %), MeOH (0.05 M), 22 °C, 12 h, in air.

para to the isopropoxy moiety of the carbene provided a much faster initiating catalyst (**87**, Figure 12) than **21**, due to the weakening of the O–Ru bond [59-61]. Its use in air was reported by Olszewski, Skowerski and co-workers in a comparison with other catalysts (see section on indenylidene complexes, below) [62].

Soon after, in 2006, the same group presented a variation of the Hoveyda–Grubbs 2nd generation catalyst, bearing a quaternary ammonium group (**54**, Figure 6) [63]. Complex **54** was used in nondegassed mixtures of MeOH/EtOH and water giving complete conversions in most cases, with short reaction times; although, requiring a high catalyst loading (5 mol %). The quaternary group increased the solubility in solvent mixtures

Table 1: RCM in water and MeOH under air.[a]

Solvent	Substrate	Product	Conversion [%][b]	
			15	**41**
MeOH	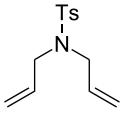	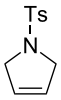	94	96
MeOH/H_2O (3:1)			29	87
MeOH/H_2O (1:1)[c]			54	90
MeOH/H_2O (1:3)[c]	**46**	**47**	77	94

[a]Reaction conditions: Catalyst **15** or **41** (5 mol %), undistilled solvent (0.05 M), 22 °C, 12 h, in air. [b]Determined by ^{1}H NMR spectroscopy. [c]Substrate not miscible with solvent [58].

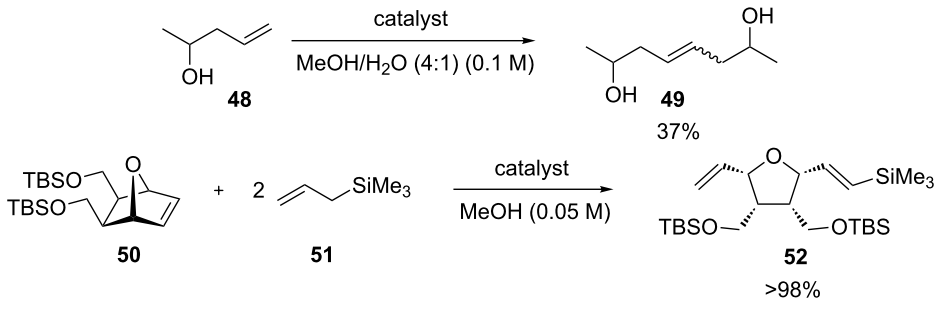

Figure 5: CM-type reactions in air using **41** as catalyst. Reaction conditions: **41** (5 mol %), 22 °C, 12 h, in air.

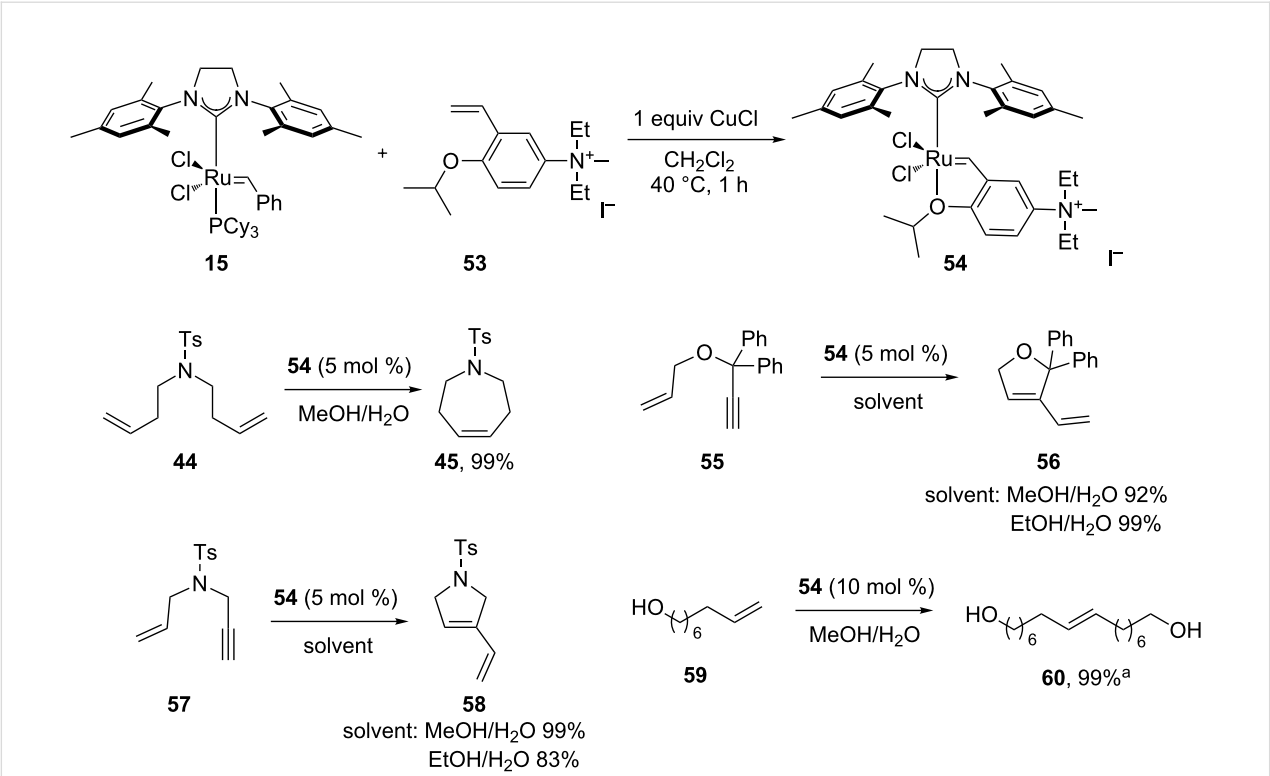

Figure 6: Grela's complex (**54**) and reaction scope in air. Reaction conditions: catalyst, substrate (0.25 mmol), nondegassed solvent (5:2; 0.02 M), 25 °C, in air, 0.5 h. GC conversion. [a]Reaction time 24 h.

and also increased the activity of the complex due to the electron-withdrawing effects of substituents.

In early 2009, Grubbs and co-workers reported the use of Hoveyda–Grubbs 2nd generation catalyst **33** (0.1 mol %) in air and in different solvents for the RCM of diethyl diallylmalonate (**29**) [64]. Conversions were found to be as low as 10% in DCM and <20% in toluene.

In 2009, Abell and Zaman reported the use of a Hoveyda–Grubbs 2nd generation ruthenium-based catalyst immobilized on PEG (**61**, Figure 7) [65]. This catalyst was soluble in dichloromethane but could be retrieved and recycled by simple exctraction with water or precipitation with ether. With a catalyst loading of 10 mol % in refluxing nondegassed dichloromethane, very high conversions were achieved in less than 1 hour for di- and trisubstituted olefins.

Towards the end of 2009, the Meier group reported the use of Grubbs (**15**), Hoveyda–Grubbs 2nd generation catalyst (**33**) and a variation of the latter (**66**, Figure 8) in the RCM of diethyl diallylmalonate (**29**) [66]. Reactions were performed with very low catalyst loading (from 2.5 to 0.04 mol %), at 30 °C, under air in nondegassed DCM, nondegassed methyl decanoate and

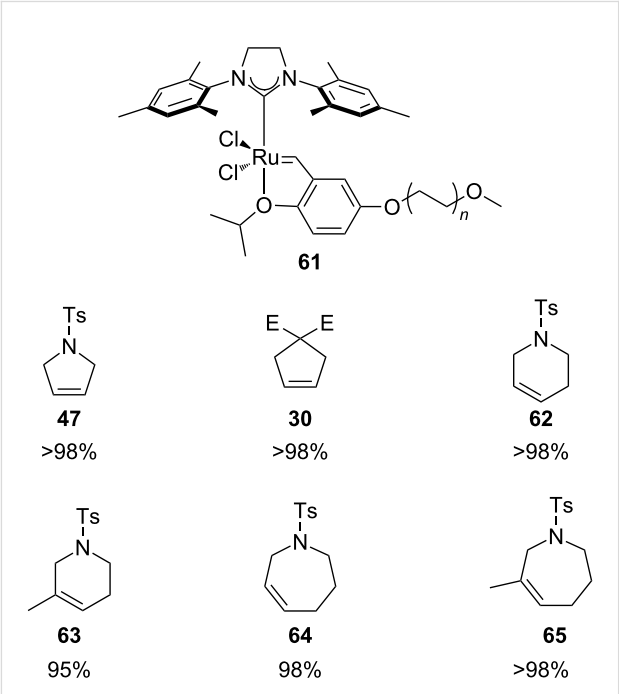

Figure 7: Abell's complex (**61**) and its RCM reaction scope in air. Reaction condition: 10 mol % of **61**, refluxing DCM in air, 0.5 h. Conversion determined by ^{1}H NMR.

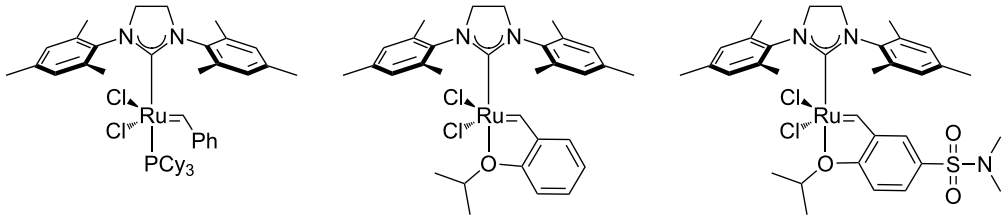

15 33 66

Figure 8: Catalysts used by Meier in air.

under solvent-free conditions in nondegassed substrates. Full conversions were achieved in the majority of cases, in both CM and RCM reactions, with all catalysts. In these reactions, catalyst **66** gave the highest performance. It should be noted that the results obtained by Meier with **33** were in contrast with the previous report by Grubbs [64].

In 2012, Grela and co-workers described the synthesis and use of 3 ammonium chloride-tagged variations of Hoveyda–Grubbs' catalyst (**67–69,** Figure 9) [67]. The catalysts were active in the isomerization of double bonds, self-metathesis, RCM and ene–yne metathesis reactions. They afforded average to high yields under air (Table 2). Reactions were performed in water at rt. Catalyst **69** was the most soluble in water; however, it did not afford the highest catalytic activity. In order to test the recyclability of the complex, diethyl diallylmalonate (**29**) was subjected to RCM reaction in refluxing DCM with 1 mol % of catalyst **69**. After reaction completion

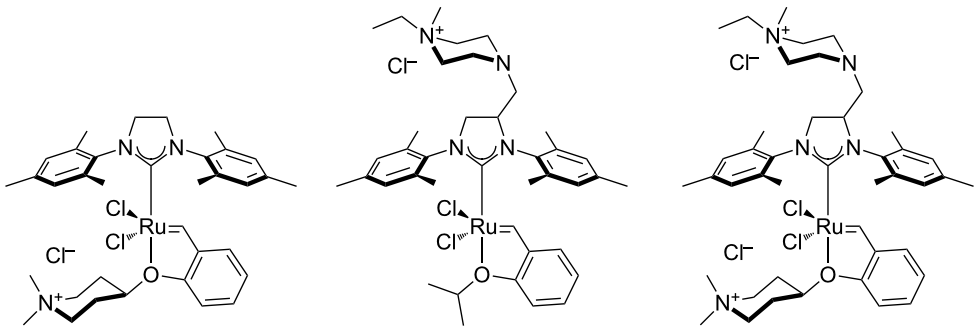

67 68 69

Figure 9: Ammonium chloride-tagged complexes.

Table 2: Metathesis reaction in water under air.

Substrate	Product	Catalyst (mol %)	Time (h)	Yield (%)[a]
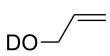 **70**	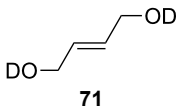 **71**	**67** (5) **68** (5) **69** (5)	24 24 24	74[b] 77[b] 38[c]
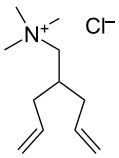 **72**	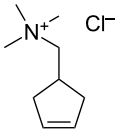 **73**	**67** (2.5) **68** (2.5) **69** (2.5)	3.5 2.5 2.5	49 96 88

[a]Yields are calculated by NMR spectroscopy. [b]*E*/*Z* = 16.7:1. [c]*E*/*Z* = 12.5:1 [67].

(97% isolated yield) and a single extraction with D_2O, (*Z*)-but-2-ene-1,4-[^{2}H]-diol was added to the water phase and isomerization to the *trans* isomer **71** was completeted after 1 h, with no decrease in activity (94% isolated yield) observed.

In early 2013, Jensen and co-workers reported a variation of the Hoveyda–Grubbs' 2nd generation catalyst bearing a sulfur-based anion (2,4,6-triphenylbenzenthiolate), replacing one of the chlorides [68]. Despite being a stable and a high *Z*-selective catalyst, it displayed no activity in air, using 0.01 mol % catalyst loading.

Later in the same year, Olszewski, Skowerski et al. reported the synthesis and use of new Scorpio-type complexes (Figure 10) [69]. These complexes presented high affinity for silica, which allowed the easy separation and recycling of the catalysts from the reaction mixture. Due to air stability, their activity in nondegassed DCM, toluene and ACS grade ethyl acetate was reported (Table 3). Complex **76b** performed slightly better in all cases, regardless of the air atmosphere and of the solvent used. With low catalyst loadings, ranging from 1 to 0.1 mol %, high to quantitative yields were achieved in all cases.

Grubbs 3rd generation catalyst

In 2002, Grubbs' and co-workers reported a variation of the 2nd generation catalyst, featuring the substitution of PCy_3 with two molecules of 3-bromopyridine (Scheme 8) [70]: Catalyst **81**, now known as Grubbs' 3rd generation catalyst, showed the highest rate of initiation reported to date for alkene metathesis reactions.

Complex **81** is used mostly for ROMP and CM reactions with electron-deficient olefins. The complex can be prepared in air but only one example of its use in air has been reported. In 2010, Tew and co-workers reported the use of **81** in the living ROMP of a hydrophilic norbornene monomer in air, leading to the formation of hydrogels [71]. Despite the living character of this reaction, the propagating catalyst was found to be inactive after 1 hour.

Indenylidene complexes

The indenylidene-bearing family of complexes has exhibited a rapid growth in use in recent years and is quickly becoming a mainstream catalyst in metathesis-type reactions (Figure 11). These complexes have received significant attention due to their high activity in olefin metathesis [72-78], their thermal stability and their ease of synthesis [77,79,80].

Complex **82** is air-stable in the solid state; however, it does not show activity in metathesis-type reactions. On the other hand, its PCy_3 counterpart **83** is as active as the Grubbs' 1st generation catalyst [73,80,81]. The NHC-bearing complexes (**74, 84–86**) showed increased activity and maintained the same thermal stability. Again, these complexes showed similar activity to the Grubbs 2nd generation catalysts [77,78], and are stable when stored under air. Nolan reported the synthesis of Grubbs' 2nd generation catalyst (**15**) from indenylidene complexes **84**, by simple reaction with styrene, avoiding the use of hazardous diazo compound **7** [82].

Towards the end of 2013, a report by Olszewski, Skowerski and co-workers showed how a variety of commercially available catalysts (Figure 12) could be employed in air with nondegassed ACS grade green solvents. Their results were in line with the ones obtained with DCM and toluene [62]. From Table 4, it can be seen how ethyl acetate at 70 °C represented an optimal solvent choice for most of the complexes.

Every catalyst afforded very high yields, in air, with activities comparable to the use of distilled and anhydrous solvents. Also reported was the cyclization of *N*-allyl-*N*-(methallyl)tosylamide (**79**) in nondegassed and undistilled ethyl acetate (ACS grade), catalyzed by **87** (0.25 mol %), at 70 °C in 1 h with a conversion of 98%.

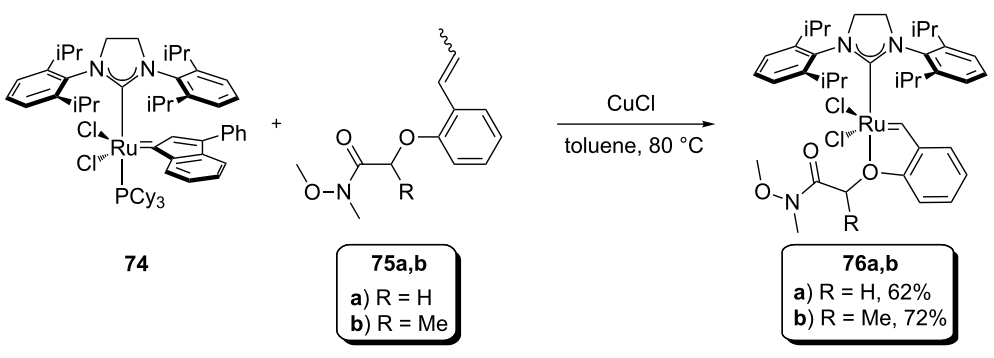

Figure 10: Scorpio-type complexes.

Table 3: Metathesis reactions catalysed by Scorpio-type complexes in air.[a]

Substrate[b]	Product[b]	Solvent (M)	Catalyst (mol %)	Time (min)	Yield (%)[c]
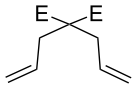 **29**	 **30**	DCM (0.05) DCM (0.05) EtOAc (0.1 M)[d]	**76a** (1) **76b** (1) **76b** (0.2)	60 30 60	94 98 >99[e]
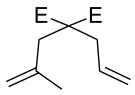 **77**	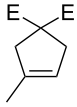 **78**	DCM (0.05) DCM (0.05)	**76a** (1) **76b** (1)	150 60	97 96
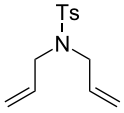 **46**	 **47**	DCM (0.05) toluene (0.1)[f]	**76b** (1) **76b** (0.1)	20 60	>98 94
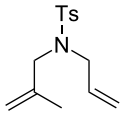 **79**	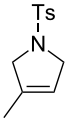 **80**	DCM (0.05) toluene (0.1)[f]	**76b** (1) **76b** (0.1)	40 60	>98 96
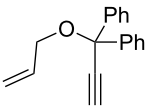 **55**	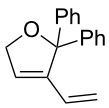 **56**	DCM (0.05) DCM (0.05) toluene (0.1)	**76a** (1) **76b** (1) **76b** (0.5)	45 30 300	99 <98 92

[a]Reaction conditions: catalyst, nondegassed DCM, reflux, *t*. [b]E = COOEt. [c]Isolated yields after column chromatography. [d]Ethyl acetate is ACS grade solvent, temperature is 40 °C. [e]Conversion determined by GC. [f]Added dropwise with a syringe pump [69].

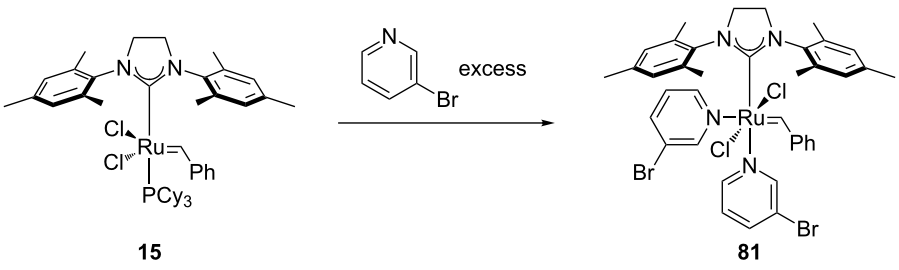

15 **81**

Scheme 8: Synthesis of Grubbs' 3rd generation catalyst.

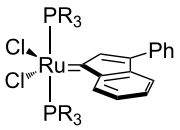

82 R = Ph
83 R = Cy

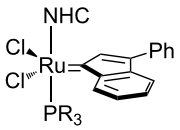

84 NHC = SIMes; R = Ph
85 NHC = SIMes; R = Cy
86 NHC = SIPr; R = Ph
74 NHC = SIPr; R = Cy

Figure 11: Indenylidene complexes.

In 2014, Grela and co-workers reported the synthesis *N,N*-unsymmetrically substituted SIMes-bearing indenylidene complexes (**93a–f** and **94**, Figure 13) [83]. They also tested their reactivity under air and in technical grade nondegassed solvents, and compared them to the activity of the commercially available catalyst **85**.

After initial screening and evaluation of their activity with the model substrate, diethyl diallylmalonate (**29**) (Table 5), **93a**, **93b**, **93d** and **93e** were found more active than **85**. When

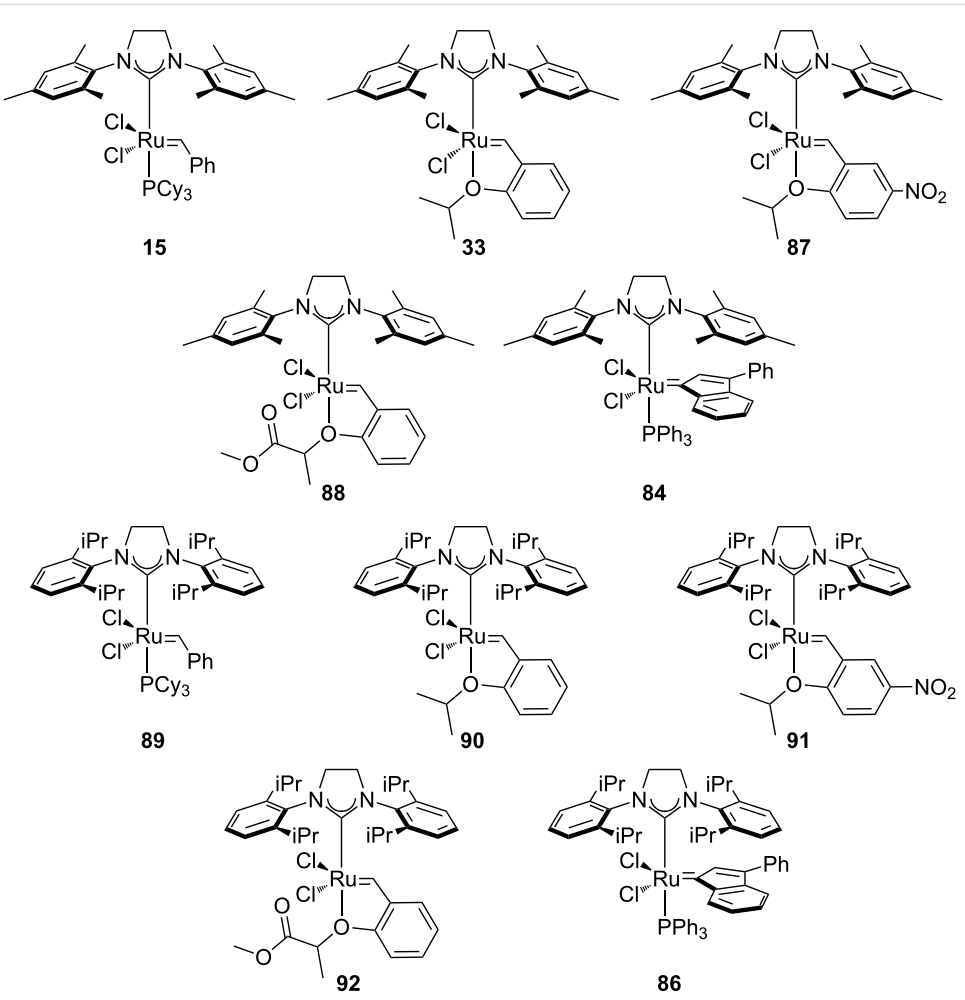

Figure 12: Commercially available complexes evaluated under air.

diethyl allyl(methallyl)malonate (**77**) and *N*,*N*-bis(methallyl)-tosylamide (**95**) were used, catalysts **93a** and **93b** performed better than others. A full scope, involving an ene–yne reaction, was carried out with these two complexes in DCM and toluene in comparison with **85**; catalyst loadings were between 1 and 2 mol % and reaction times, with the synthesised complexes, were shorter than with **85**.

Phosphite-based catalysts

In 2010, the Cazin group reported a study on the synthesis and activity of a new family of complexes (**98a–d**, Scheme 9) [84]; phophite-based complexes were thus synthesized to evaluate possible positive effects of these ligands in alkene metathesis reactions.

Their stability at high temperatures allowed their use in the RCM of bis(methallyl)tosylamide (**95**) and diethyl bis-(methallyl)malonate leading to the highest yields reported to date [85].

In 2015, the same group reported a study on the use of **98a** and other commercially available metathesis catalysts (**15**, **33**, **85**, Figure 14) [86], under various conditions. Reactions were performed under atmospheres of N_2, O_2, CO_2, air, dry air and in the presence of water to evaluate the effect of each on the performance of these catalysts.

A preliminary test on the RCM of bis(methallyl)tosylamide (**95**), using 0.1 mol % of **33**, **85** and **98a** under air and in refluxing toluene, showed a 60% conversion after 20 min for **98a**. Under these conditions, the other catalysts were completely inactive after 20 min and lead to conversions lower than 40%, when used for prolonged reaction times. After evaluation of the detrimental effects of each of the components of air on catalyst activity, a general trend could be observed: $H_2O > CO_2 \geq O_2$. In all cases, water had the most deleterious effect, whereas reactions could be performed in dry air and in N_2 atmosphere without any noticeable differences as compared to their use under inert atmosphere.

Table 4: RCM with commercially available catalysts in technical grade solvents.[a]

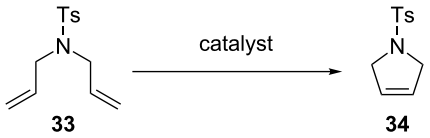

33 **34**

Catalyst	*T* (°C)	GC yield (%) AcOEt	DMC	CPME	2-MeTHF	DCM/toluene[b]
15	40	97	98	80	35	92
	70	98	98	97	95	67
87	40	94	85	79	49	96
	70	98	98	97	65	65
88	40	66	79	20	37	98
	70	99	98	60	65	61
84	40	96	98	69	38	93
	70	98	98	95	92	59
89	40	88	98	85	84	91
	70	99	98	92	97	98
91	40	96	99	97	97	88
	70	99	99	99	99	99
92	40	98	99	97	97	91
	70	99	99	99	98	99
86	40	92	98	89	93	95
	70	94	98	84	98	96

[a]Reaction conditions: Cat. 0.25 mol %, nondegassed, undistilled ACS grade solvents in air (0.1 M), 1 h. DMC: dimethyl carbonate; CPME: cyclopentyl methyl ether; 2-MeTHF: 2-methyltetrahydrofuran.[b]DCM was used at 40 °C while toluene at 70 °C [62].

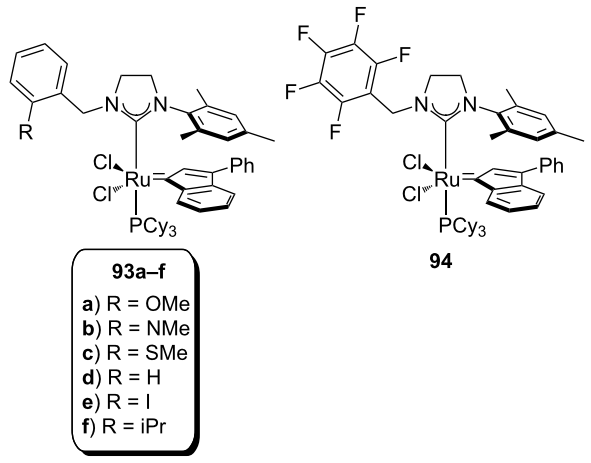

Figure 13: Grela's *N,N*-unsymmetrically substituted complexes.

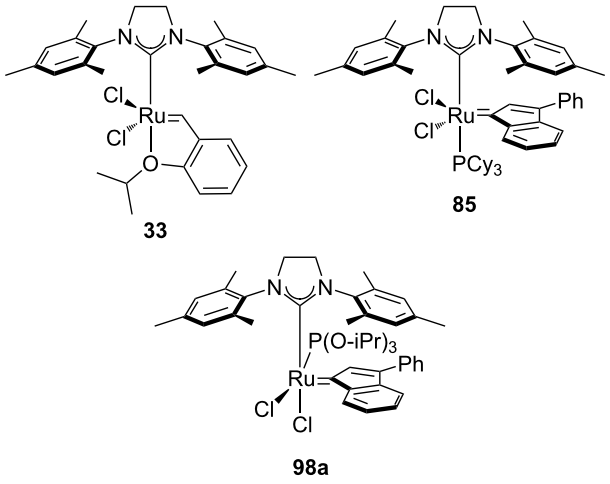

Figure 14: Catalysts used by the Cazin group.

Catalyst **98a**, with concentrations ranging from 0.05 to 0.5 mol %, exhibited the most remarkable activity in air with high to quantitative yields in the RCM, CM and ene–yne reactions. Furthermore, complexes **33** and **85** were able to perform the RCM reactions under the same conditions, with yields ranging from moderate to excellent (Figure 15).

Schiff bases

Schiff bases in metathesis are usually O,N-bidentate ligands and represent an interesting alternative family of ligands as [18,87-94]: 1) they can be produced in one high yielding step by condensation of an aldehyde and an amine, thus allowing the fine and facile tuning of ligand and catalyst steric and electronic

Table 5: RCM and ene–yne reactions catalysed by **93a–f** and **94** in air.[a]

Substrate	Product[b]	Catalyst (mol %)	*T* (°C)[c]	*t* (h)	Yield (%)[d]
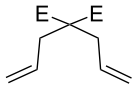 **29**	 **30**	**85** (1)	30	0.4	42
		93a (1)	30	1.7	96
		93b (1)	30	1.7	93
		93c (1)	30	1.7	7
		93d (1)	30	1.8	92
		93e (1)	30	1.7	97
		93f (1)	30	1.9	17
		94 (1)	30	0.9	90
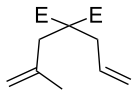 **77**	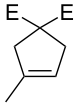 **78**	**85** (1)	30	1.7	23
		93a (1)	30	1.7	87
		93b (1)	30	1.5	72
		93d (1)	30	1.7	72
		93e (1)	30	1.5	86
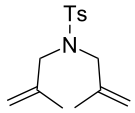 **95**	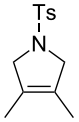 **96**	**85** (5)	30	0.4	40
		93a (5)	30	0.4	41
		93b (5)	30	0.4	38
		93d (5)	30	0.4	36
		93e (5)	30	0.4	35
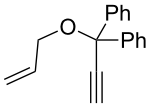 **55**	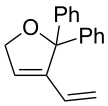 **56**	**85** (2)	30	6	94[e]
		93a (2)	30	5	96[e]
		93b (2)	30	8	96[e]

[a]Reaction conditions: Catalyst (mol %), nondegassed DCM (commercial-grade HPLC) (0.1 M) in air. [b]E = COOEt. [c]Reactions at 50 °C were performed in nondegassed toluene (commercial-grade HPLC) in air. [d]Yields determined by ^{1}H NMR. [e]Isolated yields after flash chromatography [83].

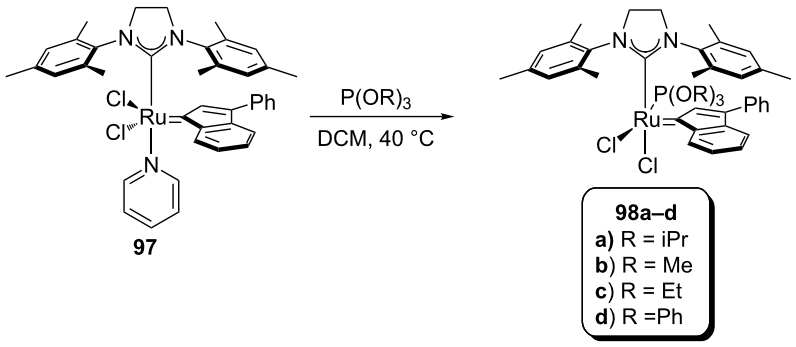

Scheme 9: Synthesis of phosphite-based catalysts.

properties; and 2) the two different donor atoms, O (hard) and N (soft), offer different features and therefore can stabilize, respectively, high and low oxidation states.

Ruthenium carbene complexes bearing Schiff bases were synthesized originally by the Grubbs' group and applied in RCM reactions [95], showing lower activity then the Grubbs 1st generation catalyst but exhibited very high termal stability (Figure 16).

In 2002 and 2003, the Verpoort group synthesized and applied a variety of Schiff base adapted complexes in RCM [87] and ROMP [87,93,94,96,97] reactions (Scheme 10). This class of complexes showed high activity and very high stability to air and water, compared to Grubbs 1st and 2nd generation catalysts [7]. RCM reactions were performed in air with 5 mol % of the catalyst, showing high yields for terminal dienes (Table 6, entry 1). In the absence of SIMes, increasing the olefin substitution led to low yields in all catalytic systems. An electron-with-

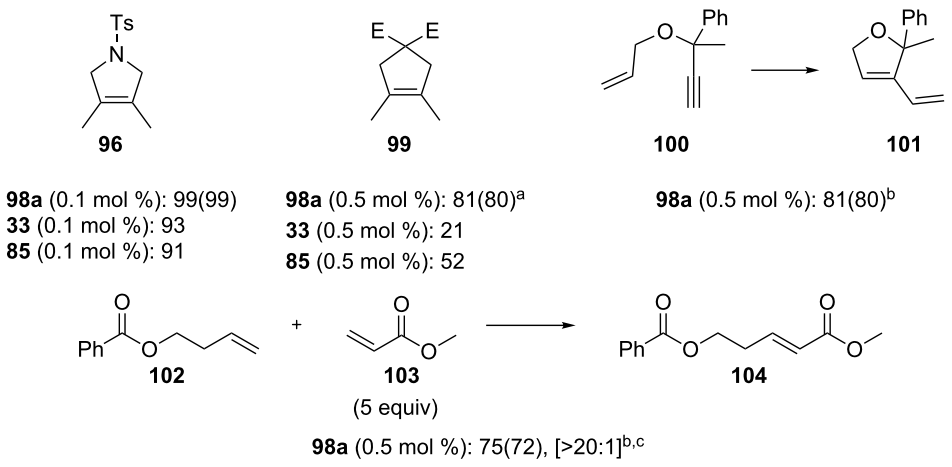

Figure 15: RCM scope in air with catalysts **33, 85** and **98a**. Reaction conditions: Catalyst, substrate (0.25 mmol), reagent-grade toluene (0.5 mL), 110 °C, in air, 3 h. E = COOEt. GC conversion and isolated yield in parentheses. [a]Isolated as a mixture, NMR yield. [b]Toluene (0.5 mL). [c]*E*/*Z* ratio determined by ^{1}H NMR.

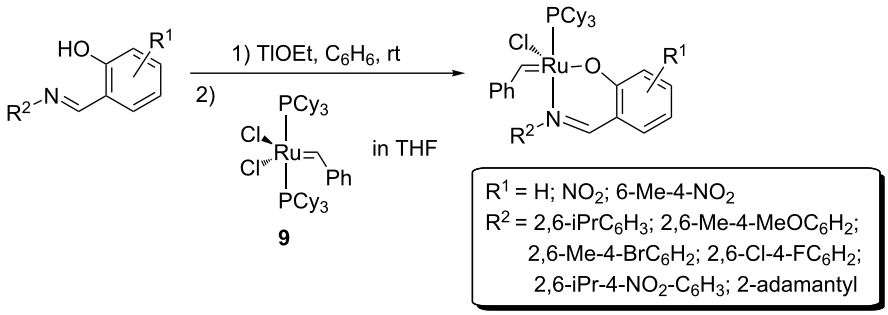

Figure 16: Synthesis of Schiff base-ruthenium complexes.

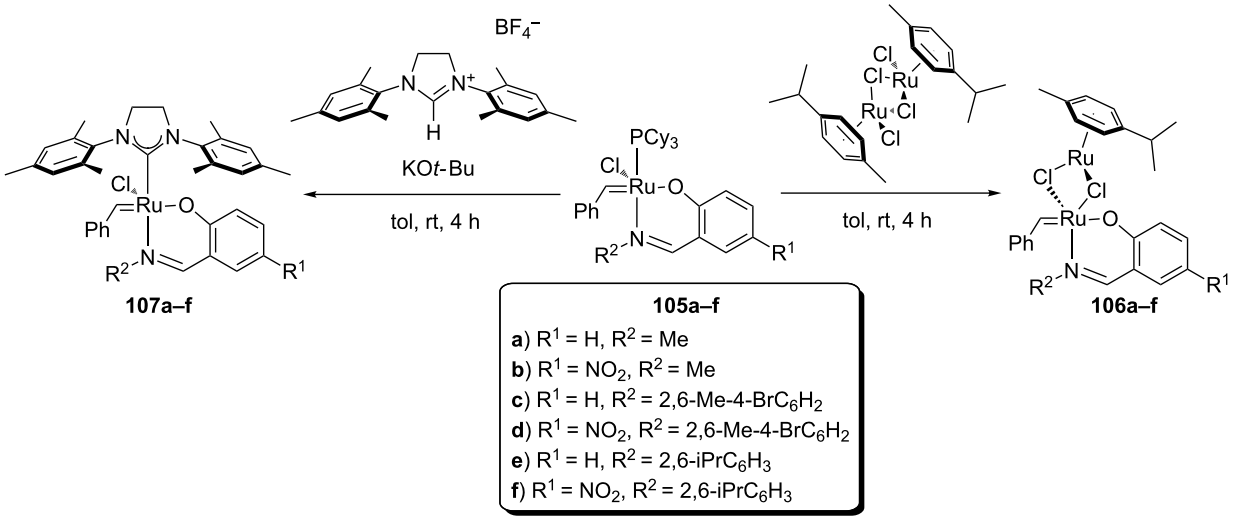

Scheme 10: Schiff base–ruthenium complexes synthesized by Verpoort.

drawing substituent on the phenyl ring and a bulky group on the imine generally lead to higher activity for both mono- and bimetallic systems. SIMes-bearing complexes are more active than monometallic systems in all cases, and more active than bimetallic systems only when the iminic substituent is less bulky (Table 6, entries 2 and 3).

In 2007, Raines et al. reported that **108b** (Scheme 11) remained intact after 8 days in C_6D_6 under air [7]. This prompted them to explore the activity of mixed Schiff–NHC complexes in RCM and ene–yne reactions using protic solvents in air.

As can be seen from Table 7, catalyst **108c**, bearing a water-soluble tag, is active in D_2O and in water/methanol mixtures under air and the presence of the tag does not influence the reactivity. Although high conversions were obtained, high catalyst loadings (5–10 mol %) of all catalysts were required.

In 2009, surely inspired by the aforementioned work, the Verpoort group reported a family of indenylidene Schiff base–ruthenium complexes (**111a–f**, Figure 17) for CM and RCM reactions in air [98]. They combined the higher thermal stability of indenylidene complexes and the tunability and stability of Schiff base ligands. These complexes were able to perform CM and RCM reactions in air with lower catayst loadings compared to **105a–f**, **106a–f**, **107a–f** and **111a–c**. RCM reactions proceeded smoothly using *N,N*-diallyltosylamide (**46**) giving, with all catalysts, quantitative yields. When a more challenging substrate (*N*-allyl-*N*-(methallyl)tosylamide, **79**) was used, a 24 h reaction time was needed in all cases, with the

Table 6: Yield (%) of RCM reactions using catalysts **105a–f**, **106a–f** and **107a–f** in air.[a]

Entry	Product[b]	Yield (%)					
		105a/106a/107a	**105b/106b/107b**	**105c/106c/107c**	**105d/106d/107d**	**105e/106e/107e**	**105f/106f/107f**
1	 **30**	100/100/100	100/100/100	100/100/100	100/100/100	100/100/100	100/100/100
2	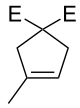 **77**	<5/13/72	<5/<5/73	<5/58/47	9/44/42	18/83/31	21/72/23
3	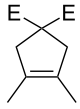 **99**	<5/6/41	<5/<5/33	<5/41/19	6/29/11	11/62/<5	17/49/<5

[a]Reaction conditions: catalyst (5 mol %), distilled C_6D_5Cl (0.05 M), 55 °C, in air for catalysts **105a–f** and 70 °C for catalysts **106a–f**, 4 h [96]. For catalysts **107a–f** undistilled C_6D_6 was used as solvent and temperature was 55 °C, 4 h, in air [97]. [b]E = COOEt.

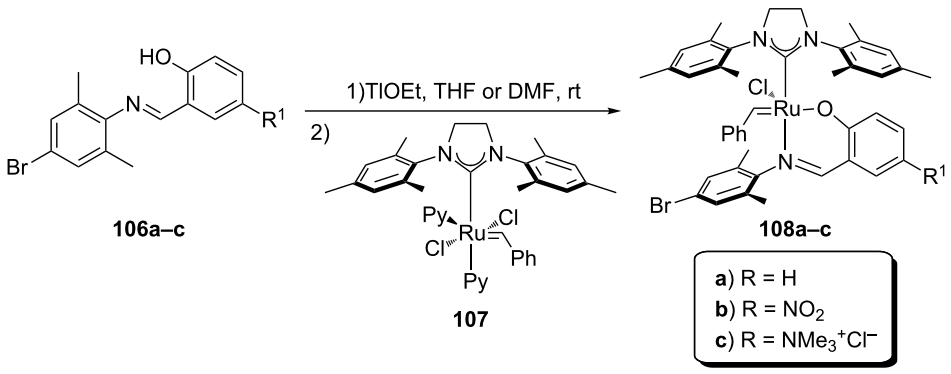

Scheme 11: Synthesis of mixed Schiff base–NHC complexes.

Table 7: RCM of representative dienes catalysed by **108a–c** under air.[a]

Substrate[b]	Product[b]	Solvent (substrate conc. [M])	Complex (mol %)	Time [h]	Conversion [%][c]
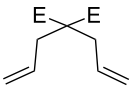 **29**	 **30**	C_6D_6 (0.1)	**108a** (5)	72	90
		C_7D_8 (0.05)	**108b** (5)	70	79
		CD_3OD (0.025)	**108b** (5)	23	94
		C_6D_6 (0.05)	**108c** (5)	40	>95
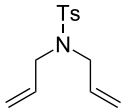 **46**	 **47**	C_6D_6 (0.05)	**108a** (5)	26	68
		C_7D_8 (0.05)	**108b** (5)	70	92
		CD_3OD (0.025)	**108b** (5)	9	>95
		CD_3OD (0.05)	**108c** (5)	6	>95
		2:1 CD_3OD/D_2O (0.025)	**108c** (5)	6	93
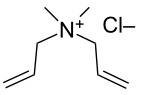 **109**	 **110**	CD_3OD (0.05)	**108c** (5)	12	79
		2:1 CD_3OD/D_2O (0.025)	**108c** (10)	6	40
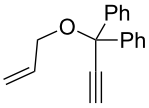 **55**	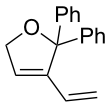 **56**	C_7D_8 (0.05)	**108a** (5)	36	93
		C_7D_8 (0.05)	**108b** (5)	18	>95
		CD_3OD (0.025)	**108b** (5)	2	90
		C_6D_6 (0.05)	**108c** (5)	5	>95
		CD_3OD (0.05)	**108c** (5)	2	>95

[a]Reaction conditions: catalyst, 55 °C. [b]E = COOEt. [c]Conversion determined by ^{1}H NMR spectroscopy. [d]80 °C.

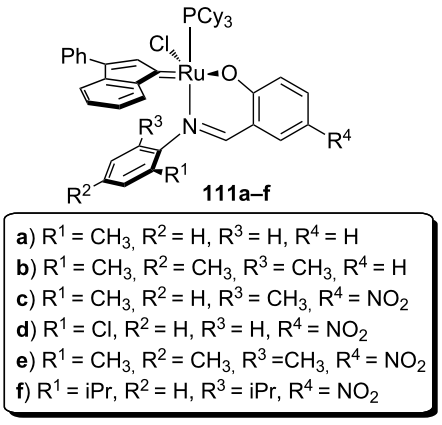

Figure 17: Veerport's indenylidene Schiff-base complexes.

Table 8: RCM of *N*-allyl-*N*-(methallyl)tosylamide (**79**) with complexes **111a–f** in air.[a]

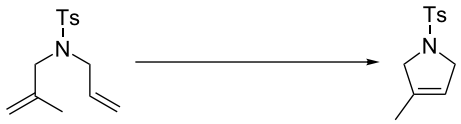

79 **80**

Catalyst (0.5 mol %)	Yield over time		
	1 h	3 h	24 h
111a	18	37	51
111b	45	67	97
111c	14	37	87
111d	87	100	100
111e	36	68	97
111f	28	55	100

[a]Reaction conditions: catalyst, CH_3Cl (0.1 M), 60 °C in air.

exception of **111d** (Table 8). This remarkable activity (higher than Hoveyda–Grubbs 2nd generation catalyst, **33**) was due to the presence of the electron-withdrawing substituents on the Schiff base.

Conclusion

Although metathesis-type reactions represent one of the most valuable strategies in modern organic synthesis, making this highly valuable tool more accessible and practical for routine use still remains a challenge. Ruthenium-based catalysts have been at the centre of recent advancements making possible their use in air, moreover these catalysts are becoming more and more stable, efficient and economically friendly with time. With the current development directed towards air and moisture stability and high performance, there is no doubt that more reports will push these reactivity/tolerance limits even further. As seen in this review, conducting metathesis-type reactions in air, in the presence of water and under high temperature has become more concrete, with several groups leading the charge [62,86].

References

1. Hoveyda, A. H.; Zhugralin, A. R. *Nature* **2007,** *450,* 243–251. doi:10.1038/nature06351
2. Malcolmson, S. J.; Meek, S. J.; Sattely, E. S.; Schrock, R. R.; Hoveyda, A. H. *Nature* **2008,** *456,* 933–937. doi:10.1038/nature07594
3. Fürstner, A. *Angew. Chem., Int. Ed.* **2000,** *39,* 3012–3043. doi:10.1002/1521-3773(20000901)39:17<3012::AID-ANIE3012>3.0.CO;2-G
4. Diesendruck, C. E.; Tzur, E.; Lemcoff, N. G. *Eur. J. Inorg. Chem.* **2009,** *2009,* 4185–4203. doi:10.1002/ejic.200900526
5. Trnka, T. M.; Grubbs, R. H. *Acc. Chem. Res.* **2001,** *34,* 18–29. doi:10.1021/ar000114f
6. Bieniek, M.; Michrowska, A.; Usanov, D. L.; Grela, K. *Chem. – Eur. J.* **2008,** *14,* 806–818. doi:10.1002/chem.200701340
7. Binder, J. B.; Guzei, I. A.; Raines, R. T. *Adv. Synth. Catal.* **2007,** *349,* 395–404. doi:10.1002/adsc.200600264
8. Lozano-Vila, A. M.; Monsaert, S.; Bajek, A.; Verpoort, F. *Chem. Rev.* **2010,** *110,* 4865–4909. doi:10.1021/cr900346r
9. Astruc, D. *New J. Chem.* **2005,** *29,* 42–56. doi:10.1039/b412198h
10. Grela, K., Ed. *Olefin Metatehsis: Theory and Practice;* John Wiley & Sons, Inc.: Hoboken, NJ, U.S.A., 2014. doi:10.1002/9781118711613
11. Leitgeb, A.; Wappel, J.; Slugovc, C. *Polymer* **2010,** *51,* 2927–2946. doi:10.1016/j.polymer.2010.05.002
12. Bielawski, C. W.; Grubbs, R. H. *Prog. Polym. Sci.* **2007,** *32,* 1–29. doi:10.1016/j.progpolymsci.2006.08.006
13. Grubbs, R. H., Ed. *Handbook of Metathesis;* Wiley-VCH: New York, NY, U.S.A., 2003. doi:10.1002/9783527619481
14. Mol, J. C. *J. Mol. Catal. A: Chem.* **2004,** *213,* 39–45. doi:10.1016/j.molcata.2003.10.049
15. Baughman, T. W.; Wagener, K. B. *Adv. Polym. Sci.* **2005,** *176,* 1–42. doi:10.1007/b101318
16. Buchmeiser, M. R. *Chem. Rev.* **2000,** *100,* 1565–1604. doi:10.1021/cr990248a
17. Lynn, D. M.; Mohr, B.; Grubbs, R. H. *J. Am. Chem. Soc.* **1998,** *120,* 1627–1628. doi:10.1021/ja9736323
18. Drozdzak, R.; Allaert, B.; Ledoux, N.; Dragutan, I.; Dragutan, V.; Verpoort, F. *Coord. Chem. Rev.* **2005,** *249,* 3055–3074. doi:10.1016/j.ccr.2005.05.003
19. Reymond, S.; Ferrié, L.; Guérinot, A.; Capdevielle, P.; Cossy, J. *Pure Appl. Chem.* **2008,** *80,* 1683–1691. doi:10.1351/pac200880081683
20. Hoveyda, A. H.; Malcolmson, S. J.; Meek, S. J.; Zhugralin, A. R. *Angew. Chem., Int. Ed.* **2010,** *49,* 34–44. doi:10.1002/anie.200904491
21. Nicolaou, K. C.; Bulger, P. G.; Sarlah, D. *Angew. Chem., Int. Ed.* **2005,** *44,* 4490–4527. doi:10.1002/anie.200500369
22. Connon, S. J.; Blechert, S. *Angew. Chem., Int. Ed.* **2003,** *42,* 1900–1923. doi:10.1002/anie.200200556
23. Požgan, F.; Dixneuf, P. H. Recent Applications Of Alkene Metathesis For Fine Chemical And Supramolecular System Synthesis. In *Metathesis Chemistry;* Imamoglu, Y.; Dragutan, V.; Karabulut, S., Eds.; NATO Science Series, Vol. 243; Springer: Berlin, Germany, 2007; pp 195–222. doi:10.1007/978-1-4020-6091-5_12
24. Mele, G. L. J.; Vasapollo, G. *Chim. Oggi* **2008,** *26,* 72–74.
25. Olszewski, T. K.; Figlus, M.; Bienek, M. *Chim. Oggi* **2014,** *32,* 22–29.
26. The Nobel Prize in Chemistry 2005. http://www.nobelprize.org/nobel_prizes/chemistry/laureates/2005/ (accessed July 13, 2015).
27. Schuster, M.; Blechert, S. *Angew. Chem., Int. Ed. Engl.* **1997,** *36,* 2036–2056. doi:10.1002/anie.199720361
28. Deshmukh, P. H.; Blechert, S. *Dalton Trans.* **2007,** 2479–2491. doi:10.1039/b703164p
29. Grubbs, R. H. *Tetrahedron* **2004,** *60,* 7117–7140. doi:10.1016/j.tet.2004.05.124
30. Schrock, R. R.; Czekelius, C. *Adv. Synth. Catal.* **2007,** *349,* 55–77. doi:10.1002/adsc.200600459
31. Novak, B. M.; Grubbs, R. H. *J. Am. Chem. Soc.* **1988,** *110,* 7542–7543. doi:10.1021/ja00230a047
32. Novak, B. M.; Grubbs, R. H. *J. Am. Chem. Soc.* **1988,** *110,* 960–961. doi:10.1021/ja00211a043
33. Marciniec, B.; Pietraszuk, C. *J. Organomet. Chem.* **1991,** *412,* C1–C3. doi:10.1016/0022-328X(91)86064-W
34. France, M. B.; Grubbs, R. H.; Mcgrath, D. V.; Paciello, R. A. *Macromolecules* **1993,** *26,* 4742–4747. doi:10.1021/ma00070a002
35. Nguyen, S. T.; Johnson, L. K.; Grubbs, R. H.; Ziller, J. W. *J. Am. Chem. Soc.* **1992,** *114,* 3974–3975. doi:10.1021/ja00036a053
36. Schwab, P.; France, M. B.; Ziller, J. W.; Grubbs, R. H. *Angew. Chem., Int. Ed. Engl.* **1995,** *34,* 2039–2041. doi:10.1002/anie.199520391
37. Nguyen, S. T.; Grubbs, R. H.; Ziller, J. W. *J. Am. Chem. Soc.* **1993,** *115,* 9858–9859. doi:10.1021/ja00074a086
38. Schwab, P.; Grubbs, R. H.; Ziller, J. W. *J. Am. Chem. Soc.* **1996,** *118,* 100–110. doi:10.1021/ja952676d
39. Weskamp, T.; Schattenmann, W. C.; Spiegler, M.; Herrmann, W. A. *Angew. Chem., Int. Ed.* **1998,** *37,* 2490–2493. doi:10.1002/(SICI)1521-3773(19981002)37:18<2490::AID-ANIE2490>3.0.CO;2-X
40. Huang, J.; Schanz, H.-J.; Stevens, E. D.; Nolan, S. P. *Organometallics* **1999,** *18,* 5375–5380. doi:10.1021/om990788y
41. Huang, J.; Stevens, E. D.; Nolan, S. P.; Petersen, J. L. *J. Am. Chem. Soc.* **1999,** *121,* 2674–2678. doi:10.1021/ja9831352
42. Scholl, M.; Trnka, T. M.; Morgan, J. P.; Grubbs, R. H. *Tetrahedron Lett.* **1999,** *40,* 2247–2250. doi:10.1016/S0040-4039(99)00217-8
43. Scholl, M.; Ding, S.; Lee, C. W.; Grubbs, R. H. *Org. Lett.* **1999,** *1,* 953–956. doi:10.1021/ol990909q
44. Chatterjee, A. K.; Grubbs, R. H. *Org. Lett.* **1999,** *1,* 1751–1753. doi:10.1021/ol991023p
45. Chatterjee, A. K.; Morgan, J. P.; Scholl, M.; Grubbs, R. H. *J. Am. Chem. Soc.* **2000,** *122,* 3783–3784. doi:10.1021/ja9939744
46. Ackermann, L.; Fürstner, A.; Weskamp, T.; Kohl, F. J.; Herrmann, W. A. *Tetrahedron Lett.* **1999,** *40,* 4787–4790. doi:10.1016/S0040-4039(99)00919-3
47. Weskamp, T.; Kohl, F. J.; Hieringer, W.; Gleich, D.; Herrmann, W. A. *Angew. Chem., Int. Ed.* **1999,** *38,* 2416–2419. doi:10.1002/(SICI)1521-3773(19990816)38:16<2416::AID-ANIE2416>3.0.CO;2-#
48. Weskamp, T.; Kohl, F. J.; Herrmann, W. A. *J. Organomet. Chem.* **1999,** *582,* 362–365. doi:10.1016/S0022-328X(99)00163-1
49. Samojłowicz, C.; Bieniek, M.; Grela, K. *Chem. Rev.* **2009,** *109,* 3708–3742. doi:10.1021/cr800524f
50. Ulman, M.; Grubbs, R. H. *J. Org. Chem.* **1999,** *64,* 7202–7207. doi:10.1021/jo9908703
51. Kingsbury, J. S.; Harrity, J. P. A.; Bonitatebus, P. J., Jr.; Hoveyda, A. H. *J. Am. Chem. Soc.* **1999,** *121,* 791–799. doi:10.1021/ja983222u
52. Grela, K.; Harutyunyan, S.; Michrowska, A. *Angew. Chem., Int. Ed.* **2002,** *41,* 4038–4040. doi:10.1002/1521-3773(20021104)41:21<4038::AID-ANIE4038>3.0.CO;2-0
53. Dowden, J.; Savovic, J. *Chem. Commun.* **2001,** *2,* 37–38. doi:10.1039/b007304k

54. Garber, S. B.; Kingsbury, J. S.; Gray, B. L.; Hoveyda, A. H. *J. Am. Chem. Soc.* **2000,** *122,* 8168–8179. doi:10.1021/ja001179g
55. Gessler, S.; Randl, S.; Blechert, S. *Tetrahedron Lett.* **2000,** *41,* 9973–9976. doi:10.1016/S0040-4039(00)01808-6
56. Van Veldhuizen, J. J.; Garber, S. B.; Kingsbury, J. S.; Hoveyda, A. H. *J. Am. Chem. Soc.* **2002,** *124,* 4954–4955. doi:10.1021/ja020259c
57. La, D. S.; Sattely, E. S.; Ford, J. G.; Schrock, R. R.; Hoveyda, A. H. *J. Am. Chem. Soc.* **2001,** *123,* 7767–7778. doi:10.1021/ja010684q
58. Connon, S. J.; Rivard, M.; Zaja, M.; Blechert, S. *Adv. Synth. Catal.* **2003,** *345,* 572–575. doi:10.1002/adsc.200202201
59. Michrowska, A.; Bujok, R.; Harutyunyan, S.; Sashuk, V.; Dolgonos, G.; Grela, K. *J. Am. Chem. Soc.* **2004,** *126,* 9318–9325. doi:10.1021/ja048794v
60. Olszewski, T. K.; Bieniek, M.; Skowerski, K.; Grela, K. *Synlett* **2013,** *24,* 903–919. doi:10.1055/s-0032-1318497
61. Honda, T.; Namiki, H.; Kaneda, K.; Mizutani, H. *Org. Lett.* **2004,** *6,* 87–89. doi:10.1021/ol0361251
62. Skowerski, K.; Białecki, J.; Tracz, A.; Olszewski, T. K. *Green Chem.* **2014,** *16,* 1125–1130. doi:10.1039/C3GC41943F
63. Michrowska, A.; Gułajski, L.; Kaczmarska, Z.; Mennecke, K.; Kirschning, A.; Grela, K. *Green Chem.* **2006,** *8,* 685–688. doi:10.1039/b605138c
64. Kuhn, K. M.; Bourg, J.-B.; Chung, C. K.; Virgil, S. C.; Grubbs, R. H. *J. Am. Chem. Soc.* **2009,** *131,* 5313–5320. doi:10.1021/ja900067c
65. Zaman, S.; Abell, A. D. *Tetrahedron Lett.* **2009,** *50,* 5340–5343. doi:10.1016/j.tetlet.2009.07.022
66. Kniese, M.; Meier, M. A. R. *Green Chem.* **2010,** *12,* 169–173. doi:10.1039/B921126H
67. Skowerski, K.; Szczepaniak, G.; Wierzbicka, C.; Gułajski, Ł.; Bieniek, M.; Grela, K. *Catal. Sci. Technol.* **2012,** *2,* 2424–2427. doi:10.1039/c2cy20320k
68. Occhipinti, G.; Hansen, F. R.; Törnroos, K. W.; Jensen, V. R. *J. Am. Chem. Soc.* **2013,** *135,* 3331–3334. doi:10.1021/ja311505v
69. Skowerski, K.; Kasprzycki, P.; Bieniek, M.; Olszewski, T. K. *Tetrahedron* **2013,** *69,* 7408–7415. doi:10.1016/j.tet.2013.06.056
70. Love, J. A.; Morgan, J. P.; Trnka, T. M.; Grubbs, R. H. *Angew. Chem., Int. Ed.* **2002,** *41,* 4035–4037. doi:10.1002/1521-3773(20021104)41:21<4035::AID-ANIE4035>3.0.CO;2-I
71. Zhang, K.; Cui, J.; Lackey, M.; Tew, G. N. *Macromolecules* **2010,** *43,* 10246–10252. doi:10.1021/ma101950f
72. Jafarpour, L.; Schanz, H.-J.; Stevens, E. D.; Nolan, S. P. *Organometallics* **1999,** *18,* 5416–5419. doi:10.1021/om990587u
73. Fürstner, A.; Guth, O.; Düffels, A.; Seidel, G.; Liebl, M.; Gabor, B.; Mynott, R. *Chem. – Eur. J.* **2001,** *7,* 4811–4820. doi:10.1002/1521-3765(20011119)7:22<4811::AID-CHEM4811>3.0.CO;2-P
74. Schmidt, B.; Wildemann, H. *J. Chem. Soc., Perkin Trans. 1* **2000,** 2916–2925. doi:10.1039/b004302h
75. Fürstner, A.; Radkowski, K. *Chem. Commun.* **2001,** *2,* 671–672. doi:10.1039/b101148k
76. Fürstner, A.; Grabowski, J.; Lehmann, C. W.; Kataoka, T.; Nagai, K. *ChemBioChem* **2001,** *2,* 60–68. doi:10.1002/1439-7633(20010105)2:1<60::AID-CBIC60>3.0.CO;2-P
77. Boeda, F.; Bantreil, X.; Clavier, H.; Nolan, S. P. *Adv. Synth. Catal.* **2008,** *350,* 2959–2966. doi:10.1002/adsc.200800495
78. Clavier, H.; Nolan, S. P. *Chem. – Eur. J.* **2007,** *13,* 8029–8036. doi:10.1002/chem.200700256
79. Öfele, K.; Tosh, E.; Taubmann, C.; Herrmann, W. A. *Chem. Rev.* **2009,** *109,* 3408–3444. doi:10.1021/cr800516g
80. Urbina-Blanco, C. A.; Guidone, S.; Nolan, S. P.; Cazin, C. S. J. Ruthenium-Indenylidene and Other Alkylidene Containing Olefin Metathesis Catalysts. In *Olefin metathesis: Theory and Practice;* Grela, K., Ed.; John Wiley & Sons, Inc.: Hoboken, NJ, U.S.A., 2014; pp 417–436. doi:10.1002/9781118711613.ch15
81. Fürstner, A.; Thiel, O. R. *J. Org. Chem.* **2000,** *65,* 1738–1742. doi:10.1021/jo991611g
82. Dorta, R.; Kelly, R. A., III; Nolan, S. P. *Adv. Synth. Catal.* **2004,** *346,* 917–920. doi:10.1002/adsc.200404047
83. Ablialimov, O.; Kędziorek, M.; Malińska, M.; Woźniak, K.; Grela, K. *Organometallics* **2014,** *33,* 2160–2171. doi:10.1021/om4009197
84. Bantreil, X.; Schmid, T. E.; Randall, R. A. M.; Slawin, A. M. Z.; Cazin, C. S. J. *Chem. Commun.* **2010,** *46,* 7115–7117. doi:10.1039/c0cc02448a
85. Bantreil, X.; Poater, A.; Urbina-Blanco, C. A.; Bidal, Y. D.; Falivene, L.; Randall, R. A. M.; Cavallo, L.; Slawin, A. M. Z.; Cazin, C. S. J. *Organometallics* **2012,** *31,* 7415–7426. doi:10.1021/om300703p
86. Guidone, S.; Songis, O.; Nahra, F.; Cazin, C. S. J. *ACS Catal.* **2015,** *5,* 2697–2701. doi:10.1021/acscatal.5b00197
87. Opstal, T.; Verpoort, F. *J. Mol. Catal. A: Chem.* **2003,** *200,* 49–61. doi:10.1016/S1381-1169(03)00099-2
88. Opstal, T.; Verpoort, F. *Synlett* **2002,** 935–941. doi:10.1055/s-2002-31892
89. Opstal, T.; Verpoort, F. *Synlett* **2003,** 314–320. doi:10.1055/s-2003-37106
90. Opstal, T.; Verpoort, F. *Tetrahedron Lett.* **2002,** *43,* 9259–9263. doi:10.1016/S0040-4039(02)02233-5
91. Drozdzak, R.; Ledoux, N.; Allaert, B.; Dragutan, I.; Dragutan, V.; Verpoort, F. *Cent. Eur. J. Chem.* **2005,** *3,* 404–416. doi:10.2478/BF02479271
92. Drozdzak, R.; Allaert, B.; Ledoux, N.; Dragutan, I.; Dragutan, V.; Verpoort, F. *Adv. Synth. Catal.* **2005,** *347,* 1721–1743. doi:10.1002/adsc.200404389
93. Opstal, T.; Verpoort, F. *Angew. Chem., Int. Ed.* **2003,** *42,* 2876–2879. doi:10.1002/anie.200250840
94. De Clercq, B.; Verpoort, F. *J. Organomet. Chem.* **2003,** *672,* 11–16. doi:10.1016/S0022-328X(03)00055-X
95. Chang, S.; Jones, L., II; Wang, C.; Henling, L. M.; Grubbs, R. H. *Organometallics* **1998,** *17,* 3460–3465. doi:10.1021/om970910y
96. De Clercq, B.; Verpoort, F. *Adv. Synth. Catal.* **2002,** *344,* 639–648.
97. De Clercq, B.; Verpoort, F. *Tetrahedron Lett.* **2002,** *43,* 9101–9104. doi:10.1016/S0040-4039(02)02247-5
98. Vila, A. M. L.; Monsaert, S.; Drozdzak, R.; Wolowiec, S.; Verpoort, F. *Adv. Synth. Catal.* **2009,** *351,* 2689–2701. doi:10.1002/adsc.200900477

BEILSTEIN JOURNAL OF ORGANIC CHEMISTRY

Ru complexes of Hoveyda–Grubbs type immobilized on lamellar zeolites: activity in olefin metathesis reactions

Hynek Balcar*, Naděžda Žilková, Martin Kubů, Michal Mazur, Zdeněk Bastl and Jiří Čejka

Full Research Paper

Open Access

Address:
J. Heyrovský Institute of Physical Chemistry, Academy of Sciences of the Czech Republic, v.v. i. Dolejškova 2155/3, 182 23 Prague 8, Czech Republic

Email:
Hynek Balcar* - hynek.balcar@jh-inst.cas.cz

* Corresponding author

Keywords:
Hoveyda–Grubbs type catalyst; hybrid catalysts; lamellar zeolites; non-covalent immobilization; olefin metathesis

Beilstein J. Org. Chem. **2015,** *11,* 2087–2096.
doi:10.3762/bjoc.11.225

Received: 12 June 2015
Accepted: 13 October 2015
Published: 04 November 2015

This article is part of the Thematic Series "Progress in metathesis chemistry II".

Guest Editor: K. Grela

Abstract

Hoveyda–Grubbs type catalysts with cationic tags on NHC ligands were linker-free immobilized on the surface of lamellar zeolitic supports (MCM-22, MCM-56, MCM-36) and on mesoporous molecular sieves SBA-15. The activity of prepared hybrid catalysts was tested in olefin metathesis reactions: the activity in ring-closing metathesis of citronellene and *N*,*N*-diallyltrifluoroacetamide decreased in the order of support MCM-22 ≈ MCM-56 > SBA-15 > MCM-36; the hybrid catalyst based on SBA-15 was found the most active in self-metathesis of methyl oleate. All catalysts were reusable and exhibited low Ru leaching (<1% of Ru content). XPS analysis revealed that during immobilization ion exchange between Hoveyda–Grubbs type catalyst and zeolitic support occurred in the case of Cl^- counter anion; in contrast, PF_6^- counter anion underwent partial decomposition.

Introduction

Immobilization of Ru alkylidene complexes (Grubbs and Hoveyda–Grubbs type catalysts) on siliceous supports represents a successful way to highly active, selective, and reusable metathesis catalysts [1-4]. Mesoporous molecular sieves (MCM-41, MCM-48, SBA-15), with large BET areas and pore volumes, proved to be very suitable supports, due to easy attachment of bulky organometallic complexes onto silica surface ensuring rapid diffusion of reactants to the active catalytic sites [5-12]. Several strategies of immobilization have been developed [1,5,13]; most of them are based on surface modification by specially designed linkers providing covalent bond linkage between the support and Ru complex. Hoveyda–Grubbs type catalysts are also capable of direct (linker-free) immobilization by means of non-covalent interac-

tions [8,14-20]. Although the character of this interaction is not completely clear, they are firm enough to ensure low Ru leaching and catalyst reusability.

Recently, we reported Hoveyda–Grubbs type catalysts bearing quaternary ammonium tag on NHC ligand (HGIIN$^+$X, where X = Cl$^-$, I$^-$, PF_6^-, or BF_4^-) and their immobilization on silica, and mesoporous molecular sieves MCM-41 and SBA-15 [21]. XPS analysis revealed that complexes were attached to the surface by non-covalent interactions and both cationic and anionic parts were present on the surface. The hybrid catalysts prepared were active in RCM of 1,7-octadiene and (−)-β-citronellene; HGIIN$^+$Cl$^-$ on SBA-15 (HGIIN$^+$Cl$^-$/SBA-15) was the most active (TON up to 16000 in RCM of citronellene). HGIIN$^+$Cl$^-$/SBA-15 proved its versatility in RCM, enyne metathesis, metathesis of methyl oleate, and cross-metathesis of electron deficient methyl acrylate with various co-substrates. The catalyst was reusable and Ru leaching was very low, not only in toluene (Ru content in product <10 ppm in most cases) but also in polar solvents (ethyl acetate, dichloromethane, leaching about 1% of Ru content in catalyst). A similar ammonium-tagged Hoveyda–Grubbs type catalyst with sterically enlarged NHC ligand supported on SBA-15 exhibited high stability and was effective in flow reactions [22].

According to our knowledge, zeolites have not been considered as perspective supports for the immobilization of Ru metathesis catalysts due to small diameters of their pores (<1 nm) not allowing to anchor appropriate alkylidene complexes in the channel system and to ensure accessibility of catalytic centers by reactants. However, new methods for the preparation of lamellar (also called two-dimensional) zeolite with high surface area and layered structure have been developed [23] and such zeolites offer the possibility of their modifications with organometallic moieties in a similar way as mesoporous molecular sieves. Limbach et al. [20] used MWW material as a support for Ru heterogeneous catalyst for cyclooctene oligomerization, however, its activity was rather low. In this article we discuss the immobilization of HGIIN$^+$Cl$^-$ and HGIIN$^+$$PF_6^-$ (Figure 1) on zeolitic supports having MWW structure: MCM-22 (three-dimensional), MCM-56 (unilamellar), and MCM-36 (pillared) and the activity of corresponding catalysts (i) in RCM of (−)-β-citronellene and *N*,*N*-diallyl-2,2,2-trifluoroacetamide (DAF), and (ii) in self-metathesis and cross-metathesis of methyl oleate.

Lamellar (two dimensional) zeolites represent a subgroup of zeolitic materials, in which one of the dimension of the crystals is usually limited to 2–3 nm and is around one unit cell [24,25]. Depending on the structure of the prepared zeolite, the individual zeolitic layers exhibit or do not exhibit micropore character. Two dimensional zeolites are usually prepared by a bottom-up hydrothermal synthesis [26]; recently also a top-down approach from germanosilicate zeolite UTL was reported [27]. The latter approach utilizes chemically selective hydrolysis of Ge–O bonds to form layers from three-dimensional zeolites [28]. Generally, two-dimensional zeolites possess BET areas above 500–600 m^2/g, which is comparable with mesoporous molecular sieves. The surface of two-dimensional zeolites can be modified with various organic ligands to induce adsorption or catalytic functionalities [29,30]. The detailed structures of zeolites MCM-22, MCM-36 and MCM-56 used as supports in this work are depicted in [31,32].

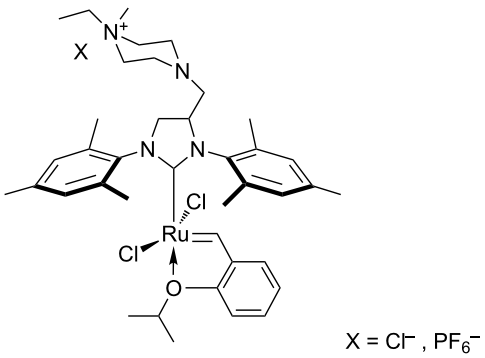

Figure 1: Hoveyda–Grubbs type catalysts used for immobilization.

Results and Discussion

Hybrid catalyst preparation and characterization

Immobilization of HGIIN$^+$X complexes proceeded smoothly by mixing their solutions with dry supports at room temperature. In the case of HGIIN$^+$Cl$^-$ and MCM-22, MCM-56, and SBA-15, the immobilization was nearly quantitative (97–99% of Ru was attached to the support, see Experimental). However, in other cases (HGIIN$^+$Cl$^-$ + MCM-36 and HGIIN$^+$$PF_6^-$ + MCM-22) only part of Ru submitted for immobilization was captured on the support under condition applied. In this way, hybrid catalysts HGIIN$^+$Cl$^-$/MCM-22 (1.1 wt % Ru), HGIIN$^+$Cl$^-$/MCM-56 (1.1 wt % Ru), HGIIN$^+$Cl$^-$/MCM-36 (0.7 wt % Ru), HGIIN$^+$$PF_6^-$/MCM-22 (0.9 wt % Ru), and HGIIN$^+$Cl$^-$/SBA-15 (1.2 wt % Ru) were prepared.

Table 1 shows textural parameters of zeolitic supports and corresponding hybrid catalysts. The attachment of Ru complex brought about a significant decrease in S_{BET} and pore volume. Especially, the micropore volume strongly decreased. Due to the molecular size of Hoveyda–Grubbs 2nd generation catalyst (1.76 × 1.35 × 1.05 nm [15]) the molecules of HGIIN$^+$Cl$^-$ cannot penetrate into micropores of MCM-22 or MCM-56 zeolites. The decrease in the micropore volume may suggest

that molecules of catalyst are located in the mouths of pores and block the access to the micropore system. X-ray diffraction patterns showed (Supporting Information File 1, Figures S1, S2, and S3) that original structure of the parent supports was preserved. As concerns $HGIIN^+Cl^-$/SBA-15, it was shown earlier [21] that the SBA-15 architecture was preserved; both S_{BET} and V values were reduced in comparison with the parent SBA-15 (from 739 m^2/g and 1.15 cm^3/g to 492 m^2/g and 0.92 cm^3/g, respectively) but the change in pore diameter was negligible (from 6.7 to 6.6 nm).

Table 1: Textural parameters of MCM-22, MCM-56, MCM-36, and corresponding hybrid catalysts.

Sample	S_{BET} (m^2/g)	S_{ext}[a] (m^2/g)	V_{mic}[b] (cm^3/g)	V_{total}[c] (cm^3/g)
MCM-22	504	121	0.174	0.429
$HGIIN^+Cl^-$/MCM-22	379	121	0.117	0.355
MCM-56	446	171	0.124	0.555
$HGIIN^+Cl^-$/MCM-56	157	119	0.015	0.324
MCM-36	658	564	0.041	0.364
$HGIIN^+Cl^-$/MCM-36	488	426	0.027	0.268

[a]External surface area, [b]micropore volume (*t*-plot method), [c]total pore volume at p/p_0 = 0.95, for evaluation of S_{BET}, the interval of p/p_0 = 0.05–0.20 was used.

The stoichiometry of the studied catalyst samples resulting from the XPS analysis is summarized in Table 2. A good agreement between the chemical composition of the neat compounds calculated from the integrated intensities of photoelectron spectra and their nominal stoichiometry was observed. For $HGIIN^+Cl^-$/SBA-15 the atomic ratio Cl/Ru = 3 indicates both cationic and anionic parts of the parent complex were present in the hybrid catalysts, as shown earlier [21]. In contrast to that, the atomic ratio Cl/Ru = 1.9 for $HGIIN^+Cl^-$/MCM-22 may indicate that Cl^- remained in a liquid phase as NaCl. For $HGIIN^+PF_6^-$/MCM-22 catalyst, the results suggest that reduction of the PF_6 anion to the PF_3 species took place in immobilized compound. In addition to it, the decrease in Cl/Ru atomic ratio to 1.3 (1.4) may indicate change in the number of Cl ligands in the coordination sphere of Ru (at least a part of catalyst molecules was affected). The low concentration of the Ru complex in $HGIIN^+PF_6^-$/MCM-22 did not allow obtaining any detailed information.

Catalyst activity in ring-closing metathesis

Hybrid catalysts were tested in ring-closing metathesis (RCM) of (−)-β-citronellene and *N*,*N*-diallyl-2,2,2-trifluoroacetamide (DAF) (Scheme 1). Figure 2 shows conversion curves of RCM of (−)-β-citronellene over $HGIIN^+Cl^-$/MCM-22, $HGIIN^+Cl^-$/MCM-56, $HGIIN^+Cl^-$/MCM-36, $HGIIN^+PF_6^-$/MCM-22, and

Table 2: Atomic concentration ratios of N, F, Cl, and P to Ru determined from XP spectra for neat $HGIIN^+X$ (X = Cl^-, PF_6^-) and hybrid catalysts $HGIIN^+Cl^-$/MCM-22, $HGIIN^+Cl^-$/SBA-15, and $HGIIN^+PF_6^-$/MCM-22. (For $HGIIN^+PF_6^-$/MCM-22 catalyst the results obtained on two independent sample preparations are displayed demonstrating the reproducibility.)

Sample	N	Cl	F	P
$HGIIN^+Cl^-$	4.2	3.0	0	0
$HGIIN^+Cl^-$/MCM-22	4.1	1.9	0	0
$HGIIN^+Cl^-$/SBA-15	4.0	3.0	0	0
$HGIIN^+PF_6^-$	3.8	1.8	6.2	1.0
$HGIIN^+PF_6^-$/MCM-22	4.2 4.0	1.3 1.4	2.9 3.2	1.2 0.85

$HGIIN^+Cl^-$/SBA-15 for comparison (data taken from ref [21] for the last catalyst). It is seen that the activities of $HGIIN^+Cl^-$/MCM-22, $HGIIN^+Cl^-$/MCM-56, and $HGIIN^+PF_6^-$/MCM-22 were rather similar but significantly higher than that of $HGIIN^+Cl^-$/SBA-15. The initial TOFs (calculated from conversion at 5 min) were 4800 h^{-1}, 5500 h^{-1}, and 2800 h^{-1} for $HGIIN^+Cl^-$/MCM-22, $HGIIN^+Cl^-$/MCM-56, and $HGIIN^+Cl^-$/SBA-15, respectively, and also the conversion after 300 min was higher for $HGIIN^+Cl^-$/MCM-22 and $HGIIN^+Cl^-$/MCM-56 (98% and 97%, respectively) than for $HGIIN^+Cl^-$/SBA-15 (81%). It demonstrates the superiority of both $HGIIN^+Cl^-$/MCM-22 and $HGIIN^+Cl^-$/MCM-56 catalysts in this reaction, originating probably from a better accessibility of catalytic centers. The conversion curve for $HGIIN^+PF_6^-$/MCM-22 was close to that for $HGIIN^+Cl^-$/MCM-22, in spite of changes of $HGIIN^+PF_6^-$ structure in the course of immobilization as indicated by XPS. Surprisingly, conversions achieved with $HGIIN^+Cl^-$/MCM-36 were lower than those achieved with $HGIIN^+Cl^-$/MCM-22 and even with $HGIIN^+Cl^-$/SBA-15, despite the pillared character of the MCM-36 support. Selectivity was 100% in all cases: only methylcyclopentene and isobutene were found as reaction products by GC–MS. Enantioselectivity was not established.

Similar dependence of catalytic activity on the type of support was found for RCM of DAF (Figure 3). The initial TOFs (calculated from conversion at 5 min) decreased in the order: $HGIIN^+Cl^-$/MCM-22 (1770 h^{-1}) > $HGIIN^+Cl^-$/MCM-56 (1440 h^{-1}) > $HGIIN^+Cl^-$/SBA-15 (990 h^{-1}) ≥ $HGIIN^+Cl^-$/MCM-36 (900 h^{-1}). Final conversions (at 180 min) were in the interval from 96% to 99%. Similarly as for RCM of (−)-β-citronellene, hybrid catalysts $HGIIN^+Cl^-$/MCM-22 and $HGIIN^+Cl^-$/MCM-56 exhibited a higher activity than $HGIIN^+Cl^-$/SBA-15. Although initial TOF for $HGIIN^+Cl^-$/SBA-15 and for $HGIIN^+Cl^-$/MCM-36 were close to each other; further progress of conversion curves indicated lower activity of $HGIIN^+Cl^-$/MCM-36 in comparison with $HGIIN^+Cl^-$/SBA-15.

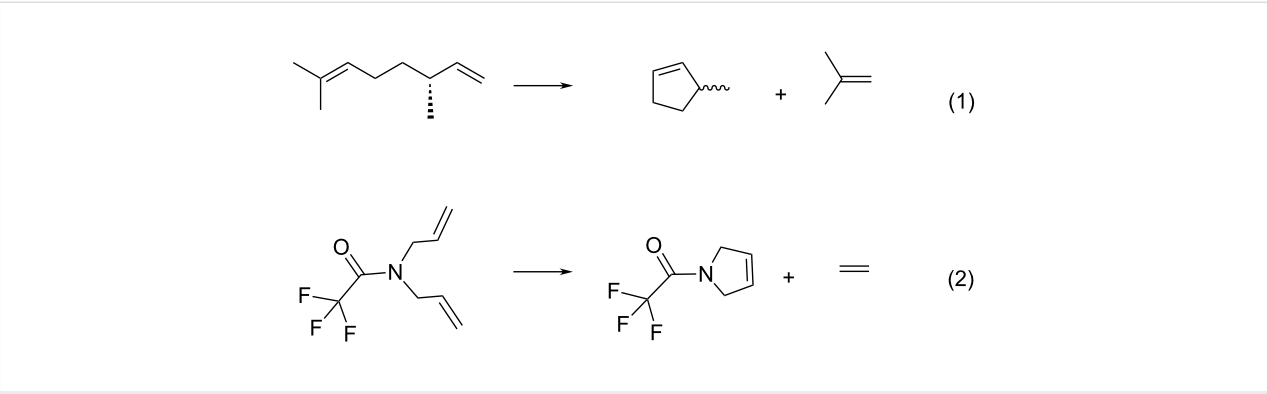

Scheme 1: RCM of (−)-β-citronellene (1) and *N*,*N*-diallyl-2,2,2-trifluoroacetamide (2).

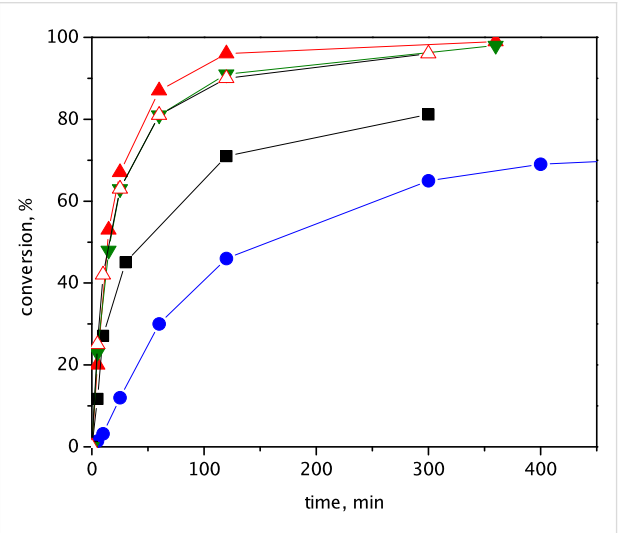

Figure 2: Conversion vs time dependence for RCM of (−)-β-citronellene over HGIIN$^+$Cl$^-$/MCM-36 (●), HGIIN$^+$Cl$^-$/SBA-15 (■), HGIIN$^+$Cl$^-$/MCM-22 (▲), HGIIN$^+$PF$_6^-$/MCM-22 (Δ), and HGIIN$^+$Cl$^-$/MCM-56 (▼). Toluene, 60 °C, molar ratio (−)-β-citronellene/Ru = 2000, c_{citr} = 0.15 mol/L.

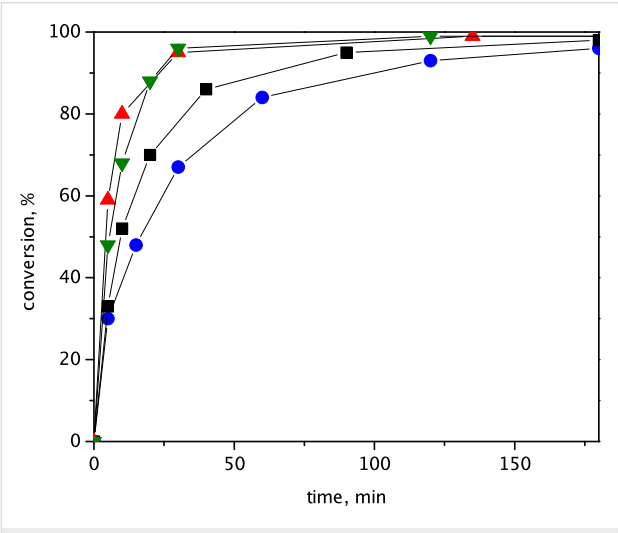

Figure 3: Conversion vs. time dependences for RCM of DAF over catalysts HGIIN$^+$Cl$^-$/MCM-22 (▲), HGIIN$^+$Cl$^-$/MCM-56 (▼), HGIIN$^+$Cl$^-$/SBA-15 (■), and HGIIN$^+$Cl$^-$/MCM-36 (●). Toluene, 30 °C, molar ratio DAF/Ru = 250, c_{DAF} = 0.15 mol/L.

The selectivity to *N*-(2-trifluoroacetyl)-2,5-dihydropyrrole was 100%.

Catalyst leaching and reusing were studied in RCM of (−)-β-citronellene. Figure 4 shows a splitting test [33] for HGIIN$^+$Cl$^-$/MCM-56. 10 min after the beginning of the reaction, a half of the liquid phase was filtered off into a parallel reactor further kept under the same reaction temperature. Metathesis reaction continued in the heterogeneous system only, which evidences no leaching of catalytically active species into the liquid phase. Ru leaching determined by elemental analysis in the reaction mixture after finishing the reaction was 0.3%, 0.1%, and 0.6% of starting amount of Ru in catalyst for HGIIN$^+$Cl$^-$/MCM-22, HGIIN$^+$Cl$^-$/MCM-56, and HGIIN$^+$Cl$^-$/MCM-36, respectively. These values correspond to 1.2, 0.4, and 2.2 ppm of Ru in the products, which is considerably lower than the Ru content in drugs recommended by the European Medicines Agency in 2007 (10 ppm for oral exposure) [34].

Results of HGIIN$^+$Cl$^-$/MCM-22 reusing are displayed in Table 3. The catalyst was used 5 times without any decrease in the conversion. Due to the very low Ru leaching level (only 0.3% of the original amount of Ru was found in the combined samples from runs 1 to 5), the conversion drop after the fifth run must be ascribed to the catalyst deactivation. The cumulative TON achieved in 7 runs was 1491. The results evidence very firm attachment of catalytically active species to the surface of zeolites and their good stability.

Catalyst activity in self-metathesis and cross-metathesis of methyl oleate

Conversion curves for self-metathesis of methyl oleate over hybrid catalysts HGIIN$^+$Cl$^-$/MCM-22, HGIIN$^+$Cl$^-$/MCM-56,

Table 3: HGIIN$^+$Cl$^-$/MCM-22 reusing in RCM of (−)-β-citronellene. Toluene, 60 °C, molar ratio (−)-β-citronellene/Ru = 1:250, c_{citr} = 0.15 mol/L, reaction time 2.5 h.

Run	1	2	3	4	5	6	7
Conversion	99.5%	99.5%	99.5%	99.5%	99.5%	72.5%	26.5%
Cumulative TON	249	498	746	995	1244	1425	1491

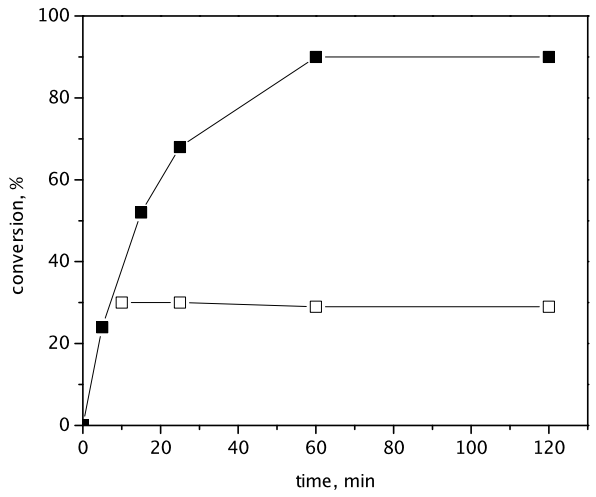

Figure 4: Splitting test for HGIIN$^+$Cl$^-$/MCM-56 in RCM of (−)-β-citronellene. Toluene, 60 °C, molar ratio (−)-β-citronellene/Ru = 2000, c_{citr} = 0.15 mol/L. Heterogeneous system (■), filtrate (□).

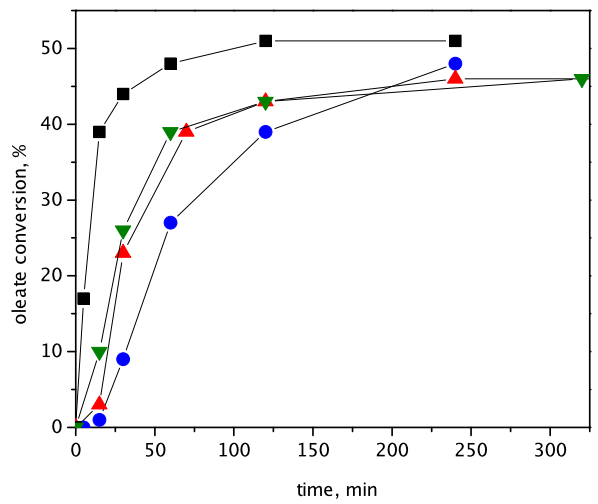

Figure 5: Self-metathesis of methyl oleate over HGIIN$^+$Cl$^-$/SBA-15 (■), HGIIN$^+$Cl$^-$/MCM-22 (▲), HGIIN$^+$Cl$^-$/MCM-56 (▼), and HGIIN$^+$Cl$^-$/MCM-36 (●). Toluene, 60 °C, molar ratio oleate/Ru = 250, c_{ol} = 0.15 mol/L.

HGIIN$^+$Cl$^-$/MCM-36, and HGIIN$^+$Cl$^-$/SBA-15 in toluene at 60 °C are depicted in Figure 5. In contrast to RCM of (−)-β-citronellene and RCM of DAF, HGIIN$^+$Cl$^-$/SBA-15 turned out to be the most active catalyst. The catalytic activity decreased in the order HGIIN$^+$Cl$^-$/SBA-15 > HGIIN$^+$Cl$^-$/MCM-56 ≈ HGIIN$^+$Cl$^-$/MCM-22 > HGIIN$^+$Cl$^-$/MCM-36. Moreover, conversion curves for catalysts supported on zeolites exhibited an induction period repeatedly (very distinct for HGIIN$^+$Cl$^-$/MCM-22 and HGIIN$^+$Cl$^-$/MCM-36). This induction period became even more pronounced when the reaction temperature decreased to 30 °C and the activity gap between HGIIN$^+$Cl$^-$/SBA-15 on one side and HGIIN$^+$Cl$^-$/MCM-22 and HGIIN$^+$Cl$^-$/MCM-56 on the other side strongly increased (Supporting Information File 1, Figure S4). With HGIIN$^+$Cl$^-$ as a homogeneous catalyst no induction period was discernable at 60 °C (see [21]), however, the conversion curve at 30 °C (Supporting Information File 1, Figure S4) suggests a short induction period similar to the reaction with HGIIN$^+$Cl$^-$/SBA-15. In all cases, octadecene and dimethyl octadecendioate were the only reaction products.

In order to elucidate the origin of the above mentioned difference in activity of HGIIN$^+$Cl$^-$/SBA-15 and HGIIN$^+$Cl$^-$/MCM-22, we performed a study of cross-metathesis (CM) of methyl oleate and *cis*-3-hexenyl acetate (Scheme 2) over these two catalysts. *cis*-3-Hexenyl acetate can be considered as a short-chain analogue of methyl oleate. Over both HGIIN$^+$Cl$^-$/SBA-15 and HGIIN$^+$Cl$^-$/MCM-22 in toluene at 30 °C, *cis*-3-hexenyl acetate reacted quickly, without any induction period, and with 100% selectivity to 3-hexene and 1,6-diacetoxy-3-hexene. The differences in the reaction rates for both catalysts were marginal (Figure S5, Supporting Information File 1). Splitting test for self-metathesis of *cis*-3-hexenyl acetate over HGIIN$^+$Cl$^-$/MCM-22 (Figure S6, Supporting Information File 1) evidenced no leaching of catalytically active species into the liquid phase, similarly to RCM of (−)-β-citronellene over HGIIN$^+$Cl$^-$/MCM-56. Figure 6 shows conversion curves for CM of methyl oleate with cis-3-hexenyl acetate (molar ratio 1:1) over both HGIIN$^+$Cl$^-$/MCM-22 and HGIIN$^+$Cl$^-$/SBA-15 together with conversion curves for self-metatheses of methyl oleate and *cis*-3-hexenyl acetate over HGIIN$^+$Cl$^-$/MCM-22. The induction period characteristic for self-metathesis of methyl oleate over HGIIN$^+$Cl$^-$/MCM-22 was minimized in CM to about 5 min for both catalysts. The reaction proceeded more quickly over HGIIN$^+$Cl$^-$/MCM-22 than over HGIIN$^+$Cl$^-$/

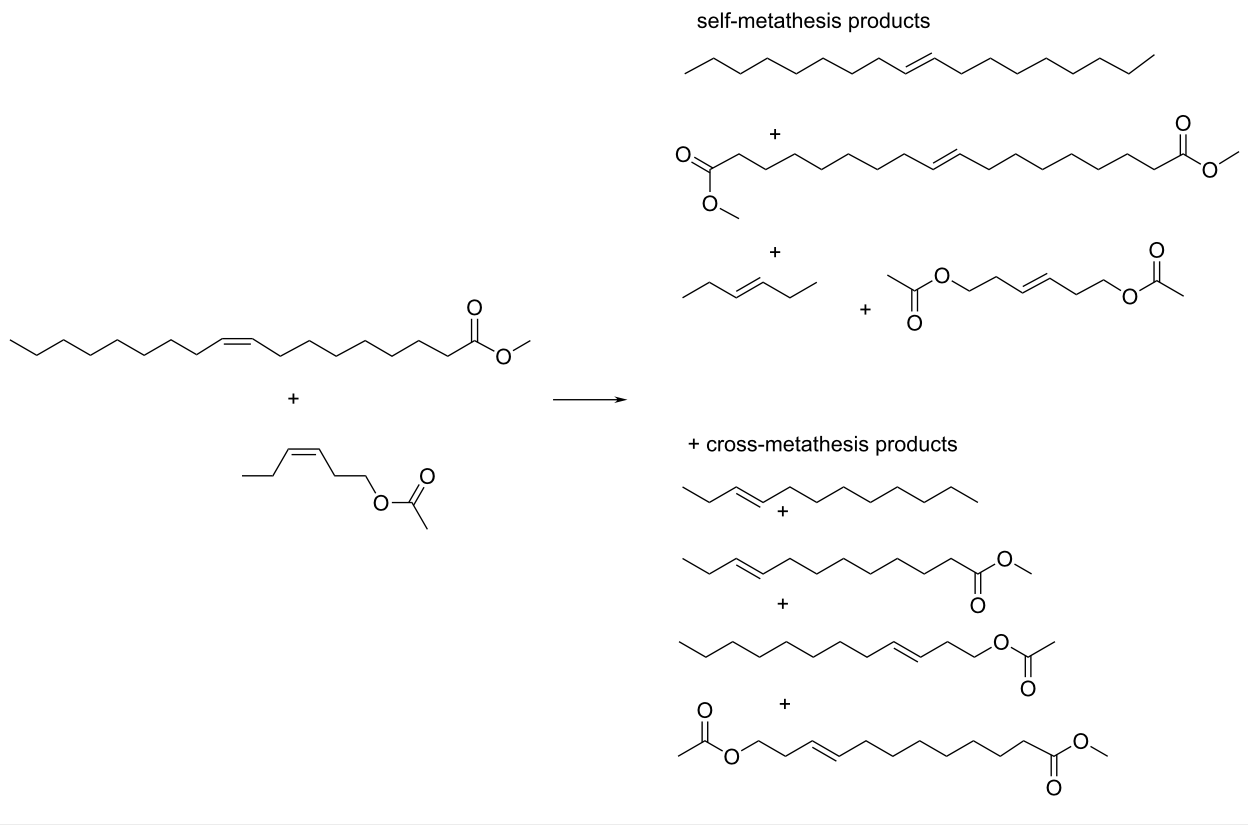

Scheme 2: Cross-metathesis of methyl oleate with *cis*-3-hexenyl acetate.

SBA-15 (cf. 31% conversion of methyl oleate at 25 min over HGIIN$^+$Cl$^-$/MCM-22 vs 25% methyl oleate conversion at 30 min over HGIIN$^+$Cl$^-$/SBA-15). At the beginning of the reaction, the consumption of *cis*-3-hexenyl acetate prevailed over that of methyl oleate, however, approaching the equilibrium, the consumptions of both reactants were practically the same. In equilibrium, about 75% of both reactants were consumed. About 23% of both methyl oleate and cis-3-hexenyl acetate were converted to the self-metathesis products (9-octadecene and 3-hexene were used for GC determination, data not given in Figure 6). The rest (52%) was converted to the cross-metathesis products according to Scheme 2. It indicates the system approached statistical cross-metathesis, in accord with the characters of both reactants (classes of reactants in CM according to Grubbs [35]).

The data presented indicated that the depressed activity of HGIIN$^+$Cl$^-$/MCM-22 in the self-metathesis of methyl oleate was not connected with a slow diffusion of the reactant to the active centers, but most probably with the slow initiation rate. If initiation starts by coordination of the substrate molecule to the Ru atom (association and interchange mechanism [36]), the steric conditions around the Ru atom may be important. The very low initiation rate with methyl oleate may implicate some restrictions in coordination of bulky molecules; we can speculate about some confinement in the coordination sphere of Ru in HGIIN$^+$Cl$^-$/MCM-22 (partial immersion of HGIIN$^+$Cl$^-$ into

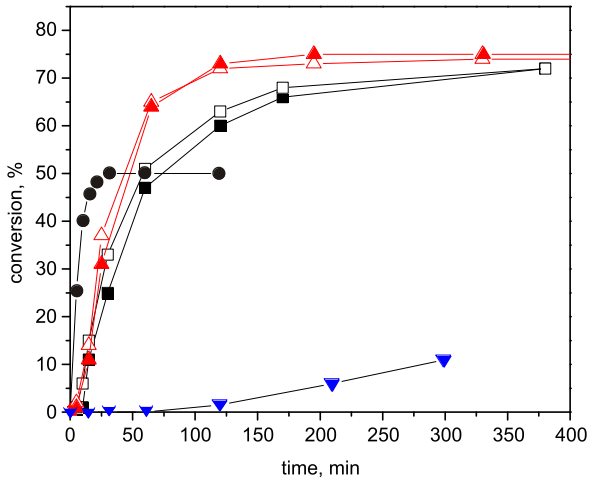

Figure 6: Conversion curves for CM of methyl oleate (full symbols) with *cis*-3-hexenyl acetate (open symbols) over HGIIN$^+$Cl$^-$/MCM-22 (▲,△), and HGIIN$^+$Cl$^-$/SBA-15 (■,□) and for self-metathesis of oleate (▼) and self-metathesis of cis-3-hexenyl acetate (●) both with HGIIN$^+$Cl$^-$/MCM-22. Toluene, 30 °C, molar ratio methyl oleate/*cis*-3-hexenyl acetate/Ru = 250/250/1, c_{ol} = c_{ac} = 0.15 mol/L.

support cavities and/or other deformation of the coordination sphere as a result of immobilization). When the initiation passed with *cis*-3-hexenyl acetate, the created catalytically active centers were able to ensure rapid propagation regardless the kind of substrate molecules.

Conclusion

Hoveyda–Grubbs type metathesis catalysts with quaternary ammonium tags on NHC ligands HGIIN$^+$Cl$^-$ and HGIIN$^+$PF$_6^-$ were immobilized on lamellar zeolites MCM-22, MCM-56, and MCM-36. Linker-free immobilizations, consisting in mixing zeolite supports with catalyst solutions and stirring the corresponding suspensions at room temperature, were successfully used. Hybrid catalysts formed (Ru content from 0.7 to 1.1 wt %) exhibited a firm attachment of Ru species to the support and high stability, which was manifested by a very low Ru leaching (from 0.1 to 0.6% of original Ru content) and possibility of catalyst reusing (five times with 99.5% conversion).

The surface stoichiometry determined from XPS indicated an ion exchange between zeolite supports (Na forms) and the Hoveyda–Grubbs type catalysts. In the case of HGIIN$^+$Cl$^-$, the unchanged cationic part of the Ru complex was suggested to be present in the hybrid catalyst and the counter anion, Cl$^-$, was suggested to remain in the liquid phase as NaCl; however, in the case of HGIIN$^+$PF$_6^-$, partial decomposition of the PF$_6^-$ anion and ligand exchange at the Ru atom most likely accompanied the immobilization. The XRD and nitrogen adsorption measurements confirmed that the layered structure of the supports was preserved in the prepared hybrid catalysts.

The activity of hybrid catalysts was studied (i) in RCM of (−)-β-citronellene and *N*,*N*-diallyl-2,2,2-trifluoroacetamide, and (ii) in self-metathesis and cross-metathesis of methyl oleate. The activity was compared with that of HGIIN$^+$Cl$^-$ linker-free immobilized on mesoporous molecular sieves SBA-15 (HGIIN$^+$Cl$^-$/SBA-15, pore diameter 6.6 nm). In RCM reactions, the activity decreased in the following order of support MCM-22 ≈ MCM-56 > SBA-15 > MCM-36. The layered structure of MCM-22 and MCM-56 most likely ensured better access of the reactants to the catalytically active centers as compared to the case of the SBA-15 based hybrid catalyst. In self-metathesis of methyl oleate, HGIIN$^+$Cl$^-$/SBA-15 was found to be the most active; the reaction over HGIIN$^+$Cl$^-$ on zeolite supports proceeded slowly and with a large induction period. In contrast to that, in the cross-metathesis of methyl oleate with *cis*-3-hexenyl acetate over HGIIN$^+$Cl$^-$/MCM-22, the induction period was negligible and the reaction rate slightly exceeded that over HGIIN$^+$Cl$^-$/SBA-15. This behavior may indicate a slow initiation by methyl oleate due to its slow coordination to the Hoveyda–Grubbs type catalysts immobilized on the zeolite supports studied.

Experimental

Materials and techniques

Ru alkylidene complexes HGIIN$^+$Cl$^-$ and HGIIN$^+$PF$_6^-$ were kindly provided by Krzysztof Skowerski (Apeiron Synthesis, Wroclaw, Poland). Zeolites MCM-22, MCM-56 and MCM-36 (Na forms) were prepared according to literature [37-39] as well as mesoporous molecular sieves SBA-15 [40]. Individual supports were calcined under following conditions: MCM-22, MCM-56 in a stream of nitrogen at 482 °C for 3 h (heating rate 1 °C/min) and further after cooling down to 100 °C under air at 540 °C for 8 h with a heating rate 1 °C/min; MCM-36 under air at 540 °C for 6 h with a heating rate 2 °C/min; SBA-15 in air at 550 °C for 6 h (heating rate 1 °C/min).

Toluene (Lach-Ner) was dried for 12 h over anhydrous Na_2SO_4, then distilled with Na, and stored over molecular sieves type 4 Å. Dichloromethane (Lach-Ner) was dried overnight over anhydrous $CaCl_2$ then distilled with CaH_2. (−)-β-citronellene (Aldrich, purity of ≥90%), *N*,*N*-diallyl-2,2,2-trifluoroacetamide (Aldrich, 98%), *cis*-3-hexenyl acetate (Aldrich, purity ≥98%), and methyl oleate (Research Institute of Inorganic Chemistry, a.s., Czech Rep., purity of 94%, with methyl palmitate, methyl stearate, and methyl linolate being the main impurities) were used after being passed through a column filled with activated alumina.

Nitrogen adsorption/desorption isotherms were measured on a Micromeritics GEMINI II 2370 volumetric Surface Area Analyzer at liquid nitrogen temperature (−196 °C) to determine the surface area and pore volume. Prior to the sorption measurements, all samples were degassed on a Micromeritics FlowPrep060 instrument under helium at 110 °C for 6 h. X-ray powder diffraction (XRD) data were obtained on a Bruker AXS D8 Advance diffractometer with a graphite monochromator and a Vantec-1 position sensitive detector using Cu Kα radiation (at 40 kV and 30 mA) in Bragg−Brentano geometry.

The X-ray photoelectron spectra (XPS) of the samples were measured using a modified ESCA 3 MkII multitechnique spectrometer equipped with a hemispherical electron analyzer operated in a fixed transmission mode. Al Kα radiation (1486.6 eV) was used for electron excitation. The binding energy scale of the spectrometers was calibrated using the Au $4f_{7/2}$ (84.0 eV) and Cu $2p_{3/2}$ (932.6 eV) photoemission lines. The pressure of residual gases in the analysis chamber during spectra acquisition was 6×10^{-9} mbar. The powder samples were spread on an aluminum surface. The spectra were measured at room temperature and collected at a detection angle of 45° with respect to the

macroscopic sample surface plane. Survey scan spectra and high-resolution spectra of overlapping Ru 3d + C 1s photoelectrons, and N 1s, Cl 2p, P 2s, and F 1s photoelectrons were measured. The spectra were curve-fitted after subtraction of the Shirley background [41] using the Gaussian−Lorentzian line shape and the damped nonlinear least-squares algorithms (software XPSPEAK 4.1) [42]. The quantification of elemental concentrations was accomplished by correcting integrated intensities of photoelectron peaks for the transmission function of the electron analyzer and the pertinent photoionization cross sections [43]. In the calculations, a homogeneous composition of the analyzed layer of the measured samples was assumed. The typical error for the quantitative analysis by XPS was approximately 10% [44].

The determination of the ruthenium content was performed by inductively coupled plasma mass spectrometry (ICP–MS) by the Institute of Analytical Chemistry (ICT, Prague, Czech Republic).

Catalyst preparation

Immobilization of $HGIIN^+X^-$ complexes was performed by stirring a mixture of complex and support in CH_2Cl_2 at room temperature (3 h) under argon atmosphere. Details are given elsewhere [21]. For immobilization, calcined (dehydrated) supports (300 °C, 3 h) were used. The amount of support, Ru complex submitted and Ru content in hybrid catalyst are given in Table 4. Catalyst prepared by immobilization of $HGIIN^+Cl^-$ on MCM-22 was labelled as $HGIIN^+Cl^-$/MCM-22; other catalysts were labelled in a similar way.

Testing of catalyst activity

Metathesis reactions were performed under Ar atmosphere in Schlenk tubes equipped with magnetic stirring bars. In a typical RCM experiment the amount of catalyst corresponding to 1 μmol of Ru was put into the reactor, then toluene (13 mL) was added and the suspension was heated to 60 °C. The reaction was started by addition of (−)-β-citronellene (2 mmol) under stirring (900 rpm). At given time intervals, samples (0.1 mL) were taken and quenched with ethyl vinyl ether, and after centrifugation, the supernatants were analyzed by gas chromatography (GC). In the cross-metathesis experiment, a mixture of methyl oleate (0.25 mmol) and *cis*-3-hexenyl acetate (0.25 mmol) was added to the suspension of catalyst (1 μmol of Ru) in toluene (1.7 mL) at 30 °C under stirring. The sampling, quenching and analysis steps were performed similarly as for RCM of (−)-β-citronellene.

A high-resolution gas chromatograph (Agilent model 6890) with a DB-5 column (length of 50 m, inner diameter of 320 μm, stationary phase thickness of 1 μm) equipped with FID detector was used for reaction product analysis. Temperature programs were: (i) from 80 °C to 260 °C with ramp 20 °C/min for (−)-β-citronellene products, and (ii) from 80 °C to 325 °C with ramps 5 °C and 20°C for methyl oleate and DAF products. Retention times (in min) were 8.63 (citronellene), 4.88 (methylcyclopentene), 19.3 (DAF), 19.7 (*N*-(2-trifluoroacetyl)-2,5-dihydropyrrole), 41.3 (methyl oleate), 33.9 (octadecene), and 57.5 (diester). *n*-Nonane was used as an internal standard, whenever required. Individual products (all are known compounds) were identified by gas chromatography and mass spectrometry (GC−MS) (ThermoFinnigan, FOCUS DSQ II Single Quadrupole). The absolute error in the determination of conversion was ±2%.

Supporting Information

Supporting Information File 1

XRD patterns of catalysts and supports, conversion curves for self-metatheses of methyl oleate and *cis*-3-hexenyl acetate, splitting experiment.
[http://www.beilstein-journals.org/bjoc/content/supplementary/1860-5397-11-225-S1.pdf]

Table 4: Amounts of support and $HGIIN^+X$ used for preparation of hybrid catalysts.

Catalyst	Weight of support (mg)	Weight of $HGIIN^+X^-$ (mg)	Ru content in catalyst (wt %)	f [a]
$HGIIN^+Cl^-$/MCM-22	250	23.9	1.1	0.97
$HGIIN^+PF_6^-$/MCM-22	140	17.8	0.9	0.66
$HGIIN^+Cl^-$/MCM-56	305	30.2	1.1	0.99
$HGIIN^+Cl^-$/MCM-36	835	87.0	0.7	0.54
$HGIIN^+Cl^-$/SBA-15	339	36.5	1.2	0.99

[a] f = fraction of Ru attached to the support.

Acknowledgements

The authors thank K. Skowerski (Apeiron Synthesis, Wroclaw, Poland) for the samples of Ru catalysts and M. Horáček (J. Heyrovský Institute, Prague) for GC–MS analysis. Financial support from Grant Agency of the Czech Republic (P106/12/0189) is gratefully acknowledged.

References

1. Buchmeiser, M. R. *Chem. Rev.* **2009,** *109,* 303–321. doi:10.1021/cr800207n
2. Copéret, C.; Basset, J.-M. *Adv. Synth. Catal.* **2007,** *349,* 78–92. doi:10.1002/adsc.200600443
3. Balcar, H.; Roth, W. J. Hybrid Catalysts for Olefin Metathesis and Related Polymerizations. In *New and Future Developments in Catalysis. Hybrid Materials, Composites, and Organocatalysts;* Suib, S. L., Ed.; Elsevier: Amsterdam, The Netherlands, 2013; pp 1–26. doi:10.1016/B978-0-444-53876-5.00001-5
4. Buchmeiser, M. R. Immobilization of Olefin Metathesis Catalysts. In *Olefin Metathesis, Theory and Practice;* Grela, K., Ed.; John Wiley & Sons, Inc.: Hoboken, NJ, USA, 2014. doi:10.1002/9781118711613.ch20
5. Balcar, H.; Čejka, J. *Coord. Chem. Rev.* **2013,** *257,* 3107–3124. doi:10.1016/j.ccr.2013.07.026
6. Bek, D.; Balcar, H.; Žilková, N.; Zukal, A.; Horáček, M.; Čejka, J. *ACS Catal.* **2011,** *1,* 709–718. doi:10.1021/cs200090e
7. Pastva, J.; Čejka, J.; Žilková, N.; Mestek, O.; Rangus, M.; Balcar, H. *J. Mol. Catal. A: Chem.* **2013,** *378,* 184–192. doi:10.1016/j.molcata.2013.06.006
8. Shinde, T.; Varga, V.; Polášek, M.; Horáček, M.; Žilková, N.; Balcar, H. *Appl. Catal., A* **2014,** *478,* 138–145. doi:10.1016/j.apcata.2014.03.036
9. Drozdzak, R.; Allaert, B.; Ledoux, N.; Dragutan, I.; Dragutan, V.; Verpoort, F. *Coord. Chem. Rev.* **2005,** *249,* 3055–3074. doi:10.1016/j.ccr.2005.05.003
10. Zhang, H.; Li, Y.; Shao, S.; Wu, H.; Wu, P. *J. Mol. Catal. A: Chem.* **2013,** *372,* 35–43. doi:10.1016/j.molcata.2013.01.034
11. Li, L.; Shi, J.-l. *Adv. Synth. Catal.* **2005,** *347,* 1745–1749. doi:10.1002/adsc.200505066
12. Elias, X.; Pleixats, R.; Man, M. W. C. *Tetrahedron* **2008,** *64,* 6770–6781. doi:10.1016/j.tet.2008.04.113
13. Dragutan, I.; Dragutan, V. *Platinum Met. Rev.* **2008,** *52,* 71–82. doi:10.1595/147106708X297477
14. Van Berlo, B.; Houthoofd, K.; Sels, B. F.; Jacobs, P. A. *Adv. Synth. Catal.* **2008,** *350,* 1949–1953. doi:10.1002/adsc.200800211
15. Yang, H.; Ma, Z.; Wang, Y.; Wang, Y.; Fang, L. *Chem. Commun.* **2010,** *46,* 8659–8661. doi:10.1039/c0cc03227a
16. Balcar, H.; Shinde, T.; Žilková, N.; Bastl, Z. *Beilstein J. Org. Chem.* **2011,** *7,* 22–28. doi:10.3762/bjoc.7.4
17. Schachner, J. A.; Cabrera, J.; Padilla, R.; Fischer, C.; van der Schaaf, P. A.; Pretot, R.; Rominger, F.; Limbach, M. *ACS Catal.* **2011,** *1,* 872–876. doi:10.1021/cs2002109
18. Cabrera, J.; Padilla, R.; Bru, M.; Lindner, R.; Kageyama, T.; Wilckens, K.; Balof, S. L.; Schanz, H.-J.; Dehn, R.; Teles, J. H.; Deuerlein, S.; Müller, K.; Rominger, F.; Limbach, M. *Chem. – Eur. J.* **2012,** *18,* 14717–14724. doi:10.1002/chem.201202248
19. Cabrera, J.; Padilla, R.; Dehn, R.; Deuerlein, S.; Gułajski, Ł.; Chomiszczak, E.; Teles, J. H.; Limbach, M.; Grela, K. *Adv. Synth. Catal.* **2012,** *354,* 1043–1051. doi:10.1002/adsc.201100863
20. Bru, M.; Dehn, R.; Teles, J. H.; Deuerlein, S.; Danz, M.; Müller, I. B.; Limbach, M. *Chem. – Eur. J.* **2013,** *19,* 11661–11671. doi:10.1002/chem.201203893
21. Pastva, J.; Skowerski, K.; Czarnocki, S. J.; Žilková, N.; Čejka, J.; Bastl, Z.; Balcar, H. *ACS Catal.* **2014,** *4,* 3227–3236. doi:10.1021/cs500796u
22. Skowerski, K.; Pastva, J.; Czarnocki, S. J.; Janoscova, J. *Org. Process Res. Dev.* **2015,** *19,* 872–877. doi:10.1021/acs.oprd.5b00132
23. Roth, W. J.; Nachtigall, P.; Morris, R. E.; Čejka, J. *Chem. Rev.* **2014,** *114,* 4807–4837. doi:10.1021/cr400600f
24. Choi, M.; Na, K.; Kim, J.; Sakamoto, Y.; Terasaki, O.; Ryoo, R. *Nature* **2009,** *461,* 246–249. doi:10.1038/nature08288
25. Eliášová, P.; Opanasenko, M.; Wheatley, P. S.; Shamzhy, M.; Mazur, M.; Nachtigall, P.; Roth, W. J.; Morris, R. E.; Čejka, J. *Chem. Soc. Rev.* **2015,** *44,* 7177–7206. doi:10.1039/c5cs00045a
26. Roth, W. J.; Čejka, J. *Catal. Sci. Technol.* **2011,** *1,* 43–53. doi:10.1039/c0cy00027b
27. Roth, W. J.; Nachtigall, P.; Morris, R. E.; Wheatley, P. S.; Seymour, V. R.; Ashbrook, S. E.; Chlubná, P.; Grajciar, L.; Položij, M.; Zukal, A.; Shvets, O.; Čejka, J. *Nat. Chem.* **2013,** *5,* 628–633. doi:10.1038/nchem.1662
28. Morris, R. E.; Čejka, J. *Nat. Chem.* **2015,** *7,* 381–388. doi:10.1038/nchem.2222
29. Zukal, A.; Dominguez, I.; Mayerová, J.; Čejka, J. *Langmuir* **2009,** *25,* 10314–10321. doi:10.1021/la901156z
30. Opanasenko, M.; Štěpnička, P.; Čejka, J. *RSC Adv.* **2014,** *4,* 65137–65162. doi:10.1039/C4RA11963K
31. Juttu, G. G.; Lobo, R. F. *Microporous Mesoporous Mater.* **2000,** *40,* 9–23. doi:10.1016/S1387-1811(00)00233-X
32. Díaz, U.; Corma, A. *Dalton Trans.* **2014,** *43,* 10292–10316. doi:10.1039/c3dt53181c
33. Phan, N. T. S.; Van Der Sluys, M.; Jones, C. W. *Adv. Synth. Catal.* **2006,** *348,* 609–679. doi:10.1002/adsc.200505473
34. European Medicines Agency, Pre-authorisation Evaluation of Medicines for Human Use, Guideline on the specification limits for residues on metal catalyst. London, January 2007.
35. Chatterjee, A. K.; Choi, T.-L.; Sanders, D. P.; Grubbs, R. H. *J. Am. Chem. Soc.* **2003,** *125,* 11360–11370. doi:10.1021/ja0214882
36. Nelson, D. J.; Manzini, S.; Urbina-Blanco, C. A.; Nolan, S. P. *Chem. Commun.* **2014,** *50,* 10355–10375. doi:10.1039/C4CC02515F
37. Kresge, C. T.; Roth, W. J.; Simmons, K. G.; Vartuli, J. C. Crystalline Oxide Material. U.S. Patent 5,229,341, June 20, 1993.
38. Fung, A. S.; Lawton, S. L.; Roth, W. J. Synthetic Layered MCM-56, Its Synthesis And Use. U.S. Patent 5,362,697, Nov 8, 1994.
39. Roth, W. J.; Kresge, C. T.; Vartuli, J. C.; Leonowicz, M. E.; Fung, A. S.; McCullen, S. B. *Stud. Surf. Sci. Catal.* **1995,** *94,* 301–308. doi:10.1016/S0167-2991(06)81236-X
40. Topka, P.; Balcar, H.; Rathouský, J.; Žilková, N.; Verpoort, F.; Čejka, J. *Microporous Mesoporous Mater.* **2006,** *96,* 44–54. doi:10.1016/j.micromeso.2006.06.016
41. Shirley, D. A. *Phys. Rev. B* **1972,** *5,* 4709–4714. doi:10.1103/PhysRevB.5.4709
42. Kwok, R. W. M.: Dept. of Chemistry, Chinese University of Hong Kong, Shatin, Hong Kong, http://www.uksaf.org/xpspeak41.zip. A freeware program.

43. Scofield, J. H. *J. Electron Spectrosc. Relat. Phenom.* **1976,** *8,* 129–137. doi:10.1016/0368-2048(76)80015-1
44. Briggs, D. J.; Grant, T., Eds. *Surface Analysis by Auger and X-Ray Photoelectron Spectroscopy;* Cromwell Press: Trowbridge, 2003.

BEILSTEIN JOURNAL OF ORGANIC CHEMISTRY

Computational study of productive and non-productive cycles in fluoroalkene metathesis

Markéta Rybáčková, Jan Hošek, Ondřej Šimůnek, Viola Kolaříková and Jaroslav Kvíčala*

Full Research Paper

Open Access

Address:
Department of Organic Chemistry, University of Chemistry and Technology, Technická 5, 166 28 Prague 6, Czech Republic

Email:
Jaroslav Kvíčala* - kvicalaj@vscht.cz

* Corresponding author

Keywords:
alkene metathesis; computation; DFT; fluoroalkene; mechanism; non-productive cycle; productive cycle

Beilstein J. Org. Chem. **2015,** *11,* 2150–2157.
doi:10.3762/bjoc.11.232

Received: 03 July 2015
Accepted: 20 October 2015
Published: 10 November 2015

This article is part of the Thematic Series "Progress in metathesis chemistry II".

Guest Editor: K. Grela

Abstract

A detailed DFT study of the mechanism of metathesis of fluoroethene, 1-fluoroethene, 1,1-difluoroethene, *cis*- and *trans*-1,2-difluoroethene, tetrafluoroethene and chlorotrifluoroethene catalysed with the Hoveyda–Grubbs 2nd generation catalyst was performed. It revealed that a successful metathesis of hydrofluoroethenes is hampered by a high preference for a non-productive catalytic cycle proceeding through a ruthenacyclobutane intermediate bearing fluorines in positions 2 and 4. Moreover, the calculations showed that the cross-metathesis of perfluoro- or perhaloalkenes should be a feasible process and that the metathesis is not very sensitive to stereochemical issues.

Introduction

Over the course of the last 20 years, alkene metathesis catalysed with homogeneous transitition metal-based precatalysts evolved into a valuable tool for organic synthetic chemists mainly due to its variability and high compatibility with functional groups. It hence became the subject of multiple books [1-3] and reviews [4-8] discussing its synthetic applications, catalysts, mechanism, regio- and stereoselectivity.

Computational chemistry proved to be extremely valuable in the study of reaction mechanisms. In particular, the use of time-efficient DFT methods for the theoretical study of alkene metathesis has been extensively reviewed [9-11] and computational results have been found to agree well with recent experimental mechanistic studies based on easily initiating ruthenium precatalysts [12,13]. A theoretical approach has been also employed in attempts to gain a better insight into the complex structure of intertwined productive and non-productive catalytic cycles of alkene metathesis [14]. In contrast to the older computations, new publications also include the initiation steps starting from metathesis precatalysts as Grubbs or Hoveyda–Grubbs 2nd generation precatalysts [15-22].

In contrast to common alkenes, the metathesis of fluoroalkenes has attracted far less attention [23]. Fluorinated modifications

have mostly concentrated on the side chain of the vinyl group [24-27] or applications of 2-fluoroalkenes [28-30]. As an exception, the reaction of the Grubbs 2nd generation catalyst with 1,1-difluoroethene gave an isolable difluoromethylene-containing ruthenium complex with very poor catalytic activity [31] and the analogous reaction of 1-fluoroalkene formed a fluoromethylene-containing complex with low catalytic activity [32,33]. Up to now, the only metathesis which included tetrafluoroethene and its analogues has been reported in a patent [34], describing the disproportionation of perfluoroalkenes and alkenes to hydrofluoroalkenes. Moreover, just recently a successful cross metathesis of perfluoroalkenes with vinyl ethers has been published [35].

The reported computations dealing with the metathesis of fluoroalkenes are also extremely scarce. Thus, the mechanism of the cross metathesis of norbornene with selected fluoro- and chloroalkenes has been studied and the higher stability of a ruthenium intermediate containing a difluoromethylene ligand has been emphasized [36,37].

A complete mechanism of alkene metathesis including initiation, productive and non-productive cycles represents a highly complex system [38], the understanding of which for fluoroalkenes is negligible. We hence report herein the results of a computational study dealing with the metathesis of most fluoroethenes with the emphasis on subsequent catalytic cycles, catalysed with the Hoveyda–Grubbs 2nd generation precatalyst (**HG2**).

Results and Discussion

In contrast to textbook pictures describing alkene metathesis as a single catalytic cycle, even a simplified system of homometathesis of 1-alkene represents a complex system, in any step of which problems can arise due to a high energetical barrier or unfavourable equilibrium. Moreover, the preference for non-productive cycles can hamper the formation of the desired product even in the absence of kinetic and thermodynamic issues (Scheme 1).

At the beginning, the starting precomplex **HG2** reacts in the initiation phase with alkene forming ruthenacyclobutane **I**, which releases 2-isopropoxystyrene and the first active catalytic species, alkylideneruthenium complex **AC**. Depending on the regioselectivity of the coordination of the second alkene molecule, the **AC** complex can form ruthenacyclobutane **PA** in the first part of productive catalytic cycle, or symmetrical ruthenacyclobutane **NA** in the first part of the non-productive catalytic cycle. While the first species **PA** reacts further to the product and methyleneruthenium complex **MC**, the non-productive ruthenacyclobutane **NA** can only return back to complex **AC**. Intermediary complex **MC** can again enter either the second part of the productive catalytic cycle closing the ring into the ruthenacyclobutane **PB**, or it can react in the non-productive

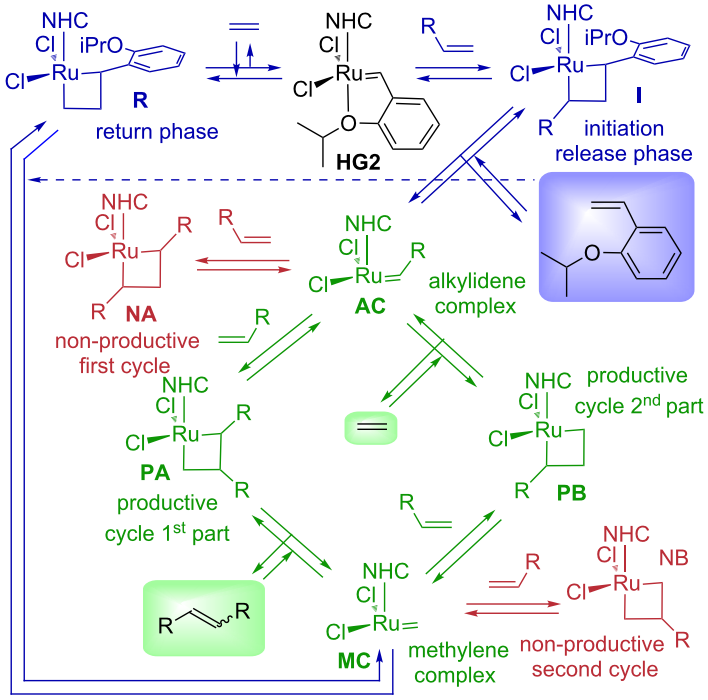

Scheme 1: Initiation, productive and non-productive cycles in alkene homometathesis.

cycle forming symmetrical ruthenacyclobutane **NB**. Finishing the productive cycle, the ruthenacyclobutane **PB** releases ethene and starts the next catalytic cycle, while the non-productive complex **NB** can again only return back to complex **MC**. It should be noted that the main aim of the development of the family of Hoveyda–Grubbs catalysts was the recycling of the catalyst. This implies a successful release-return mechanism, in which after a successful metathesis the active complexes **AC** or **MC** react with 2-isopropoxystyrene restoring the starting precatalyst **HG2**, a controversial issue, which some authors support [8,39] and the others contest [40]. Recent experiments have shown that the complex **MC** can be successfully transformed into the parent precatalyst **HG2** [41].

In our computational study, we first addressed the initiation phase of possible metathesis of a highly unsymmetrical alkene, 1,1-difluoroethene, and compared its behaviour with the already reported initiation of ethene [18,19]. Among the three possible mechanisms, interchange, dissociative and associative, the first emerged as the most energetically favourable. In contrast to the symmetrical molecule of ethene, two orientations of 1,1-difluoroethene are possible, which we arbitrarily assigned as *syn* for the coordination of difluoromethylene to ruthenium forming 2,2-difluororuthenacyclobutane intermediate **s2I** and *anti* for the coordinaton of methylene to ruthenium forming 3,3-difluororuthenacyclobutane intermediate **a2I**. The computations started from an alkene weakly coordinated to the NHC ligand without any coordination to ruthenium (structures **1a** and **2a**), and continued with the first mechanistic step, the coordination of alkene to ruthenium with partial decoordination of alkoxybenzylidene oxygen (structures **1c** and **2c**). For ethene (**1c**) and the *anti*-coordinated 1,1-difluoroethene (**a2c**), shallow minima were observed in the Gibbs free energy profile, while for the *syn* structure (**s2c**), the minimum obtained by the calculation of electronic energy changed just to inflexion when converted to free Gibbs energy at 25 °C (see Figure 1, dotted red line). At this stage only minimal relative energy differences were observed for the structures **1c** and **2c**. However, in the next step forming metallacyclobutane the transition state energy was by ca. 20 kJ/mol higher for the *syn*-coordinated 1,1-difluoroethene (**s2d**) and by another ca. 20 kJ/mol higher for the *anti*-coordinationed 1,1-difluoroethene (**a2d**) compared to ethene (**1d**), already energetically preferring the *syn*-coordination. The picture changed dramatically on the formation of metallacyclobutane (**1I** or **2I**), where 2,2-difluororuthenacyclobutane intermediate **s2I** was by 20 kJ/mol more stable than ruthenacyclobutane **s1** and by another 40 kJ/mol more stable than 3,3-difluororuthenacyclobutane **a2I**. These differences further rose for the last step of initiation, the formation of methyleneruthenium **1f** or **a2f** or difluoromethyleneruthenium **s2f**, where the relative stability of the latter was by 100 kJ/mol higher

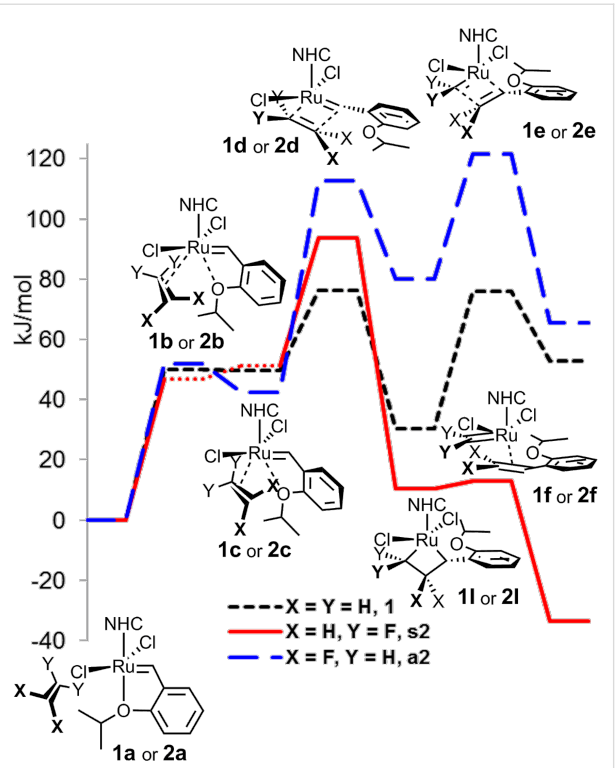

Figure 1: Initiation phase of the reaction of **HG2** with ethene (**1**) and 1,1-difluoroethene (**2**).

compared to the *anti* coordination. These results are in agreement with the previous computations of a norbornene derivative with fluoroalkenes [36,37], but are suprisingly contradictory to the experimental observations of the reaction of the Grubbs 2nd generation catalyst with 1,1-difluoroethene, where at room temperature the formation of both methylene- and difluoromethyleneruthenium complexes was observed [31].

With the additional aim to obtain the information about stereoselectivity, we next analogously computed the initation phase of the reaction of precatalyst **HG2** with 1-fluoroethene, where apart of the *syn*- and *anti*-approach, also *cis*- or *trans*- orientations of the alkene relatively to the alkoxyphenyl ring in the intermediary metallacyclobutane are possible. In the first step of the reaction, intermediary complex **3c** with partial bonding of alkene and the alkoxy group of the alkoxybenzylidene ligand to ruthenium was detected with the exception of a *syn–cis* arranged alkene, for which just a weak inflexion was observed in analogy to [42]. No large differences in the energies of transition states **3d** preceeding the formation of metallacyclobutane were found, but in analogy to the initiation of 1,1-difluoroethene, 2-fluorometallacyclobutanes **sc3I** and **st3I** with coordination of fluoromethylene to ruthenium were again more stable then the corresponding 3-fluorometallacyclobutanes **ac3I** and **at3I**. The difference is further augmented in the transition state

3e and in the final stage of the initiation, the formation of fluoromethyleneruthenium complex **s3f** or methyleneruthenium complex **a3f**. On the other hand, this difference in the energies reaches ca. 50 kJ/mol, about one half of the *syn–anti* difference for difluoromethylated complex **2AC**. We also observed significant differences in the energies for *cis*- and *trans*-ruthenacyclobutanes **c3I** and **t3I** and complexes **c3f** and **t3f**, where the *trans*-structures were more stable by 25 to 60 kJ/mol, probably due to the repulsion of fluorine with the alkoxybenzylidene oxygen (Figure 2).

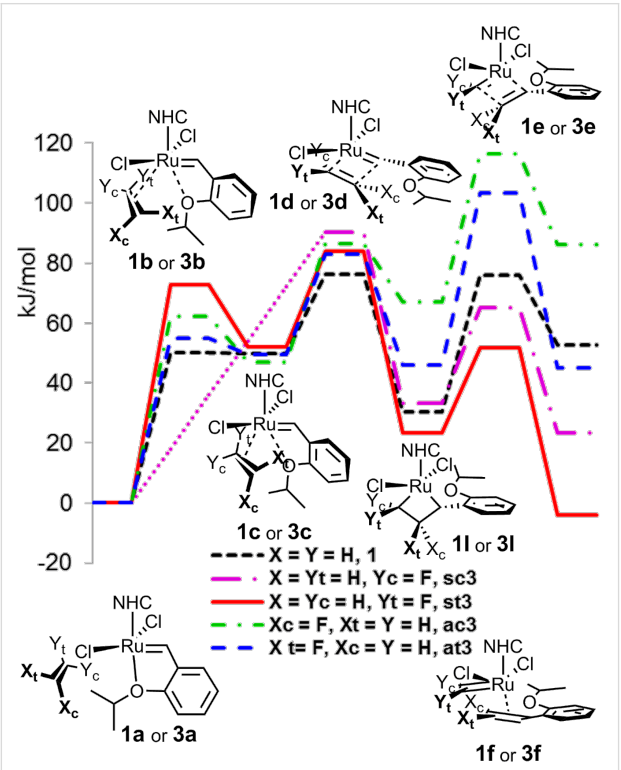

Figure 2: Initiation phase of the reaction of **HG2** with ethene (**1**) and 1-fluoroethene (**3**).

We continued our study by the computation of the first step **A** of the catalytic cycle for 1,1-difluoroethene (**2**), which started with the coordination of the starting active catalytic form **2AC** with 1,1-difluoroethene (**2**). The non-productive cycle started with the *syn*-coordination of 1,1-difluoroethene (**2**) to 1,1-difluoromethyleneruthenium complex **2AC**, leading to symmetrical metallacyclobutane **2NA** with activation energy around 65 kJ/mol and through the same transition state back to complex **2AC** and 1,1-difluoroethene (**2**). However, for the productive *anti*-coordination of 1,1-difluoroethene (**2**), no stable metallacyclobutane structure **2PC** was found (a detailed study detected only inflection on the potential energy surface), probably due to a steep rise in the energy leading through the transition state **s2i** to a highly unstable complex of methyleneruthenium with tetrafluoroethene. The comparison of the productive and non-productive cycle shows that the transition state energies differ by more than 120 kJ/mol, making thus the first part **A** of the productive cycle highly improbable and probably resulting in stopping the productive metathesis of vinylidene fluoride at all, because all active catalytic species **AC** move forth and back in the non-productive cycle (Figure 3).

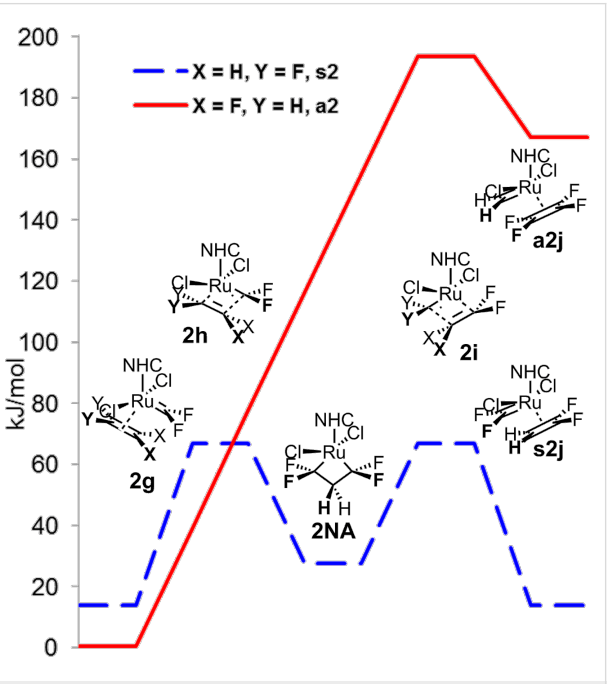

Figure 3: First part **A** of the catalytic cycle of homometathesis of 1,1-difluoroethene (**2**).

The difference in the stability of the corresponding complexes **a2j** and **s2j** can be explained partially by the π-donation of difluoromethylene carbene in analogy to [37], but also by the electron donation of the π-bond of the 1,1-difluoroethene (**2**) molecule with a high negative charge on the CH_2 group. This results in lowering of the positive charge on ruthenium and shortening of the CH_2–Ru distance (262 pm) in the **s2j** structure compared to repulsive CF_2–Ru interaction of tetrafluoroethene in the **a2j** structure with longer CF_2–Ru distance (323 pm, Figure 4).

We continued the calculations by the study of the second part **B** of the catalytic cycle of the metathesis of 1,1-difluoroethene (**2**), which starts by the decoordination of tetrafluoroethene from complex **a2j** and coordination of another molecule of 1,1-difluoroethene (**2**) to methyleneruthenium complex **MC** forming complex **2k**. While both *syn*- and *anti*-coordinations of starting complex **2k** and subsequent transition states **2l** have nearly equal energies, the subsequent non-symmetrical productive metallacyclobutane **2PB** is significantly more stable by ca.

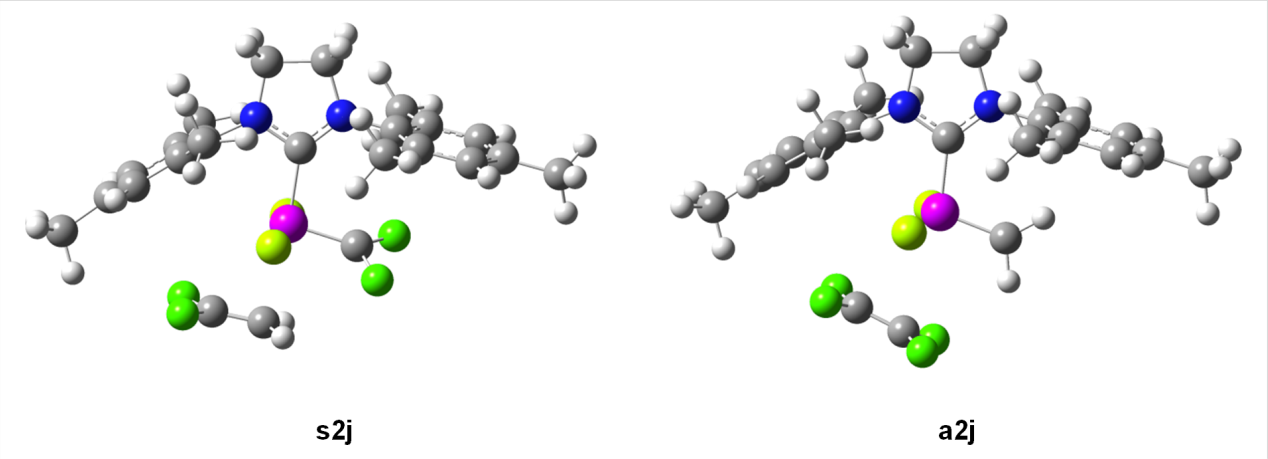

Figure 4: Computed structures of complexes **s2j** and **a2j**.

60 kJ/mol than symmetrical non-productive metallacyclobutane **2NB**. The difference in the energies was again more augmented for the subsequent transition states **2m** and finally with the alkene coordinated to the alkylidene ruthenium, where the productive complex **s2n**, a complex of ethylene with difluoro-ruthenium, is by ca. 80 kJ/mol more stable than the non-productive complex **a2n** (Figure 5). Thus, in the second part **B** of the catalytic cycle the non-productive cycle has no negative influence on the 1,1-difluoroethene (**2**) metathesis.

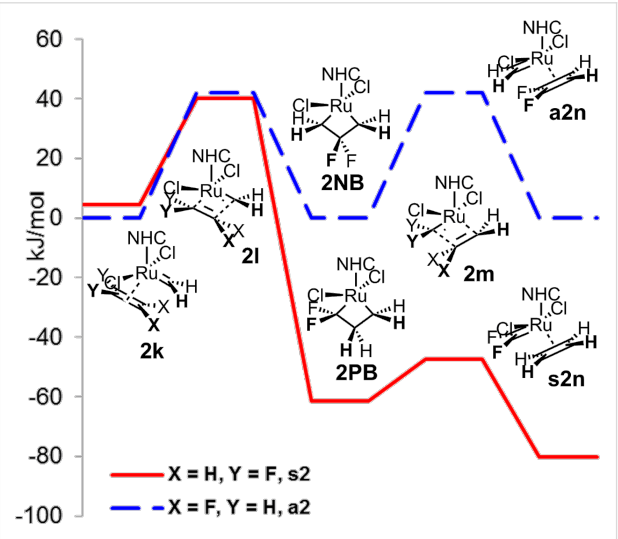

Figure 5: Second part **B** of the catalytic cycle of homometathesis of 1,1-difluoroethene (**2**).

To obtain the information about the stereoselectivity in the active catalytic cycle, we again decided to study the productive and non-productive cycles in the homometathesis of 1-fluoroethene (**3**). In the first step **A** of the catalytic cycle, a similar pattern, although less emphasized, could be observed for *syn*- and *anti*-coordination of the starting 1-fluoroethene (**3**) as in the case of 1,1-difluoroethene (**2**). Thus, the relative energies of the complexes of 1-fluoroethene (**3**) with fluoromethylene-ruthenium **3g**, as well as the subsequent transition states **3h**, differ minimally regardless of the regio- and stereoselectivity, while the intermediary symmetrical metallacyclobutane **3NA** of the non-productive cycle with the *syn*-coordination of 1-fluoroethene (**3**) shows a significantly higher stability compared to the productive *anti*-intermediate **3PA**. These differences again increased for the transition states **3i** and final complexes **3j**, preferring strongly the non-productive cycle and probably significantly slowing the possible productive metathesis. The calculations also show only low stereoselectivity with the transition states of the non-productive cycle preferring *trans*-configuration of both fluorine atoms by ca. 10 kJ/mol, while for the productive cycle the *cis*-configuration is preferred (Figure 6).

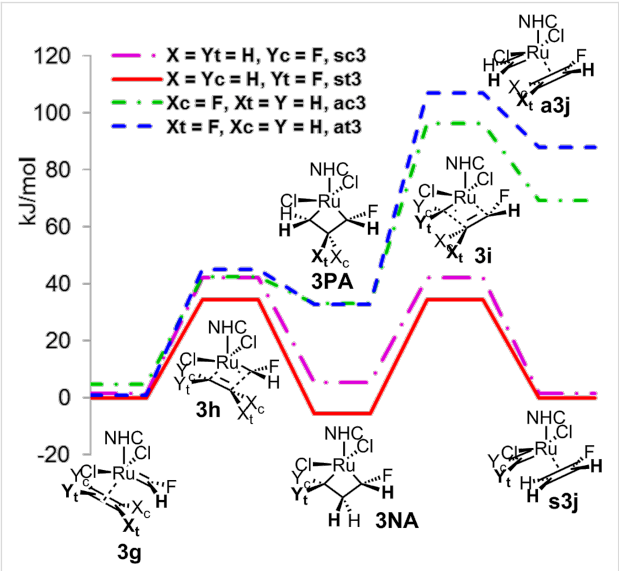

Figure 6: First part **A** of the catalytic cycle of homometathesis of 1-fluoroethene (**3**).

For the homometathesis of 1-fluoroethene (**3**), we finally studied the second part **B** of the catalytic cycle. In analogy to the homometathesis of 1,1-difluoroethene (**2**), the productive cycle is energetically more favourable, indicating that in the part **B** the non-productive cycle does not block the catalytic cycle (Figure 7).

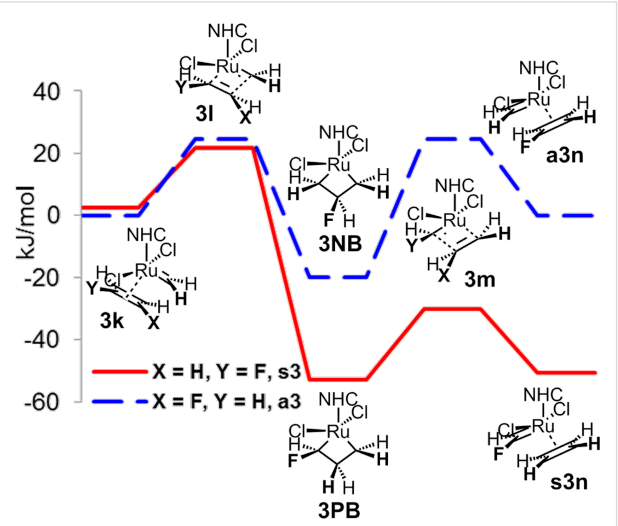

Figure 7: Second part **B** of the catalytic cycle of homometathesis of 1-fluoroethene (**3**).

The obtained results imply that the key problem in the metathesis of non-symmetrically substituted fluoroalkenes is probably not the high stability of the fluorinated methylene-ruthenium complex, but the consumption of most of the active catalytic form by the non-productive cycle proceeding through symmetrical metallacyclobutane substituted with fluorines in positions 2 and 4 of the ring.

To further confirm this hypothesis, we decided to study the active catalytic cycle of the metathesis of two perhaloethenes, tetrafluoroethene (**4**) and chlorotrifluoroethene (**5**), starting from the active catalytic form **2AC**. Due to symmetry, both parts **A** and **B** of the catalytic cycle for tetrafluoroethene (**4**) are identical and non-productive with surprisingly low transition state energy (Figure 8).

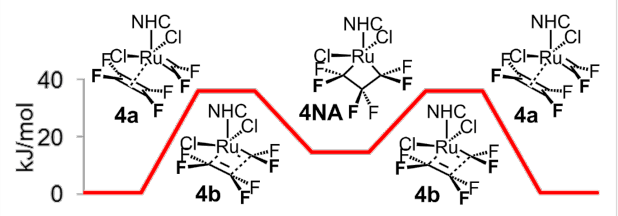

Figure 8: Non-productive catalytic cycle of homometathesis of tetrafluoroethene (**4**).

For the homometathesis of chlortrifluoroethene (**5**), the situation again becomes more complex with two parts **A** and **B** of the catalytic cycle and both productive and non-productive cycles participating. The first part **A** is in analogy to the homometathesis of tetrafluoroethene (**4**) characteristic by the low energy of the transition state, with the preference for the non-productive cycle of ca. 20 kJ/mol, i.e., much less pronounced than in the case of 1-fluoroethene (**3**) complexes (Figure 6 and Figure 9).

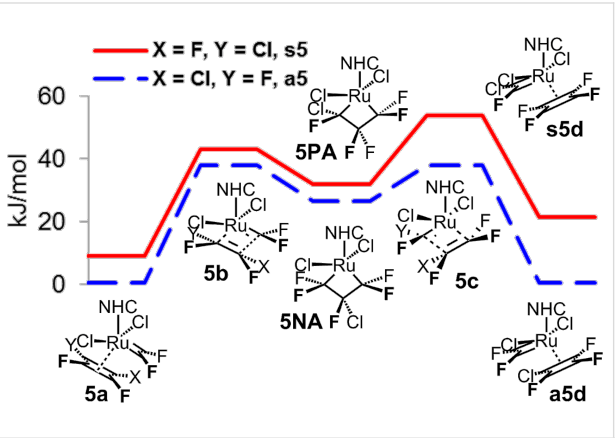

Figure 9: First part **A** of the catalytic cycle of homometathesis of chlorotrifluoroethene (**5**).

With the second part **B** of the catalytic cycle starting from a non-symmetrical chlorofluoromethyleneruthenium complex, the stereochemistry of coordination in complex **5e** became an issue with *cis*- and *trans*-ruthenacyclobutanes possible. In analogy to the homometathesis of tetrafluoroethene (**4**), the relative transition state energies were quite low with small preference for the productive cycle without any stereochemical priority (Figure 10).

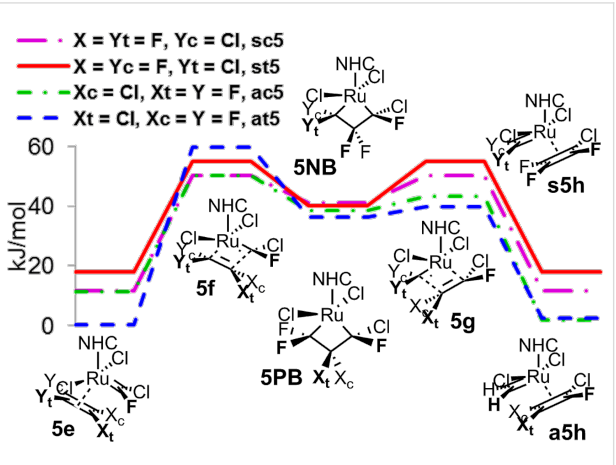

Figure 10: Second part **B** of the catalytic cycle of homometathesis of chlorotrifluoroethene (**5**).

Conclusion

Our computational study, which included the metathesis of both partially and fully fluorinated alkenes, showed that the formation of stable intermediary fluoro- or difluoromethyleneruthenium does not block the subsequent metathetic cycles. For partially fluorinated alkenes as 1,1-difluoroethene (**2**) or 1-fluoroethene (**3**), poor preparative results of metathesis can be caused by the overwhelming participation of the non-productive metathetic cycle proceeding through ruthenacyclobutanes substituted with fluorine atoms in positions 2 and 4. On the other hand, the results of computations of the catalytic cycles of both tetrafluoroethene (**4**) and chlorotrifluoroethene (**5**) indicate that their metathesis should proceed without any significant problems providing no reactive alkylideneruthenium complexes, e.g., methyleneruthenium, participates in the active catalytic cycles. Our results are in full agreement with the recently described surprisingly successful metathesis of perhaloalkenes with vinyl ethers [35], but contradicts the patent [34] which describes the successful synthesis of partially fluorinated alkenes from perfluorinated and non-fluorinated alkenes.

Computational Details

DFT calculations were performed using the Gaussian 09W program suite [43] using the resolution-of-identity approach [44], M06L pure functional [45] in analogy to [18], def2-SV(P) basis set [46] and universal def2 auxilliary basis set [47]. Vibrational frequencies were calculated for all structures to characterize them as minima or transition states. These computations gave their free Gibbs energies at 25 °C, which were used for the PES description in Figures 1–3 and Figures 5–10. Starting geometries were obtained by a careful series of preoptimization of structures **1a**–**3a** (Hoveyda–Grubbs 2nd generation precatalyst **HG2** with weakly coordinated alkene) and **1l**–**3l** (metallacyclobutane) with the most stable conformation of the isopropoxy group differing from the crystal structure of the parent precatalyst **HG2**. For all computed structures, the corresponding pdb files are listed in Supporting Information File 1 together with a table containing the total electronic and free Gibbs energies in hartrees, and the total and relative electronic and free Gibbs energies in kJ/mol.

Supporting Information

Supporting Information File 1

Table containing total electronic and free Gibbs energies in hartrees, total and relative electronic and free Gibbs energies in kJ/mol for all computed structures, as well as their coordinates in the pdb format.
[http://www.beilstein-journals.org/bjoc/content/supplementary/1860-5397-11-232-S1.pdf]

Acknowledgements

We thank the Grant Agency of the Czech Republic (grant No. 207/10/1533) for financial support. Computational resources were provided by the MetaCentrum under the program LM2010005 and the CERIT-SC under the program Centre CERIT Scientific Cloud, part of the Operational Program Research and Development for Innovations, Reg. no. CZ.1.05/3.2.00/08.0144.

References

1. Grubbs, R. H.; Wenzel, A. G.; O'Leary, D. J.; Khosravi, E., Eds. *Handbook of Organic Chemistry,* 2nd ed.; Wiley & Sons: New York, NY, U.S.A., 2015.
2. Grela, K., Ed. *Olefin Metathesis: Theory and Practice;* Wiley & Sons: New York, NY, U.S.A., 2014.
3. Cossy, J.; Arseniyadis, S.; Meyer, C.; Grubbs, R. H., Eds. *Metathesis in Natural Product Synthesis: Strategies, Substrates and Catalysts;* Wiley & Sons: New York, NY, U.S.A., 2010.
4. Koh, M. J.; Khan, R. K. M.; Torker, S.; Yu, M.; Mikus, M. S.; Hoveyda, A. H. *Nature* **2015,** *517,* 181–186. doi:10.1038/nature14061
5. Nelson, D. J.; Manzini, S.; Urbina-Blanco, C. A.; Nolan, S. P. *Chem. Commun.* **2014,** *50,* 10355–10375. doi:10.1039/C4CC02515F
6. Fürstner, A. *Science* **2013,** *341,* No. 6152. doi:10.1126/science.1229713
7. Vougioukalakis, G. C.; Grubbs, R. H. *Chem. Rev.* **2010,** *110,* 1746–1787. doi:10.1021/cr9002424
8. Bieniek, M.; Michrowska, A.; Usanov, D. L.; Grela, K. *Chem. – Eur. J.* **2008,** *14,* 806–818. doi:10.1002/chem.200701340
9. Credendino, R.; Poater, A.; Ragone, F.; Cavallo, L. *Catal. Sci. Technol.* **2011,** *1,* 1287–1297. doi:10.1039/c1cy00052g
10. Falivene, L.; Poater, A.; Cavallo, L. Tuning and Quantifying Steric and Electronic Effects of N-Heterocyclic Carbenes. In *N-Heterocyclic Carbenes: Effective Tools for Organometallic Synthesis;* Nolan, S. P., Ed.; Wiley-VCH: New York, NY, U.S.A., 2014; pp 25–38.
11. Poater, A.; Falivene, L.; Cavallo, L. Theoretical Attempts: "In Silico Olefin Metathesis"—How Can Computers Help in the Understanding of Metathesis Mechanisms and in Catalysts Development?. In *Olefin Metathesis: Theory and Practice;* Grela, K., Ed.; Wiley: New York, NY, U.S.A., 2014; pp 483–494.
12. van der Eide, E. F.; Piers, W. E. *Nat. Chem.* **2010,** *2,* 571–576. doi:10.1038/nchem.653
13. Leitao, E. M.; van der Eide, E. F.; Romero, P. E.; Piers, W. E.; McDonald, R. *J. Am. Chem. Soc.* **2010,** *132,* 2784–2794. doi:10.1021/ja910112m
14. Vummaleti, S. V. C.; Cavallo, L.; Poater, A. *Theor. Chem. Acc.* **2015,** *134,* 22–27. doi:10.1007/s00214-015-1622-x
15. Engle, K. M.; Lu, G.; Luo, S. X.; Henling, L. M.; Michael, K.; Takase, M. K.; Liu, P.; Houk, K. N.; Grubbs, R. H. *J. Am. Chem. Soc.* **2015,** *137,* 5782–5792. doi:10.1021/jacs.5b01144
16. Manzini, S.; Urbina-Blanco, C. A.; Nelson, D. J.; Poater, A.; Lebl, T.; Meiries, S.; Slawin, A. M. Z.; Falivene, L.; Cavallo, L.; Nolan, S. P. *J. Organomet. Chem.* **2015,** *780,* 43–48. doi:10.1016/j.jorganchem.2014.12.040
17. Poater, A.; Pump, E.; Vummaleti, S. V. C.; Cavallo, L. *J. Chem. Theory Comput.* **2014,** *10,* 4442–4448. doi:10.1021/ct5003863
18. Ashworth, I. W.; Hillier, I. H.; Nelson, D. J.; Percy, J. M.; Vincent, M. A. *ACS Catal.* **2013,** *3,* 1929–1939. doi:10.1021/cs400164w

19. Kvíčala, J.; Schindler, M.; Kelbichová, V.; Babuněk, M.; Rybáčková, M.; Kvíčalová, M.; Cvačka, J.; Březinová, A. *J. Fluorine Chem.* **2013,** *153,* 12–25. doi:10.1016/j.jfluchem.2013.06.001
20. Urbina-Blanco, C. A.; Poater, A.; Lebl, T.; Manzini, S.; Slawin, A. M. Z.; Cavallo, L.; Nolan, S. P. *J. Am. Chem. Soc.* **2013,** *135,* 7073–7079. doi:10.1021/ja402700p
21. Poater, A.; Falivene, L.; Urbina-Blanco, C. A.; Manzini, S.; Nolan, S. P.; Cavallo, L. *Dalton Trans.* **2013,** *42,* 7433–7439. doi:10.1039/c3dt32980a
22. Nuñez-Zarur, F.; Solans-Monfort, X.; Rodrıguez-Santiago, L.; Sodupe, M. *Organometallics* **2012,** *31,* 4203–4215. doi:10.1021/om300150d
23. Fustero, S.; Simón-Fuentes, A.; Barrio, P.; Haufe, G. *Chem. Rev.* **2015,** *115,* 871–930. doi:10.1021/cr500182a
24. Chatterjee, A. K.; Morgan, J. P.; Scholl, M.; Grubbs, R. H. *J. Am. Chem. Soc.* **2000,** *122,* 3783–3784. doi:10.1021/ja9939744
25. Imhof, S.; Randl, S.; Blechert, S. *Chem. Commun.* **2001,** 1692–1693. doi:10.1039/B105031C
26. Cuñat, A. C.; Flores, S.; Oliver, J.; Fustero, S. *Eur. J. Org. Chem.* **2011,** 7317–7323. doi:10.1002/ejoc.201101091
27. Eignerová, B.; Slavíková, B.; Buděšínský, M.; Dračínský, M.; Klepetářová, B.; Šťastná, E.; Kotora, M. *J. Med. Chem.* **2009,** *52,* 5753–5757. doi:10.1021/jm900495f
28. Marhold, M.; Stillig, C.; Fröhlich, R.; Haufe, G. *Eur. J. Org. Chem.* **2014,** 5777–5785. doi:10.1002/ejoc.201402535
29. Salim, S. S.; Bellingham, R. K.; Satcharoen, V.; Brown, R. C. D. *Org. Lett.* **2003,** *5,* 3403–3406. doi:10.1021/ol035065w
30. Guérin, D.; Gaumont, A. C.; Dez, I.; Mauduit, M.; Couve-Bonnaire, S.; Pannecoucke, X. *ACS Catal.* **2014,** *4,* 2374–2378. doi:10.1021/cs500559p
31. Trnka, T. M.; Day, M. W.; Grubbs, R. H. *Angew. Chem., Int. Ed.* **2001,** *40,* 3441–3444. doi:10.1002/1521-3773(20010917)40:18<3441::AID-ANIE3441>3.0.CO;2-7
32. Macnaughtan, M. L.; Johnson, M. J. A.; Kampf, J. W. *Organometallics* **2007,** *26,* 780–782. doi:10.1021/om061082o
33. Macnaughtan, M. L.; Gary, J. B.; Gerlach, D. L.; Johnson, M. J. A.; Kampf, J. W. *Organometallics* **2009,** *28,* 2880–2887. doi:10.1021/om800463n
34. Elsheikh, M. Y.; Bonnet, P. Process for the Manufacture of Hydrofluoroolefins via Metathesis. WO Patent 2009/003085, Dec 31, 2008.
35. Takahira, Y.; Morizawa, Y. *J. Am. Chem. Soc.* **2015,** *137,* 7031–7034. doi:10.1021/jacs.5b03342
36. Fomine, S.; Vargas Ortega, J.; Tlenkopatchev, M. A. *J. Organomet. Chem.* **2006,** *691,* 3343–3348. doi:10.1016/j.jorganchem.2006.04.021
37. Fomine, S.; Tlenkopatchev, M. A. *Appl. Catal., A* **2009,** *355,* 148–155. doi:10.1016/j.apcata.2008.12.011
38. Stewart, I. C.; Keitz, B. K.; Kuhn, K. M.; Thomas, R. M.; Grubbs, R. H. *J. Am. Chem. Soc.* **2010,** *132,* 8534–8535. doi:10.1021/ja1029045
39. Kingsbury, J. S.; Hoveyda, A. H. *J. Am. Chem. Soc.* **2005,** *127,* 4510–4517. doi:10.1021/ja042668+
40. Vorfalt, T.; Wannowius, K. J.; Thiel, V.; Plenio, H. *Chem. – Eur. J.* **2010,** *16,* 12312–12315. doi:10.1002/chem.201001832
41. Bates, J. M.; Lummis, J. A. M.; Bailey, G. A.; Fogg, D. E. *ACS Catal.* **2014,** *4,* 2387–2394. doi:10.1021/cs500539m
42. Straub, B. F. *Angew. Chem., Int. Ed.* **2005,** *44,* 5974–5978. doi:10.1002/anie.200501114
43. *Gaussian 09,* Revision D.01; Gaussian, Inc.: Wallingford, CT, U.S.A., 2009.
44. Eichkorn, K.; Treutler, O.; Öhm, H.; Häser, M.; Ahlrichs, R. *Chem. Phys. Lett.* **1995,** *240,* 283–290. doi:10.1016/0009-2614(95)00621-A
45. Zhao, Y.; Truhlar, D. G. *Theor. Chem. Acc.* **2008,** *120,* 215–241. doi:10.1007/s00214-007-0310-x
46. Weigend, F.; Ahlrichs, R. *Phys. Chem. Chem. Phys.* **2005,** *7,* 3297–3305. doi:10.1039/B508541A
47. Weigend, F. *Phys. Chem. Chem. Phys.* **2006,** *8,* 1057–1065. doi:10.1039/B515623H

License and Terms

BEILSTEIN JOURNAL OF ORGANIC CHEMISTRY

Beyond catalyst deactivation: cross-metathesis involving olefins containing *N*-heteroaromatics

Kevin Lafaye, Cyril Bosset, Lionel Nicolas, Amandine Guérinot* and Janine Cossy*

Review

Open Access

Address:
Laboratoire de Chimie Organique, Institute of Chemistry, Biology and Innovation (CBI)-UMR 8231 ESPCI ParisTech, CNRS, PSL* Research University, 10, rue Vauquelin, 75231 Paris Cedex 05, France

Email:
Amandine Guérinot* - amandine.guerinot@espci.fr;
Janine Cossy* - janine.cossy@espci.fr

* Corresponding author

Keywords:
catalyst deactivation; cross-metathesis; *N*-heteroaromatic; pyridine; ring-closing metathesis

Beilstein J. Org. Chem. **2015,** *11,* 2223–2241.
doi:10.3762/bjoc.11.241

Received: 17 July 2015
Accepted: 20 October 2015
Published: 18 November 2015

This article is part of the Thematic Series "Progress in metathesis chemistry II".

Guest Editor: K. Grela

Abstract

Alkenes containing *N*-heteroaromatics are known to be poor partners in cross-metathesis reactions, probably due to catalyst deactivation caused by the presence of a nitrogen atom. However, some examples of ring-closing and cross-metathesis involving alkenes that incorporate *N*-heteroaromatics can be found in the literature. In addition, recent mechanistic studies have focused on the rationalization of nitrogen-induced catalysts deactivation. The purpose of this mini-review is to give a brief overview of successful metathesis reactions involving olefins containing *N*-heteroaromatics in order to delineate some guidelines for the use of these challenging substrates in metathesis reactions.

Introduction

Over the past decades, metathesis has become a key reaction within the organic chemist's toolbox [1-6]. Since its infancy in the 50's, metathesis has grown in importance and, today, applications in a broad variety of areas such as natural product synthesis [7-11], polymerization [12], drug discovery [7], petrochemistry or agricultural chemistry have been reported. One of the reasons of this success is the discovery of well-defined, stable, highly chemoselective and now commercially available catalysts particularly the Grubbs catalysts 1st and 2nd generation (GI and GII) and the Grubbs–Hoveyda II catalyst (G-HII) (Figure 1) [13].

A large array of functional groups including alcohols, halides, esters, amides, carbamates and sulfonamides are compatible with the metathesis conditions [14-20]. However, the involvement of alkenes containing a nitrogen atom such as an amine or an *N*-heteroaromatic ring in metathesis reactions is still problematic and have been the subject of several research works [21-26]. Lewis basic and nucleophilic amines are supposed to interfere with the catalyst and/or intermediates, thus disrupting the catalytic cycle and preventing the process to occur (vide infra). Various approaches have been explored to allow the use of primary and secondary amines in ring-closing metathesis

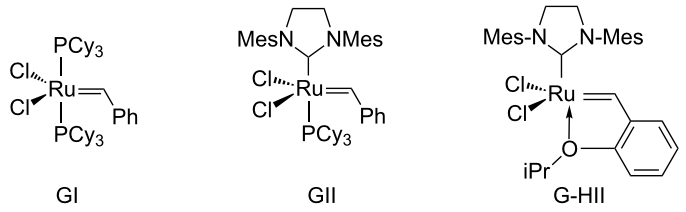

Figure 1: Some ruthenium catalysts for metathesis reactions.

(RCM) and cross-metathesis (CM), and one of them is the transformation of amines into carbamates, amides or sulfonamides [27-29]. As an alternative, metathesis reactions can be performed with olefins possessing ammonium salts that can be formed from the corresponding amines either in a preliminary step or in situ, in the presence of an acidic additive [30-35]. In addition, Lewis acids in catalytic amounts were shown to enhance the reactivity of amino compounds in metathesis reactions [36,37]. Involvement of *N*-heteroaromatics containing olefins in metathesis has been less documented. In this review, we would like to give an overview of successful metatheses involving alkenes that possess *N*-heteroaromatics in order to delineate some guidelines. Some mechanistic insights dealing with catalyst deactivation caused by amino derivatives will be first presented and discussed. RCM and CM involving alkenes possessing *N*-heteroaromatics will be then successively examined [38].

Review

Mechanistic insights into amine-induced catalyst deactivation

Recently, intensive studies dealing with ruthenium catalyst deactivation in metathesis have been published, most of them focusing on the GII catalyst [39-43]. In 2007, Grubbs et al. examined the decomposition pathways of various ruthenium methylidenes using NMR spectroscopy [44]. The methylidenes **1** and **2** derived from GI and GII had a half-life of 40 min and 5 h 40 min, respectively at 55 °C and the main byproduct $CH_3PCy_3^+Cl^-$ was identified using ^1H, ^{13}C and ^{31}P NMR data as well as HRMS data. The deactivation of the catalysts was hypothesized to go through ligand dissociation from **1** and **2** followed by a nucleophilic attack of the free phosphine on the methylidene intermediates **3** and **4** to give $CH_3PCy_3^+Cl^-$ and inactive ruthenium complexes. Similar observations were made in the absence or in the presence of ethylene in the reaction medium (Scheme 1).

Similar studies concerning the Grubbs–Hoveyda II catalyst were difficult due to the instability of the methylidene derivative that could not be isolated. Thus, the decomposition of G-HII was studied in the presence of ethylene and unidentified ruthenium hydride species were observed by ^1H NMR after 24 h. This result indicates that another mode of deactivation that does not involve a phosphine is involved in G-HII degradation (Scheme 2).

In 2009, Moore et al. studied the stability of GI and GII in the presence of *n*-butylamine using ^1H and ^{31}P NMR spectroscopy [39]. While GI decomposed within 10 min after formation of bisamino complex **7** (Scheme 3, reaction 1), GII resulted in a

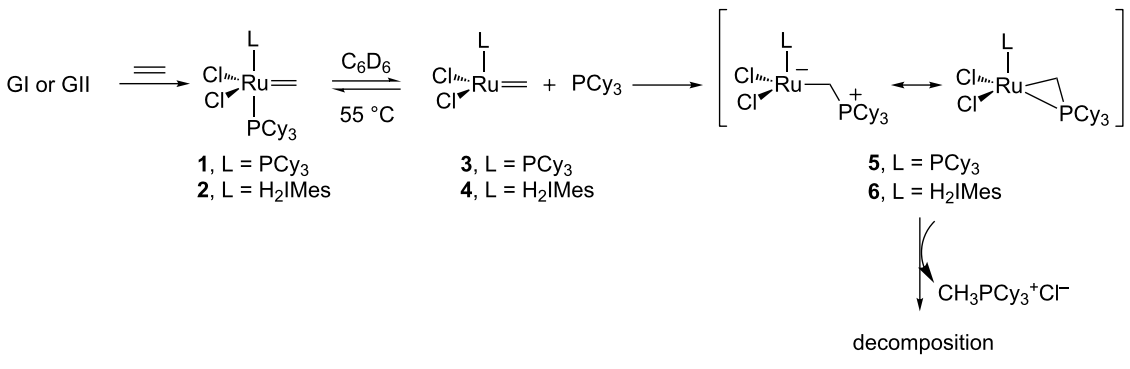

Scheme 1: Decomposition of methylidenes **1** and **2**.

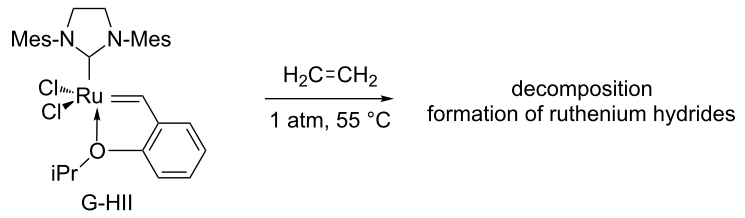

Scheme 2: Deactivation of G-HII in the presence of ethylene.

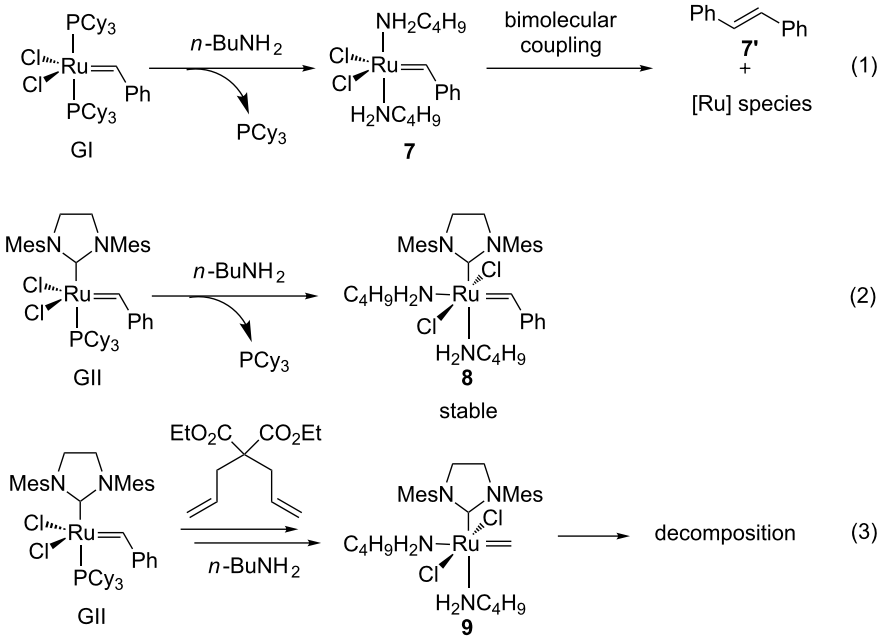

Scheme 3: Reaction between GI/GII and *n*-$BuNH_2$.

new stable bis-amino ruthenium complex **8** that was isolated and characterized using X-ray diffraction (Scheme 3, reaction 2). In both cases, free PCy_3 was observed by NMR confirming amine-induced phosphine displacement. The decomposition of GI was hypothesized to go through a bimolecular coupling from **7**. On the contrary, the bulky NHC ligand present in **8** could prevent this side reaction. However, in the presence of diethyl diallylmalonate and *n*-butylamine, GII decomposed readily probably due to an increased instability of the less hindered methylidene **9** compared to benzylidene **8** (Scheme 3, reaction 3).

Fogg et al. completed this study by focusing on amine-mediated degradation of GII and they highlighted various plausible decomposition pathways depending on the nature of the amine [45]. At first, the reaction between GII and various amines such as *n*-butylamine (**a**), pyrrolidine (**b**), morpholine (**c**) and DBU (**d**) were examined by ^{1}H NMR. As already highlighted by Moore et al., in the presence of *n*-butylamine, GII was transformed into **8** and the latter slowly decomposed (half-life = 3.5 h) to give ruthenium species and amine **10** as the major identified organic compound. This amine would come from the attack of the non-bulky *n*-butylamine on the hindered benzylidene. With more sterically hindered amines **b**–**d**, the ruthenium complexes **11b**–**d**, resulting from phosphine displacement, proved to be stable even after 24 h at 60 °C (Scheme 4).

The half-life of methylidene **2** derived from GII in the presence of the amines were then evaluated using NMR experiments [45]. The steric hindrance of the amine appeared to be a critical parameter. The non-bulky primary amine *n*-butylamine (**a**) induced a fast decomposition of the methylidene **2** (Table 1, entry 1) whereas secondary amines such as pyrrolidine (**b**) and morpholine (**c**) are less detrimental to the catalyst (Table 1, entries 2 and 3). Interestingly the sp^2 amine DBU did not induce any decomposition of the methylidene intermediate (Table 1, entry 4).

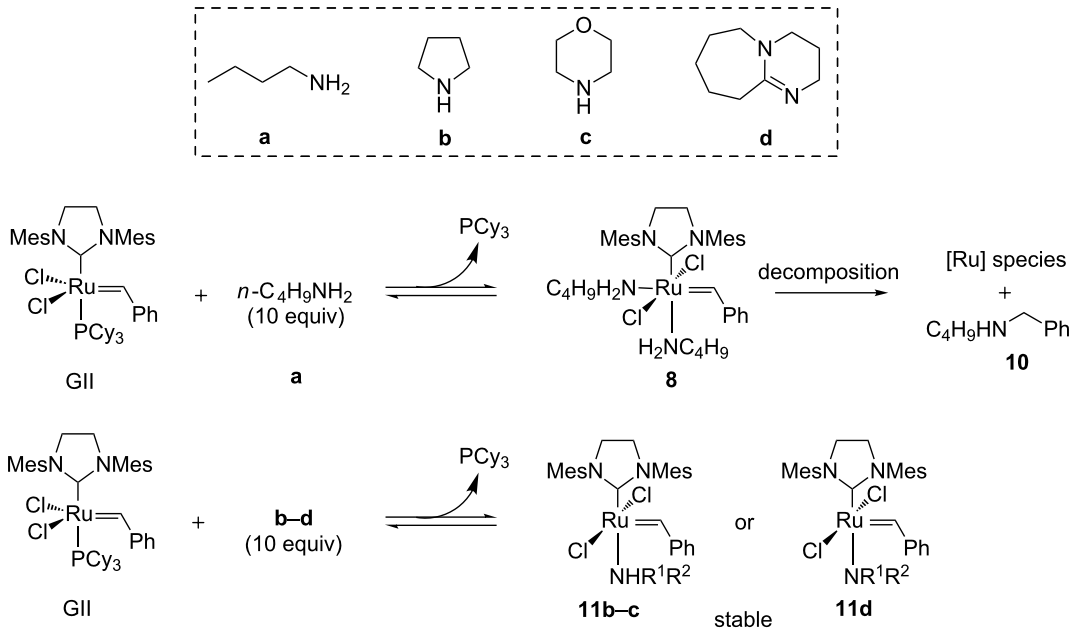

Scheme 4: Reaction of GII with amines **a**–**d**.

Table 1: Decomposition of methylidene **2** in the presence of amines **a**–**d**.

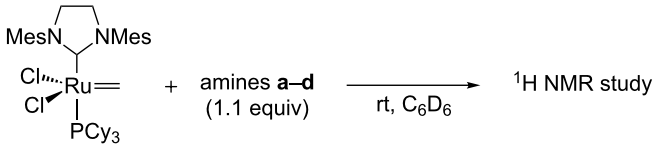

Entry	Amine	Half-life
1	*n*-$C_4H_9NH_2$ (**a**)	12 min
2	pyrrolidine (**b**)	1.5 h
3	morpholine (**c**)	14 h
4	DBU (**d**)	>24 h

In all decomposition cases, the main identified product was the phosphonium $CH_3PCy_3^+Cl^-$ that would result from a nucleophile attack of the free PCy_3 liberated through ligand exchange on the methylidene **2** (Scheme 5).

To complete their study, the authors examined the influence of the amines on the GII-catalyzed RCM of diene **13** [45]. In the presence of amines **a**–**c**, decomposition was observed and $CH_3PCy_3^+Cl^-$ was generated. Interestingly, in the presence of

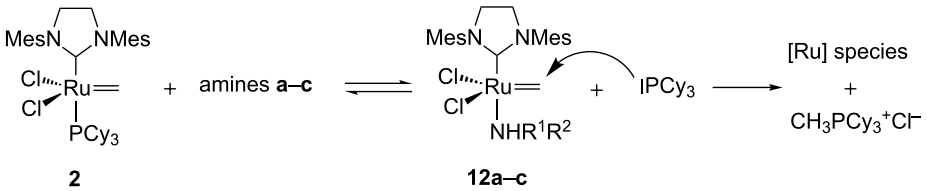

Scheme 5: Amine-induced decomposition of GII methylidene **2**.

DBU, fast decomposition of the catalyst was noticed and only the presence of free PCy_3 could be observed. According to the previous experiments, DBU was not able to decompose the methylidene resting-state and, consequently, a deprotonation of the metallacyclobutane **15** was hypothesized (Scheme 6).

The influence of pyridine as an additive on the deactivation of the metathesis catalyst has not been yet studied in detail [44]. When reacted with an excess of pyridine, the methylidene adduct **2** obtained from GII led to the formation of inactive complex **16** together with $CH_3PCy_3^+Cl^-$. These products would result from a ligand exchange followed by a nucleophilic attack of PCy_3 on the methylidene intermediate (Scheme 7).

Very recently, the amine-induced deactivation of G-HII catalyst was studied by Fogg et al. [46]. When G-HII was treated with an excess of various amines **a**–**e** (10 equiv), comparable results with those obtained with GII were obtained. In the presence of a non-bulky primary amine such as *n*-butylamine, the bis-aminobenzylidene **17** was formed and complete decomposition was noticed after 12 h at rt yielding ruthenium complex **18** and amine **10**. In the presence of secondary amines **b** and **c** and sp^2 amine **d**, ruthenium complexes **19b**–**d** possessing one amine were formed and proved to be thermally stable. When the G-HII catalyst was treated with pyridine (**e**), the stable bis-pyridyl adduct **20e** was formed in equilibrium with G-HII and no significant decomposition of the catalyst was observed (Scheme 8).

In contrast, the addition of amino additives such as pyridine, morpholine, Et_3N or DBU was shown to be detrimental to the G-HII-catalyzed dimerization of styrene (Table 2). Moderate to

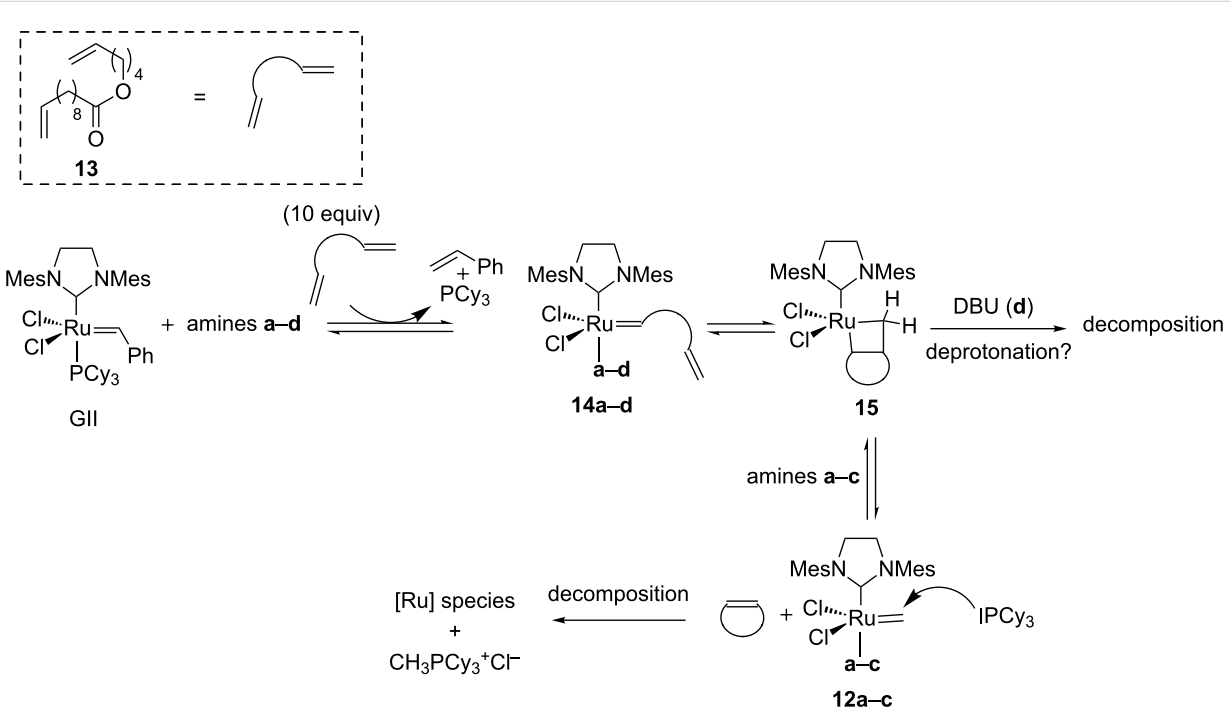

Scheme 6: Amine-induced decomposition of GII in RCM conditions.

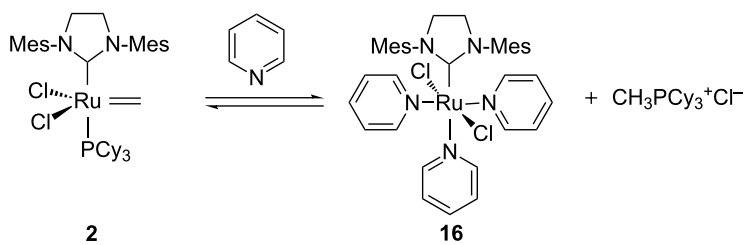

Scheme 7: Deactivation of methylidene **2** in the presence of pyridine.

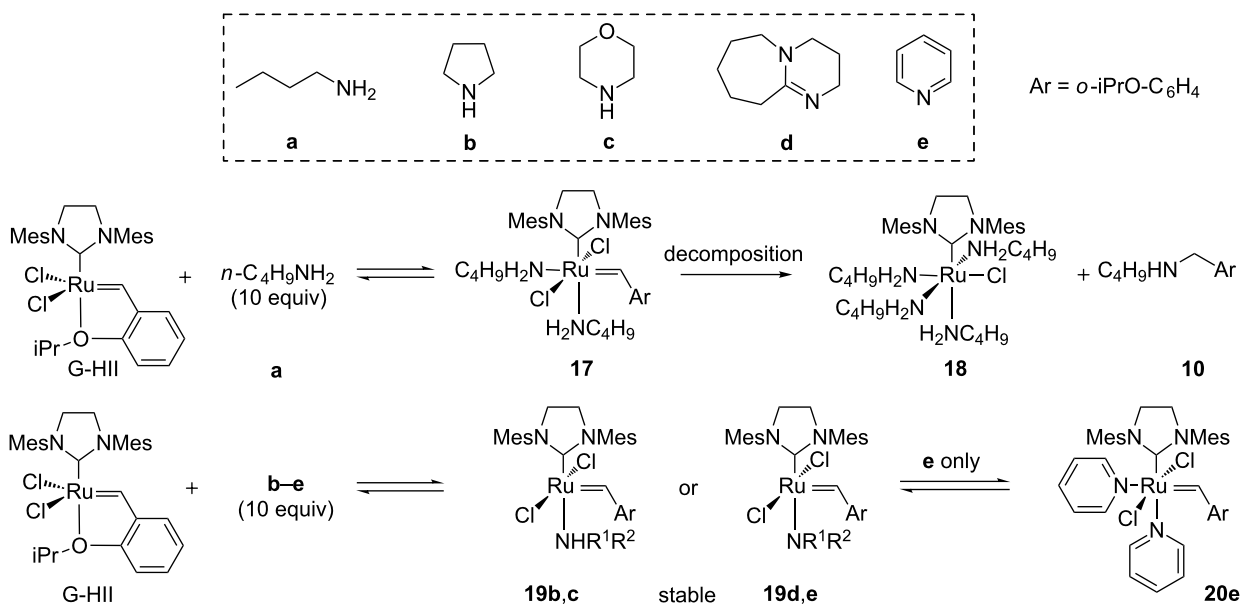

Scheme 8: Reaction of G-HII with various amines.

poor yields in stilbene **7'** were obtained and the value of the yields was correlated with the pK_a of the couple ammonium/amine. An increased Brønsted basicity of the amine seemed to induce a faster deactivation of the catalyst.

Table 2: Impact of amino additives on the CM of styrene.

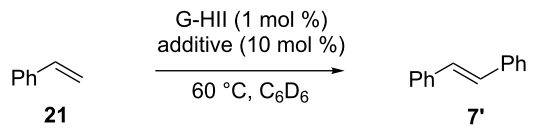

Entry	Additive	pK_a[a]	Yield
1	none	–	94%
2	pyridine	12.6	45%
3	morpholine	16.6	18%
4	Et_3N	18.5	9%
5	pyrrolidine	19.6	<5%
6	DBU	24.1	<5%

[a]pK_a of the conjugate acid in CH_3CN.

In addition, when the self-metathesis of styrene was performed in the presence of pyrrolidine, DBU or Et_3N, olefin **22** was formed as the major product (Scheme 9).

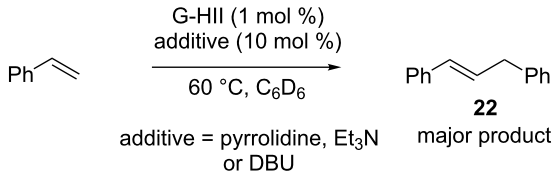

Scheme 9: Formation of olefin **22** from styrene.

To explain these observations, a deactivation mechanism involving a deprotonation of the metallacyclobutane intermediate **23** was hypothesized. The resulting anionic ruthenium complex **24** would be protonated and, after elimination, alkene **22** and unidentified ruthenium complexes would be produced (Scheme 10).

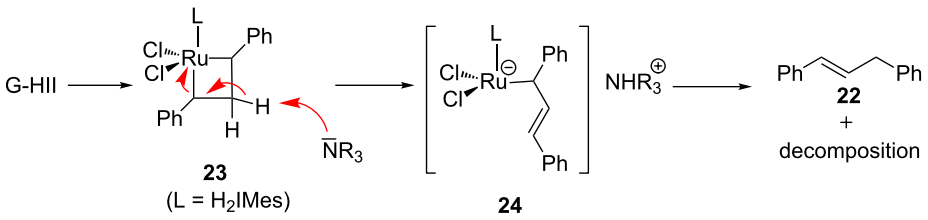

Scheme 10: Hypothetic deactivation pathway of G-HII.

According to these mechanistic investigations, several pathways are involved in the amine-induced catalyst decomposition depending on the nature of the amine and of the ruthenium complex. Non-bulky primary amines can attack directly benzylidene species and are responsible for the fast degradation of the catalyst. In the case of a phosphine-containing catalyst such as GII, secondary amines exchange with PCy_3 and the free phosphine can perform a nucleophilic attack on the methylidene intermediate triggering its decomposition. In contrast, sp^2 amines such as DBU seem rather to react with the metallacyclobutane intermediate. In the case of G-HII catalyst, a deprotonation of the metallacyclobutane is hypothesized to explain the amine-induced decomposition (Table 3). Consequently, a modulation of the Brønsted basicity and/or the nucleophilicity of the amine/*N*-heteroaromatic present on an alkene may allow its use in metathesis reactions.

Ring-closing metathesis

Formation of pyridinium/imidazolium salt prior to metathesis

Most of the examples of RCM involving substrates that possess a pyridine ring relied on the pre-requisite formation of a pyridinium salt. In 2004, Vaquero et al. reported the synthesis of dihydroquinolizium cations through RCM of dienic pyridinium salts in the presence of the GII catalyst (Scheme 11) [47]. The formation of seven- and eight-membered rings required high dilution. Few years later, the same authors showed that it was possible to oxidize 3,4-dihydroquinolizinium salts into their quinolizinium counterparts using Pd/C at high temperature (Scheme 11) [48].

This method was used to prepare polycyclic scaffolds that can be encountered in diverse alkaloid natural products such as coralyne and berberine (Scheme 12) [49].

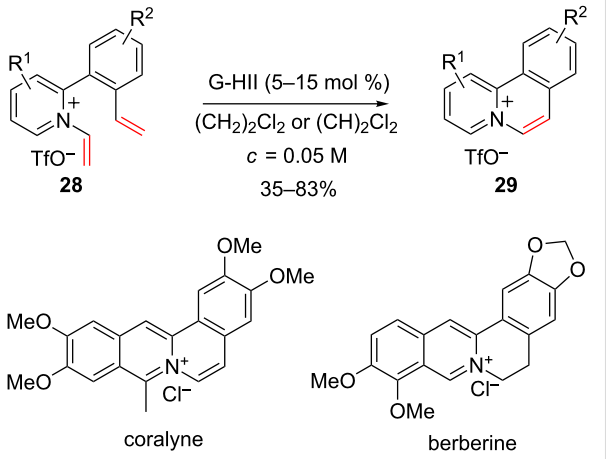

Scheme 12: Synthesis of polycyclic scaffolds using RCM.

Similarly, enyne ring-closing metathesis reactions were performed to access a variety of vinyl-3,4-dihydroquinolizinium salts (Scheme 13) [50].

In their synthetic approach towards (*R*)-(+)-muscopyridine, Fürstner and Leitner have constructed the 13-membered ring macrocycle using a RCM applied to diene **34** [51]. In order to avoid the catalyst deactivation due to the presence of the pyridine moiety, the precursor **34** was first treated with HCl to form

Table 3: Amine-induced degradation pathways of GII and G-HII.

	GII	G-HII
Primary amine	Nucleophilic attack on the benzylidene and/or methylidene **2**	Nucleophilic attack on the benzylidene and/or methylidene
Secondary amine	Ligand exchange and nucleophilic attack of free PCy_3 on the methylidene **2**	Deprotonation of the metallacyclobutane **23**
sp^2 amine	Nucleophilic attack and/or deprotonation of the metallacyclobutane **15**	Deprotonation of the metallacyclobutane **23**

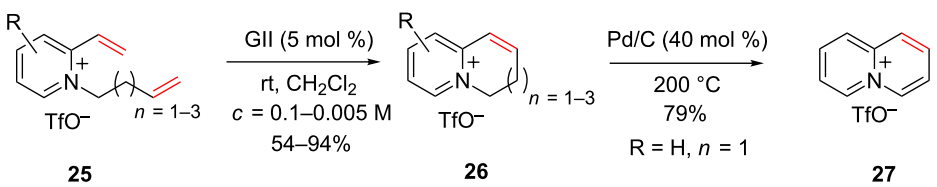

Scheme 11: RCM of dienic pyridinium salts.

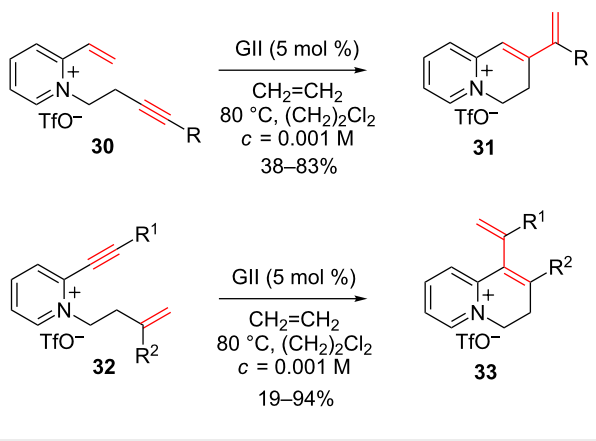

Scheme 13: Enyne ring-closing metathesis.

the corresponding hydrochloride salt which was then reacted with the ruthenium catalyst **36** under diluted conditions to deliver **35**. After reduction of the double bond, the targeted (*R*)-(+)-muscopyridine was isolated (Scheme 14).

A similar strategy was used in the synthesis of the tris-pyrrole macrocyclic pigment nonylprodigiosin [52]. A preliminary protonation of the tris-pyrrole followed by a RCM applied to **37** in the presence of the ruthenium catalyst **36** gave the macrocycle **38**, which was then transformed into the saturated derivative **39** using the Wilkinson's catalyst (Scheme 15).

The use of an acidic additive also allowed the synthesis of fused bicyclic imidazoles through a GII-catalyzed RCM reaction (Scheme 16) [53].

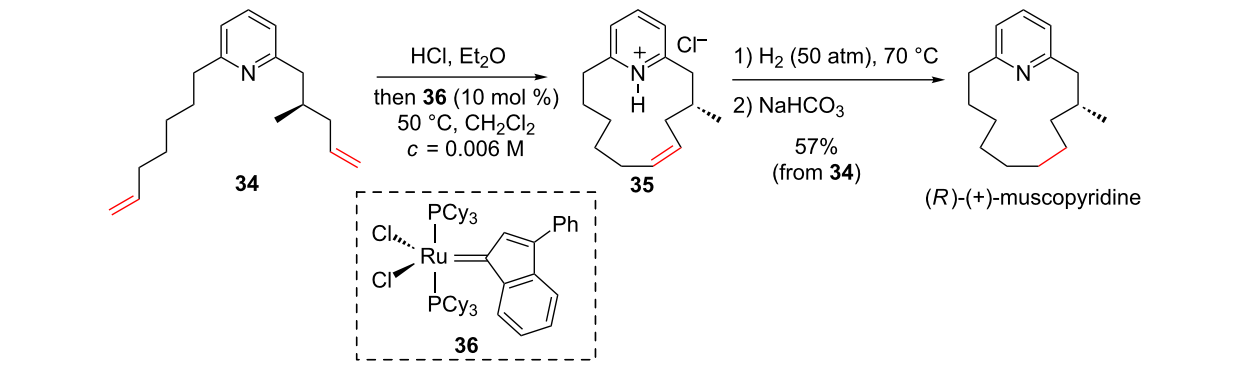

Scheme 14: Synthesis of (*R*)-(+)-muscopyridine using a RCM strategy.

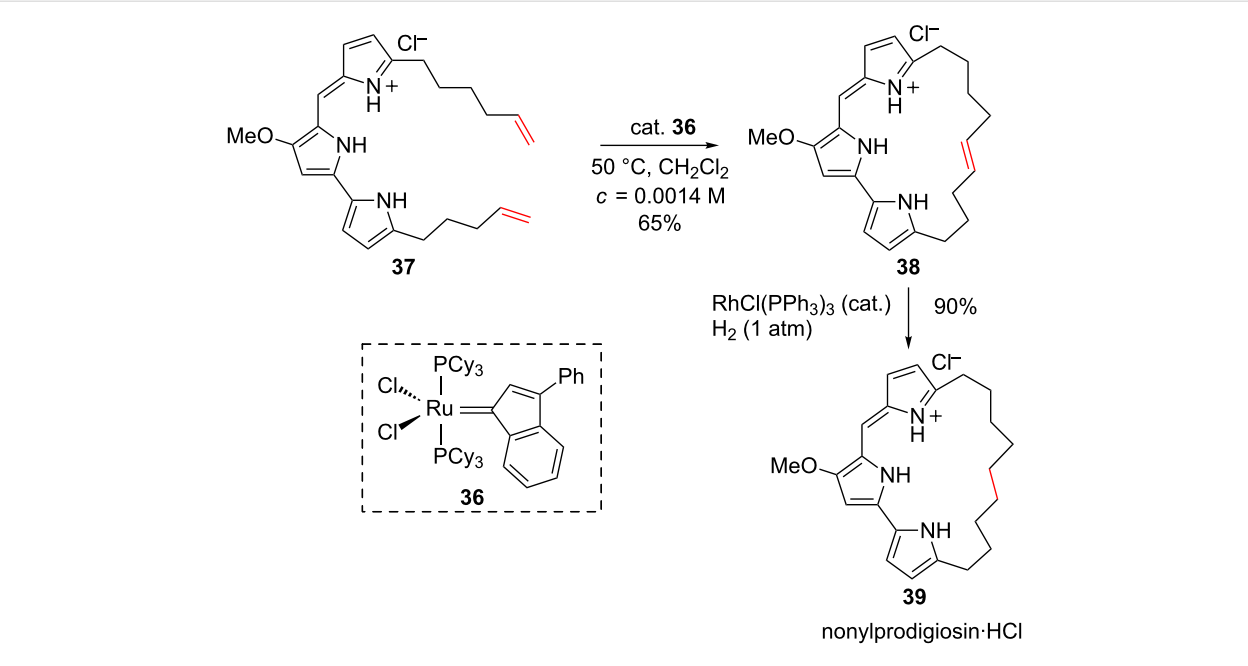

Scheme 15: Synthesis of a tris-pyrrole macrocycle.

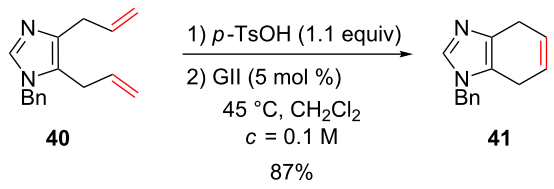

Scheme 16: Synthesis of a bicyclic imidazole.

Only few examples of RCM involving dienes that contain *N*-heteroaromatics were described on non-protonated species. In 2001, in the course of their studies towards ergot alkaloids synthesis, Martin and co-workers used a RCM to form the tetracyclic compound **43** incorporating an indole moiety. A poor yield was obtained in the presence of the GI catalyst and the more reactive Schrock complex **44** had to be used instead. Worthy of note, the indole was protected as a tosylamide and the GI deactivation may be caused by the tertiary amine (Scheme 17) [54,55].

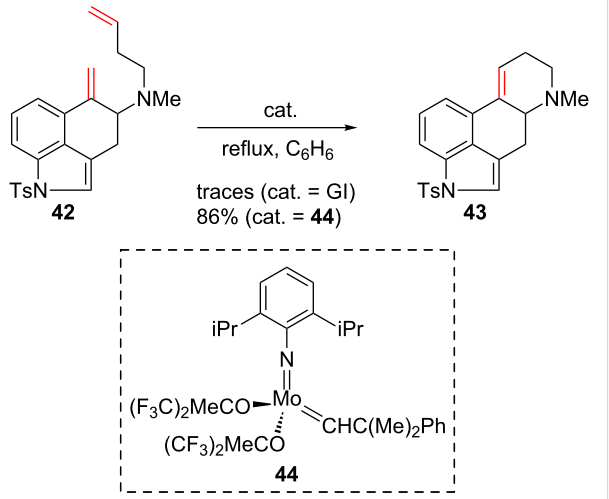

Scheme 17: RCM using Schrock's catalyst **44**.

It should be noted that *N*-heteroaromatics substituted either by bulky or electron-withdrawing groups are involved. In 2004, Billing and co-workers employed a RCM strategy to construct 1,6-pyrido-diazocine **46** with an excellent yield of 94% (Scheme 18) [56]. The presence of the two sulfonamide substituents on the pyridyl ring might decrease the basicity of the nitrogen atom thus allowing the metathesis to proceed. Steric hindrance due to the C2 substitution may also prevent the pyridine-induced catalyst deactivation.

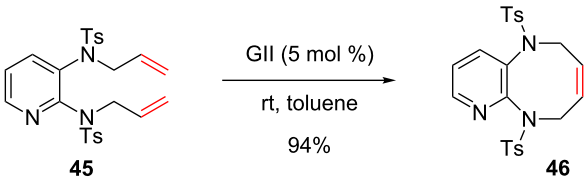

Scheme 18: Synthesis of 1,6-pyrido-diazocine **46** by using a RCM.

Grimaud et al. described the formation of fused pyrimido-azepines from bisallylic substrates using a G-HII-catalyzed RCM [57,58]. When **47** was treated with 10 mol % of G-HII at rt in toluene, the seven-membered ring product **48** was obtained, whereas at 110 °C the isomerized compound **49** was isolated (Scheme 19). It should be noted that in all cases, tetra-substituted pyrimidines were involved in the RCM and the substituents in the α position of the *N*-heteroatoms might have a role in the success of these reactions by causing steric hindrance around the nitrogen and thus preventing the catalyst deactivation.

In 2013, Moss generalized the method to the formation of azepines fused with a variety of heteroaromatics including pyrimidines, pyridines, thiazoles and pyrrazoles [59]. Interestingly, most of the heteroaryls possess a chlorine substituent but no explanation was given concerning its putative role in the success of the RCM (Scheme 20). It should be proposed that the chlorine atoms decrease the basicity of *N*-heteromatics through electron-withdrawing effects and thus reduce the catalyst deactivation. In addition, as chlorine atoms are present in the α position regarding to the nitrogen atom, steric effects cannot be neglected.

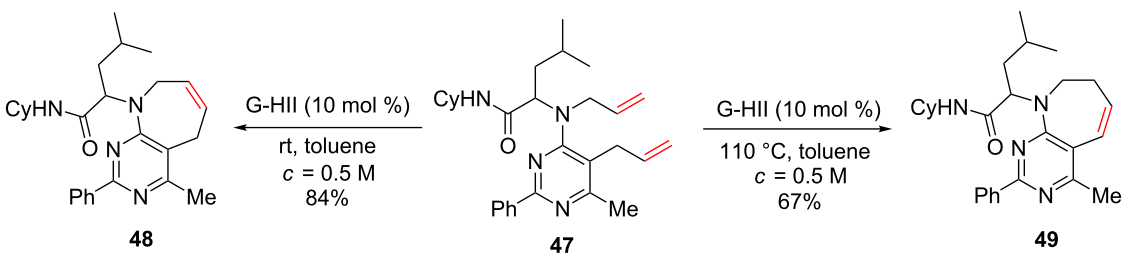

Scheme 19: Synthesis of fused pyrimido-azepines through RCM.

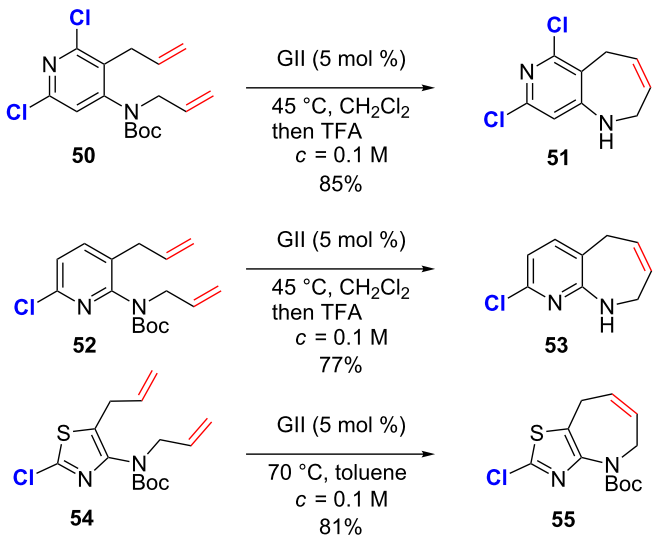

Scheme 20: RCM involving alkenes containing various *N*-heteroaromatics.

Another example of RCM involving alkenes that possess 2-chloropyridines was reported to produce dihydroisoquinoline **57** from 2,6-dichloro-3,4-diallylpyridine (**56**) [60]. The addition of benzoquinone prevented the isomerization of the double bond and it may be suspected that the presence of the two chlorine atoms significantly decreased the basicity of the pyridine (Scheme 21).

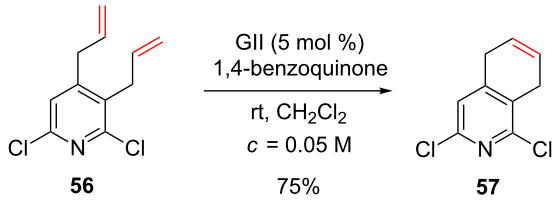

Scheme 21: Synthesis of dihydroisoquinoline using a RCM.

Tricyclic compound **59** was prepared by a RCM of diene **58** that incorporates a quinoline moiety [61]. In this case, a phenyl group was present at C2 and may be responsible for avoiding the nitrogen-induced deactivation of the catalyst by both electronic and steric effects (Scheme 22).

Macrocycles embedding *N*-heteroaromatics have been prepared using a RCM reaction. Shirbate et al. used a RCM to synthesize normuscopyridine and analogues [62]. When a diastereomeric mixture of 2,6-disubstituted pyridine **60** was treated with GI, the expected macrocycle **61** was obtained (51%) together with the dimeric cyclophane **62** (20%). The authors explained that the sulfone moieties facilitated the RCM by steering the alkenyl chains into a favorable conformation, but it also may be hypothesized that the steric hindrance caused by the sulfone groups might reduce the ability of the nitrogen atom in deactivating the ruthenium catalyst. A desulfonylation followed by a hydrogenation of the double bond afforded normuscopyridine (Scheme 23).

Other syntheses of cyclophanes using RCM were reported in the literature. Macrocycle **64** was obtained from diene **63** in good yield in the presence of the GI catalyst under diluted conditions [63]. Once again, the presence of the two alkoxy substituents at the C2 position of the pyridyl rings might not be innocent in the success of the RCM and steric hindrance may be invoked to explain the absence of catalyst deactivation (Scheme 24).

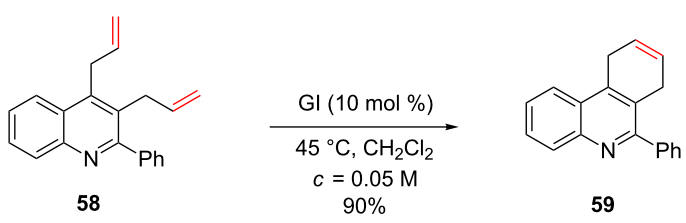

Scheme 22: Formation of tricyclic compound **59**.

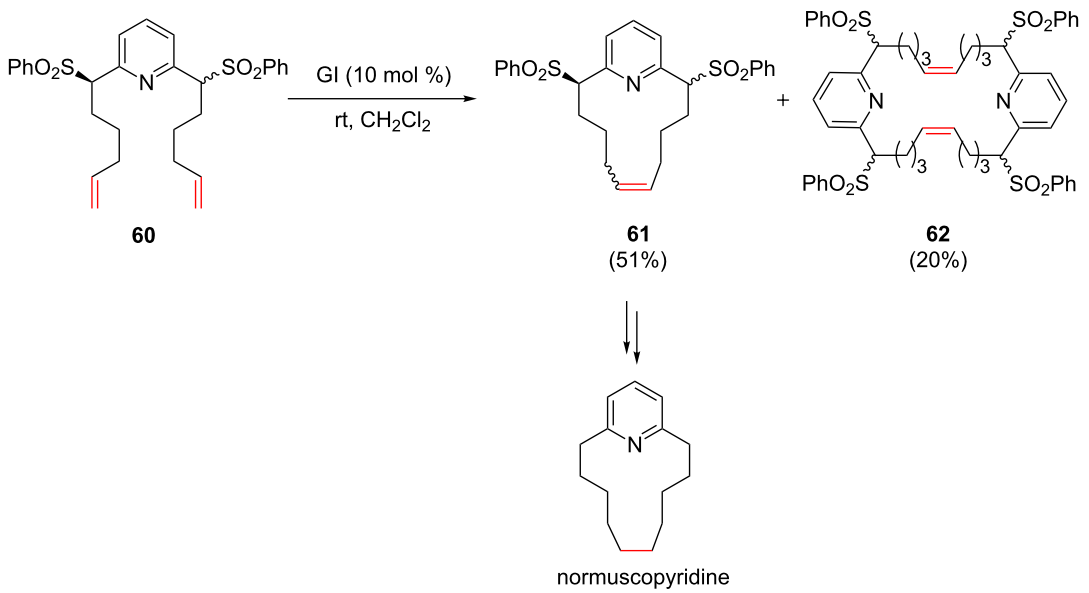

Scheme 23: RCM in the synthesis of normuscopyridine.

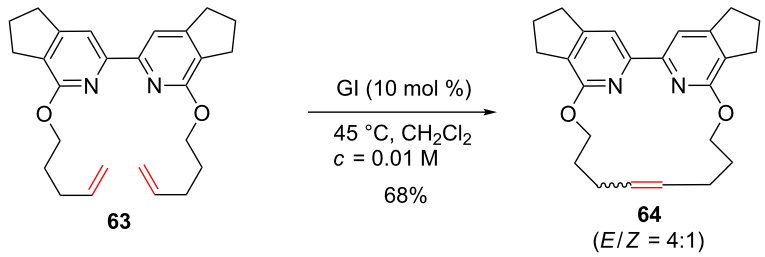

Scheme 24: Synthesis of macrocycle **64**.

Similarly, 15- to 18-membered ring macrocycles that incorporate an imidazole group were synthesized using a RCM of the corresponding dienes using GII as the catalyst (Scheme 25) [64-66].

By examining all these examples of successful RCM involving alkenes containing *N*-heteroaromatics, it seems that decreasing their Brønsted basicity and/or their nucleophilicity through the introduction of suitable electron-withdrawing and/or bulky substituents may prevent the catalyst deactivation thus allowing the metathesis to proceed.

Cross-metathesis

Examples of CM that involve an alkene containing *N*-heteroaromatics as one of the two partners are scarce [67-70]. In 2004, Zhang and co-workers planned to use a cross-metathesis

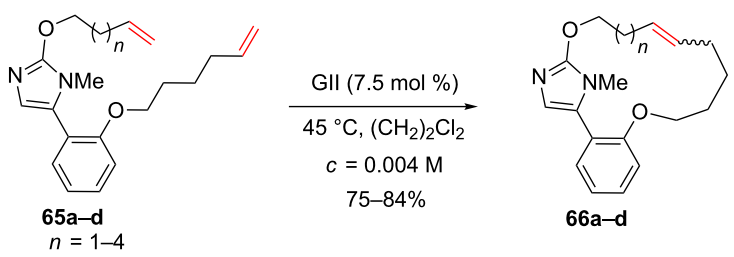

Scheme 25: Synthesis of macrocycles possessing an imidazole group.

between **67** and vinylquinoline **68** in order to synthesize ABT-773, an analogue of erythromycin possessing a 6-*O*-propenylquinoline side chain (Scheme 26) [71-74].

The cross-metathesis between **67** and vinylquinoline **68** in the presence of the GI catalyst was investigated and the authors showed that the success of the reaction required either long reaction time (168 h) (Table 4, entry 1), high catalyst loading (25 mol %) (Table 4, entry 2) or an excess of the precious macrolide (3 equiv) (Table 4, entry 3). Using an excess of the vinylquinoline **68** (5 equiv) was detrimental to the reaction as **69** was isolated in a poor yield of 23%. This observation might be explained by the deactivation of the GI catalyst caused by the quinoline (Table 4, entry 4).

In their retrosynthesis of haminol A, O'Neil et al. initially envisionned to access the trienic compound using a cross-metathesis/benzoyloxysulfone elimination sequence. The CM would involve 3-vinylpyridine **70** as one of the two partners (Scheme 27) [75].

As the 3-vinylpyridine **70** was far less precious compared to alkene **71**, it was used in excess in order to favor the CM product over homodimers. However, no reaction occurred neither with GI nor with GII catalysts and the starting materials were recovered. This absence of reactivity was attributed to the deactivation of the ruthenium catalyst due to the excess of pyridine in the reaction medium. Indeed, a successful metathesis was performed between 3-vinylpyridine (**70**) and a large excess of

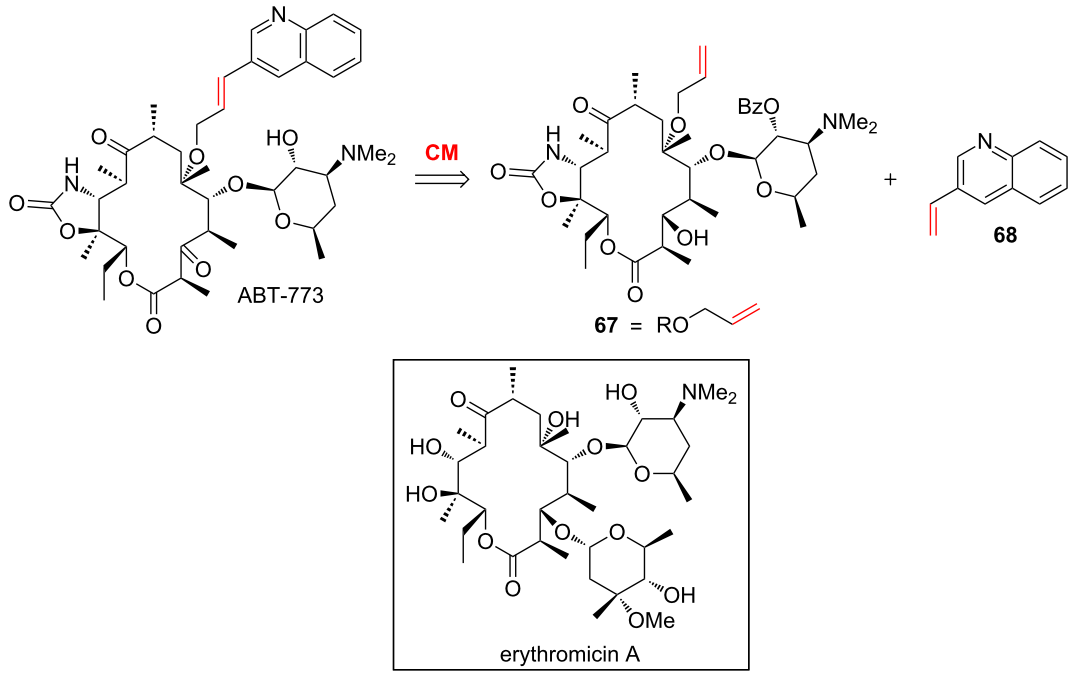

Scheme 26: Retrosynthesis of an analogue of erythromycin.

Table 4: CM between vinylquinoline and an *O*-allyl-protected erythronolide derivative.

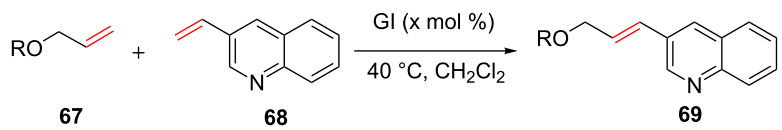

67 **68** **69**

Entry	**67** (equiv)	**68** (equiv)	Time (h)	GI (mol %)	**69** (yield)
1	1	2	168	10	71%
2	1	2	65	25	75%
3	3	1	65	10	79%
4	1	5	20	10	23%

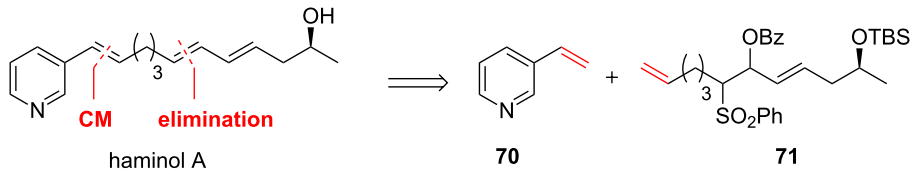

Scheme 27: Retrosynthesis of haminol A.

cis-1,4-diacetoxy-2-butene (**73**, 10 equiv) delivering the corresponding alkene **74** in 85% yield (Scheme 28).

As the use of a large excess of the functionalized alkene partner **71** was not attractive, the authors revised their synthetic strategy and finally installed the triene moiety by means of a double benzoyloxysulfone elimination applied to compound **76** which was prepared from aldehyde **77** (Scheme 29).

Aldehyde **77** was assembled by a CM between alkene **78** and crotonaldehyde (**79**). It should be noted that in this case, the CM proceeded smoothly delivering the desired olefin in 78% yield despite the presence of the pyridine. Worthy of note, the amount of crotonaldehyde added in the reaction was not given in the article (Scheme 30).

Based on NMR studies, the formation of an inactive ruthenium pyridylalkylidene **80** resulting from a reaction between GII and the vinylpyridine in excess was hypothesized to be the cause of the deactivation of the catalyst (Scheme 31). The use of a large excess of the alkene partner such as *cis*-1,4-diacetoxy-2-butene may statistically prevent the formation of **80** thus allowing the CM to occur.

In 2010, Harding et al. attempted to use reversible aqueous metathesis for the construction of a dynamic combinatorial

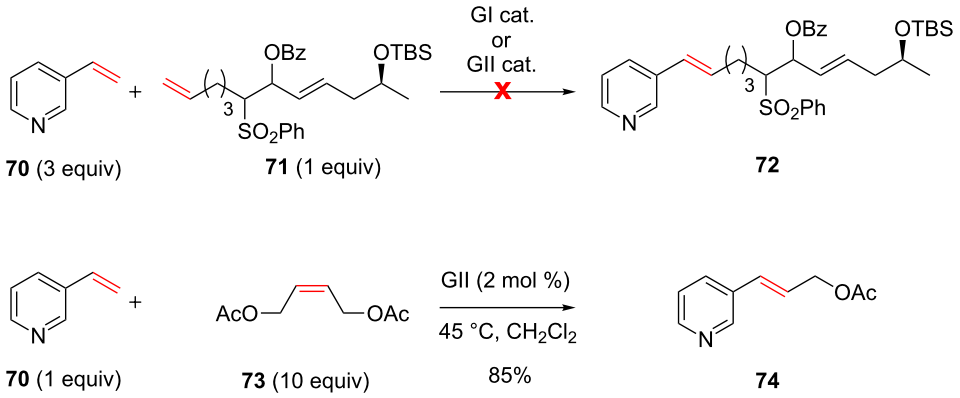

Scheme 28: CM involving 3-vinylpyridine **70** with **71** and vinylpyridine **70** with **73**.

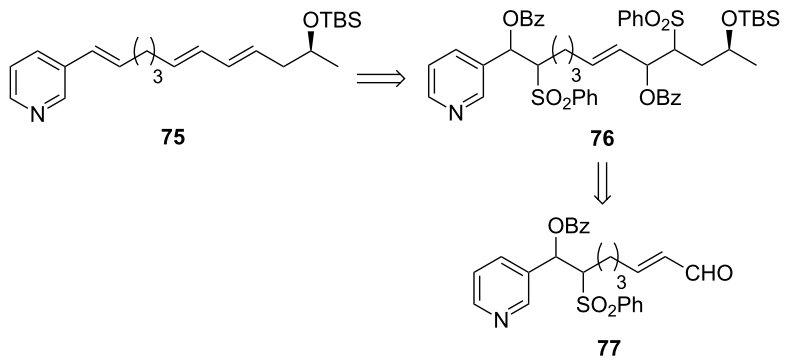

Scheme 29: Revised retrosynthesis of haminol A.

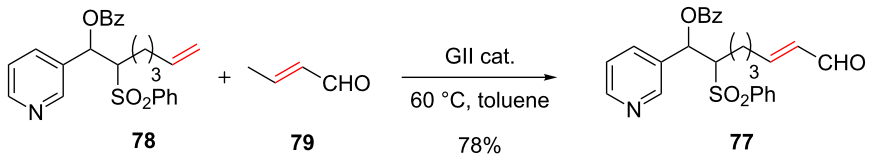

Scheme 30: CM between **78** and crotonaldehyde.

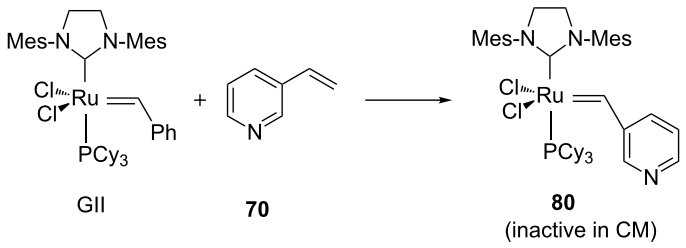

Scheme 31: Hypothesized deactivation pathway.

library aimed at identifying DNA ligands [76]. Toward that goal, biologically relevant conditions were selected (rt, *t*-BuOH/H_2O) and CM involving allyl sulfides that contain functional groups commonly found in DNA-intercalators and *N*-heteroaromatics were investigated. When a quinoline was present on the allylic sulfide, allylic alcohol was found to be the unique suitable partner among the tested olefins. In addition, 20 equiv of allylic alcohol were required and the CM product was obtained in a moderate 53% yield. Cross-metathesis of **81** with amide **83** or alkene **85** gave no conversion (Scheme 32).

In the presence of a quinoxaline moiety on the allyl sulfide, the CM reaction with allylic alcohol delivered **88** in a low 31% yield and when an alkene containing a phenanthroline was used, no reaction occurred. By the light of the previously reported observations, these results could be imputed to the deactivation

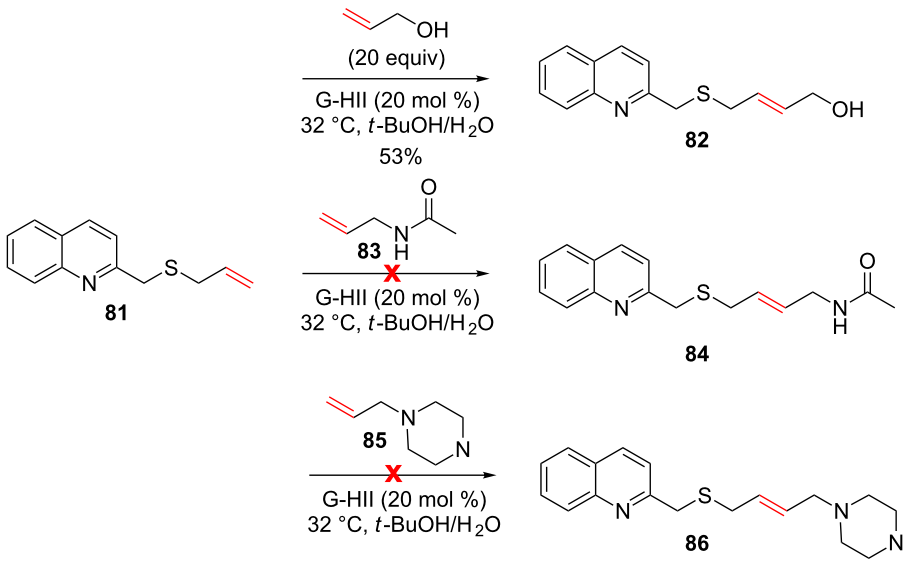

Scheme 32: CM involving an allyl sulfide containing a quinoline.

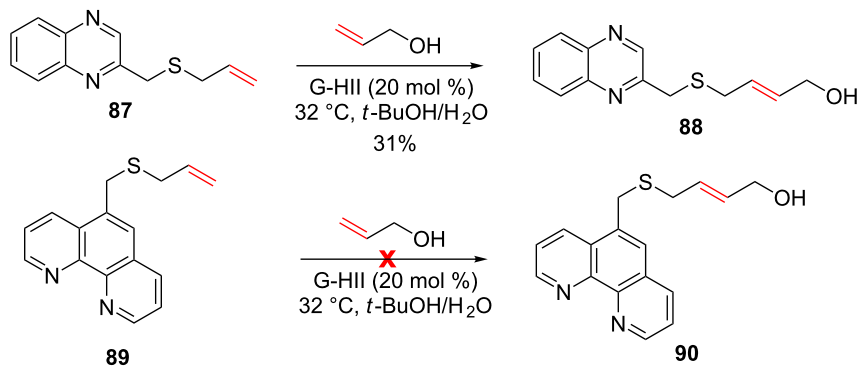

Scheme 33: CM involving allylic sulfide possessing a quinoxaline or a phenanthroline.

of the ruthenium catalyst caused by *N*-heteroaromatics (Scheme 33).

One of the rare successful example of CM involving alkene containing a pyridine moiety was reported by Sarpong et al. in their total synthesis of (±)-lyconadin A [77]. Alkene **91** was coupled with ethyl acrylate (5 equiv) using a catalytic amount of the G-HII catalyst to give **92** with a very good yield of 88% (Scheme 34).

It should be noted that, in this case, the pyridyl ring is substituted by a methoxy group and a bromide and these substituents might be non-innocent in the success of the CM. The presence of 2 substituents at C2 and C6 may cause steric hindrance and the bromine atom at C3 may decrease the basicity of the nitrogen atom through inductive effect. Indeed, in a recent study published by our group, it was demonstrated that successful CM involving alkenes that contain *N*-heteroaromatics could be performed by the introduction of a suitable electron-withdrawing group on the *N*-heteroaryl ring [78]. When olefin **93**, bearing a pyridine without any substituent at C2 or C6, was treated with methyl acrylate in the presence of G-HII catalyst no reaction took place and the starting material was fully recovered. By contrast, the presence of a chlorine substituent at C2 on the pyridyl ring restored the reactivity of the olefin in the CM as the expected product was isolated in 84% yield (Scheme 35). We hypothesized that the presence of the chlorine atom modulates the Lewis and/or Brønsted basicity of the nitrogen atom, thus preventing the deactivation of the ruthenium catalyst (vide infra).

Various substituents on the pyridyl ring such as halides, trifluoromethyl or triflate groups were found to be suitable basicity modulators and the alkenes containing the corresponding disubstituted pyridines were efficiently coupled to methyl acrylate by utilizing a CM reaction. In addition, steric hindrance next to the nitrogen atom could also play a role by decreasing the nucleophilicity of the nitrogen as attested by the formation of alkene **98f** in a moderate 52% yield (Scheme 36).

This strategy was applied to the formation of a broad variety of disubstituted olefins containing *N*-heteroaromatic moieties such as pyridines, pyrimidines, imidazoles and pyrazoles (Scheme 37).

From the selected examples discussed above, we tried to delineate some trends regarding to the use of alkenes possessing *N*-heteroaromatics in RCM and CM. In RCM, GI and GII are

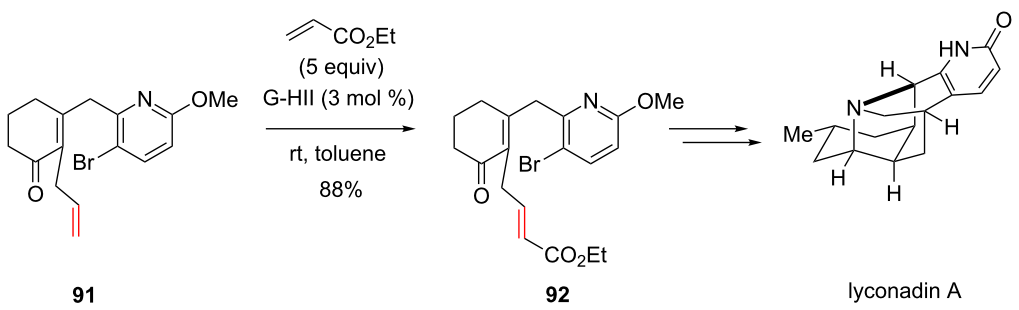

Scheme 34: CM between an acrylate and a 2-methoxy-5-bromo pyridine.

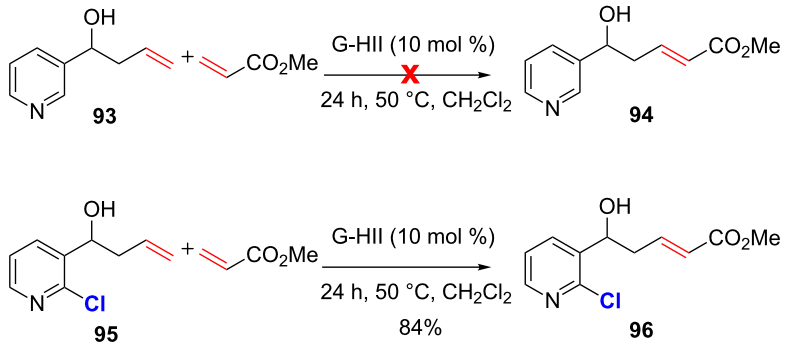

Scheme 35: Successful CM of an alkene containing a 2-chloropyridine.

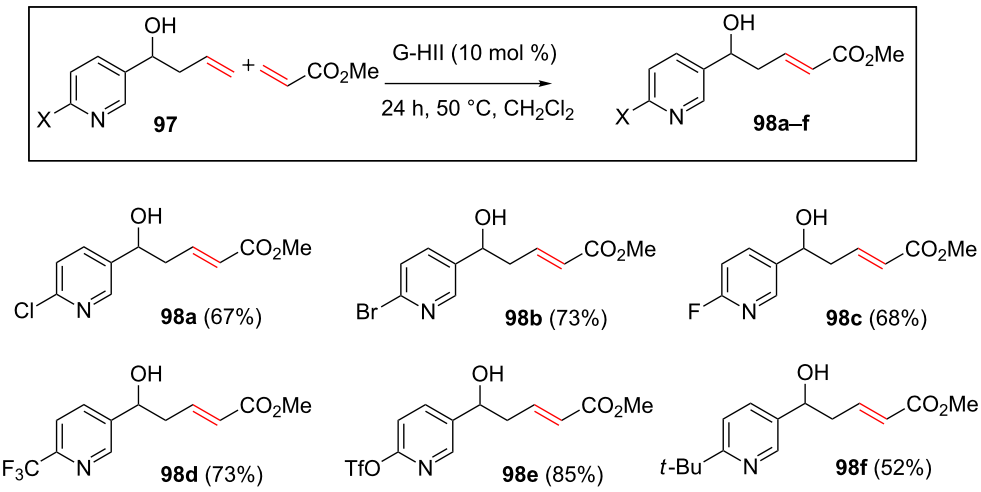

Scheme 36: Variation of the substituent on the pyridine ring.

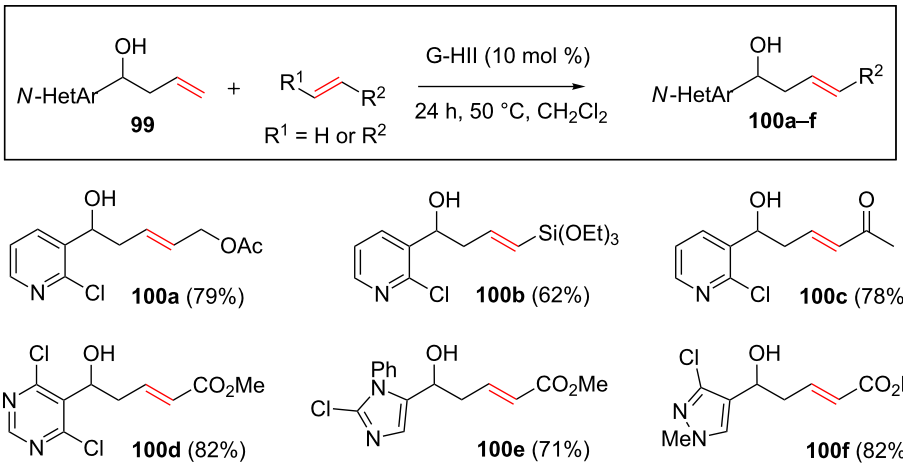

Scheme 37: CM involving alkenes containing a variety of *N*-heteroaromatics.

usually preferred and diluted conditions are recommended to avoid dimerization. The most studied strategy allowing the use of olefins bearing *N*-heteroaromatics is the formation of the *N*-heteroaromatic salt prior to metathesis. The salt can be either isolated before metathesis or formed in situ using acidic additives. Alternatively, introduction of bulky and/or electron-withdrawing substituents on the *N*-heteroaromatic ring allows the metathesis to proceed by preventing nitrogen-induced catalyst deactivation. However, no general study dealing with the influence of the *N*-heteroaromatic substituents on the outcome of the RCM has been led so far. In CM, G-HII may be considered as the most potent catalyst even if some examples involving GII catalyst are described in the literature. Two strategies can be adopted to use olefins possessing *N*-heteroaromatics as one of the partner. When the second partner is non-expensive, it can be introduced in large excess thus avoiding the *N*-heteroaromatic induced catalyst deactivation. As an alternative, bulky and/or electron-withdrawing substituents can be introduced on the *N*-heteroaromatic to reduce the basicity of the nitrogen atom and thus the deactivation. This strategy appears as the most promising especially as a simple chlorine substituent is sufficient to allow the metathesis to proceed (Table 5).

Conclusion

N-Heteroaromatics are known to have a deleterious impact on metathesis by inducing ruthenium catalysts deactivation. Based on NMR and kinetic mechanistic studies, Lewis and/or Brønsted basicity of amines appeared to be responsible for the degradation of the catalyst. The most common solution proposed to circumvent the problem is the protonation of the nitrogen atom of *N*-heteroaromatics prior to the metathesis that can then be carried out using the corresponding salts. By close examination of the successful metatheses involving alkenes that possess non-protonated *N*-heteroaromatics, the presence of electron-withdrawing and/or bulky substituents on the heteroarene was noticed to be beneficial. These substituents can allow a fine tuning of the basicity and/or nucleophilicity of the nitrogen thus preventing the catalyst deactivation. By unravelling catalyst deactivation pathways, mechanistic investigations could help to extend the scope of the metathesis reactions to alkenes containing *N*-heteroaromatics, thus overcoming one major barrier to the widespread use of metathesis, particularly for industrial purposes.

References

1. Fürstner, A. *Alkene Metathesis in Organic Synthesis;* Springer: Berlin, 1998.
2. Grubbs, R. H.; Wenzel, A. G.; O'Leary, D. J.; Khosravi, E., Eds. *Handbook of Metathesis,* 2nd ed.; Wiley-VCH: Weinheim, 2015. doi:10.1002/9783527674107
3. Grela, K. *Olefin Metathesis. Theory and Practise;* Wiley, 2014. doi:10.1002/9781118711613
4. Fürstner, A. *Angew. Chem., Int. Ed.* **2000,** *39,* 3012. doi:10.1002/1521-3773(20000901)39:17<3012::AID-ANIE3012>3.0.CO;2-G
5. Connon, S. J.; Blechert, S. *Angew. Chem., Int. Ed.* **2003,** *42,* 1900. doi:10.1002/anie.200200556
6. Fürstner, A. *Science* **2013,** *341,* 1229713. doi:10.1126/science.1229713
7. Saito, A.; Hanzawa, Y. *Metathesis Reactions in Drug and Natural Products. Stereoselective Synthesis of Drugs and Natural Products;* Wiley, 2013.
8. Cossy, J.; Arseniyadis, S.; Meyer, C. *Metathesis in Natural Product Synthesis: Strategies, Substrates and Catalysts;* Wiley-VCH: Weinheim, 2010. doi:10.1002/9783527629626.fmatter
9. Cossy, J.; Arseniyadis, S., Eds. *Modern Tools for the Synthesis of Complex Bioactive Molecules;* Wiley, 2012. doi:10.1002/9781118342886
10. Nicolaou, K. C.; Bulger, P. G.; Sarlah, D. *Angew. Chem., Int. Ed.* **2005,** *44,* 4490. doi:10.1002/anie.200500369
11. Dassonneville, B.; Delaude, L.; Demonceau, A.; Dragutan, I.; Dragutan, V.; Etsè, K. S.; Hans, M. *Curr. Org. Chem.* **2013,** *17,* 2609. doi:10.2174/1385272811317220006
12. Bielawski, C. W.; Grubbs, R. H. *Prog. Polym. Sci.* **2007,** *32,* 1. doi:10.1016/j.progpolymsci.2006.08.006
13. Nolan, S.; Clavier, H. *Chem. Soc. Rev.* **2010,** *39,* 3305. doi:10.1039/b912410c
14. Chatterjee, A. K.; Choi, T.-L.; Sanders, D. P.; Grubbs, R. H. *J. Am. Chem. Soc.* **2003,** *125,* 11360. doi:10.1021/ja0214882
15. Hoye, T. R.; Zhao, H. *Org. Lett.* **1999,** *1,* 1123. doi:10.1021/ol990947+
16. Lin, Y. A.; Davis, B. G. *Beilstein J. Org. Chem.* **2010,** *6,* 1219. doi:10.3762/bjoc.6.140
17. Yun, J. I.; Kim, H. R.; Kim, S. K.; Kim, D.; Lee, J. *Tetrahedron* **2012,** *68,* 1177. doi:10.1016/j.tet.2011.11.064
18. Choi, T.-L.; Chatterjee, A. K.; Grubbs, R. H. *Angew. Chem., Int. Ed.* **2001,** *40,* 1277. doi:10.1002/1521-3773(20010401)40:7<1277::AID-ANIE1277>3.0.CO;2-E
19. Hoveyda, H. R.; Vézina, M. *Org. Lett.* **2005,** *7,* 2113. doi:10.1021/ol050387g
20. Donohoe, T. J.; Race, N. J.; Bower, J. F.; Callens, C. K. A. *Org. Lett.* **2010,** *12,* 4094. doi:10.1021/ol101681r
21. Compain, P. *Adv. Synth. Catal.* **2007,** *349,* 1829. doi:10.1002/adsc.200700161

Table 5: Metathesis involving alkenes that contain *N*-heteroaromatics.

Metathesis	Cat.	Conditions	Strategies
RCM	GI or GII	diluted	* *N*-heteroaromatic salt formation prior to CM
CM	G-HII		* Non *N*-heteroaromatic partner in large excess * Bulky and/or electron withdrawing substituent on the *N*-heteroaromatic

22. Chattopadhyay, S. K.; Karmakar, S.; Biswas, T.; Majumdar, K. C.; Rahaman, H.; Roy, B. *Tetrahedron* **2007,** *63,* 3919. doi:10.1016/j.tet.2007.01.063
23. Felpin, F.-X.; Lebreton, J. *Eur. J. Org. Chem.* **2003,** 3693. doi:10.1002/ejoc.200300193
24. Compain, P.; Hazelard, D. *Top. Heterocycl. Chem.* **2015,** 1. doi:10.1007/7081_2014_139
25. Wang, H.; Goodman, S. N.; Dai, Q.; Stockdale, G. W.; Clark, W. M., Jr. *Org. Process Res. Dev.* **2008,** *12,* 226. doi:10.1021/op700288p
26. Yee, N. K.; Farina, V.; Houpis, I. N.; Haddad, N.; Frutos, R. P.; Gallou, F.; Wang, X.-J.; Wei, X.; Simpson, R. D.; Feng, X.; Fuchs, V.; Xu, Y.; Tan, J.; Zhang, L.; Xu, J.; Smith-Keenan, L. L.; Vitous, J.; Ridges, M. D.; Spinelli, E. M.; Johnson, M.; Donsbach, K.; Nicola, T.; Brenner, M.; Winter, E.; Kreye, P.; Samstag, W. *J. Org. Chem.* **2006,** *71,* 7133. doi:10.1021/jo060285j
27. Nomura, H.; Richards, C. J. *Org. Lett.* **2009,** *11,* 2892. doi:10.1021/ol900880w
28. Yoshida, K.; Kawagoe, F.; Hayashi, K.; Horiuchi, S.; Imamoto, T.; Yanagisawa, A. *Org. Lett.* **2009,** *11,* 515. doi:10.1021/ol8023117
29. Dragutan, I.; Dragutan, V.; Demonceau, A. *RSC Adv.* **2012,** *2,* 719. doi:10.1039/C1RA00910A
30. Fu, G. C.; Nguyen, S. T.; Grubbs, R. H. *J. Am. Chem. Soc.* **1993,** *115,* 9856. doi:10.1021/ja00074a085
31. Kirkland, T. A.; Lynn, D. M.; Grubbs, R. H. *J. Org. Chem.* **1998,** *63,* 9904. doi:10.1021/jo981678o
32. Woodward, C. P.; Spiccia, N. D.; Jackson, W. R.; Robinson, A. J. *Chem. Commun.* **2011,** *47,* 779. doi:10.1039/C0CC03716H
33. Nash, A.; Soheili, A.; Tambar, U. K. *Org. Lett.* **2013,** *15,* 4770. doi:10.1021/ol402129h
34. Malik, M.; Witkowski, G.; Ceborska, M.; Jarosz, S. *Org. Lett.* **2013,** *15,* 6214. doi:10.1021/ol403063v
35. Cheng, X.; Waters, S. P. *Org. Lett.* **2010,** *12,* 205. doi:10.1021/ol902455y
36. Vedrenne, E.; Dupont, H.; Oualef, S.; Elkaïm, L.; Grimaud, L. *Synlett* **2005,** 670. doi:10.1055/s-2005-862375
37. Shafi, S.; Kędziorek, M.; Grela, K. *Synlett* **2011,** 124. doi:10.1055/s-0030-1259083
38. This mini-review is restricted to metathesis involving alkenes containing *N*-heteroaromatics. Metathesis reactions involving olefins that include primary or secondary amines have been reviewed elsewhere, see [21].
39. Wilson, G. O.; Porter, K. A.; Weissman, H.; White, S. R.; Sottos, N. R.; Moore, J. S. *Adv. Synth. Catal.* **2009,** *351,* 1817. doi:10.1002/adsc.200900134
40. Sanford, M. S.; Love, J. A.; Grubbs, R. H. *Organometallics* **2001,** *20,* 5314. doi:10.1021/om010599r
41. Bolton, S. L.; Williams, J. E.; Sponsler, M. B. *Organometallics* **2007,** *26,* 2485. doi:10.1021/om061098e
42. Bates, J. M.; Lummiss, J. A. M.; Bailey, G. A.; Fogg, D. E. *ACS Catal.* **2014,** *4,* 2387. doi:10.1021/cs500539m
43. Lummiss, J. A. M.; McClennan, W. L.; McDonald, R.; Fogg, D. E. *Organometallics* **2014,** *33,* 6738. doi:10.1021/om501011y
44. Hong, S. H.; Wenzel, A. G.; Salguero, T. T.; Day, M. W.; Grubbs, R. H. *J. Am. Chem. Soc.* **2007,** *129,* 7961. doi:10.1021/ja0713577
45. Lummiss, J. A. M.; Ireland, B. J.; Sommers, J. M.; Fogg, D. E. *ChemCatChem* **2014,** *6,* 459. doi:10.1002/cctc.201300861
46. Ireland, B. J.; Dobigny, B.; Fogg, D. E. *ACS Catal.* **2015,** *5,* 4690. doi:10.1021/acscatal.5b00813
47. Núñez, A.; Cuadro, A. M.; Alvarez-Builla, J.; Vaquero, J. J. *Org. Lett.* **2004,** *6,* 4125. doi:10.1021/ol048177b
48. Núñez, A.; Abarca, B.; Cuadro, A. M.; Alvarez-Builla, J.; Vaquero, J. J. *J. Org. Chem.* **2009,** *74,* 4166. doi:10.1021/jo900292b
49. Núñez, A.; Cuadro, A. M.; Alvarez-Builla, J.; Vaquero, J. J. *Org. Lett.* **2007,** *9,* 2977. doi:10.1021/ol070773t
50. Núñez, A.; Cuadro, A. M.; Alvarez-Builla, J.; Vaquero, J. J. *Chem. Commun.* **2006,** 2690. doi:10.1039/B602420C
51. Fürstner, A.; Leitner, A. *Angew. Chem., Int. Ed.* **2003,** *42,* 308. doi:10.1002/anie.200390103
52. Fürstner, A.; Grabowski, J.; Lehmann, C. W. *J. Org. Chem.* **1999,** *64,* 8275. doi:10.1021/jo991021i
53. Chen, Y.; Rasika Dias, H. V.; Lovely, C. J. *Tetrahedron Lett.* **2003,** *44,* 1379. doi:10.1016/S0040-4039(02)02864-2
54. Lee, K. L.; Goh, J. B.; Martin, S. F. *Tetrahedron Lett.* **2001,** *42,* 1635. doi:10.1016/S0040-4039(01)00002-8
55. Baker, S. R.; Cases, M.; Keenan, M.; Lewis, R. A.; Tan, P. *Tetrahedron Lett.* **2003,** *44,* 2995. doi:10.1016/S0040-4039(03)00389-7
56. van Otterlo, W. A.; Morgans, G. L.; Khanye, S. D.; Aderibigbe, B. A. A.; Michael, J. P.; Billing, D. G. *Tetrahedron Lett.* **2004,** *45,* 9171. doi:10.1016/j.tetlet.2004.10.108
57. El Kaïm, L.; Grimaud, L.; Oble, J. *J. Org. Chem.* **2007,** *72,* 5835. doi:10.1021/jo070706c
58. Majumdar, K. C.; Mondal, S.; Ghosh, D. *Synthesis* **2010,** 1176. doi:10.1055/s-0029-1219228
59. Moss, T. A. *Tetrahedron Lett.* **2013,** *54,* 993. doi:10.1016/j.tetlet.2012.12.042
60. van den Hoogenband, A.; den Hartog, J. A. J.; Faber-Hilhorst, N.; Lange, J. H. M.; Terpstra, J. W. *Tetrahedron Lett.* **2009,** *50,* 5040. doi:10.1016/j.tetlet.2009.06.101
61. Luo, J.; Huo, Z.; Fu, J.; Jin, F.; Yamamoto, Y. *Org. Biomol. Chem.* **2015,** *13,* 3227. doi:10.1039/C4OB02567A
62. Kotha, S.; Waghule, G. T.; Shirbate, M. E. *Eur. J. Org. Chem.* **2014,** 984. doi:10.1002/ejoc.201301493
63. Branowska, D.; Rykowski, A. *Tetrahedron* **2005,** *61,* 10713. doi:10.1016/j.tet.2005.08.081
64. Van Den Berge, E.; Pospíšil, J.; Trieu-Van, T.; Collard, L.; Robiette, R. *Eur. J. Org. Chem.* **2011,** 6649. doi:10.1002/ejoc.201100805
65. Halland, N.; Blum, H.; Buning, C.; Kohlmann, M.; Lindenschmidt, A. *ACS Med. Chem. Lett.* **2014,** *5,* 193. doi:10.1021/ml4004556
See for other syntheses of macrocyles possessing *N*-heteroaromatics using RCM.
66. Rudd, M. T.; Butcher, J. W.; Nguyen, K. T.; McIntyre, C. J.; Romano, J. J.; Gilbert, K. F.; Bush, K. J.; Liverton, N. J.; Holloway, M. K.; Harper, S.; Ferrara, M.; DiFilippo, M.; Summa, V.; Swestock, J.; Fritzen, J.; Carroll, S. S.; Burlein, C.; DiMuzio, J. M.; Gates, A.; Graham, D. J.; Huang, Q.; McClain, S.; McHale, C.; Stahlhut, M. W.; Black, S.; Chase, R.; Soriano, A.; Fandozzi, C. M.; Taylor, A.; Trainor, N.; Olsen, D. B.; Coleman, P. J.; Ludmerer, S. W.; McCauley, J. A. *ChemMedChem* **2015,** *10,* 727. doi:10.1002/cmdc.201402558
67. Luo, G.; Dubowchik, G. M.; Macor, J. E.; Chen, L. CGRP Receptors Antagonists. PCT International Application WO 2012154354, Nov 15, 2012.
And [68-70]. See for some other examples of CM involving alkenes containing *N*-heteroaromatics, that are not discussed in the review.
68. Corte, J. R.; Fang, T.; Decicco, C. P.; Pinto, D. J. P.; Rossi, K. A.; Hu, Z.; Jeon, Y.; Quan, M. L.; Smallheer, J. M.; Wang, Y.; Yang, W. Macrocycles as Factor Xia Inhibitors. PCT International Application WO 2011100401, Aug 18, 2011.

69. Defossa, E.; Goerlitzer, J.; Klabunde, T.; Drosou, V.; Stengelin, S.; Haschke, G.; Herling, A.; Bartoschek, S. 4,5-Diphenyl-pyrimidinyl-oxy or -mercapto substituted carboxylic acids, methods for the production and use thereof as medicaments. PCT International Application WO 2007131619, Nov 22, 2007.
70. Ksander, G. M.; Meredith, E.; Monovich, L. G.; Papillon, J.; Firooznia, F.; Hu, Q.-Y. Condensed Imidazolo Derivatives for the Inhibition of Aldosterone and Aromatase. PCT International Application WO 2007024945, March 1, 2007.
71. Hsu, M. C.; Junia, A. J.; Haight, A. R.; Zhang, W. *J. Org. Chem.* **2004,** *69,* 3907. doi:10.1021/jo049737n
72. Or, Y. S.; Ma, Z.; Clark, R. F.; Chu, D. T.; Plattner, J. J.; Griesgaber, G. 6-*O*-Substituted Ketolides Having Antibacterial Activity. U.S. Patent 5,866,549, Feb 2, 1999.
And [73,74]. See for ABT-773 which was an anti-infective candidate developed at Abbott Laboratories.
73. Or, Y. S.; Ma, Z.; Clark, R. F.; Chu, D. T.; Plattner, J. J.; Griesgaber, G. 6-*O*-Substituted Antibacterial Erythromycin Ketolides and Methods of Making. U.S. Patent 6,028,181, Feb 22, 2000.
74. Or, Y. S.; Ma, Z.; Clark, R. F.; Chu, D. T.; Plattner, J. J.; Griesgaber, G. 6-*O*-Substituted Antibacterial Erythromycin Ketolides and Methods of Making. U.S. Patent 6,075,133, June 16, 2000.
75. Storvick, J. M.; Ankoudinova, E.; King, B. R.; Van Epps, H.; O'Neil, G. W. *Tetrahedron Lett.* **2011,** *52,* 5858. doi:10.1016/j.tetlet.2011.08.153
76. Hunter, L.; Condie, G. C.; Harding, M. M. *Tetrahedron Lett.* **2010,** *51,* 5064. doi:10.1016/j.tetlet.2010.07.105
77. Bisai, A.; West, S. P.; Sarpong, R. *J. Am. Chem. Soc.* **2008,** *130,* 7222. doi:10.1021/ja8028069
78. Lafaye, K.; Nicolas, L.; Guérinot, A.; Reymond, S.; Cossy, J. *Org. Lett.* **2014,** *16,* 4972. doi:10.1021/ol502016h

License and Terms

BEILSTEIN JOURNAL OF ORGANIC CHEMISTRY

Recent advances in metathesis-derived polymers containing transition metals in the side chain

Ileana Dragutan*[1], Valerian Dragutan*[1], Bogdan C. Simionescu*[2], Albert Demonceau[3] and Helmut Fischer[4]

Review

Open Access

Address:
[1]Institute of Organic Chemistry, Romanian Academy, 202B Spl. Independentei, POBox 35-108, Bucharest 060023, Romania, [2]Petru Poni Institute of Macromolecular Chemistry, Romanian Academy, Iasi, Romania, [3]Macromolecular Chemistry and Organic Catalysis, Institute of Chemistry (B6a), University of Liège, Sart Tilman, Liège 4000, Belgium and [4]Department of Chemistry, University of Konstanz, Konstanz, Germany

Email:
Ileana Dragutan* - idragutan@yahoo.com; Valerian Dragutan* - vdragutan@yahoo.com; Bogdan C. Simionescu* - bcsimion@icmpp.ro

* Corresponding author

Keywords:
advanced materials; metallopolymers; metathesis; ROMP; transition metals

Beilstein J. Org. Chem. **2015,** *11,* 2747–2762.
doi:10.3762/bjoc.11.296

Received: 03 August 2015
Accepted: 30 November 2015
Published: 28 December 2015

This article is part of the Thematic Series "Progress in metathesis chemistry II".

Guest Editor: K. Grela

Abstract

This account critically surveys the field of side-chain transition metal-containing polymers as prepared by controlled living ring-opening metathesis polymerization (ROMP) of the respective metal-incorporating monomers. Ferrocene- and other metallocene-modified polymers, macromolecules including metal-carbonyl complexes, polymers tethering early or late transition metal complexes, etc. are herein discussed. Recent advances in the design and syntheses reported mainly during the last three years are highlighted, with special emphasis on new trends for superior applications of these hybrid materials.

Introduction

The fast growing interest in metal-containing polymers (metallopolymers) as advanced hybrid materials spurred prolific research in the worldwide organometallic and polymer scientific communities [1-4]. The variety of metals and the diversity of organic polymers allow tailoring metallopolymers so as to reach the desired physical and chemical properties suitable for progressive applications [5-7]. These functional hybrid materials are highly appreciated for their superior behaviour in catalysis, optics as well as for their magnetic, mechanical and thermal attributes. Structurally, metallopolymers are endowed with linear, cross-linked, hyperbranched, star or dendritic polymer architectures containing metals ranging from the main groups to transition metals and lanthanides which are embedded into the main chain or appended to the side chains of the polymer [8-11]. This make-up would confer an optimal set of capabilities that recommend them for diverse emerging applica-

tion areas, e.g., as electro-optical and magnetic devices, for energy storage, nanomaterials, sensing, catalytic and drug-delivery systems [6,12-14].

Numerous synthetic routes have been explored to achieve the synthesis of these targets presently accessible through controlled and living polymerization techniques including controlled radical polymerizations (CRP) such as atom transfer radical polymerization (ATRP), nitroxide-mediated polymerization (NMP) and reversible addition–fragmentation chain transfer (RAFT) polymerization [15,16], living ionic polymerizations, specifically ring-opening polymerization (ROP) [17], as well as migration insertion polymerization (MIP) [18], acyclic diene metathesis polymerization (ADMET) [19,20] and ring-opening metathesis polymerization (ROMP) [21-27]. These synthetic strategies ensure metal incorporation from the corresponding metal-containing monomers into the polymer in a precise, predetermined mode. With the advent of new metathesis catalysts endowed with a high activity and chemoselectivity and good tolerance towards many functionalities [28-30], ROMP with Mo and Ru catalysts has become a very practical methodology in organic, polymer and materials chemistry. ROMP is also the method of choice for obtaining new and diverse metallopolymers [31-34].

The present contribution aims to provide an overview of selected developments in metathesis-based synthesis and applications of polymers containing transition metals in the side chain evidencing recent work published since our earlier review on this topic [34]. Metallopolymers are herein classified according to the nature of the transition metal and its binding mode to the organic moiety. Information on the physical characteristics of these materials is also included, with a focus on their present and future practical applications. Taking advantage of the considerable reactivity of ring-strained norbornenes and congeners and of their easy functionalization with many organic and organometallic groups it became possible to synthesize a broad range of polymers and copolymers by ROMP [35,36]. On the other hand it is well-known that ferrocene and numerous transition metal sandwich complexes exhibit great redox stability that allows fine tuning of their properties and applications in electrochemistry, sensing, catalysis, nanomaterials, etc. [37-40]. Not surprisingly, therefore, attention of researchers has turned first on metallopolymers containing ferrocene [33,34,41-43].

Review

Iron-containing polymers

Following the first successful application of Mo–alkylidene catalysts by Schrock and coworkers [42] in ROMP to ferrocene-appended monomers as well as the rapid expansion of Grubbs Ru metathesis catalysts [28-30], a vast number of iron-containing polymers have been synthesized by ROMP up to now [33,34,42,43].

In a compelling work, Astruc et al. [44] reported a biologically relevant type of new homopolymers (e.g., **2**, Scheme 1) and block copolymers provided with amidoferrocenyl groups linked through a tetraethylene glycol side chain. These interesting metallopolymers were readily prepared through living ROMP initiated by the Grubbs 3rd generation catalyst which proved

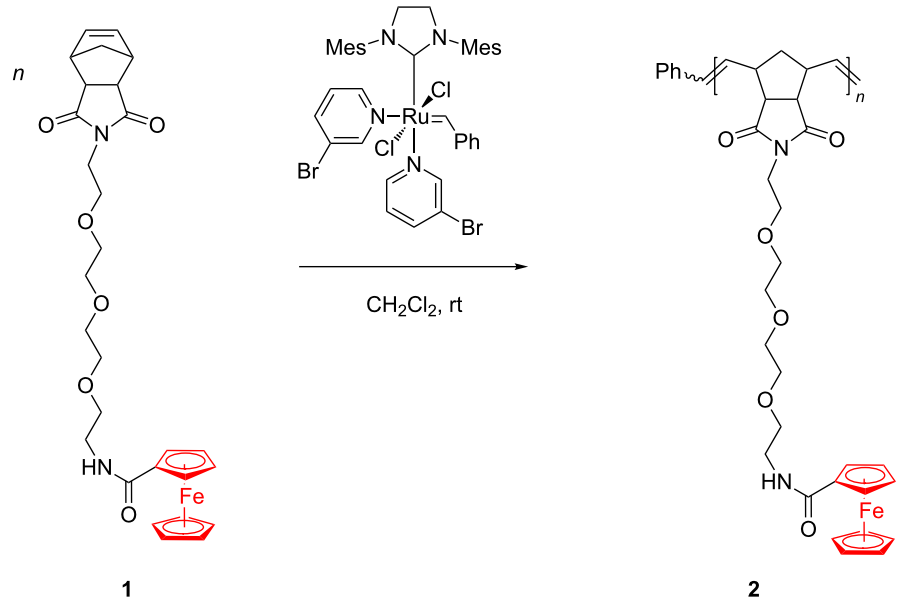

1 2

Scheme 1: Synthesis of homopolymers containing ferrocenyl and tetraethylene glycol groups.

quite active and tolerant toward the monomer endowed with multiple functionalities (Scheme 1).

By precisely controlling the living polymerization process, they succeeded in varying the number of amidoferrocenyl motifs in the polymers within pre-established limits. Such polymers and block copolymers were used to prepare modified Pt electrodes with high stability and good qualitative sensing of ATP^{2-} anions. It was supposed that the triethylene glycol domains in the block copolymers favor the amidoferrocene–ATP interactions by encapsulation. Astruc assumed that during the recognition process different H-bonding modes arise in the supramolecular polymeric network, i.e., an intramolecular H bonding with the β- and γ-phosphate groups of ATP^{2-} and an intermolecular H bond between the α-phosphate and another amidoferrocenyl group. Redox properties of polycationic copolymers containing the complex $[Fe(\eta^5\text{-}C_5H_5)(\eta^6\text{-}C_6Me_6)][PF_6]$ have been recently revealed as potential electron-transfer reagents provided with a high stability [45].

On extending their research to the areas of anion sensing and nanomaterials, the Astruc group accomplished an efficient synthesis, by ROMP with Grubbs 3rd generation catalyst, of redox-robust triazolylbiferrocenyl (trzBiFc) polymers **4** bearing the organometallic group in the side chain (Scheme 2) [46,47].

Here again, the Grubbs 3rd generation catalyst was very active and highly tolerant towards the biferrocene and triaza functionalities. Noteworthy, the oxidation of the polymer **4** with ferricenium hexafluorophosphate led to a stable biferrocenium polymer while oxidation with Au(III) or Ag(I) allowed the formation of networks with nanosnake morphology, consisting of mixed-valent Fe(II)–Fe(III) polymers that encapsulate metal (Au or Ag) nanoparticles (NPs). These polymers were suitable for obtaining modified Pt electrodes with good sensing affinities for ATP^{2-} and Pd(II) cations. The importance of such results lies in the multi-electron properties of these side-chain BiFc polymers that have not been much studied so far although the outstanding stability of the biferrocenium motifs recommends them for designing new redox reactions, eventually leading to value-added nanomaterials. Along a different line, in a recent, inventive work Astruc and coworkers [48] demonstrated that triazolylbiferrocenyl-containing polymers can effectively stabilize palladium nanoparticles (PdNPs) affording highly active catalysts for Suzuki–Miyaura coupling reactions.

Cobalt-containing polymers

The incorporation of other late transition metals such as cobalt into polymers soon emerged as an efficient and rapid method for the production of nanostructured materials of scientific and practical importance for microelectronics, catalysis, biology and medicine (vide infra). Tang et al. [49] were the first to apply the ROMP strategy to synthesize the well-defined, high molecular weight cobaltocenium-containing polymer **6** (Scheme 3).

Under ambient conditions, the Grubbs 3rd generation catalyst induced polymerization of **5** in a living manner leading to a product with low polydispersity (1.12) and high molecular weight (167,000 $g \cdot mol^{-1}$). By substituting the PF_6^- anion with BPh_4^-, Cl^- or an anion exchange resin (chloride-form), the authors demonstrated that the nature of the anion is important for the polymer properties. They found that polymer **6** was soluble in water and various organic solvents when the counteranion was chloride. Subsequently, these authors copolymer-

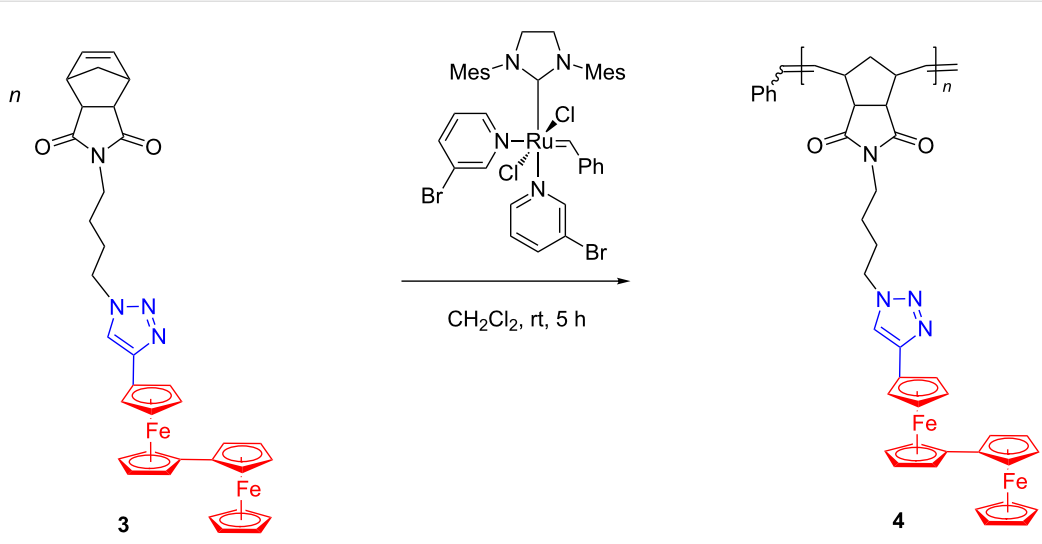

Scheme 2: Synthesis of redox-robust triazolylbiferrocenyl polymers **4**.

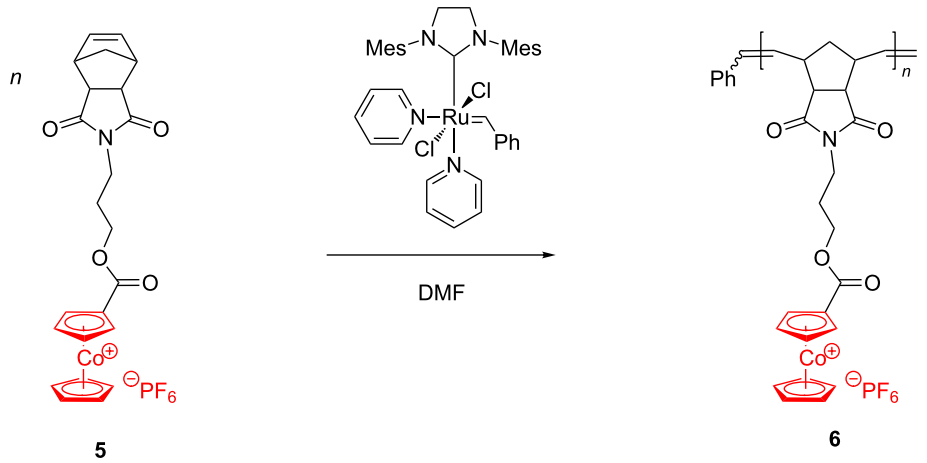

Scheme 3: Synthesis of cobaltocenium-containing polymers by ROMP.

ized **6** with norbornene-2-carboxylic acid, using Grubbs 3rd generation catalyst, to prepare diblock copolymer **7**, in which one block contains cobaltocenium units while the other block comprises an organic chain only [50] (Scheme 4).

By the same technique, polymer **6** was further copolymerized with a cobaltocenium-BPh_4 monomer and a cobaltocenium-Cl monomer affording, respectively, the new diblock copolymers **8** (X = PF_6, Y = BPh_4 or Cl). Self-assembly of these block copolymers into core–shell spherical micelles was successfully conducted and, by UV/ozonolysis or thermal pyrolysis generating antiferromagnetic CoO species, some of these micelles could be converted into inorganic nanoparticles.

With the aim at extending the application of metallopolymers as heterogeneous macromolecular catalysts for living radical polymerizations, Tang et al. [51] produced the cobalt-containing polymer **10** by ROMP of the norbornene monomer **9**, derivatized with triazolyl and cyclopentadienylcobalt-1,3-cyclopentadiene moieties (Scheme 5).

The triazolyl unit was first attached to the η^4-cyclopentadiene CpCo(I) complex by click reaction of the corresponding alkyne precursor and then the triazolyl-Co scaffold was incorporated into the norbornene monomer **9** by conventional esterification. It is important to note that the cyclopentadienyl-cobalt-1,3-cyclopentadiene, an isoelectronic 18-electron species to ferrocene and cobaltocenium, was well tolerated by the Grubbs 3rd generation ROMP catalyst. The polymerization of **9** proceeded in a controlled and living manner under ambient conditions. Polymer **10** was successfully employed as an organometallic catalyst in the atom-transfer radical polymerization of methyl methacrylate or styrene to obtain poly(methyl methacrylate) and polystyrene devoid of colored traces of catalyst, a very important requirement for special applications, e.g., in dentistry, medical devices, housewares, and food packaging. In another

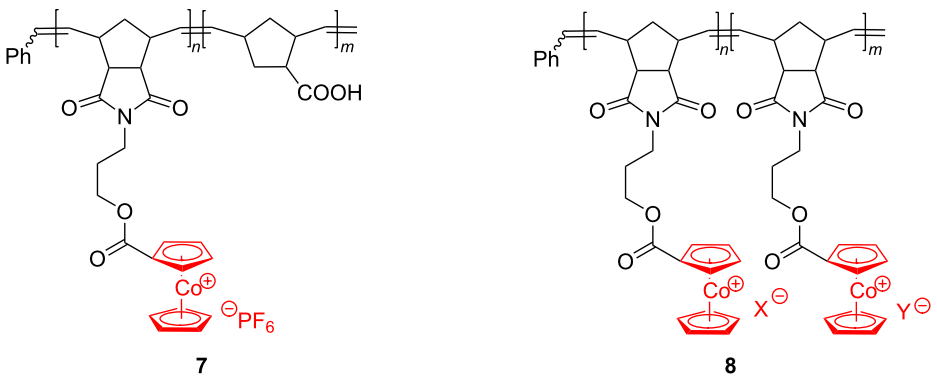

Scheme 4: Cobaltocenium-appending copolymers by the ROMP approach (X = PF_6, Y = BPh_4 or Cl).

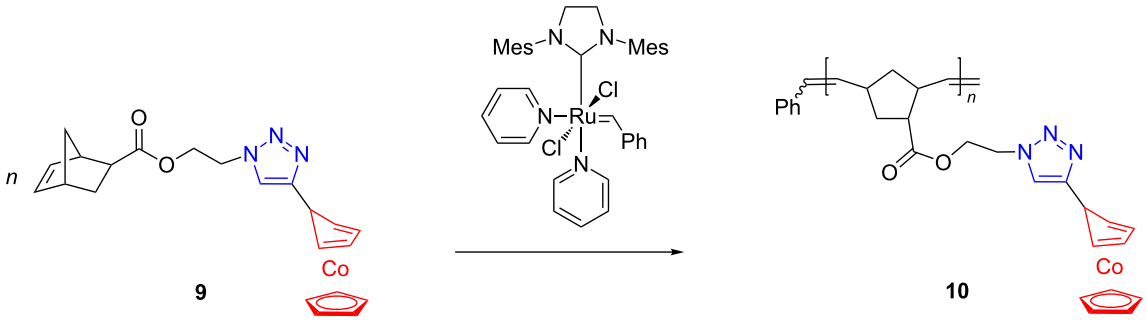

Scheme 5: Cobalt-containing polymers by click and ROMP approach.

recent study, Tang and coworkers [52] performed a quantitative analysis of counterion exchange in cobaltocene-containing polyelectrolytes that are accessible by an initial ROMP, and subsequently derivatized with cobalt motifs. These results appear to be relevant for self-assembly and drug-delivery systems with this type of polyelectrolytes.

An interesting cobalt-containing diblock copolymer, bearing a dicobalt hexacarbonyl complex coordinated to an alkyne, with a constant block ratio was proposed as a new magnetic material by Tew et al. [53]. Their procedure involved the synthesis of a first block polymer, **12**, by ROMP of monomer **11** using Grubbs 3rd generation catalyst. The second block polymer was created by the addition of the cobalt-containing monomer to the reaction mixture containing **12** to continue the ROMP. Diblock copolymer **13**, with a defined block ratio, could be obtained by the variation of the polymerization time (Scheme 6).

In this process, the ruthenium initiator proved to well tolerate the dicobalt hexacarbonyl complex embedded in the monomer. By controlled heating of the cobalt-containing block copolymers, robust, room temperature ferromagnetic (RTF) materials have been obtained.

By two alternative ROMP protocols, both starting from 5-formyl-2-norbornene (**14**) and using the Grubbs 3rd generation catalyst, Astruc and coworkers [54] successfully prepared new redox-active cobalticenium-tethered polyelectrolytes of type **17**. According to the first protocol, the norbornene monomer containing an enamine-cobalticenium group (**16**) was first prepared by hydroamination of the ethynyl cobalticenium with *n*-butylamine-substituted norbornene **15**. Next, **16** was polymerized to **17**, by ROMP under mild conditions (Scheme 7A). In the second approach, first, the monomer **14** was polymerized to **17a**, followed by functionalization of the latter with *n*-butylamine to yield **17b**, and finally this organic polymer hydroaminated the ethynyl cobalticenium to produce **17** (Scheme 7B). Both protocols embody an elegant and original ROMP-based access to cobalticenium-containing polyelectrolytes.

Ruthenium-, iridium-, osmium- and rhodium-containing polymers

ROMP syntheses of homopolymers and block copolymers bearing bipyridine–ruthenium complexes starting from norbornene or oxanorbornene functionalized with Ru complexes have been reported by several authors [55,56]. In these investigations it was revealed that the Ru catalysts are active initiators

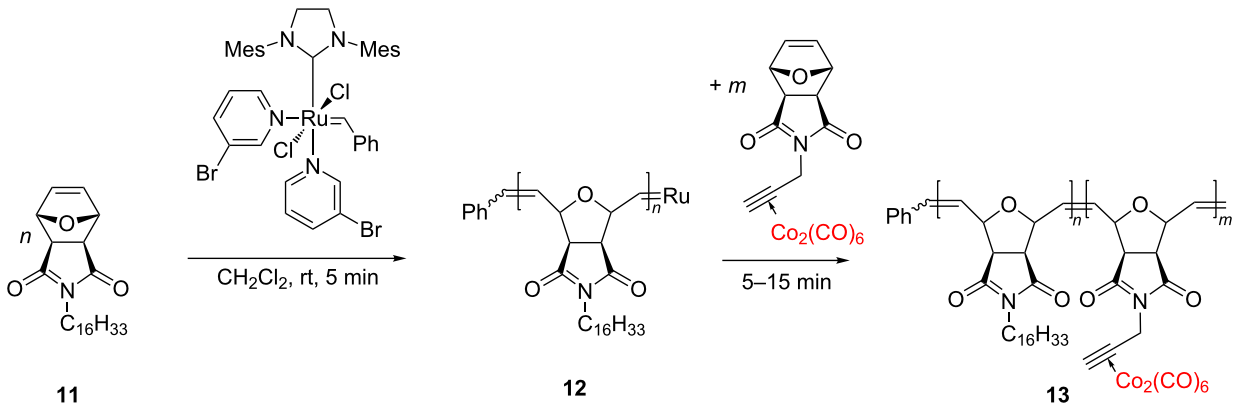

Scheme 6: Synthesis of new cobalt-integrating block copolymers.

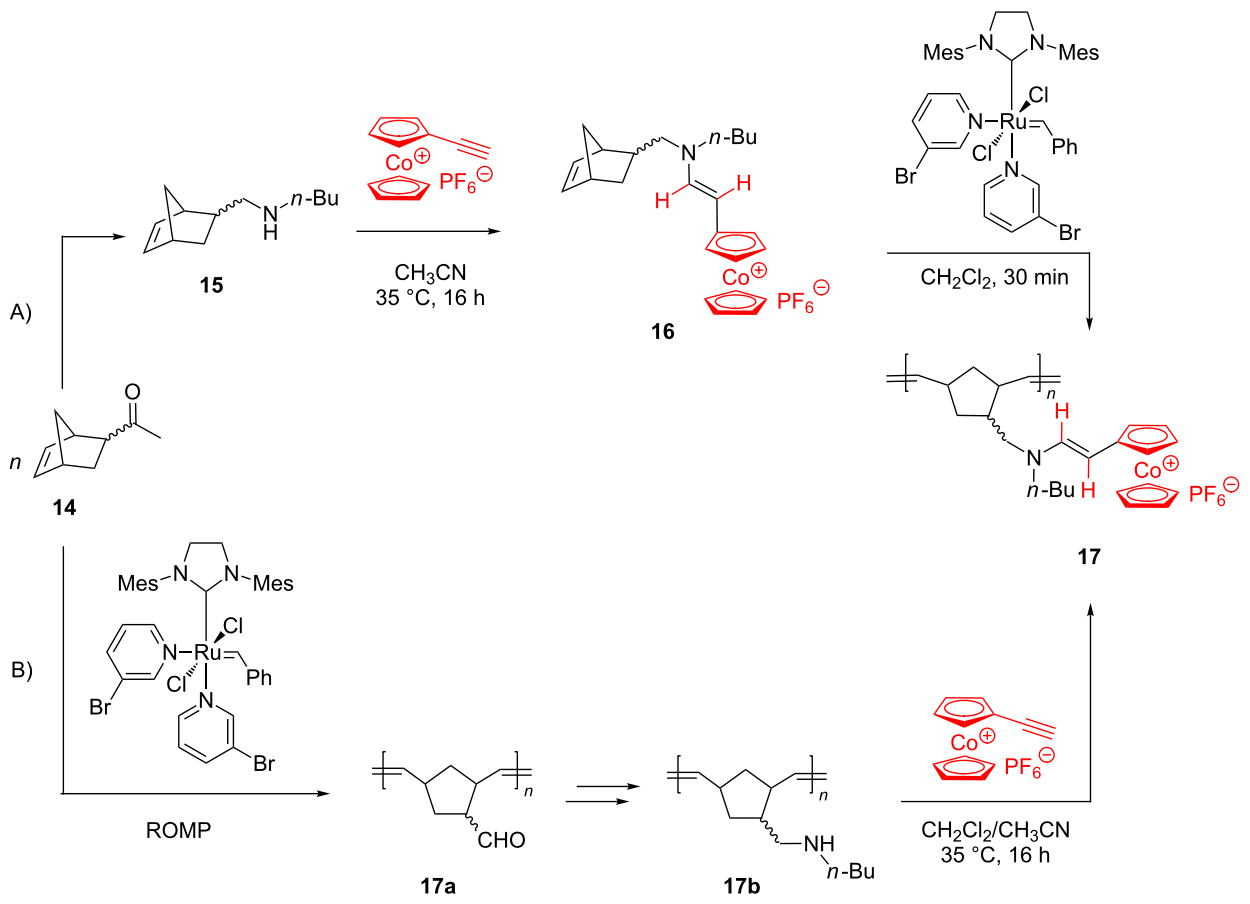

Scheme 7: Two alternative routes for the synthesis of redox-active cobalticenium-tethered polyelectrolytes.

in producing, in a living polymerization manner, well-defined polymers containing Ru in the side chains. Again, the best results were obtained with the Grubbs 3rd generation catalyst. Along this line, Sleiman et al. [56] prepared an array of oxanorbornene monomers tethered with ruthenium–bipyridine motifs (e.g., **18**–**20**, Scheme 8) and used them to prepare homopolymers (Scheme 9), diblock- (Scheme 10) and triblock copolymers (Scheme 11).

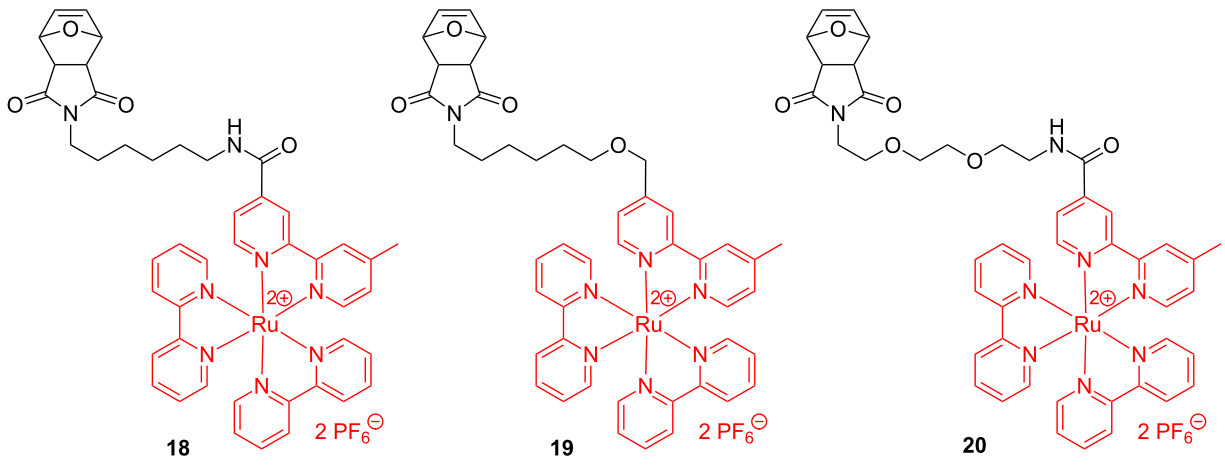

Scheme 8: Oxanorbornene monomers for the synthesis of Ru-containing polymers by ROMP.

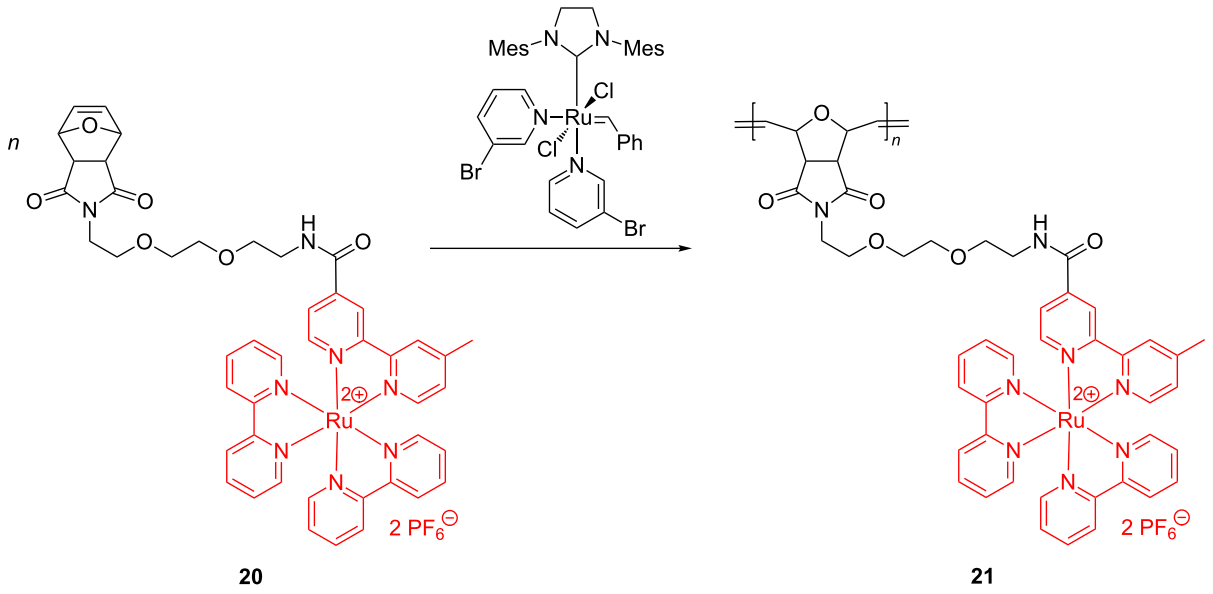

Scheme 9: ROMP synthesis of Ru-containing homopolymers.

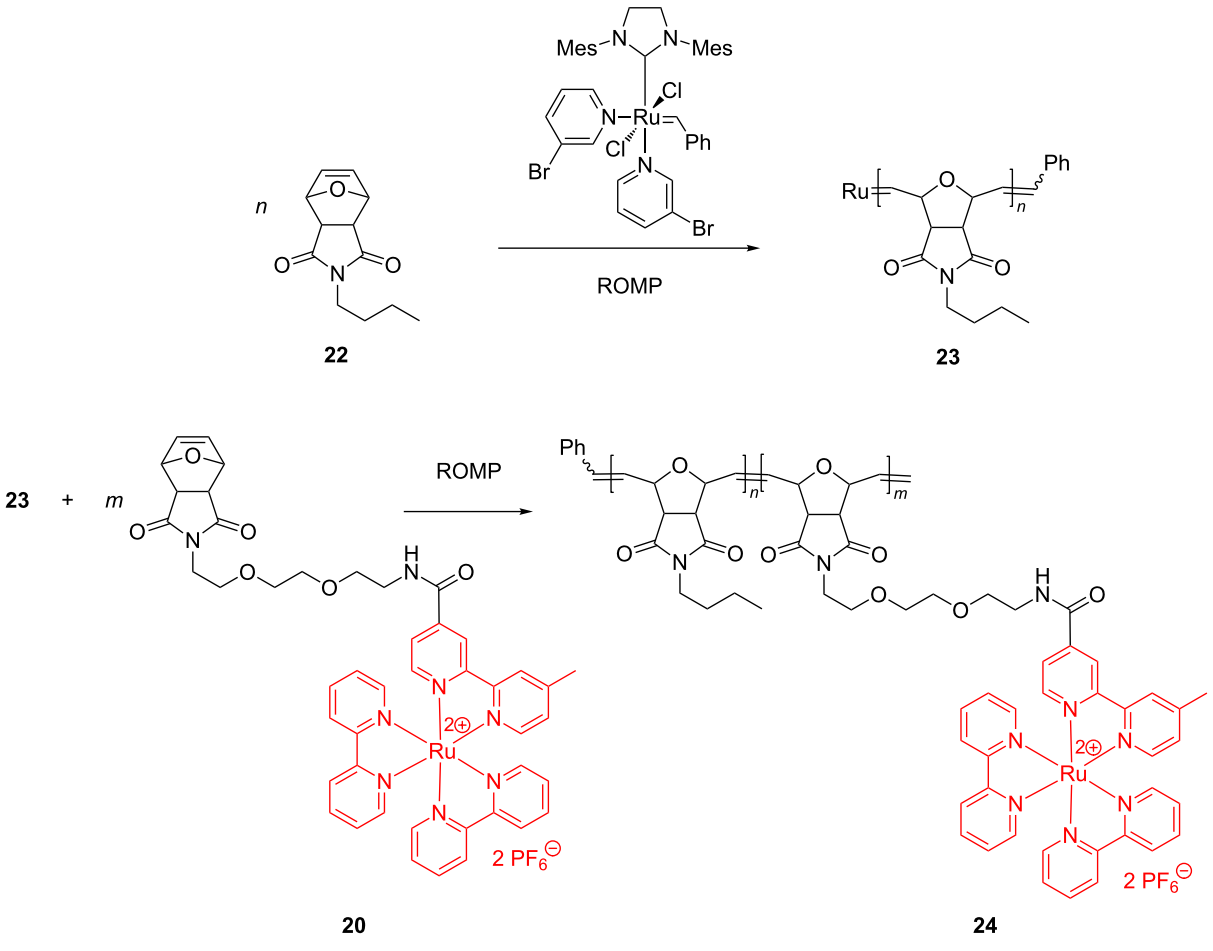

Scheme 10: Synthesis of diblock copolymers incorporating ruthenium.

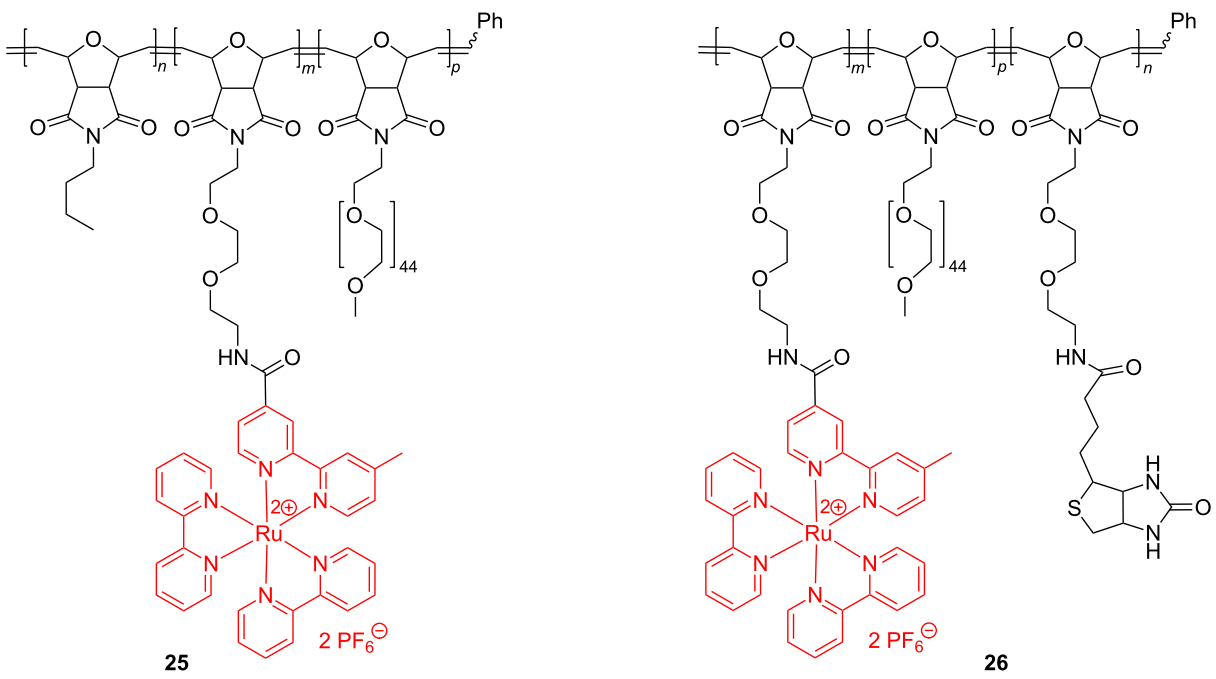

Scheme 11: Synthesis of Ru triblock copolymers.

In an in-depth exploration of the synthesis of diblock copolymers **24**, Sleiman developed a step-wise procedure: in the first step, the ruthenium catalyst induced polymerization of the bicyclic monomer **22** to homopolymer **23**, followed by polymerization of the additional comonomer **20** at the Ru site of **23** to yield the copolymer **24** (Scheme 10).

Based on their potential application as tools for biological detection and signal amplification, amphiphilic Ru-modified triblock copolymers have been produced from biocompatible and bioconjugatable oxanorbornene monomers. By extending the above ROMP methodology, Sleiman et al. managed to synthesize the Ru triblock copolymers **25** and **26** (Scheme 11), and examined their self-assembling into micelles in aqueous media to evaluate them as luminescent markers of biological molecules.

The production of metal-cation-based anion exchange membranes from ROMP polymers was first reported by Tew et al. [57]. The ROMP reaction, induced here by the Grubbs 2nd generation catalyst, implied the copolymerization of a norbornene monomer (**27**) functionalized with a water-soluble bis(terpyridine)ruthenium(II) complex, with dicyclopentadiene as a cross-linking agent (Scheme 12). In the resulted copolymer

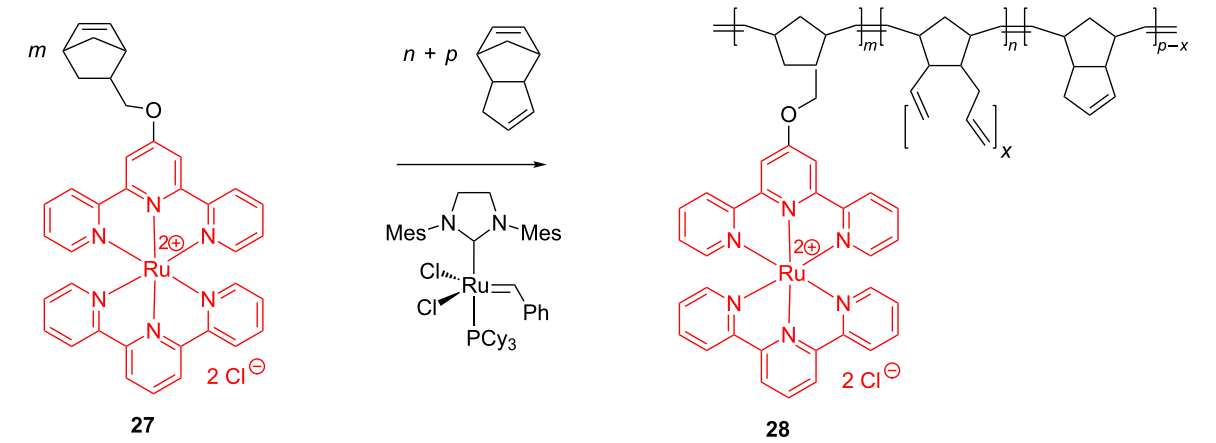

Scheme 12: Synthesis of cross-linked Ru-containing triblock copolymers.

28 each Ru complex is associated with two counteranions (chloride), which represents a novelty versus most cation-based membranes provided with single cation–anion pairs. Cross-linking with dicyclopentadiene ensured a high mechanical stability of the copolymer. The film cast from **28** displayed an anion conductivity and mechanical properties similar to those of the traditional quaternary ammonium-based anion exchange membranes. In addition, the film exhibited high methanol and base tolerance making it suitable for applications in fuel cells and anion-conducting devices.

Owing to their high phosphorescent propensity, complexes based on iridium have been grafted onto polymers for the application as light-emitting diodes (LEDs) [58]. In an earlier research, in order to obtain iridium-containing polymers by the ROMP route, Weck and coworkers [59] polymerized monomers **29** and *mer*-**31**, in the presence of Grubbs 3rd generation catalyst, to the fully soluble ROMP homopolymers **30** and *mer*-**32** (Scheme 13).

Later on, while investigating the self-assembly of transition metal-containing polymers, Sleiman et al. [60] expanded the field by preparing ROMP-able oxanorbornene monomers having iridium and osmium bipyridines attached by an extended organic linker (Scheme 14).

The triblock copolymers obtained through a sequential ROMP of the corresponding monomers, appended to Ir bipyridine

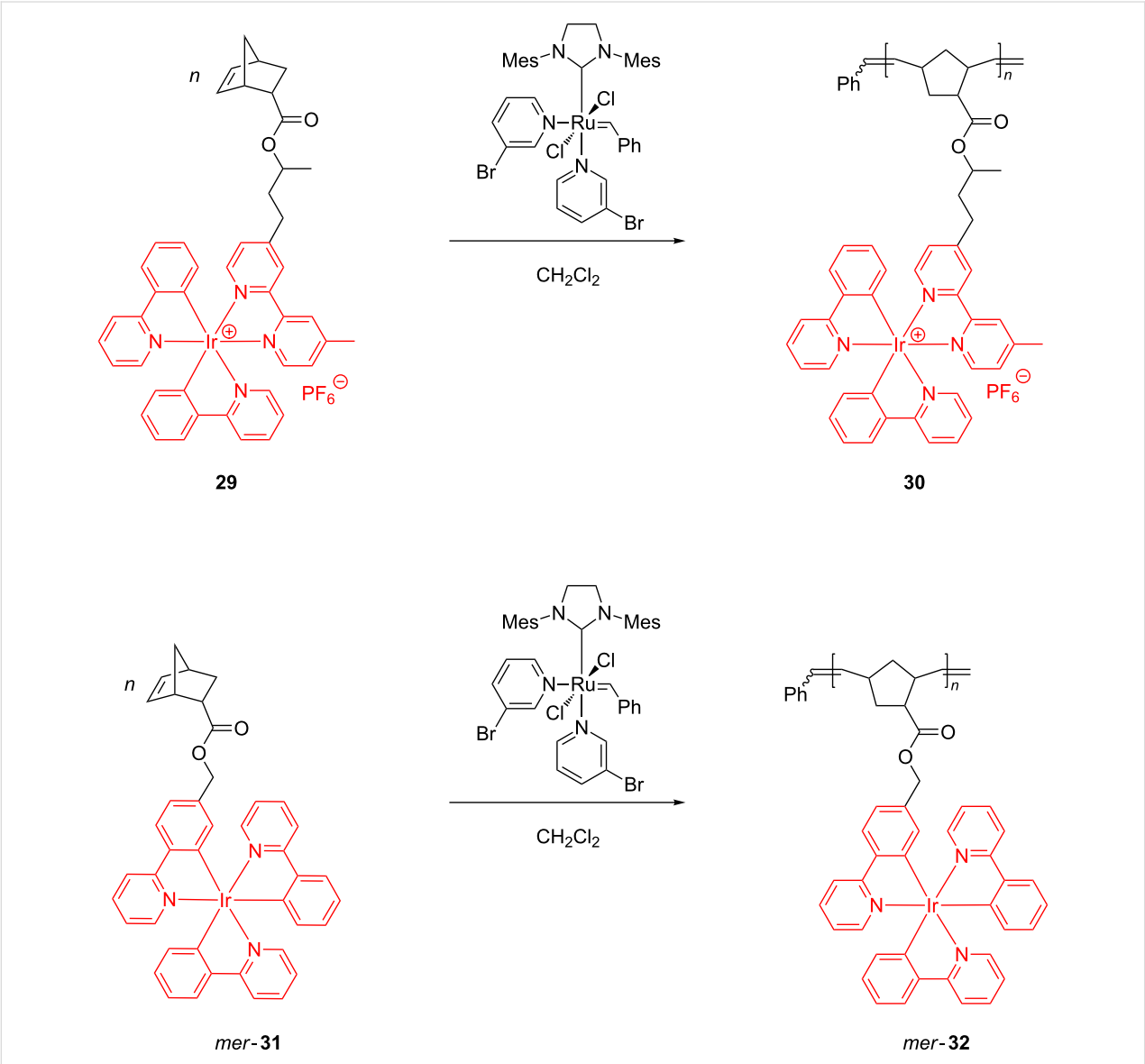

Scheme 13: Synthesis of Ir-containing homopolymers by ROMP.

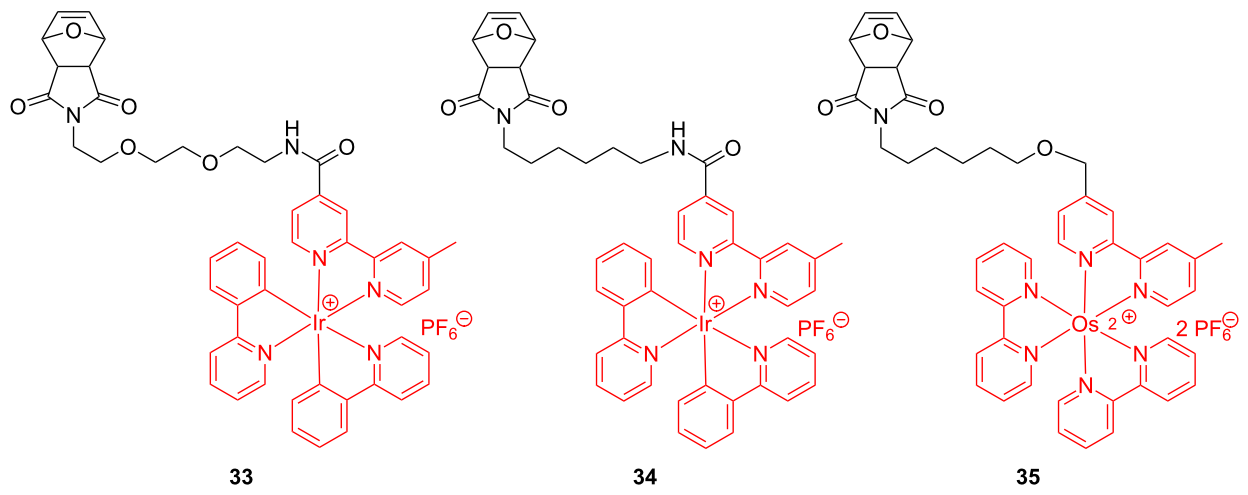

Scheme 14: Monomers for Ir- and Os-containing ROMP polymers.

complexes, oligoethylene glycol and biotin entities, have been examined by fluorescence spectroscopy for their self-assembling behavior and biodetection capability (Scheme 15).

In a very interesting work, Blechert, Buchmeiser and coworkers [61] copolymerized norborn-5-ene-(*N*,*N*-dipyrid-2-yl)carbamide with *exo*,*exo*-[2-(3-ethoxycarbonyl-7-oxabicyclo[2.2.1]hept-5-en-2-carbonyloxy)ethyl]trimethylammonium iodide to polymer **38**, using the Schrock Mo catalyst. By further reaction with $[Rh(COD)Cl]_2$ (COD = cycloocta-1,5-diene), polymer **38** gave the Rh(I)-appended block copolymer **39** (Scheme 16).

Remarkably, in water, this Rh-containing block copolymer readily generated micelles and could be thus successfully employed as a Rh-immobilized catalyst for the hydroformylation of 1-octene.

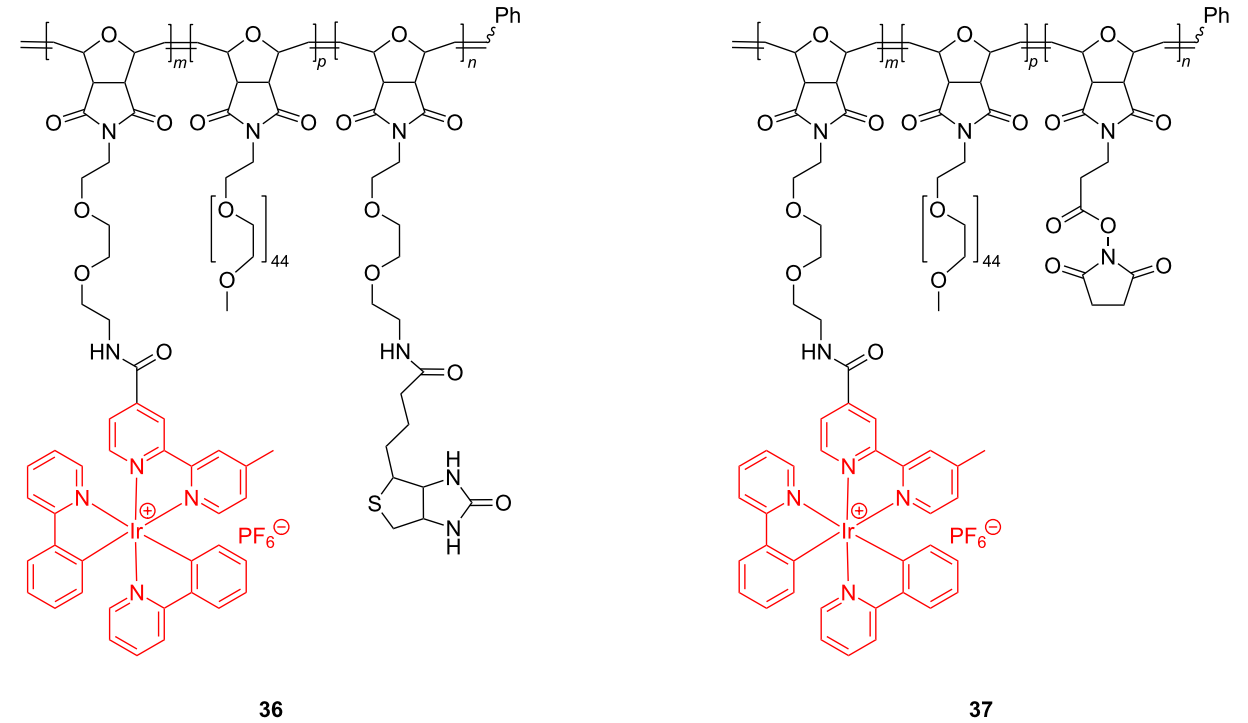

Scheme 15: ROMP block copolymers integrating Ir in their side chains.

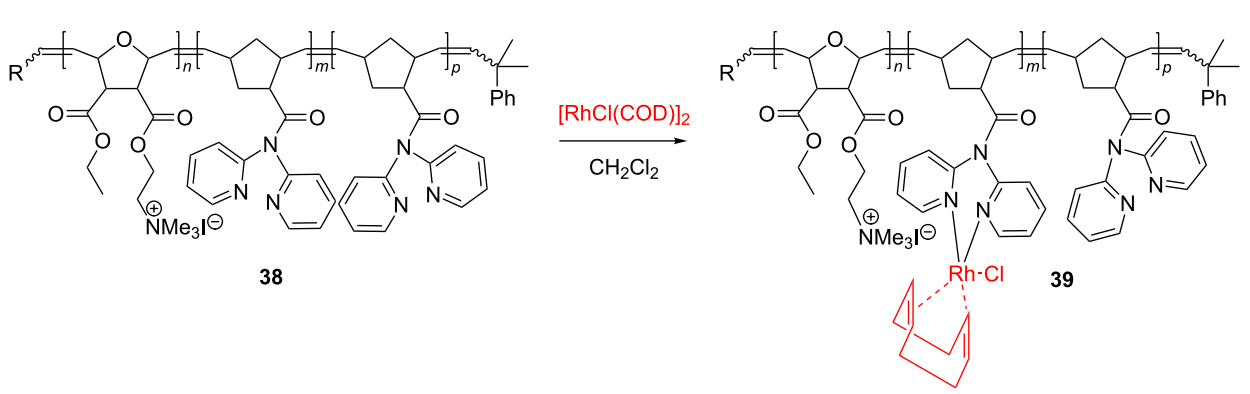

Scheme 16: Synthesis of Rh-containing block copolymers.

Very recently, Matyjaszewski, Tang and coworkers [62] reported the first synthesis of norbornene monomers substituted with rhodocenium units and their controlled polymerization, by two parallel routes (ROMP and RAFT), to rhodocenium-containing metallopolymers. ROMP of both triazolyl-rhodocenium monomers, **40** and **42**, proceeded productively and in a living fashion to yield amphiphilic metallopolymers **41** and **43** (Scheme 17).

Polymers **41** and **43** have been evaluated for their counterion exchange properties and self-assembling tendency revealing a promising application profile. The point of interest here is that rhodocenium exhibits different chemical and physical properties from cobaltocenium. A novel immobilized Rh catalytic system in which the metal is embedded, by means of the 5,5-dinorimido BINAP ligand, into the polymer, obtained from alternating ROMP of cyclooctene with the Grubbs first

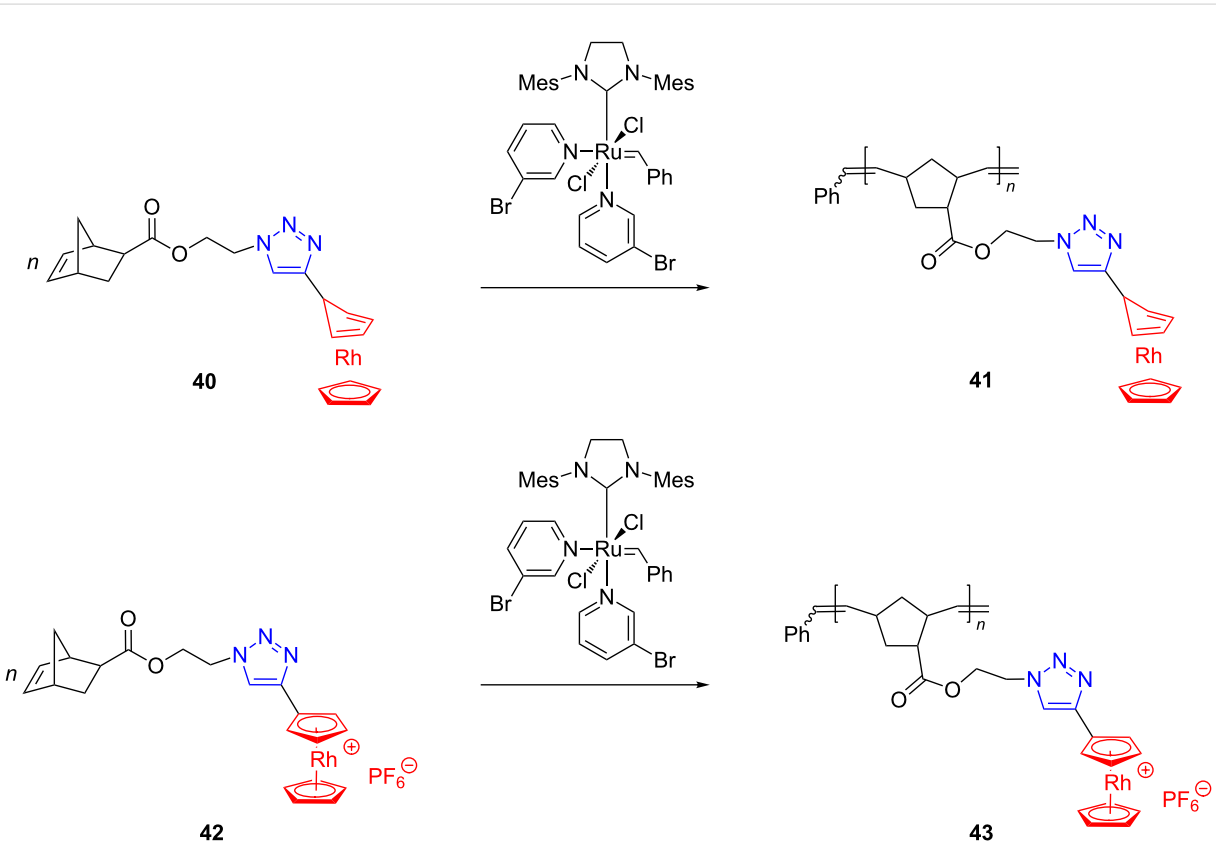

Scheme 17: Access to rhodocenium-containing metallopolymers by ROMP.

generation catalyst, has been disclosed in a patent by Bergens et al. [63]. This catalytic system allowed the intramolecular cycloisomerization of enynes with high yields and turnover numbers.

Copper-containing polymers

A copper(I) complex containing a norbornene substituted with the 2-(pyridin-2-yl)-1*H*-benzimidazole ligand, **44**, developed by Il'icheva et al. [64], came to the attention of the scientific community involved in the area. The complex was used to access Cu-containing homopolymers **45** and copolymers **47** under metathesis polymerization with the Grubbs 3rd generation catalyst (Scheme 18 and Scheme 19). Further variations in the spacer subunit from a norbornene carbazole comonomer **46** enabled fine-tuning of the physical and chemical properties of the copolymer **47**.

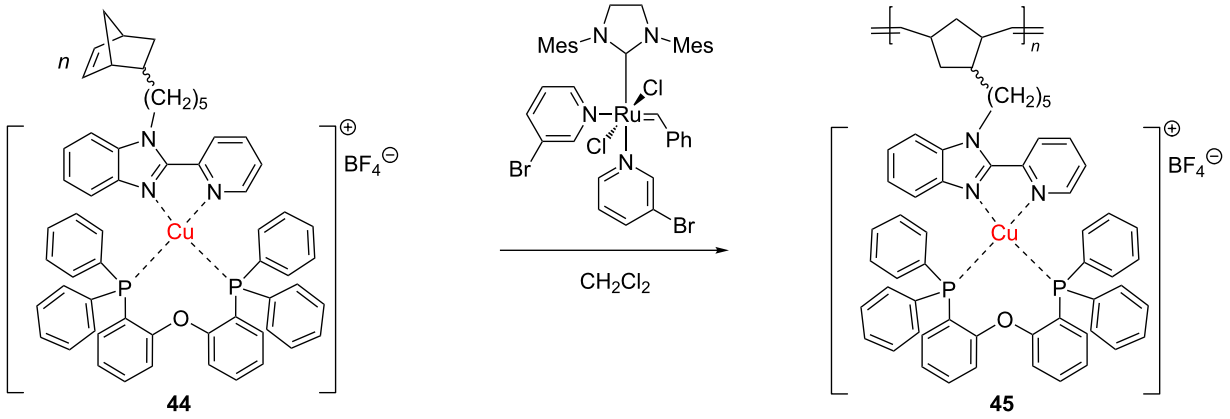

Scheme 18: Synthesis of homopolymers equipped with Cu coordination centers.

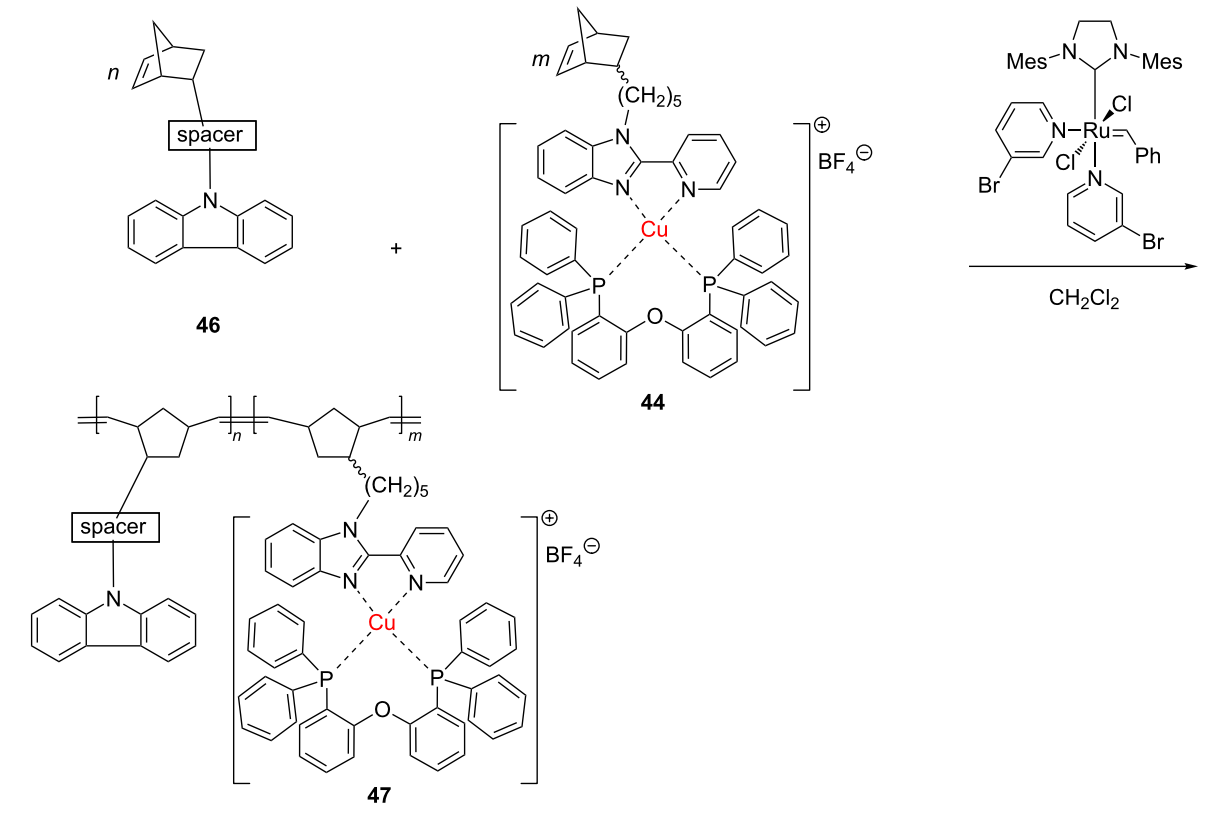

Scheme 19: Synthesis of Cu-containing copolymers (spacer = –$(CH_2)_5$–; >C=O).

These materials, in which Cu is tethered to the polymeric backbone by an organic linker, exhibited notable luminescent characteristics. The same research group subsequently introduced other new copper(I) complexes, ligating norbornene-substituted phenanthroline, that were polymerized by ROMP (Grubbs 3rd generation catalyst) to yield copolymers with valuable photo- and electroluminescent properties [65]. This kind of hybrid structure may induce high performance in LED devices.

Early transition metal-containing polymers

In contrast to the numerous polymers including late transition metals discussed so far, only few representatives of early transition metals attached to ROMP polymers have been disclosed recently. Thus, Wang et al. [66] communicated the ROMP synthesis of the first polynorbornene bearing a polyoxometalate (POM) cluster in the side chain (Scheme 20).

According to their concept, the norbornene monomer containing a trivanadium-substituted Wells–Dawson-type polyoxotungstate (POM) (**48**) was polymerized quantitatively to **49** in a living and controlled process under promotion of Grubbs 3rd generation catalyst. It should be remarked that this Grubbs catalyst favored the polymerization under mild reaction conditions and tolerated very well the bulky POM cluster attached to the monomer. The obtained hybrid materials are promising candidates for the production of high-performance catalysts based on poly(polyoxometalate)s.

Lanthanide-containing polymers

Recently, new polynorbornenes of type **53**, functionalized with terpyridine and carbazole moieties and integrating a europium complex in the pendant chains, were described by Rozhkov et al. [67]. They were obtained by a metathesis copolymerization with Grubbs 3rd generation catalyst as the key step (Scheme 21).

In a first approach the copolymer **52** was coordinated with europium thenoyl trifluoroacetonate to yield copolymers **53** with different ratios between the purely organic and europium-containing units. Alternatively, similar coordination copolymers were prepared by copolymerizing the europium complex of the terpyridine monomer **51** with the carbazole-substituted norbornene **50**. In solution or in thin film these Eu-containing products exhibited important metal-centered photoluminescence recommending them for novel applications.

Unveiling and rationalizing the interactions between the metal and the organic polymer backbone and/or side chains is crucial for ensuring the desired properties for the hybrid material [68]. Indeed, when appraising luminescence of a series of polynorbornenes attaching various homoleptic bi- or trinuclear lanthanide salen complexes (with La, Nd, Yb, Er, Gd or Tb), Lü et al. [69,70] established that, only in the case of Nd and Yb metallopolymers, the luminescent emissions are strongly retained versus those of the respective monomers in solution.

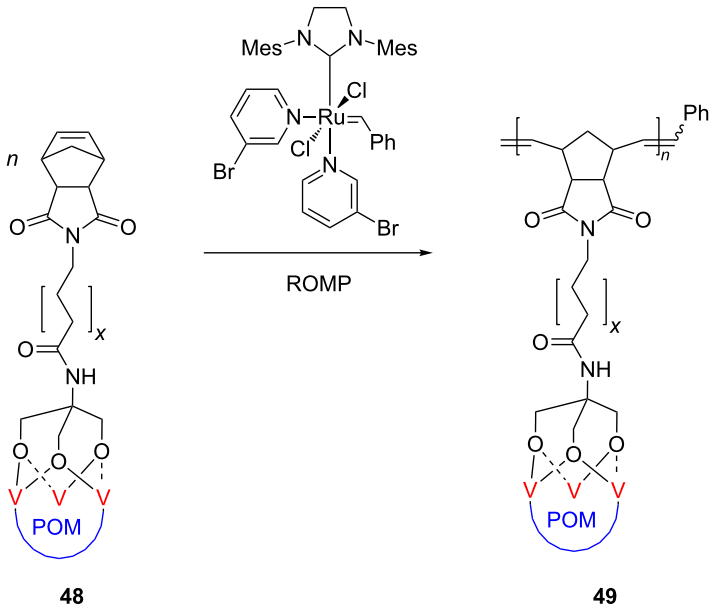

48 49

Scheme 20: Synthesis of polynorbornene bearing a polyoxometalate (POM) cluster in the side chain.

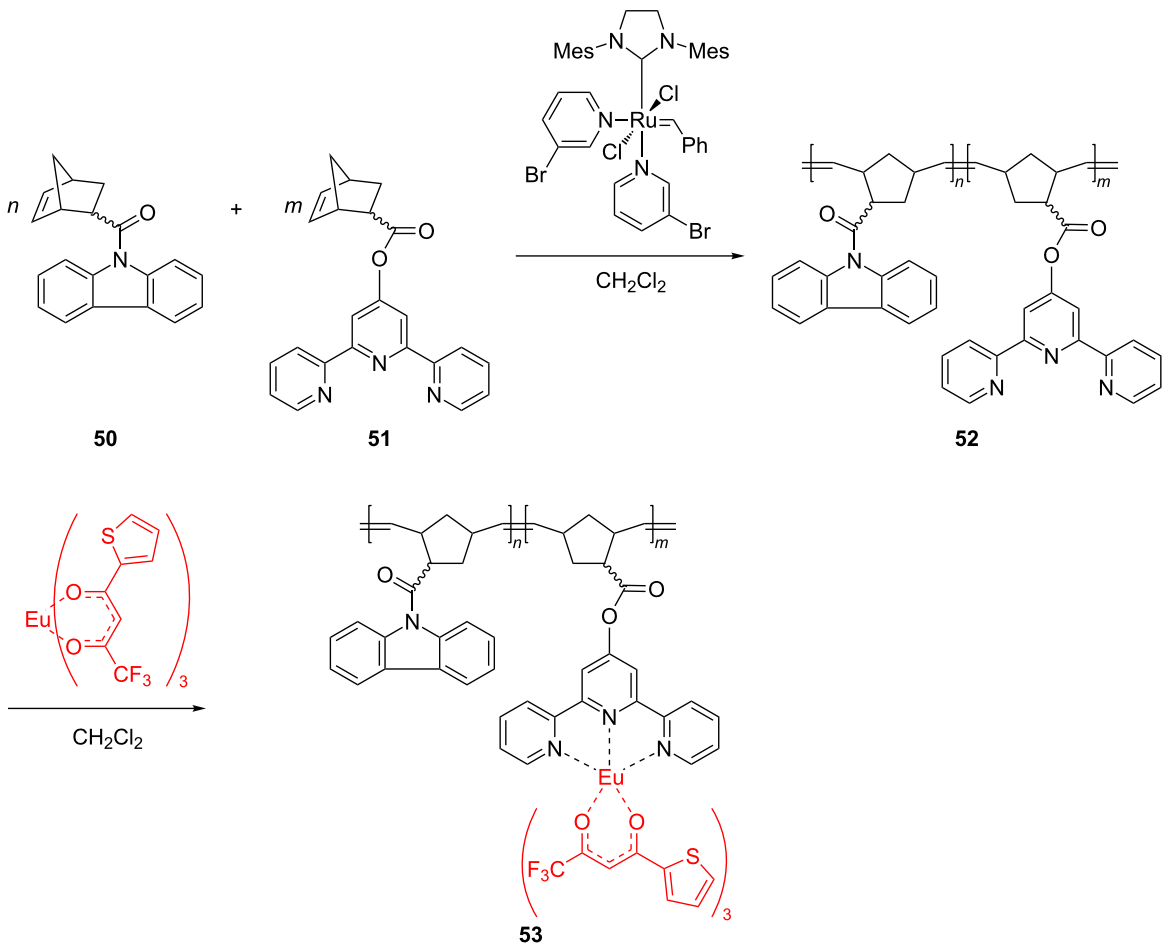

Scheme 21: Synthesis of Eu-containing copolymers by a ROMP-based route.

Conclusion

This review highlights ingenious ways in which a large variety of transition metals could be attached to organic polymer side-chains thus prompting the appearance of extraordinary new physical properties (optical, electrical, conducting, catalytic, magnetic, biological, etc.), most of which were not detained before by either the metal or the organic counterpart. Such distinguishing features recommend these privileged scaffolds as important hybrid materials having a strong impact on a host of current high-tech applications, as fuel cells, light-emitting diodes (LED), magnetic nanomaterials, catalysts, biosensors, for energy generation and storage. The mainstay of the synthesis of these engineered metallopolymers is living ROMP, the key step advantageously executed either with Schrock's or Grubbs latest generation catalysts, and easier to be precisely controlled versus other techniques used for the preparation of metallopolymers.

Acknowledgements

The authors gratefully acknowledge support from the Romanian Academy and Ministry of Education and Research, as well as from Wallonie–Bruxelles International (WBI), the Direction générale des Relations extérieures de la Région wallonne, and the Fonds de la Recherche scientifique. Special thanks are due to the Referees and to the Editors of the *Beilstein Journal of Organic Chemistry* for their helpful comments and suggestions.

References

1. Manners, I. *Synthetic Metal Containing Polymers;* Wiley-VCH: Weinheim, Germany, 2004. doi:10.1002/3527601686
2. Abd-El-Aziz, A. S.; Manners, I., Eds. *Frontiers in Transition Metal Containing Polymers;* John Wiley & Sons: Hoboken, New Jersey, USA, 2007.
3. Russell, A. D.; Musgrave, R. A.; Stoll, L. K.; Choi, P.; Qiu, H.; Manners, I. *J. Organomet. Chem.* **2015,** *784,* 24–30. doi:10.1016/j.jorganchem.2014.10.038

4. Abd-El-Aziz, A. S.; Agatemor, C.; Etkin, N. *Macromol. Rapid Commun.* **2014,** *35,* 513–559. doi:10.1002/marc.201300826
5. Schacher, F. H.; Rupar, P. A.; Manners, I. *Angew. Chem., Int. Ed.* **2012,** *51,* 7898–7921. doi:10.1002/anie.201200310
6. Whittell, G. R.; Hager, M. D.; Schubert, U. S.; Manners, I. *Nat. Mater.* **2011,** *10,* 176–188. doi:10.1038/nmat2966
7. Breul, A. M.; Kübel, J.; Häupler, B.; Friebe, C.; Hager, M. D.; Winter, A.; Dietzek, B.; Schubert, U. S. *Macromol. Rapid Commun.* **2014,** *35,* 747–751. doi:10.1002/marc.201300806
8. Cao, K.; Murshid, N.; Wang, X. *Macromol. Rapid Commun.* **2015,** *36,* 586–596. doi:10.1002/marc.201400563
9. Rapakousiou, A.; Djeda, R.; Grillaud, M.; Li, N.; Ruiz, J.; Astruc, D. *Organometallics* **2014,** *33,* 6953–6962. doi:10.1021/om501031u
10. Mavila, S.; Diesendruck, C. E.; Linde, S.; Amir, L.; Shikler, R.; Lemcoff, N. G. *Angew. Chem., Int. Ed.* **2013,** *52,* 5767–5770. doi:10.1002/anie.201300362
11. Dragutan, V.; Dragutan, I.; Fischer, H. *J. Inorg. Organomet. Polym. Mater.* **2008,** *18,* 18–31. doi:10.1007/s10904-007-9185-5
12. Mavila, S.; Rozenberg, I.; Lemcoff, N. G. *Chem. Sci.* **2014,** *5,* 4196–4203. doi:10.1039/c4sc01231c
13. Abd-El-Aziz, A. S.; Strohm, E. A. *Polymer* **2012,** *53,* 4879–4921. doi:10.1016/j.polymer.2012.08.024
14. Eloi, J.-C.; Chabanne, L.; Whittell, G. R.; Manners, I. *Mater. Today* **2008,** *11,* 28–36. doi:10.1016/S1369-7021(08)70054-3
15. Yan, Y.; Zhang, J.; Qiao, Y.; Ganewatta, M.; Tang, C. *Macromolecules* **2013,** *46,* 8816–8823. doi:10.1021/ma402039u
16. Hadadpour, M.; Gwyther, J.; Manners, I.; Ragogna, P. J. *Chem. Mater.* **2015,** *27,* 3430–3440. doi:10.1021/acs.chemmater.5b00752
17. Baljak, S.; Russell, A. D.; Binding, S. C.; Haddow, M. F.; O'Hare, D.; Manners, I. *J. Am. Chem. Soc.* **2014,** *136,* 5864–5867. doi:10.1021/ja5014745
18. Wang, X.; Cao, K.; Liu, Y.; Tsang, B.; Liew, S. *J. Am. Chem. Soc.* **2013,** *135,* 3399–3402. doi:10.1021/ja400755e
19. Ding, L.; Wang, C.; Lin, L.; Zhu, Z. *Macromol. Chem. Phys.* **2015,** *216,* 761–769. doi:10.1002/macp.201400579
20. Bachler, P. R.; Wagener, K. B. *Monatsh. Chem.* **2015,** *146,* 1053–1061. doi:10.1007/s00706-015-1479-7
21. Autenrieth, B.; Jeong, H.; Forrest, W. P.; Axtell, J. C.; Ota, A.; Lehr, T.; Buchmeiser, M. R.; Schrock, R. R. *Macromolecules* **2015,** *48,* 2480–2492. doi:10.1021/acs.macromol.5b00123
22. Dragutan, I.; Dragutan, V.; Demonceau, A. *Molecules* **2015,** *20,* 17244–17274. doi:10.3390/molecules200917244
23. Rosebrugh, L. E.; Marx, V. M.; Keitz, B. K.; Grubbs, R. H. *J. Am. Chem. Soc.* **2013,** *135,* 10032–10035. doi:10.1021/ja405559y
24. Elling, B. R.; Xia, Y. *J. Am. Chem. Soc.* **2015,** *137,* 9922–9926. doi:10.1021/jacs.5b05497
25. Eissa, A. M.; Khosravi, E. *Macromol. Chem. Phys.* **2015,** *216,* 964–976. doi:10.1002/macp.201400604
26. Dragutan, V.; Dragutan, I.; Dimonie, M. Tuning Product Selectivity in ROMP of Cycloolefins with W-Based Catalytic Systems. In *Green Metathesis Chemistry: Great Challenges in Synthesis, Catalysis and Nanotechnology;* Dragutan, V.; Demonceau, A.; Dragutan, I.; Finkelshtein, E. S., Eds.; Springer-Verlag: New York, 2010; pp 383–390. doi:10.1007/978-90-481-3433-5_24
27. Gutekunst, W. R.; Hawker, C. J. *J. Am. Chem. Soc.* **2015,** *137,* 8038–8041. doi:10.1021/jacs.5b04940
28. Grubbs, R. H.; Wenzel, A. G.; O'Leary, D. J.; Khosravi, E., Eds. *Handbook of Metathesis,* 2nd ed.; Wiley-VCH: Weinheim, Germany, 2015.
29. Grela, K. *Beilstein J. Org. Chem.* **2010,** *6,* 1089–1090. doi:10.3762/bjoc.6.124
30. Levin, E.; Mavila, S.; Eivgi, O.; Tzur, E.; Lemcoff, N. G. *Angew. Chem., Int. Ed.* **2015,** *54,* 12384–12388. doi:10.1002/anie.201500740
31. Zeits, P. D.; Fiedler, T.; Gladysz, J. A. *Chem. Commun.* **2012,** *48,* 7925–7927. doi:10.1039/C2CC32150E
32. Wappel, J.; Grudzień, K.; Barbasiewicz, M.; Michalak, M.; Grela, K.; Slugovc, C. *Monatsh. Chem.* **2015,** *146,* 1153–1160. doi:10.1007/s00706-015-1494-8
33. Hardy, C. G.; Zhang, J.; Yan, Y.; Ren, L.; Tang, C. *Prog. Polym. Sci.* **2014,** *39,* 1742–1796. doi:10.1016/j.progpolymsci.2014.03.002
34. Dragutan, I.; Dragutan, V.; Fischer, H. *J. Inorg. Organomet. Polym. Mater.* **2008,** *18,* 311–324. doi:10.1007/s10904-008-9213-0
35. Yampolskii, Yu.; Starannikova, L.; Belov, N.; Bermeshev, M.; Gringolts, M.; Finkelshtein, E. *J. Membr. Sci.* **2014,** *453,* 532–545. doi:10.1016/j.memsci.2013.11.002
36. Bang, A.; Mohite, D.; Saeed, A. M.; Leventis, N.; Sotiriou-Leventis, C. *J. Sol-Gel Sci. Technol.* **2015,** *75,* 460–474. doi:10.1007/s10971-015-3718-0
37. Hardy, C. G.; Ren, L.; Ma, S.; Tang, C. *Chem. Commun.* **2013,** *49,* 4373–4375. doi:10.1039/c2cc36756d
38. Zhou, J.; Whittell, G. R.; Manners, I. *Macromolecules* **2014,** *47,* 3529–3543. doi:10.1021/ma500106x
39. Zha, Y.; Thaker, H. D.; Maddikeri, R. R.; Gido, S. P.; Tuominen, M. T.; Tew, G. N. *J. Am. Chem. Soc.* **2012,** *134,* 14534–14541. doi:10.1021/ja305249b
40. AL-Badri, Z. M.; Maddikeri, R. R.; Zha, Y.; Thaker, H. D.; Dobriyal, P.; Shunmugam, R.; Russell, T. P.; Tew, G. N. *Nat. Commun.* **2011,** *2,* 482. doi:10.1038/ncomms1485
41. Hardy, C. G.; Ren, L.; Zhang, J.; Tang, C. *Isr. J. Chem.* **2012,** *52,* 230–245. doi:10.1002/ijch.201100110
42. Albagli, D.; Bazan, G.; Wrighton, M. S.; Schrock, R. R. *J. Am. Chem. Soc.* **1992,** *114,* 4150–4158. doi:10.1021/ja00037a017
43. Amer, W. A.; Wang, L.; Amin, A. M.; Ma, L.; Yu, H. *J. Inorg. Organomet. Polym. Mater.* **2010,** *20,* 605–615. doi:10.1007/s10904-010-9373-6
44. Gu, H.; Rapakousiou, A.; Castel, P.; Guidolin, N.; Pinaud, N.; Ruiz, J.; Astruc, D. *Organometallics* **2014,** *33,* 4323–4335. doi:10.1021/om5006897
45. Gu, H.; Ciganda, R.; Hernandez, R.; Castel, P.; Zhao, P.; Ruiz, J.; Astruc, D. *Macromolecules* **2015,** *48,* 6071–6076. doi:10.1021/acs.macromol.5b01603
46. Rapakousiou, A.; Deraedt, C.; Gu, G.; Salmon, L.; Belin, C.; Ruiz, J.; Astruc, D. *J. Am. Chem. Soc.* **2014,** *136,* 13995–13998. doi:10.1021/ja5079267
47. Rapakousiou, A.; Deraedt, C.; Irigoyen, J.; Wang, Y.; Pinaud, N.; Salmon, L.; Ruiz, J.; Moya, S.; Astruc, D. *Inorg. Chem.* **2015,** *54,* 2284–2299. doi:10.1021/ic5028916
48. Deraedt, C.; Rapakousiou, A.; Gu, H.; Salmon, L.; Ruiz, J.; Astruc, D. *J. Inorg. Organomet. Polym. Mater.* **2015,** *25,* 437–446. doi:10.1007/s10904-014-0161-6
49. Ren, L.; Zhang, J.; Bai, X.; Hardy, C. G.; Shimizu, K. D.; Tang, C. *Chem. Sci.* **2012,** *3,* 580–583. doi:10.1039/C1SC00783A
50. Ren, L.; Zhang, J.; Hardy, C. G.; Ma, S.; Tang, C. *Macromol. Rapid Commun.* **2012,** *33,* 510–516. doi:10.1002/marc.201100732

51. Yan, Y.; Zhang, J.; Wilbon, P.; Qiao, Y.; Tang, C. *Macromol. Rapid Commun.* **2014,** *35,* 1840–1845. doi:10.1002/marc.201400365
52. Zhang, J.; Pellechia, P. J.; Hayat, J.; Hardy, C. G.; Tang, C. *Macromolecules* **2013,** *46,* 1618–1624. doi:10.1021/ma4000013
53. Zha, Y.; Maddikeri, R. R.; Gido, S. P.; Tew, G. N. *J. Inorg. Organomet. Polym. Mater.* **2013,** *23,* 89–94. doi:10.1007/s10904-012-9744-2
54. Wang, Y.; Rapakousiou, A.; Astruc, D. *Macromolecules* **2014,** *47,* 3767–3774. doi:10.1021/ma5007864
55. Hadjichristidis, N.; Pitsikalis, M.; Iatrou, H. *Adv. Polym. Sci.* **2005,** *189,* 1–124. doi:10.1007/12_005
56. Sankaran, N. B.; Rys, A. Z.; Nassif, R.; Nayak, M. K.; Metera, K.; Chen, B.; Bazzi, H. S.; Sleiman, H. F. *Macromolecules* **2010,** *43,* 5530–5537. doi:10.1021/ma100234j
57. Zha, Y.; Disabb-Miller, M. L.; Johnson, Z. D.; Hickner, M. A.; Tew, G. N. *J. Am. Chem. Soc.* **2012,** *134,* 4493–4496. doi:10.1021/ja211365r
58. Xu, F.; Kim, H. U.; Kim, J.-H.; Jung, B. J.; Grimsdale, A. C.; Hwang, D.-H. *Prog. Polym. Sci.* **2015,** *47,* 92–121. doi:10.1016/j.progpolymsci.2015.01.005
59. Carlise, J. R.; Wang, X. Y.; Weck, M. *Macromolecules* **2005,** *38,* 9000–9008. doi:10.1021/ma0512298
60. Metera, K. L.; Hänni, K. D.; Zhou, G.; Nayak, M. K.; Bazzi, H. S.; Juncker, D.; Sleiman, H. F. *ACS Macro Lett.* **2012,** *1,* 954–959. doi:10.1021/mz3001644
61. Pawar, G. M.; Weckesser, J.; Blechert, S.; Buchmeiser, M. R. *Beilstein J. Org. Chem.* **2010,** *6,* No. 28. doi:10.3762/bjoc.6.28
62. Yan, Y.; Deaton, T. M.; Zhang, J.; He, H.; Hayat, J.; Pageni, P.; Matyjaszewski, K.; Tang, C. *Macromolecules* **2015,** *48,* 1644–1650. doi:10.1021/acs.macromol.5b00471
63. Bergens, S. H.; Sullivan, A. D.; Hass, M. Heterogenous rhodium metal catalysts. U.S. Patent 8,962,516 B2, Feb 24, 2015.
64. Il'icheva, A. I.; Barinova, Yu. P.; Bochkarev, L. N.; Il'ichev, V. A. *Russ. J. Appl. Chem.* **2012,** *85,* 1711–1717. doi:10.1134/S1070427212110146
65. Barinova, Yu. P.; Ilicheva, A. I.; Bochkarev, L. N.; Ilichev, V. A.; Kurskii, Yu. A. *Russ. J. Gen. Chem.* **2013,** *83,* 72–79. doi:10.1134/S107036321301012X
66. Miao, W.-K.; Yan, Y.-K.; Wang, X.-L.; Xiao, Y.; Ren, L.-J.; Zheng, P.; Wang, C.-H.; Ren, L.-X.; Wang, W. *ACS Macro Lett.* **2014,** *3,* 211–215. doi:10.1021/mz5000202
67. Rozhkov, A. V.; Bochkarev, L. N.; Basova, G. V.; Abakumov, G. A. *Russ. J. Appl. Chem.* **2012,** *85,* 1930–1938. doi:10.1134/S1070427212120233
68. Nguyen, M. T.; Holliday, B. J. *Chem. Commun.* **2015,** *51,* 8610–8613. doi:10.1039/c5cc01719j
69. Feng, W.; Zhang, Y.; Zhang, Z.; Su, P.; Lü, X.; Song, J.; Fan, D.; Wong, W.-K.; Jones, R. A.; Su, C. *J. Mater. Chem. C* **2014,** *2,* 1489–1499. doi:10.1039/c3tc31814a
70. Zhang, Z.; Feng, H.; Liu, L.; Yu, C.; Lü, X.; Zhu, X.; Wong, W.-K.; Jones, R. A.; Pan, M.; Su, C. *Dalton Trans.* **2015,** *44,* 6229–6241. doi:10.1039/C5DT00141B

License and Terms